

Earth Resources

ACCESSION NUMBER RANGES

Accession numbers cited in this Supplement fall within the following ranges.

STAR (N-10000 Series)	N85-15657 – N85-22341
-----------------------	-----------------------

IAA (A-10000 Series)	A85-19102 – A85-30222
----------------------	-----------------------

This bibliography was prepared by the NASA Scientific and Technical Information Facility operated for the National Aeronautics and Space Administration by RMS Associates.

SPECIAL NOTICE

FOREIGN TECHNOLOGY INDEX IN THIS ISSUE

Documents referred to in this bibliography whose country of intellectual origin is other than the United States are listed in the Foreign Technology Index (see page D-1).

A great deal of excellent scientific and technical work is done throughout the world. To the extent that U.S. researchers, engineers, and industry can utilize what is done in foreign countries, we save our resources. We can thus increase our country's productivity.

We are testing out this approach by helping readers bring foreign technology into focus. We would like to know whether it is useful, and how it might be improved.

Check below, tear out, fold, staple, and return this sheet.

Foreign Technology Index:

- ☐ Isn't useful, so should be discontinued.
- ☐ Is useful, but other sources can be used.
- ☐ Is useful and should be continued.
- ☐ Suggestions for improvements to future issues:

Name (optional) _____

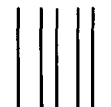
Organization (optional) _____

National Aeronautics and
Space Administration

Washington, D.C.
20546

Official Business
Penalty for Private Use, \$300

FIRST CLASS MAIL



Postage and Fees Paid
National Aeronautics and
Space Administration
NASA-451

National Aeronautics & Space Administration
NASA Headquarters Mail Code NIT-2
Washington, D.C. 20546

NASA

EARTH RESOURCES

A CONTINUING BIBLIOGRAPHY WITH INDEXES

Issue 46

A selection of annotated references to unclassified reports and journal articles that were introduced into the NASA scientific and technical information system and announced between April 1 and June 30, 1985 in

- *Scientific and Technical Aerospace Reports (STAR)*
- *International Aerospace Abstracts (IAA).*



Scientific and Technical Information Branch

1985

National Aeronautics and Space Administration

Washington, DC

This supplement is available as NTISUB/038/093 from the National Technical Information Service (NTIS), Springfield, Virginia 22161 at the price of \$12.50 domestic; \$25.00 foreign for standing orders. Please note: Standing orders are subscriptions which do not terminate at the end of a year, as do regular subscriptions, but continue indefinitely unless specifically terminated by the subscriber.

INTRODUCTION

The technical literature described in this continuing bibliography may be helpful to researchers in numerous disciplines such as agriculture and forestry, geography and cartography, geology and mining, oceanography and fishing, environmental control, and many others. Until recently it was impossible for anyone to examine more than a minute fraction of the Earth's surface continuously. Now vast areas can be observed synoptically, and changes noted in both the Earth's lands and waters, by sensing instrumentation on orbiting spacecraft or on aircraft.

This literature survey lists 467 reports, articles, and other documents announced between April 1 and June 30, 1985 in *Scientific and Technical Aerospace Reports (STAR)*, and *International Aerospace Abstracts (IAA)*.

The coverage includes documents related to the identification and evaluation by means of sensors in spacecraft and aircraft of vegetation, minerals, and other natural resources, and the techniques and potentialities of surveying and keeping up-to-date inventories of such riches. It encompasses studies of such natural phenomena as earthquakes, volcanoes, ocean currents, and magnetic fields; and such cultural phenomena as cities, transportation networks, and irrigation systems. Descriptions of the components and use of remote sensing and geophysical instrumentation, their subsystems, observational procedures, signature and analyses and interpretive techniques for gathering data are also included. All reports generated under NASA's Earth Resources Survey Program for the time period covered in this bibliography will also be included. The bibliography does not contain citations to documents dealing mainly with satellites or satellite equipment used in navigation or communication systems, nor with instrumentation not used aboard aerospace vehicles.

The selected items are grouped in nine categories. These are listed in the Table of Contents with notes regarding the scope of each category. These categories were especially chosen for this publication, and differ from those found in *STAR* and *IAA*.

Each entry consists of a standard bibliographic citation accompanied by an abstract. The citations include the original accession numbers from the respective announcement journals.

Under each of the nine categories, the entries are presented in one of two groups that appear in the following order:

- IAA* entries identified by accession number series A85-10,000 in ascending accession number order;

- STAR* entries identified by accession number series N85-10,000 in ascending accession number order.

After the abstract section, there are seven indexes:

- subject, personal author, corporate source, foreign technology, contract number, report/ accession number, and accession number.

AVAILABILITY OF CITED PUBLICATIONS

IAA ENTRIES (A85-10000 Series)

All publications abstracted in this Section are available from the Technical Information Service, American Institute of Aeronautics and Astronautics, Inc. (AIAA), as follows: Paper copies of accessions are available at \$8.50 per document. Microfiche⁽¹⁾ of documents announced in *IAA* are available at the rate of \$4.00 per microfiche on demand. Standing order microfiche are available at the rate of \$1.45 per microfiche for *IAA* source documents.

Minimum air-mail postage to foreign countries is \$2.50 and all foreign orders are shipped on payment of pro-forma invoices.

All inquiries and requests should be addressed to AIAA Technical Information Service. Please refer to the accession number when requesting publications.

STAR ENTRIES (N85-10000 Series)

One or more sources from which a document announced in *STAR* is available to the public is ordinarily given on the last line of the citation. The most commonly indicated sources and their acronyms or abbreviations are listed below. If the publication is available from a source other than those listed, the publisher and his address will be displayed on the availability line or in combination with the corporate source line.

Avail: NTIS. Sold by the National Technical Information Service. Prices for hard copy (HC) and microfiche (MF) are indicated by a price code preceded by the letters HC or MF in the *STAR* citation. Current values for the price codes are given in the tables on page viii.

Documents on microfiche are designated by a pound sign (#) following the accession number. The pound sign is used without regard to the source or quality of the microfiche.

Initially distributed microfiche under the NTIS SRIM (Selected Research in Microfiche) is available at greatly reduced unit prices. For this service and for information concerning subscription to NASA printed reports, consult the NTIS Subscription Section, Springfield, Va. 22161.

NOTE ON ORDERING DOCUMENTS: When ordering NASA publications (those followed by the * symbol), use the N accession number. NASA patent applications (only the specifications are offered) should be ordered by the US-Patent-Appl-SN number. Non-NASA publications (no asterisk) should be ordered by the AD, PB, or other *report* number shown on the last line of the citation, not by the N accession number. It is also advisable to cite the title and other bibliographic identification.

Avail: SOD (or GPO). Sold by the Superintendent of Documents, U.S. Government Printing Office, in hard copy. The current price and order number are given following the availability line. (NTIS will fill microfiche requests, as indicated above, for those documents identified by a # symbol.)

Avail: NASA Public Document Rooms. Documents so indicated may be examined at or purchased from the National Aeronautics and Space Administration, Public Document Room (Room 126), 600 Independence Ave., S.W., Washington, D.C. 20546, or public document rooms located at each of the NASA research centers, the NASA Space Technology Laboratories, and the NASA Pasadena Office at the Jet Propulsion Laboratory.

(1) A microfiche is a transparent sheet of film, 105 by 148 mm in size containing as many as 60 to 98 pages of information reduced to micro images (not to exceed 26:1 reduction)

- Avail: DOE Depository Libraries. Organizations in U.S. cities and abroad that maintain collections of Department of Energy reports, usually in microfiche form, are listed in *Energy Research Abstracts*. Services available from the DOE and its depositories are described in a booklet, *DOE Technical Information Center - Its Functions and Services* (TID-4660), which may be obtained without charge from the DOE Technical Information Center.
- Avail: Univ. Microfilms. Documents so indicated are dissertations selected from *Dissertation Abstracts* and are sold by University Microfilms as xerographic copy (HC) and microfilm. All requests should cite the author and the Order Number as they appear in the citation.
- Avail: USGS. Originals of many reports from the U.S. Geological Survey, which may contain color illustrations, or otherwise may not have the quality of illustrations preserved in the microfiche or facsimile reproduction, may be examined by the public at the libraries of the USGS field offices whose addresses are listed in this introduction. The libraries may be queried concerning the availability of specific documents and the possible utilization of local copying services, such as color reproduction.
- Avail: HMSO. Publications of Her Majesty's Stationery Office are sold in the U.S. by Pendragon House, Inc. (PHI), Redwood City, California. The U.S. price (including a service and mailing charge) is given, or a conversion table may be obtained from PHI.
- Avail: BLL (formerly NLL): British Library Lending Division, Boston Spa, Wetherby, Yorkshire, England. Photocopies available from this organization at the price shown. (If none is given, inquiry should be addressed to the BLL.)
- Avail: Fachinformationszentrum, Karlsruhe. Sold by the Fachinformationszentrum Energie, Physik, Mathematik GMBH, Eggenstein Leopoldshafen, Federal Republic of Germany, at the price shown in deutschmarks (DM).
- Avail: Issuing Activity, or Corporate Author, or no indication of availability. Inquiries as to the availability of these documents should be addressed to the organization shown in the citation as the corporate author of the document.
- Avail: U.S. Patent and Trademark Office. Sold by Commissioner of Patents and Trademarks, U.S. Patent and Trademark Office, at the standard price of 50 cents each, postage free.
- Avail: ESDU. Pricing information on specific data, computer programs, and details on ESDU topic categories can be obtained from ESDU International Ltd. Requesters in North America should use the Virginia address while all other requesters should use the London address, both of which are on page vii.
- Other availabilities: If the publication is available from a source other than the above, the publisher and his address will be displayed entirely on the availability line or in combination with the corporate author line.

PUBLIC COLLECTIONS OF NASA DOCUMENTS

DOMESTIC: NASA and NASA-sponsored documents and a large number of aerospace publications are available to the public for reference purposes at the library maintained by the American Institute of Aeronautics and Astronautics, Technical Information Service, 555 West 57th Street, 12th Floor, New York, New York 10019.

EUROPEAN: An extensive collection of NASA and NASA-sponsored publications is maintained by the British Library Lending Division, Boston Spa, Wetherby, Yorkshire, England for public access. The British Library Lending Division also has available many of the non-NASA publications cited in *STAR*. European requesters may purchase facsimile copy or microfiche of NASA and NASA-sponsored documents, those identified by both the symbols # and * from ESA — Information Retrieval Service European Space Agency, 8-10 rue Mario-Nikis, 75738 CEDEX 15, France.

FEDERAL DEPOSITORY LIBRARY PROGRAM

In order to provide the general public with greater access to U.S. Government publications, Congress established the Federal Depository Library Program under the Government Printing Office (GPO), with 50 regional depositories responsible for permanent retention of material, inter-library loan, and reference services. Over 1,300 other depositories also exists. A list of the regional GPO libraries appears on the inside back cover.

ADDRESSES OF ORGANIZATIONS

American Institute of Aeronautics and
Astronautics

Technical Information Service
555 West 57th Street, 12th Floor
New York, New York 10019

British Library Lending Division,
Boston Spa, Wetherby, Yorkshire,
England

Commissioner of Patents and
Trademarks
U S Patent and Trademark Office
Washington, D C 20231

Department of Energy
Technical Information Center
P O Box 62
Oak Ridge, Tennessee 37830

ESA-Information Retrieval Service
ESRIN
Via Galileo Galilei
00044 Frascati (Rome) Italy

ESDU International, Ltd.
1495 Chain Bridge Road
McLean, Virginia 22101

ESDU International, Ltd
251-259 Regent Street
London, W1R 7AD, England

Fachinformationszentrum Energie, Physik,
Mathematik GMBH
7514 Eggenstein Leopoldshafen
Federal Republic of Germany

Her Majesty's Stationery Office
P O. Box 569, S E 1
London, England

NASA Scientific and Technical Information
Facility
P O Box 8757
B W I Airport, Maryland 21240

National Aeronautics and Space
Administration
Scientific and Technical Information
Branch (NIT-1)
Washington, D C 20546

National Technical Information Service
5285 Port Royal Road
Springfield, Virginia 22161

Pendragon House, Inc
899 Broadway Avenue
Redwood City, California 94063

Superintendent of Documents
U S Government Printing Office
Washington, D C 20402

University Microfilms
A Xerox Company
300 North Zeeb Road
Ann Arbor, Michigan 48106

University Microfilms, Ltd
Tylers Green
London, England

U S. Geological Survey Library
National Center – MS 950
12201 Sunrise Valley Drive
Reston, Virginia 22092

U S Geological Survey Library
2255 North Gemini Drive
Flagstaff, Arizona 86001

U S Geological Survey
345 Middlefield Road
Menlo Park, California 94025

U S Geological Survey Library
Box 25046
Denver Federal Center, MS 914
Denver, Colorado 80225

NTIS PRICE SCHEDULES

Schedule A

STANDARD PAPER COPY PRICE SCHEDULE

(Effective January 1, 1983)

Price Code	Page Range	North American Price	Foreign Price
A01	Microfiche	\$ 4 50	\$ 9 00
A02	001-025	7 00	14 00
A03	026-050	8 50	17 00
A04	051-075	10 00	20 00
A05	076-100	11 50	23 00
A06	101-125	13 00	26 00
A07	126-150	14 50	29 00
A08	151-175	16 00	32 00
A09	176-200	17 50	35 00
A10	201-225	19 00	38 00
A11	226-250	20 50	41 00
A12	251-275	22 00	44 00
A13	276-300	23 50	47 00
A14	301-325	25 00	50 00
A15	326-350	26 50	53 00
A16	351-375	28 00	56 00
A17	376-400	29 50	59 00
A18	401-425	31 00	62 00
A19	426-450	32 50	65 00
A20	451-475	34 00	68 00
A21	476-500	35 50	71 00
A22	501-525	37 00	74 00
A23	526-550	38 50	77 00
A24	551-575	40 00	80 00
A25	576-600	41 50	83 00
A99	601-up	-- 1	-- 2

1/ Add \$1 50 for each additional 25 page increment or portion thereof for 601 pages up

2/ Add \$3 00 for each additional 25 page increment or portion thereof for 601 pages and more

Schedule E

EXCEPTION PRICE SCHEDULE

Paper Copy & Microfiche

Price Code	North American Price	Foreign Price
E01	\$ 6 50	\$ 13 50
E02	7 50	15 50
E03	9 50	19 50
E04	11 50	23 50
E05	13 50	27 50
E06	15 50	31 50
E07	17 50	35 50
E08	19 50	39 50
E09	21 50	43 50
E10	23 50	47 50
E11	25 50	51 50
E12	28 50	57 50
E13	31 50	63 50
E14	34 50	69 50
E15	37 50	75 50
E16	40 50	81 50
E17	43 50	88 50
E18	46 50	93 50
E19	51 50	102 50
E20	61 50	123 50

E-99 - Write for quote

N01	35 00	45 00
-----	-------	-------

TABLE OF CONTENTS

	Page
Category 01 Agriculture and Forestry	1
Includes crop forecasts, crop signature analysis, soil identification, disease detection, harvest estimates, range resources, timber inventory, forest fire detection, and wildlife migration patterns.	
Category 02 Environmental Changes and Cultural Resources	13
Includes land use analysis, urban and metropolitan studies, environmental impact, air and water pollution, geographic information systems, and geographic analysis.	
Category 03 Geodesy and Cartography	15
Includes mapping and topography.	
Category 04 Geology and Mineral Resources	20
Includes mineral deposits, petroleum deposits, spectral properties of rocks, geological exploration, and lithology.	
Category 05 Oceanography and Marine Resources	26
Includes sea-surface temperature, ocean bottom surveying imagery, drift rates, sea ice and icebergs, sea state, fish location	
Category 06 Hydrology and Water Management	42
Includes snow cover and water runoff in rivers and glaciers, saline intrusion, drainage analysis, geomorphology of river basins, land uses, and estuarine studies.	
Category 07 Data Processing and Distribution Systems	45
Includes film processing, computer technology, satellite and aircraft hardware, and imagery.	
Category 08 Instrumentation and Sensors	55
Includes data acquisition and camera systems and remote sensors.	
Category 09 General	70
Includes economic analysis.	
Subject Index	A-1
Personal Author Index	B-1
Corporate Source Index	C-1
Foreign Technology Index	D-1
Contract Number Index	E-1
Report/Accession Number Index	F-1
Accession Number Index	G-1

TYPICAL CITATION AND ABSTRACT FROM STAR

NASA SPONSORED DOCUMENT → **N85-15248*** # Utah Univ, Salt Lake City Center for Remote Sensing and Cartography
NASA ACCESSION NUMBER → **AN INTEGRATED LANDSAT/ANCILLARY DATA CLASSIFICATION OF DESERT RANGELAND**
TITLE → **K P PRICE, M K RIDD, and J. A. MEROLA 1984 8 p**
AUTHORS → Sponsored in part by Utah Dept. of Agriculture ERTS
CONTRACT OR GRANT → (Contract NAGW-95)
REPORT NUMBER → (E85-10046, NASA-CR-174222; NAS 1 26-174222) Avail: NTIS HC A02/MF A01 CSCL 08B
AVAILABLE ON MICROFICHE
CORPORATE SOURCE
PUBLICATION DATE
AVAILABILITY SOURCE
COSATI CODE

Range inventorying methods using LANDSAT MSS data, coupled with ancillary data were examined. The study area encompassed nearly 20,000 acres in Rush Valley, Utah. The vegetation is predominately desert shrub and annual grasses, with some annual forbs. Three LANDSAT scenes were evaluated using a Kauth-Thomas brightness/greenness data transformation (May, June, and August dates). The data was classified using a four-band maximum-likelihood classifier. A print map was taken into the field to determine the relationship between print symbols and vegetation. It was determined that classification confusion could be greatly reduced by incorporating geomorphic units and soil texture (coarse vs fine) into the classification. Spectral data, geomorphic units, and soil texture were combined in a GIS format to produce a final vegetation map identifying 12 vegetation types.

Author

TYPICAL CITATION AND ABSTRACT FROM IAA

NASA SPONSORED DOCUMENT → **A85-17493*** National Aeronautics and Space Administration.
AIAA ACCESSION NUMBER → Lyndon B Johnson Space Center, Houston, Tex
TITLE → **EVALUATION OF PROCEDURES TO CORRECT FOR VARIABLE VIEWING AND ILLUMINATION GEOMETRY WHEN OBSERVING A NON-LAMBERTIAN SURFACE THROUGH THE ATMOSPHERE**
AUTHORS → **V S. WHITEHEAD (NASA, Johnson Space Center, Houston, TX), W. R. JOHNSON, M. L. MATHEWS, and N. C. HORVATH (Lockheed Engineering and Management Services Co., Inc., Houston, TX)** IN: 1983 International Geoscience and Remote Sensing Symposium (IGARSS '83), San Francisco, CA, August 31-September 2, 1983, Digest Volume 1. New York, Institute of Electrical and Electronics Engineers, Inc., 1983, 6 p. refs
MEETING → **MEETING DATE**
AUTHOR'S AFFILIATION

Data from the Advanced Very High Resolution Radiometer aboard the NOAA polar orbiting satellite are being operationally applied to provide estimates of vegetation cover and/or condition over a large part of the earth by the USDA. The wide scan angle (+ or - 54 deg) of this system permits daily views of the earth when used to its limits. Five-day repetitive coverage is acquired, assuming cloud-free conditions, in current operations which limit the use of the scan to the center + or - 14 deg of swath. While use of the full scan width would provide clear acquisitions frequent enough to monitor crop development and condition even with normal cloudiness, these off-nadir data are made difficult to interpret due to the non-Lambertian nature of the surface, enhanced effect of the atmosphere, inclusion of subpixel and thin invisible clouds in the scene, and differences in illumination across the scene; all of which contribute to variations in observed reflected radiation. Some approaches to provide corrections for these effects are discussed here.

Author

EARTH RESOURCES

A Continuing Bibliography (Issue 46)

JULY 1985

01

AGRICULTURE AND FORESTRY

Includes crop forecasts, crop signature analysis, soil identification, disease detection, harvest estimates, range resources, timber inventory, forest fire detection, and wildlife migration patterns.

A85-20573

AN EXAMPLE OF LANDSAT COST EFFECTIVENESS IN MAPPING LAND-COVER

I. L. THOMAS (General Technology Systems, Ltd., Brentford, Middx, England; Department of Scientific and Industrial Research, Physics and Engineering Laboratory, Lower Hutt, New Zealand), N. P. CHING (Department of Lands and Survey, New Zealand Forest Service, Wellington, New Zealand), and V. M. BENNING (Department of Lands and Survey, Wellington, New Zealand) *Earth-Oriented Applications of Space Technology* (ISSN 0277-4488), vol. 4, no. 4, 1984, p. 261-264. refs

Landsat 2 satellite data was acquired over an agricultural and forestry primary producing region of the North Island of New Zealand, and the IBM Earth Resources Management package was used to produce classification maps of the area selected for study. The results from two independently conducted land-cover and forestry projects are presented. These results indicate that the Landsat/computer analysis system is able to make a valid, timely, and impartial contribution to the management process. Classification confidence levels of 94.5 and 81.4 percent were achieved for land-cover discrimination to level II and level III/IV for forest-class discrimination using a single Landsat image. A comparison made between a multi-department conventional survey in the same area and the land-cover and forestry results derived using Landsat data, indicates an 80 percent savings in manpower and an 85 percent reduction in total costs. M.D

A85-21050

ANALYSIS OF ACIR TRANSPARENCIES OF CITRUS TREES WITH A PROJECTING SPECTRAL DENSITOMETER

G. J. EDWARDS (Florida, University, Lake Alfred, FL) and C. H. BLAZQUEZ (Florida, University, Cocoa Beach, FL) *Photogrammetric Engineering and Remote Sensing* (ISSN 0099-1112), vol. 51, Jan 1985, p. 95-98. refs

Ratios of selected spectral densitometric values of citrus tree images on aerial color infrared (ACIR) transparencies were determined using a set of three instruments: Dokumator DL-2 Microfilm Reader, a Visible Monochromator, and an Auto-Photometer. Plots of film density for citrus tree images had two peaks, one at 490 to 500 nm and another at 600 to 610 nm. The ratios of the film density at these two peaks were lower for healthy trees than for stressed trees. A linear regression of the photointerpretation (PI) versus the ratio values for 60 tree images gave a correlation coefficient of 0.85 Author

A85-21174* National Aeronautics and Space Administration Goddard Space Flight Center, Greenbelt, Md

AFRICAN LAND-COVER CLASSIFICATION USING SATELLITE DATA

C. J. TUCKER, T. E. GOFF (NASA, Goddard Space Flight Center, Greenbelt, MD), and J. R. G. TOWNSHEND (Reading, University, Reading, Berks, England) *Science* (ISSN 0036-8075), vol. 227, Jan 25, 1985, p. 369-375. refs

Data from the advanced very high resolution radiometer sensor on the National Oceanic and Atmospheric Administration's operational series of meteorological satellites were used to classify land cover and monitor vegetation dynamics for Africa over a 19-month period. There was a correspondence between seasonal variations in the density and extent of green leaf vegetation and the patterns of rainfall associated with the movement of the Intertropical Convergence Zone. Regional variations, such as the 1983 drought in the Sahel of western Africa, were observed. Integration of the weekly satellite data with respect to time for a 12-month period produced a remotely sensed estimate of primary production based upon the density and duration of green leaf biomass. Eight of the 21-day composited data sets covering an 11-month period were used to produce a general land-cover classification that corresponded well with those of existing maps. Author

A85-22420* National Aeronautics and Space Administration Goddard Space Flight Center, Greenbelt, Md.

EFFECT OF HELIOTROPISM ON THE BIDIRECTIONAL REFLECTANCE OF IRRIGATED COTTON

J. B. SCHUTT, D. S. KIMES (NASA, Goddard Space Flight Center, Earth Resources Branch, Greenbelt, MD), and W. W. NEWCOMB (Republic Management Systems, Landover, MD) *Remote Sensing of Environment* (ISSN 0034-4257), vol. 17, Feb 1985, p. 13-25 refs

The dynamic behavior of cotton leaves is described using gyroscopic coordinates. Angular movements represented as pitching, rolling, and yawing are used to follow the movement of leaf normals and their instantaneous relationships to the sun on an individual basis. A sensitivity analysis establishes that the angle between a leaf normal and the sun is most affected by changes in pitch and roll. Plots of the phase angle gamma averaged by quadrant show the pronounced heliotropic behavior of cotton leaves. Plots of pitch versus roll averaged by quadrant demonstrate the differential behavior of cotton leaves relative to the position of the sun. These results are used to interpret sections taken from bidirectional reflectance curves obtained using 0.57-0.69 micron band in terms of the evolution of gamma from sunrise until noon. The measured and experimental values of gamma are in reasonable agreement. Forescattered and backscattered extinctions are observed to have distinct leaf normal directions. C.D

A85-23694

VISUAL INTERPRETATION OF SAR IMAGES OF TWO AREAS IN THE NETHERLANDS

TH. A. DE BOER (Centre for Agrobiological Research, Wageningen, Netherlands) IN: *Satellite microwave remote sensing* Chichester, West Sussex, England, Ellis Horwood, Ltd., 1983, p. 299-305.

SAR images with a resolution of 25 m and a scale of 1:250,000 recorded in October 1978, after the crops were harvested, are

examined for detection of soil use and of the ground-water level in grassland areas, and are compared to previous SLAR images of the same areas. The two areas under consideration are: one surrounding the town of Wolvega (province of Friesland) and the Oostelijk Flevoland area. Seven density classes are distinguished, and the corresponding arable areas are defined. It is found that ditches filled with water and oriented parallel to the satellite's track frequently have distinctly higher backscatter than those with a different orientation; this feature is also observed for green belts, dikes, ditch-side vegetation, river banks, and road-side trees.

L.T.

A85-23752

ANGULAR AND SPATIAL VARIABILITY OF VISIBLE AND NIR SPECTRAL DATA [VARIABILITE ANGULAIRE ET SPATIALE DES DONNEES SPECTRALES DANS LE VISIBLE ET LE PROCHE INFRAROUGE]

G. GUYOT (Institut National de la Recherche Agronomique, Montfavet, Vaucluse, France) IN: Spectral signatures of objects in remote sensing; International Conference, 2nd, Bordeaux, France, September 12-16, 1983, Reports. Versailles, Institut National de la Recherche Agronomique, 1984, p. 27-44. In French. refs

Techniques for taking into account and applying the angular and spatial variability of visible and NIR data on vegetation cover and surface morphology obtained with high-resolution remote sensors such as Landsat TM and SPOT are discussed and illustrated in a review of recent field experiments and model simulations. Consideration is given to the effects of the view angle, the geometric structure of vegetation, the sun position, the turbidity of the atmosphere, and the physiological and phenological condition of the cover vegetation. The feasibility of combining vertical and oblique views to facilitate the identification of certain classes of surface objects is examined.

T.K.

A85-23753* State Univ. of New York, Binghamton.

ESTIMATION OF AGRONOMIC VARIABLES USING SPECTRAL SIGNATURES

N. S. GOEL and R. L. THOMPSON (New York, State University, Binghamton, NY) IN: Spectral signatures of objects in remote sensing; International Conference, 2nd, Bordeaux, France, September 12-16, 1983, Reports. Versailles, Institut National de la Recherche Agronomique, 1984, p. 45-53. NASA-supported research. refs

Techniques for the determination of leaf area index or leaf angle distribution from remote-sensing canopy-reflectance (CR) measurements are developed on the basis of empirical models relating CR to parameters such as soil and vegetation spectral properties, solar flux, and viewing angle. A general procedure for inverting CR models is presented and applied to the models of Suits (1972), Verhoef and Bunnik (1981), and Norman (1979) in the IR range. Numerical results for a soybean canopy are compared in a table, and the error sensitivity of the inverted models is shown to be relatively high, requiring the use of ancillary data such as soil reflectance, leaf reflectance, and leaf transmittance.

T.K.

A85-23754* Purdue Univ., Lafayette, Ind.

LIGHT POLARIZATION MEASUREMENTS - A METHOD TO DETERMINE THE SPECULAR AND DIFFUSE LIGHT-SCATTERING PROPERTIES OF BOTH LEAVES AND PLANT CANOPIES

V. C. VANDERBILT and L. GRANT (Purdue University, West Lafayette, IN) IN: Spectral signatures of objects in remote sensing; International Conference, 2nd, Bordeaux, France, September 12-16, 1983, Reports. Versailles, Institut National de la Recherche Agronomique, 1984, p. 55-66. refs
(Contract NAG5-269; NAS9-14970)

The contributions of diffuse and specular reflection to the total canopy reflection of sunlight are determined experimentally for wheat at two stages of development using spectroradiometer measurements obtained at 13 wavelengths in the 480-720-nm range with a polarizing film in maximum and minimum signal-amplitude positions. The data and computation techniques

are presented in tables, diagrams, and graphs, and the need to take specular reflection into account in constructing models of light/canopy interaction is stressed

T.K.

A85-23756

THE MEASUREMENT OF BIDIRECTIONAL REFLECTANCES BY ANALYSIS OF LANDSAT IMAGES [LA MESURE DE REFLECTANCES BIDIRECTIONNELLES PAR ANALYSE DES IMAGES LANDSAT]

F. CAVAYAS, G. ROCHON (Universite Laval, Sainte-Foy, Quebec, Canada), and P. TEILLET (Canada Centre for Remote Sensing, Ottawa, Canada) IN: Spectral signatures of objects in remote sensing; International Conference, 2nd, Bordeaux, France, September 12-16, 1983, Reports. Versailles, Institut National de la Recherche Agronomique, 1984, p. 123-130. In French.

Techniques for the estimation of bidirectional reflectance of ground features from Landsat MSS images are described and demonstrated. The theoretical model takes the effects of atmospheric attenuation and backscatter into account and attempts to correct for the slope and orientation of the topography, as determined from an aerial-laser-ranging digital terrain model. An application to several types of forest cover is shown, and a Lambertian approximation is found to estimate reflectance to within 5 deg from MSS bands 4 and 5 at slopes less than 20 deg. For bands 6 and 7 and for slopes above 20 deg, a model which accounts for the anisotropy of the bidirectional reflectance is proposed, but more ground-truth data are required for its evaluation

T.K.

A85-23757

COMPARATIVE SEASONAL EVOLUTION OF THE SPECTRAL SIGNATURES OF BROAD-LEAVED AND CONIFEROUS TREES FROM LANDSAT DATA COMPARISON WITH OTHER PERENNIAL SURFACES [EVOLUTIONS SAISONNIERES COMPAREES DES SIGNATURES SPECTRALES DE FEUILLUS ET DE CONIFERES A PARTIR DE DONNEES LANDSAT COMPARAISON AVEC D'AUTRES MILIEUX PERENNES]

R. CHAUME and A. COMBEAU (Office de la Recherche Scientifique et Technique d'Outre-Mer, Bondy, Seine-Saint-Denis, France) IN: Spectral signatures of objects in remote sensing; International Conference, 2nd, Bordeaux, France, September 12-16, 1983, Reports. Versailles, Institut National de la Recherche Agronomique, 1984, p. 131-139. In French.

A85-23758

ANALYSIS OF GROUND RADIOMETRIC MEASUREMENTS IN THE RICE-GROWING SITE AT TAMANI (REPUBLIC OF MALI) - EFFECT OF CERTAIN YIELD PARAMETERS ON THE SPECTRAL SIGNATURE [ANALYSE DE MESURES RADIOMETRIQUES AU SOL SUR LE SITE RIZICOLE DE TAMANI (REP. DU MALI) - INFLUENCE DE CERTAINS PARAMETRES DE RENDEMENT SUR LE COMPORTEMENT SPECTRAL]

G. M. FERRARI and J. M. GREGOIRE (Commission of the European Communities, Joint Research Centre, Ispra, Italy) IN: Spectral signatures of objects in remote sensing; International Conference, 2nd, Bordeaux, France, September 12-16, 1983, Reports. Versailles, Institut National de la Recherche Agronomique, 1984, p. 193-200. In French. refs

A85-23760

DETERMINATION OF REFLECTANCES OF TROPICAL VEGETATION BY COMBINED METHODS OF RADIOMETRY AND PHOTOMETRY

M. C. MUEKSCH (Bonn, Universitaet, Bonn, West Germany) IN: Spectral signatures of objects in remote sensing; International Conference, 2nd, Bordeaux, France, September 12-16, 1983, Reports. Versailles, Institut National de la Recherche Agronomique, 1984, p. 287-294. refs

Iterative algorithms for calculating the 500-850-nm reflectance of tropical vegetation from in situ or remote-sensing radiometric and photometric data are developed and demonstrated. Four semiempirical localized models are shown in block diagrams and

described: one using radiometric signals converted to energy units, one using the raw voltages and a humidity-modified Rayleigh atmosphere, one using horizontal photometric data calibrated by observing the nonturbid horizon in the direction of the test object, and one using vertical photometric data (from satellite images) with standard reference objects and a standard Rayleigh atmosphere. Sample results from measurements on shrubs, grasslands, and bare soils in East Africa (-8 to -10 deg S) are presented in graphs and briefly characterized, the reliability of the models is estimated as 1-5 percent. T.K.

A85-23762

COMPARISON OF SPOT HRV AND LANDSAT-4 TM FOR CROP INVENTORIES [COMPARAISON DE SPOT-HRV ET DE LANDSAT-4-TM POUR L'INVENTAIRE DE CULTURES]

G. SAINT, A. PODAIRE (Centre National d'Etudes Spatiales, Toulouse, France), P. CORDIER, P. FOURNIER, and J. MEYER-ROUX (Ministere de l'Agriculture, Paris, France) IN: Spectral signatures of objects in remote sensing, International Conference, 2nd, Bordeaux, France, September 12-16, 1983, Reports Versailles, Institut National de la Recherche Agronomique, 1984, p. 331-340 In French.

The results of a simulation of the SPOT high-resolution visible-range (HRV) instrument and the Landsat Thematic Mapper (TM), using an airborne Daedalus scanner over a 2500-ha area of SW France on four days during spring and summer, 1981, are reported and analyzed. The test area contains three sites with hills, plains, plateau, and valleys and small fields of winter wheat, corn, sorghum, colza, and sunflowers, as well as some small amounts of other crops, natural grasslands, vineyards, and forests. The results are presented in tables, graphs, and histograms and characterized statistically. The value of interband correlations is demonstrated, and the importance of the green bands (1 and 2) in the superior performance of the TM in classifying crops spectrally similar on one day is stressed. The higher resolution of the HRV is found to give more accurate one-day area estimates for easily distinguished crops and better multitemporal comparisons. T.K.

A85-23763

ESTIMATION OF WHEAT PRODUCTION ON THE BASIS OF LANDSAT CHANNEL 5 AND 7 RADIOMETRIC MEASUREMENTS [ESTIMATION DE LA PRODUCTION DU BLE A PARTIR DE MESURES RADIOMETRIQUES DANS LES CANAUX 5 ET 7 DE LANDSAT]

F. BARET (Institut Technique des Cereales et Fourrages, Manosque, Alpes-de-Haute-Provence, France), G. GUYOT, and J. N. MIGUET (Institut National de la Recherche Agronomique, Montfavet, Vaucluse, France) IN: Spectral signatures of objects in remote sensing; International Conference, 2nd, Bordeaux, France, September 12-16, 1983, Reports Versailles, Institut National de la Recherche Agronomique, 1984, p. 373-382. In French. refs

The feasibility of using Landsat images to monitor the maturation of wheat in a dry climate is investigated experimentally using in situ radiometers to simulate channels 5 and 7. Radiometric and biological measurements for four varieties of winter wheat and one of hard wheat grown with natural rainfall and for one variety of winter wheat grown with three degrees of irrigation are obtained from a site in SE France and analyzed statistically. Special attention is given to the critical period near the end of maturation when the water content of the grain remains constant: it is found that the length of this period can be detected radiometrically. An empirical relation between the final yield of wheat and the rate of decrease of the normalized difference of the reflectance measured in the two channels is established for the winter wheat Talent T.K.

A85-23765

ESTIMATION OF EVAPOTRANSPIRATION ON THE BASIS OF THERMAL IR [ESTIMATION DE L'EVAPOTRANSPIRATION A PARTIR DE L'INFRA-ROUGE THERMIQUE]

B. SEGUIN (Institut National de la Recherche Agronomique, Montfavet, Vaucluse, France) IN: Spectral signatures of objects in remote sensing, International Conference, 2nd, Bordeaux, France, September 12-16, 1983, Reports Versailles, Institut National de la Recherche Agronomique, 1984, p. 427-446. In French. refs

The use of remotely sensed thermal-IR data to determine the evaporation from bare soils, the transpiration from leaves, or the evapotranspiration from vegetative canopies is discussed in a review of theoretical and empirical models and data-reduction procedures. The value of satellite measurements in bridging the gap between local-scale and synoptic-scale methods is indicated; the physical relationship between surface temperature and evaporation is explained; local-scale models based on simulations or on the combination of the energy-balance equation with the aerodynamic formulation of the sensible heat flux are examined, their application to data from such satellites as NOAA, HCMM, and Meteosat is considered; typical data are presented graphically; and regional-scale simulations are surveyed. The need for further detailed studies of various types of developed canopies (such as wheat, corn, orchards, and forests) and for longer-time-scale observations is stressed T.K.

A85-23767

EFFECTS OF THE EXPERIMENTAL ERRORS AND CONDITIONS ON THE ESTIMATION OF THERMAL INERTIA AND EVAPOTRANSPIRATION FROM METEOSAT DATA [INFLUENCE DES CONDITIONS DE MESURE SUR L'ESTIMATION DE L'INERTIE THERMIQUE ET DE L'EVAPOTRANSPIRATION A PARTIR DES DONNEES METEOSAT]

A. ABDELLAOUI, F. BECKER, E. OLORY-HECHINGER, and M. RAFFY (Strasbourg I, Universite, Strasbourg, France) IN: Spectral signatures of objects in remote sensing; International Conference, 2nd, Bordeaux, France, September 12-16, 1983, Reports Versailles, Institut National de la Recherche Agronomique, 1984, p. 475-484. In French. Research supported by the Centre National d'Etudes Spatiales and ESA. refs

A85-23771

USE OF HCMM THERMAL IMAGES IN THE STUDY OF MICROCLIMATES IN A MOUNTAINOUS REGION [UTILISATION DES THERMOGRAPHIES HCMM DANS L'ETUDE DES MICROCLIMATS EN REGION MONTAGNEUSE]

J. P. LAGOUARDE (Institut National de la Recherche Agronomique, Montfavet, Vaucluse, France) IN: Spectral signatures of objects in remote sensing; International Conference, 2nd, Bordeaux, France, September 12-16, 1983, Reports Versailles, Institut National de la Recherche Agronomique, 1984, p. 535-544. In French. refs

The effect of topography on HCMM satellite thermal images is studied for a fir forest in the northeast region of the Central Massif (Bois Noirs, Monts du Forez) and on Mont Ventoux which exhibits a heterogeneous vegetation (ranging from forests to bare soil). A linear relationship between surface temperature (without any atmospheric correction) and height for the fir forest is developed. The effects of slope and orientation, expressed through the insolation index, are neutralized by the presence of the forest. The same comparison, repeated for Mont Ventoux, shows that the soil/vegetation cover is an important source of variability, and the correlation coefficients between the surface temperature and insolation, which are nonexistent for the fir forest, are found to increase for Mont Ventoux. It is concluded that height and soil/vegetation cover have an influence on daytime thermal images. A comparison between the daytime surface temperature of three types of coniferous plantations in Monts du Beaujolais, with and without a correction of the effect of height, is presented M.D.

A85-23772

MICROWAVE PROPERTIES OF VEGETATION CANOPIES - AN OVERVIEW

F. T. ULABY (Kansas, University, Lawrence, KS) IN: Spectral signatures of objects in remote sensing; International Conference, 2nd, Bordeaux, France, September 12-16, 1983, Reports . Versailles, Institut National de la Recherche Agronomique, 1984, p. 565-576. refs

This paper provides an overview of approaches and techniques that can be used to determine the microwave dielectric, scattering, and emission properties of sub-canopy elements such as stalks, leaves, and fruit. The lack of adequate information regarding these properties has thus far been the limiting factor in the development of models capable of relating the microwave observables, i.e., the radar scattering coefficient and radiometer brightness temperature, to the physical parameters of the canopy and its soil background. It is hoped that through experiments of the type described in this paper it will be possible to establish the relationships necessary to the construction of physically meaningful models. Author

A85-23774

RELATIONS BETWEEN THE RADAR BACKSCATTER COEFFICIENT AND THE CHARACTERISTICS OF A VEGETATION CANOPY - ANALYSIS OF THE EFFECT OF STRUCTURE [RELATIONS ENTRE LE COEFFICIENT DE RETRODIFFUSION RADAR ET LES CARACTERISTIQUES D'UN COUVERT VEGETAL - CONSIDERATIONS SUR L'EFFET DE LA STRUCTURE]

T. LE TOAN, A. LOPES, and A. MALAVALD (Centre d'Etude Spatiale des Rayonnements, Toulouse, France) IN: Spectral signatures of objects in remote sensing, International Conference, 2nd, Bordeaux, France, September 12-16, 1983, Reports Versailles, Institut National de la Recherche Agronomique, 1984, p. 601-615. In French. refs

A85-23775

CLASSIFICATION OF VEGETATION TYPES BY ANALYSIS OF X-BAND AND C-BAND RADAR IMAGES [CLASSIFICATION DE DIFFERENTS TYPES DE VEGETATION PAR L'ANALYSE D'IMAGES RADAR EN BANDE X ET C]

D. BEGIN, C. J. GIRARD, C. DUBE, R. BROCHU, and F. BONN (Sherbrooke, Universite, Sherbrooke, Quebec, Canada) IN: Spectral signatures of objects in remote sensing; International Conference, 2nd, Bordeaux, France, September 12-16, 1983, Reports Versailles, Institut National de la Recherche Agronomique, 1984, p. 619-626. In French.

The use of X-band and C-band radar images to classify vegetative cover is investigated on the basis of airborne images obtained over the experimental farm at Lennoxville, Quebec, Canada, in October, 1982. The 65,536 dynamic-amplitude levels of the digital images are reduced to 256 levels (comparable to those of Landsat images), corrected for differential illumination by a three-stage procedure, filtered to reduce graininess, and analyzed in terms of both the spectral signatures of 10 predetermined ground-cover types (including three types of forest, clover pasture, water areas, and five types of field crops) and the spatial variance. Although the signatures are found to be statistically different (by the Student t test) in at least one of the bands, only rough division into forest, field, and water areas is possible using standard Euclidean-distance classification algorithms, and inclusion of the spatially inhomogeneous variance images only degrades the classification accuracy. The need for more refined analytical procedures is indicated. T.K.

A85-23782* National Aeronautics and Space Administration Lyndon B. Johnson Space Center, Houston, Tex

USE OF SATELLITE DATA IN AGRICULTURAL SURVEYS

F. G. HALL and A. G. HOUSTON (NASA, Johnson Space Center, Earth Sciences and Applications Div., Houston, TX) IN: Spectral signatures of objects in remote sensing, International Conference, 2nd, Bordeaux, France, September 12-16, 1983, Reports . Versailles, Institut National de la Recherche Agronomique, 1984, p. 723-738. refs

The state-of-the-art of crop surveying by satellite is reviewed with an emphasis on the signature extension problem. Registration and preprocessing procedures are discussed with reference to: normalization of the radiometric values of each scene for scene-to-scene differences; registration techniques, implemented at the NASA Johnson Space Center, capable of 0.5 pixel root-mean-square error; and current research in this direction. Data transformation and modeling techniques applied to the Landsat MSS images and a solution for the field-to-field variations of the greenness and brightness temporal trajectories are included. Finally, a review of the mixture decomposition method of labeling and estimating the areal proportions is given. L.T.

A85-23787

SPECTRAL RESPONSE OF DIFFERENT AGRICULTURAL AND PERIURBAN LAND-USE UNITS IN THE SPECTRAL WINDOWS AT 1.55-1.75 AND 2.08-2.35 MICRONS [LA REPONSE SPECTRALE DE DIVERSES UNITES D'UTILISATION DU SOL EN MILIEU AGRICOLE ET PERIURBAIN DANS LES FENETRES SPECTRALES 1,55-1,75 ET 2,08-2,35 MICRONS]

M. CARIGNAN, P. VINCENT, O. DUPONT, L. CHARBONNEAU, and F. BONN (Sherbrooke, Universite, Sherbrooke, Quebec, Canada) IN: Spectral signatures of objects in remote sensing; International Conference, 2nd, Bordeaux, France, September 12-16, 1983, Reports . Versailles, Institut National de la Recherche Agronomique, 1984, p. 783-792. In French. Research supported by the Ministere de l'Agriculture du Quebec and Natural Sciences and Engineering Research Council of Canada. refs

A85-25181* National Aeronautics and Space Administration. Marshall Space Flight Center, Huntsville, Ala.

SATELLITE PASSIVE MICROWAVE RAIN RATE MEASUREMENT OVER CROPLANDS DURING SPRING, SUMMER AND FALL

R. W. SPENCER (NASA, Marshall Space Flight Center, Huntsville, AL, Wisconsin University, Madison, WI) Journal of Climate and Applied Meteorology (ISSN 0733-3021), vol 23, Nov. 1984, p. 1553-1562. refs
(Contract NOAA-NA-80SAC00742)

Rain-rate algorithms for spring, summer and fall that have been developed from comparisons between the brightness temperatures measured by the Nimbus-7 Scanning Multichannel Microwave Radiometer (SMMR) and rain rates derived from operational WSR-57 radars over land are described. Data were utilized from a total of 25 SMMR passes and 234 radars, resulting in about 12,000 observations of about 1600 sq/km areas. Multiple correlation coefficients of 0.63, 0.80 and 0.75 are achieved for the spring, summer and fall algorithms, respectively. Most of this information is in the form of multifrequency contrast in brightness temperature, which is interpreted as a measurement of the degree to which the land-emitted radiation is attenuated by the rain systems. The SMMR 37-GHz channel has more information on rain rate than any other channel. By combining the lower frequency channels with the 37-GHz observations, variations in land and precipitation thermometric temperatures can be removed, leaving rain attenuation as the major effect on brightness temperature. Polarization screening at 37 GHz is found to be sufficient to screen out cases of wet ground, which is only important when the ground is relatively vegetation free. Heavy rain cases are found to be significant part of the algorithms' success, because of the strong microwave signatures (low-brightness temperatures) that result from the presence of precipitation-sized ice in the upper portions of heavily precipitating storms. If IR data are combined with the

summer microwave data, an improved (0.85) correlation with radar rain rates is achieved
Author

A85-25656

IDENTIFICATION OF THE STRUCTURE OF SOIL-VEGETATION COVER USING AERIAL AND SPACE IMAGES [VYIAVLENIE STRUKTURY POCHVENNO-RASTITEL'NOGO POKROVA S POMOSHCH'U AERO- I KOSMICHESKIKH SNIMKOV]

S. M. GOROZHANKINA and V. D. KONSTANTINOV (Akademiia Nauk SSSR, Institut Lesa i Drevesiny, Krasnoyarsk, USSR) *Issledovanie Zemli iz Kosmosa* (ISSN 0205-9614), Nov.-Dec 1984, p. 42-52. In Russian. refs

The paper describes a method for the identification and mapping of the structure of the vegetation and soil cover of taiga landscapes on the basis of aerial and space photographs in the scale range from 1:10,000,000 to 1:15,000. Meteor-satellite photographs of western Siberia are used. The main features of mega-, macro-, meso-, and micro-structures are characterized.
B.J.

A85-25670

SPECTRAL CHARACTERIZATION OF VEGETATION CANOPIES IN THE VISIBLE AND NIR - APPLICATION TO REMOTE SENSING [CARACTERISATION SPECTRALE DES COUVERTS VEGETAUX DANS LE VISIBLE ET LE PROCHE INFRAROUGE - APPLICATION A LA TELEDETECTION]

G. GUYOT (Institut National de la Recherche Agronomique, Montfavet, Vaucluse, France) *Societe Francaise de Photogrammetrie et de Teledetection, Bulletin* (ISSN 0244-6014), no. 95, 1984, p. 5-22. In French. refs

The 400-1300-nm spectral signatures of plants and plant structures, the factors which influence these signatures, and their application to the satellite remote sensing of crops and other vegetation are reviewed. The effects of plant anatomical structure, age, water content, mineral deficiencies, and parasite attacks, soil properties, crop orientation and arrangement; image area, sun angle; viewing angle; cloud cover, and wind speed are briefly characterized and illustrated with graphs. The spectral bands of Landsat MSS and TM and of SPOT are defined and compared with the plant signatures, and statistical, analytical, spatial-variability, and combined vertical/oblique-viewing approaches to the interpretation of satellite remote-sensing data are examined.
T.K.

A85-26931

ESTIMATION OF THE VEGETATION CONTRIBUTION TO THE 1.65-2.22 MICRON RATIO IN AIRBORNE THEMATIC-MAPPER IMAGERY OF THE VIRGINIA RANGE, NEVADA

C. D. ELVIDGE and R. J. P. LYON (Stanford University, Stanford, CA) *International Journal of Remote Sensing* (ISSN 0143-1161), vol. 6, Jan. 1985, p. 75-88. Research supported by the Shell Companies Foundation. refs

Previous investigations have successfully used the 1.65/2.22 micron ratio to map the concentration of hydroxyl-bearing minerals in imagery of sparsely vegetated terrain. However, difficulties arise in applying this ratio to semiarid regions where there is a wide variation in vegetation density. Besides mapping the mineralogic features of interest, the 1.65/2.22 micron ratio also maps the density of vegetation by responding to leaf water content. A technique has been developed to estimate the vegetation contribution to this ratio based on the near-IR/red ratio. The technique has proved useful in mapping supergene alteration in the Virginia Range, Nevada
Author

A85-26932

THE UTILITY OF DATA FROM VARIOUS AIRBORNE SENSORS FOR SOIL MAPPING

R. S. DWIVEDI (National Remote Sensing Agency, Hyderabad, India) *International Journal of Remote Sensing* (ISSN 0143-1161), vol. 6, Jan. 1985, p. 89-100

A comparative study of soil maps prepared for part of the Anantapur District (southern India), using panchromatic black-and-white and false-color airphotographs and airborne Modular Multispectral Scanner (MMS) data, has revealed that a

better soil map in terms of soilscape boundary delineation can be prepared from false-color airphotographs with less field checking compared with black-and-white airphotographs. MMS data offers certain advantages over false-color airphotographs in respect of soilscape boundary delineation. However, it suffers from the limitation of grouping the picture elements with similar spectral response into one category, even if they represent two different categories on the ground. An accuracy as high as 96.4 per cent was achieved from color infrared airphotographs as against 95.5 and 78 per cent from black-and-white airphotographs and MMS data, respectively. Nevertheless, soil maps prepared from these databases have been found to be better than a conventional soil map on the same scale.
Author

A85-26933

AUTOMATED MEASUREMENTS OF TERRAIN REFLECTION AND HEIGHT VARIATIONS USING AN AIRBORNE INFRARED LASER SYSTEM

H. SCHREIER (British Columbia, University, Vancouver, Canada), J. LOUGHEED (Davis Engineering, Ltd., Ottawa, Canada), C. TUCKER (Department of National Defence, Ottawa, Canada), and D. LECKIE (Petawawa National Forestry Institute, Chalk River, Ontario, Canada) *International Journal of Remote Sensing* (ISSN 0143-1161), vol. 6, Jan. 1985, p. 101-113. Research supported by the Defence Research Establishment. refs

A pulsed near-infrared laser system was converted to determine laser height and reflection values in airborne operations. The laser produces precise traces of the terrain and vegetation canopy and tree measurements can readily be made in open forests since the laser beam frequently penetrates openings in the canopy cover. The reflection measurements were useful in discriminating between vegetation type and density. Using the combined laser height, laser reflection and reflection variability parameters, it was possible to arrive at a simple semiautomated terrain classification which allowed a distinction between conifer and broadleaf forests and terrain with low-growing vegetation cover. The classification of individual trees into coniferous and broadleaf of different height classes is demonstrated. The data is in digital form and can be incorporated into geographic information systems. Considering that these measurements were made at a single wavelength (904 nm), it is clearly evident that high-resolution vegetation surveys are possible in the near future using multiple or tunable lasers.
Author

A85-26934* National Aeronautics and Space Administration. Goddard Space Flight Center, Greenbelt, Md.

THE POTENTIAL OF SATELLITE REMOTE SENSING OF ECOLOGICAL CONDITIONS FOR SURVEY AND FORECASTING DESERT-LOCUST ACTIVITY

C. J. TUCKER (NASA, Goddard Space Flight Center, Earth Resources Branch, Greenbelt, MD), J. U. HIELKEMA, and J. ROFFEY (United Nations, Food and Agriculture Organization, Rome, Italy) *International Journal of Remote Sensing* (ISSN 0143-1161), vol. 6, Jan. 1985, p. 127-138. refs

A85-26936

SOIL SLAKING AND THE POSSIBILITIES TO RECORD WITH INFRARED LINE SCANNING

J. G. LAMERS (Research Station for Arable Farming and Field Production of Vegetables, Lelystad, Netherlands) *International Journal of Remote Sensing* (ISSN 0143-1161), vol. 6, Jan. 1985, p. 153-165. refs

Extended areas of light textured soil may deteriorate when weather and cultural practices are favorable for slaking. In 1979 newly reclaimed polder soil slaked and in 1980 was slaked artificially. The soil surface roughness, pore volume and water infiltration rate decreased with slaking, whereas soil moisture content and penetration resistance were increased. These changes in soil characteristics decreased soil surface radiant temperature by + or - 2 deg C, while differences in reflectance were small, in the afternoon of a sunny day when soil moisture content was high or medium. Slaked fields were easily detected in spring by the use of infrared line scanning, while possibilities using aerial

photography were uncertain. Under dry soil conditions false color photography may be preferred to thermal imagery. Differences early in the morning were not measurable Author

A85-26939* National Aeronautics and Space Administration
Goddard Space Flight Center, Greenbelt, Md.

EXPERIMENTAL EVIDENCE FOR SPRING AND AUTUMN WINDOWS FOR THE DETECTION OF GEOBOTANICAL ANOMALIES THROUGH THE REMOTE SENSING OF OVERLYING VEGETATION

M. L. LABOVITZ (NASA, Goddard Space Flight Center, Geophysics Branch, Greenbelt, MD, Systems and Applied Sciences Corp., Scientific Systems Div., Hyattsville, MD), E. J. MASUOKA, R. BELL (NASA, Goddard Space Flight Center, Geophysics Branch, Greenbelt, MD), R. F. NELSON (NASA, Goddard Space Flight Center, Earth Resources Branch, Greenbelt, MD), C. A. LARSEN, L. K. HOOKER (Maryland, University, College Park, MD), and K. W. TROENSEGAARD (Callahan Mining Corp., Charlottesville, VA) International Journal of Remote Sensing (ISSN 0143-1161), vol 6, Jan 1985, p. 195-216 refs

It is pointed out that in many regions of the world, vegetation is the predominant factor influencing variation in reflected energy in the 0.4-2.5 micron region of the spectrum. Studies have, therefore, been conducted regarding the utility of remote sensing for detecting changes in vegetation which could be related to the presence of mineralization. The present paper provides primarily a report on the results of the second year of a multiyear study of geobotanical-remote-sensing relationships as developed over areas of sulfide mineralization. The field study has a strong experimental design basis. It is preceded by first delineating the boundaries of a large geographic region which satisfied a set of previously enumerated field-site criteria. Within this region, carefully selected pairs of mineralized and nonmineralized test sites were examined over the growing season. The experiment is to provide information about the spectral and temporal resolutions required for remote-sensing-geobotanical exploration. The obtained results are evaluated. G.R

A85-26942

INTERNATIONAL SYMPOSIUM ON MICROWAVE SIGNATURES IN REMOTE SENSING, 3RD, TOULOUSE, FRANCE, JANUARY 16-20, 1984, PROCEEDINGS

R. K. MOORE, ED (Kansas, University, Lawrence, KS) and E. SCHANDA, ED. (Bern, Universitaet, Bern, Switzerland) Symposium sponsored by the International Union of Radio Science. International Journal of Remote Sensing (ISSN 0143-1161), vol 6, Feb. 1985, 108 p. For individual items see A85-26943 to A85-26948.

Measurement methods and modeling of microwave backscattering and emission signatures in remote sensing are discussed. Topics examined include the determination of backscatter sources in surface-type targets, the determination of the sources of scattering from vegetation canopies at 10 GHz, and experimental relationships between microwave emission and vegetation features. Consideration is also given to the measurement of radar backscattering from rough soil surfaces using linear and circular polarizations, soil-moisture-content estimation from radar survey data during the sowing campaign, and a computationally efficient maximum-likelihood classifier employing prior probabilities for remotely-sensed data. M.D.

A85-26947

SOIL MOISTURE CONTENT ESTIMATION BY RADAR SURVEY DATA DURING THE SOWING CAMPAIGN

E. N. ZOTOVA (Akademiia Nauk SSSR, Institut Radiotekhniki i Elektroniki, Moscow, USSR) and A. G. GELLER (Moskovskii Gosudarstvennyi Universitet, Moscow, USSR) (International Union of Radio Science, International Symposium on Signatures in Remote Sensing, 3rd, Toulouse, France, Jan 16-20, 1984.) International Journal of Remote Sensing (ISSN 0143-1161), vol 6, Feb. 1985, p. 353-364. refs

The results of experimental studies of arable land plots during the spring sowing campaign with the aid of K band side-looking

airborne radar (SLAR) are given. The possibility of estimating the productive moisture content in soil in 0-50 and 0-100 cm layers by radar-survey data and soil indication functions are shown in bare soil and winter crop plots using volumetric free moisture content as the measurement parameter. Author

A85-29908

INVESTIGATION OF SALTY SOLIS AND SALINES ON THE BASIS OF SPACE REMOTE-SENSING METHODS [IZUCHENIE ZASOLENNYKH ZEMEL' I SOLONCHAKOV S POMOSHCH'IU KOSMICHESKIKH METODOV]

E. A. MAMEDOV (Akademiia Nauk Azerbaidzhanskoi SSR, Nauchno-Proizvodstvennoe Ob'edinenie Kosmicheskikh Issledovani, Baku, Azerbaidzhan SSR) Issledovanie Zemli iz Kosmosa (ISSN 0205-9614), Jan-Feb 1985, p. 60-65. In Russian. refs

A85-29910

DETERMINATION OF SOIL MOISTURE CONTENT BY MICROWAVE RADIOMETRY WITH THE USE OF A PRIORI INFORMATION [OPREDELENIE VLAGOSODERZHANIIA POCHOVGRUNTOV SVCH-RADIOMETRICHESKIM METODOM S PRIVLECHENIEM APRIORNOI INFORMATSII]

E. A. REUTOV and A. M. SHUTKO (Akademiia Nauk SSR, Institut Radiotekhniki i Elektroniki, Moscow, USSR) Issledovanie Zemli iz Kosmosa (ISSN 0205-9614); Jan.-Feb. 1985, p. 73-87. In Russian. refs

Theoretical and experimental studies of the microwave emission characteristics of nonuniformly wet soils were conducted. The dependence of spectral radio-brightness contrast on the parameters of the permittivity (moisture) profile is obtained. The emission characteristics of soils with different moisture profiles were measured by a microwave radiometer at wavelengths of 2.5, 18, and 30 cm. A method for determining moisture-profile parameters and total moisture content in soil at a depth of one meter is proposed which is based on the joint utilization of remote microwave radiometry data and a priori information about the water-physical properties of the soil. B. J.

A85-29911

RADAR MAPPING OF THE MOISTURE OF OPEN SOILS [RADIOLOKATSIONNOE KARTIROVANIE VLAZHNOСТИ OTKRYTYKH POCHV]

N. N. KRUPENIO (Vsesoiuznyi Nauchno-Issledovatel'skii Tsentr AIUS-Agroresursy, Moscow, USSR) Issledovanie Zemli iz Kosmosa (ISSN 0205-9614), Jan.-Feb. 1985, p. 88-93. In Russian. refs

Airborne sidelooking radar with a 60-100 m resolution was used for the moisture mapping of open soils (i.e., without vegetation cover) in the 0-10 cm layer in the Stavropol'sk region of the USSR. The difference between the moisture value obtained by the remote radar measurements and that obtained by direct thermoweight measurements did not exceed 2 wt percent in the 9-30 percent moisture variation range. B.J.

A85-29969

COMPUTING THE FOLIAGE ANGLE DISTRIBUTION FROM CONTACT FREQUENCY DATA

D. R. JACKETT and R. S. ANDERSEN (Commonwealth Scientific and Industrial Research Organization, Div. of Mathematics and Statistics, Canberra, Australia) IN: Computational techniques and applications: CTAC-83, Proceedings of the International Conference, Sydney, Australia, August 28-31, 1983. Amsterdam, North-Holland, 1984, p. 863-872. refs

The mathematical implications of Miller's (1965) inversion formula for the computation of the foliage angle distribution from contact frequency data are discussed. The inversion formula can be used to determine the structure and status of plant canopies through indirect measurement by satellite. The computational aspects of substituting the known angle density function $g(\alpha)$ for the azimuthally averaged mean canopy projection function $f(\beta)$ in stochastic models of the interaction of sunlight and leaves are considered. Some advantages of computational

schemes based on contact frequency functionals instead of foliage density functionals are identified. I.H.

A85-30086* Environmental Research Inst. of Michigan, Ann Arbor.

AN ANALYSIS OF SPECTRAL DISCRIMINATION BETWEEN CORN AND SOYBEANS USING A ROW CROP REFLECTANCE MODEL

G. H. SUITS (Michigan, Environmental Research Institute, Ann Arbor, MI) Remote Sensing of Environment (ISSN 0034-4257), vol 17, April 1985, p. 109-116 NASA-sponsored research Previously announced in STAR as N84-10642. refs

Reflectance calculations of soybeans and corn crops at two times during the growing season indicate that the high sensitivity of the thematic mapper mid-infrared band to exposed bare soil between soybean rows is most likely responsible for early season spectral discrimination of corn and soybean crops by this band.

Author

A85-30089* National Aeronautics and Space Administration. Goddard Space Flight Center, Greenbelt, Md

EFFECT OF VEGETATION ON SOIL MOISTURE SENSING OBSERVED FROM ORBITING MICROWAVE RADIOMETERS

J R WANG (NASA, Goddard Space Flight Center, Laboratory for Oceans, Greenbelt, MD) Remote Sensing of Environment (ISSN 0034-4257), vol. 17, April 1985, p 141-151. refs

The microwave radiometric measurements made by the Skylab 1.4 GHz radiometer and by the 6.6 GHz and 10.7 GHz channels of the Nimbus-7 Scanning Multichannel Microwave Radiometer were analyzed to study the large-area soil moisture variations of land surfaces. Two regions in Texas, one with sparse and the other with dense vegetation covers, were selected for the study. The results gave a confirmation of the vegetation effect observed by ground-level microwave radiometers. Based on the statistics of the satellite data, it was possible to estimate surface soil moisture in about five different levels from dry to wet conditions with a 1.4 GHz radiometer, provided that the biomass of the vegetation cover could be independently measured. At frequencies greater than about 6.6 GHz, the radiometric measurements showed little sensitivity to moisture variation for vegetation-covered soils. The effects of polarization in microwave emission were studied also.

Author

A85-30090

THERMAL STRUCTURE OF AN AGRICULTURAL REGION AS SEEN BY NOAA-7 AVHRR

F CHEEVASUVIT, O. TACONET, D. VIDAL-MADJAR (CNRS and CNET, Centre de Recherches en Physique de l'Environnement Terrestre et Planetaire, Issy-les-Moulineaux, Hauts-de-Seine, France), and H. MAITRE (Ecole Nationale Supérieure des Telecommunications, Paris, France) Remote Sensing of Environment (ISSN 0034-4257), vol. 17, April 1985, p. 153-163 Research supported by the Centre National d'Etudes Spatiales. refs

Using a split and merge image segmentation algorithm on NOAA-7 AVHRR channel four data, the thermal structure of an agricultural homogeneous region (the Beauce Plateau in France) around midday is studied during 1982. It is shown that the image homogeneous areas can be identified with known natural regions hills, forests, and the Beauce Plateau. The Beauce Plateau has a thermal structure divided into three or more areas depending on the season. Those areas are very well correlated with regions of equal soil water availability.

Author

A85-30091

EARTH OBSERVATION MODELING BASED ON LAYER SCATTERING MATRICES

W. VERHOEF (Nationaal Lucht- en Ruimtevaartlaboratorium, Amsterdam, Netherlands) Remote Sensing of Environment (ISSN 0034-4257), vol 17, April 1985, p 165-178 refs

The differential equations describing radiative transfer in vegetative canopies as given by Suits (1972) are generalized and solved to derive a layer scattering matrix. Layer scattering matrices

can be applied to the calculation of optical parameters for multilayer ensembles according to the Adding method. The application to atmospheric scattering is demonstrated by explaining path radiance, and other quantities in terms of elements from a layer scattering matrix and a surface reflectance matrix. By combining scattering matrices originating from atmospheric layers with those from earth objects, earth observation models can be constructed. These may become valuable tools in the study of various remote sensing problems.

Author

A85-30092* National Aeronautics and Space Administration Lyndon B Johnson Space Center, Houston, Tex.

COMPARATIVE STUDY OF SUITS AND SAIL CANOPY REFLECTANCE MODELS

G. D. BADHWAR (NASA, Johnson Space Center, Houston, TX), W. VERHOEF, and N. J. J. BUNNIK (Nationaal Lucht- en Ruimtevaartlaboratorium, Amsterdam, Netherlands) Remote Sensing of Environment (ISSN 0034-4257), vol. 17, April 1985, p. 179-195. NASA-supported research. refs

A detailed understanding of the relationships between the canopy reflectance and the characteristics of canopy elements is an important factor for the full exploitation of the potential of remote sensing from aircraft and spacecraft altitudes to map vegetation and estimate key agronomic parameters such as the leaf area index (LAI) and biomass (BM). Suits (1972) idealized the canopy geometry by replacing each plant component with three orthogonal projections of that component. Verhoef and Bunnik (1981) extended the Suits model, henceforth called the SAIL (Scattering from Arbitrarily Inclined Leaves) model, by removing certain constraints. The present investigation is concerned with an evaluation of the performance of the Suits and SAIL models, taking into account two data sets on soybean and corn. It was found that the tested models have significant deficiencies. However, the performance of the SAIL model is better than that of the Suits model because it provides a more realistic description of the canopy architecture.

G.R.

A85-30093* National Aeronautics and Space Administration Lyndon B. Johnson Space Center, Houston, Tex.

APPLICATION OF THEMATIC MAPPER DATA TO CORN AND SOYBEAN DEVELOPMENT STAGE ESTIMATION

G. D. BADHWAR and K. E. HENDERSON (NASA, Johnson Space Center, Earth Sciences and Applications Div., Houston, TX) Remote Sensing of Environment (ISSN 0034-4257), vol 17, April 1985, p. 197-201. refs

A model, utilizing direct relationship between remotely sensed spectral data and the development stage of both corn and soybeans has been proposed and published previously (Badhwar and Henderson, 1981, and Henderson and Badhwar, 1984). This model was developed using data acquired by instruments mounted on trucks over field plots of corn and soybeans as well as satellite data from Landsat. In all cases, the data was analyzed in the spectral bands equivalent to the four bands of Landsat multispectral scanner (MSS). In this study the same model has been applied to corn and soybeans using Landsat-4 Thematic Mapper (TM) data combined with simulated TM data to provide a multitemporal data set in TM band intervals. All data (five total acquisitions) were acquired over a test site in Webster County, Iowa from June to October 1982. The use of TM data for determining development state is as accurate as with Landsat MSS and field plot data in MSS bands. The maximum deviation of 0.6 development stage for corn and 0.8 development stage for soybeans is well within the uncertainty with which a field can be estimated with procedures used by observers on the ground in 1982.

Author

N85-16241*# Purdue Univ., Lafayette, Ind. Lab. for Applications of Remote Sensing

VARIATION IN SPECTRAL RESPONSE OF SOYBEANS WITH RESPECT TO ILLUMINATION, VIEW, AND CANOPY GEOMETRY

K. J. RANSON, L. L. BIEHL, and M. E. BAUER (Minnesota Univ.)
31 Jul. 1984 27 p refs ERTS
(Contract NAS9-16528)

(E85-10040; NASA-CR-171821; NAS 1.26:171821;

LARS-TR-073184) Avail: NTIS HC A03/MF A01 CSCL 02C

Comparisons of the spectral response for incomplete (well-defined row structure) and complete (overlapping row structure) canopies of soybeans indicated a greater dependence on Sun and view geometry for the incomplete canopies. Red and near-IR reflectance for the incomplete canopy decreased as solar zenith angle increased for a nadir view angle until the soil between the plant rows was completely shaded. Thereafter for increasing solar zenith angle, the red reflectance leveled off and the near-IR reflectance increased. A 'hot spot' effect was evident for the red and near-IR reflectance factors. The 'hot spot' effect was more pronounced for the red band based on relative reflectance value changes. The ratios of off-nadir to nadir acquired data reveal that off-nadir red band reflectance factors more closely approximated straightdown measurements for time periods away from solar noon. Normalized difference generally approximated straightdown measurements during the middle portion of the day. R.S.F.

N85-16242*# Purdue Univ., Lafayette, Ind. Lab. for Applications of Remote Sensing.

SPECTRAL ESTIMATORS OF ABSORBED PHOTOSYNTHETICALLY ACTIVE RADIATION IN CORN CANOPIES

K. P. GALLO, C. S. T. DAUGHTRY, and M. E. BAUER (Minnesota Univ.) 29 Jun. 1984 20 p refs ERTS
(Contract NAS9-16528)

(E85-10041; NASA-CR-171822; NAS 1.26:171822;

LARS-TR-062984) Avail: NTIS HC A02/MF A01 CSCL 02C

Most models of crop growth and yield require an estimate of canopy leaf area index (LAI) or absorption of radiation. Relationships between photosynthetically active radiation (PAR) absorbed by corn canopies and the spectral reflectance of the canopies were investigated. Reflectance factor data were acquired with a LANDSAT MSS band radiometer. From planting to silking, the three spectrally predicted vegetation indices examined were associated with more than 95% of the variability in absorbed PAR. The relationships developed between absorbed PAR and the three indices were evaluated with reflectance factor data acquired from corn canopies planted in 1979 through 1982. Seasonal cumulations of measured LAI and each of the three indices were associated with greater than 50% of the variation in final grain yields from the test years. Seasonal cumulations of daily absorbed PAR were associated with up to 73% of the variation in final grain yields. Absorbed PAR, cumulated through the growing season, is a better indicator of yield than cumulated leaf area index. Absorbed PAR may be estimated reliably from spectral reflectance data of crop canopies. R.S.F.

N85-16246*# Utah Univ., Salt Lake City Center for Remote Sensing and Cartography.

AN INTEGRATED REMOTE SENSING APPROACH FOR IDENTIFYING ECOLOGICAL RANGE SITES

R. A. JAYNES 1983 10 p refs Sponsored in part by Utah Div. of State Lands and Forestry ERTS
(Contract NAGW-95)

(E85-10050; NASA-CR-174226; NAS 1.26:174226) Avail: NTIS HC A02/MF A01 CSCL 08B

A model approach for identifying ecological range sites was applied to high elevation sagebrush-dominated rangelands on Parker Mountain, in south-central Utah. The approach utilizes map information derived from both high altitude color infrared photography and LANDSAT digital data, integrated with soils, geological, and precipitation maps. Identification of the ecological range site for a given area requires an evaluation of all relevant

environmental factors which combine to give that site the potential to produce characteristic types and amounts of vegetation. A table is presented which allows the user to determine ecological range site based upon an integrated use of the maps which were prepared. The advantages of identifying ecological range sites through an integrated photo interpretation/LANDSAT analysis are discussed. Author

N85-16247*# National Aeronautics and Space Administration Earth Resources Labs., Bay St. Louis, Miss.

RELATIONSHIP BETWEEN FOREST CLEARING AND BIOPHYSICAL FACTORS IN TROPICAL ENVIRONMENTS: IMPLICATIONS FOR THE DESIGN OF A FOREST CHANGE MONITORING APPROACH

S. A. SADER and A. T. JOYCE Sep 1984 25 p refs
Original contains imagery. Original photography may be purchased from the EROS Data Center, Sioux Falls, S.D. 57198 ERTS
(E85-10051; NASA-TM-87405; NSTL/ERL-230; NAS 1.15:87405)
Avail: NTIS HC A02/MF A01 CSCL 05B

The relationship between forest clearing, biophysical factors (e.g. ecological zones, slope gradient, soils), and transportation network in Costa Rica was analyzed. The location of forested areas at four reference dates (1940, 1950, 1961, and 1977) as derived from aerial photography and LANDSAT MSS data was digitized and entered into a geographically-referenced data base. Ecological zones as portrayed by the Holdridge Life Zone Ecology System, and the location of roads and railways were also digitized from maps of the entire country as input to the data base. Information on slope gradient and soils was digitized from maps of a 21,000 square kilometer area. The total area of forest cleared over four decades are related to biophysical factors was analyzed within the data base and deforestation rates and trends were tabulated. The relationship between forest clearing and ecological zone and the influence of topography, soils, and transportation network are presented and discussed. R.S.F.

N85-16253*# Rice Univ., Houston, Tex.

NONPARAMETRIC ANALYSIS OF MINNESOTA SPRUCE AND ASPEN TREE DATA AND LANDSAT DATA

D. W. SCOTT and R. JEE /in Texas A and M Univ. Proc. of the 2nd Ann. Symp on Math. Pattern Recognition and Image Analysis Program p 27-49 1984 refs
Original contains imagery. Original photography may be purchased from the EROS Data Center, Sioux Falls, S.D. 57198 ERTS
Avail: NTIS HC A25/MF A01 CSCL 12A

The application of nonparametric methods in data-intensive problems faced by NASA is described. The theoretical development of efficient multivariate density estimators and the novel use of color graphics workstations are reviewed. The use of nonparametric density estimates for data representation and for Bayesian classification are described and illustrated. Progress in building a data analysis system in a workstation environment is reviewed and preliminary runs presented. M.G.

N85-16256*# Texas Univ., Austin. Center for Statistical Sciences.

SPATIAL ESTIMATION FROM REMOTELY SENSED DATA VIA EMPIRICAL BAYES MODELS

J. R. HILL, D. V. HINKLEY, H. KOSTAL, and C. N. MORRIS /in Texas A and M Univ. Proc. of the 2nd Ann. Symp on Math. Pattern Recognition and Image Analysis Program p 115-135 1984 refs ERTS

Avail: NTIS HC A25/MF A01 CSCL 12A

Multichannel satellite image data, available as LANDSAT imagery, are recorded as a multivariate time series (four channels, multiple passovers) in two spatial dimensions. The application of parametric empirical Bayes theory to classification of, and estimating the probability of, each crop type at each of a large number of pixels is considered. This theory involves both the probability distribution of imagery data, conditional on crop types, and the prior spatial distribution of crop types. For the latter Markov models indexed by estimable parameters are used. A broad outline of the general theory reveals several questions for further research.

Some detailed results are given for the special case of two crop types when only a line transect is analyzed. Finally, the estimation of an underlying continuous process on the lattice is discussed which would be applicable to such quantities as crop yield. M.G.

N85-16259*# Southern Methodist Univ., Dallas, Tex Dept. of Statistics

EXPLORING THE USE OF STRUCTURAL MODELS TO IMPROVE REMOTE SENSING AGRICULTURAL ESTIMATES

R. F. GUNST and M. Y. LAKSHMINARAYANAN *In* Texas A and M Univ Proc of the 2nd Ann. Symp. on Math. Pattern Recognition and Image Analysis Program p 175-203 1984 refs ERTS
Avail: NTIS HC A25/MF A01 CSCL 02C

Satellite estimates of agricultural characteristics often are not sufficiently precise for reliable use in small geographical regions. The precision of estimates of agricultural characteristics such as crop proportions and leaf area indexes can be increased by modeling ground observations as a function of satellite estimates. Linear regression models using least squares estimators of the model parameters are most often advocated as an appropriate methodology, however, least squares estimation requires that the predictor variables are measured without error, an unreasonable assumption for this application. An alternative estimation methodology which assumes that both the response variables (ground observations) and the predictor variables (satellite estimates) are measured with error involves the use of linear structural models. The application of linear structural models to the estimation of agricultural characteristics using satellite spectral measurements is examined
Author

N85-16260*# National Aeronautics and Space Administration. Lyndon B. Johnson Space Center, Houston, Tex.

CALIBRATION OR INVERSE REGRESSION: WHICH IS APPROPRIATE FOR CROP SURVEYS USING LANDSAT DATA?

R. S. CHHIKARA (Lockheed Engineering and Management Services Co., Inc., Houston, Tex.) and A. G. HOUSTON *In* Texas A and M Univ Proc. of the 2nd Ann. Symp. on Math. Pattern Recognition and Image Analysis Program p 205-243 1984 refs Sponsored in part by Dept of Agriculture (Contract NAS9-15800)
Avail: NTIS HC A25/MF A01 CSCL 02C

Calibration and inverse regression estimators of crop proportions are investigated where the auxiliary variable is obtained from binary classification of multivariate LANDSAT data. The appropriate model relating classifier proportions and ground observed proportions for a given crop type is the calibration model. Under this model the inverse regression estimator is superior to the calibration estimator in estimating the crop acreage or proportion for a region of interest.
Author

N85-16269*# Environmental Research Inst of Michigan, Ann Arbor.

GROWTH/REFLECTANCE MODEL INTERFACE FOR WHEAT AND CORRESPONDING MODEL Final Report, Mar. - Dec. 1984

G. H. SUITS, R. SIERON, and J. ODENWELLER Dec 1984 30 p refs ERTS (Contract NAS5-83)
(E85-10058; NASA-CR-174230; NAS 1 26 174230; ERIM-166500-4-F) Avail: NTIS HC A03/MF A01 CSCL 02C

The use of modeling to explore the possibility of discovering new and useful crop condition indicators which might be available from the Thematic Mapper and to connect these symptoms to the biological causes in the crop is discussed. A crop growth model was used to predict the day to day growth features of the crop as it responds biologically to the various environmental factors. A reflectance model was used to predict the character of the interaction of daylight with the predicted growth features. An atmospheric path radiance was added to the reflected daylight to simulate the radiance appearing at the sensor. Finally, the digitized data sent to a ground station were calculated. The crop under investigation is wheat
M.G.

N85-16290# Forest Service, New Orleans, La. Southern Forest Experiment Station

FOREST AREA ESTIMATES FROM LANDSAT MSS AND FOREST INVENTORY PLOT DATA

R. A. BIRDSEY, W. F. MILLER, J. CLARK, and R. H. SMITH Sep. 1984 12 p refs
(PB85-105617/GAR, FSRP/SO-211) Avail: NTIS HC A02/MF A01 CSCL 02F

Forest area estimates for Puerto Rico from LANDSAT multispectral scanner data were compared with area estimates derived from black and white aerial photographs. These estimates for forest resource evaluation are discussed. The sampling error for LANDSAT data was nearly twice the sampling error for photointerpreted data.
GRA

N85-16362# Instituto de Pesquisas Espaciais, Sao Jose dos Campos (Brazil).

THE MANAGEMENT OF ATMOSPHERIC RESOURCES IN FOOD PRODUCTION

F. C. DEALMEIDA *In* WMO Climate Conf. for Latin America and the Caribbean p 214-219 1984 refs
Avail: NTIS MF A01; print copy available at WMO, Geneva SWFR65

The concept of atmospheric resources management is presented as a system capable of collecting, controlling, and disseminating in time to be used by the farm manager. The importance of economic return from the use of meteorological data in a food production system is emphasized. The applications are illustrated by a frost damage example in which the frost probability level is used by the farm manager to reach a decision of whether to turn on the frost protection system or not. Such a system based on digitally processed infrared satellite images is being tested in Brazil.
Author (ESA)

N85-17228*# Purdue Univ., Lafayette, Ind

MICROWAVE AND OPTICAL REMOTE SENSING OF FOREST VEGETATION

R. M. HOFFER, M. E. BAUER, L. L. BIEHL, and R. P. MROCZYNSKI *In* JPL The SIR-B Sci. Invest Plan 3 p 1 Jul 1984
Avail: NTIS HC A10/MF A01 CSCL 02F

The objectives and anticipated results of a study to define the strengths and limitations of microwave (SIR-B) and optical (Thematic Mapper) data, singly and in combination, for the purpose of characterizing forest cover types and condition classes are described. Other specific objectives include: (1) the assessment of the effectiveness of a contextual classification algorithm (SECHO), (2) evaluation of the utility of different look angles of SAR data in determining differences in stand density of commercial forests, and (3) the determination of the effectiveness of the L-band HH polarized SIR-B data in differentiating forest-stand densities.
M.G.

N85-17240*# Jet Propulsion Lab., California Inst. of Tech., Pasadena.

DEVELOPMENT AND EVALUATION OF TECHNIQUES FOR USING COMBINED MICROWAVE AND OPTICAL IMAGE DATA FOR VEGETATION STUDIES

J. F. PARIS, B. N. ROCK, and S. Y. HSU (Susquehanna Resource and Environment, Inc.) *In* JPL The SIR-B Sci. Invest Plan 3 p 1 Jul. 1984
Avail: NTIS HC A10/MF A01 CSCL 02F

Techniques for using combined image data from the Shuttle Imaging Radar (SIR-B) and the LANDSAT Thematic Mapper (TM) or Multispectral Scanner (MSS) for studies of irrigated crops, and boreal and deciduous forests are developed and evaluated. The effects of the structure and composition of crop canopies and soil surfaces on multiangle L-band HH (Horizontal polarization for transmission and reception) backscattering and on optical reflectance (in TM or MSS bands viewed at the nadir) are investigated. The relative accuracy of digital, calibrated SIR-B image data and LANDSAT TM or MSS image data is evaluated. Textural

01 AGRICULTURE AND FORESTRY

information extraction-techniques are developed for radar and optical image analysis B W

N85-17246*# California Univ., Santa Barbara.
THE EXTENSION OF AN INVERTIBLE CONIFEROUS FOREST CANOPY REFLECTANCE MODEL USING SIR-B AND LANDSAT DATA

D. S. SIMONETT and A. H. STRAHLER (City Univ. of New York) /n JPL The SIR-B Invest. Plan 4 p 1 Jul 1984 refs Avail NTIS HC A10/MF A01 CSCL 02F

Using a 23-cm radar system, an invertible coniferous canopy reflectance model is extended. The extension involves the joint use of shuttle imaging radar (SIR-B) multilook angle data, the multispectral scanner (MSS), and the thematic mapper (TM) on LANDSAT. B.W.

N85-17251*# Lund Technical Univ. (Sweden)
GROUND TRUTH FOR SIR-B IMAGES OBTAINED BY SIR SYSTEM 8 IMPULSE RADAR

P. ULRIKSEN, H. OTTERSTEN (Research Inst. of National Defence), C. G. BORG (Swedish Space Corp., Solna), S. AXELSSON (Saab-Scania, Linköping), and B. EKENGREN (Ericsson Radio System) /n JPL The SIR-B Sci. Invest Plan 4 p 1 Jul 1984 refs

Avail: NTIS HC A10/MF A01 CSCL 17I

Verification of suspected penetration by means of three dimensional information on the features in the SIR-B images will be investigated. The Great Alvar is a well documented area, especially in geology and ecology, and should provide a good opportunity to evaluate the data. B.G.

N85-17252*# National Aeronautics and Space Administration. Goddard Space Flight Center, Greenbelt, Md.

REMOTE SENSING OF SOIL MOISTURE

J. R. WANG, J. C. SHIUE, T. J. SCHMUGGE, P. CUDDAPAH, T. J. JACKSON (Dept. of Agriculture, Beltsville, Md.), and T. MO (Computer Sciences Corp., Silver Spring, Md.) /n JPL The SIR-B Sci. Invest. Plan 4 p 1 Jul 1984 refs

Avail: NTIS HC A10/MF A01 CSCL 08M

Four major objectives are proposed (1) to study the sensitivity of active and passive microwave remote sensing approaches to soil moisture variations; (2) to investigate the effect of vegetation cover on microwave backscatter and emission; (3) to test theoretical models of microwave backscatter and emission from a natural terrain against the observations obtained from SIR-B and aircraft radiometer flights, and (4) to estimate vegetation biomass with airborne visible and infrared sensors B.G.

N85-17400*# National Aeronautics and Space Administration. Goddard Space Flight Center, Greenbelt, Md.

NORTH AMERICAN VEGETATION PATTERNS OBSERVED WITH THE NOAA-7 ADVANCED VERY HIGH RESOLUTION RADIOMETER

S. N. GOWARD, C. J. TUCKER, and D. G. DYE 1985 29 p refs Prepared in cooperation with Maryland Univ., College Park Original contains imagery. Original photography may be purchased from the EROS Data Center, Sioux Falls, S.D. 57198 ERTS (Contract NCC5-26)

(E85-10062; NASA-TM-87402, NAS 1.15.87402) Avail: NTIS HC A03/MF A01 CSCL 02C

Spectral vegetation index measurements derived from remotely sensed observations show great promise as a means to improve knowledge of land vegetation patterns. The daily, global observations acquired by the advanced very high resolution radiometer, a sensor on the current series of U.S. National Oceanic and Atmospheric Administration meteorological satellites, may be particularly well suited for global studies of vegetation. Preliminary results from analysis of North American observations, extending from April to November 1982, show that the vegetation index patterns observed correspond to the known seasonality of North American natural and cultivated vegetation. Integration of the observations over the growing season produced measurements that are related to net primary productivity patterns of the major

North American natural vegetation formations. Regions of intense cultivation were observed as anomalous areas in the integrated growing season measurements. Significant information on seasonality, annual extent and interannual variability of vegetation photosynthetic activity at continental and global scales can be derived from these satellite observations. Author

N85-17401*# Maryland Univ., College Park
ANALYSIS OF TERRESTRIAL CONDITIONS AND DYNAMICS Progress Report, 1 Aug. 1983 - 31 Aug. 1984

S. N. GOWARD, Principal Investigator 31 Aug. 1984 17 p refs ERTS

(Contract NCC5-26)

(E85-10063; NASA-CR-174312, NAS 1.26:174312) Avail: NTIS HC A02/MF A01 CSCL 05B

Land spectral reflectance properties for selected locations, including the Goddard Space Flight Center, the Wallops Flight Facility, a MLA test site in Cambridge, Maryland, and an acid test site in Burlington, Vermont, were measured. Methods to simulate the bidirectional reflectance properties of vegetated landscapes and a data base for spatial resolution were developed. North American vegetation patterns observed with the Advanced Very High Resolution Radiometer were assessed. Data and methods needed to model large-scale vegetation activity with remotely sensed observations and climate data were compiled. B.G.

N85-17402*# Maryland Univ., College Park. Dept. of Geography.

SHORTWAVE INFRARED DETECTION OF VEGETATION

S. N. GOWARD, Principal Investigator 1985 19 p refs Sponsored by NASA ERTS

(E85-10064; NASA-CR-174313, NAS 1.26:174313) Avail: NTIS HC A02/MF A01 CSCL 02C

The potential of short wave infrared (SWIR) measurements in vegetation discrimination is further substantiated through a discussion of field studies and an examination of the physical bases which cause SWIR measurements to vary with the vegetation type observed. The research reported herein supported the AGRISTARS program objective to incorporate TM measurements in the analysis of agricultural activity. Field measurements on corn and soybeans in Iowa were conducted, and the mean and variance of canopy reflectance were computed for each observation date. The Suits canopy reflectance model was used to evaluate possible explanations of the observed corn/soybeans reflectance patterns /39/. The SWIR measurements were shown to effectively discriminate corn and soybeans on the basis of leaf absorption properties. R.S.F.

N85-18447# Sandia Labs., Albuquerque, N. Mex.
TEST PLAN FOR THE FOREST-ECHO EXPERIMENT

D. A. JELINEK Jul. 1984 12 p refs

(Contract DE-AC04-76DP-00789)

(DE84-017175; SAND-83-2195) Avail: NTIS HC A02/MF A01

A test plan to determine the characteristics of the average radar echo from a number of forested terrains is described. The data required to do this will be obtained by using a very narrow pulse width (20 ns) radar and associated hardware on board a helicopter. Data will be taken as the helicopter makes straight and level passes over each terrain at a number of altitudes. Both deciduous and conifer forests will be overflown at different times of the year to determine the effect of seasonal changes. The hardware that will be used and the procedure that will be followed to gather the data are described. The theoretical statistical characteristics of the radar's video output and the amount of intrapulse and interpulse correlation expected are given. DOE

N85-19321# Joint Publications Research Service, Arlington, Va.
CNES, INRA DO JOINT REMOTE-SENSING RESEARCH
In its Worldwide Rept. Telecommun. Policy, Res and Develop
 (JPRS-TTP-85-006) p 54-55 26 Feb. 1985 Transl into ENGLISH
 from Electron Actualites (Paris), 16 Nov 1984 p 21
 Avail. NTIS HC A04/MF A01

One year before the launching of the French remote-sensing satellite Spot 1, the authorities and organizations concerned are actively preparing to take full advantage of the data it will supply to benefit agriculture. To that end, the Ministry of Agriculture created a Commission on Remote-Sensing which acts as a coordinator for the various departments of the ministry and the teaching and research institutions it supervises. Activities of the Commission are reported. A R H

N85-19485*# National Aeronautics and Space Administration
 Earth Resources Labs., Bay St. Louis, Miss.
**ANALYSIS OF DATA ACQUIRED BY SYNTHETIC APERTURE
 RADAR AND LANDSAT MULTISPECTRAL SCANNER OVER
 KERSHAW COUNTY, SOUTH CAROLINA, DURING THE
 SUMMER SEASON**

S. T. WU Mar 1983 46 p refs Sponsored by NASA, USDA,
 Dept. of Commerce, Dept. of the Interior, and Agency for
 International Development Original contains color imagery.
 Original photography may be purchased from the EROS Data
 Center, Sioux Falls, S.D. 57198 ERTS

(Contract PROJ. AGRISTARS)
 (E85-10071; NASA-TM-87413, NSTL/ERL-213; DC-Y2-04374;
 NAS 1.15:87413) Avail: NTIS HC A03/MF A01 CSCL 05B

Data acquired by synthetic aperture radar (SAR) and LANDSAT
 multispectral scanner (MSS) were processed and analyzed to derive
 forest-related resources inventory information The SAR data were
 acquired by using the NASA aircraft X-band SAR with linear (HH,
 VV) and cross (HV, VH) polarizations and the SEASAT L-band
 SAR. After data processing and data quality examination, the three
 polarization (HH, HV, and VV) data from the aircraft X-band SAR
 were used in conjunction with LANDSAT MSS for multisensor data
 classification. The results of accuracy evaluation for the SAR, MSS
 and SAR/MSS data using supervised classification show that the
 SAR-only data set contains low classification accuracy for several
 land cover classes. However, the SAR/MSS data show that
 significant improvement in classification accuracy is obtained for
 all eight land cover classes. These results suggest the usefulness
 of using combined SAR/MSS data for forest-related cover mapping.
 The SAR data also detect several small special surface features
 that are not detectable by MSS data. A R.H.

N85-19487*# Utah Univ., Salt Lake City. Center for Remote
 Sensing and Cartography.
**AN INTEGRATED GIS/REMOTE SENSING DATA BASE IN
 NORTH CACHE SOIL CONSERVATION DISTRICT, UTAH: A
 PILOT PROJECT FOR THE UTAH DEPARTMENT OF
 AGRICULTURE'S RIMS (RESOURCE INVENTORY AND
 MONITORING SYSTEM)**

D. J. WHEELER, M. K. RIDD, and J. A. MEROLA Dec 1984
 56 p refs ERTS
 (Contract NAGW-95)

(E85-10073; NASA-CR-174400; NAS 1.26:174400; CRSC-84-8)
 Avail: NTIS HC A04/MF A01 CSCL 05B

A basic geographic information system (GIS) for the North
 Cache Soil Conservation District (SCD) was sought for selected
 resource problems. Since the resource management issues in the
 North Cache SCD are very complex, it is not feasible in the initial
 phase to generate all the physical, socioeconomic, and political
 baseline data needed for resolving all management issues A
 selection of critical variables becomes essential. Thus, there are
 four specific objectives: (1) assess resource management needs
 and determine which resource factors are most fundamental for
 building a beginning data base; (2) evaluate the variety of data
 gathering and analysis techniques for the resource factors selected,
 (3) incorporate the resulting data into a useful and efficient digital
 data base; and (4) demonstrate the application of the data base
 to selected real world resource management issues. B G

N85-19488*# California Univ., Berkeley Space Sciences Lab.
**ANALYSIS OF THE QUALITY OF IMAGE DATA REQUIRED BY
 THE LANDSAT-4 THEMATIC MAPPER AND MULTISPECTRAL
 SCANNER Final Technical Report, 3 Jan. 1983 - 31 Dec. 1984**
 R. N. COLWELL, Principal Investigator 31 Dec 1984 151 p
 refs Original contains color imagery Original photography may
 be purchased from the EROS Data Center, Sioux Falls, S D 57198
 ERTS

(Contract NAS5-27377)

(E85-10074; NASA-CR-174401; NAS 1.26:174401) Avail: NTIS
 HC A08/MF A01 CSCL 05B

The spatial, geometric, and radiometric qualities of LANDSAT
 4 thematic mapper (TM) and multispectral scanner (MSS) data
 were evaluated by interpreting, through visual and computer means,
 film and digital products for selected agricultural and forest cover
 types in California. Multispectral analyses employing Bayesian
 maximum likelihood, discrete relaxation, and unsupervised
 clustering algorithms were used to compare the usefulness of TM
 and MSS data for discriminating individual cover types. Some of
 the significant results are as follows (1) for maximizing the
 interpretability of agricultural and forest resources, TM color
 composites should contain spectral bands in the visible,
 near-reflectance infrared, and middle-reflectance infrared regions,
 namely TM 4 and TM 5 and must contain TM 4 in all cases
 even at the expense of excluding TM 5; (2) using enlarged TM
 film products, planimetric accuracy of mapped points was within
 91 meters (RMSE east) and 117 meters (RMSE north); (3) using
 TM digital products, planimetric accuracy of mapped points was
 within 12.0 meters (RMSE east) and 13.7 meters (RMSE north);
 and (4) applying a contextual classification algorithm to TM data
 provided classification accuracies competitive with Bayesian
 maximum likelihood. Author

N85-19494*# Purdue Univ., Lafayette, Ind. Lab for Applications
 of Remote Sensing

**GROWTH AND REFLECTANCE CHARACTERISTICS OF
 WINTER WHEAT CANOPIES**

L. D. HINZMAN, M. E. BAUER (Minnesota Univ.), and C. S. T.
 DAUGHTRY 14 Nov. 1984 21 p refs ERTS
 (Contract NAS9-16528)

(E85-10080; NASA-CR-171843, NAS 1.26:171843,
 LARS-TR-111484) Avail: NTIS HC A02/MF A01 CSCL 02C

A valuable input to crop growth and yield models would be
 estimates of current crop condition. If multispectral reflectance
 indicates crop condition, then remote sensing may provide an
 additional tool for crop assessment. The effects of nitrogen
 fertilization on the spectral reflectance and agronomic
 characteristics of winter wheat (*Triticum aestivum* L.) were
 determined through field experiments. Spectral reflectance was
 measured during the 1979 and 1980 growing seasons with a
 spectroradiometer. Agronomic data included total leaf N
 concentration, leaf chlorophyll concentration, stage of development,
 leaf area index (LAI), plant moisture, and fresh and dry phytomass.
 Nitrogen deficiency caused increased visible, reduced near infrared,
 and increased middle infrared reflectance These changes were
 related to lower levels of chlorophyll and reduced leaf area in the
 N-deficient plots. Green LAI, an important descriptor of wheat
 canopies, could be reliably estimated with multispectral data. The
 potential of remote sensing in distinguishing stressed from healthy
 crops is demonstrated Evidence suggests multispectral imagery
 may be useful for monitoring crop condition. R S F.

N85-19495*# Purdue Univ., Lafayette, Ind. Lab. for Applications
 of Remote Sensing.

**TECHNIQUES FOR MEASURING INTERCEPTED AND
 ABSORBED PAR IN CORN CANOPIES**

K. P. GALLO and C. S. T. DAUGHTRY 14 Nov. 1984 20 p
 refs ERTS

(Contract NAS9-16528)

(E85-10081; NASA-CR-171842; NAS 1.26:171842;
 LARS-TR-111284) Avail: NTIS HC A02/MF A01 CSCL 02C

The quantity of radiation potentially available for photosynthesis
 that is captured by the crop is best described as absorbed

01 AGRICULTURE AND FORESTRY

photosynthetically active radiation (PAR). Absorbed PAR (APAR) is the difference between descending and ascending fluxes. The four components of APAR were measured above and within two planting densities of corn (*Zea mays* L.) and several methods of measuring and estimating APAR were examined. A line quantum sensor that spatially averages the photosynthetic photon flux density provided a rapid and portable method of measuring APAR. PAR reflectance from the soil (Typic Argiaquoll) surface decreased from 10% to less than 1% of the incoming PAR as the canopy cover increased. PAR reflectance from the canopy decreased to less than 3% at maximum vegetative cover. Intercepted PAR (1 - transmitted PAR) generally overestimated absorbed PAR by less than 4% throughout most of the growing season. Thus intercepted PAR appears to be a reasonable estimate of absorbed PAR.

A.R.H.

N85-19496*# Hunter Coll., New York. Dept. of Geology and Geography.

PRELIMINARY EVALUATION OF THE AIRBORNE IMAGING SPECTROMETER FOR VEGETATION ANALYSIS Final Report

A. H. STRAHLER and C. E. WOODCOCK Mar 1984 32 p refs. Sponsored by NASA. Prepared for JPL, Pasadena, Calif. Original contains color illustrations (Contract JPL-956585)

(NASA-CR-174440, JPL-9950-956, NAS 1.26:174440) Avail: NTIS HC A03/MF A01 CSCL 02C

The primary goal of the project was to provide ground truth and manual interpretation of data from an experimental flight of the Airborne Infrared Spectrometer (AIS) for a naturally vegetated test site. Two field visits were made, one trip to note snow conditions and temporally related vegetation states at the time of the sensor overpass, and a second trip following acquisition of prints of the AIS images for field interpretation. Unfortunately, the ability to interpret the imagery was limited by the quality of the imagery due to the experimental nature of the sensor.

B.W.

N85-21736*# Environmental Research Inst. of Michigan, Ann Arbor.

THEMATIC MAPPER SPECTRAL DIMENSIONALITY AND DATA STRUCTURE

E. P. CRIST and R. C. CICONE *In its* LANDSAT-4 Sci. Characterization Early Results, Vol. 3, Pt 2 p 443-466 Jan. 1985 refs ERTS

(Contract NAS5-16538)

Avail: NTIS HC A25/MF A01 CSCL 05B

A simulated LANDSAT 4 TM and MSS data set, representing three crops over three growing seasons and a wide variety of soil types, was used to evaluate the structure of TM data and to compare its characteristics to those of MSS data. TM bands 2, 3, and 4, transformed to tasseled cap-like coordinates, provide an equivalent data space to MSS tasseled cap data, with greater dynamic range and no apparent loss of information resulting from the exclusion of the 0.9 to 1.1 micron region. Data from the six reflective TM bands (excluding the thermal band) primarily occupy two planes and a transition zone between them. The plane of vegetation is comparable to the MSS tasseled cap plane, while the plane of soils and transition zone provide a new dimension of information unavailable from the MSS. This added dimension offers promise of improved ability to determine the relative mix of vegetation and soil in the sensor field of view and to estimate soil moisture status. The improvement in spectral characteristics of the TM over the MSS, not to mention the greater spatial resolution, have resulted in a significant increase in the information content of the data.

R.S.F.

N85-21747*# Environmental Research Inst. of Michigan, Ann Arbor. Infrared and Optics Div.

INVESTIGATIONS OF VEGETATION AND SOILS INFORMATION CONTAINED IN LANDSAT THEMATIC MAPPER AND MULTISPECTRAL SCANNER DATA Final Report

E. CRIST, R. LAURIN, J. E. COLWELL, and R. J. KAUTH Dec. 1984 117 p refs ERTS

(Contract NAS9-16538)

(E85-10082; NASA-CR-171857, NAS 1.26:171857;

ERIM-160300-101-F) Avail: NTIS HC A06/MF A01 CSCL 05B

An extension of the TM tasseled cap transformation to reflectance factor data is presented, and the basic concepts underlying the tasseled cap transformations are described. The ratio of TM bands 5 and 7, and TM tasseled cap wetness, are both shown to offer promise of direct detection of available soil moisture. Some effects of organic matter and other soil characteristics or constituents on TM tasseled cap spectral response are also considered.

A.R.H.

N85-21748*# National Oceanic and Atmospheric Administration, Columbia, Mo.

NOAA-AISC USER'S GUIDE FOR IMPLEMENTING CERES MAIZE MODEL FOR LARGE AREA YIELD ESTIMATION

J. LARRABEE and T. HODGES Jan. 1985 21 p. Sponsored by NASA, USDA, Dept. of Commerce, Dept. of the Interior, and Agency for International Development ERTS

(Contract PROJ. AGRISTARS)

(E85-10083; NASA-CR-175518; YM-15-00401; JSC-20237, NAS 1.26:175518) Avail: NTIS HC A02/MF A01 CSCL 02C

The subroutines used by the CERES (Crop Estimation through Resource and Environment Synthesis) to simulate the phenological development, growth, and economic yield of corn using soil and daily meteorological data are described.

A.R.H.

N85-21749*# National Oceanic and Atmospheric Administration, Columbia, Mo.

USER'S GUIDE TO THE TAMW WHEAT MODEL AS IMPLEMENTED ON THE IBM 360/195 COMPUTER

J. LARRABEE and T. HODGES Jan. 1985 11 p. Sponsored by NASA, USDA, Dept. of Commerce, Dept. of the Interior, and Agency for International Development ERTS

(Contract PROJ. AGRISTARS)

(E85-10084; NASA-CR-175519; YM-15-00402; JSC-20238; NAS 1.26:175519) Avail: NTIS HC A02/MF A01 CSCL 02C

The implementation of the Texas A&M wheat simulation model on the IBM 360/195 computer is described. Local changes were made to the model using a wide variety of meteorological data sources. The FORTRAN code was more modularized and made easier to understand.

A.R.H.

N85-21750*# National Oceanic and Atmospheric Administration, Columbia, Mo.

NOAA-AISC USER'S GUIDE FOR IMPLEMENTING CERES WHEAT MODEL FOR LARGE AREA YIELD ESTIMATION

J. LARRABEE and T. HODGES Jan. 1985 27 p. Sponsored by NASA, USDA, Dept. of Commerce, Dept. of the Interior, and Agency for International Development ERTS

(Contract PROJ. AGRISTARS)

(E85-10085; NASA-CR-175520; YM-15-00400; JSC-20236, NAS 1.26:175520) Avail: NTIS HC A03/MF A01 CSCL 02C

Subroutines used by the CERES (Crop Estimation through Resource and Environment Synthesis) to simulate crop phenological development, growth, and final yield from soil as well as daily meteorological data are described.

Author

N85-21751*# National Oceanic and Atmospheric Administration, Columbia, Mo.

ESTIMATING SOLAR RADIATION FOR PLANT SIMULATION MODELS

T. HODGES, V. FRENCH, and S. LEDUC Jan 1985 23 p refs Sponsored by NASA, USDA, Dept. of Commerce, Dept. of the Interior, and Agency for International Development ERTS (Contract PROJ AGRISTARS) (E85-10089; NASA-CR-175524; YM-15-00403; JSC-20239; NAS 1.26:175524) Avail: NTIS HC A02/MF A01 CSCL 02C

Five algorithms producing daily solar radiation surrogates using daily temperatures and rainfall were evaluated using measured solar radiation data for seven U.S. locations. The algorithms were compared both in terms of accuracy of daily solar radiation estimates and terms of response when used in a plant growth simulation model (CERES-wheat). Requirements for accuracy of solar radiation for plant growth simulation models are discussed. One algorithm is recommended as being best suited for use in these models when neither measured nor satellite estimated solar radiation values are available. A R.H.

N85-21752*# California Univ., Berkeley Space Sciences Lab. **REMOTE SENSING RESEARCH FOR AGRICULTURAL APPLICATIONS Progress Report, 1 Feb. 1983 - 31 Dec. 1984**

R. N. COLWELL, Principal Investigator, S. L. WALL, L. H. BECK, S. D. DEGLORIA, P. R. RITTER, R. W. THOMAS, A. J. TRAVLOS, and E. FAKHOURY (California Univ., Davis) 31 Dec. 1984 60 p refs ERTS (Contract NCC2-205)

(E85-10090; NASA-CR-175525; NAS 1.26:175525) Avail: NTIS HC A04/MF A01 CSCL 02C

Materials and methods used to characterize selected soil properties and agricultural crops in San Joaquin County, California are described. Results show that: (1) the location and widths of TM bands are suitable for detecting differences in selected soil properties, (2) the number of TM spectral bands allows the quantification of soil spectral curve form and magnitude; and (3) the spatial and geometric quality of TM data allows for the discrimination and quantification of within field variability of soil properties. The design of the LANDSAT based multiple crop acreage estimation experiment for the Idaho Department of Water Resources is described including the use of U.C. Berkeley's Survey Modeling Planning Model. Progress made on Peditor software development on MIDAS, and cooperative computing using local and remote systems is reported as well as development of MIDAS microcomputer systems. A R.H.

02

ENVIRONMENTAL CHANGES AND CULTURAL RESOURCES

Includes land use analysis, urban and metropolitan studies, environmental impact, air and water pollution, geographic information systems, and geographic analysis.

A85-20570

ON THE APPLICATION OF METEOROLOGICAL SATELLITE IMAGERY FOR MONITORING THE ENVIRONMENT

G. E. HUNT (Imperial College of Science and Technology, London, England) Earth-Oriented Applications of Space Technology (ISSN 0277-4488), vol. 4, no. 4, 1984, p. 239-245 Research supported by the Science and Engineering Research Council of England refs

Meteorological satellites now routinely monitor the earth and provide measurements of the atmosphere, ocean and land surface which are used for studies of weather and climate. In this paper a review is given of current knowledge, with particular emphasis directed towards remote sensing of clouds, atmospheric energetics, mesoscale meteorology and radiation budget. Author

A85-20644#

STUDY ON A REGIONAL GEOGRAPHICAL INFORMATION SYSTEM AND APPLICATION MODEL

J. HE, S. YEN, T. CHI, and S.-X. ZHAO (Chinese Academy of Sciences, Institute of Remote Sensing Application, Beijing, People's Republic of China) United Nations, International Meeting of Experts on Remote Sensing Information Systems, Feldafing and Oberpfaffenhofen, West Germany, May 7-11, 1984, Paper. 21 p. refs

A technique for the development of a regional geographical information system (RGIS) by using remote-sensing data, computer technique, and traditional geoscience research methods is presented. The paper is divided into four parts: introduction, system design and technique procedure, system architecture and implementation, and system function and application. Author

A85-20647#

NEEDS AND ACCESSIBILITY OF DEVELOPING COUNTRIES FOR/TO REMOTE SENSING INFORMATION SYSTEMS

R. E. GALEANO and H. DIEDERIX (Centro Interamericano de Fotointerpretacion, Bogota, Colombia) United Nations, International Meeting of Experts on Remote Sensing Information Systems, Feldafing and Oberpfaffenhofen, West Germany, May 7-11, 1984, Paper 12 p. refs

The development and use of remote sensing technology in a part of the Latin American and Caribbean region has been limited because of severe restrictions on the availability of basic data and the means of processing these data. The implementation of a regional program to develop, promote, and transfer remote sensing technology and applications is necessary if this powerful tool is to be used effectively. The aim of this presentation is to briefly give some idea not only about the problems of the developing countries in the remote sensing field, but also about the solutions to these problems by means of a structured program with regional scope. Author

A85-20747

MASMAP, DESIGN FOR A PROJECT-ORIENTED GEO-INFORMATION PROGRAM PACKAGE FOR URBAN UPGRADING SCHEMES

C. A. DE BRUIJN (International Institute for Aerial Survey and Earth Sciences, Enschede, Netherlands) ITC Journal (ISSN 0303-2434), no. 2, 1984, p. 95-103. refs

MASMAP (Mapping and Analysis with Small format Aerial Photography) is a computer software system being designed specifically for urban upgrading projects in developing countries. The information requirements of planners/administrators have been carefully analyzed to determine what information is needed in each project stage and in what format it will be most useful. The system also takes into account the programming skills of the eventual users. It assumes the availability of small format aerial photographs complemented by limited ground surveys. Author

A85-20748

METHOD FOR SEQUENTIAL ANALYSIS OF SPATIAL DEVELOPMENT IN A RURAL-URBAN FRINGE ZONE

H. T. J. LUTCHMAN (International Institute for Aerial Survey and Earth Sciences, Enschede, Netherlands) ITC Journal (ISSN 0303-2434), no. 2, 1984, p. 104-111. refs

The method used in a partly exploratory, partly hypothesis-testing survey carried out in the southern rural-urban fringe of Paramaribo, Surinam, is described. A process approach was followed using sequential aerial photographs taken at 11 year intervals. Aerial photographs were the primary data source, supplemented by local knowledge of the area. Usemap, a gridcell based, computer aided geo-information system, was used to store and sort the data and produce the resulting maps. Author

02 ENVIRONMENTAL CHANGES AND CULTURAL RESOURCES

A85-20749

POPULATION ESTIMATION FROM AERIAL PHOTOS FOR NON-HOMOGENEOUS URBAN RESIDENTIAL AREAS

V. F. L. POLLE (International Institute for Aerial Survey and Earth Sciences, Enschede, Netherlands) ITC Journal (ISSN 0303-2434), no 2, 1984, p. 116-122 refs

Aerial photo interpretation can be useful for estimating populations in fast-growing newly built-up areas in Third World cities. Reliable results can be obtained, however, only if the housing areas which are homogeneous with respect to physical characteristics are also homogeneous with respect to population densities. Case studies from Teheran and Colombo are used to illustrate different methods in different situations. Standard deviations from census data are approximately 20 percent, but standard deviations of 30 to 50 percent are not exceptional. Planners/geographers should study their local situations to judge under which conditions these standard deviations are acceptable.

Author

A85-24950

AMERICAN CONGRESS ON SURVEYING AND MAPPING AND AMERICAN SOCIETY OF PHOTOGRAMMETRY, FALL CONVENTION, SALT LAKE CITY, UT, SEPTEMBER 19-23, 1983, TECHNICAL PAPERS

Falls Church, VA, American Society of Photogrammetry and American Congress on Surveying and Mapping, 1983, 752 p. No individual items are abstracted in this volume.

The technology and application of photogrammetry, surveying, and cartography are discussed in reviews and reports and illustrated with tables, diagrams, and maps. Topics examined include stereometric cameras, multifrequency radar interpretation, land-cover classification from Landsat TM data, the optimization of space radars for geological analysis in tropical environments, photogrammetric robot vision, and the use of remote sensing for monitoring sandhill-crane populations. Consideration is given to an albedo-texture model for detecting change in semiarid environments from Landsat MSS data, thematic line-printer maps from Landsat data, tests of quality and precision in aerial photography, and microwave measurements of moisture gradients in the upper soil profile.

T.K.

A85-25070

THE SECULAR PERIOD BEHAVIOR OF 38 RR LYRAE STARS IN THE LMC GLOBULAR CLUSTER NGC 2257

J. M. NEMEC (Dominion Astrophysical Observatory, Victoria, British Columbia, Canada; Washington, University, Seattle, WA; Observatorio Interamericano de Cerro Tololo, La Serena, Chile), M. L. HAZEN-LILLER (Harvard-Smithsonian Center for Astrophysics, Cambridge, MA; Dominion Astrophysical Observatory, Victoria, British Columbia, Canada), and J. E. HESSER (Dominion Astrophysical Observatory, Victoria, British Columbia, Canada; Observatorio Interamericano de Cerro Tololo, La Serena, Chile) Astrophysical Journal Supplement Series (ISSN 0067-0049), vol. 57, Feb. 1985, p. 329-348. Research supported by the Dominion Astrophysical Observatory, Observatorio Interamericano de Cerro Tololo, and Harvard-Smithsonian Center for Astrophysics refs (Contract NSF AST-83-14961)

The secular period behavior of 38 RR Lyrae stars in the LMC globular cluster NGC 2257 is investigated using new PDS and visual photometry of plates taken during 1951-61 and recent photometry of CTIO plates taken during 1971-82. Accurate periods, light curves, and phases of maximum light are derived for the cluster variables. The period behavior of the stars is derived under the assumption that the periods are either constant or changing uniformly with time. Detailed remarks on all the NGC 2257 variables are made. As a check on the reduction procedures, period change rates are also derived for 15 RR Lyrae stars in four galactic globular clusters and the results are compared with previously derived results. Period change rate distributions and mean period change rates as a function of position in the color-magnitude diagram and RR Lyrae type are derived and compared with galactic globular cluster stars.

C.D.

A85-26935

AN EXAMINATION OF SOME PROBLEMS AND SOLUTIONS IN MONITORING URBAN AREAS FROM SATELLITE PLATFORMS

B. C. FORSTER (New South Wales, University, Kensington, Australia) International Journal of Remote Sensing (ISSN 0143-1161), vol. 6, Jan. 1985, p. 139-151. refs

A discussion of the benefits of satellite remote sensing to urban studies is followed by a consideration of resolution requirements and associated problems. Problems include loss of contextual clues for interpretation, heterogeneity of cover surfaces, temporal differences in atmospheric effects and registration of different scenes. A number of solutions to these problems are considered, such as the use of reference surfaces for atmospheric corrections and the use of targetted control points for temporal change monitoring. The specific advantages of high-resolution satellite data are particularly considered.

Author

A85-27984

THE 1982 EL CHICHON VOLCANO ERUPTIONS - A SATELLITE PERSPECTIVE

M. MATSON (NOAA, National Environmental Satellite, Data, and Information Service, Washington, DC) Journal of Volcanology and Geothermal Research (ISSN 0377-0273), vol. 23, 1984, p. 1-10 refs

The March 28, April 3, and April 4, 1982 eruptions of El Chichon Volcano were detected and monitored using the GOES and NOAA-6 environmental satellites. The satellite data provided information about the height and dispersal of the eruption plume and subsequent ash cloud on each of these dates. Based on the satellite data it was concluded that the March 28 eruption, the second of two eruptions on April 3, and the April 4 eruption injected material into the stratosphere at heights between 17 and 31 km.

Author

A85-29907

COMPREHENSIVE DESERTIFICATION MAPS AND METHODS FOR MAKING SUCH MAPS ON THE BASIS OF SPACE PHOTOGRAPHS [KOMPLEKSNIYE KARTY OPUSTYNIVANIYA I METODIKA IKH SOSTAVLENIIA PO KOSMICHESKIM SNIMKAM]

N. G. KHARIN (Akademiia Nauk Turkmenskoi SSR, Institut Pustyn', Ashkhabad, Turkmen SSR) Issledovanie Zemli iz Kosmosa (ISSN 0205-9614), Jan.-Feb. 1985, p. 52-59. In Russian refs

Quantitative criteria of desertification are proposed, and a method for the compilation of desertification maps on the basis of space remote sensing data is developed. The desertification aspects include the current status, the rate and inherent risk of desertification, and the effect of animals and humans on the environment. Landsat and Soyuz-22 data on southeast Turkmenistan are considered.

B.J.

A85-30088* National Aeronautics and Space Administration Goddard Space Flight Center, Greenbelt, Md.

EFFECT OF LANDSAT THEMATIC MAPPER SENSOR PARAMETERS ON LAND COVER CLASSIFICATION

D. L. TOLL (NASA, Goddard Space Flight Center, Earth Resources Branch, Greenbelt, MD) Remote Sensing of Environment (ISSN 0034-4257), vol. 17, April 1985, p. 129-140 refs

Selected sensor parameter differences between TM and MSS were assessed through classification performance of a suburban/regional test site. Overall classification accuracy of a seven-band Landsat TM scene in comparison to MSS yielded an improvement in accuracy from 74.8 percent to 83.2 percent. To study the possible causes for the difference in classification performance, key sensor parameter differences between MSS and TM, including: (1) spatial resolution (30 m for TM versus 80 m for MSS), (2) quantization level (256 levels for TM versus 64 for MSS), and (3) spectral regions (seven bands in four major spectral regions for TM versus four bands in two regions for MSS), were evaluated. Landsat TM data were processed to stimulate all possible combinations of these MSS and TM parameters, yielding a three-factor design with two levels per factor. The results indicated that the added spectral regions (TM 1, TM 5, and TM

7) and to a lesser degree the increase in quantization level to eight bits produced the improved TM classification accuracy. However, in this study, the higher 30 m spatial resolution of TM contributed to a reduced classification accuracy from increased within-field variability or class heterogeneity. Author

N85-16245*# Utah Univ., Salt Lake City.
DETECTING AGRICULTURAL TO URBAN LAND USE CHANGE FROM MULTI-TEMPORAL MSS DIGITAL DATA
 M. K. RIDD, J. A. MEROLA, and R. A. JAYNES 1983 10 p refs ERTS
 (Contract NAGW-95)
 (E85-10049, NASA-CR-174225, NAS 1.26:174225) Avail NTIS HC A02/MF A01 CSCL 05B

Conversion of agricultural land to a variety of urban uses is a major problem along the Wasatch Front, Utah. Although LANDSAT MSS data is a relatively coarse tool for discriminating categories of change in urban-size plots, its availability prompts a thorough test of its power to detect change. The procedures being applied to a test area in Salt Lake County, Utah, where the land conversion problem is acute are presented. The identity of land uses before and after conversion was determined and digital procedures for doing so were compared. Several algorithms were compared, utilizing both raw data and preprocessed data. Verification of results involved high quality color infrared photography and field observation. Two data sets were digitally registered, specific change categories internally identified in the software, results tabulated by computer, and change maps printed at 1:24,000 scale. R.S.F

N85-19486*# Utah Univ., Salt Lake City. Center for Remote Sensing and Cartography.
ASSESSMENT OF LANDSAT FOR RANGELAND MAPPING, RUSH VALLEY, UTAH
 M. K. RIDD, K. P. PRICE, and G. E. DOUGLASS Dec 1984 38 p ERTS
 (Contract NAGW-95)
 (E85-10072; NASA-CR-174399; NAS 1.26 174399, CRSC-84-9) Avail NTIS HC A03/MF A01 CSCL 08B

The feasibility of using LANDSAT MSS (multispectral scanner) data to identify and map cover types for rangeland, and to determine comparative condition of the ecotypes was assessed. A supporting objective is to assess the utility of various forms of aerial photography in the process. If rangelands can be efficiently mapped with Landsat data, as supported by appropriate aerial photography and field data, then uniform standards of cover classification and condition may be applied across the rangelands of the state. Further, a foundation may be established for long-term monitoring of range trend, using the same satellite system over time. Author

N85-19502# Instituto de Pesquisas Espaciais, Sao Jose dos Campos (Brazil)
THE SHARING OF REMOTE SENSING TECHNIQUES IN BRAZILIAN GEOGRAPHIC RESEARCH [A PARTICIPACAO DAS TECNICAS DE SENSORIAMENTO REMOTO NA PESQUISA GEOGRAFICA BRASILEIRA]
 E. M. L. D. NOVO Oct. 1984 18 p refs In PORTUGUESE, ENGLISH summary Submitted for publication
 (INPE-3307-PRE/617) Avail: NTIS HC A02/MF A01

Some observations about how the Brazilian geographical community was dealing with remote sensing are presented. The remote sensing technical communication published by geographical journals and the frequency of geographers who attended to the 1st and 2nd Brazilian symposium of Remote Sensing are evaluated. Results present a contradiction between the relative high geographers attendance to the remote sensing symposia and the small scientific production related to this subject. Results also suggested that the academic geographical community should increase its interest on remote sensing, so as to improve remote sensing applications to geographical research. Author

N85-20517# National Oceanic and Atmospheric Administration, Washington, D. C. National Environmental Satellite, Data and Information Service.

EARTH OBSERVATIONS AND THE POLAR PLATFORM
 J. H. MCELROY and S. R. SCHNEIDER Jan 1985 21 p refs (NOAA-TR-NESDIS-18) Avail. NTIS HC A02/MF A01

The Polar Platform component of NASA's Space Station Project may be used for operational monitoring of the oceans, land surfaces, atmosphere and space environment. Issues addressed include data and sensor requirements, platform configuration, platform servicing, international participation, communications and research support. Author

N85-21754*# Utah Univ., Salt Lake City. Center for Remote Sensing and Cartography
BUILDING A FUNCTIONAL, INTEGRATED GIS/REMOTE SENSING RESOURCE ANALYSIS AND PLANNING SYSTEM
 M. K. RIDD and D. J. WHEELER 1985 2 p Sponsored by NASA ERTS
 (E85-10092, NASA-CR-175527, NAS 1.26:175527) Avail: NTIS HC A02/MF A01 CSCL 05B

To be an effective tool for resource analysis and planning, a geographic information system (GIS) needs to be integrated with a digital remote sensing capability. To be truly functional, the paired system must be driven by grass roots local needs. A case study couched in a Soil Conservation District in northern Utah is presented. Agency representatives determined that the most fundamental data sets to be entered into the GIS system analysis system in the first round were land use/land cover, geomorphic/soil unit data; hydrologic unit data; and digital terrain. The least expensive and best ways to obtain these data were determined. Data were acquired and formatted to enter the state's PRIME/ARC-INFO GIS, and are being interrogated for resource management decisions related to such issues as agricultural preservation, urban expansion, soil erosion control, and dam siting. A.R.H

N85-21890# Meteorological Research Inst., Tokyo (Japan). Upper Atmosphere Physics Div.
ON THE P1 DATA FROM GMS-SEM
 T. NAGAI In Meteorological Satellite Center Meteorol Satellite Center Tech. Note No. 10, 1984 p 37-46 Nov 1984 refs
 Avail. NTIS HC A05/MF A01:

The count rate of the lowest energy channel P1 (1.2-4 MeV protons nominal) of the space environment monitor on the Geostationary Meteorological Satellite is compared with the proton intensity derived from U.S. spacecraft observations. It is found that the channel P1 count rate is almost always abnormally high. It is also found that the channel P1 count rate corresponds feature by feature to the energetic electron intensity derived from channel EL (2 MeV electrons). This analysis indicates that energetic electrons are a significant contaminant in the proton channel P1. Author

03

GEODESY AND CARTOGRAPHY

Includes mapping and topography.

A85-20035#
THE PARTICIPATION OF THE NETHERLANDS IN THE NASA CRUSTAL DYNAMICS PROJECT [DE NEDERLANDSE DEELNAME AAN NASA'S CRUSTAL DYNAMICS PROJECT]
 L. AARDOOM and K. F. WAKKER Ruimtevaart, vol. 33, Dec 1984, p 215-224 In Dutch

The contributions of Netherlands institutions to the Crustal Dynamics Project begun by NASA in 1981 and to related international projects are surveyed. The fundamental principles of plate tectonics are introduced and illustrated with maps, the

advantages, history, and organization satellite of geodetic observation programs are reviewed, and the orbital computation techniques developed to derive station positions are briefly characterized. Primary participants include the Delft Technical University Section for Spacecraft Orbital Mechanics and the Satellite Geodesy Observatory at Kootwijk (using its newly acquired modular transportable laser-ranging systems), with efforts concentrated on movements of the plates of the eastern Mediterranean. Preparations for performing laser-ranging measurements from remote locations are under way T.K

A85-21107* National Aeronautics and Space Administration. Goddard Space Flight Center, Greenbelt, Md.

SATELLITE MAGNETIC ANOMALIES OVER SUBDUCTION ZONES - THE ALEUTIAN ARC ANOMALY

S C CLARK, H FREY, and H H THOMAS (NASA, Goddard Space Flight Center, Geophysics Branch, Greenbelt, MD) *Geophysical Research Letters* (ISSN 0094-8276), vol. 12, Jan. 1985, p 41-44. refs

Positive magnetic anomalies seen in MAGSAT average scalar anomaly data overlying some subduction zones can be explained in terms of the magnetization contrast between the cold subducted oceanic slab and the surrounding hotter, nonmagnetic mantle. Three-dimensional modeling studies show that peak anomaly amplitude and location depend on slab length and dip. A model for the Aleutian Arc anomaly matches the general trend of the observed MAGSAT anomaly if a slab thickness of 7 km and a relatively high (induced plus viscous) magnetization contrast of 4 A/m are used. A second source body along the present day continental margin is required to match the observed anomaly in detail, and may be modeled as a relic slab from subduction prior to 60 m.y. ago Author

A85-23700

THE ALTIMETRIC GEOID IN THE NORTH SEA

J BRENNER and D LELGEMANN (Institut fuer Angewandte Geodasie, Frankfurt am Main, West Germany) IN: *Satellite microwave remote sensing*. Chichester, West Sussex, England, Ellis Horwood, Ltd., 1983, p. 403-417. Research supported by the Universitaet Hannover. refs

Seasat altimeter data are analyzed in the North Sea Altimeter Project to estimate the precision of mean sea surface heights by adjusting the altimeter profiles and to determine the accuracy of this height through comparison with a gravimetric geoid. Time-dependent effects, such as tides, are accounted for in computing the geoid function by including a number of collinear passes in the adjustment. Within the accuracy limitations of the GGNS3 gravimetric geoid, the comparison confirmed the accuracy of the Seasat altimetry to be better than + or - 24 cm. The precision of mean sea-surface determination for regional areas is within + or - 10 cm, which agrees with the noise level of the instrument. L.T.

A85-25662

MINIMIZATION OF THE EFFECT OF THE EARTH'S CURVATURE IN THE PROJECTIVE TRANSFORMATION OF SPACE IMAGES INTO PHOTOPLANS AND PHOTOMAPS [MINIMIZATSIIA VLIANIYA KRIVIZNY ZEMLI PRI PROEKTIVNOM PREOBRAZOVANII KOSMICHESKIKH SNIMKOV V FOTOPLANY I FOTOKARTY]

A. M. KUZINA, N. S. RAMM, and A. P. SKORODUMOV (Proizvodstvenno Geologicheskoe Ob'edinenie Aerogeologiya, Leningrad, USSR) *Issledovanie Zemli iz Kosmosa* (ISSN 0205-9614), Nov.-Dec. 1984, p. 101-106. In Russian. refs

A85-25689

MATHEMATICAL MODELLING OF THE GEOMAGNETIC FIELD AND SECULAR VARIATION, AND ITS APPLICATIONS; PROCEEDINGS OF THE SYMPOSIUM, HAMBURG, WEST GERMANY, AUGUST 15-27, 1983

D. R. BARRACLOUGH, ED (British Geological Survey, Edinburgh, Scotland) Symposium sponsored by the International Association of Geomagnetism and Aeronomy Physics of the Earth and Planetary Interiors (ISSN 0031-9201), vol. 37, Jan. 1985, 93 p. For individual items see A85-25690 to A85-25693.

Some of the topics discussed include: the assessment of near-surface accuracy of the International Geomagnetic Reference Field (IGRF 80) model of the main geomagnetic field; application of the IGRF 80 to large sets of marine magnetometer data, and the sensitivity of cosmic ray trajectory calculations to geomagnetic field model representations. Consideration is also given to: a test of main IGRF 80 main field and secular variation in Europe; the perpendicular error effect in DGRF model proposals; a comparison of planetary reference fields over Italy; and the characteristics of secular variation of the geomagnetic field from 1964-1981 in Romania. Some additional topics include: the characteristics of the geomagnetic field and its secular variation in and near China in the past 20 years, the effects of the nonuniform distribution of magnetic observatory data on secular variation models; and earth magnetic field modeling and its relation to geological evolution and structure. I.H

A85-26401*# National Aeronautics and Space Administration. Goddard Space Flight Center, Greenbelt, Md.

INTRODUCTION TO THE SPECIAL ISSUE - A PERSPECTIVE ON MAGSAT RESULTS

R. A. LANGE (NASA, Goddard Space Flight Center, Greenbelt, MD) *Journal of Geophysical Research* (ISSN 0148-0227), vol. 90, Feb. 28, 1985, p. 2441-2444. refs

A85-26408* National Aeronautics and Space Administration. Goddard Space Flight Center, Greenbelt, Md.

THE NEAR-EARTH MAGNETIC FIELD AT 1980 DETERMINED FROM MAGSAT DATA

R. A. LANGE (NASA, Goddard Space Flight Center, Greenbelt, MD; Cambridge University, Cambridge, England) and R. H. ESTES (Business and Technological Systems, Inc., Seabrook, MD) *Journal of Geophysical Research* (ISSN 0148-0227), vol. 90, Feb. 28, 1985, p. 2495-2509. Previously announced in STAR as N84-31733. refs

Data from the Magsat spacecraft for November 1979 through April 1980 and from 91 magnetic observatories for 1978 through 1982 are used to derive a spherical harmonic model of the earth's main magnetic field and its secular variation. Constant coefficients are determined through degree and order 13 and secular variation coefficients through degree and order 10. The first degree external terms and corresponding induced internal terms are given as a function of Dst. Preliminary modeling using separate data sets at dawn and dusk local time showed that the dusk data contains a substantial field contribution from the equatorial electrojet current. The final data set is selected first from dawn data and then augmented by dusk data to achieve a good geographic data distribution for each of three time periods: (1) November/December, 1979, (2) January/February, 1980; (3) March/April, 1980. A correction for the effects of the equatorial electrojet is applied to the dusk data utilized. The solution included calculation of fixed biases, or anomalies, for the observation data. Author

A85-26409* National Science Foundation, Washington, D.C
A REVIEW OF PROBLEMS AND PROGRESS IN STUDIES OF SATELLITE MAGNETIC ANOMALIES

M. A. MAYHEW (NSF, Washington, DC), B. D. JOHNSON (NASA, Goddard Space Flight Center, Geophysics Branch, Greenbelt, MD, MacQuarie University, North Ryde, New South Wales, Australia), and P. J. WASILEWSKI (NASA, Goddard Space Flight Center, Laboratory for Extraterrestrial Physics, Greenbelt, MD) *Journal of Geophysical Research* (ISSN 0148-0227), vol. 90, Feb. 28, 1985, p. 2511-2522. Research supported by MacQuarie University. refs

(Contract NAS5-26328, NAS5-26616, NAS5-26074)

A review is conducted of studies performed during the Magsat project. The obtained data are considered, taking into account questions of data availability, aspects of orbit attitude determination, ionospheric noise, a field model, and an anomaly field presentation. Models for interpretation are discussed, giving attention to forward modeling, and equivalent layer inverse modeling. In an evaluation of rock property constraints, the magnetic bottom is discussed along with Curie points, metamorphism and magnetization, and the direction of magnetization. G.R.

A85-26411
MEAN IONOSPHERIC FIELD CORRECTION FOR MAGSAT DATA

M. YANAGISAWA (Tokyo, University, Tokyo, Japan) and M. KONO (Tokyo Institute of Technology, Tokyo, Japan) *Journal of Geophysical Research* (ISSN 0148-0227), vol. 90, Feb. 28, 1985, p. 2527-2536. refs

The determination of crustal magnetic anomalies on the basis of satellite data requires a suitable correction procedure, taking into account the ionospheric field. The present investigation is concerned with the correction required to obtain meaningful magnetic anomaly maps from the Magsat data. An approximation, called the mean ionospheric field correction (MIFC), is presented, giving attention to a strong dependence of the disturbance field at the twilight meridians on the local dip latitude. The magnetospheric and induction fields are discussed along with details regarding the ionospheric field, and the implementation of the mean ionospheric field correction. G.R.

A85-26412
ON THE IDENTIFICATION OF MAGSAT ANOMALY CHARTS AS CRUSTAL PART OF THE INTERNAL FIELD

J. MEYER, J.-H. HUFEN, M. SIEBERT (Goettingen, Universitaet, Goettingen, West Germany), and A. HAHN (Niedersaechsisches Landesamt fuer Bodenforschung, Hanover, West Germany) *Journal of Geophysical Research* (ISSN 0148-0227), vol. 90, Feb. 28, 1985, p. 2537-2541. Research supported by the Deutsche Forschungsgemeinschaft. refs

It is pointed out that geomagnetic anomalies are defined as deviations of the measured internal field from some reference field regarded as normal. The main field, originating in the earth's core, is commonly considered the reference field, and the anomalies are defined as the field which originates in the crust. Thus, satellite anomaly charts are meant to represent the crustal part of the internal magnetic field. In the determination of the geomagnetic anomalies, the core field, which is represented by a specific model, is subtracted from the measured field. Such a procedure is formally justified by the shape of the spatial energy density spectrum of the internal field. Attention is given to the spatial spectrum of the field, and the crustal model field. It is found that an important crustal part is removed by the usual method of constructing anomaly charts. Approaches for correcting this situation are discussed. G.R.

A85-26413* National Aeronautics and Space Administration
 Goddard Space Flight Center, Greenbelt, Md
COMPARISON BETWEEN THE RECENT U.S. COMPOSITE MAGNETIC ANOMALY MAP AND MAGSAT ANOMALY DATA

C. C. SCHNETZLER, P. T. TAYLOR, R. A. LANGE (NASA, Goddard Space Flight Center, Greenbelt, MD), W. J. HINZE (Purdue University, West Lafayette, IN), and J. D. PHILLIPS (U.S. Geological Survey, Reston, VA) *Journal of Geophysical Research* (ISSN 0148-0227), vol. 90, Feb. 28, 1985, p. 2543-2548. refs

The present investigation is concerned with a comparison of Magsat data with a Composite Magnetic Anomaly Map (CMAM) of the conterminous U.S. reported by Zietz (1982). The investigation was initiated to test the validity of the satellite measurements, and to provide insights into error or problems in either data set. It is found that upward continuation of the digital CMAM data is not in qualitative agreement with the Magsat map. However, if a least squares fit polynomial surface is taken out prior to upward continuation, there is improved quantitative agreement between a residual CMAM and Magsat. Causes for the remaining differences between the residual, upward continued CMAM and the Magsat map are also considered. G.R.

A85-26414* Lamont-Doherty Geological Observatory, Palisades, N. Y.

INTERMEDIATE-WAVELENGTH MAGNETIC ANOMALY FIELD OF THE NORTH PACIFIC AND POSSIBLE SOURCE DISTRIBUTIONS

J. L. LABRECQUE, S. C. CANDE, and R. D. JARRARD (Lamont-Doherty Geological Observatory, Palisades, NY) *Journal of Geophysical Research* (ISSN 0148-0227), vol. 90, Feb. 28, 1985, p. 2549-2564. Previously announced in STAR as N83-14596. refs

(Contract NAS5-25891; NSF OCE-83-17174)

A technique that eliminates external field sources and the effects of strike aliasing was used to extract from marine survey data the intermediate wavelength magnetic anomaly field for (B) in the North Pacific. A strong correlation exists between this field and the Magsat field although a directional sensitivity in the Magsat field can be detected. The intermediate wavelength field is correlated to tectonic features. Island arcs appear as positive anomalies of induced origin likely due to variations in crustal thickness. Seamount chains and oceanic plateaus also are manifested by strong anomalies. The primary contribution to many of these anomalies appears to be due to a remanent magnetization. The source parameters for the remainder of these features are presently unidentified and ambiguous. Results indicate that the sea surface field is a valuable source of information for secular variation analysis and the resolution of intermediate wavelength source parameters. Author

A85-26415
SEAFLOOR SPREADING ANOMALIES IN THE MAGSAT FIELD OF THE NORTH ATLANTIC

J. L. LABRECQUE (Lamont-Doherty Geological Observatory, Palisades, NY) and C. A. RAYMOND (Lamont-Doherty Geological Observatory, Palisades; Columbia University, New York, NY) *Journal of Geophysical Research* (ISSN 0148-0227), vol. 90, Feb. 28, 1985, p. 2565-2575. Navy-supported research. refs

(Contract NSF OCE-83-17174)

The Magsat mission has stimulated new research aimed at resolving and quantifying the sources of intermediate-wavelength magnetic anomalies in the 4000- to 400-km band pass. The present investigation is mainly concerned with studies on the ocean basins. Attention is given to seafloor spreading anomalies at satellite altitude and a modified seafloor magnetization model. It is shown that the Magsat anomaly field over the North Atlantic can be modeled by a surprisingly simple crustal magnetization distribution whose elements have been observed in other studies of the surface field. The Magsat anomalies make it possible to map, on a regional basis, the high magnetization over the Cretaceous Quiet Zone, the anomalous skewness of the Cretaceous crustal anomalies, and the enhanced susceptibility of the younger oceanic crust. G.R.

A85-26416

MAGSAT SCALAR MAGNETIC ANOMALIES AT NORTHERN HIGH LATITUDES

R. L. COLES (Department of Energy, Mines, and Resources, Div of Seismology and Geomagnetism, Ottawa, Canada) *Journal of Geophysical Research* (ISSN 0148-0227), vol. 90, Feb. 28, 1985, p. 2576-2582. refs

A new scalar magnetic anomaly map derived from Magsat data at high northern latitudes shows important correlations with major geologic and tectonic features. Positive magnetic anomalies over some high-grade metamorphic Precambrian terranes contrast with negative anomalies over lower-grade Precambrian terranes. A positive anomaly is associated with the Aleutian arc-trench system, a region of active plate convergence. Negative anomaly fields are associated with the Nansen-Gakkel Ridge, a region of plate accretion in the Arctic Basin, with its extension into the seismically active Cherskiy Mountains in eastern Siberia, and with the Labrador Sea, an extinct spreading center. However, a positive anomaly occurs over Iceland, on the mid-Atlantic spreading ridge system, and an intense positive anomaly occurs over the Alpha Ridge in the Arctic Basin. The relations among the Magsat orbit, the rotation of the earth, and the movements of the auroral oval have major effects on the spatial distribution of acceptable data and, therefore, on map resolution. Author

A85-26417

MAGSAT VERTICAL FIELD ANOMALIES ABOVE 40 DEG N FROM SPHERICAL CAP HARMONIC ANALYSIS

G. V. HAINES (Department of Energy, Mines, and Resources, Div of Seismology and Geomagnetism, Ottawa, Canada) *Journal of Geophysical Research* (ISSN 0148-0227), vol. 90, Feb. 28, 1985, p. 2593-2598. refs

A spherical cap harmonic analysis has been done on selected Magsat vertical field anomaly data north of 40 deg N, and the resulting map is shown at 6700 and 6900 km, the lower and upper limits in radial distance of the Magsat satellite. Geodetic altitudes for these two radial distances range from 331 and 531 km, respectively, at 40 deg N to 343 and 543 km, respectively, at 90 deg N. C.D.

A85-26418

SCALAR MAGNETIC ANOMALIES OF CANADA AND NORTHERN UNITED STATES DERIVED FROM MAGSAT DATA

J. ARKANI-HAMED, W. E. S. URQUHART, and D. W. STRANGWAY (Toronto, University, Toronto, Canada) *Journal of Geophysical Research* (ISSN 0148-0227), vol. 90, Feb. 28, 1985, p. 2599-2608. Research supported by the Natural Sciences and Engineering Research Council of Canada. refs

The total magnetic field of the earth over Canada and the northern United States is sampled along individual orbits of the magnetometer satellite (Magsat) on the basis of data extracted from the Magsat chronicle tapes. The procedures employed for sampling and analyzing the data are described. The analysis leads to a scalar magnetic anomaly map by suppressing the contributions of both the internal and external magnetic fields of the earth. General features of the anomalies are discussed, and the treatment of the dawn-dusk asymmetry associated with the external magnetic field is described. A band-limited scalar magnetic anomaly map derived after suppression of the dawn-dusk asymmetry effects is described, and a preliminary interpretation of the anomalies is given. C.D.

A85-26422*# National Aeronautics and Space Administration. Goddard Space Flight Center, Greenbelt, Md

MAGSAT AND POGO MAGNETIC ANOMALIES OVER THE LORD HOWE RISE EVIDENCE AGAINST A SIMPLE CONTINENTAL CRUSTAL STRUCTURE

H. FREY (NASA, Goddard Space Flight Center, Geophysics Branch, Greenbelt, MD) *Journal of Geophysical Research* (ISSN 0148-0227), vol. 90, Feb. 28, 1985, p. 2631-2639. refs

Magsat average scalar and POGO reduced-to-pole magnetic anomaly data both show prominent positive signatures over the Lord Howe Rise. Although generally assumed to be continental in

nature, the Lord Howe Rise cannot simply be submerged ordinary continental crust, which would produce a negative anomaly contrast with respect to the surrounding higher susceptibility oceanic crust. Three-dimensional modeling of the plateau, using the known crustal structure and assuming an induced origin for the satellite elevation anomaly, leads to a model in which the lowest crustal layer in an otherwise 'continental' crustal structure has an unusually high susceptibility in the range cgs 0.008-0.010 (SI 0.10-0.13). Replacement or alteration of the lowest layer by a high-susceptibility rock type may be related to the subsidence of the plateau.

Author

A85-26476

COSMIC INTERPOLATION OF TERRESTRIAL POTENTIAL VALUES

K. ARNOLD and D. SCHOEPS (Deutsche Akademie der Wissenschaften, Zentralinstitut fuer Physik der Erde, Potsdam, East Germany) *Gerlands Beitrage zur Geophysik* (ISSN 0016-8696), vol. 93, no. 6, 1984, p. 409-422. refs

It is shown that the values of the gravity potential at the surface of the earth can be interpolated between the data of the satellite altimetry by cosmic methods. This requires the observation of a low-low mission of two satellites. The method seems to offer also a way to determine the topography of the oceans. Author

A85-27386

A COMPARISON BETWEEN GEOS 1 MAGNETIC-FIELD MEASUREMENTS AND SOME MODELS OF THE GEOMAGNETIC FIELD

E. AMATA, M. CANDIDI, R. ORFELI, and C. SIGNORINI (CNR, Istituto di Fisica dello Spazio Interplanetario, Frascati, Italy) *Nuovo Cimento C, Serie 1* (ISSN 0390-5551), vol. 7 C, July-Aug. 1984, p. 397-412. refs

The GEOS 1 satellite recorded geomagnetic field data for comparison with the predictions of four models of the field. The models were based on the earth's dipole tilt and magnetopause currents, the magnetospheric current distribution and a fixed solar wind impingement angle, on Explorer 33, 34, 41 and 43 data and the dipole tilt angle, and current distributions and the dipole tilt angle. The data covered quiet intervals from May-December 1977 in terms of the dayside three field components and the field direction as measured from a 2127 x 38,645 km orbit. Accuracies consistently within 3 percent were obtained with the Olsen-Pfitzer (1974) 6th order model, which assumed the fixed solar wind approach angle. M.S.K.

A85-28011* National Aeronautics and Space Administration. Goddard Space Flight Center, Greenbelt, Md.

UNITED STATES CRUSTAL THICKNESS

R. J. ALLENBY and C. C. SCHNETZLER (NASA, Goddard Space Flight Center, Geophysics Branch, Greenbelt, MD) *Tectonophysics* (ISSN 0040-1951), vol. 93, 1983, p. 13-31. refs

The thickness of the crust, the thickness of the basal (intermediate or lower) crustal layer, and the average velocity at the top of the mantle have been mapped using all available deep-penetrating seismic-refraction profiles in the conterminous United States and surrounding border areas. These profiles are indexed to their literature data sources. The more significant long wavelength anomalies on the three maps are briefly discussed and analyzed. An attempt to use Bouguer gravity to validate mantle structure was inconclusive. Author

A85-28012* National Aeronautics and Space Administration. Goddard Space Flight Center, Greenbelt, Md.

ESTIMATION OF LOWER CRUST MAGNETIZATION FROM SATELLITE DERIVED ANOMALY FIELD

C. C. SCHNETZLER and R. J. ALLENBY (NASA, Goddard Space Flight Center, Geophysics Branch, Greenbelt, MD) *Tectonophysics* (ISSN 0040-1951), vol. 93, 1983, p. 33-45. refs

Various lines of evidence point to the lower crust as the source of the long-wavelength magnetic anomaly field measured by the POGO and Magsat satellites. Using seismically determined lower crust thicknesses and equivalent source inversion of the satellite

anomaly data, magnetization for the lower crust for much of the United States has been calculated. The average magnetization for two hundred sixty-six 150 x 150 km areas is 3.5 A/m with a standard deviation of 1.1 A/m. These values are consistent with laboratory measurements of mafic-ultramafic rocks expected in the lower crust, and in agreement with previous estimates of lower crust magnetization based on long-wavelength aeromagnetic data. Average lower crust thickness for the same areas is 18.2 km ($\sigma = 6.4$). Thus, over large regions, it appears that variation in magnetization and variation in magnetic layer thickness contribute almost equally in causing the anomaly field variation at satellite altitude. Author

A85-29000

DETERMINATION OF THE HEIGHTS OF POINTS OF A PLACE ON THE BASIS OF RADAR-SURVEY DATA [K VOPROSU OPREDELENIIA VYSOT TOCHEK MESTNOSTI PO MATERIALAM RADIOLOKATSIONNOI S'EMKI]

P. V. BELIKOV, V. G. ELIUSHKIN, and B. V. PRONIN. *Geodeziia i Aerofotos'emka* (ISSN 0536-101X), no. 6, 1984, p. 84-89. In Russian. refs

The possibility of using information about terrain relief obtained on the basis of overlapping radar photographs with known external-orientation elements forming a stereopair is assessed with reference to the determination of place-point heights. It is shown that it is possible to use a stereopair of radar photographs to obtain relief information with the aim of producing maps with a scale of 1:100,000. B.J.

A85-30013

METHODS OF SPACE GEODESY AND ITS ROLE IN EARTH STUDIES [METODY GEODEZJI KOSMICZNEJ I JEJ ROLA W BADANIACH ZIEMI]

W. BARAN (Akademia Rolniczo-Techniczna, Olsztyn, Poland). *Postepy Astronautyki* (ISSN 0373-5982), vol. 17, no. 2, 1984, p. 7-19. In Polish. refs

The current trends and techniques of satellite-based observations are reviewed, and the possibilities afforded by the use of these techniques for solving problems in space geodesy are discussed. Some results of the satellite-based studies of the earth's gravitational field are examined. V.L.

N85-17234*# Jet Propulsion Lab., California Inst. of Tech., Pasadena.

SIR-B CARTOGRAPHY AND STEREO TOPOGRAPHIC MAPPING

M. KOBRICK, F. LEBER (Inst. for Image Processing and Computer Graphics), J. RAGGAM (Image Processing and Computer Graphics), G. DOMIK (Image Processing and Computer Graphics), R. WELCH (Georgia Univ., Athens), H. CARR (Naval Observatory, Washington, D.C.), J. HAMMAK (Naval Observatory, Washington, D.C.), V. KAUPP (Arkansas Univ., Fayetteville), H. C. MACDONALD (Arkansas Univ., Fayetteville), W. P. WAITE (Arkansas Univ., Fayetteville) et al. *In its* The SIR-B Sci. Invest. Plan 3 p. 1 Jul. 1984

Avail: NTIS HC A10/MF A01 CSCL 08B

The SIR-B mapping experiment which will evaluate the utility of SAR images taken singularly, in pairs, and in combination with other data sets for cartographic, topographic, and thematic mapping, and determine the optimum configuration of a SAR system for future mapping mission is outlined. SIR-B is the first orbital imaging radar mission which will incorporate maintenance of geometric image fidelity along with careful calibration and documentation of internal timing and frequency parameters. This along and the multiple incidence angle images of the same target which are necessary for stereoscopy and topographic mapping, make it the ideal opportunity for cartographic experimentation. It is emphasized that comprises a significant part of the overall experiment objectives. E.A.K.

N85-17407# Royal Inst. of Tech., Stockholm (Sweden) Dept of Photogrammetry

MATHEMATICAL ASPECTS OF DIGITAL TERRAIN INFORMATION; REPORT FROM INTERNATIONAL SOCIETY FOR PHOTOGRAMMETRY AND REMOTE SENSING (ISPRS) WORKING GROUP 3:3, 1980 - 1984

K. TORLEGAARD. *In its* Papers of the 15th Intern. Soc. for Photogrammetry and Remote Sensing (ISPRS) Congr. p. 1-5 1984

Avail: NTIS HC A05/MF A01

An international comparative test was organized in order to study the relations between methods for sampling the terrain in a photogrammetric stereomodel, approximation (interpolation and filtering) of the terrain surface, accuracy of derived (resampled) elevations from a digital elevation model (DEM), and the type of terrain. Ten participants measured DEMs and resampled elevations in check points for six test areas. The test areas were studied as to ways to classify the type of terrain with respect to its elevations. Author (ESA)

N85-18437 Texas Univ., Austin

USING THE GLOBAL POSITIONING SYSTEM (GPS) PHASE OBSERVABLE FOR RELATIVE GEODESY: MODELING, PROCESSING, AND RESULTS Ph.D. Thesis

B. W. REMONDI 1984 324 p

Avail: Univ. Microfilms Order No. DA8421790

Performing centimeter-level relative positioning geodesy (translocation), using L-band signals from Global Positioning System (GPS) satellites, was research. Specifically, signal phase was the data measurement. A detailed model of the observable was developed; existing methods of processing the data were developed and extended, new methods of processing the phase observable were developed and compared. Algorithmic development, data, processing run streams, and results are included. Dissert. Abstr.

N85-18440 Bayerische Akademie der Wissenschaften, Munich (West Germany).

ACTIVITIES REPORT OF THE DEPARTMENT OF APPLIED RESEARCH 78 FOR SATELLITE GEODESY OF THE TECHNICAL UNIVERSITY, MUNICH Annual Report, 1983 [DIE ARBEITEN DES SONDERFORSCHUNGSBEREICHES 78 SATELLITENGEOAESIE DER TECHNISCHE UNIVERSITAET MUENCHEN]

M. SCHNEIDER 1984 272 p refs. In GERMAN (ASTRON-GEODAE-ARB-45; ISBN-3-7696-9788-X; ISSN-0340-7691) Avail. Issuing Activity

Geodesy, laser landmarking, radiointerferometry, and microwave metrology research is summarized. Topics discussed include: range finding, mobile laser range determination, construction of a reception station for radiointerferometry, microwave measurements, geopotential, Earth-Moon interaction, kinematic geodetic coordinates, and geophysical application of interferometric methods.

Author (ESA)

N85-20505*# National Aeronautics and Space Administration. Goddard Space Flight Center, Greenbelt, Md. **GEOMETRIC ACCURACY ASSESSMENT OF LANDSAT-4 MULTISPECTRAL SCANNER (MSS) DATA**

M. L. IMHOFF and W. L. ALFORD. *In its* LANDSAT-4 Sci. Characterization Early Results, Vol. 1 p. 143-158 Jan. 1985 ERTS

Avail: NTIS HC A10/MF A01 CSCL 08E

Standard LANDSAT 4 MSS data for Washington, DC was analyzed to characterize the geodetic, temporal registration, and band-to-band registration accuracy of standard P-format MSS image data. Geodetic accuracy was assessed by comparing geodetic verification points selected from U.S. Geological Survey (USGS) topographic triangles against the corresponding LANDSAT 4 image feature locations. Cross-correlation was used to evaluate band-to-band and temporal registration accuracy. The geometric accuracies of LANDSAT 4 MSS data are excellent. The geodetic registration accuracy appears very good. The LANDSAT data closely match the USGS map products with image-to-map offset

03 GEODESY AND CARTOGRAPHY

errors of 5 (57 x 57 m) pixels. Temporal registration accuracy is also quite good although results from this analysis do not meet specifications. The specifications for temporal registration are 0.3 sensor (82 x 82 m) pixel or 24.6 m 90 percent of the time. The results show that the 90 percent error figure for temporal registration is 0.68 (57 x 57 m) pixel or 38.8 meters. Band-to-band registration could be considered to meet specifications. The registration error between the bands having naturally higher correlations between information content (bands 1 and 2 and bands 3 and 4) proved to meet specifications 14.2m and 13.7m, respectively.

R.S.F.

N85-21746*# EROS Data Center, Sioux Falls, S. Dak.
**GEODETIC ACCURACY OF LANDSAT 4 MULTISPECTRAL
SCANNER AND THEMATIC MAPPER DATA**

J. M. THORMODSGARD and D. J. DEVRIES *In its* LANDSAT-4
Sci. Characterization Early Results, Vol 3, Pt. 2 p 581-590 Jan
1985 ERTS

Avail: NTIS HC A25/MF A01 CSCL 05B

Conclusive statements concerning the geodetic accuracy of LANDSAT 4 data, based on such a small sampling of scenes, is impossible. However, the results provide a few interesting observations. For example, LANDSAT 4 multispectral band scanner (MSS) system corrected errors were larger than were expected based on the knowledge of the geometric accuracy of the data from LANDSAT 2 and 3. Also, the thematic mapper (TM) system corrected scenes were more accurate than the MSS scenes by a factor of three. As the spacecraft platform for these two sensors is the same, this result cannot be explained, but a comparison of concurrently acquired MSS and TM data might clarify this situation. Finally, the single MSS ground control point (GCP) corrected product evaluated had good geodetic accuracy considering the poor distribution of the two GCP's applied in the registration

Author

N85-21761# Admiralty Research Establishment, Portland
(England)

**THE IMAGING OF INTERNAL WAVES BY THE SEASAT-A
SYNTHETIC APERTURE RADAR**

M. M. BAGG and K. I. JOHNSON Aug. 1984 34 p
(AD-A149808; ARE/TN-720/84; DRIC-BR-93397) Avail: NTIS
HC A03/MF A01 CSCL 08C

This paper presents results derived from a study of some 5 million square kilometers of optical survey processed SEASAT-SAR imagery of the northeast Atlantic. In the study, markings attributed to internal wave activity were collected on maps together with the relevant bathymetry and surface meteorology. Simple analysis techniques have been applied systematically to compare the very large data sets involved. The characteristics of the internal wave features are also discussed. A small portion of the imagery is studied and discussed in greater detail as a case study. GRA

N85-21766# National Geodetic Survey, Rockville, Md.
**HYBRID METHOD OF MAPPING AND PHOTOGEODETIC
CONTROL NETWORK DENSIFICATION**

R. ADLER Oct. 1984 22 p refs
(PB85-133775, NOAA-TM-NOS-NGS-41) Avail: NTIS HC
A02/MF A01 CSCL 08E

During the past few years, tremendous progress has been made in aerial triangulation by block adjustment with additional parameters. This method has achieved reliability and accuracy not considered possible only a decade ago. The paper postulates that photogeodetic control densification is economically viable, especially when performed in conjunction with well defined mapping tasks. Satellite geodesy, by means of the NAVSTAR Global Positioning System, is also discussed. This recently operational system is revolutionizing the approach to geodetic control densification by attaining survey results of centimeter level accuracy. Author (GRA)

N85-22323*# National Aeronautics and Space Administration,
Washington, D. C. The Planetary Cartography Working Group.

**PLANETARY CARTOGRAPHY IN THE NEXT DECADE (1984 -
1994)**

1984 71 p refs

(NASA-SP-475; NAS 1.21:475) Avail: NTIS HC \$10.00/MF A01
CSCL 03A

The cartographic products required to support science and planetary exploration during the next 10 years were assessed. Only major map series or first order maps needed to characterize the surface physiography of a planet or satellite were considered. Included in these considerations are maps needed as bases for plotting geologic, geophysical, and atmospheric phenomena and for planning future planetary exploration. These products consist of three types of maps: controlled photomosaics, shaded relief maps, and topographic contour maps.

E.A.K.

04

GEOLOGY AND MINERAL RESOURCES

Includes mineral deposits, petroleum deposits, spectral properties of rocks, geological exploration, and lithology.

A85-21047

**DETERMINING STRETCH PARAMETERS FOR LITHOLOGIC
DISCRIMINATION ON LANDSAT MSS BAND-RATIO IMAGES**

D. H. KNEPPER, JR. and G. L. RAINES (U.S. Geological Survey,
Denver, CO) Photogrammetric Engineering and Remote Sensing
(ISSN 0099-1112), vol 51, Jan. 1985, p. 63-70.

A key factor in preparing band-ratio images of Landsat multispectral scanner (MSS) data for discriminating rock and soil units is the determination of the proper contrast stretches to enhance spectral variations that are related to lithologic differences. In and regions with little vegetation, histograms of band ratios show the spectral properties mostly of rocks and soils; however, as vegetation and water bodies become more abundant, the histograms no longer reflect the spectral properties of only rocks and soils, and determining appropriate contrast stretches for lithologic discrimination is more difficult. A method has been developed to routinely exclude the effects of vegetation and water from band-ratio histograms that does not require intensive investigator participation. With the exclusion of vegetation and water, the remaining pixels included in the histograms are presumed to represent rocks and soils.

Author

A85-21975* Jet Propulsion Lab., California Inst. of Tech.,
Pasadena

MEASURING SPECTRA OF ARID LANDS

A. B. KAHLE (California Institute of Technology, Jet Propulsion
Laboratory, Pasadena, CA) IN: Deserts and arid lands. The
Hague, Martinus Nijhoff Publishers, 1984, p. 195-217. refs

The principles, instrumentation and data acquisition and interpretation techniques employed in multispectral remote sensing for geological applications are surveyed. Sensing is based on exact measurements of electromagnetic radiation interacting with atoms and molecules in the sensed scene. Absorbed radiation can be used to identify elements in the near-IR bands and emitted or reflected energy can be sensed in the mid- and far-IR. Sunlight normally serves as the exciting source. Wavelength absorbance and emittance characteristics are distinct for the various elements and molecules such as transition metal ions, water, carbonates, etc. The bands for identifying different materials are determined in the laboratory, followed by ground truth field tests. Several hand-held radiometers and spectrometers have been developed for the field trials. Each instrument usually has a limited detection range and serves for developing a data base for subtle distinctions among contiguous minerals with similar radiometric signatures. The data serve for calibrating first airborne and then satellite sensors,

e.g. the Landsat MSS and Thematic Mapper Instruments are also being tested using the Orbiter as the test platform. M.S.K.

A85-22422

MAPPING OF LANDFORMS FROM LANDSAT IMAGERY - AN EXAMPLE FROM EASTERN NEW SOUTH WALES, AUSTRALIA
C. F. PAIN (New South Wales, University, Kensington, Australia)
Remote Sensing of Environment (ISSN 0034-4257), vol. 17, Feb. 1985, p. 55-65. refs

A85-23766

THERMAL-INERTIA MAPPING FROM SPACE [LA CARTOGRAPHIE SPATIALE D'INERTIE THERMIQUE]
K. WATSON (U.S. Geological Survey, Denver, CO) IN: Spectral signatures of objects in remote sensing, International Conference, 2nd, Bordeaux, France, September 12-16, 1983, Reports Versailles, Institut National de la Recherche Agronomique, 1984, p. 459-473. refs

The application of satellite-remote-sensing thermal images to the identification of structural features, the discrimination of geologic materials by thermal-inertia mapping, and the construction of heat-flux models is demonstrated using HCMM 500-m-resolution images obtained with site repetition rate 16 days at 1.30 PM and 2:30 AM local time over the western U.S. The data-analysis approach and procedures are described, and sample results are presented graphically and characterized in detail. The limitations imposed by the HCMM repetition rate, cloud cover, the lack of global coverage, the relatively low spatial resolution, and registration problems are examined and shown to be more significant than the level of thermal resolution, which is considered adequate for the sophistication of current flux models. T.K.

A85-23785

GEOMORPHOLOGY AND REMOTE SENSING: NUMERICAL INVENTORY OF OBJECTS IN LANDSAT, SPOT SIMULATION, AND SIR-A DATA APPLICATIONS TO THE MOPTI-BANDIAGARA (MALI) REGION [GEOMORPHOLOGIE ET TELEDETECTION: L'INVENTAIRE NUMERIQUE DES OBJETS DANS LES DONNEES LANDSAT, SIMULATION SPOT ET SIR-A APPLICATIONS A LA REGION DE MOPTI-BANDIAGARA /MALI/]

C. BARDINET (Ecole Normale Supérieure des Jeunes Filles, Paris; Paris, Ecole Nationale Supérieure des Mines, Valbonne, Alpes-Maritimes, France), M. BENARD, J. M. MONGET, M. SAAIDI (Paris, Ecole Nationale Supérieure des Mines, Valbonne, Alpes-Maritimes, France), and J. TRICART (CNRS, Paris, France) IN: Spectral signatures of objects in remote sensing, International Conference, 2nd, Bordeaux, France, September 12-16, 1983, Reports Versailles, Institut National de la Recherche Agronomique, 1984, p. 763-770. In French. refs

A85-23790

CLASSIFICATION OF THE GEOLOGICAL ENVIRONMENTS OF ANTICOSTI ISLAND - AN APPROACH USING A LANDSAT-4 SPECTRAL SIMULATION [CLASSIFICATION DES ENVIRONNEMENTS GEOLOGIQUES DE L'ILE D'ANTICOSTI - UNE APPROCHE UTILISANT UNE SIMULATION SPECTRALE DU SATELLITE LANDSAT-4]

S. PERRAS, F. BONN, and Q. H. J. GWYN (Sherbrooke, Université, Sherbrooke, Québec, Canada) IN: Spectral signatures of objects in remote sensing; International Conference, 2nd, Bordeaux, France, September 12-16, 1983, Reports Versailles, Institut National de la Recherche Agronomique, 1984, p. 831-839. In French. Research supported by the Ministère de l'Éducation du Québec; Natural Science and Engineering Research Council of Canada (Contract NSERC-7526)

A spectral simulation of TM bands 2, 3, 4, and 6 (2.08 to 2.35 microns) is used to study nine geological environments on Anticosti Island. By using TM bands 2 and 3, three water-depth zones are identified in the sea environment. Peat bogs and string bogs are identifiable using TM bands 3 and 6, whereas TM bands 3 and 4, which are found to be sensitive to high chlorophyll content, are

used to identify tree-covered bogs. The two most extensive environments in the study area, bedrock and shallow water deposits, both of which are identified by TM band 3, are covered with arborescent vegetation. The final environment consists of littoral and fluvial deposits, and an accurate identification of this environment is achieved through TM band 6 which is reflected by the bare material but absorbed by the water. Better results in identifying the various environments are obtained by using certain band ratios: the modified vegetation index (TM4-TM3/TM4+TM3) and the algorithm (TM6-Biomass/TM6+Biomass) M.D.

A85-23792

GENERATION OF A LANDSAT-HCMM COMBINED IMAGE AND ITS APPLICATION TO GEOLOGICAL CARTOGRAPHY [GENERATION D'UNE IMAGE LANDSAT-HCMM COMBINEE - APPLICATION A LA CARTOGRAPHIE GEOLOGIQUE]

Y. RABU, M. ABRAMS, W. NIBLACK (IBM France, S.A., Centre Scientifique, Paris, France), and J. CHOROWICZ (Paris VI, Université, Paris, France) IN: Spectral signatures of objects in remote sensing; International Conference, 2nd, Bordeaux, France, September 12-16, 1983, Reports Versailles, Institut National de la Recherche Agronomique, 1984, p. 849-855. In French

A85-23793* Jet Propulsion Lab., California Inst. of Tech., Pasadena.

CHARACTERISTICS OF PLAYA DEPOSITS AS SEEN ON SIR-A, SEASAT AND LANDSAT COREGISTERED DATA [CARACTERISTIQUES DE DEPOTS DE SEBKHA OBSERVEES SUR DES IMAGES SIR-A, SEASAT ET LANDSAT]

PH. REBILLARD and M. NARAGHI (California Institute of Technology, Jet Propulsion Laboratory, Pasadena, CA) IN: Spectral signatures of objects in remote sensing; International Conference, 2nd, Bordeaux, France, September 12-16, 1983, Reports Versailles, Institut National de la Recherche Agronomique, 1984, p. 857-863. NASA-supported research.

A classification technique currently under development has been applied for the qualitative study of a playa located in Northeastern Algeria using coregistered SIR-A, Seasat and Landsat MSS 7 data. This classification which is texture based can be applied to only single band imagery at this time. The first results are very encouraging and reach conclusions similar to those obtained with more time consuming classifiers. The signature of each class is well expressed for the Landsat picture. Misclassifications occur with the SIR-A or Seasat images. Author

A85-25655

ANALYSIS OF MESOFRACTURES ACCORDING TO SPACE IMAGES - CURRENTS TRENDS IN THE EXPLORATION FOR OIL AND GAS DEPOSITS [ANALIZ MEZOTRESHCHINOVATOSTI PO KOSMICHESKIM SNIMKAM AKTUAL'NOE NAPRAVLENIE IZUCHENIYA NEFTIANYKH I GAZOVYKH MESTOROZHDENII]
G. I. AMURSKII, G. A. ABRAMENOK, and N. N. SOLOVEV (Vsesoiuznyi Nauchno-Issledovatel'skii Institut Prirodnykh Gazov, Moscow, USSR) Issledovanie Zemli iz Kosmosa (ISSN 0205-9614), Nov.-Dec. 1984, p. 36-41. In Russian. refs

A85-26419

EXTRACTION OF MAGNETIC ANOMALIES OF CRUSTAL ORIGIN FROM MAGSAT DATA OVER THE AREA OF THE JAPANESE ISLANDS

I. NAKAGAWA, T. YUKUTAKE, and N. FUKUSHIMA (Tokyo, University, Tokyo, Japan) Journal of Geophysical Research (ISSN 0148-0227), vol. 90, Feb. 28, 1985, p. 2609-2615. refs

A85-26420*# National Aeronautics and Space Administration. Goddard Space Flight Center, Greenbelt, Md
AN ESTIMATION OF CONTINENTAL CRUST MAGNETIZATION AND SUSCEPTIBILITY FROM MAGSAT DATA FOR THE CONTERMINOUS UNITED STATES

C. C. SCHNETZLER (NASA, Goddard Space Flight Center, Geophysics Branch, Greenbelt, MD) Journal of Geophysical Research (ISSN 0148-0227), vol. 90, Feb. 28, 1985, p. 2617-2620. refs

The Magsat-derived magnetic anomaly field over the United States was inverted to magnetization in a seismically determined variable-thickness lower crust. The results are quite similar to those obtained from a previous inversion of POGO data. The average magnetization is 3.45 ± 1.0 A/m, which gives a bulk magnetic susceptibility of $8.7 \pm 2.4 \times 10^{-6}$ to the -2nd (SI units) for the lower crustal layer consistent with a mafic composition. These values are also consistent with previous estimates of lower crustal magnetization from aeromagnetic data and with laboratory measurements of mafic rock susceptibilities. Author

A85-26421* Manitoba Univ., Winnipeg.
CRUSTAL STRUCTURE OF THE CHURCHILL-SUPERIOR BOUNDARY ZONE BETWEEN 80 AND 98 DEG W LONGITUDE FROM MAGSAT ANOMALY MAPS AND STACKED PASSES

D. H. HALL, T. W. MILLAR (Manitoba, University, Winnipeg, Canada), and I. A. NOBLE (Texaco Canada Resources, Ltd., Calgary, Alberta, Canada) Journal of Geophysical Research (ISSN 0148-0227), vol. 90, Feb. 28, 1985, p. 2621-2630. Research supported by the Department of Energy, Mines and Resources of Canada, Natural Sciences and Engineering Research Council of Canada, and NASA. refs

A modeling technique using spherical shell elements and equivalent dipole sources has been applied to Magsat signatures at the Churchill-Superior boundary in Manitoba, Ontario, and Ungava. A large satellite magnetic anomaly (12 nT amplitude) on POGO and Magsat maps near the Churchill-Superior boundary was found to be related to the Richmond Gulf aulacogen. The averaged crustal magnetization in the source region is 5.2 A/m. Stacking of the magnetic traces from Magsat passes reveals a magnetic signature (10 nT amplitude) at the Churchill-Superior boundary in an area studied between 80 deg W and 98 deg W. Modeling suggests a steplike thickening of the crust on the Churchill side of the boundary in a layer with a magnetization of 5 A/m. Signatures on aeromagnetic maps are also found in the source areas for both of these satellite anomalies. Author

A85-26423* National Aeronautics and Space Administration. Goddard Space Flight Center, Greenbelt, Md.
VISCOUS REMANENT MAGNETIZATION MODEL FOR THE BROKEN RIDGE SATELLITE MAGNETIC ANOMALY

B. D. JOHNSON (NASA, Goddard Space Flight Center, Geophysics Branch, Greenbelt, MD; MacQuarie University, North Ryde, New South Wales, Australia) Journal of Geophysical Research (ISSN 0148-0227), vol. 90, Feb. 28, 1985, p. 2640-2646. Research supported by MacQuarie University. refs

An equivalent source model solution of the satellite magnetic field over Australia obtained by Mayhew et al. (1980) showed that the satellite anomalies could be related to geological features in Australia. When the processing and selection of the Magsat data over the Australian region had progressed to the point where interpretation procedures could be initiated, it was decided to start by attempting to model the Broken Ridge satellite anomaly, which represents one of the very few relatively isolated anomalies in the Magsat maps, with an unambiguous source region. Attention is given to details concerning the Broken Ridge satellite magnetic anomaly, the modeling method used, the Broken Ridge models, modeling results, and characteristics of magnetization. G.R.

A85-27943* Geosat Committee, Inc., San Francisco, Calif.
FRONTIERS FOR GEOLOGICAL REMOTE SENSING FROM SPACE; GEOSAT WORKSHOP, 4TH, FLAGSTAFF, AZ, JUNE 12-17, 1983, REPORT

F. B. HENDERSON, ED. (Geosat Committee, Inc., San Francisco, CA) and B. N. ROCK, ED. (California Institute of Technology, Jet Propulsion Laboratory, Pasadena, CA) Workshop sponsored by the Geosat Committee, Inc. Falls Church, VA, American Society of Photogrammetry, 1983, 87 p. For individual items see A85-27944 to A85-27948.

Consideration is given to: the applications of near-infrared spectroscopy to geological reconnaissance and exploration from space; imaging systems for identifying the spectral properties of geological materials in the visible and near-infrared; and Thematic Mapper (TM) data analysis. Consideration is also given to descriptions of individual geological remote sensing systems, including: GEO-SPAS; SPOT; the Thermal Infrared Multispectral Scanner (TIMS); and the Shuttle Imaging Radars A and B (SIR-A and SIR-B). Additional topics include the importance of geobotany in geological remote sensing; achromatic holographic stereograms from Landsat MSS data; and the availability and applications of NOAA's non-Landsat satellite data archive. I.H.

A85-27944
NEAR-INFRARED SPECTROSCOPY IN GEOLOGICAL RECONNAISSANCE AND EXPLORATION

J. W. SALISBURY, B. BAILEY (U.S. Geological Survey, Reston, VA), W. BUCKINGHAM (Gulf Science and Technology Co., Pittsburgh, PA), W. COLLINS (Geophysical and Environmental Research, Inc., New York, NY), and S. MARSH (Sun Exploration and Production Co., Dallas, TX) IN: Frontiers for geological remote sensing from space; Geosat Workshop, 4th, Flagstaff, AZ, June 12-17, 1983, Report. Falls Church, VA, American Society of Photogrammetry, 1983, p. 1-11.

The applications of near-infrared spectroscopy to geological remote-sensing and exploration are discussed. Attention is given to the current status of laboratory methods for the identification of individual rocks and minerals according to their infrared spectra. The effects of particle size differences and overlapping or concentrated absorption spectra on the accuracy of infrared surveys of clay-containing regions are considered. A number of recommendations are presented for improvements in data reduction and instrument calibration techniques. Spectral data from the Thematic Mapper (TM) instrument onboard the Landsat 4 satellite is given as an example. I.H.

A85-27945* Geological Survey, Reston, Va.
IMAGING SYSTEMS FOR THE DELINEATION OF SPECTRAL PROPERTIES OF GEOLOGIC MATERIALS IN THE VISIBLE AND NEAR-INFRARED

S. E. MARSH (Sun Exploration and Production Co., Dallas, TX), M. H. PODWYSOCKI (U.S. Geological Survey, Reston, VA), A. F. H. GOETZ, G. VANE (California Institute of Technology, Jet Propulsion Laboratory, Pasadena, CA), P. N. SLATER (Arizona, University, Tucson, AZ), and T. E. TOWNSEND IN: Frontiers for geological remote sensing from space, Geosat Workshop, 4th, Flagstaff, AZ, June 12-17, 1983, Report. Falls Church, VA, American Society of Photogrammetry, 1983, p. 13-20.

The current status of imaging systems for the identification of the spectral properties of geologic minerals in the visible and near infrared ranges is reviewed. The technical characteristics of the most important instruments are given, including the MSS and TM, the Airborne Imaging Spectrometer, (AIS) the Airborne Visible/Infrared Imaging Spectrometer (AVIRIS), and the Shuttle Imaging Spectrometer Experiment (SISEX). It is pointed out that none of the current systems have sufficient spectral resolution to identify mineralogy on the basis of absorption characteristics in the visible, near-infrared or shortwave-infrared bands. The development of new systems with higher spectral resolution is discussed. I.H.

A85-27946* National Aeronautics and Space Administration, Washington, D. C.

THEMATIC MAPPER DATA ANALYSIS

M. SETTLE (NASA, Washington, DC), P. CHAVEZ, H. H. KIEFFER (U.S. Geological Survey, Flagstaff, AZ), J. R. EVERETT (Earth Satellite Corp., Chevy Chase, MD), A. B. KAHLE (California Institute of Technology, Jet Propulsion Laboratory, Pasadena, CA), C. A. KITCHO (Woodward-Clyde Consultants, San Francisco, CA), N. M. MILTON (U.S. Geological Survey, Reston, VA), and D. A. MOUAT (NASA, Ames Research Center, Moffett Field, CA) IN Frontiers for geological remote sensing from space; Geosat Workshop, 4th, Flagstaff, AZ, June 12-17, 1983, Report . Falls Church, VA, American Society of Photogrammetry, 1983, p. 21-26

The geological applications of remote sensing technology are discussed, with emphasis given to the analysis of data from the Thematic Mapper (TM) instrument onboard the Landsat 4 satellite. The flight history and design characteristics of the Landsat 4/TM are reviewed, and some difficulties encountered in the interpretation of raw TM data are discussed, including the volume of data, residual noise, detector-to-detector striping; and spatial misregistration between measurements. Preliminary results of several geological, lithological, geobotanical mapping experiments are presented as examples of the geological applications of the TM, and some areas for improving the quality of TM imagery are identified. I.H.

A85-27948* National Aeronautics and Space Administration Ames Research Center, Moffett Field, Calif

THE IMPORTANCE OF GEOBOTANY IN GEOLOGICAL REMOTE SENSING APPLICATIONS

D. A. MOUAT (NASA, Ames Research Center, Moffett Field, CA), W. COLLINS (Geophysical and Environmental Research, Inc., New York, NY), C. ELVIDGE, R. J. P. LYON (Stanford University, Stanford, CA), M. L. LABOVITZ (NASA, Goddard Space Flight Center, Greenbelt, MD), N. M. MILTON (U.S. Geological Survey, Reston, VA), J. PARRISH (California Institute of Technology, Jet Propulsion Laboratory, Pasadena, CA; Pennsylvania State University, Philadelphia, PA), B. N. ROCK (California Institute of Technology, Jet Propulsion Laboratory, Pasadena, CA), D. E. WICKLAND (Savannah River Ecology Laboratory, Savannah, GA), and G. K. ARP IN Frontiers for geological remote sensing from space; Geosat Workshop, 4th, Flagstaff, AZ, June 12-17, 1983, Report . Falls Church, VA, American Society of Photogrammetry, 1983, p. 57-64.

A description of the different effects of variations in ground cover vegetation on remote sensing data in geological and prospecting applications is presented. The different variations are divided into three categories: structural, taxonomic and spectral. Structural variations include changes in the physical appearance of ground cover which may be detectable by a remote sensing instrument. Taxonomic variations occur in those plant communities which are associated with specific geological regions. Spectral variations are due to specific geochemical stresses which may be useful in characterizing geological features at a site. The need for a general scheme for the interpretation of geobotanical remote sensing data is discussed. Geosat data for the field reflectance spectra of different tree species in West Virginia are presented as examples. I.H.

A85-28400

SPACE REMOTE-SENSING DATA IN GEOLOGY [KOSMICHESKAIA INFORMATSIYA V GEOLOGIIA]

V. G. TRIFONOV, ED., V. I. MAKAROV, ED., I. U. G. SAFONOV, ED., and P. V. FLORENSKII Moscow, Izdatel'stvo Nauka, 1983, 536 p. In Russian. No individual items are abstracted in this volume.

The topics discussed include the use of mathematical methods for the solution of geological problems in remote sensing applications; the correlation of space and geologic-geophysical information; and a neotectonic and geomorphological analysis of coastal areas. Consideration is also given to modern and recent geological processes in the continental shelves, the lineaments of

the Turanian plate, the great circular structures of the Upper Juna-Kolyma orogenic region, and the transcontinental lineaments in Eurasia according to data from remote sensing satellites. Among additional topics discussed are: the use of space images for the study of linear ore-controlling and ore-concentrating structures; the application of space images for studies of ore-field and ore-deposits near Lake Baikal, Siberia; and the petroleum and gas provinces of old and young geological platforms I.H.

A85-28999

THE USE OF SALYUT-5 PHOTOGRAPHS FOR REGIONAL GEOMORPHOLOGICAL MAPPING [ISPOL'ZOVANIE KOSMICHESKIKH SOIMKOV S OPS 'SALIUT-5' PRI REGIONAL'NOM GEOMORFOLOGICHESKOM KARTOGRAFIROVANII]

G. G. BAKAI and E. M. NIKOLAEVA (Moskovskii Institut Inzhenerov Geodezii, Aerofotos'emki i Kartografi, Moscow, USSR) Geodeziia i Aerofotos'emka (ISSN 0536-101X), no. 6, 1984, p. 73-78. In Russian.

A series of photographs taken from Salyut-5 was used for the small-scale geomorphological mapping of the Aral Sea region, the Syrdar' valley, and the Karatau ridge. A large number of terrain elements (particularly the large-area elements) have been represented on the geomorphological map. The map has a large information content and exhibits great detail in the contour drawing, which indicates that small-scale space photographs can be used effectively in the thematic mapping of large and complex regions of Central Asia. B.J.

A85-29405

PROSPECTING FROM THE SKIES

G. GRAFF High Technology (ISSN 0277-2981), vol. 5, March 1982, p. 48-53.

Such natural resources as iron oxides, clay minerals, calcite, and quartz, as well as the chlorophyll cycle in plants and the water content of soils, can be assessed through airborne and satellite-borne sensors, on the basis of surface reflectance characteristics. Typical of the sensors in question are the Landsat thematic mapper. Geological data can also be acquired by means of synthetic aperture radars, which establish the existence of the fracture zones at which metal ores or hydrocarbons are frequently found. Current generation remote sensors use aircraft or spacecraft motion to cover one axis of a two-dimensional image, while generating the other axis one-line-at-a-time by means of a scanner. Attention is given to spectrometric analysis methods for multispectral sensor images. O.C.

A85-29904

METHODS FOR THE STUDY OF RECENT TECTONICS ON THE BASIS OF REMOTE SENSING AND GROUND DATA [METODY IZUCHENIIA NOVEISHEI TEKTONIKI PO MATERIALAM DISTANTSIONNYKH I NAZEMNYKH ISSLEDOVANI]

A. A. FREIDLIN, E. G. FARRAKHOV, and L. F. VOLCHEGURSKII (Proizvodstvennoe Geologicheskoe Ob'edinenie Aerogeologia, Moscow, USSR) Issledovanie Zemli iz Kosmosa (ISSN 0205-9614), Jan.-Feb. 1985, p. 32-38. In Russian.

Methods for the complex study of tectonic formations to the east of the near-Caspian depression have been developed on the basis of the interpretation of space (Salyut-4) and aerial photographs in conjunction with other types of geological and geophysical data. This approach led to the determination of: (1) the location and structure of recent tectonic zones; (2) the correlation of interpreted elements of relief and deep tectonic characteristics of the region; (3) the connection between oil deposits and tectonic and neotectonic activity; and (4) the role of tectonic processes in the formation of dispersed-sand massifs in the eastern Caspian region. B.J.

04 GEOLOGY AND MINERAL RESOURCES

A85-29905

POSSIBILITIES OF USING REMOTE-SENSING METHODS TO IMPROVE THE EFFICIENCY OF OIL AND GAS EXPLORATION [VOZMOZHNOСТИ PRIMENENIYA DISTANTSIONNYKH METODOV DLYA POVYSHENIYA EFFEKTIVNOSTI NEFTEGAZOPOISKOVYKH RABOT]

M. KH ISHANOV, V. I. IUSHIN, A. K. GAIKOVA, and G. N. MALESHENKOV (Gosudarstvennyi Nauchno-Issledovatel'skii i Proizvodstvennyi Tsentr Priroda, Proizvodstvennoe Ob'edinenie Tadzhikneft', Dushanbe, Tadzhik SSR) Issledovanie Zemli iz Kosmosa (ISSN 0205-9614), Jan-Feb 1985, p. 39-46. In Russian. refs

A85-29912

IDENTIFICATION OF HOMOGENEOUS REGIONS WITH INCOMPATIBLE BOUNDARIES ON AN IMAGE [VYDELENIE NA IZOBRAZHENII ODNORODNYKH OBLASTEI S NEPOLNYMI GRANITSAMI]

A. A. ZLATOPOLSKII (Proizvodstvennoe Geologicheskoe Ob'edinenie Aerogeologiya, Moscow, USSR) Issledovanie Zemli iz Kosmosa (ISSN 0205-9614), Jan-Feb 1985, p. 94-102. In Russian. refs

An image segmentation method according to identified parts of region boundaries is proposed in the framework of the interpretation of remote-sensing images. Results of a theoretical analysis of a structure generated by a distance transformation are presented, and an algorithm based on the structure is formulated. An example of the application of the algorithm to geological image analysis is examined. B.J.

A85-30087

IMAGE-SCALE AND LOOK-DIRECTION EFFECTS ON THE DETECTABILITY OF LINEAMENTS IN RADAR IMAGES

Y. YAMAGUCHI (Geological Survey of Japan, Tsukuba, Ibaraki, Japan) Remote Sensing of Environment (ISSN 0034-4257), vol. 17, April 1985, p. 117-127.

The effects of image-scale and radar look-direction on the detectability of lineaments are investigated using synthetic aperture radar images of the Japanese Islands. To make clear the optimum image-scale, various kinds of image data including Landsat images and aerial photographs were interpreted. The result indicates that lineament interpretation can be performed most efficiently if $R \times S = 0.1$ mm, where R is the ground resolution and S is the image-scale. The value of 0.1 mm corresponds to the limitation of human eyes. Then, selective enhancement of lineaments caused by radar shadowing was examined by using a topographic model, which was modified from the model of Wise (1969) to fit dissected topographic relief in mature stage of the Japanese Islands. That is, a lineament corresponds to a straight valley of the second order, on whose walls small valleys of the first order develop. Optimum shadow enhancements is achieved when the strike of the lineament is ranging from 20 deg to 30 deg to the radar look-direction. Author

N85-16248*# Instituto de Pesquisas Espaciais, Sao Jose dos Campos (Brazil).

INTEGRATED ANALYSIS OF REMOTE SENSING PRODUCTS FROM BASIC GEOLOGICAL SURVEYS [ANALISE INTEGRADA DOS PRODUTOS DE SENSORIAMENTO REMOTO EM LEVANTAMENTOS GEOLOGICOS BASICOS]

E. DASILVAFAGUNDESFILHO, Principal Investigator Aug. 1984 12 p refs In PORTUGUESE; ENGLISH summary Presented at the 33rd Congr. Brasil. de Geol. Sponsored by NASA ERTS (E85-10052; NASA-CR-174188; NAS 1.26:174188, INPE-3243-PRE/589) Avail: NTIS HC A02/MF A01 CSCL 05B

Recent advances in remote sensing led to the development of several techniques to obtain image information. These techniques as effective tools in geological mapping are analyzed. A strategy for optimizing the images in basic geological surveying is presented. It embraces as integrated analysis of spatial, spectral, and temporal data through photopic (color additive viewer) and computer

processing at different scales, allowing large areas survey in a fast, precise, and low cost manner. Author

N85-17215*# Cornell Univ., Ithaca, N.Y.

TECTONIC, VOLCANIC, AND CLIMATIC GEOMORPHOLOGY STUDY OF THE SIERRAS PAMPEANAS ANDES, NORTHWESTERN ARGENTINA

A. L. BLOOM, M. R. STRECKER, and E. J. FIELDING In JPL The SIR-B Sci. Invest. Plan 4 p 1 Jul 1984 refs Avail: NTIS HC A10/MF A01 CSCL 17I

A proposed analysis of Shuttle Imaging Radar-B (SIR-B) data extends current research in the Sierras Pampeanas and the Puna of northwestern Argentina to the determination - by the digital analysis of mountain-front sinuosity - of the relative age and amount of fault movement along mountain fronts of the late-Cenozoic Sierras Pampeanas basement blocks; the determination of the age and history of the boundary across the Andes at about 27° S latitude between continuing volcanism to the north and inactive volcanism to the south; and the determination of the age and extent of Pleistocene glaciation in the High Sierras, as well as the comparative importance of climatic change and tectonic movements in shaping the landscape. The integration of these studies into other ongoing geology projects contributes to the understanding of landform development in this active tectonic environment and helps distinguish between climatic and tectonic effects on landforms. R.J.F.

N85-17226*# National Aeronautics and Space Administration. Lyndon B. Johnson Space Center, Houston, Tex

GEOLOGICAL, STRUCTURAL, AND GEOMORPHOLOGICAL ANALYSES FROM SIR-B

J. W. HEAD, III, P. J. MOUGINIS-MARK (Hawaii Univ., Honolulu), S. H. ZISK (Haystack Observatory, Westford, Mass.), R. A. F. GRIEVE, A. R. PETERFREUND, and K. D. SULLIVAN In JPL The SIR-B Sci. Invest. Plan 6 p 1 Jul 1984 refs Prepared in cooperation with Brown Univ., Providence, R.I. Avail: NTIS HC A10/MF A01 CSCL 08G

A Shuttle Imaging Radar-B (SIR-B) study designed to develop a better understanding of the application of radar in geological studies is described. The specific objectives for deltaic environments include the examination of delta morphology and the intertidal zone, the surface expression of shallow bathymetry, the characterization of vegetation cover, and the water balance of the delta. In impact crater environments, the goals include the establishment of the radar characteristics of exposed craters and the application of this knowledge to test for the detectability of very poorly exposed craters. M.G.

N85-17232*# Arkansas Univ., Fayetteville.

EVALUATION OF THE L-BAND SCATTERING CHARACTERISTICS OF VOLCANIC TERRAIN IN AID OF LITHOLOGIC IDENTIFICATION, ASSESSMENT OF SIR-B CALIBRATION, AND DEVELOPMENT OF PLANETARY GEOMORPHIC ANALOGS

V. H. KAUPP, W. P. WAITE, H. C. MACDONALD, P. J. MOUGINIS-MARK (Hawaii Univ., Honolulu), and S. H. ZISK (Haystack Observatory, Westford, Mass.) In JPL The SIR-B Sci. Invest. Plan 3 p 1 Jul 1984 Avail: NTIS HC A10/MF A01 CSCL 08K

The objectives of the Shuttle Imaging Radar-B (SIR-B) scattering study and calibration investigation of volcanic terrain are to delineate textural and structural features, to evaluate the L-band scattering characteristics, and to assess SIR-B calibration. Specific tasks are outlined and expected results are summarized. M.G.

N85-17236*# National Aeronautics and Space Administration. Goddard Space Flight Center, Greenbelt, Md
STRUCTURAL INVESTIGATION OF THE CANADIAN SHIELD BY ORBITAL RADAR AND LANDSAT

P. D. LOWMAN, JR., H. W. BLODGET, W. J. WEBSTER, JR., S. PAIA (Ontario Centre for Remote Sensing), V. H. SINGHROY (Ontario Centre for Remote Sensing), and V. R. SLANEY (RADARSAT Project Office) /In JPL The SIR-B Sci. Invest. Plan 4 p 1 Jul. 1984 refs

Avail NTIS HC A10/MF A01 CSCL 08G

Canadian Shield were studied by orbital radar. The primary objective of the study is scientific, to investigate and clarify the tectonic relationships of the Churchill, Superior, and Grenville Provinces, concentrating on their geologic boundaries, the Nelson and Grenville Fronts. Theories about its origin range from in-situ regional metamorphism to tectonic sutures resulting from terrain accretion. The SIR-B investigation clarifies this problem. Secondary objectives are technique development, and include: (1) evaluation of the use of orbital radar in high altitude Precambrian terrains; (2) evaluation of look-azimuth biasing in radar and LANDSAT imagery, and (3) investigation of the synergistic use of radar, LANDSAT, and geophysical data in Precambrian studies. E.A.K.

N85-17237*# National Aeronautics and Space Administration. Goddard Space Flight Center, Greenbelt, Md
STRUCTURAL INVESTIGATION OF THE GRENVILLE PROVINCE BY RADAR AND OTHER IMAGING AND NONIMAGING SENSORS

P. D. LOWMAN, JR., H. W. BLODGET, W. J. WEBSTER, JR., S. PAIA (Ontario Centre for Remote Sensing), V. H. SINGHROY (Ontario Centre for Remote Sensing), and V. R. SLANEY (RADARSAT Project Office) /In JPL The SIR-B Sci. Invest. Plan 4 p 1 Jul. 1984 refs

Avail: NTIS HC A10/MF A01 CSCL 17I

The structural investigation of the Canadian Shield by orbital radar and LANDSAT, is outlined. The area includes parts of the central metasedimentary belt and the Ontario gneiss belt, and major structures as well-expressed topographically. The primary objective is to apply SIR-B data to the mapping of this key part of the Grenville orogen, specifically ductile fold structures and associated features, and igneous, metamorphic, and sedimentary rock (including glacial and recent sediments). Secondary objectives are to support the Canadian RADARSAT project by evaluating the baseline parameters of a Canadian imaging radar satellite planned for late in the decade. The baseline parameters include optimum incidence and azimuth angles. The experiment is to develop techniques for the use of multiple data sets. E.A.K.

N85-17241*# Analytic Sciences Corp., Reading, Mass.
INVESTIGATION OF SIR-B IMAGES FOR LITHOLOGIC MAPPING

J. T. PARR and R. V. SAILOR /In JPL The SIR-B Sci. Invest. Plan 2 p 1 Jul. 1984 refs

Avail: NTIS HC A10/MF A01 CSCL 08B

It is immediately apparent from the examination of almost any synthetic aperture radar (SAR) data that the radar return is primarily a function of the topographic relief. Yet radar reflectance is dependent on both surface roughness and the dielectric constant of the surface material. These two parameters can in many cases be related to lithologic units. Thus, if the first-order terrain effects due to topographic relief could (in essence) be removed from the radar image, the SAR data might well be used for lithologic discrimination. Such an approach is evaluated. Landsat Thematic Mapper data along with ground truth are used to define training cells that characterize the various lithologic units in the area. By aggregating the radar data for these cells, curves of radar reflectance versus local incidence are estimated. The curves are then used to classify the test area. The results are compared with lithologic classification based upon multi-spectral (visible and infrared) data. B.W.

N85-17244*# Jet Propulsion Lab., California Inst. of Tech., Pasadena.

APPLICATION AND CALIBRATION OF THE SUBSURFACE MAPPING CAPABILITY OF SIR-B IN DESERT REGIONS

G. G. SCHABER, J. F. MCCAULEY, C. S. BREED, M. J. GROlier, B. ISSAWI (Egyptian Geological Survey and Mining Authority), C. V. HAYNES (Arizona Univ., Tucson), W. MCHUGH (GAI Consultants), A. S. WALKER (Geological Survey, Reston, Va.), and R. BLOM /In its The SIR-B Sci. Invest. Plan 5 p 1 Jul. 1984 refs Prepared in cooperation with Geological Survey, Flagstaff, Ariz

Avail NTIS HC A10/MF A01 CSCL 08B

The penetration capability of the shuttle imaging radar (SIR-B) sensor in desert regions is investigated. Refined models to explain this penetration capability in terms of radar physics and regional geologic conditions are devised. The sand-buried radar-rivers discovered in the Western Desert in Egypt and Sudan are defined. Results and procedures developed during previous SIR-A investigation of the same area are extrapolated. Author

N85-17248*# Nevada Univ., Reno.

ANALYSIS OF SIR-B RADAR ILLUMINATION OF GEOMETRY FOR DEPTH OF PENETRATION AND SURFACE FEATURE AND VEGETATION DETECTION, NEVADA AND CALIFORNIA

J. V. TARANIK, D. B. SLEMMONS, E. J. BELL, M. BORENGASSER, T. P. LUGASKI, H. VREELAND, P. VREELAND, E. KLEINER, F. F. PETERSON, and H. KLEIFORTH /In JPL The SIR-B Sci. Invest. Plan 3 p 1 Jul. 1984

Avail NTIS HC A10/MF A01 CSCL 02F

The measurement capability provided by the Shuttle Imaging Radar (SIR-B) was used to determine: (1) the relationships between radar illumination geometry and depth of penetration in different climatic and physiographic environments in Nevada, and, (2) the relationships between radar illumination geometry and detection and analysis of structural features in different climatic and physiographic environments in Nevada. B.G.

N85-17249*# Massachusetts Inst of Tech., Cambridge.

DELINEATION OF MAJOR GEOLOGIC STRUCTURES IN TURKEY USING SIR-B DATA

M. N. TOKSOZ, G. H. PETTINGILL, P. FORD, and L. GULEN /In JPL The SIR-B Sci. Invest. Plan 3 p 1 Jul. 1984 refs

Avail: NTIS HC A10/MF A01 CSCL 08G

Shuttle Imaging Radar-B (SIR-B) images of well mapped segments of major faults, such as the North Anatolian Fault (NAF) and East Anatolian Fault (EAF) will be studied to identify the prominent signatures that characterize the fault zones for those specific regions. The information will be used to delineate the unmapped fault zones in areas with similar geological and geomorphological properties. The data obtained from SIR-B images will be compared and correlated with the LANDSAT thematic mapper and seismicity alignments based on well constrained earthquake epicenters. B.G.

N85-19497*# Texas Univ., Dallas.

SIR-A IMAGERY IN GEOLOGIC STUDIES OF THE SIERRA MADRE ORIENTAL, NORTHEASTERN MEXICO. PART 1 (REGIONAL STRATIGRAPHY): THE USE OF MORPHOSTRATIGRAPHIC UNITS IN REMOTE SENSING MAPPING

J. F. LONGORIA and O. H. JIMENEZ 1985 37 p refs Sponsored by NASA Prepared for JPL, Pasadena, Calif (Contract JPL-956432)

(NASA-CR-175457; JPL-9950-983; NAS 1.26:175457) Avail: NTIS HC A03/MF A01 CSCL 08B

SIR-A imagery was used in geological studies of sedimentary terrains in the Sierra Madre Oriental, northeastern Mexico. Geological features such as regional strike and dip, bedding, folding and faulting were readily detected on the image. The recognition of morphostructural units in the imagery, coupled with field verification, enabled geological mapping of the region at the scale of 1:250,000. Structural profiling lead to the elaboration of a morphostructural map allowing the recognition of an echelon folds

and field trends which were used to postulate the ectonic setting of the region. Author

N85-19498* Texas Univ., Dallas.

POST-CARBONIFEROUS TECTONICS IN THE ANADARKO BASIN, OKLAHOMA: EVIDENCE FROM SIDE-LOOKING RADAR IMAGERY

K C NIELSEN and R J STERN 1985 18 p refs Submitted for publication Sponsored by NASA Prepared for JPL, Pasadena, Calif.

(Contract JPL-956430)

(NASA-CR-175458, JPL-9950-982; NAS 1.26 175458;

UTD-CONTRIB-471) Avail: NTIS HC A02/MF A01 CSCL 171

The Anadarko Basin of western Oklahoma is a WNW-ESE elongated trough filled with of Paleozoic sediments. Most models call for tectonic activity to end in Pennsylvanian times. NASA Shuttle Imaging Radar revealed a distinctive and very straight lineament set extending virtually the entire length of the Anadarko Basin. The lineaments cut across the relatively flat-lying Permian units exposed at the surface. The character of these lineaments is seen most obviously as a tonal variation. Major streams, including the Washita and Little Washita rivers, appear to be controlled by the location of the lineaments. Subsurface data indicate the lineaments may be the updip expression of a buried major fault system, the Mountain View fault. Two principal conclusions arise from this analysis: (1) the complex Mountain View Fault system appears to extend southeast to join the Reagan, Sulphur, and/or Mill Creek faults of the Arbuckle Mountains, and (2) this fault system has been reactivated in Permian or younger times.

R.S.F

N85-21757* EROS Data Center, Sioux Falls, S. Dak.

LANDSAT 4 INVESTIGATIONS OF THEMATIC MAPPER AND MULTISPECTRAL SCANNER APPLICATIONS Quarterly Report

D T LAUER, Principal Investigator 27 Feb 1985 3 p ERTS

(Contract NASA ORDER S-10757-C)

(E85-10095; NASA-CR-175530; NAS 1 26:175530;

PCN902-91548) Avail: NTIS HC A02/MF A01 CSCL 05B

Structural and stratigraphic characteristics of the Drum Mountains in Utah were obtained using LANDSAT 5 TM data that were digitally enhanced using band ratioing, principal components analysis, and spatial filtering techniques. Color ratioing composite images proved most useful for distinguishing between and identifying exposure of hydroxyl bearing hydrothermally altered inclusive rocks and bleached contact metamorphic rocks dominated by calc-silicate mineral assemblages. The amount and detail of geologic information interpreted from TM images is more significant than that from MSS and in geologic maps. Enhanced LANDSAT 5 TM data also identified and mapped hydrothermal alteration and distinguished between altered and unaltered limonitic assemblages in the Tonopah, Nevada quadrangle. A.R.H.

05

OCEANOGRAPHY AND MARINE RESOURCES

Includes sea-surface temperature, ocean bottom surveying imagery, drift rates, sea ice and icebergs, sea state, fish location

A85-19417* Miami Univ., Fla.

CENTER OF MASS ESTIMATION IN CLOSED VORTICES - A VERIFICATION IN PRINCIPLE AND PRACTICE

S B. HOOKER and D. B. OLSON (Miami, University, Miami, FL) Journal of Atmospheric and Oceanic Technology (ISSN 0739-0572), vol. 1, Sept. 1984, p. 247-255. refs

(Contract NAGW-273; NSF OCE-80-18736, NSF OCE-80-16991; N00014-80-C-0042)

The problem of tracking closed mesoscale vortices using center of mass estimation techniques is studied. Three estimators are evaluated using data from a warm core Gulf Stream ring. The

comparisons show that a method based on the intersection of perpendicular bisectors and one using a least-squares fit of a conic section perform comparably. The perpendicular bisector algorithm is used in conjunction with a Gaussian ring model and a star-shaped survey pattern to produce an expected error curve as a function of vortex translation, survey speed and vortex size. For typical ring parameters, center estimation is usually possible to within \pm or \pm 5 km. The feasibility of using differing data sets to construct a history of ring motion based on a coordinate system moving with the ring is also investigated. In this way, the validity of using satellite-derived data and drifter trajectories to estimate the center of mass of a mesoscale feature is assessed. The results of the analysis demonstrate that the location of the deeper structure of the ring and the surface expression are sufficiently well correlated to permit dynamically relevant calculations based on surface measurements. It is shown that satellite-derived data can be used to approximate the center of mass trajectory to within the error in the individual center estimates for the period analyzed. The Lagrangian-drifter-derived centers are offset from the center of mass trajectory in a manner consistent with kinematic arguments.

Author

A85-19420* National Aeronautics and Space Administration. Langley Research Center, Hampton, Va.

AN INTERCALIBRATION OF METEOSAT-1 AND GOES-2 VISIBLE AND INFRARED MEASUREMENTS

D. R. BROOKS, P. MINNIS (NASA, Langley Research Center, Atmospheric Sciences Div., Hampton, VA), C. F. ENGLAND, and G. E. HUNT (Imperial College of Science and Technology, London, England) Journal of Atmospheric and Oceanic Technology (ISSN 0739-0572), vol. 1, Sept. 1984, p. 283-286.

An intercomparison between radiative parameters determined from visible and infrared channels of the Meteosat-1 and GOES-2 geosynchronous satellites has been carried out using data obtained over the central Atlantic Ocean for 5 November 1978. Hourly visible-infrared measurement pairs at a nominal resolution of 5 km (Meteosat) or 8 km (GOES) have been stored in 1 deg x 1 deg longitude-latitude regions. For the infrared intercomparisons, the GOES 11.5 micron radiance has been compared to Meteosat infrared counts. The scatter in partly cloudy regions is interpreted as being caused by meteorological differences arising from differences in measurement time between the two data sets. For the visible intercomparison, the GOES measurements for clear and cloudy scenes have first been converted with the aid of scene-dependent angular reflectance and albedo models to estimates of the filtered shortwave radiance that GOES would have measured had it been in the Meteosat position. This value has then been compared to Meteosat counts for the shortwave channel. The results indicate that earlier Meteosat calibrations made from airplane overflights of a limited variety of surfaces are applicable to much larger areas of cloud and ocean. Author

A85-19428

REMOTE SENSING BY RADAR ALTIMETRY

C C. KILGUS, J L. MACARTHUR, and P. V. K. BROWN (Johns Hopkins University, Laurel, MD) Johns Hopkins APL Technical Digest (ISSN 0270-5214), vol. 5, Oct.-Dec. 1984, p. 341-345.

The satellite radar altimeter was found to be a versatile and powerful tool for the remote sensing of the oceans. Thus, data from the Geos-C and Seasat-1 altimeters have supported research in geodesy, bathymetry, mesoscale oceanography, tides, ice topography, winds and waves. The radar altimeter is a conceptually simple instrument, which employs a short-pulse radar that measures the distance between the satellite orbit and the subsatellite point on the ocean's surface with the precision of a few centimeters. The Geosat-A altimeter will produce the dense data set required for geodesy. Future altimeters will incorporate redundancy for long life and dual-frequency operation to remove ionospheric effects. It is pointed out that the multibeam altimeter under development will provide the spatial and temporal sampling required for the remote sensing of mesoscale oceanography. G.R.

A85-19429* Applied Physics Lab., Johns Hopkins Univ., Laurel, Md.

PREDICTING DANGEROUS OCEAN WAVES WITH SPACEBORNE SYNTHETIC APERTURE RADAR

R. C. BEAL (Johns Hopkins University, Applied Physics Laboratory, Laurel, MD) Johns Hopkins APL Technical Digest (ISSN 0270-5214), vol. 5, Oct-Dec. 1984, p. 346-359 Research sponsored by the Johns Hopkins University, U.S. Navy, and NASA. refs

It is pointed out that catastrophes, related to the occurrence of strong winds and large ocean waves, can consume more lives and property than most naval battles. The generation of waves by wind are considered, Pierson et al. (1955) have incorporated statistical concepts into a wave forecast model. The concept of an 'ocean wave spectrum' was introduced, with the wind acting independently on each Fourier component. However, even after 30 years of research and debate, the generation, propagation, and dissipation of the spectrum under arbitrary conditions continue to be controversial. It has now been found that spaceborne SAR has a surprising ability to precisely monitor spatially evolving wind and wave fields. Approaches to overcome certain weaknesses of the SAR method are discussed, taking into account the second Shuttle Imaging Radar experiment, and a possible long-term solution provided by Spectrasat. Spectrasat should be a low-altitude (200 to 250 km) satellite with active drag compensation. G.R.

A85-20086

SPACE RADAR OBSERVATIONS OF SMALL-SCALE FORMATIONS ON THE OCEAN SURFACE [RADIOFIZICHESKIE NABLIUDENIYA IZ KOSMOSA MEZOMASSHTABNYKH OBRAZOVANIY NA POVERKHNOSTI OKEANA]

A. I. KALMYKOV, A. P. PICHUGIN, V. N. TSYMBAL, and V. P. SHESTOPALOV (Akademiia Nauk Ukrainskii SSR, Institut Radiofiziki i Elektroniki, Kharkov, Ukrainian SSR) Akademiia Nauk SSSR, Doklady (ISSN 0002-3264), vol. 279, no. 4, 1984, p. 860-862. In Russian

Cosmos-1500 sidelooking radar (SLR) observations of formations on the ocean surface are considered, and radar photographs of sections of the Sea of Okhotsk and the Pacific Ocean, as well as of typhoon Ida at the shoreline of Japan are presented. It is concluded that satellite-borne SLR observations make it possible to detect previously unobserved small-scale formations on the ocean surface, and to investigate large-scale active phenomena that play an important role in the interaction of the ocean and atmosphere. B J

A85-20486* National Aeronautics and Space Administration, Goddard Space Flight Center, Greenbelt, Md

AIRCRAFT AND SATELLITE MEASUREMENT OF OCEAN WAVE DIRECTIONAL SPECTRA USING SCANNING-BEAM MICROWAVE RADARS

F. C. JACKSON (NASA, Goddard Space Flight Center, Laboratory for Oceans, Greenbelt, MD), W. T. WALTON (NASA, Goddard Space Flight Center, Laboratory for Oceans, Greenbelt; Maryland, University, College Park, MD), and P. L. BAKER (Computer Technology Associates, McLean, VA; Computer Sciences Corp., Silver Spring, MD) Journal of Geophysical Research (ISSN 0148-0227), vol. 90, Jan. 20, 1985, p. 987-1004. NASA-supported research. Previously announced in STAR as N83-13544. refs

A microwave radar technique for remotely measuring the vector wave number spectrum of the ocean surface is described. The technique which employs short-pulse, noncoherent radars in a conical scan mode near vertical incidence, is shown to be suitable for both aircraft and satellite application, the technique was validated at 10 km aircraft altitude, where we have found excellent agreement between buoy and radar-inferred absolute wave height spectra. Author

A85-20487* National Aeronautics and Space Administration, Goddard Space Flight Center, Greenbelt, Md.

A COMPARISON OF IN SITU AND AIRBORNE RADAR OBSERVATIONS OF OCEAN WAVE DIRECTIONALITY

F. C. JACKSON (NASA, Goddard Space Flight Center, Greenbelt, MD), W. T. WALTON (NASA, Goddard Space Flight Center, Greenbelt; Maryland, University, College Park, MD), and C. Y. PENG (Science Systems and Applications, Inc., Seabrook, MD) Journal of Geophysical Research (ISSN 0148-0227), vol. 90, Jan. 20, 1985, p. 1005-1018. NASA-supported research. refs

The directional spectrum of a fully arisen, about 3 m sea as measured by an experimental airborne radar, the NASA K(u)-band radar ocean wave spectrometer (ROWS), is compared to reference pitch-roll buoy data and to the classical SWOP (stereo wave observations project) spectrum for fully developed conditions. The ROWS spectrum, inferred indirectly from backscattered power measurements at 5-km altitude, is shown to be in excellent agreement with the buoy spectrum. Specifically, excellent agreement is found between the two nondirectional height spectra, and mean wave directions and directional spreads as functions of frequency. A comparison of the ROWS and SWOP spectra shows the two spectra to be very similar, in detailed shape as well as in terms of the gross spreading characteristics. Both spectra are seen to exhibit bimodal structures which accord with the Phillips' (1958) resonance mechanism. This observation is thus seen to support Phillips' contention that the SWOP modes were indeed resonance modes, not statistical artifacts. Author

A85-20492

AN ALGORITHM TO MEASURE SEA ICE CONCENTRATION WITH MICROWAVE RADIOMETERS

C. T. SWIFT (Massachusetts, University, Amherst, MA), L. S. FEDOR (NOAA, Wave Propagation Laboratory, Boulder, CO), and R. O. RAMSEIER (Atmospheric Environmental Service, Ice Research and Development, Ottawa, Canada) Journal of Geophysical Research (ISSN 0148-0227), vol. 90, Jan. 20, 1985, p. 1087-1099. refs

An algorithm is developed which uses two microwave radiometer channels to estimate quantitative fractions of first-year and multiyear sea ice types. The algorithm is applied to data obtained from satellite sensors, and the data trends are used to refine values of the emissivities. The algorithm was tested, and results were in reasonable agreement with visual observations, where mixtures of first-year sea ice and multiyear sea ice were known to coexist. However, on a synoptic basis the satellite estimates differ from visual and radar means of classifying ice that has survived at least one melt season (old ice). A possible explanation for the discrepancy is that the emissivity of sea ice changes over time periods longer than one melt season. Author

A85-21145* Texas Univ., Austin

NEOTECTONICS OF THE CARIBBEAN

P. MANN (Texas, University, Austin, TX) and K. BURKE (Lunar and Planetary Institute; Houston, University, Houston, TX) Reviews of Geophysics and Space Physics (ISSN 0034-6853), vol. 22, Nov 1984, p. 309-362. refs
(Contract NAG5-155, NASW-3389)

Burke et al. (1980) have considered geologic and seismic data from Jamaica, while Mann et al. (1984) have examined data from Hispaniola. The present investigation is concerned with the neotectonics of the entire Caribbean region, taking into account the recent results in the northeastern Caribbean and a more comprehensive compilation of seismicity and neotectonic structures from other areas than has been available to most previous authors. It is hoped that this study will complement seismic network results in helping to pinpoint areas of seismic hazard. It is also intended to provide a framework for high-precision geodetic surveys of Caribbean plate motion using measurements from satellites and astronomical observations. G.R.

A85-21669

INVESTIGATION OF KRASNOVODSK BAY ON THE BASIS OF SPACE PHOTOGRAPHS [OPYT ISSLEDOVANIYA AKVATORII KRASNOVODSKOGO ZALIVA S ISPOL'ZOVANIEM KOSMICHESKIKH FOTONIMKOV]
V. A. MUSATOV and E. M. KISELEV Geodeziya i Kartografiya (ISSN 0016-7126), Oct. 1984, p. 40-44. In Russian.

A85-21960

ADVANCES IN MICROWAVE REMOTE SENSING OF THE OCEAN AND ATMOSPHERE
P. C. PANDEY and T. A. HARIHARAN (Indian Space Research Organization, Space Applications Centre, Ahmedabad, India) Indian Academy of Sciences, Proceedings (Earth and Planetary Sciences) (ISSN 0370-0089), vol. 93, Aug. 1984, p. 257-282. refs

This article reviews the current state-of-the-art and future prospects of the microwave techniques for remote sensing of the earth's atmosphere and ocean. Geophysical parameters and their relationship with measured thermal microwave radiation is established through radiative transfer processes. The atmospheric temperature profile obtained from microwave sounding unit (MSU) onboard TIROS-N series of satellites is operational and is used for numerical weather prediction. The demonstrated applications of scanning multichannel microwave radiometer (SMMR) onboard most recent and advanced Seasat satellite are highlighted. The capability of Seasat active sensors for monitoring ocean parameters have also been indicated. Feasible applications of microwave techniques e.g., moisture profile with advanced moisture sounder (AMSU), and surface pressure from multifrequency active microwave pressure sounder (MPS) are also described. Finally, the recent and advanced microwave limb sounding (MLS) technique and its applications to upper atmospheric research has been reviewed. Author

A85-22171*# National Aeronautics and Space Administration, Goddard Space Flight Center, Greenbelt, Md
THE HARP PROBE - AN IN SITU BRAGG SCATTERING SENSOR

E. MOLLO-CHRISTENSEN, N. E. HUANG, S. R. LONG (NASA, Goddard Space Flight Center, Greenbelt, MD), and L. F. BLIVEN (Oceanic Hydrodynamics, Inc., Salisbury, MD) Journal of Atmospheric and Oceanic Technology (ISSN 0739-0572), vol. 1, Dec. 1984, p. 358-371. refs

A wave sensor, consisting of parallel, evenly spaced capacitance wires, whose output is the sum of the water surface deflections at the wires, has been built and tested in a wave tank. The probe output simulates Bragg scattering of electromagnetic waves from a water surface with waves; it can be used to simulate electromagnetic probing of the sea surface by radar. The study establishes that the wave probe, called the 'Harp' for short, will simulate Bragg scattering and that it can also be used to study nonlinear wave processes. Author

A85-22175

EVALUATION OF THE OCEAN/ATMOSPHERE THERMAL INTERACTION IN THE ATLANTIC FGGE AREA [OTSENKA TEPLOVOGO VZAIMODEISTVIA OKEANA I ATMOSFERY NA ATLANTICHESKOM POLIGONE PGEP]

V. V. BELEVICH (Gosudarstvennyi Okeanograficheskii Institut, Odessa, Ukrainian SSR) Meteorologiya i Gidrologiya (ISSN 0130-2906), Dec. 1984, p. 102-107. In Russian. refs

External thermal equilibrium and its components are analyzed using over 9000 hourly meteorological observations and 240 cloud images transmitted from Meteor-2-series satellites. The thermal interaction characteristics included the ocean surface thermal balance and the enthalpy of the upper 50 m of the ocean. Using GATE and FGGE data, seasonal and annual variations of thermal interaction parameters are examined with respect to the intratropical convergence zone (ITCZ) location. It is noted that the ITCZ axis shifted along 29 degrees W from 2-3 degrees S for winter observation and from 7-8 degrees S for summer observations. L.T

A85-22423

SEPARATING CLOUDS FROM OCEAN IN INFRARED IMAGES
K. A. KELLY (Woods Hole Oceanographic Institution, Woods Hole, MA, California, University, La Jolla, CA) Remote Sensing of Environment (ISSN 0034-4257), vol. 17, Feb. 1985, p. 67-83. NSF-sponsored research. refs
(Contract N00014-75-C-0300)

A nearly automatic sorting procedure for infrared images of the ocean surface is described. Three basic techniques are used in the sorting procedure: a threshold test, a comparison of two infrared channels of the same image, and a uniformity test on a subset of the image. The effectiveness and limitations of each technique are discussed. The sorting procedure consists of two algorithms which do not rely on a visible channel and thus sort both daytime and nighttime images. An application example is given. The characteristics of signals emitted by nonocean surfaces and methods for detecting clouds are also discussed. C.D.

A85-23644

AIRBORNE MICROWAVE MEASUREMENTS OF THE SOUTHERN GREENLAND ICE SHEET

C. T. SWIFT, P. S. HAYES, J. S. HERD (Massachusetts, University, Amherst, MA), W. L. JONES (Satellite Television Corp., Princeton, NJ), and V. E. DELNORE (Kertron International, Hampton, VA) Journal of Geophysical Research (ISSN 0148-0227), vol. 90, Feb. 10, 1985, p. 1983-1994. refs

Microwave remote sensing measurements were collected over Greenland with the NASA C-130 aircraft used as a platform. The principal instruments were a C band radiometer and an X band scatterometer, which simultaneously collected both active and passive microwave remote sensing data. The results indicate that subsurface inhomogeneities control the scattering and emission process, including anisotropic effects. The results strongly suggest that microwave remote sensing techniques can provide a relative measure of the density and orientation of the volume scatters. Author

A85-23676

SATELLITE MICROWAVE REMOTE SENSING

T. D. ALLAN, ED (Institute of Oceanographic Sciences, Wormley, Surrey, England) Chichester, West Sussex, England, Ellis Horwood, Ltd., 1983, 523 p. For individual items see A85-23677 to A85-23707.

A comprehensive review of the performance of SEASAT, the first satellite to carry a suite of microwave remote sensors dedicated to a study of the sea surface, is presented. SEASAT's four microwave sensors - the radar altimeter, synthetic aperture radar (SAR), wind scatterometer, and scanning multifrequency radiometer, are treated. The results of comparisons made between the wind and wave fields measured by surface ship and buoy during JASIN (a multiship air-sea interaction experiment in the Northeast Atlantic) and by satellite sensors are described. The output of the altimeter over the North Sea is compared with models of the area. A physical treatment of SAR imagery of ocean waves is presented along with more mathematical analyses. A preview is given of Europe's first microwave remote sensing satellite due for launch in 1979/88. C.D.

A85-23677

A REVIEW OF SEASAT

T. D. ALLAN (Institute of Oceanographic Sciences, Wormley, Sussex, England) IN: Satellite microwave remote sensing. Chichester, West Sussex, England, Ellis Horwood, Ltd., 1983, p. 15-44. refs

The performance of SEASAT sensors is reviewed. The physical principles underlying the different sensor operations are described, including the data processing. Sample scenes are shown and discussed. The sensors reviewed include the radar altimeter, the Synthetic Aperture Radar (SAR), the wind scatterometer, and the Scanning Multichannel Microwave Radiometer. The SAR is emphasized, covering the imaging of ocean waves, Fourier transforms of SAR wave imagery, and SAR imagery of internal waves, slicks, and streaks. The results of comparing wind and

wave fields from SEASAT sensors and JASIN ships are summarized. C.D.

A85-23681

VALIDATION AND APPLICATIONS OF SASS OVER JASIN

T. H. GUYMER (Institute of Oceanographic Sciences, Godalming, Surrey, England) IN: Satellite microwave remote sensing Chichester, West Sussex, England, Ellis Horwood, Ltd., 1983, p. 87-104 refs

The results of a comparison of SEASAT and JASIN measurements of near-surface winds are described. The probable causes of an anomaly are discussed, and some examples of the usage of such data in the Northeast Atlantic are presented. It is concluded that the accuracy of the SEASAT scatterometer winds is at least as great as that obtained with conventional surface-based instrumentation, with much superior spatial sampling. The anomaly in question indicates that care is needed in interpreting SASS data when close to heavy rain cells. The value of the SASS in interpreting SAR images is demonstrated. C.D.

A85-23682

IMAGING OCEAN SURFACE WAVES BY SYNTHETIC APERTURE RADAR - A REVIEW

W. ALPERS (Hamburg, Universitaet; Max-Planck-Institut fuer Meteorologie, Hamburg, West Germany) IN: Satellite microwave remote sensing Chichester, West Sussex, England, Ellis Horwood, Ltd., 1983, p. 107-119 refs

The effect on SAR performance of motion of the ocean surface is discussed. Basic concepts of the SAR ocean wave imaging mechanism as based on the two-scale scattering and hydrodynamic model are reviewed. A brief description is given of the cross-section modulation due to hydrodynamic and electromagnetic interaction. The effect of target motion on SAR imaging is analyzed and the results are applied to ocean surface wave imaging. C.D.

A85-23683

CAN OPTICAL MEASUREMENTS HELP IN THE INTERPRETATION OF RADAR BACKSCATTER?

M. S. LONGUET-HIGGINS (Cambridge University, Cambridge; Institute of Oceanographic Sciences, Wormley, Surrey, England) IN: Satellite microwave remote sensing Chichester, West Sussex, England, Ellis Horwood, Ltd., 1983, p. 121-127

The possibility of deriving information from remote observations at optical wavelengths about the 'long-wave short-wave interaction' phenomenon in the backscatter of electromagnetic radiation from the sea surface in the X and L bands. A two-scale model of this effect, in which the backscatter depends on the spectral density of sea surface waves at wavelengths of a few centimeters and on how the intensity of these waves is related locally to the longer waves that are present, is summarized and compared with observation. It is concluded that the theory does give results in quantitative agreement with observation. C.D.

A85-23685

THE EFFECT OF A MOVING SEA SURFACE ON SAR IMAGERY

M. J. TUCKER (Institute of Oceanographic Sciences, Taunton, Somerset, England) IN: Satellite microwave remote sensing Chichester, West Sussex, England, Ellis Horwood, Ltd., 1983, p. 147-154.

The interaction of the moving sea surface with the aperture synthesis process, which allows the one wave-imaging mechanism which operates only with an SAR, is discussed. Basic concepts, including Bragg resonance with or without long waves present, the primary scene element, azimuthal offsets due to range velocities, and the linearity of the aperture synthesis process, are first summarized. The effect of sea surface velocities on wave imaging is described for two extreme cases for which analytic solutions are available, a long low swell travelling azimuthally and a short-wavelength sea with no swell. C.D.

A85-23686

THEORY OF SAR OCEAN WAVE IMAGING

S. ROTHERAM (General Electric Co., PLC, Chelmsford, Essex, England) IN: Satellite microwave remote sensing Chichester, West Sussex, England, Ellis Horwood, Ltd., 1983, p. 155-186. ESA-supported research

The relation between waves on the sea surface and features in SAR images is discussed. The foundations of the relevant theory are presented, describing sea surface representations and electromagnetic scattering theory. Analytical results on the problem of explaining SAR images of a given sea surface are given for both linear and nonlinear imaging. Linear inverse theory, a tentative theory which ignores speckle, noise, and nonlinearity, is also discussed. Alternative ways for constructing SAR images, including phase, autocorrelation function, and refocused images, are pointed out. A case study of a SEASAT SAR image whose spectrum shows both harmonics and banding is presented. The linear inverse theory is applied to the image in a reconstruction of the sea surface. C.D.

A85-23688

EFFECT OF DEFOCUSING ON THE IMAGES OF OCEAN WAVES

K. OUCHI (Imperial College of Science and Technology, London, England) IN: Satellite microwave remote sensing Chichester, West Sussex, England, Ellis Horwood, Ltd., 1983, p. 209-222. refs

The effect of defocusing on the images of ocean waves propagating in an arbitrary direction are examined, taking into account the spatial and temporal dependence of small-scale and large-scale ocean waves. Expressions for the local mean intensity and contrast of the images of ocean waves propagating in an arbitrary direction are derived and discussed. It is shown that if the reference signal of the SAR processor is matched to a stationary point target, the images of waves are always defocused, irrespective of their propagation direction. The images can be enhanced by applying a defocused reference signal, and the amount of defocus depends on the phase velocity and propagation direction of ocean waves. C.D.

A85-23690

THE USE OF SEASAT-SAR DATA IN OCEANOGRAPHY AT THE IFF

A. WADSWORTH, C. ROBERTSON, and D. DESTAERKE (Institut Francais de Petrole, Rueil Malmaison, Hauts-de-Seine, France) IN: Satellite microwave remote sensing Chichester, West Sussex, England, Ellis Horwood, Ltd., 1983, p. 235-245. refs

Results from a variety of SEASAT studies are briefly reviewed. Investigations involving the measurement of sea state, current detection, imaging of sea bottom features, study of internal waves, and monitoring of hydrocarbon pollution are considered. C.D.

A85-23691

EXPRESSIONS OF BATHYMETRY ON SEASAT SYNTHETIC RADAR IMAGES

D. W. S. LODGE (Royal Aircraft Establishment, Space and New Concepts Dept., Farnborough, Hants., England) IN: Satellite microwave remote sensing Chichester, West Sussex, England, Ellis Horwood, Ltd., 1983, p. 247-260.

A correlation between the state of the ocean surface (fraction of a millimeter depth) and deep-water tidal processes is examined on the basis of Seasat SAR data. Radar images of regions around the Fair Isle and nearby Foulda, and Straits of Dover and Thames Estuary Approaches are analyzed with respect to diffraction and refraction of the gravity waves for depths up to 1000 m. It is noted that, in deep water, internal waves propagating from discontinuities on the sea bed appear as detectable surface modulations; in shallow water with depths less than about 50 m, the tidal flow over the undulations of the sea bed can also modulate the surface roughness in a way detectable by radar. L.T.

A85-23692

TIDAL CURRENT BEDFORMS INVESTIGATED BY SEASAT

N. H. KENYON (Institute of Oceanographic Sciences, Wormley, Surrey, England) IN: Satellite microwave remote sensing. Chichester, West Sussex, England, Ellis Horwood, Ltd., 1983, p. 261-270. refs

Seasat SAR seafloor images, specifically those of the Bristol Channel (UK) and the Southern Bight of the North Sea, are analyzed in order to assess the possibility of using SAR to study sedimentary processes and geological modeling techniques. The discovery of the current-parallel streaks, made possible by SAR data, is noted to be of significance in explaining the formation of longitudinal bedforms and in measuring current orientation. The SAR is also suggested to offer greater accuracy in measuring bedform trends than shipborne acoustic methods, thus allowing the effects of Coriolis force on bedform trends to be investigated more effectively. L.T.

A85-23695

ALTIMETER MEASUREMENTS OF OCEAN TOPOGRAPHY

D. E. CARTWRIGHT and G. A. ALCOCK (Institute of Oceanographic Sciences, Bidston, Birkenhead, England) IN: Satellite microwave remote sensing. Chichester, West Sussex, England, Ellis Horwood, Ltd., 1983, p. 309-319. refs

Recent progress in satellite altimeter measurement of the topographical features of the world oceans is considered. Attention is given to the increased precision of distance measurements from the Seasat altimeter relative to Skylab and GEOS-3 measurements. Preliminary Seasat data for the removal of tides in the North Sea and for variations in semidiurnal tides in the central North Atlantic Ocean are analyzed, and the results are discussed in detail. A series of contour maps of the ocean regions is provided. I.H.

A85-23696

A SURVEY OF SOME RECENT SCIENTIFIC RESULTS FROM THE SEASAT ALTIMETER

J. R. APEL (Johns Hopkins University, Laurel, MD) IN: Satellite microwave remote sensing. Chichester, West Sussex, England, Ellis Horwood, Ltd., 1983, p. 321-335. refs

It is pointed out that the radar altimeter on Seasat was a remarkable instrument in many ways, yielding a variety of information on geophysical phenomena such as sea surface topography, wave heights, and wind speeds. Attention is given to sea surface topography, observations of currents, wave height observations, wind speed measurements, and details regarding the three types of basic measurements performed with the altimeter. For the basic types of measurements, much ancillary information as well as highly sophisticated mathematical algorithms are needed in order to arrive at the geophysical quantities of interest. G.R.

A85-23699

GRAVITY FIELD INVESTIGATION IN THE NORTH SEA

R. RUMMEL, G. L. STRANG VAN HEES, and H. W. VERSLUIS (Delft, Technische Hogeschool, Delft, Netherlands) IN: Satellite microwave remote sensing. Chichester, West Sussex, England, Ellis Horwood, Ltd., 1983, p. 389-402. refs

The gravity field of the North Sea region is characterized on the basis of shipborne gravimetry and 10-cm-precision Seasat altimeter measurements. The geophysical situation in the region (accumulated sediments, fault-bounded troughs or grabens, and vestiges of previous orogenic activity) is surveyed; the data are presented graphically, the reduction and analysis procedures are discussed; and the resulting free-air-gravimetric-anomaly and sea-surface-height maps are shown to be qualitatively correlated with the main geological features of the area. T.K.

A85-23701

WAVE MEASUREMENTS WITH THE SEASAT RADAR ALTIMETER - A REVIEW

D. J. WEBB (Institute of Oceanographic Sciences, Wormley, Surrey, England) IN: Satellite microwave remote sensing. Chichester, West Sussex, England, Ellis Horwood, Ltd., 1983, p. 419-424. refs

MacArthur (1976, 1978) has described the design and the operation of the radar altimeter used by the Seasat satellite, while Hancock et al. (1980) have discussed the algorithms employed for processing the data. It is pointed out that the accurate measurement of distance and wave-height using a radar altimeter, depends on the use of a very short radar pulse. The pulse must be powerful enough to make its detection possible. For Seasat the required combination of power and resolution was obtained by using a long (3.2 microseconds) swept-frequency pulse. The returned signal was correlated with a replica of the transmitted signal, and Fourier transformed to give the effective returned pulse from a transmitted pulse of only 3.2 ns duration. Attention is given to calibration tests, research studies, and future ideas regarding directional spectra and wave climate. G.R.

A85-23702

SWELL PROPAGATION IN THE NORTH ATLANTIC OCEAN USING SEASAT ALTIMETER

N. M. MOGNARD (Centre National d'Etudes Spatiales, Groupe de Recherches de Geodesie Spatiale, Toulouse, France) IN: Satellite microwave remote sensing. Chichester, West Sussex, England, Ellis Horwood, Ltd., 1983, p. 425-437. refs

A method to compute minimum swell heights from the SEASAT altimeter measurements is presented and applied to compute a global mean swell map for three months of SEASAT lifetime. This map is the first picture of a mean swell field over the world ocean ever obtained. Swell propagation patterns in the North Atlantic ocean are analyzed for September-October 1978, when the ocean was starting to be influenced by deep atmospheric depressions originating in the Arctic regions. C.D.

A85-23703

USE OF OCEAN SKEWNESS MEASUREMENTS IN CALCULATING THE ACCURACY OF ALTIMETER HEIGHT MEASUREMENTS

G. WHITE (Royal Aircraft Establishment, Space Dept., Farnborough, Hants, England) IN: Satellite microwave remote sensing. Chichester, West Sussex, England, Ellis Horwood, Ltd., 1983, p. 439-449. refs

A85-23704

SPATIAL VARIATION OF SIGNIFICANT WAVE-HEIGHT

P. G. CHALLENGER (Institute of Oceanographic Sciences, Wormley, Surrey, England) IN: Satellite microwave remote sensing. Chichester, West Sussex, England, Ellis Horwood, Ltd., 1983, p. 451-460. refs

The variation of significant wave height (H_s) in space has so far not received any attention, and a number of questions arise regarding such a variation. The altimeter data from the Seasat satellite give a suitable database for initiating study concerned with providing answers to these questions. To remove temporal variation, measurements are needed which were made at the same location at different times. For obtaining insight into spatial variability per se, it is best to consider a track in the open ocean. Such a track has been selected, taking into account significant wave-height along eight passes. There was considerable variation in the values from pass to pass. The significance of the obtained data is evaluated, giving attention to small-scale variation, large-scale variation, and a comparison of satellite data with data provided by OWS Lima, which is fitted with a Shipborne Wave Recorder. The mean significant wave-height along a track of 2100 km appears to be constant. The need for more data is pointed out. G.R.

A85-23706**THE EVALUATION OF SMMR RETRIEVAL ALGORITHMS**

C. R. FRANCIS, D. P. THOMAS, and E. P. L. WINDSOR (British Aerospace, PLC, Dynamics Group, Bristol, England) IN: Satellite microwave remote sensing. Chichester, West Sussex, England, Ellis Horwood, Ltd., 1983, p. 481-498. Research supported by the Department of Industry. refs

The present investigation is concerned with the development of a retrieval algorithm for sea surface parameters in the case of data provided by the Scanning Multichannel Microwave Radiometer (SMMR) on the satellite Nimbus-7. Attention is given to the development of an iterative algorithm, as an alternative to the linear approach adopted for the routine production of geophysical data. An evaluation of the natural microwave emissions from the ocean and atmosphere requires information regarding the geophysical parameters which influence the emissions. A model of the radiative transfer processes which estimates the observed microwave spectrum resulting from a given set of geophysical parameters has been generated. The environmental model is discussed, taking into account a general description, an ocean model, and an atmospheric model. An evaluation of the iterative algorithm is also conducted. G.R.

A85-23707**STATUS AND FUTURE PLANS FOR ERS-1**

G. DUCHOSSOIS (ESA, Paris, France) IN: Satellite microwave remote sensing. Chichester, West Sussex, England, Ellis Horwood, Ltd., 1983, p. 501-514.

The current status of ERS-1, the ocean and ice remote-sensing satellite being developed by ESA for Ariane launch to a 777-km sun-synchronous circular orbit of inclination 98.1 deg in late 1987 for a 2-3-yr life, is surveyed, and plans for the multisatellite ERS program in the 1990s are discussed. ERS-1 employs the SPOT multimission platform to carry a payload which includes a C-band active microwave package (SAR, wave scatterometer, and wind scatterometer), a Ku-band radar altimeter, laser retroreflectors for ground tracking, and a probably three-channel IR along-track scanning radiometer. The data-processing system operates in high and low bit-rate modes to provide raw data, quick annotated raw and system-corrected data, quick-look data, and quick thematic products to a wide variety of users via either land lines or satellite links from the ground segment, which comprises a management and control facility at ESOC and a data-acquisition, telemetry, tracking, and command station at Kiruna. The nominal performance parameters of the platform and the payload instruments are listed in an appendix. T.K.

A85-23755**LIDAR APPLICATIONS IN REMOTE SENSING OF OCEAN PROPERTIES**

D. DIEBEL-LANGOHR, K. GUENTHER, and R. REUTER (Oldenburg, Universitaet, Oldenburg, West Germany) IN: Spectral signatures of objects in remote sensing, International Conference, 2nd, Bordeaux, France, September 12-16, 1983, Reports. Versailles, Institut National de la Recherche Agronomique, 1984, p. 71-80. refs

The physical principles governing the use of lidar devices to determine the depth, chlorophyll-a, organic matter, tracer dye, or oil concentration; and Raman scattering of a water column by remote sensing are explained, and the airborne device developed at the Universitaet Oldenburg is briefly characterized. This device comprises a high-power 308-nm excimer laser pumping an amplified dye laser tunable from 350 to 680 nm at pulse width 8 nsec, a 40-cm Cassegrain telescope, dichroic beamsplitters, narrowband interference filters, photomultiplier detectors, a transient digitizer with sampling rate 2 nsec, and a control microcomputer. A drawing and block diagram of the device and some sample data are shown, and the possibility of remote lidar sensing of water temperature profiles, sound velocity, and hydrosol compositions is considered. T.K.

A85-24076**SIMULTANEOUS RADIOMETRIC AND RADAR ALTIMETRIC MEASUREMENTS OF SEA MICROWAVE SIGNATURES**

S. P. GAGARIN, A. A. KALINKEVICH, B. G. KUTUZA (Akademii Nauk SSSR, Institut Radiotekhniki i Elektroniki, Moscow, USSR), A. I. BASKAKOV, and V. A. TEREKHOV (Moskovskii Energeticheskii Institut, Moscow, USSR) IEEE Journal of Oceanic Engineering (ISSN 0364-9059), vol. OE-9, Dec. 1984, p. 325-328. refs

The advantages provided by the combined use of a polarization microwave radiometer and a short-pulse radar altimeter for sea roughness monitoring are discussed. A brief analysis of the potential of each device taken separately is carried out, which shows the advisability of their combination. The method and the results of the experiment performed with an airborne K-band radiometer and an altimeter are described. It is shown that, in regions of fully developed roughness, a correlation exists between the polarization characteristics of the microwave radiation by the sea surface and the rms sea waveheight as measured by the altimeter. Correlation is not found in regions where the roughness is not developed. Therefore, the combination of the two instruments makes it possible to sense the regions of fully developed sea roughness. Author

A85-24077**RADIOPHYSICAL TECHNIQUES EMPLOYED FOR SEA ICE INVESTIGATIONS**

A. A. KURSKAIA and B. G. KUTUZA (Akademii Nauk SSSR, Institut Radiotekhniki i Elektroniki, Moscow, USSR) IEEE Journal of Oceanic Engineering (ISSN 0364-9059), vol. OE-9, Dec. 1984, p. 329-332. refs

Experimental data on emissivity and backscattering properties of sea ice are presented. Measurements were conducted in east and west Soviet regions of the Arctic Ocean during recent years with the IL-18 airborne laboratory and the AN-2 aircraft. The equipment installed on board the aircraft provided simultaneous X-band side looking airborne radar (SLAR) images and radiometric data at wavelengths from 0.8 to 30 cm along the flight paths. Use of these measurements for sea ice studies is discussed. Author

A85-24078**POLARIZATION EFFECTS IN SEA-ICE SIGNATURES**

C. MAETZLER (Bern, Universitaet, Bern, Switzerland), R. O. RAMSEIER (Department of the Environment, Atmospheric Environment Service, Ottawa, Canada), and E. SVENDSEN (Bergen, Universitet, Bergen, Norway) IEEE Journal of Oceanic Engineering (ISSN 0364-9059), vol. OE-9, Dec. 1984, p. 333-338. refs

Observations of microwave emissivities of multiyear sea ice showed anomalies at horizontal polarization in the frequency range from 5 to 35 GHz during the Norwegian Remote Sensing Experiment (NORSEX) in September and October 1979. The effect can be explained by layers of solid ice present in the dry snow cover throughout the NORSEX area. A special experiment made on a typical multiyear floe confirms this explanation. Since the results also indicate that at 94 GHz the layers do not affect the radiation, a dual-polarized radiometer in the 90-GHz window is a promising sea-ice sensor. Author

A85-24079**MICROWAVE SIGNATURES OF THE SEA ICE IN THE EAST GREENLAND CURRENT**

N. SKOU and L. T. PEDERSEN (Danmarks Tekniske Højskole, Lyngby, Denmark) IEEE Journal of Oceanic Engineering (ISSN 0364-9059), vol. OE-9, Dec. 1984, p. 339-343. refs

Airborne microwave radiometer measurements at 5, 17, and 34 GHz have been carried out over the East Greenland Current. Sea ice signatures have been established for some of the basic ice types like first-year ice and multiyear ice. Other signatures have been experienced like that of presumably very old arctic ice and signatures associated more with the snow cover on the ice than with the ice itself. During MIZEX-83 measurements of total ice concentration were carried out. Author

A85-24080

INTERPRETATION OF AIRCRAFT SEA ICE MICROWAVE DATA

V. V. BOGORODSKII and A. N. DAROVSKIKH (Glavnoe Upravlenie Gidrometeorologicheskoi Sluzhby SSSR, Arkticheskii i Antarkticheskii Nauchno-Issledovatel'skii Institut, Leningrad, USSR) IEEE Journal of Oceanic Engineering (ISSN 0364-9059), vol. OE-9, Dec. 1984, p. 344-346.

This paper deals with the Bayesian classifier and its application for a radiometric discrimination of sea ice types. Microwave data used for these studies have been acquired from a dual-frequency passive nadir-looking radiometer which records radiation from earth at wavelengths of 1.6 and 3.2 cm. In addition, a photographic system and IR radiometer operating at 8-14 microns were used in aircraft experiments. Empirical brightness temperature probability distributions for water surface and several ice types for spring (March-April) and autumn (September-October) are given. It is shown that, in order to improve a radiometric discrimination and at the same time to maintain the spatial resolution, it is necessary to use nonlinear low-frequency filtering. Author

A85-24083

THE EFFECT OF A SNOW COVER ON MICROWAVE BACKSCATTER FROM SEA ICE

Y.-S. KIM, R. G. ONSTOTT, and R. K. MOORE (University of Kansas Center for Research, Inc., Lawrence, KS) IEEE Journal of Oceanic Engineering (ISSN 0364-9059), vol. OE-9, Dec. 1984, p. 383-388. refs

The present investigation of the effect of snow cover on sea ice takes into account both the backscattering contribution and the temperature effect of the snow cover. The backscattering coefficient of the snow-covered sea ice was calculated. In the calculation, empirical equations derived by Ulaby et al (1982) were used to describe the effect of snow cover on natural surfaces. The net effect of dry snow cover on smooth first-year ice is found to be severe, while that on multiyear ice is found to be smaller. The higher temperature at the upper surface of sea ice due to the presence of an insulating layer of snow was found to cause a minor effect on the backscattering coefficient, at least for air temperature below about -20 C. G.R

A85-24524* National Aeronautics and Space Administration, Washington, D. C.

ICE SHEET MARGINS AND ICE SHELVES

R. H. THOMAS (NASA, Washington, DC; California Institute of Technology, Jet Propulsion Laboratory, Pasadena, CA) IN: Climate processes and climate sensitivity. Volume 5. Washington, DC, American Geophysical Union (Geophysical Monograph, No. 29), 1984, p. 265-274. refs

The effect of climate warming on the size of ice sheet margins in polar regions is considered. Particular attention is given to the possibility of a rapid response to warming on the order of tens to hundreds of years. It is found that the early response of the polar regions to climate warming would be an increase in the area of summer melt on the ice sheets and ice shelves. For sufficiently large warming (5-10C) the delayed effects would include the breakup of the ice shelves by an increase in ice drainage rates, particularly from the ice sheets. On the basis of published data for periodic changes in the thickness and melting rates of the marine ice sheets and fjord glaciers in Greenland and Antarctica, it is shown that the rate of retreat (or advance) of an ice sheet is primarily determined by bedrock topography; the basal conditions of the grounded ice sheet, and the ice shelf condition downstream of the grounding line. A program of satellite and ground measurements to monitor the state of ice sheet equilibrium is recommended. I.H.

A85-24551

LARGE-SCALE OCEANOGRAPHIC EXPERIMENTS AND SATELLITES; PROCEEDINGS OF THE ADVANCED RESEARCH WORKSHOP, PORTO VECCHIO, CORSE, FRANCE, OCTOBER 3-7, 1983

C. GAUTIER, ED. (California, University, La Jolla, CA) and M. FIEUX, ED. (Museum National d'Histoire Naturelle, Paris, France) Workshop supported by NATO and University of California. Dordrecht, D. Reidel Publishing Co. (NATO ASI Series, No. C128), 1984, 297 p. For individual items see A85-24552 to A85-24560.

A collection of papers on large-scale oceanographic experiments, altimetry, satellite sea surface temperature studies, satellite wind and stress studies, and satellite surface heat flux investigations is presented. Individual topics addressed include: sampling strategy for altimeter measurements of the global statistics of mesoscale eddies, eddy kinetic energy distribution in the southern ocean from SEASAT altimeter and drifting buoys, and satellite measurements of sea surface temperature for climate research. Also discussed are: satellite sea surface temperature determination from microwave and infrared radiometry, scatterometer versus surface measurements of wind speed and stress over the ocean, summary of wind data available from satellites, large-scale surface heat fluxes, and earth radiation budget observations. C.D.

A85-24553

A SAMPLING STRATEGY FOR ALTIMETER MEASUREMENTS OF THE GLOBAL STATISTICS OF MESOSCALE EDDIES

F. P. BRETHERTON (National Center for Atmospheric Research, Boulder, CO) IN: Large-scale oceanographic experiments and satellites; Proceedings of the Advanced Research Workshop, Porto Vecchio, Corse, France, October 3-7, 1983. Dordrecht, D. Reidel Publishing Co., 1984, p. 27-40. refs

The value and feasibility of using satellite altimetry to estimate mesoscale eddy statistics are discussed. The choice and treatment of spectral ranges and the treatment of spectra are briefly considered, and the signals to be expected in the altimetry are described. The analytical procedures to be applied to the data are briefly discussed, and sources of error are considered in some detail, including corrections for vertically integrated electron density in the ionosphere, for tropospheric water vapor, for sea-state bias, for residual geoid, and for sample size. It is concluded that repeat tracks to an accuracy of 10 km every 3-5 days are needed for an observing period of at least six months, with simultaneous measurement of the sea state. Recommendations are made as to development of analytical procedures, ancillary measurements, orbit tradeoffs, in situ observations, and data management. C.D.

A85-24554

EDDY KINETIC ENERGY DISTRIBUTION IN THE SOUTHERN OCEAN FROM SEASAT ALTIMETER AND FGGE DRIFTING BUOYS

N. DANIAULT (Centre National pour l'Exploitation des Oceans, Centre Oceanologique de Bretagne, Brest, France), Y. MENARD (Centre National d'Etudes Spatiales, Groupe de Recherches de Geodesie Spatiale, Toulouse, France), and J. GONELLA (Museum National d'Histoire Naturelle, Paris, France) IN: Large-scale oceanographic experiments and satellites; Proceedings of the Advanced Research Workshop, Porto Vecchio, Corse, France, October 3-7, 1983. Dordrecht, D. Reidel Publishing Co., 1984, p. 41-56. refs

A85-24555

SATELLITE MEASUREMENTS OF SEA-SURFACE TEMPERATURE FOR CLIMATE RESEARCH

P. J. MINNETT, A. M. ZAVODY, and D. T. LLEWELLYN-JONES (Science and Engineering Research Council, Rutherford Appleton Laboratory, Didcot, Oxon, England) IN: Large-scale oceanographic experiments and satellites; Proceedings of the Advanced Research Workshop, Porto Vecchio, Corse, France, October 3-7, 1983. Dordrecht, D. Reidel Publishing Co., 1984, p. 57-85. refs

Factors determining the accuracy with which the sea surface temperature can be measured from space using infrared

radiometers are discussed. These include the clear atmosphere radiative effects, contamination of the signal by clouds in the field of view, and sun glitter at the 3.7 micron 'atmospheric window'. The effects of near-surface vertical temperature gradients caused by surface heat loss (the skin effect) and by solar heating (the diurnal thermocline) are also discussed. A review of present measurement capabilities is made and a brief description is given of the Along Track Scanning Radiometer (ATSR), which will fly on the European satellite ERS-1 to provide accurate measurements of sea surface temperature using a multiangle, multichannel technique to overcome the effects of the clear atmosphere

Author

A85-24556

SATELLITE SEA SURFACE TEMPERATURE DETERMINATION FROM MICROWAVE AND INFRARED RADIOMETRY

R. L. BERNSTEIN (California, University, La Jolla, CA) IN: Large-scale oceanographic experiments and satellites; Proceedings of the Advanced Research Workshop, Porto Vecchio, Corse, France, October 3-7, 1983. Dordrecht, D. Reidel Publishing Co., 1984, p. 87-98. refs

Recent progress in the radiometric determination of sea surface temperature from satellite-based instruments is reviewed. Infrared and microwave measurement results are described and their ability to dramatically improve knowledge of the sea surface temperature relative to shipboard techniques is demonstrated using results for the eastern tropical Pacific. Some speculations extrapolating recent trends five to ten years into the future are made. C.D.

A85-24557

WIND SPEED AND STRESS OVER THE OCEAN - SCATTEROMETER VERSUS SURFACE MEASUREMENTS

W. G. LARGE (National Center for Atmospheric Research, Boulder, CO) IN: Large-scale oceanographic experiments and satellites; Proceedings of the Advanced Research Workshop, Porto Vecchio, Corse, France, October 3-7, 1983. Dordrecht, D. Reidel Publishing Co., 1984, p. 117-124. refs

The study of scatterometer winds is briefly addressed. The status of microwave scatterometry is summarized indicating the important issues now facing scatterometer investigations. Empirical algorithms used in this field are briefly described, and two surface measurement programs designed to advance scatterometry by addressing the important issues in the field are outlined. C.D.

A85-24558

A SUMMARY OF THE WIND DATA AVAILABLE FROM SATELLITES FROM THE PAST HISTORY TO FUTURE SENSORS

D. WYLIE and B. HINTON (Wisconsin, University, Madison, WI) IN: Large-scale oceanographic experiments and satellites; Proceedings of the Advanced Research Workshop, Porto Vecchio, Corse, France, October 3-7, 1983. Dordrecht, D. Reidel Publishing Co., 1984, p. 125-146. refs

The relative advantages and disadvantages of the five different types of satellite wind sensing methods are discussed, and the prospects for wind information on future satellites are outlined. The five methods are: cloud motion measurements, sun glitter reflection from the sea surface, measurements of thermally emitted microwaves from the ocean surface, reflection of radar pulses off the surface from an altimeter, and radar reflections from a multidirectional scatterometer. Past and current usages of these methods are summarized and their sampling characteristics and accuracy are discussed. C.D.

A85-24739* General Software Corp., Landover, Md.

THE DIURNAL VARIATION OF ATLANTIC OCEAN TROPICAL CYCLONE CLOUD DISTRIBUTION INFERRED FROM GEOSTATIONARY SATELLITE INFRARED MEASUREMENTS

J. STERANKA (General Software Corp., Landover, MD), E. B. RODGERS (NASA, Goddard Space Flight Center, Laboratory for Atmospheric Sciences, Greenbelt, MD), and R. C. GENTRY (Clemson University, Clemson, SC) Monthly Weather Review (ISSN 0027-0644), vol. 112, Nov. 1984, p. 2338-2344. NASA-supported research. refs

A85-24945* Georgia Inst. of Tech., Atlanta.

PERFORMANCE OF AN AIRBORNE IMAGING 92/183 GHZ RADIOMETER DURING THE BERING SEA MARGINAL ICE ZONE EXPERIMENT (MIZEX-WEST)

J. A. GAGLIANO, J. J. MCSHEEHY (Georgia Institute of Technology, Atlanta, GA), and D. J. CAVALIERI (NASA, Goddard Space Flight Center, Greenbelt, MD) IN: Millimeter wave technology II, Proceedings of the Meeting, San Diego, CA, August 23, 24, 1983. Bellingham, WA, SPIE - The International Society for Optical Engineering, 1983, p. 164-170. refs (Contract NAS5-27385)

An airborne imaging 92/183 GHz radiometer was recently flown onboard NASA's Convair 990 research aircraft during the February 1983 Bering Sea Marginal Ice Zone Experiment (MIZEX-WEST). The 92 GHz portion of the radiometer was used to gather ice signature data and to generate real-time millimeter wave images of the marginal ice zone. Dry atmospheric conditions in the Arctic resulted in good surface ice signature data for the 183 GHz double sideband (DSB) channel situated + or - 8.75 GHz away from the water vapor absorption line. The radiometer's beam scanner imaged the marginal ice zone over a + or - 45 degrees swath angle about the aircraft nadir position. The aircraft altitude was 30,000 feet (9.2 km) maximum and 3,000 feet (0.92 km) minimum during the various data runs. Calculations of the minimum detectable target (ice) size for the radiometer as a function of aircraft altitude were performed. In addition, the change in the atmospheric attenuation at 92 GHz under varying weather conditions was incorporated into the target size calculations. A radiometric image of surface ice at 92 GHz in the marginal ice zone is included. Author

A85-25351* National Aeronautics and Space Administration, Wallops Flight Center, Wallops Island, Va.

THE USE OF AIRBORNE LASERS IN TERRESTRIAL AND WATER ENVIRONMENTS

W. B. KRABILL (NASA, Wallops Flight Center, Wallops Island, VA), L. E. LINK (U.S. Army, Corps of Engineers, Vicksburg, MS), and R. N. SWIFT (EG&G Washington Analytical Services Center, Inc., Pocomoke City, MD) IN: Optical engineering for cold environments, Proceedings of the Meeting, Arlington, VA, April 7, 8, 1983. Bellingham, WA, SPIE - The International Society for Optical Engineering, 1983, p. 201-207. refs

This document has the objective to provide some information regarding the applications for which an airborne laser system can be utilized. The considered data have been collected with the NASA Airborne Oceanographic Lidar (AOL), operational since 1977 as a flying laser laboratory. The most basic mode of operation of the AOL involves operation as a profiler. The data collected are similar to those which would be collected by a ground survey party. In the fluorosensing mode, pulsed laser light is used to induce fluorescence in various pigments contained in land and water targets. A capability for reliably mapping bottom geometry in clear ocean water to depths of 10-12 meters was also demonstrated, while other studies are related to the utilization of the AOL for synoptic mapping of surface layer concentrations of chlorophyll and other photopigments contained in phytoplankton. G.R.

A85-25594

ULTRASHORT-WAVE RADAR SUBSURFACE SOUNDING OF SEA ICE AND EARTH COVERS [RADIOLOKATSIONNOE PODPOVERKHNOSTNOE ZONDIROVANIE MORSKOGO L'DA I ZEMNYKH POKROVOV NA UL'TRAKOROTKIKH VOLNAKH]
M. I. FINKELSHEIN (Akademiia Nauk SSSR, Vestnik (ISSN 0002-3442), no. 9, 1984, p. 20-28. In Russian.

A85-25651

FEATURES CHARACTERIZING THE DEVELOPMENT OF MUSHROOM-SHAPED CURRENTS IN THE OCEAN, REVEALED BY AN ANALYSIS OF SATELLITE IMAGERY [NEKOTORYE ZAKONOMERNOSTI RAZVITIIA GRIBOVIDNYKH TECHENII V OKEANE, VYIAVLENNYE PUTEM ANALIZA SPUTNIKOVYKH IZOBRAZHENII]

A. I. GINZBURG and K. N. FEDOROV (Akademiia Nauk SSSR, Institut Okeanologii, Moscow, USSR) Issledovanie Zemli iz Kosmosa (ISSN 0205-9614), Nov.-Dec. 1984, p. 3-13. In Russian. refs

The appearance, development, and structure of mushroom-shaped currents (MCs) in the upper layers of the ocean are analyzed on the basis of Meteor-satellite remote-sensing data. The MCs are found to form regular tightly packed patterns in cases when several jet currents going in different directions are developing simultaneously in a limited area. Current hypotheses concerning sources of locally applied momentum generating the MCs are examined. A relationship between the appearance of the MCs and the quasi-steady anticyclonic circulation in the southwestern part of the Sea of Okhotsk is noted. Examples of MCs arising from water exchange through straits are given, and the effect of seasonal factors on the formation and visibility from space of MC structures is considered. B.J.

A85-25654

INTERPRETATION OF SPACE IMAGES OF THE SEA SURFACE USING THE SVIT DIGITAL-PROCESSING COMPLEX [DESHIFROVANIE KOSMICHESKIKH IZOBRAZHENII MORSKOI POVERKHNOSTI S ISPOL'ZOVANIEM KOMPLEKSA TSIFROVOI OBRABOTKI SVIT]

G. A. GRISHIN, I. U. P. ILIN, A. B. NELEPO, A. V. PEREVOZCHIKOV, N. I. BOLDYREV, and R. V. ILINSKII (Akademiia Nauk Ukrainsoi SSR, Morskoj Gidrofizicheskii Institut, Sevastopol, Ukrainian SSR, Akademiia Nauk SSSR, Institut Kosmicheskikh Issledovani, Moscow, USSR) Issledovanie Zemli iz Kosmosa (ISSN 0205-9614), Nov.-Dec. 1984, p. 28-35. In Russian. refs

The SVIT complex was used for the digital processing of multispectral-scanner images of the northwestern Black Sea obtained with the Meteor satellite from August 31 to September 2, 1983. Three quasi-homogeneous zones were identified on the basis of the multimodal character of histograms of the sea surface brightness distribution. Numerical calculations and hydrological data show that these zones correspond to transformed river waters with different salinities. Their summer eastward spreading from estuary fronts is shown to occur under the effect of wind-induced currents. B.J.

A85-25658

DOUBLE-ANGLE METHOD FOR MEASURING OCEAN SURFACE TEMPERATURE IN THE INFRARED [DVUKHUGLOVOI METOD IZMERENIIA TEMPERATURY POVERKHNOSTI OKEANA V INFRAKRASNOM DIAPAZONE SPEKTRA]

V. P. VLASOV and A. B. KARASEV (Moskovskii Fiziko-Tekhnicheskii Institut, Moscow, USSR) Issledovanie Zemli iz Kosmosa (ISSN 0205-9614), Nov.-Dec. 1984, p. 59-68. In Russian. refs

The feasibility of the double-angle (DA) method for the satellite remote sensing of ocean surface temperature in the infrared is demonstrated. Optimal angles of sight and optimal spectral intervals of sensitivity of the measuring instrumentation are chosen which minimize the total error of the method with allowance for the main factors of the problem (i.e., the earth surface, the atmosphere, and the instrumentation). It is shown that, compared with the double-spectral method, the DA method makes it possible to

account for the effect of the atmosphere almost fully, although in some cases the temperature-measurement error can exceed 1 K. The total error of the two-channel method under optimal conditions amounts to 0.15 K. B.J.

A85-25661

TRANSFORMATION OF SEA-WAVE SPECTRUM INTO A SYNTHETIC-APERTURE-RADAR IMAGE SPECTRUM [O PREEBRAZOVANII SPEKTRA MORSKOGO VOLNENIIA V SPEKTR IZOBRAZHENIIA RADIOLOKATORAMI S SINTEZIROVANNOI APERTUROI]

A. V. IVANOV and A. V. MOSHKOV (Akademiia Nauk SSSR, Institut Radiotekhniki i Elektroniki, Moscow, USSR) Issledovanie Zemli iz Kosmosa (ISSN 0205-9614), Nov.-Dec. 1984, p. 91-100. In Russian. refs

A85-27441

REMOTE SENSING TECHNIQUES FOR MONITORING OF POLLUTION IN COASTAL WATERS - POTENTIAL APPLICATION TO SAUDI ARABIA

A. M. ISHAQ (University of Petroleum and Minerals, Dhahran, Saudi Arabia) Arabian Journal for Science and Engineering (ISSN 0377-9211), vol. 10, Jan. 1985, p. 15-26. refs

The state of the art of remote sensing technology for the monitoring and assessment of marine pollution problems including oil spills is discussed, with an emphasis on its application to Saudi Arabia. Sources of marine pollution, including sewage sludge, industrial waste, and oil spills that occur off the Saudi coast are described and the use of remote sensing to detect them is addressed. Multispectral imagery in the visible portion of the spectrum is effective for detecting and monitoring pollutants that have light scattering and/or absorbing properties different from normal ocean constituents. A combination of optical-multispectral, microwave, and laser fluorescence remote sensing systems on aircraft offers the best potential for both qualitative and quantitative detection and monitoring of oil spills in the marine environment. C.D.

A85-27701

ABYSSAL EDDIES NEAR THE GULF STREAM

E. KELLEY and G. L. WEATHERLY (Florida State University, Tallahassee, FL) Journal of Geophysical Research (ISSN 0148-0227), vol. 90, March 20, 1985, p. 3151-3159. refs (Contract N00014-82-0404)

A comparison is made of long (8-12) months records of three near-bottom current meters with satellite-derived frontal positions of Gulf Stream meanders and rings. Energetic fluctuations with time scales 0(30-90 days) coincide with, and most probably result from, the movement of Gulf Stream meanders and rings. Author

A85-27704

VARIATIONS IN ATMOSPHERIC MIXING HEIGHT ACROSS OCEANIC THERMAL FRONTS

S. A. HSU (Louisiana State University, Baton Rouge, LA), R. FETT (U.S. Navy, Naval Environmental Prediction Research Facility, Monterey, CA), and P. E. LA VIOLETTE (U.S. Navy, Naval Ocean Research and Development Activity, Bay St. Louis, MS) Journal of Geophysical Research (ISSN 0148-0227), vol. 90, March 20, 1985, p. 3211-3224. Navy-supported research. refs

When an oceanic thermal front is under the influence of an atmospheric high-pressure system, differences in atmospheric mixing height across the front exist, mainly because of the gradient in the sea-surface temperature (SST). To study and estimate these differences, an analytical model based on a basic thermodynamic equation is devised. The model states that $\Delta H = K \Delta T$, where ΔH and ΔT are the difference in the mixing height in meters and SST in degrees Celsius across the front, respectively, and K (in m/C) is related to the entrainment coefficient, wind speed, transfer coefficient for sensible heat flux, local change of the potential temperature in the mixed layer, advection due to winds, and radiative processes due to clouds. On the basis of pertinent field experiments conducted over the Gulf Stream, in the Korea Strait, and over the Alboran Sea, the composite value

of K is found to be approximately 38 m C. The limitation of using a constant K is discussed. Author

A85-27705

STRUCTURE AND SEASONAL CHARACTERISTICS OF THE GASPÉ CURRENT

J. BENOIT (Mobil Oil Canada, Ltd., St John's, Newfoundland; Quebec, Université, Rimouski, Canada), M. I. EL-SABH (Quebec, Université, Rimouski, Canada), and C. L. TANG (Bedford Institute of Oceanography, Dartmouth, Nova Scotia, Canada) Journal of Geophysical Research (ISSN 0148-0227), vol. 90, March 20, 1985, p. 3225-3236. Research supported by the Bedford Institute of Oceanography, Natural Sciences and Engineering Research Council of Canada, and Ministère de l'Éducation du Québec. refs

It is pointed out that the Gaspé Current is a strong coastal jet flowing seaward along the coast of Gaspé Peninsula of Quebec. Its formation has been determined to be buoyancy induced, the source of the buoyancy being the river runoff from the St. Lawrence estuary. The Gaspé Current can frequently be identified in infrared satellite images as a narrow band of cold surface water running parallel to the shore. The present investigation has the objective to study the gross properties of the Gaspé Current and examine the changes in the properties from June to November. It is pointed out that the results may not represent the mean seasonal variations, since only one year's data were used. However, the data are useful for an understanding of the dynamics of buoyancy-driven boundary currents. G.R.

A85-27710*

LAGRANGIAN OBSERVATIONS OF SURFACE CIRCULATION AT THE EMPEROR SEAMOUNT CHAIN

A. C. VASTANO (Texas A&M University, College Station, TX), D. E. HAGAN (California Institute of Technology, Jet Propulsion Laboratory, Pasadena, CA), and G. J. McNALLY (California, University, Scripps Institution of Oceanography, La Jolla, CA) Journal of Geophysical Research (ISSN 0148-0227), vol. 90, March 20, 1985, p. 3325-3331. refs (Contract N00014-75-C-0537)

In a Kuroshio tracking experiment initiated in February 1977, two satellite-reporting buoys, drogued to 100-m depth, were released southeast of Kuyshu Island, Japan. These drifters crossed the Shatskiy Rise in the Kuroshio extension during May and October and then traversed the Emperor Seamount Chain. Although they reached the chain 117 days apart, their movements near the seamounts display remarkably similar patterns, demonstrating upstream meanders in the surface flow; cyclonic eddy activity immediately west of the chain, passage through the same gap associated with the Jingu and Nintoku seamounts; and a wavelike pattern present over the Hess Rise east of the chain. One drifter exhibited cyclonic eddy motion east of the chain in the lee of the Kinmei Seamount. Author

A85-27736

IMPROVEMENT OF THE ACCURACY OF RADAR MEASUREMENTS OF SEA-ICE THICKNESS BY CEPSTRAL PROCESSING OF REFLECTED SIGNALS [POVYSHENIE TOCHNOSTI RADIOLOKATSIONNYKH IZMERENII TOLSHCHINY MORSKOGO L'DA PUTEM KEPSTRAL'NOI OBRABOTKI OTRAZHENNYKH SIGNALOV]

V. V. BOGORODSKII, V. I. BOIARSKII, and A. G. OGANESIAN Radiotekhnika i Elektronika (ISSN 0033-8494), vol. 30, Feb. 1985, p. 291-297. In Russian. refs

It is proposed that cepstral methods of reflected-signal processing be used to improve the accuracy of existing techniques of remote radar measurement of sea-ice thickness. The good potential of these methods is demonstrated using reflected signals produced by a digital simulator, the expected rms error of thickness measurement in the range of 0.1 to 2 meters amounted to 6 percent. The algorithms developed were used to analyze radar signals obtained in drifting-station measurements and in flights over Arctic ice; the rms error of thickness measurement did not exceed 10 percent. B.J.

A85-27841

ADVANCED SAR SYSTEM MAPS ARCTIC REGIONS

A. NICHOLS, J. WILHELM, T. GAFFIELD (Michigan, Environmental Research Institute, Ann Arbor, MI), R. INKSTER, and S. LEUNG (Intera Technologies, Ltd., Calgary, Alberta, Canada) Microwaves & RF (ISSN 0745-2993), vol. 24, March 1985, p. 80, 81, 82, 85

The STAR-1 (Sea and Ice Terrain Assessment Radar) system has been designed to provide high-quality fine-resolution Synthetic Aperture Radar (SAR) imagery for ice and terrain-surveillance applications. Other requirements were related to the possibility of an installation in a small aircraft, a wide-swath mapping capability, and the ability to process data on board the aircraft in order to minimize postflight data accessing time. Since 1983, the STAR-1 has been installed aboard a twin-engine turboprop aircraft operating in the Beaufort Sea. Impressive data have been obtained for oil exploration support and for navigation in the considered areas. Attention is given to the SAR imaging system, the aircraft serving as the platform for the SAR system, real-time results, the X-band radar, and a number of images obtained. G.R.

A85-28005*

SCRIPPS INSTITUTION OF OCEANOGRAPHY, LA JOLLA, CALIF. ESTIMATING OCEAN PRIMARY PRODUCTION FROM SATELLITE CHLOROPHYLL - INTRODUCTION TO REGIONAL DIFFERENCES AND STATISTICS FOR THE SOUTHERN CALIFORNIA BIGHT

R. W. EPPLEY, E. STEWART (California, University, Scripps Institution of Oceanography, La Jolla, CA), M. R. ABBOTT (California Institute of Technology, Jet Propulsion Laboratory, Pasadena, CA), and U. HEYMAN (Uppsala Universitet, Uppsala, Sweden, California, University, Scripps Institution of Oceanography, La Jolla, CA) Journal of Plankton Research (ISSN 0142-7873), vol. 7, no. 1, 1985, p. 57-70. NSF-supported research. refs (Contract NAGW-458; DE-AT03-82ER-60031)

A85-28007*

JET PROPULSION LAB., CALIFORNIA INST. OF TECH., PASADENA.

DETERMINATION OF MONTHLY MEAN HUMIDITY IN THE ATMOSPHERIC SURFACE LAYER OVER OCEANS FROM SATELLITE DATA

W. T. LIU (California Institute of Technology, Jet Propulsion Laboratory, Pasadena, CA) and P. P. NIILER (California Institute of Technology, Jet Propulsion Laboratory, Pasadena; California, University, Scripps Institution of Oceanography, La Jolla, CA) Journal of Physical Oceanography (ISSN 0022-3670), vol. 14, Sept. 1984, p. 1451-1457. NASA-supported research. refs (Contract NSF OCE-78-20766)

A simple statistical technique is described to determine monthly mean marine surface-layer humidity, which is essential in the specification of surface latent heat flux, from total water vapor in the atmospheric column measured by space-borne sensors. Good correlation between the two quantities was found in examining the humidity soundings from radiosonde reports of mid-ocean island stations and weather ships. The relation agrees with that obtained from satellite (Seasat) data and ship reports averaged over 2 deg areas and a 92-day period in the North Atlantic and in the tropical Pacific. The results demonstrate that, by using a local regression in the tropical Pacific, total water vapor can be used to determine monthly mean surface layer humidity to an accuracy of 0.4 g/kg. With a global regression, determination to an accuracy of 0.8 g/kg is possible. These accuracies correspond to approximately 10 to 20 W/sq m in the determination of latent heat flux with the bulk parameterization method, provided that other required parameters are known. Author

A85-28022* National Aeronautics and Space Administration, Washington, D. C.

SATELLITE OBSERVATIONS OF SEA ICE

R. H. THOMAS (NASA, Washington, DC; California Institute of Technology, Jet Propulsion Laboratory, Pasadena, CA) IN: Oceans '84: Industry, Government, Education - Design for the future, Proceedings of the Conference, Washington, DC, September 10-12, 1984. New York, Institute of Electrical and Electronics Engineers, Inc., 1984, p. 950-955. NASA-supported research refs

Attention is given to techniques developed by NASA for the satellite acquisition of polar ice cover data, as well as for the spotlighting of selected ice cover areas in order to reveal detailed ice pack features. Of the visible, IR and microwave sensors available aboard satellites, only microwave units operate day and night and in all weather conditions to provide global synoptic coverage. Microwave may be either passive or active; the former include the Electrically Scanning Microwave Radiometer aboard Nimbus-5 and the Scanning Multichannel Microwave Radiometer of Seasat and Nimbus-7, while the latter are represented by synthetic aperture radars and radar altimeters aboard Seasat.

O.C.

A85-28027* Jet Propulsion Lab., California Inst. of Tech., Pasadena.

MAPPING OF GLACIAL LANDFORMS FROM SEASAT RADAR IMAGES

J. P. FORD (California Institute of Technology, Jet Propulsion Laboratory, Pasadena, CA) Quaternary Research (ISSN 0033-5894), vol. 22, Nov. 1984, p. 314-327. NASA-supported research. refs

Glacial landforms in the drumlin drift belt of Ireland and the Alaska Range can be identified and mapped from Seasat synthetic-aperture radar (SAR) images. Drumlins cover 60 percent of the Ireland scene. The width/length ratio of individual drumlins can be measured on the SAR images, allowing regional differences in drumlin shape to be mapped. This cannot be done with corresponding Landsat multispectral scanner (MSS) images because of lower spatial resolution and because of shadowing effects that vary seasonally. The Alaska scene shows the extent and nature of morphological features such as medial and lateral moraines, stagnant ice, and fluted ground moraine in glaciated valleys. Perception of these features on corresponding Landsat MSS images is limited by seasonal differences in solar illumination. Because SAR is not affected by such differences or by cloud cover, it is particularly well suited for monitoring glacial movement. The disadvantage of distorted high-relief features on Seasat SAR images can be reduced in future SAR systems by modifying the radar illumination geometry

Author

A85-28119#

SATELLITE DATA COMMUNICATION SYSTEM FOR NEAR REAL-TIME PROCESSING AND DISTRIBUTION OF MARINE FISHERY RESEARCH DATA

K. J. SAVASTANO (NOAA, Southeast Fisheries Center, Miami, FL) and L. B. STOGNER IN: SOUTHEASTCON '83; Proceedings of the Region 3 Conference and Exhibit, Orlando, FL, April 11-13, 1983. New York, Institute of Electrical and Electronics Engineers, Inc., 1983, p. 516-519.

A85-28783

AIRBORNE DOPPLER ESTIMATES OF THE AIR MOTIONS ASSOCIATED WITH A DEVELOPING, SEA-BREEZE INDUCED, MESOSCALE PRECIPITATION LINE

D. P. JORGENSEN, R. W. BURPEE, and K. C. BELLE (NOAA, Hurricane Research Div., Miami, FL) IN: Conference on Radar Meteorology, 21st, Edmonton, Alberta, Canada, September 19-23, 1983, Preprints. Boston, MA, American Meteorological Society, 1983, p. 670-674. refs

A85-28788* National Aeronautics and Space Administration, Goddard Space Flight Center, Greenbelt, Md.

SIMULTANEOUS OCEAN CROSS-SECTION AND RAINFALL MEASUREMENTS FROM SPACE WITH A NADIR POINTING RADAR

D. ATLAS and R. MENEGHINI (NASA, Goddard Space Flight Center, Laboratory for Atmospheric Sciences, Greenbelt, MD) IN: Conference on Radar Meteorology, 21st, Edmonton, Alberta, Canada, September 19-23, 1983, Preprints. Boston, MA, American Meteorological Society, 1983, p. 719-726. refs

A modified version of the surface-target-attenuation radar described by Meneghini et al. (1983) is proposed which permits simultaneous measurement of ocean radar cross sections and path-average rain rates using a nadir-pointing satellite-borne microwave radar. The basic concept is explained and illustrated, the equations describing the data reduction are derived; some preliminary numerical computations based on a 7.5-m-diameter 10-kW 1.33-microsec-pulse radar operating at 1.87 cm from an altitude of 500 km are performed, and the major error sources (mismatches between rain scattering volumes and additional multipath contributions) and limitations (nadir pointing) are discussed. It is suggested that the system could provide a nadir calibration for wide-swath observing systems such as scanning microwave radiometers.

T.K

A85-29703* Jet Propulsion Lab., California Inst. of Tech., Pasadena.

A SURVEY OF OCEANOGRAPHIC SATELLITE ALTIMETRIC MISSIONS

G. H. BORN (California Institute of Technology, Jet Propulsion Laboratory, Pasadena, CA; Texas, University, Austin, TX), D. B. LAME (California Institute of Technology, Jet Propulsion Laboratory, Pasadena, CA), and J. L. MITCHELL (California Institute of Technology, Jet Propulsion Laboratory, Pasadena, CA; U.S. Navy, Naval Ocean Research and Development Activity, Bay St. Louis, MS) Marine Geodesy (ISSN 0149-0419), vol. 8, no. 1-4, 1984, p. 3-16.

Consideration is given to the potential benefits of satellite altimetry measurements for oceanographic studies. The technical specifications and instrument payloads of past and future satellite altimetric satellite missions are described in a table. The missions include SKYLAB (1973); GEOS-3 (1975); and SEASAT (1978). Consideration is also given to the NROSS (1988); GEOSAT-4 (1984), and POSEIDON (1987-88) satellite missions

I.H.

A85-29704

THE POTENTIAL FOR OCEAN PREDICTION AND THE ROLE OF ALTIMETER DATA

H. E. HURLBURT (U.S. Navy, Naval Ocean Research and Development Activity, Bay St. Louis, MS) Marine Geodesy (ISSN 0149-0419), vol. 8, no. 1-4, 1984, p. 17-66. Navy-supported research. refs

A scheme for global ocean prediction forecasting based on satellite altimetry data is described. The data requirements of a global ocean forecasting system are identified. The issues of model design and data assimilation are examined within the context of current US Navy efforts to develop an accurate ocean prediction capability. The unique contributions of satellite altimetry data to surface and subsurface forecasts of meandering currents, eddies, and frontal locations are identified. It is pointed out that satellite altimetry data may extend the reliability of ocean surface and subsurface forecasts to a period of several months

I.H.

A85-29705

OBSERVING GLOBAL OCEAN CIRCULATION WITH SEASAT ALTIMETER DATA

B. C. DOUGLAS, R. W. AGREEN, and D. T. SANDWELL (NOAA, National Ocean Service, Rockville, MD) Marine Geodesy (ISSN 0149-0419), vol. 8, no. 1-4, 1984, p. 67-83. refs

A nondynamic algorithm for correcting the geocentric radius of the SEASAT orbit has been developed. This scheme reduces the satellite altitude error to a few decimeters and requires only weak a priori knowledge of sea surface undulations. Application has

been made to a single three-day period during which SEASAT took global altimeter measurements of sea surface topography with geographic resolution of 900 km at the equator. The resulting corrected SEASAT ephemeris then enabled computation of a sea surface largely free of the 2 to 7 m error that would otherwise arise from error in the ephemeris distributed with the SEASAT data. Subsequent subtraction of GEM L2 geoid heights from this sea surface has yielded ocean dynamic heights in reasonable qualitative and quantitative agreement with values obtained from oceanographic data. The fact that results of this quality could be obtained from only one three-day arc of SEASAT data demonstrates the potential of satellite altimetry for determining global ocean circulation. The results also show that the solution to the problem of ephemeris error is to be found by considering both dynamic and nondynamic orbit determination methods

Author

A85-29706

ON THE DETERMINATION OF THE DEFLECTION OF THE VERTICAL BY SATELLITE ALTIMETRY

A. B. WATTS (Meteorological College, Kashiwa, Chiba, Japan, Lamont-Doherty Geological Observatory, Palisades, NY), K. HORAI (Lamont-Doherty Geological Observatory, Palisades; Columbia University, New York, NY), and N. M. RIBE (Yale University, New Haven, CT; Lamont-Doherty Geological Observatory, Palisades, NY) Marine Geodesy (ISSN 0149-0419), vol. 8, no. 1-4, 1984, p. 85-127. refs

(Contract N00014-80-C-0098)

SEASAT altimeter data were used to derive the deflection of the vertical in an area of the Pacific Ocean in the vicinity of the Izu-Bonin and Mariana Trenches. The rms difference in the magnitude and direction of the deflection of 13 intersections of SEASAT repeat orbital tracks were + or - 1.9 arcsec, and + or - 14.9 deg, respectively. Some possible geophysical mechanisms for the observed variations are identified. Deflections were also estimated in two other regions of the Pacific Ocean using altimeter data: one in the region of the Magellan Seamounts and one in the vicinity of the Line Islands. In general, the measured deflections were largest (up to 25 arcsec) in the region of the Magellan Seamounts and smallest (up to 10 arcsec) in the region of the Line Islands. It is concluded that satellite altimeter measurements can be used to determine the deflection of the vertical at sea at crossovers of ascending and descending orbital tracks. I.H.

A85-29707

WORLD OCEAN MEAN MONTHLY WAVES, SWELL, AND SURFACE WINDS FOR JULY THROUGH OCTOBER 1978 FROM SEASAT RADAR ALTIMETER DATA

N. M. MOGNARD, C. BROSSIER (Centre National des Etudes Spatiales, Groupe de Recherche de Geodesie Spatiale, Toulouse, France), and W. J. CAMPBELL (U.S. Geological Survey, Tacoma, WA) Marine Geodesy (ISSN 0149-0419), vol. 8, no. 1-4, 1984, p. 159-181. refs

A85-29708

SWELL IN THE PACIFIC OCEAN OBSERVED BY SEASAT RADAR ALTIMETER

N. M. MOGNARD (Centre National des Etudes Spatiales, Groupe de Recherche de Geodesie Spatiale, Toulouse, France) Marine Geodesy (ISSN 0149-0419), vol. 8, no. 1-4, 1984, p. 183-210. refs

Synoptic observations of ocean swell generation propagation, and dissipation have been obtained from SEASAT radar altimeter data. Wave height and surface wind speed measurements were also deduced from altimeter data. The observations were used to develop three-day average swell maps of the Pacific Ocean for the period from June to October, 1978. Regional differences in the northward propagation and dissipation patterns of separate swell events were analyzed, and the results are discussed in detail. It is found that the maps generally agreed with swell propagation data from conventional pressure transducer measurements. I.H.

A85-29712* National Aeronautics and Space Administration. Wallops Flight Center, Wallops Island, Va.

ELECTROMAGNETIC BIAS OF 36-GHZ RADAR ALTIMETER MEASUREMENTS OF MSL

E. J. WALSH, D. W. HANCOCK, III, D. E. HINES (NASA, Wallops Flight Center, Wallops Island, VA), and J. E. KENNEY (U.S. Navy, Naval Research Laboratory, Washington, DC) Marine Geodesy (ISSN 0149-0419), vol. 8, no. 1-4, 1984, p. 265-296. refs

(Contract N00024-83-C-5301)

The data reduction techniques used to determine the magnitude of electromagnetic (EM) bias in radar altimeter measurements of mean sea level (MSL) area described. Particular attention is given to the bias reduction scheme developed specifically for the Surface Contour Radar (SCR) instrument of the Ocean Topography Experiment (TOPEX). The SCR makes it possible to determine the amount of the backscattered power due to EM reflectance per unit area by measuring both the return power and elevation. Variations of backscattered power for different sea states are determined as a function of displacement of the MSL. On the basis of the recent SCR observations from aircraft, a standard error due to EM bias is predicted for MSL measurements performed with a satellite altimeter radar operating at a frequency of 36 GHz. The obtained standard error was 1 percent for regions with waves 1.9-5.5 meters in height. I.H.

A85-29713* Naval Research Lab., Washington, D. C.

ELECTROMAGNETIC BIAS OF 10-GHZ RADAR ALTIMETER MEASUREMENTS OF MSL

L. W. CHOY, D. L. HAMMOND, and E. A. ULIANA (U.S. Navy, Naval Research Laboratory, Washington, DC) Marine Geodesy (ISSN 0149-0419), vol. 8, no. 1-4, 1984, p. 297-312. NASA-supported research. Previously announced in STAR as N83-25708. refs

(Contract AIR TASK A370370G/058C/2, NAVY PROJECT RR1452-SB-000)

Electromagnetic bias, the small difference that exists between the radar measured mean sea level and the geometric mean sea level is an important issue in high precision satellite altimetry. Present day satellite altimetry has achieved, with SEASAT-1, a precision of 5 cm rms in the range measurement. Future altimeter designs are expected to improve the range measurement precision to cm rms. In order to exploit the capability of these precise radar altimeters are marine geodesy and oceanography, it is necessary to understand and account for all of the known biases in the range measurement. The electromagnetic bias or the EM bias, which has been attributed to the observed fact that ocean wave troughs tend to be better reflectors of nadir viewing microwave radar energy than ocean wave crests, can be observed with high resolution airborne radar. This report presents the results of the EM bias measurements made by NRL using an airborne radar altimeter operating at 10 GHz with a 1 ns range resolution. Data were taken for various sea states and wind conditions. The experimental results are compared with current theories. Author

A85-29714* National Aeronautics and Space Administration. Wallops Flight Center, Wallops Island, Va.

THE REFLECTION OF AIRBORNE UV LASER PULSES FROM THE OCEAN

F. E. HOGE, W. B. KRABILL (NASA, Wallops Flight Center, Wallops Island, VA), and R. N. SWIFT (EG&G Washington Analytical Services Center, Inc., Pocomoke City, MD) Marine Geodesy (ISSN 0149-0419), vol. 8, no. 1-4, 1984, p. 313-344. refs

It is experimentally shown here for the first time that the normalized laser backscatter cross-section of the sea surface is a function of elevation or height position on the ocean wave. All data were taken off-nadir, resulting in incidence angles of about 6.5 deg measured relative to the normal to mean sea level (MSL). In the limited data sets analyzed to date, the normalized backscatter cross-section was found to be higher in wave crest regions and lower in wave troughs for a swell-dominated sea over which the wind speed was 5 m/s. The reverse was found to be the case for a sea that was driven by a 14 m/s wind. These isolated results show that the MSL, as measured by an off-nadir and/or

05 OCEANOGRAPHY AND MARINE RESOURCES

multibeam type satellite laser altimeter, will be found above, at, or below the true MSL, depending on the local sea conditions existing in the footprint of the altimeter. Airborne nadir-pointed laser altimeter data for a wide variety of sea conditions are needed before a final determination can be made of the effect of sea state on the backscatter cross-section as measured by a down-looking satellite laser system. Author

A85-29715* Applied Physics Lab., Johns Hopkins Univ., Laurel, Md.

AN ANALYSIS OF A SATELLITE MULTIBEAM ALTIMETER

G. B. BUSH, E. B. DOBSON, R. MATYSKIELA, C. C. KILGUS (Johns Hopkins University, Applied Physics Laboratory, Laurel, MD), and E. J. WALSH (NASA, Wallops Flight Center, Wallops Island, VA) *Marine Geodesy* (ISSN 0149-0419), vol. 8, no. 1-4, 1984, p. 345-384. refs

Since the GEOS-3 and SEASAT-1 radar altimeters measured altitude over a narrow swath along the satellite subtrack, ocean current and mesoscale feature maps could only be generated after a large number of satellite revolutions. The present paper analyzes a new multibeam altimeter technique that has the potential to cover wide swaths. The multibeam altimeter uses two antenna elements, simple parabolic dishes with offset feeds, deployed cross-track on singly hinged booms into a fixed measurement geometry to generate an interferometer pattern over the desired swath extent. Range gating allows the isolation of a single interferometric lobe, and the desired altitude measurements are extracted by using a modified altitude tracker design. Implementing this sensor on future altimetry missions would allow the timely generation of ocean current and mesoscale feature maps for the first time. Author

A85-29716* National Aeronautics and Space Administration. Goddard Space Flight Center, Greenbelt, Md.
REGIONAL MEAN SEA SURFACES BASED ON GEOS-3 AND SEASAT ALTIMETER DATA

J. G. MARSH (NASA, Goddard Space Flight Center, Geodynamics Branch, Greenbelt, MD), R. E. CHENEY (NOAA, National Geodetic Survey, Rockville, MD), J. J. MCCARTHY, and T. V. MARTIN (EG & G Washington, Analytical Services Center, Inc., Riverdale, MD) *Marine Geodesy* (ISSN 0149-0419), vol. 8, no. 1-4, 1984, p. 385-402. refs

Altimetric sea surfaces provide a basis for detailed analyses of the earth's gravity, crustal structure, and the oceanic surface circulation. Long-term mean surfaces have been computed for the Bering Sea, Northwest Atlantic Ocean, and Gulf of Mexico based on a combination of the entire SEASAT (three-month) and GEOS-3 (3.5-year) altimeter data sets. The number of available passes ranged from 558 in the gulf to 1396 in the Atlantic. The large amount of data in these areas, coupled with the increased constraint provided by the combination of data from two orbital inclinations, has permitted the accurate removal of the effects of radial ephemeris error through crossing arc adjustments. The precision of these regional mean sea surfaces is approximately 15 cm, with horizontal resolutions approaching 25 km. Author

A85-29903

DETERMINATION OF THE PHYSICAL PARAMETERS OF SEA ICE ON THE BASIS OF REMOTE MICROWAVE MEASUREMENTS IN THE 0.3-18 CM RANGE [OPREDELENIE FIZICHESKIKH PARAMETROV MORSKOGO L'DA PO DANNYM DISTANTSIONNYKH SVCH-IZMERENII V DIAPAZONE 0.3-18 SM]

V. I. RAIZER, I. G. ZAITSEVA, V. M. ANISKOVICH, and V. S. ETKIN (Akademiia Nauk SSSR, Institut Kosmicheskikh Issledovani, Moscow, USSR) *Issledovanie Zemli iz Kosmosa* (ISSN 0205-9614), Jan.-Feb. 1985, p. 23-31. In Russian. refs

Brightness temperature spectra of young sea-ice formations in the Arctic were obtained with an airborne radiometer at wavelengths of 0.3, 0.8, 1.35, 8, and 18 cm during October 30 to November 4, 1983. The following physical parameters of the young ice were determined on the basis of a numerical simulation of the emission characteristics: thickness, and temperature, salinity, and density

profiles. In the physical algorithm, the ice structure is assumed to be a stratified dielectric consisting of pure ice containing ellipsoidal conducting inclusions and gas bubbles (brine layers), the contribution of these layers to the microwave emission is investigated on the basis of a numerical method. Author

A85-29915

REMOTE-SENSING OBSERVATIONS OF ADVECTIVE EDDIES IN THE CENTRAL PART OF THE BALTIC SEA [AEROKOSMICHESKIE NABLIUDENIIA ADVEKTIVNO-VIKHREVIKH OBRAZOVANII V TSENTRAL'NOI CHASTI BALTIISKOGO MORIA]

I. A. BYCHKOVA, S. V. VIKTOROV, V. V. VINOGRADOV, V. N. LOSINSKII, and KH. IU. BROZIN (Gosudarstvennyi Okeanograficheskii Institut, Leningrad, USSR; Deutsche Akademie der Wissenschaften, Institut fuer Meereskunde, Rostock, East Germany) *Issledovanie Zemli iz Kosmosa* (ISSN 0205-9614), Jan.-Feb. 1985, p. 118-122. In Russian. refs

N85-15960# Kansas Univ. Center for Research, Inc., Lawrence Remote Sensing Lab.

INTERMEDIATE RESULTS OF RADAR BACKSCATTER MEASUREMENTS FROM SUMMER SEA ICE

S. GOGINENI, R. G. ONSTOTT, R. K. MOORE, and J. CHANCELLOR. Jul 1984. 51 p.
(Contract N00014-76-C-1105)
(AD-A147212; RSL-TR-3311-2) Avail: NTIS HC A04/MF A01 CSCI 20N

A helicopter-borne scatterometer (HELOSCAT) was used to measure radar backscatter from sea ice under summer conditions near Mould Bay, N.W.T., Canada, in June and July 1982. These measurements were made at selected frequencies between 1 and 17 GHz, and at angles between 5 deg and 60 deg with like and cross-polarizations. Multiyear ice (MYI) can be distinguished from first-year ice (FYI) using the profiles acquired by flying the helicopter along selected scan lines at 5.2, 9.6 and 13.6 GHz during early and late summer. Because of wet snow and ice on the surface, producing reduced volume scatter, there is lower backscatter from MYI during summer than during winter. Because of superimposed ice, the backscatter from FYI during early summer is slightly higher than that during other seasons. Its backscatter is higher than that of MYI for the early part of summer, but as summer progresses, FYI backscatter reduces and eventually becomes lower than that from MYI. Results indicate that higher frequencies in Ku- and X-bands are not better than lower frequencies in C-band for discriminating basis ice types during summer. Backscatter from MYI and FYI increased with frequency, and the contrast between FYI and MYI increased with decreasing frequency during late summer. GRA

N85-16239# Joint Publications Research Service, Arlington, Va.
SATELLITE PHOTOGRAPHS SUGGEST ARCTIC VOLCANO

Y. MASURENKOV and O. DZYUBA. In *its* USSR Rept.: Earth Sci. (JPRS-UES-84-008) p. 99-100. 13 Dec 1984. Transl. into ENGLISH from *Izv. (Moscow)*, 31 May 1984. p. 6. Avail: NTIS HC A06

Satellite photographs have registered a foggy trail over the Arctic Ocean on several occasions. The activities of a Soviet expedition to Bennett Island in the Arctic are described briefly. Evidence of volcanic activity on the island and on the ocean bottom around it is discussed. The foggy trail above the sea that a satellite could sense is attributed to the action of lava from a volcano. R.S.F.

N85-16281# Naval Ocean Research and Development Activity, Bay St. Louis, Miss.

BIO-OPTICAL VARIABILITY IN THE ALBORAN SEA AS ASSESSED BY NIMBUS-7 COASTAL ZONE COLOR SCANNER Final Report

P. E. LAVIOLETTE and R. A. ARNONE Aug. 1984 32 p
(Contract F59-553)
(AD-A147909; NORDA-TN-283) Avail NTIS HC A03/MF A01 CSCL 08A

An international oceanographic experiment, was conducted in 1982 in the Alboran Sea in which a specialized portion was dedicated to examining the spatial and temporal variability of bio-optical properties around the Alboran Sea Gyre. The circulation of the Alboran Sea, as characterized by Atlantic Inflow (through the Strait of Gibraltar), The Alboran Gyre, and coastal water masses, was analyzed through use of Nimbus-7 Coastal Zone Color Scanner (CZCS) imagery, NOAA-7 Advanced Very High Resolution Radiometer (AVHRR) imagery, and aircraft and ship data. Diffuse attenuation coefficients calculated from CZCS data are in agreement with the ship data. A strong correlation between the surface temperature and ocean color fronts was observed in the two satellite imagery sets. A 6-day sequence of CZCS imagery shows that significant changes in the diffuse attenuation coefficient and phytoplankton pigment concentration occurred in the frontal regions. These changes are attributed to the bio-optical horizontal and vertical variations that occurred within the first attenuation length.

Author (GRA)

N85-16282# Naval Ocean Research and Development Activity, Bay St. Louis, Miss.

SATELLITE DEFINITION OF THE BIO-OPTICAL AND THERMAL VARIATION OF COASTAL EDDIES ASSOCIATED WITH THE AFRICAN CURRENT Final Report

R. A. ARNONE and P. E. LAVIOLETTE Sep. 1984 24 p
(AD-A147910; NORDA-TN-291) Avail NTIS HC A02/MF A01 CSCL 08C

The circulation of the African oceanic currents along the north coasts of Morocco, Algeria, and Tunisia are shown by numerous seasonal satellite imagery as a series of complex anticyclonic eddies. An eastward propagation of the eddy field indicates a significant net transport. Turbulent shear flow of the African current interacting with the coast results in the advection of coastal waters into the offshore waters of the eddy field. The biological activity and chemical reactions spawned by the interaction of offshore and coastal water properties are clearly observed in the Coastal Zone Color Scanner (CZCS) by ocean color changes. High suspended sediments concentrations from the coastal waters were observed to border the periphery of the eddies. Sea surface temperature shown by NOAA-7 AVHRR imagery also illustrate complex flow although in some imagery the ocean color imaging better defines the patterns. Applications of both visible and ocean color imagery are suggested as a method of determining the flow patterns. Originator-supplied keywords include: Satellite imagery, and Western Mediterranean.

GRA

N85-17212*# Institute of Oceanographic Sciences, Wormley (England)

THE INTERPRETATION OF SIR-B IMAGERY OF SURFACE WAVES AND OTHER OCEANOGRAPHIC FEATURES USING IN-SITU, METEOROLOGICAL SATELLITE, AND INFRARED SATELLITE DATA

T. ALLAN, T. GUYMER, and P. MULLER (Imperial Coll., London)
In JPL The SIR-B Sci Invest. Plan 13 p 1 Jul 1984 refs
Avail: NTIS HC A10/MF A01 CSCL 17I

The overall aim is to interpret Shuttle Imaging Radar-B imagery of selected ocean areas near the United Kingdom using available data from ships and buoys, with particular emphasis on understanding the mechanisms involved in the backscattering of microwaves from the sea surface and their relationship to surface gravity waves. The secondary objective is to use a multispectral approach to study sea-surface expressions such as slicks, internal waves, and eddies. Data acquisition, handling, and analysis approaches and expected results are discussed.

R.J.F.

N85-17213*# National Aeronautics and Space Administration, Goddard Space Flight Center, Greenbelt, Md

THE SPATIAL EVOLUTION OF THE DIRECTIONAL WAVE SPECTRUM IN THE SOUTHERN OCEAN: ITS RELATION TO EXTREME WAVES IN AGULHAS CURRENT

R. C. BEAL, A. GOLDFINGER, D. IRVINE, F. MONALDO, D. TILLEY (ERIM, Ann Arbor), R. SHUCHMAN (NOAA, Washington, D.C.), D. LYZENGA (ERIM, Ann Arbor), J. LYDEN (ERIM, Ann Arbor), P. DELEONIBUS (NOAA, Washington, D.C.), C. RUFENACH (Cape Town Univ.) et al. In JPL The SIR-B Sci Invest Plan 4 p 1 Jul 1984 refs Prepared in cooperation with APL, Laurel, Md
Avail: NTIS HC A10/MF A01 CSCL 17I

An experiment using the Shuttle Imaging Radar-B (SIR-B) to monitor certain properties of the ocean wave directional spectrum and to track the long swell systems as they propagate northward to encounter the Agulhas near the southeastern coast of Africa is discussed. The experiment is designed around the unique capability of SIR-B to overcome key limitations of the Seasat synthetic aperture radar data set, and to extend the existing Seasat results into new areas. Ocean wave systems will be tracked. The variable-incidence-angle capability to examine wave imaging quality will be utilized. Doppler current measurements will be attempted. An effort will be made to verify that the lower range-to-velocity ratio of SIR-B will lead to the improved response of azimuth-traveling wave systems.

R.J.F.

N85-17231*# Illinois Univ., Urbana

INTERLOBATE COMPARISON OF GLACIAL-DEPOSITIONAL STYLE AS EVIDENCED BY SMALL-RELIEF GLACIAL LANDSCAPE FEATURES IN ILLINOIS, INDIANA, AND OHIO, UTILIZING SIR-B

W. H. JOHNSON, N. K. BLEUER (Geological Survey, Bloomington, Ind.), G. S. FRASER (Geological Survey, Bloomington, Ind.), and S. M. TOTTON (Hanover Coll., Ind.) In JPL The SIR-B Sci Invest. Plan 3 p 1 Jul 1984 refs
Avail: NTIS HC A10/MF A01 CSCL 08L

The objectives and expected results of an investigation of the use of the Shuttle Imaging Radar-B (SIR-B) as a basic tool in the recognition and mapping of glacial landforms are discussed. The main goals are (1) to evaluate the ability of SIR-B to delineate varying sizes, shapes, and relief of surface forms; (2) to compare and contrast SIR-B imagery with selected Seasat SAR imagery; (3) to utilize SIR-B imagery synergistically with available SEASAT SAR, LANDSAT RBV, and other imagery sources to identify and map suites of glacial landforms; and (4) eventually to interpret the suites in terms of ice dynamics and conditions of deglaciation, to relate them to the stratigraphic record, and to evaluate interactions of the major lobes and sublobes.

M.G.

N85-17233*# Royal Aircraft Establishment, Farnborough (England).

THE INVESTIGATION OF SELECTED OCEANOGRAPHIC APPLICATIONS OF SPACEBORNE SYNTHETIC-APERTURE RADAR

G. E. KEYTE, B. C. BARBER, M. B. BARNES, G. C. WHITE, M. BAGG (Admiralty Underwater Weapons Establishment), B. DOLIER (City of London Polytechnic), and N. LYNN (Royal Naval Coll.) In JPL The SIR-B Sci Invest. Plan 6 p 1 Jul 1984
Avail: NTIS HC A10/MF A01 CSCL 08C

Synthetic aperture radar images obtained from Seasat and SIR-A showed that a number of oceanographic features were imaged in considerable detail, like internal waves, large ocean waves, bathymetric features, eddies, and slicks. The imaging mechanisms however, are not well understood, and for both SEASAT and SIR-A there are few supporting sea surface measurements to assist in the study of these imaging mechanisms. The SIR-B will conduct three separate experiments to provide a better understanding of the use of spaceborne SAR for imaging: (1) internal waves, (2) ocean surface waves, and (3) shallow water bathymetry. These experiments are chosen because they lead to possible applications for microwave remote sensing of the ocean surface and give a better understanding of the microwave/sea surface imaging mechanism.

E.A.K.

05 OCEANOGRAPHY AND MARINE RESOURCES

N85-17235*# International Inst. for Aerial Survey and Earth Sciences, Enschede (Netherlands).

MONITORING OF THE TIDAL DYNAMICS OF THE DUTCH WADDENSEA BY SIR-B

B. N. KOOPMANS, D. VANDERZEE, A. T. VERSTAPPEN, T. WOLDAI, and H. HOSCHITITZKY *In* JPL The SIR-B Sci. Invest. Plan 4 p 1 Jul. 1984 refs

Avail: NTIS HC A10/MF A01 CSCL 08C

The potential of LANDSAT data, covering the entire tidal flats at a certain, known, tidal situation, was assessed. It was discovered that the data cannot be used for systematic survey because of the long interval between subsequent passes, weather conditions often interfere with recording, and of the lack of correlation between passes and the tidal situation. The objective is to overcome the problems by using (1) the synoptic view obtained by SIR-B, which has the potential of surveying large areas of the flats simultaneously; (2) the all-weather capability of the microwave system; (3) the recording during consecutive days, which results in a straightforward correlation with the tidal cycle and the picturing of different tidal stages; and (4) the multiangle incidence of SIR-B to analyze the bottom configuration of submerged parts of the flats. The use of a weather independent monitoring device, such as radar, an improvement in the monitoring technique of tidal coastal areas. E.A.K.

N85-17274# Mitre Corp., McLean, Va
SEASAT 3 AND 4

K. CASE, C. CALLAN, R. DASHEN, R. DAVIS, W. MUNK, J. VESECKY, K. WATSON, and F. ZACHARIASEN Aug 1984 141 p

(Contract F19628-84-C-0001)

(AD-A148343, JSR-84-203) Avail NTIS HC A07/MF A01 CSCL 17I

JASON continues its theoretical investigation of understanding the origin of the ship wakes seen by the SEASAT radar. The present effort incorporates the new experimental results from the Georgia Strait and the Gulf of Alaska experiments. These experiments appear to rule out the internal wave hypothesis; they also seem to indicate that the Kelvin Wake (here defined in the most general sense to include non-linear processes as well as interactions with the turbulent wake) is rather different than conventional Kelvin wake theory would predict. Nonetheless, a model which seems to be at least qualitatively reasonable can be constructed. The generation of ship wakes (surface or internal) and their detection by radar is a complicated phenomenology involving various branches of physics, hydrodynamics and oceanography. Nevertheless, with the exception of the inner, small angle part of the Kelvin wake, we believe that the theoretical understanding of the problem is adequate to support the conclusions reached in the report. Author (GRA)

N85-17404*# National Aeronautics and Space Administration, Goddard Space Flight Center, Greenbelt, Md.

ALTIMETRY, ORBITS AND TIDES

O. L. COLOMBO Nov. 1984 183 p refs ERTS

(E85-10066; NASA-TM-86180; NAS 1 15-86180) Avail: NTIS HC A09/MF A01 CSCL 05B

The nature of the orbit error and its effect on the sea surface heights calculated with satellite altimetry are explained. The elementary concepts of celestial mechanics required to follow a general discussion of the problem are included. Consideration of errors in the orbits of satellites with precisely repeating ground tracks (SEASAT, TOPEX, ERS-1, POSEIDON, amongst past and future altimeter satellites) are detailed. The theoretical conclusions are illustrated with the numerical results of computer simulations. The nature of the errors in this type of orbits is such that this error can be filtered out by using height differences along repeating (overlapping) passes. This makes them particularly valuable for the study and monitoring of changes in the sea surface, such as tides. Elements of tidal theory, showing how these principles can be combined with those pertinent to the orbit error to make direct maps of the tides using altimetry are presented. Author

N85-17416# Naval Ocean Research and Development Activity, Bay St Louis, Miss.

THE USE OF PRINCIPAL COMPONENTS ANALYSIS TECHNIQUES NIMBUS-7 COASTAL ZONE COLOR SCANNER DATA TO DEFINE MESOSCALE OCEAN FEATURES THROUGH A WARM HUMID ATMOSPHERE Final Report

R. J. HOLYER and P. E. LAVIOLETTE Apr. 1984 78 p Original contains color illustrations

(AD-A148567, NORDA-60) Avail. NTIS HC A05/MF A01 CSCL 08J

The Nimbus-7 Coastal Zone Color Scanner (CZCS) has the unique potential to remotely sense mesoscale ocean features through warm, humid atmospheres that are opaque to thermal infrared sensors. The major obstacle to the use of these data is the masking effect of sunlight backscattered by the atmosphere. This study details a new atmospheric correction method, employing principal component analysis techniques, that effectively removes the atmospheric radiance from CZCS images of the ocean. The method has the advantage of ease of use and, hence, allows the CZCS data to be incorporated into routine naval environmentally-oriented operations. The study shows the method to be especially effective in the descriptive analyses of mesoscale oceanic phenomena. Four examples of the use of the technique are presented for three different ocean areas. GRA

N85-17506# Department of the Navy, Washington, D. C.

A METHOD FOR DETERMINING MESOSCALE DYNAMIC TOPOGRAPHY Patent Application

J. L. MITCHELL, inventor (to Navy) 22 Feb. 1984 13 p

(AD-D011412; US-PATENT-APPL-SN-582412) Avail NTIS HC A02/MF A01 CSCL 08J

A method for determining mesoscale dynamic topography places a satellite altimeter into a properly selected, exact repeating orbit. The proper mesoscale sampling strategy depends upon the nature of the frequency/wavenumber response of the mesoscale ocean which is different in different regions of the global ocean. The result is altimetry data completely free of geoid contamination and having an order of magnitude alleviation of the problem of temporal undersampling. Author (GRA)

N85-18443*# National Aeronautics and Space Administration, Goddard Space Flight Center, Greenbelt, Md.

DATA REPORT ON VARIATIONS IN THE COMPOSITION OF SEA ICE DURING MIZEX/EAST'83 WITH THE NIMBUS-7 SMMR

P. GLOERSEN Dec 1984 144 p

(NASA-TM-86170; NAS 1.15:86170) Avail: NTIS HC A07/MF A01 CSCL 08L

Data acquired with the scanning multichannel microwave radiometer (SMMR) on board the Nimbus-7 satellite for a six-week period including the 1983 MIZEX in Fram Strait were analyzed with the use of a previously developed procedure for calculating sea ice concentration, multiyear fraction, and ice temperature. These calculations can be compared with independent observations made on the surface and from aircraft in order to check the validity of the calculations based on SMMR data. The calculation of multiyear fraction, which was known earlier to be invalid near the melting point of sea ice, was of particular interest during this period. The indication of multiyear ice was found to disappear a number of times, presumably corresponding to freeze/thaw cycles which occurred in this time period. Both grid-print maps and grey-scale images of total sea ice concentration and multiyear sea ice fraction for the entire period are included. Author

N85-19503# Titan Systems, Inc., Vienna, Va.
NAUTICAL CHARTING WITH REMOTELY SENSED IMAGERY, VOLUME 1
 J. PASSAUER, M. RAGUSKY, J. KORAK, and W. COVER Nov 1984 191 p 2 Vol
 (Contract DMA800-83-C-0056)
 (AD-A149361, AD-F300533) Avail: NTIS HC A09/MF A01
 CSCL 08B

Organized in two volumes, this study is designed as a guide and reference for the hydrographic cartographer in using remotely sensed imagery to delineate coastal areas and that phenomena associated with coastal areas. Volume 1 is the basic text, covering charts and missions, coastal geomorphology, coastal classification, oceanography, remote sensing and hydrographic charting. It contains a glossary, a list of abbreviations and acronyms, and a bibliography applicable to both volumes. Volume 2 supports Volume 1, under a parallel plan of organization, by presenting case studies using imagery examples with analysis. GRA

N85-19504# Titan Systems, Inc., Vienna, Va.
NAUTICAL CHARTING WITH REMOTELY SENSED IMAGERY. VOLUME 2: CASE STUDIES
 J. PASSAUER, M. RAGUSKY, J. KORAK, and W. COVER Nov. 1984 187 p 2 Vol
 (Contract DMA800-83-C-0056)
 (AD-A149362; AD-F300533) Avail: NTIS HC A09/MF A01
 CSCL 08F

Organized in two volumes each of which can be used separately, this study is designed as a guide and reference for the hydrographic cartographer in using remotely sensed imagery to chart coastal and shallow sea features. Volume I is the basic text, covering charts and missions, coastal geomorphology, coastal classification, oceanography, remote sensing, and hydrographic charting. It contains a glossary, a list of abbreviations and acronyms, and a bibliography applicable to both volumes. Volume II is designed to stand alone and present case studies using world-wide imagery examples with analysis. Examples of imagery range from archival to the latest imagery available at the compilation deadline including the European Space Agency Metric Camera and the NASA Large Format Camera. Imagery acquired from high altitude aircraft were also included. GRA

N85-19594# Army Cold Regions Research and Engineering Lab., Hanover, N. H.
MIZEX (MARGINAL ICE ZONE PROGRAM): A PROGRAM FOR MESOSCALE AIR-ICE-OCEAN INTERACTION EXPERIMENTS IN ARCTIC MARGINAL ICE ZONES. 5. MIZEX 84. SUMMER EXPERIMENT PI (PRINCIPAL INVESTIGATOR) PRELIMINARY REPORTS
 O. M. JOHANNESSEN and D. A. HORN Oct 1984 185 p
 (AD-A148986; AD-E301513; CRREL-SR-84-29) Avail: NTIS HC A09/MF A01 CSCL 08J

The marginal ice zone program (MIZEX) which goal it is to understand the mesoscale processes which dictate the advance and retreat of the ice margin is outlined. The field coordinator's overview, and preliminary reports for the MIZEX 84 Summer experiment are reported. The following categories are summarized: oceanography, ice reconnaissance and formation, meteorology, remote sensing, acoustics, and biology. GRA

N85-20619# Coast Guard Research and Development Center, Groton, Conn
ATLAS OF THE BEAUFORT SEA Final Report
 I. M. LISSAUER, L. E. HACHMEISTER, and B. J. MORSON Oct. 1984 182 p
 (AD-A149545; CGR/DC-17/84, USCG-D-33-84) Avail: NTIS HC A09/MF A01 CSCL 08C

This is a reference document on oceanography, meteorology, ice and climatology. The oceanography section contains information for circulation, tides, riverine input, ice conditions, storm surges and bathymetry of the Alaskan Beaufort Sea. From review of information on meteorology, climate, ice conditions, and oceanography, maps have been generated showing circulation in

two typical wind conditions: ENE wind at 10 knots and NW storm wind at 30 knots. These maps show tides, storm surges, bathymetry and river discharges as well as charts of mean ice drift over time. The meteorology section contains information on winds, storm surges and waves. Included is a rapid manual forecast system for estimating the height of a storm surge. The ice section gives information on the ice zones, including the annual ice cycle within the nearshore area, the freezing and breakup of nearshore ice, and the movement of the pack ice. The climatology section includes information on the arctic climate, temperature information (including wind chill charts), visibility, and precipitation. GRA

N85-21723* National Aeronautics and Space Administration. Pasadena Office, Calif
METHOD OF MEASURING SEA SURFACE WATER TEMPERATURE WITH A SATELLITE INCLUDING WIDEBAND PASSIVE SYNTHETIC-APERTURE MULTICHANNEL RECEIVER Patent

J. M. STACEY, inventor (to NASA) (JPL, California Inst. of Tech., Pasadena) 12 Feb. 1985 11 p Filed 6 May 1982 Supersedes N82-26523 (20 - 17, p 2390) Sponsored by NASA
 (NASA-CASE-NPO-15651-1, NAS 1.71:NPO-15651-1, US-PATENT-4,499,470, US-PATENT-APPL-SN-375620; US-PATENT-CLASS-343-352, US-PATENT-CLASS-374-122)
 Avail US Patent and Trademark Office CSCL 14B

A wideband passive synthetic-aperture multichannel receiver with an antenna is mounted on a satellite which travels in an orbit above the Earth passing over large bodies of water, e.g., the Atlantic Ocean. The antenna is scanned to receive signals over a wide frequency band from each incremental surface area (pixel) of the water which are related to the pixel's sea temperature. The received signals are fed to several channels which are tuned to separate selected frequencies. Their outputs are fed to a processor with a memory for storage. As the antenna points to pixels within a calibration area around a buoy of known coordinates, signals are likewise received and stored. Exactly measured sea temperature is received from the buoy. After passing over several calibration areas, a forward stepwise regression analysis is performed to produce an expression which selects the significant from the insignificant channels and assigns weights (coefficients) to them. The expression is used to determine the sea temperature at each pixel based on the signals received therefrom. Wind temperature, pressure, and wind speed at each pixel can also be calculated.

Official Gazette of the U.S. Patent and Trademark Office

N85-21753*# City Coll. of the City Univ. of New York Inst. of Marine and Atmospheric Sciences.
OCEANOGRAPHIC AND METEOROLOGICAL RESEARCH BASED ON THE DATA PRODUCTS OF SEASAT Final Technical Report
 W. J. PIERSON, JR. Mar. 1985 21 p refs ERTS
 (Contract NAGW-266)
 (E85-10091, NASA-CR-175526, NAS 1.26.175526) Avail: NTIS HC A02/MF A01 CSCL 05B

Reservations were expressed concerning the sum of squares wind recovery algorithm and the power law model function. The SAS sum of squares (SOS) method for recovering winds from backscatter data leads to inconsistent results when V pol and H pol winds are compared. A model function that does not use a power law and that accounts for sea surface temperature is needed and is under study both theoretically and by means of the SASS mode 4 data. Aspects of the determination of winds by means of scatterometry and of the utilization of vector wind data for meteorological forecasts are elaborated. The operational aspect of an intermittent assimilation scheme currently utilized for the specification of the initial value field is considered with focus on quantifying the absolute 12-hour linear displacement error of the movement of low centers. A.R.H.

05 OCEANOGRAPHY AND MARINE RESOURCES

N85-21758* # Washington Univ., Seattle. NASA Science Working Group for the Special Sensor Microwave Imager (SSM/I). **PASSIVE MICROWAVE REMOTE SENSING FOR SEA ICE RESEARCH**

Dec. 1984 69 p refs Sponsored by NASA Original contains color illustrations (NASA-CR-175570; NAS 1.26:175570) Avail NTIS HC A04/MF A01 CSCL 08L

Techniques for gathering data by remote sensors on satellites utilized for sea ice research are summarized. Measurement of brightness temperatures by a passive microwave imager converted to maps of total sea ice concentration and to the areal fractions covered by first year and multiyear ice are described. Several ancillary observations, especially by means of automatic data buoys and submarines equipped with upward looking sonars, are needed to improve the validation and interpretation of satellite data. The design and performance characteristics of the Navy's Special Sensor Microwave Imager, expected to be in orbit in late 1985, are described. It is recommended that data from that instrument be processed to a form suitable for research applications and archived in a readily accessible form. The sea ice data products required for research purposes are described and recommendations for their archival and distribution to the scientific community are presented. B.G.

N85-21767# National Geodetic Survey, Rockville, Md. **ALONG-TRACK DEFLECTION OF THE VERTICAL FROM SEASAT: GERCO (GENERAL BATHYMETRIC CHART OF THE OCEANS) OVERLAYS**

D. T. SANDWELL Oct. 1984 14 p refs (PB85-129641; NOAA-TM-NOS-NGS-40) Avail: NTIS HC A02/MF A01 CSCL 08E

To provide easy access to the large number of SEASAT altimeter observations, the National Geodetic Survey has produced overlays for the General Bathymetric Chart of the Oceans (GEBCO). Each of the 32 overlays displays along track deflection of the vertical for either ascending or descending altimeter passes. In poorly charted southern ocean areas the complete coverage by the SEASAT altimeter reveals many previously undetected features of the seafloor. Author (GRA)

N85-21891# Meteorological Satellite Center, Tokyo (Japan) **THE DEVELOPMENT OF IMAGE PROCESSING OF NOAA AVHRR DATA AND ITS APPLICATION TO SEA SURFACE TEMPERATURE**

M. TOKUNO and S. TAKAHASHI *In its* Meteorol. Satellite Center Tech. Note No. 10, 1984 p 47-56 Nov. 1984 refs Avail: NTIS HC A05/MF A01

Satellite data from the Advanced Very High Resolution Radiometer (AVHRR) on board NOAA have been used to detect areas of clouds or to investigate surface conditions. In order to use NOAA AVHRR imagery effectively, a system was developed to display the imagery on an Image Processing Console (IPC). The system has the following functions: (1) enlarging or compressing the image; (2) constructing the image by the enhancement conversion table; and (3) monochrome or pseudo color display of the image. As an example of its application, features of sea surface temperature patterns were studied three times in the ocean off the Sanriku Shore. A large warm eddy detached from the Kuroshio was noticed. Author

N85-21920# Colorado School of Mines, Golden. Dept. of Geophysics. **RESEARCH ON OCEAN FLOOR ELECTRICAL SURVEYS Final Report**

G. V. KELLER and A. A. KAUFMAN 1 Oct. 1984 37 p (Contract N00014-80-C-0768) (AD-A149831) Avail NTIS HC A03/MF A01 CSCL 08N

An important problem faced by the U.S. Navy is that of detecting submarines at greater ranges with airborne magnetic sensors than can now be done. One of the limits to the range at which detection is possible is the confusion of submarine-generated signals with natural-field pulsations of the Earth's magnetic fields. One approach

to the removal of the natural magnetic noise is that of monitoring the fluctuations at a moving airborne system. This requires two assumptions: the magnetic field of variations are coherent over the range on which cancellation is accomplished, and the correlation between magnetic field effects at the two sites is not dependent on the geology at either the mobile station or the reference site. Experience with geophysical surveys indicates that coherency of the magnetic field does exist; but, also, in water depths up to several thousand feet, the magnetic field is dependent upon geology at the observation site. This leads to a requirement for a method to evaluate the effect of subsea geology on local micropulsation behavior. In the research described in this report, three general categories of subsea electrical surveys were reviewed: direct current resistivity surveys, magnetotelluric soundings, and seafloor based electromagnetic system. GRA

N85-22143# Wisconsin Univ., Madison Marine Studies Center. **AN AIRBORNE INFRARED THERMAL SCANNING SYSTEM FOR EASY USE ON NAVY P-3 AIRCRAFT Final Report**

T. GREEN, III, M. J. GREEN, and F. L. SCARPACE 1 Sep 1984 66 p

(Contract N00014-79-C-0066)

(AD-A149690) Avail NTIS HC A04/MF A01 CSCL 17E

This report describes an infrared scanning system which allows almost any Navy P-3 aircraft to be used to obtain maps of sea-surface temperature (SST), and can thus be readily used to provide SST data for many oceanographic experiments. Although a few minor changes need to be made (e.g., adjusting the low-pass filter of the video, and completing the realtime data display software), the device is essentially ready to be put into use. This scanning system will probably be most helpful when operated as part of a larger program, and in areas demanding either frequent coverage, or long flight times. The scale of the phenomena under investigation should probably be at most 50-100 km, and SST should, of course, be indicative of the dynamics of the processes. Such a system would seem to be almost essential to a research program when the SST gradients are sharp, and changing rapidly in time. The sensing device is mounted in a wing pod, and the data are sent optically to recording equipment located in the cabin. The system can be installed on a P-3 in a few hours, and involves no airframe modifications. It has been tested in flight only minor changes are needed to make it fully operational. GRA

06

HYDROLOGY AND WATER MANAGEMENT

Includes snow cover and water runoff in rivers and glaciers, saline intrusion, drainage analysis, geomorphology of river basins, land uses, and estuarine studies

A85-21046

DEVELOPMENT OF WATER QUALITY MODELS APPLICABLE THROUGHOUT THE ENTIRE SAN FRANCISCO BAY AND DELTA

S. KHORRAM (North Carolina State University, Raleigh, NC) Photogrammetric Engineering and Remote Sensing (ISSN 0099-1112), vol. 51, Jan. 1985, p. 53-62. Research supported by the University of California. refs

A85-21130

A COMPARATIVE ANALYSIS OF SOME PREDICTION METHODS FOR RAIN ATTENUATION STATISTICS IN EARTH-TO-SPACE LINKS

G. MACCHIARELLA (CNR, Centro di Studio per le Telecomunicazioni Spaziali, Milan, Italy) Radio Science (ISSN 0048-6604), vol. 20, Jan.-Feb. 1985, p. 35-49. refs

The results of a comparison among six prediction methods of rain attenuation statistics developed in the United States, Europe, and Japan are presented. The models have been tested through

attenuation at 11.6 GHz and rainfall data collected in Italy at Fucino, Gera Lario, and Spino d'Adda during the SIRIO experiment during 1978-1982. Author

A85-23786

INFLUENCE OF SPATIAL VARIABILITY OF SOIL HYDRAULIC CHARACTERISTICS ON SURFACE PARAMETERS OBTAINED FROM REMOTE-SENSING DATA IN THERMAL INFRARED AND MICROWAVES [INFLUENCE DE LA VARIABILITE SPATIALE DES CARACTERISTIQUES HYDRAULIQUES DES SOLS SUR LES PARAMETRES DE SURFACE OBTENUS A PARTIR DE DONNEES DE TELEDETECTION DANS L'INFRA-ROUGE THERMIQUE ET LES MICRO-ONDES]

Y. BRUNET (Institut National de la Recherche Agronomique, Montfavet, Vaucluse, France) and M. VAUCLIN (Grenoble, Institut de Mecanique, Saint-Martin-d'Heres, Isere, France) IN: Spectral signatures of objects in remote sensing, International Conference, 2nd, Bordeaux, France, September 12-16, 1983, Reports. Versailles, Institut National de la Recherche Agronomique, 1984, p. 771-781. In French. refs

A85-24082

RETRIEVAL OF SNOW WATER EQUIVALENT FROM NIMBUS-7 SMMR DATA EFFECT OF LAND-COVER CATEGORIES AND WEATHER CONDITIONS

M. T. HALLIKAINEN (Helsinki University of Technology, Espoo, Finland) IEEE Journal of Oceanic Engineering (ISSN 0364-9059), vol. OE-9, Dec 1984, p. 372-376 refs

The effect of the four major surface types in Finland (forests, boglands, farmlands, and water or ice) on the microwave brightness temperature of snow-covered areas is investigated. Nimbus-7 Scanning Multichannel Microwave Radiometer (SMMR) data are employed to derive the response of each surface type. An algorithm to retrieve the water equivalent of snow cover from Nimbus-7 SMMR data is tested in different dry snow conditions. Author

A85-25352

AIRBORNE SNOW WATER EQUIVALENT AND SOIL MOISTURE MEASUREMENT USING NATURAL TERRESTRIAL GAMMA RADIATION

T. R. CARROLL and J. C. SCHAAKE, JR. (NOAA, National Weather Service, Minneapolis, MN) IN: Optical engineering for cold environments; Proceedings of the Meeting, Arlington, VA, April 7, 8, 1983. Bellingham, WA, SPIE - The International Society for Optical Engineering, 1983, p. 208-213. refs

Airborne measurements of the natural terrestrial gamma radiation flux near the soil surface are used to infer mean areal snow water equivalent and soil moisture values. Terrestrial gamma radiation data are sensed from a lowflying aircraft over a network of 400 flight lines (each approximately 6 sq/km) in the upper Midwest. The airborne data are used to make real-time airborne snow water equivalent and soil moisture measurements in the region to support the National Weather Service hydrologic forecasting program. Ground-based snow cover data collected along 20 calibration flight lines indicate that airborne snow water equivalent values can be calculated with an RMS error of 0.88 cm. Ground-based soil moisture data collected along 155 calibration flight lines indicate that airborne soil moisture values for the upper 20 cm can be calculated with an RMS error of 3.9 percent soil moisture. Approximately 80 percent of the error is due to airborne instrumentation sensitivity while only 20 percent of the error results from flight line calibration using groundbased soil moisture data. Author

A85-26930

MONITORING AFRICA'S LAKE CHAD BASIN WITH LANDSAT AND NOAA SATELLITE DATA

S. R. SCHNEIDER, D. F. MCGINNIS, JR., and G. STEPHENS (NOAA, National Environmental Satellite Data and Information Service, Washington, DC) International Journal of Remote Sensing (ISSN 0143-1161), vol. 6, Jan 1985, p. 59-73. refs

Data from the Landsat and NOAA polar orbiting satellites are used to analyse the Lake Chad basin in Africa. AVHRR

measurements spanning the November 1981-November 1982 period are used to monitor lake boundaries, vegetation growth and surface temperature patterns. Historical Landsat data from the 1972-1981 period are studied to track changes in lake and basin boundaries. Observations of lake conditions, as viewed from satellites, are related to the recent climate record. Author

A85-29218*

National Aeronautics and Space Administration
Goddard Space Flight Center, Greenbelt, Md
DETECTION OF LOWLAND FLOODING USING ACTIVE MICROWAVE SYSTEMS

J. P. ORMSBY, B. J. BLANCHARD (NASA, Goddard Space Flight Center, Hydrological Sciences Branch, Greenbelt, MD), and A. J. BLANCHARD (Texas A&M University, College Station, TX) Photogrammetric Engineering and Remote Sensing (ISSN 0099-1112), vol. 51, March 1985, p. 317-328. refs

The development of radar systems with longer wavelengths (greater than 3 cm) has provided new possibilities regarding the utilization of radar. Thus, it has been found that the interpretation of data from radar images can be a valuable classification aid for applications related to water resources. In the case of an interpreter accustomed to photographic or visible/infrared images, an evaluation of radar images presents some problems, because the radar is sensing a set of surface characteristics which have little influence on visible/infrared systems. Detectable features in radar images caused by differences in dielectric properties are usually associated with the water content of either soils or vegetation. The present paper is concerned with studies which were initiated in 1976. The studies had the objective to define the magnitude of the effects on radar data caused by flood waters under vegetation. The obtained results indicate the feasibility to detect flood conditions beneath a forest canopy, and to obtain an improved definition of the land-water boundary. G.R.

A85-29219

REMOTE SENSING OF WATER QUALITY IN THE NEUSE RIVER ESTUARY, NORTH CAROLINA

S. KHORRAM and H. M. CHESHIRE (North Carolina State University, Raleigh, NC) Photogrammetric Engineering and Remote Sensing (ISSN 0099-1112), vol. 51, March 1985, p. 329-341. Research supported by the University of North Carolina. refs

A85-29220

MONITORING WATER QUALITY CONDITIONS IN A LARGE WESTERN RESERVOIR WITH LANDSAT IMAGERY

J. P. VERDIN (U.S. Bureau of Reclamation, Denver, CO) Photogrammetric Engineering and Remote Sensing (ISSN 0099-1112), vol. 51, March 1985, p. 343-353. refs

Seven Landsat multispectral scanner scenes were processed to portray water quality conditions in Flaming Gorge Reservoir, a large Bureau of Reclamation impoundment in Utah and Wyoming. Concurrent surface sampling data were available for four of the seven scenes. A deterministic approach employing an atmospheric radiative transfer model was used to account for effects of sun angle and atmosphere in the Landsat imagery. This permitted the development of water quality predictive regression equations using surface sampling data from all four dates at once. It also permitted the estimation of reservoir conditions for the three scenes for which no concurrent surface sampling was carried out. The two equations, providing estimates of Secchi transparency and chlorophyll a concentration, were used to monitor the year-to-year spatial variation of trophic zones in the reservoir. Author

A85-29906

DETERMINATION OF WATER SURFACES IN NORTHWEST BOHEMIA ON THE BASIS OF SATELITE DATA [OPREDELENIE VODNYKH POVERKHNOSTEI V SEVERO-ZAPADNOI CHEKHII PO SPUTNIKOVYIM DANYM]

K. KIRKHNER, I. A. KOLARZH, and S. PLAKHI (Ceskoslovenska Akademie Ved, Geograficky Ustav, Brno; Ceske Vysoke Ucení Technické, Prague, Czechoslovakia) Issledovanie Zemli iz Kosmosa (ISSN 0205-9614), Jan.-Feb 1985, p. 47-51. In Russian.

N85-16273*# National Aeronautics and Space Administration. Goddard Space Flight Center, Greenbelt, Md.

SIMULTANEOUS OCEAN CROSS-SECTION AND RAINFALL MEASUREMENTS FROM SPACE WITH A NADIR-POINTING RADAR

R. MENEGHINI and D. ATLAS Nov. 1984 46 p refs (NASA-TM-86167; NAS 1.15.86167) Avail: NTIS HC A03/MF A01 CSCL 04B

A method to determine simultaneously the rainfall rate and the normalized backscattering cross section of the surface was evaluated. The method is based on the mirror reflected power, $p_{sub m}$ which corresponds to the portion of the incident power scattered from the surface to the precipitation, intercepted by the precipitation, and again returned to the surface where it is scattered a final time back to the antenna. Two approximations are obtained for $P_{sub m}$ depending on whether the field of view at the surface is either much greater or much less than the height of the reflection layer. Since the dependence of $P_{sub m}$ on the backscattering cross section of the surface differs in the two cases, two algorithms are given by which the path averaged rain rate and normalized cross section are deduced. The detectability of $P_{sub m}$, the relative strength of other contributions to the return power arriving simultaneous with $P_{sub m}$, and the validity of the approximations used in deriving $P_{sub m}$ are discussed E.A.K.

N85-17216*# Jet Propulsion Lab., California Inst of Tech., Pasadena.

DEFORESTATION, FLOODPLAIN DYNAMICS, AND CARBON BIOGEOCHEMISTRY IN THE AMAZON BASIN

M. L. BRYAN, T. DUNNE (Washington Univ., Seattle), J. RICHEY (Washington Univ., Seattle), J. MELACK (California Univ., Santa Barbara), D. SIMONETT (California Univ., Santa Barbara), and G. WOODWELL (Marine Biological Lab., Woods Hole, Mass.) In its The SIR-B Sci. Invest Plan 7 p 1 Jul. 1984 refs Avail: NTIS HC A10/MF A01 CSCL 171

Three aspects of the physical geographic environment of the Amazon Basin are considered. (1) deforestation and reforestation, (2) floodplain dynamics, and (3) fluvial geomorphology. Three independent projects are coupled in this experiment to improve the in-place research and to ensure that the Shuttle Imaging Radar-B (SIR-B) experiment stands on a secure base of ongoing work. Major benefits to be obtained center on: (1) areal and locational information, (2) data from various depression angles, and (3) digital radar signatures. Analysis will be conducted for selected sites to define how well SIR-B data can be used for: (1) definition of extent and location of deforestation in a tropical moist forest, (2) definition and quantification of the nature of the vegetation and edaphic conditions on the (floodplain) of the Amazon River, and (3) quantification of the accuracy with which the geometry and channel shifting of the Amazon River may be mapped using SIR-B imagery in conjunction with other remote sensing data R.J.F.

N85-17239*# Kansas Univ Center for Research, Inc., Lawrence.

INFORMATION FOR SPACE RADAR DESIGNERS: REQUIRED DYNAMIC RANGE VS RESOLUTION AND ANTENNA CALIBRATION USING THE AMAZON RAIN FOREST

R. K. MOORE and V. S. FROST In JPL The SIR-B Sci. Invest. Plan 3 p 1 Jul. 1985 refs

Avail: NTIS HC A10/MF A01 CSCL 02F

Calibration of the vertical pattern of the antennas for the SEASAT scatterometer was accomplished using the nearly-uniform radar return from the Amazon rain forest. A similar calibration will be attempted for the SIR-B antenna. Thick calibration is important to establish the radiometric calibration across the swath of the SIR-B, and the developed methodology will provide an important tool in the evaluation of future spaceborne imaging radars. This calibration was made by the very-wide-beam SEASAT scatterometer antennas because at 14.65 GHz the scattering coefficient of the rain forest is almost independent of angle of incidence. It is expected that the variation in scattering coefficient for the rain forest across the relatively narrow vertical beam of the SIR-B will be very small; even at L band the forest should be essentially impenetrable for radar signals, the volume scatter from the treetops will predominate as at higher frequencies. The basic research elements include. (1) examination of SIR-B images over the rain forest to establish the variability of the scattering coefficient at finer resolutions than that of the SEASAT scatterometer; (2) analysis of the variability of SIR-B data detected prior to processing for either azimuth compression or; possibly, range compression so that averages over relatively large footprints can be used; (3) processing of data of the form of (2) using algorithms that can recover the vertical pattern of the antenna. E.A.K.

N85-19221*# Wisconsin Univ., Madison. Dept of Meteorology. **RESOLUTION ENHANCEMENT OF MULTICHANNEL MICROWAVE IMAGERY FROM THE NIMBUS-7 SMMR FOR MARITIME RAINFALL ANALYSIS**

W. S. OLSON, C. L. YEH, J. A. WEINMAN, and R. T. CHIN 1985 29 p refs

(Contract NAGW-380)

(NASA-CR-174367; NAS 1.26:174367) Avail: NTIS HC A03/MF A01 CSCL 20N

A restoration of the 37, 21, 18, 10.7, and 6.6 GHz satellite imagery from the scanning multichannel microwave radiometer (SMMR) aboard Nimbus-7 to 22.2 km resolution is attempted using a deconvolution method based upon nonlinear programming. The images are deconvolved with and without the aid of prescribed constraints, which force the processed image to abide by partial a priori knowledge of the high-resolution result. The restored microwave imagery may be utilized to examine the distribution of precipitating liquid water in marine rain systems. Author

N85-19568*# South Dakota School of Mines and Technology, Rapid City. Inst. of Atmospheric Sciences.

RAIN VOLUME ESTIMATION OVER AREAS USING SATELLITE AND RADAR DATA Semiannual Report, 1 Jul. - 31 Dec. 1984

A. A. DONEAUD and T. H. VONDERHAAR 15 Mar 1985 25 p (Contract NAG5-386)

(NASA-CR-174434; NAS 1.26:174434) Avail: NTIS HC A02/MF A01 CSCL 04B

An investigation of the feasibility of rain volume estimation using satellite data following a technique recently developed with radar data called the Arera Time Integral was undertaken. Case studies were selected on the basis of existing radar and satellite data sets which match in space and time. Four multicell clusters were analyzed. Routines for navigation remapping and smoothing of satellite images were performed. Visible counts were normalized for solar zenith angle. A radar sector of interest was defined to delineate specific radar echo clusters for each radar time throughout the radar echo cluster lifetime. A satellite sector of interest was defined by applying small adjustments to the radar sector using a manual processing technique. The radar echo area, the IR maximum counts and the IR counts matching radar echo areas were found to evolve similarly, except for the decaying phase

of the cluster where the cirrus debris keeps the IR counts high
Author

N85-20606# Colorado Univ., Boulder. Cooperative Inst. for Research in Environmental Sciences.

LAKE ICE OCCURRENCE AS A POSSIBLE DETECTOR OF ATMOSPHERIC CO₂ EFFECTS ON CLIMATE Progress Report, 1 Dec. 1983 - 30 Nov. 1984

R. G. BARRY Nov 1984 5 p refs

(Contract DE-AC02-83ER-60106)

(DE85-002951, DOE/ER-60106/1) Avail NTIS HC A02/MF A01

Temporal patterns of the freeze-up and break-up of lakes in middle and high latitudes were analyzed to determine the usefulness of such data as an integrative index of thermal trends that are expected as a result of CO₂ induced climatic effects. High correlations exist between daily mean air temperatures during approximately 80 days prior to these events and the freeze-up/break-up dates, confirming the value of lake ice data as an index of thermal regime during the transition seasons. A change in freeze-up date of plus or minus 6 (plus or minus 4) days corresponds to a plus or minus 1(0)C temperature change. Break-up dates show lower correlations although decadal averages show greater coherence than for freeze-up. A spatial array of lake-ice conditions monitored by satellite could serve as a useful tool for early detection of possible CO₂-induced perturbations.

DOE

07

DATA PROCESSING AND DISTRIBUTION SYSTEMS

Includes film processing, computer technology, satellite and aircraft hardware, and imagery.

A85-20084

RING STRUCTURES OBSERVED ON SPACE RADAR IMAGES OF THE EARTH [KOL'TSEVYE STRUKTURY NA RADIOLOKATSIONNYKH IZOBRAZHENIIAKH ZEMLI IZ KOSMOSA]

V. P. SHESTOPALOV, I. U. G. SPIRIDONOV, A. I. KALMYKOV, and A. P. PICHUGIN (Akademiia Nauk Ukrainskoi SSR, Institut Radiofiziki i Elektroniki, Kharkov, Ukrainian SSR) Akademiia Nauk SSSR, Doklady (ISSN 0002-3264), vol. 279, no. 4, 1984, p. 835-837. In Russian.

Remote-sensing images of the Western Sahara obtained with the Cosmos-1500 3-cm-wavelength sidelooking radar were compared with multispectral photographs of the same territory. The radar, but not the multispectral system, observed a ring structure with a diameter of about 35 km at 21 deg N, 11 deg W. It is suggested that this structure is hidden by sand and is therefore not observable by optical imaging. The implication of this finding for the geological interpretation of space remote-sensing images is discussed in detail.

B J.

A85-20572

THE INTEGRATED USE OF DIGITAL CARTOGRAPHIC DATA AND REMOTELY SENSED IMAGERY

D. R. CATLOW (Natural Environment Research Council, Thematic Information Service, Swindon, Wilts., England), R. J. PARSELL, and B. K. WYATT (Natural Environment Research Council, Institute of Terrestrial Ecology, Bangor, Wales) Earth-Oriented Applications of Space Technology (ISSN 0277-4488), vol. 4, no. 4, 1984, p. 255-260. refs

Recent work carried out at the Thematic Information Service of the UK Natural Environment Research Council is described. Digital cartographic data is integrated with remotely sensed imagery by a technique involving vector data transfer and the conversion of the cartographic data into a raster format. The encoded raster

cartographic data can be used, in the form of digital map overlays, to assess the success of any geometrical correction of the imagery, improve visual interpretation of the imagery; evaluate the results of a thematic classification; and in a more integrated form, to define areas of interest and stratify a classification. An example of the combined use of digital cartographic data and Landsat MSS imagery by scientists from the Institute of Terrestrial Ecology for monitoring land cover change in mid Wales is given. M D.

A85-20750

AUTOMATIC PRODUCTION OF DTM DATA USING DIGITAL OFF-LINE TECHNIQUE

B. MAKAROVIC (International Institute for Aerial Survey and Earth Sciences, Enschede, Netherlands) (International Society for Photogrammetry and Remote Sensing, Congress, Rio de Janeiro, Brazil, June 1984) ITC Journal (ISSN 0303-2434), no. 2, 1984, p. 135-141. refs

A review is presented of the state-of-the-art in digital off-line technique for production of DTMs. The main process stages, their interactions and operations are outlined. Data structure, strategy, algorithms and techniques of image matching are strongly interrelated. Performance can be improved by optimizing the overall process and by carrying out some pre- and post-processing operations. Moreover, use can be made of multiple sets of image data, multi-stage strategy, external data and collective processing.

Author

A85-21048* Jet Propulsion Lab., California Inst. of Tech., Pasadena.

CALCULATION OF THERMAL INERTIA FROM DAY-NIGHT MEASUREMENTS SEPARATED BY DAYS OR WEEKS

A. B. KAHLE and R. E. ALLEY (California Institute of Technology, Jet Propulsion Laboratory, Pasadena, CA) Photogrammetric Engineering and Remote Sensing (ISSN 0099-1112), vol. 51, Jan. 1985, p. 73-75 NASA-supported research. refs

The calculation of the thermal inertia of an area from remotely sensed data involves the measurement of the surface albedo and the determination of the diurnal temperature range of the surface in image format. The temperature-range image is calculated from surface thermal radiance measured as near as possible to the time of maximum surface temperature and (predawn) surface minimum temperature. Ordinarily, both surface-temperature images are measured within the same 12-hour period. If this is impossible, then the measurement of the predawn surface radiance within a 36-hour period has been considered to be adequate, although less satisfactory. The problems arising in connection with the impossibility to conduct measurements within the same 12-hour period are studied, and suggestions are made for cases in which only relative thermal inertia across an area is required. In such cases investigators should consider using the best day-night temperature pairs available, even if not acquired within a 12 to 36 hour period.

G R.

A85-21138

ON THE SEPARABILITY OF VARIOUS CLASSES FROM THE GOES VISIBLE AND INFRARED DATA

A. A. TSONIS (Department of the Environment, Atmospheric Environment Service, Downsview, Ontario, Canada) Journal of Climate and Applied Meteorology (ISSN 0733-3021), vol. 23, Oct. 1984, p. 1393-1410. refs

The spatial and spectral characteristics of the GOES visible and infrared images are examined. From that analysis, a scheme is developed which identifies and separates the following classes: clear skies/no snow cover, clear skies/snow cover and clouds. Clouds are then classified as high or low broken clouds and overcast. The scheme is tested for various weather situations. Comparison of the classification results with reports from ground synoptic stations and maps reflects an average accuracy of approximately 72 percent, and a higher accuracy (approximately 87 percent) when high or low broken clouds and overcast are considered as one class (i.e., clouds). The differentiation between clouds and snow, or no snow-covered ground has been found to

07 DATA PROCESSING AND DISTRIBUTION SYSTEMS

be very satisfactory, even in cases of temperature inversions.

Author

A85-22678* Rochester Inst. of Tech., N. Y.

COMPARISON OF MODELLED AND EMPIRICAL ATMOSPHERIC PROPAGATION DATA

J. R. SCHOTT and J. D. BIEGEL (Rochester Institute of Technology, Rochester, NY) IN: Infrared technology IX; Proceedings of the Ninth Annual Meeting, San Diego, CA, August 23-25, 1983 Bellingham, WA, SPIE - The International Society for Optical Engineering, 1983, p. 45-52. Previously announced in STAR as N83-32146. refs

(Contract NAS5-27323)

The radiometric integrity of TM thermal infrared channel data was evaluated and monitored to develop improved radiometric preprocessing calibration techniques for removal of atmospheric effects. Modelled atmospheric transmittance and path radiance were compared with empirical values derived from aircraft underflight data. Aircraft thermal infrared imagery and calibration data were available on two dates as were corresponding atmospheric radiosonde data. The radiosonde data were used as input to the LOWTRAN 5A code which was modified to output atmospheric path radiance in addition to transmittance. The aircraft data were calibrated and used to generate analogous measurements. These data indicate that there is a tendency for the LOWTRAN model to underestimate atmospheric path radiance and transmittance as compared to empirical data. A plot of transmittance versus altitude for both LOWTRAN and empirical data is presented.

A.R.H

A85-23144* National Aeronautics and Space Administration, Langley Research Center, Hampton, Va.

EVALUATION OF AN EXPERIMENTAL SYSTEM FOR SPACEBORNE PROCESSING OF MULTISPECTRAL IMAGE DATA

B. D. MEREDITH, N. D. MURRAY (NASA, Langley Research Center, Hampton, VA), R. J. LABAUGH (Martin Marietta Aerospace, Denver, CO), and J. V. AANSTOOS (Research Triangle Institute, Research Triangle Park, NC) Optical Engineering (ISSN 0091-3286), vol. 24, Jan.-Feb. 1985, p. 189-196. refs

An experimental data processing system has been developed to demonstrate the feasibility of processing high speed, multispectral image data on board the spacecraft. The design incorporates real-time processing with adaptable operation in an expandable architecture. The experimental hardware is coupled to test support and computing equipment to provide a laboratory tool for evaluating and demonstrating each of the processing functions as well as the overall system operation. An evaluation of the high speed processor was conducted to ensure that the desired system throughput was achieved without sacrificing processing accuracy. A description of the system is presented along with the results of the test and evaluation activity. Author

A85-23679

SEASAT - A KEY ELEMENT OF THE EARTHNET PROGRAMME

L. MARELLI (ESA, European Space Research Institute, Frascati, Italy) IN: Satellite microwave remote sensing Chichester, West Sussex, England, Ellis Horwood, Ltd., 1983, p. 59-65.

The development and some features of SEASAT are discussed. The goals of the EARTHNET program of which SEASAT is a part are first outlined, and the pioneering days of SEASAT are recalled. The development of the SAR processing element is reviewed, and the SEASAT evaluation activities are summarized. Finally, some programs based on SEASAT are briefly described. C.D

A85-23684

SOME PROPERTIES OF SAR SPECKLE

B. C. BARBER (Royal Aircraft Establishment, Farnborough, Hants., England) IN: Satellite microwave remote sensing. Chichester, West Sussex, England, Ellis Horwood, Ltd., 1983, p. 129-145. refs

The power spread function of a conventional digital SAR processor is derived, including the phase terms. It is shown that even for scatterers embedded in a flat surface the resulting image speckle has circular normal first-order statistics. It is concluded that surface roughness may have little effect on the type of first-order statistics of speckle, in contrast to the speckle obtained in optical imagery. An example is given where the second order statistics in the azimuth direction do seem to be affected by the scatterer, the Doppler spectrum being peaked around the center of the synthetic aperture. C.D.

A85-23689

THE CANADIAN SAR EXPERIENCE

R. K. RANEY (Canada Centre for Remote Sensing, Radarsat Project Office, Ottawa, Canada) IN: Satellite microwave remote sensing. Chichester, West Sussex, England, Ellis Horwood, Ltd., 1983, p. 223-234. refs

The Canadian experience with aircraft and spacecraft SAR, as demonstrated in the SEASAT and SURSAT projects, is briefly described, and the digital processing of the SAR data is described. The results of the projects demonstrated the technical feasibility of a spaceborne SAR and ground reception and processing system capable of providing high-resolution images from space. It is concluded that spaceborne SAR data can significantly assist meeting Canada's needs for surveillance information by providing information on ice coverage, type, and drift. Digital techniques for processing SAR data is found to offer significantly higher quality data and processing flexibility than optical techniques. The future of the Canadian SAR program is discussed, with emphasis on the RADARSAT project. C.D.

A85-23769

INVENTORY OF GEOGRAPHICALLY HOMOGENEOUS ZONES BY SPECTRAL MODELING OF DIACHRONIC METEOSAT ALBEDO OR COMBINED ALBEDO/THERMAL-CHANNEL DATA - APPLICATIONS TO THE MAGHREB AND TO SAHELIAN AFRICA [L'INVENTAIRE DES ZONES HOMOGENES GEOGRAPHIQUES PAR MODELISATION SPECTRALE DE DONNEES METEOSAT DIACHRONIQUES DANS L'ALBEDO OU COMBINEES AVEC LE CANAL THERMIQUE - APPLICATIONS AU MAGHREB ET A L'AFRIQUE SAHELIENNE]

C. BARDINET (Ecole Normale Supérieure de Jeunes Filles, Paris; Paris, Ecole Nationale Supérieure des Mines, Valbonne, Alpes-Maritimes, France), M. BENARD, D. CANO, and J. M. MONGET (Paris, Ecole Nationale Supérieure des Mines, Valbonne, Alpes-Maritimes, France) IN: Spectral signatures of objects in remote sensing; International Conference, 2nd, Bordeaux, France, September 12-16, 1983, Reports. Versailles, Institut National de la Recherche Agronomique, 1984, p. 495-502. In French. refs

A85-23779

RADARGRAMMETRY OF SHUTTLE IMAGING RADAR-B EXPERIMENT

S. S. C. WU (U.S. Geological Survey, Flagstaff, AZ) IN: Spectral signatures of objects in remote sensing; International Conference, 2nd, Bordeaux, France, September 12-16, 1983, Reports. Versailles, Institut National de la Recherche Agronomique, 1984, p. 661-665.

The future benefits of the Shuttle Imaging Radar-B (SIR-B) experiment, which is a part of the OSTA-3 earth observation experiments scheduled by NASA for August 1984, are examined. SIR-B will allow the area of interest to be viewed from six incidence angles ranging from 15 to 60 deg with resolution ranging between 58 and 17 m from side to side of the surveyed area. By modifying the plotter software, stereo models using SIR-B images are expected to be established. Standard errors of position measurements are predicted to range from 12 to 76 m, depending

on the combination of different incidence angles. Maps at scales of 1:125,000 to 1:50,000 are anticipated, thus meeting the National Map Accuracy standards. Optimum radar incidence angles and illumination geometries for terrestrial and extraterrestrial missions with side-looking radar are determined. L.T.

A85-23783* National Aeronautics and Space Administration. Goddard Space Flight Center, Greenbelt, Md
REGIONAL ANALYSIS FROM DATA FROM HETEROGENEOUS PIXELS - REMOTE SENSING OF TOTAL DRY MATTER PRODUCTION IN THE SENEGALESE SAHEL

C. J. TUCKER (NASA, Goddard Space Flight Center, Earth Resources Branch, Greenbelt, MD), C. VANPRAET, A. GASTON, and E. BOERWINKEL (Ecosystems Pastoraux, Dakar, Senegal) IN: Spectral signatures of objects in remote sensing; International Conference, 2nd, Bordeaux, France, September 12-16, 1983, Reports. Versailles, Institut National de la Recherche Agronomique, 1984, p. 739-747. refs

Nine predominantly cloud-free NOAA-7 advanced very high resolution radiometer images were obtained during a three-month period during the 1981 rainy season in the Sahel of Senegal. The 0.55-0.68 and 0.725-1.10-micron channels were used to form the normalized difference green leaf density vegetation index and the 11.5-12.5-micron channel was used as a cloud mask for each of the nine images. Changes in the normalized difference values among the various dates were closely associated with precipitation events. Six of the images spanning an eight-week period were used to generate a cumulative integrated index. Ground biomass samplings in the 30,000 sq km study area were used to assign total dry biomass classes to the cumulative index. Author

A85-23788
INDEPENDENT VARIABLES IN REMOTE SENSING AS A FUNCTION OF LANDCOVER TYPE [NOTION DE VARIABLES INDEPENDANTES EN TELEDETECTION EN FONCTION DU TYPE DE PAYSAGE]

C. LALLEMAND and G. LEGENDRE (Institut Francais du Petrole, Rueil-Malmaison, Hauts-de-Seine, France) IN: Spectral signatures of objects in remote sensing; International Conference, 2nd, Bordeaux, France, September 12-16, 1983, Reports. Versailles, Institut National de la Recherche Agronomique, 1984, p. 801-814. In French

An analysis of the spectral signatures of different homogeneous areas of a digital image, recorded by the Landsat IV Thematic Mapper (TM) scanner, is considered. The area that is studied is north of Memphis, TN. Statistics relative to the Karhunen-Loeve transformation are studied for the following types of landscape: forests, water (rivers and lakes), towns, agricultural areas, swamp areas, and bare soil. The relative responses for each type of area and each wavelength are calculated, and correlations between the seven spectral bands of the TM image are discussed. It is shown that the large number of variables in the TM makes simultaneous comparisons between wavelengths difficult. The statistics are used to establish rules for choosing wavelength combinations that will lead to uncorrelated variables for images recorded by the Landsat TM and MSS scanners. M.D.

A85-23791
INTERPRETATION OF THERMAL INFRARED DATA TO AUGMENT SPECTRAL SIGNATURES [INTERPRETATION DE DONNEES INFRAROUGE THERMIQUES POUR PRECISER LES SIGNATURES SPECTRALES]

J. PRICE (U.S. Department of Agriculture, Hydrology Laboratory, Beltsville, MD) IN: Spectral signatures of objects in remote sensing; International Conference, 2nd, Bordeaux, France, September 12-16, 1983, Reports. Versailles, Institut National de la Recherche Agronomique, 1984, p. 841-848. refs

Advanced Very High Resolution Radiometer thermal IR data from NOAA satellites are evaluated in conjunction with visible-to-near IR reflectances, meteorological data, and land use maps. A quantitative analysis of IR data for surface energy balance yields reasonable results which are consistent with earlier work. An examination of Landsat data and conventional land use maps

indicates that at the hundreds-of-km scale of the NOAA image maps, variability is associated with topography, differences in soil characteristics and farming practices, cities and residential areas, etc. The inclusion of these factors in the analysis will require the extraction of map-type data from large, centralized data bases. O.C.

A85-24258
RESOURCE MEASUREMENT SYSTEM

A. MARTENS, K. KRECKEL, and R. MCHAIL (Bausch and Lomb, Inc., Rochester, NY) IN: Airborne reconnaissance VII, Proceedings of the Meeting, San Diego, CA, August 23, 24, 1983. Bellingham, WA, SPIE - The International Society for Optical Engineering, 1983, p. 68-70.

The Resource Measurement System (RMS) has been developed to aid in the gathering of quantitative data from thematic map images on the basis of image analysis and computer graphics technologies. The RMS employs a popular personal computer and its software, thereby maximizing its utility. RMS operates in semiautomatic fashion, with the user tracing the outlines of features or objects of interest in photographs, maps, or drawings placed over a digitizing table. Point locations of the boundaries of these features are stored in the system memory during the tracing process, and RMS then acts on these inputs to generate a variety of planimetric dimensional measurements of the features in question. O.C.

A85-24277
MULTISPECTRAL DATA COMPRESSION USING STAGGERED DETECTOR ARRAYS

R. T. GRAY and B. R. HUNT (Arizona, University, Tucson, AZ) IN: Applications of digital image processing VI; Proceedings of the Meeting, San Diego, CA, August 23-26, 1983. Bellingham, WA, SPIE - The International Society for Optical Engineering, 1983, p. 54-59. refs
 (Contract AF-AFOSR-81-0170)

A multispectral image data compression scheme has been investigated in which a scene is imaged onto a detector array whose elements vary in spectral sensitivity. The elements are staggered such that the scene is undersampled within any single spectral band, but is sufficiently sampled by the total array. Compression thus results from transmitting only one spectral component of a scene at any given array coordinate. High-resolution reconstructions are achieved by a space-variant minimum-mean-square spectral regression estimate of the missing pixels of each band from the adjacent samples of other bands. Digital simulations show that spectral regressions of mosaic array data provide reconstruction errors comparable to second-order differential pulse code modulation (DPCM). When the mosaic data is itself encoded by DPCM, the accuracy of spectral regression is superior to direct DPCM for equivalent bit rates. Author

A85-24285
DETERMINATION OF VISUAL RANGE FROM LANDSAT DATA
 R. S. DENNEN (U.S. Department of the Interior, Service Center, Denver, CO) IN: Applications of digital image processing VI; Proceedings of the Meeting, San Diego, CA, August 23-26, 1983. Bellingham, WA, SPIE - The International Society for Optical Engineering, 1983, p. 148-156. refs

The present investigation has the objective to establish a procedure for estimating baseline visibility on the basis of an employment of Landsat radiometric data. The visibility estimates considered make use of the relation between visibility and the contrast an observer would see between two objects. Objects can no longer be distinguished, when the contrast between two objects is reduced to some threshold value. Attention is given to a definition of visibility, satellite radiance, atmospheric radiance measurements, ground measurements, Landsat MSS data, aircraft data, and the determination of the scattering constants. The relationships and the method developed are based on a single scattering model for the in-welling radiance at the airborne sensor. G.R.

A85-24521*

EROS MAIN IMAGE FILE - A PICTURE PERFECT DATABASE FOR LANDSAT IMAGERY AND AERIAL PHOTOGRAPHY

R. F. JACK (NASA/University of Kentucky, Technology Applications Program, Lexington, KY) Database (ISSN 0162-4105), vol. 7, Feb. 1984, p. 35-52.

The Earth Resources Observation System (EROS) Program was established by the U.S. Department of the Interior in 1966 under the administration of the Geological Survey. It is primarily concerned with the application of remote sensing techniques for the management of natural resources. The retrieval system employed to search the EROS database is called INORAC (Inquiry, Ordering, and Accounting). A description is given of the types of images identified in EROS, taking into account Landsat imagery, Skylab images, Gemini/Apollo photography, and NASA aerial photography. Attention is given to retrieval commands, geographic coordinate searching, refinement techniques, various online functions, and questions regarding the access to the EROS Main Image File. G R

A85-24740

DRAMATIC CONTRAST BETWEEN LOW CLOUDS AND SNOW COVER IN DAYTIME 3.7 MICRON IMAGERY

S. Q. KIDDER (Illinois State Water Survey, Champaign, Illinois, University, Urbana, IL) and H.-T. WU (Illinois, University, Urbana, IL) Monthly Weather Review (ISSN 0027-0644), vol. 112, Nov. 1984, p. 2345, 2346 (Contract NSF ATM-83-05502)

A85-25350* National Aeronautics and Space Administration. Goddard Space Flight Center, Greenbelt, Md.

OBSERVATIONS OF THE EARTH USING NIGHTTIME VISIBLE IMAGERY

J. L. FOSTER (NASA, Goddard Space Flight Center, Earth Survey Applications Div., Greenbelt, MD) IN: Optical engineering for cold environments; Proceedings of the Meeting, Arlington, VA, April 7, 8, 1983. Bellingham, WA, SPIE - The International Society for Optical Engineering, 1983, p. 187-193. refs

The earth as viewed from space in visible light at night reveals some features not easily discernible during the day such as aurora, forest fires, city lights and gas flares. In addition, those features having a high albedo such as snow and ice can be identified on many moonlit nights nearly as well as they can in sunlight. The Air Force DMSP satellites have been operating in the visible wavelengths at night since the mid 1960s. Most all other satellites having optical sensors are incapable of imaging at night. Imaging systems having improved light sensitivity in the visible portion of the spectrum should be considered when planning future earth resources satellite missions in order to utilize nighttime as well as daytime visual observations. Author

A85-25653

EFFECT OF METEOROLOGICAL CONDITIONS ON THE CHARACTERISTICS OF SPACE RADAR IMAGES OF THE EARTH SURFACE [VLIANIE METEOSLOVIV NA KHAKTERISTIKI RADIOLOKATSIONNYKH IZOBRAZHENII ZEMNOI POVERKHNOSTI IZ KOSMOSA]

IU. G. SPIRIDONOV and A. P. PICHUGIN (Akademiia Nauk Ukrainskoi SSR, Institut Radiofiziki i Elektroniki, Kharkov, Ukrainian SSR) Issledovanie Zemli iz Kosmosa (ISSN 0205-9614), Nov.-Dec. 1984, p. 21-27. In Russian. refs

A theoretical study of the effect of meteorological conditions on the character of space radar images of the earth surface is presented with reference to the sidelooking radar aboard the Cosmos-1500 satellite. It is shown that, at a wavelength of 3-cm, cloud cover has practically no effect on the determination of surface characteristics. It is concluded that only distortions due to zones of precipitation with an intensity exceeding 20 mm/h should be considered in the interpretation of radar images of the earth surface. B.J.

A85-25660

FEATURES OF THE DIGITAL PROCESSING OF RADAR IMAGES OBTAINED WITH THE SIDELOOKING RADAR OF THE COSMOS-1500 SATELLITE [OSOBENNOSTI TSIFROVOI OBRABOTKI RADIOIZOBRAZHENII, POLUCHENNYKH RLS BO ISZ 'KOSMOS-1500']

A. P. PICHUGIN, L. V. ELENSKII, V. B. EFIMOV, A. I. KALMYKOV, and A. S. KUREKIN (Akademiia Nauk Ukrainskoi SSR, Institut Radiofiziki i Elektroniki, Kharkov, Ukrainian SSR) Issledovanie Zemli iz Kosmosa (ISSN 0205-9614), Nov.-Dec. 1984, p. 82-90. In Russian. refs

A description is given of the method for the digital processing of radar remote-sensing images of the earth surface obtained with the Cosmos-1500 sidelooking radar. Processing algorithms for determining the quantitative characteristics of signals reflected from the earth surface are presented, the calibration levels being taken into account; and processing results are given. It is concluded that the proposed processing method can be used to obtain absolute values of the specific effective scattering area and contrasts of radar images, which makes it possible to determine the characteristics of the surfaces studied (e.g., ice layers and surface-wind fields). B.J.

A85-25671

DIGITAL CORRELATION OF IMAGES ALONG QUASI-EPIPOLAR LINES BY SUCCESSIVE APPROXIMATIONS [CORRELATION NUMERIQUE D'IMAGES QUELCONQUES SELON LES LIGNES QUASI-EPIPOLAIRES, PAR APPROXIMATIONS SUCCESSIVES]

G. DE MASSON DAUTUME Societe Francaise de Photogrammetrie et de Teledetection, Bulletin (ISSN 0244-6014), no. 95, 1984, p. 23-32. In French.

Digital procedures for the correlation of remotely sensed images of various types are developed and demonstrated, with a focus on the case of simulated SPOT images. The approach used combines the quasi-epipolar-line preliminary resampling method and elastic-grid technique of de Masson d'Autume (1978 and 1979) to iteratively reduce the differences between two images and is applicable even where no ground-truth control points are available. For images with very different radiometric characteristics a reduction to contour lines is performed to facilitate registration. A series of images demonstrating the application of the procedure to 1:60,000 aerial photographs is shown. T.K.

A85-26294

THE INFLUENCE OF A SCATTERING MEDIUM ON THE QUALITY OF AN OPTICAL IMAGE [VLIANIE RASSEIVAIUSHCHEI SREDY NA KACHESTVO OPTICHESKOGO IZOBRAZHENIIA]

L. P. VOLNISTOVA and A. S. DROFA (Gosudarstvennyi Komitet SSSR po Gidrometeorologii i Kontroliu Prirodnoi Sredy, Institut Eksperimental'noi Meteorologii, Obninsk, USSR) Akademiia Nauk SSSR, Izvestiia, Fizika Atmosfery i Okeana (ISSN 0002-3515), vol. 21, Jan. 1985, p. 50-57. In Russian. refs

Image quality as a function of the scattering-medium layer position relative to the self-luminous object under observation is experimentally studied for purposes of aerial and space photography and television. The laboratory environment consisted of a 6-m long light path with a fluoroplastic film (50 microns thick) as a scattering medium. The experimental data are shown to be in agreement with theoretical conclusions based on the linear-system theory. The large discrepancies among the previous studies on the subject are suggested to be caused by the disregard of distortion of the Fourier-transformed image function resulting from the finiteness of the receiver sighting angle in an optical system. L.T.

A85-26641

EVALUATION OF AIRCRAFT MSS ANALYTICAL BLOCK ADJUSTMENT

J. C. MCGLONE (H. Dell Foster Associates, San Antonio, TX) and E. M. MIKHAIL (Purdue University, West Lafayette, IN) Photogrammetric Engineering and Remote Sensing (ISSN 0099-1112), vol. 51, Feb. 1985, p. 217-225. refs (Contract NOAA-04-7-158-44128)

It is pointed out that most recent work on the geometric rectification of aircraft multispectral scanner (MSS) data has, except for a few instances, involved only single strips. Although there are often good reasons for using only single strips, there are also advantages for an employment of overlapping strips of data. The block adjustment of sidelapping MSS data essentially follows the standard photogrammetric technique of block adjustment. Details concerning the formulation of the adjustment procedure and the evaluation statistics are discussed along with MSS block adjustment tests. The test results are examined, taking into account the results of accuracy tests and precision tests. It is found that the number of sections into which the strips are divided has a significant effect on the accuracy and precision of the adjustment. G.R.

A85-26948

A COMPUTATIONALLY-EFFICIENT MAXIMUM-LIKELIHOOD CLASSIFIER EMPLOYING PRIOR PROBABILITIES FOR REMOTELY-SENSED DATA

P. M. MATHER (Nottingham, University, Nottingham, England) (International Union of Radio Science, International Symposium on Signatures in Remote Sensing, 3rd, Toulouse, France, Jan. 16-20, 1984.) International Journal of Remote Sensing (ISSN 0143-1161), vol. 6, Feb. 1985, p. 369-376

A time-efficient method for evaluating the maximum-likelihood classifier for Landsat MSS data is described and its extension to the case of unequal prior probabilities is summarized, following Shlien (1975) and Strahler (1980). The use of unequal prior probabilities is demonstrated by example and it is shown that, where classes are well separated, then the effect of including prior probability estimates is negligible, but where classes are closely related, then the choice of prior probability estimate can have considerable effect. Author

A85-27827

LAND CLUTTER MODELS FOR RADAR DESIGN AND ANALYSIS

D. K. BARTON (ANRO Engineering Consultants, Lexington, MA) IEEE, Proceedings (ISSN 0018-9219), vol. 73, Feb. 1985, p. 198-204. refs

Land clutter reflectivity has been described in the literature for many types of terrain, viewed by radars of different frequencies at different grazing angles. Significant gaps remain in the published data, especially for ground-based radars viewing the terrain at grazing incidence, and for bistatic situations where one path is at grazing incidence. An analytical model is proposed here which predicts many of the observed trends in data, as functions of range, antenna height, terrain roughness, and radar wavelength. By comparing measured data to the model, better correlations among data sets taken under different conditions can be obtained, and better understanding of the underlying propagation and scattering phenomena achieved. Author

A85-28973

INVESTIGATION OF THE PROPERTIES OF NATURAL OBJECTS BY THE CANONICAL-CORRELATION METHOD [OB IZUCHENII SVOISTV PRIRODNYKH OB'EKTOV METODOM KANONICHESKOI KORRELIATsii]

V. A. KOTTSOV and V. I. IUROV Geodeziia i Kartografiia (ISSN 0016-7126), Jan. 1985, p. 31-34. In Russian.

The canonical-correlation method (CCM) was used to analyze Soyuz-22 multispectral-scanner data obtained in September 1976. A determination was made of the weight coefficients of sampling ensembles of random objects and maximum values of brightness for a maximum value of the canonical-correlation coefficient. It is concluded that the CCM has features which make it suitable for

processing multispectral-scanner data. In particular, the CCM can be used effectively to define the interrelationship between observations in different spectral bands from space and on the ground in reference areas. B.J.

A85-29217

INTEGRATION OF THE SPOT PANCHROMATIC CHANNEL INTO ITS MULTISPECTRAL MODE FOR IMAGE SHARPNESS ENHANCEMENT

G. CLICHE, F. BONN (Sherbrooke, Universite, Sherbrooke, Quebec, Canada), and P. TEILLET (Canada Centre for Remote Sensing, Ottawa, Canada) Photogrammetric Engineering and Remote Sensing (ISSN 0099-1112), vol. 51, March 1985, p. 311-316. Research supported by the Ministere de l'Education du Quebec. refs

By integrating SPOT's panchromatic channel with 10-m resolution into its multiband channels with 20-m resolution, it is possible to produce a high resolution image suitable for photointerpretation. Three different integration algorithms have been tested on simulated SPOT data in order to produce color composite images using SPOT's multispectral mode (three channels) in combination with its 10-m resolution panchromatic mode. The algorithm that gave the best visual results used a different integration formula for the near infrared channel than for the green and red channels, due to the fact that the panchromatic is less correlated with the infrared than with the visible channels. The result looks very similar to a color infrared air-photo with high resolution and good spectral information quality. Author

A85-29221

THE EFFECTS OF IMAGE NOISE ON DIGITAL CORRELATION PROBABILITY

M. EHLERS (Georgia, University, Athens, GA, Hannover, Universitaet, Hanover, West Germany) Photogrammetric Engineering and Remote Sensing (ISSN 0099-1112), vol. 51, March 1985, p. 357-365. refs

In image processing operations related to remote sensing applications, digital techniques are employed as standard methods. However, there is also an increase in the utilization of digital image evaluation in 'conventional' photogrammetry. According to these developments, automatic components are substituted for the human operator. One central problem is related to the automation of the human eye's capability, particularly with respect to stereoscopic viewing and object identification. Techniques for solving this problem are based on the use of correlation techniques. In remote sensing, the main problem is related to the probability of the correlation function, and the identification of homologous points is very difficult. One difficulty is caused by noise contamination. The present investigation is concerned with the effects of image quality on correlation probability, taking into account the determination of the correlation function with the smallest probability of failure. Formulas are presented for correlation probability and image signal-to-noise ratio. G.R.

A85-29913

SEGMENTATION OF HALF-TONE REMOTE-SENSING IMAGES BY THE LEVEL LINES METHOD [SEGMENTATsiiA POLUTONOVYKH AEROKOSMICHESKIKH IZOBRAZHENII METODOM LINII UROVNIA]

D. E. MINSKII and M. M. FEIGIN (Institut Soizgiprovodkhoz, Moscow, USSR) Issledovanie Zemli iz Kosmosa (ISSN 0205-9614), Jan-Feb. 1985, p. 103-112. In Russian. refs

The advantages and disadvantages of segmentation methods for half-tone multicontour images are examined. A mathematical model of a continuous scalar field is used to develop an edge detection method based on the comparative analysis of the boundary and the characteristic grey-scale function. The corresponding algorithm is described along with its implementation in a system for the preliminary interpretation of remote-sensing data for purposes of land-reclamation mapping. A segmentation of a photograph taken from Soyuz-22 is considered as an example. B.J.

07 DATA PROCESSING AND DISTRIBUTION SYSTEMS

A85-29914

THE USE OF A PRIORI ESTIMATION OF THE CONDITIONS OF THE OBSERVATION OF THE EARTH SURFACE FROM SPACE FOR A RATIONAL SELECTION OF THE TIME AT WHICH THE SURVEY IS CONDUCTED [ISPOL'ZOVANIE APRIORNOI OTSENKI USLOVII NABLIUDENIIA ZEMNOI POVERKHNOSTI IZ KOSMOSA DLIYA RATSIONAL'NOGO VYBORA VREMENI PROVEDENIIA S'EMKI]

N. V. KAPITONOVA and E. L. LUKASHEVICH (Gosudarstvennyi Nauchno-Issledovatel'skii i Proizvodstvennyi Tsentr Priroda, USSR) Issledovanie Zemli iz Kosmosa (ISSN 0205-9614), Jan.-Feb. 1985, p. 113-117. In Russian.

N85-16251*# Texas A&M Univ., College Station Dept. of Mathematics.

PROCEEDINGS OF THE SECOND ANNUAL SYMPOSIUM ON MATHEMATICAL PATTERN RECOGNITION AND IMAGE ANALYSIS PROGRAM Final Report, 16 Jul. 1983 - 15 Jul. 1984

L. F. GUSEMAN, JR., Principal Investigator 1984 595 p refs Symp. held in Houston, Tex., 6-8 Jun. 1984 Original contains imagery. Original photography may be purchased from the EROS Data Center, Sioux Falls, S.D. 57198 ERTS (Contract NAS9-16664)

(E85-10056; NASA-CR-171819; NAS 1 26:171819) Avail: NTIS HC A25/MF A01 CSCL 12A

Several papers addressing image analysis and pattern recognition techniques for satellite imagery are presented. Texture classification, image rectification and registration, spatial parameter estimation, and surface fitting are discussed.

N85-16252*# National Aeronautics and Space Administration. Lyndon B. Johnson Space Center, Houston, Tex.

ESTIMATING LOCATION PARAMETERS IN A MIXTURE

R. P. HEYDORN and M. V. MARTIN (Lockheed Engineering and Management Services Co., Inc.) In Texas A and M Univ. Proc. of the 2nd Ann. Symp. on Math. Pattern Recognition and Image Analysis Program p 1-26 1984 refs ERTS

Avail: NTIS HC A25/MF A01 CSCL 12A

The problem of estimating the parameters in a finite mixture is considered. The approach is based on an integral equation formulation of the form $h_{sub t}(x) = \int (limits b \text{ and } a) f(x-y) g_{sub t}(y) dy$ where $h_{sub t}$ is a smoothed version of h and $g_{sub t}$ is a prior function that tends to be concentrated on the translation values. A solution for $g_{sub t}$ that uses the method of regularization and one based on a posterior operator approach is considered. Numerical simulations are presented to bring out some of the estimation and numerical problems of these approaches.

M.G

N85-16254*# Jet Propulsion Lab., California Inst. of Tech., Pasadena

TEXTURE CLASSIFICATION USING AUTOREGRESSIVE FILTERING

W. M. LAWTON and M. LEE In Texas A and M Univ. Proc. of the 2nd Ann. Symp. on Math. Pattern Recognition and Image Analysis Program p 51-99 1984 refs Original contains imagery. Original photography may be purchased from the EROS Data Center, Sioux Falls, S.D. 57198 ERTS

Avail: NTIS HC A25/MF A01 CSCL 12A

A general theory of image texture models is proposed and its applicability to the problem of scene segmentation using texture classification is discussed. An algorithm, based on half-plane autoregressive filtering, which optimally utilizes second order statistics to discriminate between texture classes represented by arbitrary wide sense stationary random fields is described. Empirical results of applying this algorithm to natural and synthesized scenes are presented and future research is outlined. Author

N85-16255*# Houston Univ., Tex. Dept. of Mathematics **BAYESIAN ESTIMATION OF NORMAL MIXTURE PARAMETERS**

C. PETERS In Texas A and M Univ. Proc. of the 2nd Ann. Symp. on Math. Pattern Recognition and Image Analysis Program p 101-114 1984 refs ERTS

Avail: NTIS HC A25/MF A01 CSCL 12A

A Bayesian, or penalized maximum likelihood, approach to the problem of estimating the parameters of a mixture of multivariate normal distributions is proposed. The Bayesian formulation eliminates the problem of singularities in the likelihood function and results in an attractive EM-like procedure. Although the question of consistency is not settled, it is suggested that the proposed method has certain advantages over both the constrained and unconstrained maximum likelihood procedures. Author

N85-16257*# Texas A&M Univ., College Station Center for Approximation Theory.

MULTIVARIATE SPLINE METHODS IN SURFACE FITTING

L. F. GUSEMAN, JR., Principal Investigator and L. L. SCHUMAKER In its Proc. of the 2nd Ann. Symp. on Math. Pattern Recognition and Image Analysis Program p 137-163 1984 refs ERTS

Avail: NTIS HC A25/MF A01 CSCL 12A

The use of spline functions in the development of classification algorithms is examined. In particular, a method is formulated for producing spline approximations to bivariate density functions where the density function is described by a histogram of measurements. The resulting approximations are then incorporated into a Bayesian classification procedure for which the Bayes decision regions and the probability of misclassification is readily computed. Some preliminary numerical results are presented to illustrate the method. Author

N85-16258*# Texas A&M Univ., College Station.

AUTOREGRESSIVE SPECTRAL ESTIMATION FOR TWO DIMENSIONAL TIME SERIES

H. J. NEWTON and W. B. SMITH In its Proc. of the 2nd Ann. Symp. on Math. Pattern Recognition and Image Analysis Program p 165-174 1984 refs ERTS

Avail: NTIS HC A25/MF A01 CSCL 12A

The method of determining asymptotic confidence bands for autoregressive spectra due to Newton and Pagano is extended to the case of data observed in the plane. One Quadrant Autoregressive Models are used as a basis for the method.

Author

N85-16261*# Maryland Univ., College Park. Center for Automation Research

EVIDENCE ACCUMULATION FOR SPATIAL REASONING

T. MATSUYAMA, V. S. S. HWANG, and L. S. DAVIS In Texas A and M Univ. Proc. of the 2nd Ann. Symp. on Math. Pattern Recognition and Image Analysis Program p 245-302 1984 refs Previously announced as N84-29302 Original contains imagery. Original photography may be purchased from the EROS Data Center, Sioux Falls, S.D. 57198 ERTS

Avail: NTIS HC A25/MF A01 CSCL 12A

The evidence accumulation process of an image understanding system is described enabling the system to perform top-down(goal-oriented) picture processing as well as bottom-up verification of consistent spatial relations among objects. Author

N85-16262*# Kansas Univ., Lawrence. Telecommunications and Information Sciences Lab.

POWER SPECTRAL ENSITY OF MARKOV TEXTURE FIELDS

K. S. SHANMUGAN and J. C. HOLTZMAN In Texas A and M Univ. Proc. of the 2nd Ann. Symp. on Math. Pattern Recognition and Image Analysis Program p 303-307 1984 refs ERTS (Contract NAS9-16664)

Avail: NTIS HC A25/MF A01 CSCL 12A

Texture is an important image characteristic. A variety of spatial domain techniques were proposed for extracting and utilizing textural features for segmenting and classifying images. for the

most part, these spatial domain techniques are ad hoc in nature. A markov random field model for image texture is discussed. A frequency domain description of image texture is derived in terms of the power spectral density. This model is used for designing optimum frequency domain filters for enhancing, restoring and segmenting images based on their textural properties Author

N85-16263*# Purdue Univ., Lafayette, Ind. School of Civil Engineering

RECTIFICATION OF SINGLE AND MULTIPLE FRAMES OF SATELLITE SCANNER IMAGERY USING POINTS AND EDGES AS CONTROL

F C PADERES, JR., E M. MIKHAIL, and W FOERSTNER (Stuttgart Univ., West Germany) /n Texas A and M Univ. Proc. of the 2nd Ann. Symp. on Math. Pattern Recognition and Image Analysis Program p 309-400 1984 refs ERTS (Contract NAS9-16664)

Avail: NTIS HC A25/MF A01 CSCL 12A

Rectification of single and overlapping multiple scanner frames produced by such satellite-borne scanners as the LANDSAT MSS was carried out using a newly developed comprehensive parametric model. Tests with both simulated and real image data demonstrate conclusively that this model in general is superior to the widely used polynomial model, and that the simultaneous rectification of overlapping frames using least squares techniques yields a high accuracy than single frame rectification due to the inclusion of tie points between the image frames. Used to control, edges or lines, which are much more likely to be found in images, can replace conventional control points and can easily be implemented into the least squares approach. An efficient algorithm for finding corresponding points in image pairs was developed which can be used for determining tie points between image frames and thus increase the economy of the whole rectification procedure

Author

N85-16264*# National Aeronautics and Space Administration. Earth Resources Labs., Bay St Louis, Miss.

THE INFLUENCE OF THE NUMBER OF GROUND CONTROL POINTS ON THE SCENE-TO-MAP REGISTRATION ACCURACY

D D. DOW /n Texas A and M Univ. Proc. of the 2nd Ann. Symp. on Math. Pattern Recognition and Image Analysis Program p 401-426 1984 refs ERTS

Avail: NTIS HC A25/MF A01 CSCL 05B

The optimum number of ground control points required to rectify a full scene or a portion of a LANDSAT MSS scene was investigated using data from southeastern Louisiana/southwestern Mississippi and eastern Kansas. The ground control points utilized were randomly distributed across the partial or full scene. This work suggests that 24 ground control points are more than adequate to rectify a partial or full scene of LANDSAT MSS data. The error incurred in choosing ground control points representing artificial versus natural features was also studied Author

N85-16265*# Boston Univ., Mass. Dept. of Geography.

IMAGE VARIANCE AND SPATIAL STRUCTURE IN REMOTELY SENSED SCENES

C E. WOODCOCK and A. H. STRAHLER (City Univ. of New York) /n Texas A and M Univ. Proc. of the 2nd Ann. Symp. on Math. Pattern Recognition and Image Analysis Program p 427-465 1984 refs Original contains imagery. Original photography may be purchased from the EROS Data Center, Sioux Falls, S.D. 57198 ERTS

Avail: NTIS HC A25/MF A01 CSCL 05B

Digital images derived by scanning air photos and through acquiring aircraft and spacecraft scanner data were studied. Results show that spatial structure in scenes can be measured and logically related to texture and image variance. Imagery data were used of a South Dakota forest; a housing development in Canoga Park, California, an agricultural area in Mississippi, Louisiana, Kentucky, and Tennessee; the city of Washington, D.C., and the Klamath National Forest. Local variance, measured as the average standard deviation of brightness values within a three-by-three moving window, reaches a peak at a resolution cell size about two-thirds

to three-fourths the size of the objects within the scene. If objects are smaller than the resolution cell size of the image, this peak does not occur and local variance simply decreases with increasing resolution as spatial averaging occurs. Variograms can also reveal the size, shape, and density of objects in the scene. R.S.R.

N85-16266*# SRI International Corp., Menlo Park, Calif. Artificial Intelligence Center.

IMAGE-TO-IMAGE CORRESPONDENCE: LINEAR STRUCTURE MATCHING

G. B. SMITH and H C WOLF /n Texas A and M Univ. Proc. of the 2nd Ann. Symp. on Math. Pattern Recognition and Image Analysis Program p 467-487 1984 refs Original contains imagery. Original photography may be purchased from the EROS Data Center, Sioux Falls, S.D. 57198 ERTS (Contract NAS9-16664; MDA903-83-C-0027)

Avail: NTIS HC A25/MF A01 CSCL 12A

The task of matching images of a scene was examined when images are taken from very different vantage points, when there is considerable scale change, and when the image orientations are unknown. The linear structures in the scene were used as the basis of the correspondence procedure. The problem of describing the linear structures in a manner that is invariant relative to the variations that can occur among images is considered. A method of finding the best description of the linear structures is discussed. Author

N85-16267*# Maryland Univ., College Park.

ANALYSIS OF SUBPIXEL REGISTRATION

C A BERENSTEIN, L N KANAL, D LAVINE, E C. OLSON, and E. SLUD /n Texas A and M Univ. Proc. of the 2nd Ann. Symp. on Math. Pattern Recognition and Image Analysis Program p 489-594 1984 refs Prepared in cooperation with LNK Corp., Silver Spring, Md. ERTS

Avail: NTIS HC A25/MF A01 CSCL 12A

The area of subpixel accuracy in image registration and edge detection was studied. Two main directions of research were pursued, edge detection and matching based on the digital geometry of edges, and random field models for probabilistic analysis of registration error. In the edge detection approach, error bounds and error probabilities were computed using theoretical models. Algorithms were developed and tests on simulated imagery. The methods appear promising for high accuracy edge position estimation and registration, though further refinement of the procedures is required. Using random field models, a statistical measure of the quality of the cross correlation peak as an estimate of the offset between a sensed and a reference image was developed. Simulations were performed to determine the validity of this estimate with real imagery and to study the results of interpolating digital correlation functions to estimate the translation offset to subpixel accuracy Author

N85-17229*# Commonwealth Scientific and Industrial Research Organization, Wembley (Australia)

EVALUATION OF SIR-B IMAGERY FOR GEOLOGIC AND GEOMORPHIC MAPPING, HYDROLOGY, AND OCEANOGRAPHY IN AUSTRALIA

F R HONEY, C. J. SIMPSON (Bureau of Mineral Resources, Canberra, Australia), J. HUNTINGTON, R. HORWITZ, G. BYRNE, and C. NILSSON /n JPL The SIR-B Sci Invest Plan 3 p 1 Jul. 1984 refs

Avail: NTIS HC A10/MF A01 CSCL 17G

The objectives of a study to evaluate the potential of Shuttle Imaging Radar-B (SIR-B) imagery for various applications are outlined. Specific goals include the development of techniques for registration multiple acquisition, varied illumination, and incidence-angle SIR-B imagery, and a model for estimation of the relative contributions to the backscattered radiation of topography, surface roughness, and dielectric and conductivity components; (2) the evaluation of SIR-B imagery for delineation of agricultural lands affected by secondary salinity in the southwest and southeast agricultural regions of Australia, (3) the development of techniques for application of SIR-B imagery for geologic, geomorphologic and

07 DATA PROCESSING AND DISTRIBUTION SYSTEMS

soils mapping and mineral exploration; and (4) the evaluation of the use of SIR-B imagery in determining ocean currents, current shear patterns, internal waves and bottom features for specific locations off the Australian coast. M.G

N85-17242*# National Aeronautics and Space Administration. Goddard Space Flight Center, Greenbelt, Md

AUTOMATIC TERRAIN ELEVATION MAPPING AND REGISTRATION

H. K. RAMAPRIYAN, C. W. MURRAY, J. P. STRONG, and H. W. BLODGET *In JPL The SIR-B Sci. Invest. Plan 3 p 1 Jul 1984 refs*

Avail: NTIS HC A10/MF A01 CSCL 08B

Optimum radar illumination geometries for stereoscopic analysis of surface topography are determined. Correlation and image processing experiments on synthetic aperture radar (SAR) data for improved information extraction are conducted. Model of the geometry of the multiple SIR-B views of the Earth are developed the sensitivity of the derived terrain altitude data to the various system parameters is established. The limits of accuracy of terrain data achievable with shuttle imaging radar (SIR-B) are derived. Algorithms for matching multiple SIR-B images to generate digital terrain maps are developed. Finally, the use of such terrain maps in geometric correction and registration of SIR-B and LANDSAT Thematic Mapper data is demonstrated B.W.

N85-17243*# New South Wales Univ., Kensington (Australia). **AUSTRALIAN MULTIEXPERIMENTAL ASSESSMENT OF SIR-B (AMAS)**

J. A. RICHARDS, B. C. FORSTER, A. K. MILNE, G. R. TAYLOR, and J. C. TRINDER *In JPL The SIR-B Sci. Invest. Plan 3 p 1 Jul 1984 refs*

Avail: NTIS HC A10/MF A01 CSCL 17I

The utility of SIR-B data for analysis of surface properties and subsurface morphology in three arid regions of Australia is investigated. This study area is located in western New South Wales. It contains extensive aeolian and alluvially derived depositional plains and is the site of the University's Arid Zone Research Station; it is well-mapped and surveyed. Radar backscatter is mapped and evaluated against known terrain conditions. Relative components of surface and subsurface return are determined with a view to identifying structural properties of surface and subsurface morphology. The capability of microwave remote sensing in locating likely groundwater sources in the Bancannia Basin, near Fowler's Gap is assessed. B.W.

N85-17256*# Kansas Univ. Center for Research, Inc., Lawrence. Telecommunications and Information Sciences Lab.

INFORMATION EXTRACTION AND TRANSMISSION TECHNIQUES FOR SPACEBORNE SYNTHETIC APERTURE RADAR IMAGES Final Technical Report

V. S. FROST, L. YUROVSKY, E. WATSON, K. TOWNSEND, S. GARDNER, D. BOBERG, J. WATSON, G. J. MINDEN, and K. S. SHANMUGAN Dec. 1984 274 p refs

(Contract NAGW-381)

(NASA-CR-174341; NAS 1.26-174341; FTR-596-5) Avail: NTIS HC A12/MF A01 CSCL 17I

Information extraction and transmission techniques for synthetic aperture radar (SAR) imagery were investigated. Four interrelated problems were addressed. An optimal tonal SAR image classification algorithm was developed and evaluated. A data compression technique was developed for SAR imagery which is simple and provides a 5:1 compression with acceptable image quality. An optimal textural edge detector was developed. Several SAR image enhancement algorithms have been proposed. The effectiveness of each algorithm was compared quantitatively.

Author

N85-17408# Royal Inst. of Tech., Stockholm (Sweden). Dept. of Photogrammetry.

A COMPARATIVE TEST OF PHOTOGRAMMETRICALLY SAMPLED DIGITAL ELEVATION MODELS

K. TORLEGAARD, A. OESTMAN, and R. LINDGREN *In its Papers of the 15th Intern. Soc. for Photogrammetry and Remote Sensing (ISPRS) Congr. p 6-23 1984 refs*

Avail: NTIS HC A05/MF A01

An international comparative test studied relations between methods for data acquisition, interpolation, resulting accuracy and type of terrain. Six test areas varying from smooth rolling farmland to very steep mountains with forest in the valleys were selected. Fifteen organizations produced digital elevation models (DEMs) from aerial photographs in scales 1:4000 to 1:30,000. The DEMs were used to derive elevations in a set of check points, the locations of which were unknown when the DEM was measured. The elevations of these check points were then compared with their true values. Systematic errors can originate from the reconstruction of the stereomodel, from the interpolation of the DEM, and from effects of vegetation height. The size and distribution of the errors are presented. Errors of functions of the DEM (e.g., slope and curvature) are also studied. Author (ESA)

N85-17417# General Electric Co., Lanham, Md. Space Systems Div.

INTERACTIVE DIGITAL IMAGE PROCESSING FOR TERRAIN DATA EXTRACTION Final Technical Report, Nov. 1983 - Sep. 1984 on Phase 5

H. HEYDT, V. KARKHANIS, and C. PETERSON Sep. 1984 70 p

(Contract DAAK70-79-C-0153)

(AD-A148580; ETL-0374) Avail: NTIS HC A04/MF A01 CSCL 20F

Some techniques were investigated for extracting terrain surface roughness data from digital aerial imagery. Measurement of tonal changes in the imagery is one feasible approach. A digital image data base was assembled containing 10 image planes, 4096 x 4096 pixels/plane, 8 bits/pixel. The planes contain Landsat Thematic Mapper image data, four digitized aerial photos which were rectified, registered to the Thematic Mapper image and mosaicked, and digitized aerial radar imagery, all for the same scene. From the digital photomosaic, open water and forested areas were extracted using a gray level-texture classification.

GRA

N85-19490*# EROS Data Center, Sioux Falls, S. Dak.

LANDSAT 4 INVESTIGATION OF THEMATIC MAPPER AND MULTISPECTRAL SCANNER APPLICATIONS Quarterly Report

D. T. LAUER, Principal Investigator 6 Nov 1984 3 p

(Contract NASA ORDER S-10757-C)

(E85-10076; NASA-CR-174403; NAS 1.26-174403,

PCN902-91548) Avail: NTIS HC A02/MF A01 CSCL 05B

A comparison of methods for selecting optimum TM band combinations for visual interpretation of data are examined. Two statistical methods and visual interpretation by experienced photointerpreters are compared using photographic chips of 1:250,000 scale prints and the digital equivalent of the chips. A mosaic of TM data of the Great Salt Lake area of Utah was done. The filtering process was reviewed since the results were not satisfactory. B.G.

N85-19493*# Instituto de Pesquisas Espaciais, Sao Jose dos Campos (Brazil).

BRAZILIAN REMOTE SENSING RECEIVING, RECORDING AND PROCESSING GROUND SYSTEMS IN THE 1980'S

N. D. J. PARADA, Principal Investigator Oct. 1984 15 p Presented at the 18th Intern. Symp. of the Environ., Paris, 1-5 Oct. 1984. Sponsored by NASA ERTS

(E85-10079, NASA-CR-174406, NAS 1.26-174406,

INPE-3312-PRE/619) Avail: NTIS HC A02/MF A01 CSCL 05B

A ground station was built in Brazil to receive, record, and process TM data from LANDSAT satellites. The receiving/recording

subsystem and the processing subsystem are discussed. Functional design specifications for the facility are addressed. R.S.F.

N85-20497*# National Aeronautics and Space Administration. Goddard Space Flight Center, Greenbelt, Md.

SUMMARY OF MSS CHARACTERIZATION INVESTIGATIONS

W. L. ALFORD and M. L. IMHOFF *In its* LANDSAT-4 Sci. Characterization Early Results, Vol. 1 p 1-8 Jan. 1985 ERTS Avail: NTIS HC A10/MF A01 CSCL 14B

The geometric quality of LANDSAT MSS data processed by the MSS image processing system (MIPS) is discussed. The accuracy of systematic and geodetic corrections done to MSS scenes is considered along with temporal and band to band registration accuracy. A comparison of scene to scene registration accuracies achievable within the LANDSAT 2/3 series with those between LANDSAT 4 and the LANDSAT 2/3 series is mentioned. Radiometric characterization of MSS data is also addressed. Spectral characteristics, banding characteristics, and woodgrain noise pattern are discussed. R.S.F.

N85-20498*# National Aeronautics and Space Administration. Goddard Space Flight Center, Greenbelt, Md.

RADIOMETRIC ACCURACY ASSESSMENT OF LANDSAT 4 MULTISPECTRAL SCANNER DATA

W. L. ALFORD and M. L. IMHOFF *In its* LANDSAT-4 Sci. Characterization Early Results, Vol. 1 p 9-22 Jan. 1985 Original contains imagery. Original photography may be purchased from the EROS Data Center, Sioux Falls, S.D. 57198 ERTS Avail: NTIS HC A10/MF A01 CSCL 05B

The LANDSAT 4 mission has unique characteristics relative to previous LANDSAT missions. The effects of these changes on the character of MSS radiometric data were explored. The histogram calibration process made a significant reduction of the channel differences within a band. If this improvement proves consistent over a wide radiometric range and persists over time, LANDSAT 4 MSS may not have the banding problems that plagued previous MSS instruments. For a simultaneous overpass of LANDSAT 3 and 4, uniform test areas were selected that were common in both data sets. Significant differences in radiance values between the two satellites were observed when R sub max and R sub min were used to compute absolute radiance values. Ground truth should be used to determine new values. A woodgrain appearing pattern is apparent in the MSS images that were not apparent in previous MSS's. It is believed to be caused by many different frequency components, most of which originate from a common source. R.S.F.

N85-20501*# Canada Centre for Remote Sensing, Ottawa (Ontario)

RADIOMETRIC CALIBRATION AND GEOCODED PRECISION PROCESSING OF LANDSAT-4 MULTISPECTRAL SCANNER PRODUCTS BY THE CANADA CENTRE FOR REMOTE SENSING

J. MURPHY, D. BENNETT, and F. E. GUERTIN *In* NASA. Goddard Space Flight Center LANDSAT-4 Sci. Characterization Early Results, Vol. 1 p 77-118 Jan. 1985 refs ERTS Avail: NTIS HC A10/MF A01 CSCL 05B

The methodology used to perform radiometric calibration and precision geometric correction of standard LANDSAT 4 MSS products is described. It is shown how the same algorithms are used to radiometrically correct and to place on a calibrated radiance scale the data from all four LANDSAT satellites. To assess the reliability of absolute calibration, the minor variations observed in the LANDSAT 4 calibration data are discussed. Comparison of overlapping LANDSAT 3 and LANDSAT 4 scenes acquired at the same time is proposed. The concept of geocoded products is reviewed. It is shown that the geometric correction model developed to precision-process the MSS data from the earlier LANDSAT satellites can generate LANDSAT 4 MSS geocoded products with comparable geodetic accuracy. The results are seen as preliminary and are expected to be refined and augmented as more LANDSAT 4 data are acquired and processed. R.S.F.

N85-20503*# Georgia Univ., Athens Dept of Geography

GEOMETRIC ACCURACY OF LANDSAT-4 MSS IMAGE DATA

R. WELCH and E. L. USERY *In* NASA. Goddard Space Flight Center LANDSAT-4 Sci. Characterization Early Results, Vol. 1 p 123-132 Jan. 1985 refs Previously announced as N83-27322 ERTS (Contract NAS5-27383)

Avail: NTIS HC A10/MF A01 CSCL 08B

Analyses of the LANDSAT-4 MSS image data of North Georgia provided by the EDC in CCT-p formats reveal that errors of approximately + or - 30 m in the raw data can be reduced to about + or - 55 m based on rectification procedures involving the use of 20 to 30 well-distributed GCPs and 2nd or 3rd degree polynomial equations. Higher order polynomials do not appear to improve the rectification accuracy. A subscene area of 256 x 256 pixels was rectified with a 1st degree polynomial to yield an RMSE sub xy value of + or - 40 m, indicating that USGS 1:24,000 scale quadrangle-sized areas of LANDSAT-4 data can be fitted to a map base with relatively few control points and simple equations. The errors in the rectification process are caused by the spatial resolution of the MSS data, by errors in the maps and GCP digitizing process, and by displacements caused by terrain relief. Overall, due to the improved pointing and attitude control of the spacecraft, the geometric quality of the LANDSAT-4 MSS data appears much improved over that of LANDSAT-1, -2 AND -3 M.G.

N85-20504*# EROS Data Center, Sioux Falls, S. Dak

GEODETTIC ACCURACY OF LANDSAT 4 MULTISPECTRAL SCANNER AND THEMATIC MAPPER DATA

J. M. THORMODSGARD and D. J. DEVRIES *In* NASA. Goddard Space Flight Center LANDSAT-4 Sci. Characterization Early Results, Vol. 1 p 133-142 Jan. 1985 ERTS

Avail: NTIS HC A10/MF A01 CSCL 08E

The geodetic accuracy of LANDSAT 4 data from both the MSS and TM processing systems was evaluated. The procedure was based on comparing the calculated image location, computed with the geodetic referencing algorithms, with the true image location visually located on a display device. Results of the testing of geodetic accuracy of three MSS scenes (Washington, DC, central Alabama, and Los Angeles, CA) and two TM scenes (Aberdeen, SD and Galesburg, IL) are presented. The calculated and actual image locations of the ground control points are shown. The offset between the calculated and actual image location, as well as the offset vector magnitude or pixel error, are given. R.S.F.

N85-20507*# General Electric Co., Lanham, Md. Space Div.

LS-4 MSS GEOMETRIC CORRECTION: METHODS AND RESULTS

J. BROOKS, E. KIMMER, and J. SU *In* NASA. Goddard Space Flight Center LANDSAT-4 Sci. Characterization Early Results, Vol. 1 p 177-200 Jan. 1985 ERTS

Avail: NTIS HC A10/MF A01 CSCL 12A

Methods and results of the effort that fine-tuned both the software and data base and assessed the geometric performance of the calibrated LANDSAT 4 system are described. The systematic correction data surface, the geodetic correction data surface, and the MSS filter that links them are discussed. R.S.F.

N85-20511*# General Electric Co., Philadelphia, Pa.

AN OVERVIEW OF THE THEMATIC MAPPER GEOMETRIC CORRECTION SYSTEM

E. P. BEYER *In* NASA. Goddard Space Flight Center LANDSAT-4 Sci. Characterization Early Results, Vol. 2, Pt. 1 p 87-146 Jan. 1985 refs ERTS

(Contract NAS5-25300)

Avail: NTIS HC A21/MF A01 CSCL 08B

The processing concepts which form the basis of the NASA TM geometric correction system are summarized. This system serves to place TM image samples onto an output coordinate system which is related to a map projection. The flight segment includes the TM instrument, attitude measurement devices, attitude control, and ephemeris processing. A spacecraft formatter combines the necessary on-board computer information and

07 DATA PROCESSING AND DISTRIBUTION SYSTEMS

angular displacement sensor samples into a 32-kilobit per second telemetry stream called payload correction data. These data are downlinked on a telemetry channel and included with TM wideband data. Ground segment processes performed include: payload correction, control point processing, and geometric correction (resampling) A.R.H.

N85-20512*# National Aeronautics and Space Administration. Goddard Space Flight Center, Greenbelt, Md.

TM DIGITAL IMAGE PRODUCTS FOR APPLICATIONS

J. L. BARKER, F. J. GUNTHER (Computer Sciences Corp., Silver Spring, Md.), R. B. ABRAMS (Computer Sciences Corp., Silver Spring, Md.), and D. L. BALL (Computer Sciences Corp., Silver Spring, Md.) *In its* LANDSAT-4 Sci. Characterization Early Results, Vol. 2, Pt. 1 p 147-220 Jan. 1985 refs Original contains imagery. Original photography may be purchased at the EROS Data Center, Sioux Falls, S.D. 57198 ERTS
Avail. NTIS HC A21/MF A01 CSCL 08B

LANDSAT-4 TM images recorded on computer compatible tapes (CCTs) are currently available in the following tape formats (1) raw rectified data (CCT-BT); (2) calibrated data (CCT-AT); and (3) geometrically corrected data (CCT-PT). These formats represent different steps in the process of producing fully-corrected TM data. The CCT-BT images are rectified from telemetry format to image format, but are uncorrected radiometrically and geometrically; they are generally used for internal transportation of data from one ground processing system to another. The CCT-AT images have had data from faulty channels replaced and all data radiometrically calibrated to produce an archive image; they are available to researchers for radiometric characterization. The final products, the CCT-PT images, have been resampled by cubic convolution procedures to provide a geometrically corrected image using satellite ephemeris data. The CCT-PT image is the one to which all of the various radiometric and geometric corrections have been applied; this is the product that is the product that is available to all users. A.R.H.

N85-20513*# Canada Centre for Remote Sensing, Ottawa (Ontario)

CANADIAN PLANS FOR THEMATIC MAPPER DATA

W. M. STROME, F. E. GUERTIN, A. B. COLLINS, and D. G. GOODENOUGH *In* NASA. Goddard Space Flight Center LANDSAT-4 Sci. Characterization Early Results, Vol. 2, Pt. 1 p 221-234 Jan. 1985 refs ERTS
Avail. NTIS HC A21/MF A01 CSCL 08B

To improve the quality of data obtained from remote sensing satellites, and thereby improve Canada's resource management capability, facilities were to enable them to receive, record, process, distribute and analyze TM and MSS data from LANDSAT-4. The CCT format used was changed to the standard format family to make it compatible with other ground stations. All MSS data are now in that format. The antenna, at Prince Albert were modified to receive TM X-band data and a transcription system was added to convert high density digital tape to CCT format. A bulk processing system is being developed to provide geometrically corrected MSS, TM, and SPOT products. Methods are being investigated for integrating multiple pixel data from different satellites and other sources using a digital image analysis system that is being established. A cost benefits study is also underway. A.R.H.

N85-21726*# Rochester Inst. of Tech., N. Y. School of Photographic Arts and Sciences.

EVALUATION OF THE RADIOMETRIC INTEGRITY OF LANDSAT 4 THEMATIC MAPPER BAND 6 DATA

J. R. SCHOTT *In its* LANDSAT-4 Sci. Characterization Early Results, Vol. 3, Pt. 2 p 221-231 Jan. 1985 refs Original contains imagery. Original photography may be purchased from the EROS Data Center, Sioux Falls, S.D. 57198 ERTS
Avail. NTIS HC A25/MF A01 CSCL 14B

Probably the most generally accepted method for processing radiometric data from space is to correct the observed radiance or apparent temperature to a surface radiance or temperature value using atmospheric propagation models. As part of NASA's

Heat Capacity Mapping Mission (HCMM) experiment the atmospheric propagation models were used in reverse in an attempt to evaluate the post launch radiometric response of the radiometer. Techniques successfully used to radiometrically calibrate the HCMM sensor were extended. The HCMM experiment is described and used as a base for the evaluation of the TM band 6 (infrared) sensor. A.R.H.

N85-21728*# Department of Energy, Mines, and Resources, Ottawa (Ontario).

A PRELIMINARY ASSESSMENT OF LANDSAT-4 THEMATIC MAPPER DATA

D. G. GOODENOUGH, E. A. FLEMING, and K. DICKINSON *In its* LANDSAT-4 Sci. Characterization Early Results, Vol. 3, Pt. 2 p 257-273 Jan. 1985 refs ERTS
Avail. NTIS HC A25/MF A01 CSCL 08B

The geometric errors for image to map rectification of one Thematic Mapper (TM) scene of an area near Windsor, Ontario were studied. The scene had been produced on computer compatible tape by NASA and contained radiometric and system corrections for geometric distortions. The geometric properties of TM photographic imagery permitted very good fitting to map detail using simple scaling techniques to localized areas and, using simple scaling, the overall geometry remained with 500 meters or 0.4 mm at the image scale of 1:1,141,600. An affine transformation, permitting differential scaling, slightly improves the fit to about 400 meters or 0.35 mm at image scale. The imagery shows promise of having the needed additional resolution and spectral discrimination to provide map revision information in urban-rural areas where the MSS sensor is considered inadequate. The late-season prairie image, however, did not hold such promise, and judgement must be reserved until images are acquired at other seasons in this particular geographic area. A.R.H.

N85-21731*# Purdue Univ., Lafayette, Ind. Lab. for Applications of Remote Sensing.

EVALUATION OF THE RADIOMETRIC QUALITY OF THE TM DATA USING CLUSTERING, LINEAR TRANSFORMATIONS AND MULTISPECTRAL DISTANCE MEASURES

L. A. BARTOLUCCI, M. E. DEAN, and P. E. ANUTA *In its* LANDSAT-4 Sci. Characterization Early Results, Vol. 3, Pt. 2 p 321-358 Jan. 1985 refs Original contains imagery. Original photography may be purchased from the EROS Data Center, Sioux Falls, S.D. 57198 ERTS
Avail. NTIS HC A25/MF A01 CSCL 05B

The radiometric quality of LANDSAT 4 TM data for the classification and identification of Earth surface features was evaluated. Techniques employed in the evaluation included clustering, data compression (linear transformations), multispectral distance measures, and hierarchical classification methods. TM and MSS data for the Chicago, Illinois test site were studied. In order to determine the radiometric quality of the TM thermal data for temperature mapping of surface water, a test site was selected within the area covered by the TM scene (Scene ID: 40101-16025) gathered over Illinois. This site was chosen because it includes a surface water body with a large range of temperatures, i.e., a cooling pond for the Dresden nuclear power plant and the junction of two rivers. R.S.F.

N85-21739*# Geological Survey, Reston, Va.

A PRELIMINARY EVALUATION OF LANDSAT-4 THEMATIC MAPPER DATA FOR THEIR GEOMETRIC AND RADIOMETRIC ACCURACIES

M. H. PODWYSOCKI, N. FALCONE, L. U. BENDER, and O. D. JONES *In its* LANDSAT-4 Sci. Characterization Early Results, Vol. 3, Pt. 2 p 492-512 Jan. 1985 refs Previously announced as N83-32136 Original contains imagery. Original photography may be purchased from the EROS Data Center, Sioux Falls, S.D. 57198 ERTS
Avail. NTIS HC A25/MF A01 CSCL 05B

Some LANDSAT thematic mapper data collected over the eastern United States were analyzed for their whole scene geometric accuracy, band to band registration and radiometric

accuracy. Band ratio images were created for a part of one scene in order to assess the capability of mapping geologic units with contrasting spectral properties. Systematic errors were found in the geometric accuracy of whole scenes, part of which were attributable to the film writing device used to record the images of film. Band to band registration showed that bands 1 through 4 were registered to within one pixel. Likewise, bands 5 and 7 also were registered to within one pixel. However, bands 5 and 7 were misregistered with bands 1 through 4 by 1 to 2 pixels. Band 6 was misregistered by 4 pixels to bands 1 through 4. Radiometric analysis indicated two kinds of banding, a modulo-16 stripping and an alternate light dark group of 16 scanlines. A color ratio composite image consisting of TM band ratios 3/4, 5/2, and 5/7 showed limonitic clay rich soils, limonitic clay poor soils, and nonlimonitic materials as distinctly different colors on the image.

Author

N85-21743*# National Aeronautics and Space Administration. Ames Research Center, Moffett Field, Calif.

ASSESSMENT OF THEMATIC MAPPER BAND-TO-BAND REGISTRATION BY THE BLOCK CORRELATION METHOD

D. H. CARD, R. C. WRIGLEY, F. C. MERTZ (Technicolor Government Services, Inc., Moffett Field, Calif.), and J. R. HALL (Technicolor Government Services, Inc., Moffett Field, Calif.) *In its* LANDSAT-4 Sci. Characterization Early Results, Vol. 3, Pt. 2 p 553-564 Jan. 1985 refs Previously announced as N83-33286 ERTS

Avail: NTIS HC A25/MF A01 CSCL 05B

Rectangular blocks of pixels from one band image were statistically correlated against blocks centered on identical pixels from a second band image. The block pairs were shifted in pixel increments both vertically and horizontally with respect to each other and the correlation coefficient to the maximum correlation was taken as the best estimate of registration error for each block pair. For the band combinations of the Arkansas scene studied, the misregistration of TM spectral bands within the noncooled focal plane lie well within the 0.2 pixel target specification. Misregistration between the middle IR bands is well within this specification also. The thermal IR band has an apparent misregistration with TM band 7 of approximately 3 pixels in each direction. The TM band 3 has a misregistration of approximately 0.2 pixel in the across-scan direction and 0.5 pixel in the along-scan direction, with both TM bands 5 and 7.

A.R.H.

N85-21744*# Geological Survey, Flagstaff, Ariz.

TESTS OF LOW-FREQUENCY GEOMETRIC DISTORTIONS IN LANDSAT 4 IMAGES

R. M. BATSON and W. T. BORGESON *In its* LANDSAT-4 Sci. Characterization Early Results, Vol. 3, Pt. 2 p 565-570 Jan. 1985 Original contains imagery. Original photography may be purchased from the EROS Data Center, Sioux Falls, S.D. 57198 ERTS

Avail: NTIS HC A25/MF A01 CSCL 05B

The geometric characteristics of LANDSAT 4 images were studied. The extent of image distortion caused by the physical process of writing the LANDSAT 4 images on film was determined. The geometric accuracies inherent in the digital images themselves were characterized. Test materials consisted of film images of test targets generated by the laser beam recorders (LBR), the Optronics Photowrite film writer, and digital image films of a strip 600 lines deep across the full width of band 5 of the Washington, D.C. Thematic Mapper scene. The tests were made by least squares adjustment of an array of measured image points to a corresponding array of control points. The film test array consists of 25 test points, and the image test array consists of 60 test points, resulting in a model that can be used to characterize the low frequency, random geometric distortions of the images. The tests were not suitable for examining jitter or similar high-frequency distortions.

B.G.

N85-21755*# Rochester Inst. of Tech., N. Y. Coll. of Graphic Arts and Photography.

LANDSAT 4 BAND 6 DATA EVALUATION Quarterly Report

15 Mar. 1985 4 p ERTS

(Contract NAS5-27323)

(E85-10093; NASA-CR-175528; NAS 1.26:175528; QR-10) Avail: NTIS HC A02/MF A01 CSCL 05B

Comparison of underflight data with satellite estimates of temperature revealed significant gain calibration errors. The source of the LANDSAT 5 band 6 error and its reproducibility is not yet adequately defined. The error can be accounted for using underflight or ground truth data. When underflight data are used to correct the satellite data, the residual error for the scene studied was 1.3K when the predicted temperatures were compared to measured surface temperature.

A.R.H.

08

INSTRUMENTATION AND SENSORS

Includes data acquisition and camera systems and remote sensors.

A85-19363#

METHODOLOGICAL STUDY OF SPECTRAL BAND SELECTION FOR MULTISPECTRAL REMOTE SENSING

Q. TONG, G. TIAN, and Y. MAO Chinese Society of Astronautics, Journal, no. 2, 1983, p. 1-13. In Chinese, with abstract in English. refs

Based on laboratory and field measurements, the spectral reflectances taken from fifteen species of the earth object about plant, soil, rock, and water were studied in order to select the optimum spectral bands of multispectral remote sensing. The data of the reflectance have been analyzed by means of T test, S method, and the test of grouping in a sequence of alternative and other statistical methods, and the data were processed by computer. According to the analysis, the corresponding spectral bands of multispectral remote sensing are as follows: 0.44-0.51, 0.53-0.62, 0.63-0.70, 0.74-0.80 microns, where the last band might extend to longer wavelengths. Comparison of the selected spectral bands in this work with some bands used in several important spaceflight activities abroad provides a very considerable coincidence.

Author

A85-19608#

THE SPACE ENVIRONMENT MONITORS ONBOARD GOES

J. A. JOSELYN and R. N. GRUBB (NOAA, Space Environment Laboratory, Boulder, CO) American Institute of Aeronautics and Astronautics, Aerospace Sciences Meeting, 23rd, Reno, NV, Jan. 14-17, 1985. 6 p. refs (AIAA PAPER 85-0238)

The first Geostationary Operational Environmental Satellite (GOES) was launched in April 1974. Since that time, eight similar satellites have been built and deployed to meet the operational requirement of the National Oceanic and Atmospheric Administration (NOAA). Each GOES contains a visible and infrared spin scan radiometer (VISSR) or an atmospheric sounder (VAS), a space environment monitor (SEM), and a communications subsystem which includes data relay from ground-based data collection platforms which can be interrogated by command. It is pointed out that the VAS or VISSR systems provide hemispheric imaging and information for the National Weather Service. The space environment monitors are discussed, taking into account the energetic particle sensor, the high energy proton and alpha particle detector, the magnetometer, and the solar X-ray instrument. Attention is also given to the satellite broadcast system.

G.R.

A85-19998

DETERMINATION OF THE EXTERNAL-ORIENTATION ELEMENTS OF AERIAL AND SPACE PHOTOGRAPHS IN THE REMOTE SENSING OF DYNAMIC PROCESSES AND PHENOMENA [OPREDELENIE ELEMENTOV VNESHNEGO ORIENTIROVANNIA AEROKOSMICHESKIKH SNIMKOV PRI DISTANTSIONNOM IZUCHENII DINAMICHESKIKH PROTSESSOV I IAVLENIII]

V. B. DUBINOVSKII (Moskovskii Institut Inzhenerov Geodezii, Aerofotos'emki i Kartografii, Moscow, USSR) and A. A. MOROZOV (Geodeziia i Aerofotos'emka (ISSN 0536-101X), no. 5, 1984, p. 66-70. In Russian.

A85-20081

COMPLEX STUDIES OF THE ENVIRONMENT BY OPTICAL AND RADAR METHODS [KOMPLEKSNIYE ISSLEDOVANNIA PRIRODNOI SREDY OPTICHESKIM I RADIOLOKATSIONNYM METODAMI]

V. P. SHESTOPALOV, V. I. DRANOVSKII, V. B. EFIMOV, A. I. KALMYKOV, A. P. PICHUGIN, A. S. SELIVANOV, IU. G. SPIRIDONOV, IU. M. TUCHIN, and B. E. KHYMYROV (Akademiia Nauk Ukrainkoi SSR, Institut Radiofiziki i Elektroniki, Kharkov, Ukrainian SSR) Akademiia Nauk SSSR, Doklady (ISSN 0002-3264), vol. 279, no. 3, 1984, p. 621-623. In Russian. refs

The use of optical and radar techniques for observing the earth from space is discussed. In particular, attention is given to the use of low-resolution optomechanical scanners and sidelooking radar on board the Kosmos-1500 satellite for monitoring the land and ocean ice cover over large areas. The radar system operates in the 3-cm band; data are processed on board the satellite and then transmitted to the ground stations over the standard communication channels in the meter (136 MHz) and decimeter (460 MHz) bands. Images of an area in the Antarctic are presented. V.L.

A85-20568

STATUS AND PLANS FOR THE SPOT PROGRAM AND THE LAUNCH OF SPOT. I - ITS ON-GROUND PROCESSING AND DATA DISSEMINATION TO USERS

A. FONTANEL (SPOT IMAGE, Toulouse, France) Earth-Oriented Applications of Space Technology (ISSN 0277-4488), vol. 4, no. 4, 1984, p. 221-225.

The SPOT system which involves high resolution remote sensing of the earth's surface is discussed. The principal characteristics of SPOT include a circular orbit at 832 km, two identical sensors with a pointing capability of 27 deg east or west of the orbital plane, two spectral channels, panchromatic and multispectral, and direct broadcasting at 8 GHz at a rate of 50 Mb/s. The data acquisition and distribution system is designed to meet the user needs and is managed by a commercial corporation called SPOT IMAGE. The SPOT ground segment consists of a satellite mission and a control center operated by CNES, and two main ground receiving stations and a network of regional receiving stations around the world. A computerized SPOT catalogue system includes statistical calculations concerning image characteristics and scene selection, and analyzes users' data requests, records and manages data orders, and manages the data acquisition programs. A SPOT data simulation program, initiated in order to prepare the user community to the use and analysis of SPOT images, is also considered. M.D.

A85-20571

MICROCOMPUTER SYSTEMS FOR SATELLITE IMAGE PROCESSING

D. C. FERNS (Nigel Press Associates, Ltd., Edenbridge, Kent, England) Earth-Oriented Applications of Space Technology (ISSN 0277-4488), vol. 4, no. 4, 1984, p. 247-254. refs

The use of microcomputers for the interactive processing and display of satellite imagery is reviewed. A simple introduction is presented to the principal hardware characteristics which influence system performance, with direct reference to user requirements for processing imagery from the Landsat and SPOT satellites. The satellite image processing software which is available on

microcomputer systems is considered with respect to the algorithms which are most widely used, and the geographical information systems which are currently under development. Although microcomputers cannot universally replace large mainframe installations, they will have an increasingly important role as intelligent workstations, particularly in computer networks. Commercially available turnkey systems are reviewed, and it is envisaged that the increasing performance and relatively lower costs of such microcomputer systems will be a major contributing factor to the more widespread operational use of satellite imagery and geographical information systems. Author

A85-20643#

REMOTE SENSING DEVELOPMENT IN THE PEOPLE'S REPUBLIC OF CHINA

W. CHEN, S. YANG, L. FU, and L. ZHENG (National Remote Sensing Center, People's Republic of China) United Nations, International Meeting of Experts on Remote Sensing Information Systems, Feldafing and Oberpfaffenhofen, West Germany, May 7-11, 1984, Paper. 6 p.

Aspects of the development of remote sensing in China are discussed. Basic research and experimentation and remote sensing sensor development in China are considered, and remote sensing image processing techniques and applications relevant to China are addressed. The activities of Chinese remote sensing organizations are described, and short-term planning for remote sensing technology in China is summarized. C.D.

A85-22424* Arizona Univ., Tucson.

SURVEY OF MULTISPECTRAL IMAGING SYSTEMS FOR EARTH OBSERVATIONS

P. N. SLATER (Arizona, University, Tucson, AZ) Remote Sensing of Environment (ISSN 0034-4257), vol. 17, Feb. 1985, p. 85-102. refs

(Contract NAG5-196)

Fifty-six multispectral imaging systems are described in terms of their instantaneous fields of view, spectral bands, fields of view, and number of quantization levels. These systems have been used during the past decade for earth resources studies from aircraft or spacecraft, or are currently in the proposal or design and development stage. Author

A85-22681

THE THEMATIC MAPPER - INSTRUMENT OVERVIEW AND PRELIMINARY ON-ORBIT RESULTS

J. L. ENGEL (Santa Barbara Research Center, Goleta, CA) IN: Infrared technology IX; Proceedings of the Ninth Annual Meeting, San Diego, CA, August 23-25, 1983. Bellingham, WA, SPIE - The International Society for Optical Engineering, 1983, p. 75-84.

An overview description of the Thematic Mapper (flown aboard Landsat 4) is given, including a comparison of the TM and the multispectral scanner, and descriptions of the TM scanner, and optical system and detector projection on ground track. System performance is evaluated with respect to spectral coverage, radiometric sensitivity, square wave response, dynamic band-to-band registration, and geometric accuracy; and preliminary on-orbit results are assessed, with particular emphasis on data classification accuracy. Early results indicate that the performance of the TM is consistent with the prelaunch results, and that the utility is meeting or exceeding expectations. B.J.

A85-22682

LARGE SCAN MIRROR ASSEMBLY OF THE NEW THEMATIC MAPPER DEVELOPED FOR LANDSAT 4 EARTH RESOURCES SATELLITE

C. J. STARKUS (Hughes Aircraft Co., El Segundo, CA) IN: Infrared technology IX; Proceedings of the Ninth Annual Meeting, San Diego, CA, August 23-25, 1983. Bellingham, WA, SPIE - The International Society for Optical Engineering, 1983, p. 85-92.

This paper reviews mechanical aspects in the development of a large, oscillating scan mirror mechanism that featured a remarkably low level of structural vibration for the impact energies involved in mirror oscillation. Another feature was that energy lost

during impact was returned to the mirror by applying torque only during the instant of impact. Because the duration of impact was only about 0.010 second, it was critical that energy losses be minimal since there was not much time to restore them. Solutions to these critical mechanical problems constituted a major milestone in the development of object-space scanning sensors. Author

A85-22711

SYNTHETIC APERTURES - AN OVERVIEW

J. S. FENDER (USAF, Weapons Laboratory, Kirtland AFB, NM) IN: Synthetic aperture systems, Proceedings of the Meeting, San Diego, CA, August 25, 26, 1983. Bellingham, WA, SPIE - The International Society for Optical Engineering, 1984, p. 2-7. refs

An aperture is synthesized by combining separate optical systems to function as a single large aperture. Specifically, a synthetic aperture is a phased array of independent optical systems which together form a common image field with a resolution which exceeds that produced by any single element. Attention is given to the pupil function which describes the phase and amplitude variations across a synthetic aperture, the diffracting screen, far field irradiance, a synthetic aperture formed by six identical circular elements, techniques for achieving and maintaining matched optical paths, and examples of astronomical synthetic apertures. G.R.

A85-23678

SEASAT-DATA ACQUISITION AND PROCESSING BY THE ROYAL AIRCRAFT ESTABLISHMENT

D. HARDY (Royal Aircraft Establishment, Farnborough, Hants., England) IN: Satellite microwave remote sensing. Chichester, West Sussex, England, Ellis Horwood, Ltd., 1983, p. 45-57

The preparation for and execution of the SEASAT data acquisition and processing operations are described. The characteristics and role in data acquisition of the Tracking and Command Station (TCS) antenna at Oakhanger, UK are addressed, and the software used for processing is briefly described. Block diagrams are shown of the TCS system and of the configuration of the remote sensing data center at Farnborough. C.D.

A85-23693

SEASAT OVER LAND

P. H. MARTIN-KAYE, M. MCDONOUGH (Hunting Geology and Geophysics Ltd., Borehamwood, Herts., England), and G. C. DEANE (Hunting Technical Services, Ltd., Borehamwood, Herts., England) IN: Satellite microwave remote sensing. Chichester, West Sussex, England, Ellis Horwood, Ltd., 1983, p. 271-298. Research supported by the National Remote Sensing Centre of Farnborough. refs

It is pointed out that the Seasat satellite, launched by NASA in 1978, presented the first opportunity of evaluating some potentially important land applications of a satellite-borne Synthetic Aperture Radar (SAR) system. Such possible applications include the monitoring of soil moisture and crop state for crop yield forecasting. The results of the considered evaluation are particularly significant for areas in which an occurrence of cloudy conditions is often an obstacle for an employment of other forms of remote sensing techniques. The Seasat receiving station at Oakhanger, England, recorded some 272 minutes of data from 53 passes of Seasat. The SAR data represent imagery of approximately 11 million sq km between Greenland and North Africa, of which about 20 percent are overland images. Geological studies are discussed, taking into account United Kingdom study areas, Iceland, and a comparison between Seasat and Landsat images. In a discussion of land use studies, attention is given to test sites in the UK, the evaluation of the imagery, and conclusions. G.R.

A85-23705

THE SCANNING MULTICHANNEL MICROWAVE RADIOMETER - AN ASSESSMENT

P. K. TAYLOR (Institute of Oceanographic Sciences, Wormley, Surrey, England) IN: Satellite microwave remote sensing. Chichester, West Sussex, England, Ellis Horwood, Ltd., 1983, p. 463-480. refs

The operational performance of the Scanning Multichannel Microwave Radiometer (SMMR) instrument carried by the Seasat oceanographic satellite is evaluated. A general description of the operation of the instrument is presented, and a list is given of the microwave frequencies used to measure sea surface temperature, surface wind, water vapor content, and rain rate. SMMR data for the above parameters are compared with information from the NOAA-5 meteorological satellite in a series of contoured maps. It is shown that the SMMR is capable of quantitative measurements of sea surface temperature, surface wind speed, and total atmospheric water vapor which agree well with surface measurements. Recommendations are offered with respect to increasing measurement accuracies in the future. I.H.

A85-23751

SPECTRAL SIGNATURES OF OBJECTS IN REMOTE SENSING; INTERNATIONAL CONFERENCE, 2ND, BORDEAUX, FRANCE, SEPTEMBER 12-16, 1983, REPORTS [SIGNATURES SPECTRALES D'OBJETS EN TELEDETECTION; COLLOQUE INTERNATIONAL, 2ND, BORDEAUX, FRANCE, SEPTEMBER 12-16, 1983, ACTES]

G. GUYOT, ED. and M. VERBRUGGHE, ED. (Institut National de la Recherche Agronomique, Montfavet, Vaucluse, France) Conference supported by the Centre National d'Etudes Spatiales and Institut National de la Recherche Agronomique Versailles, Institut National de la Recherche Agronomique (INRA, Colloques, No. 23), 1984, 939 p. In French and English. For individual items see A85-23752 to A85-23795

The signatures of terrestrial surfaces in the UV, visible, NIR, thermal-IR, and microwave spectral regions observed by remote sensing, mainly from satellites, are characterized in reviews and reports. Topics examined include the angular and spatial variability of spectral data, polarization measurements, applications of lidar to the remote sensing of the oceans, the use of radiometry and photometry to determine tropical-vegetation reflectance, thermal-inertia mapping from space, and the calibration of microwave remote sensors. Consideration is given to the angular radar response to surface and subsurface soil moisture at 9.5 GHz, the use of combined data from different spectral regions, the bands of the planned SPOT satellite, and spectral inputs to agrometeorological crop-growth/yield models. T.K.

A85-23759

DEVELOPMENT OF A SPOT-SIMULATION RADIOMETER [MISE AU POINT D'UN RADIOMETRE DE SIMULATION DE SPOT]

G. GUYOT, J. F. HANOCQ (Institut National de la Recherche Agronomique, Montfavet, Vaucluse, France), J. P. BUIS (Cimel Electronique, Paris, France), and G. SAINT (Centre National d'Etudes Spatiales, Toulouse, France) IN: Spectral signatures of objects in remote sensing; International Conference, 2nd, Bordeaux, France, September 12-16, 1983, Reports. Versailles, Institut National de la Recherche Agronomique, 1984, p. 233-242. In French.

The design and performance of a three-channel interchangeable-filter ground-truth radiometer capable of simulating the performance of the SPOT instruments in the 400-1100-nm range are reported. The radiometer comprises a radiance head with aperture angles 12 and 1 deg, a sky-irradiance head with diffusing windows, and a compact control, display, and data-storage unit with a 20,000-point A/D converter. Block diagrams, photographs and tables and graphs of sample field data are shown, and the radiometer is found to provide accurate and applicable data with no need for zero and gain adjustments. T.K.

A85-23768

STUDY OF THE CORRELATION BETWEEN THE IRT BAND OF THE NOAA AVHRR AND THE FACTORS CONDITIONING THE THERMAL BEHAVIOR OF BIOCLIMATIC AREAS ON A REGIONAL SCALE [RECHERCHE SUR LA CORRELATION ENTRE LA BANDE IRT DU AVHRR DE NOAA ET LES PARAMETRES CONDITIONNANT LE COMPORTEMENT THERMIQUE DES TERROIRS BIOCLIMATIQUES A L'ECHELLE REGIONALE]

I. ANGLADE (Toulouse II, Université, Toulouse, France) IN: Spectral signatures of objects in remote sensing; International Conference, 2nd, Bordeaux, France, September 12-16, 1983, Reports Versailles, Institut National de la Recherche Agronomique, 1984, p. 485-493. In French. refs

A85-23780* Kansas Univ. Center for Research, Inc., Lawrence **SURFACE SCATTERING EFFECTS AT DIFFERENT SPECTRAL REGIONS [EFFETS DE DIFFUSION DE SURFACE POUR DIFFERENTES REGIONS DU SPECTRE]**

A. K. FUNG (University of Kansas Center for Research, Inc., Lawrence, KS) IN: Spectral signatures of objects in remote sensing, International Conference, 2nd, Bordeaux, France, September 12-16, 1983, Reports Versailles, Institut National de la Recherche Agronomique, 1984, p. 693-707 refs (Contract NAG5-268; DAAG29-80-K-0018)

The development of theoretical models of rough surface scattering in different frequency regions is reviewed. The applications of the models to four different types of rough surface scattering are presented. The four categories of surface roughness effects are: (1) where the angular distribution of first-order average incoherent scattered power is proportional to the roughness spectrum of the surface; (2) where the horizontal roughness scale is less than the incident wavelength; (3) where both the horizontal and vertical roughness scales are large compared to the incident wavelength, and (4) scattering in the specular direction is dominated by large-scale roughness, and scattering in the opposite direction is dominated by small-scale roughness. Acoustic, optical and microwave scattering measurements from rough surfaces are presented which illustrate the four types of scattering behavior.

I. H.

A85-23781

DEMONSTRATION, ANALYSIS, AND CORRECTION OF ATMOSPHERIC EFFECTS ON LANDSAT OR SPOT MULTISPECTRAL DATA [MISE EN EVIDENCE, ANALYSE ET CORRECTION DES EFFETS ATMOSPHERIQUES SUR LES DONNEES MULTISPECTRALES DE LANDSAT OU SPOT]

P. Y. DESCHAMPS, P. DUHAUT, M. C. ROUQUET, and D. TANRE (Centre National d'Etudes Spatiales, Département d'Etudes Thématiques, Toulouse, Lille I, Université, Villeneuve-d'Ascq, Nord, France) IN: Spectral signatures of objects in remote sensing; International Conference, 2nd, Bordeaux, France, September 12-16, 1983, Reports Versailles, Institut National de la Recherche Agronomique, 1984, p. 709-722. In French. refs

The effect of atmospheric aerosols on the mean reflectances and standard errors of Landsat MSS channel 4, 5, 6, and 7 images of the same area (in the Loire valley, France) obtained on two successive days in 1976 is shown; a theoretical model taking gas absorption and diffusion into account is developed; and a statistical procedure for correcting the diffusion effect when the optical thickness and atmospheric reflectance are known is presented and demonstrated on the same images. The limitations of the water-surface calibration technique of Rochon et al. (1977) are indicated.

T.K.

A85-23784*

National Aeronautics and Space Administration Goddard Space Flight Center, Greenbelt, Md. **SPECTRAL SIGNATURES OF SOIL, SNOW AND SEA ICE AS OBSERVED BY PASSIVE MICROWAVE AND THERMAL INFRARED TECHNIQUES**

T. SCHMUGGE (NASA, Goddard Space Flight Center, Hydrological Sciences Branch, Greenbelt, MD) IN: Spectral signatures of objects in remote sensing; International Conference, 2nd, Bordeaux, France, September 12-16, 1983, Reports Versailles, Institut National de la Recherche Agronomique, 1984, p. 749-762 refs

There have been many passive microwave observations of soil, snow, and sea ice surfaces made during the past several years. These measurements have been from tower, aircraft, and spacecraft platforms covering the wavelength range from 0.8 cm to 50 cm. Based on these data it can be concluded that the longer wavelengths (greater than 5 cm) are more effective for soil moisture observations because of a greater capability to penetrate vegetation, while the shorter wavelengths (1 to 3 cm) are best for snow and sea ice observations since the dominant process is volume scattering by the ice grains in the snow and the brine cells in sea ice. Because it is the intensity of a thermal emission process that is being measured, thermal infrared measurements are necessary to separate the emissivity and temperature effects in the microwave emission.

Author

A85-23789

EXPERIMENTS CONCERNING RADIOMETRIC MEASUREMENTS AND NATURAL-OBJECT INDICATORS IN ORDER TO APPLY CORRECTIONS TO RECORDINGS OF SATELLITE REMOTE SENSING [EXPERIENCES CONCERNANT LES DETERMINATIONS RADIOMETRIQUES ET D'INDICATEURS DES OBJETS NATURELS EN VUE DE L'APPLICATION DE CORRECTIONS AUX ENREGISTREMENTS SATELLITAIRES DE TELEDETECTION]

N. OPRESCU (Institut de Constructii, Bucharest, Rumania) and E. MANDESCU (Commission Roumaine pour les Activités Spatiales, Bucharest, Rumania) IN: Spectral signatures of objects in remote sensing, International Conference, 2nd, Bordeaux, France, September 12-16, 1983, Reports Versailles, Institut National de la Recherche Agronomique, 1984, p. 815-822. In French. refs

A85-23794

THEMATIC EVALUATION OF SPOT SPECTRAL BANDS [EVALUATION THEMATIQUE DES BANDES SPECTRALES DE SPOT]

G. SAINT, F. LAVENU (Centre National d'Etudes Spatiales, Toulouse, France), R. ZBINDEN (Ecole Normale Supérieure, Montrouge, Hauts-de-Seine, France), and J. CHOROWICZ (Paris VI, Université, Paris, France) IN: Spectral signatures of objects in remote sensing; International Conference, 2nd, Bordeaux, France, September 12-16, 1983, Reports Versailles, Institut National de la Recherche Agronomique, 1984, p. 881-888 In French.

The results of some studies on SPOT simulated data are analyzed in order to show the correspondence between the characteristics of the system and its missions. An evaluation of the characteristics is presented for the following two domains: renewable resources (agriculture and vegetation) and land use in coastal and urban zones. Radiometric measurements are carried out either by means of wide-band radiometers, identical to those of SPOT, or by using spectroradiometers which permit an integration over the spectral bands of HRV. The radiometric studies show that the choice of three spectral bands at a resolution of 20 m allows detailed mapping of land use and the coastal environment.

M.D.

A85-23795

**REVIEW OF EARTH OBSERVATION SATELLITE PROGRAMS
[REVUE DES PROGRAMMES DE TELEDETECTION
SATELLITE]**

F. J. DOYLE (International Society for Photogrammetry and Remote Sensing, Reston, VA) IN: Spectral signatures of objects in remote sensing; International Conference, 2nd, Bordeaux, France, September 12-16, 1983, Reports. Versailles, Institut National de la Recherche Agronomique, 1984, p. 889-898.

A review of international photogrammetry and remote sensing programs is presented. General descriptions are given of the status of current instrumentation and information processing technology in the USSR, the US, Japan, and India. Particular emphasis is given to a description of the Metric Camera (MC) experiment to be carried out during the Spacelab mission of the Space Shuttle.

I.H.

A85-24081

**THE ANALYSIS OF BACKSCATTERING PROPERTIES FROM
SAR DATA OF MOUNTAIN REGIONS**

H. ROTT (Innsbruck, Universitaet, Innsbruck, Austria) (International Union of Radio Science, International Symposium on Microwave Signatures in Remote Sensing, 3rd, Toulouse, France, Jan. 16-20, 1984) IEEE Journal of Oceanic Engineering (ISSN 0364-9059), vol. OE-9, Dec. 1984, p. 347-355. Research supported by the Fonds zur Foerderung der Wissenschaftlichen Forschung and Bundesministerium fuer Wissenschaft und Forschung of Austria. refs

Possibilities and problems for the extraction of backscattering coefficients from airborne and spaceborne Synthetic Aperture Radar (SAR) data are discussed. Corrections for system errors and for imaging geometry are described. Examples are given for airborne SAR data acquired in the X and C-bands over a test site in the Austrian Alps and for Seasat SAR data of glacierized areas in Iceland. From these data, backscattering coefficients have been derived on a relative scale for wet snow, glacier ice, and several ice-free surfaces. Data of in situ measurements on surface roughness and on dielectric parameters are presented for interpretation purposes and as the basis for backscatter modeling. The SAR-derived results are compared with theoretical backscattering calculations which were based on the Kirchhoff model for surface scattering and on the Born approximation for snow volume scattering.

Author

A85-24246#

**AIRCRAFT MEASUREMENTS FOR CALIBRATION OF AN
ORBITING SPACECRAFT SENSOR**

W. A. HOVIS, J. S. KNOLL, and G. R. SMITH (NOAA, National Environmental Satellite, Data, and Information Service, Washington, DC) Applied Optics (ISSN 0003-6935), vol. 24, Feb. 1, 1985, p. 407-410.

Satellite sensor calibration is readily established by means of simultaneous measurements along the satellite view vector from a calibrated instrument aboard a high altitude aircraft, so that the satellite sensor prelaunch radiance calibration can be compared with the in-orbit radiance values produced by comparison with the simultaneous aircraft data. The present aircraft measurements were made over the Atlantic Ocean, off the east coast of the U.S., and the comparison of prelaunch and in-orbit data indicated a 25-percent degradation in the Nimbus 7 Coastal Zone Color Scanner's channel 1.

O.C.

A85-24654

**THE POTENTIAL OF SOLAR POWER SATELLITES FOR
DEVELOPING COUNTRIES**

N. JASENTULIYANA and R. A. LUDWIG (United Nations, Outer Space Affairs Div., New York, NY) Space Solar Power Review (ISSN 0191-9067), vol. 4, 1983, p. 291-300. refs

The basic political, economic and technical aspects of a solar power satellite system (SPS) for the Third World are briefly discussed. It is shown that the development of a SPS system could contribute significantly to economic growth in developing countries by reducing the costs of energy to a level commensurate

with the rest of the world. Attention is given to the INTELSAT program as a model of a satellite system which serves the economic interests of the Third World without compromising the economic interests of the more developed nations.

I.H.

A85-25182*# National Aeronautics and Space Administration. Goddard Space Flight Center, Greenbelt, Md.

**COMMENTS ON 'INFERENCE OF CLOUD TEMPERATURE AND
THICKNESS BY MICROWAVE RADIOMETRY FROM SPACE'**

H.-Y. M. YEH (NASA, Goddard Space Flight Center, Laboratory for Atmospheric Sciences, Greenbelt, MD) Journal of Climate and Applied Meteorology (ISSN 0733-3021), vol. 23, Nov 1984, p. 1579.

The method proposed by Pandey et al. (1983) for estimating the temperature differential and thickness of clouds from microwave data obtained with the scanning multichannel microwave radiometers of the Seasat and Nimbus-7 satellites is examined critically. It is pointed out that both the thicknesses and the temperature differentials derived from them may not be meaningful unless accurate measurements of cloud-top height (from IR radiometry) and reliable data on liquid-water content are available. It is suggested that the good fits obtained in generating regression coefficients for the proposed method may be artifacts of the fixed or limited-range liquid-water densities of the cloud models used. With respect to cloud-top height, the need to quantify and account for differences in the fields of view and spatial resolutions of the IR and microwave radiometers, as undertaken for the case of precipitating clouds by Yeh and Liou (1983), is stressed.

T.K.

A85-25344

**OPTICAL ENGINEERING FOR COLD ENVIRONMENTS;
PROCEEDINGS OF THE MEETING, ARLINGTON, VA, APRIL 7,
8, 1983**

G. W. AITKEN, ED. (U.S. Army, Cold Regions Research and Engineering Laboratory, Hanover, NH) Meeting sponsored by SPIE - The International Society for Optical Engineering. Bellingham, WA, SPIE - The International Society for Optical Engineering (SPIE Proceedings, Volume 414), 1983, 231 p. For individual items see A85-25345 to A85-25354.

Optical hardware for cold environments are discussed, taking into account data needs for characterizing winter obscuration, cold environment fogs and measurements, a portable ice crystal replicator for use in snowfall transmission studies, a technique for measuring the mass concentration of falling snow, instruments used for snow characterization in support of SNOW-ONE-A and SNOW-ONE-B, the characterization of snow for evaluation of its effect on electromagnetic wave propagation, a visible and near-infrared scanning photometer for field measurements of spectral albedo and irradiance under polar conditions, and progress in methods of measuring the free water content of snow. Other subjects explored are related to electro-optical/infrared systems and effects, millimeter wave systems and effects, and remote sensing systems. Attention is given to the use of airborne lasers in terrestrial and water environments, the Landsat-4 thematic mapper (TM) for cold environments, millimeter-wave propagation through snow, and the characterization of ice particles in the atmosphere.

G.R.

A85-25347

**PERFORMANCE OF A COHERENT LIDAR REMOTE SENSOR
IN SNOW AND FOG**

R. M. HARDESTY (NOAA, Wave Propagation Laboratory, Boulder, CO) IN: Optical engineering for cold environments; Proceedings of the Meeting, Arlington, VA, April 7, 8, 1983. Bellingham, WA, SPIE - The International Society for Optical Engineering, 1983, p. 108-113. refs

Since spring 1981, a pulsed CO₂ coherent optical radar (lidar) was used in studies concerned with the laser-based remote sensing of atmospheric parameters. The primary objective of these studies is related to an investigation of the feasibility of the Windsat concept. This concept involves the measurement of the global wind field from space using a satellite-mounted scanning coherent optical radar system. Attention is given to a description of the optical

radar, aspects of measurement and analysis procedure, the obtained results, and seasonal effects on the performance of the optical radar
G R.

A85-25349* National Aeronautics and Space Administration. Goddard Space Flight Center, Greenbelt, Md. **LANDSAT-4 THEMATIC MAPPER (TM) FOR COLD ENVIRONMENTS**

J C. GERVIN, V. V. SALOMONSON (NASA, Goddard Space Flight Center, Greenbelt, MD), and H. L. MCKIM (U.S. Army, Cold Regions Research and Engineering Laboratory, Hanover, NH) IN: Optical engineering for cold environments, Proceedings of the Meeting, Arlington, VA, April 7, 8, 1983. Bellingham, WA, SPIE - The International Society for Optical Engineering, 1983, p. 179-186. refs

Landsat-4 was launched into a near-polar, sun-synchronous orbit on July 16, 1982. It is the largest and most complex of NASA's earth resources satellites. Landsat-4's instrument payload includes two remote sensors. The Multispectral Scanner Subsystem (MSS) is an electro-optical scanning radiometer with four spectral bands in the visible and near infrared, which was also carried aboard Landsats 1, 2, and 3. The second sensor, the Thematic Mapper (TM), represents a more advanced remote sensing instrument than the MSS. It uses a scanning mirror assembly to collect data from a 15.4 deg angle on both forward and reverse scans. It is pointed out that the improved spatial, spectral, and radiometric characteristics of TM have significant implications for satellite remote sensing in cold environments. The expected improvements are discussed, giving attention to snow, ice, water, soil, and land cover
G.R.

A85-25659 **CORRELATION OF SPECTRAL BRIGHTNESSES MEASURED USING MULTISPECTRAL SPACE IMAGES [O KORRELIATSII SPEKTRAL'NYKH IARKOSTEI, IZMERENNYKH PO MNOGOZONAL'NYM KOSMICHESKIM SNIMKAM]**

V. A. KOTTSOV and E. A. GORBUSHINA (Akademiya Nauk SSSR, Institut Kosmicheskikh Issledovaniy, Moscow, USSR) Issledovanie Zemli iz Kosmosa (ISSN 0205-9614), Nov.-Dec. 1984, p. 78-81. In Russian. refs

The correlation of the spectral-brightness parameters of ground objects as measured by satellite multispectral remote-sensing systems is considered with reference to photographs of the USSR taken with the Soyuz-22 MKF-6 camera. The occurrence of false correlation in the case of observations made over a large territory is noted, and it is shown that this false correlation can be reduced by the use of normalized parameters
B.J.

A85-25855# **REALTIME PROCESSOR OF SAR SYSTEMS**

R. SCHOTTER Dornier-Post (English Edition) (ISSN 0012-5563), no. 4, 1984, p. 29-31.

Attention is given to potential applications of a synthetic aperture radar (SAR) real time processor which was developed for Space Shuttle-based earth sensing, and which may prove useful in military surveillance, ocean wave studies, ship movements in territorial waters, land conservation, geology, and mineralogical prospecting. The SAR processor's signal processing task is characterized by complex algorithms and large quantities of raw data/time unit. A 'pipeline' configuration has been judged optimal for this type of processing, and it will consist of digital hardware modules for Fourier transform, digital filtering, two-dimensional image memory, and complex multiplication
O C

A85-26393# **INVESTIGATIONS OF THE ACCURACY OF THE DIGITAL PHOTOGRAMMETRY SYSTEM DPS, A RIGOROUS THREE DIMENSIONAL COMPILATION PROCESS FOR PUSH BROOM IMAGERY**

O. HOFMANN (Messerschmitt-Boelkow-Blohm GmbH, Munich, West Germany) International Society for Photogrammetry and Remote Sensing, International Congress on Photogrammetry and Remote Sensing, 15th, Rio de Janeiro, Brazil, June 17-29, 1984, Paper. 8 p
(MBB-UA-753/83-OE)

MBB developed a new concept for a digital stereo-scanner with three line sensor arrays working on the push broom principle and a suitable analytical compilation method. It delivers the orientation data of the camera along the flight trajectory of aircraft, spacecraft, or missiles, the three-dimensional coordinates of the digital elevation model (DEM), ortho- and stereo-orthophotos and geometrically rectified multispectral images. The procedure involves a digital correlation process and does not need, beside the scanner data, any additional information with the exception of a few control points for the absolute orientation. Special stabilizations or measurements of flight data are not required. By computer simulated models the accuracy of the process was tested

Author

A85-26642 **TERRAIN AND LOOK ANGLE EFFECTS UPON MULTISPECTRAL SCANNER RESPONSE**

C. J. STOHR (Illinois State Geological Survey, Champaign, IL) and T. R. WEST (Purdue University, West Lafayette, IN) Photogrammetric Engineering and Remote Sensing (ISSN 0099-1112), vol. 51, Feb. 1985, p. 229-235. Sponsorship: U.S. Department of Transportation. refs
(Contract DOT-FH-7565)

Statistical analysis of airborne multispectral scanner (MSS) data of a pasture show that the effects of the sun-scanner look angle and terrain elements vary between spectral regions and wavelength bands. Shorter wavelength bands experienced the greatest influence, reflective infrared the least. Shorter wavelengths are most affected by the sun-scanner look angle alone.
Author

A85-26927 **THE INFLUENCE OF SATELLITE SPECTRAL SENSOR RESPONSE ON THE ANALYSIS OF SATELLITE IMAGERY AT HIGH LATITUDES**

K. P. SHINE (Oxford University, Oxford, Liverpool, University, Liverpool, England) and A. HENDERSON-SELLERS (Liverpool, University, Liverpool, England) International Journal of Remote Sensing (ISSN 0143-1161), vol. 6, Jan. 1985, p. 29-34. refs
(Contract NSF ATM-80-18898)

Many polar-orbiting satellites used in high-latitude work employ instruments which sense only narrow regions of the solar spectrum. A radiative transfer scheme is used to illustrate the differences between broad-band albedos and those calculated using the spectral response of the NOAA-6 AVHRR channel 1 and DMSP visible sensors. The albedo contrast between snow/no snow is shown to be exaggerated by the satellite sensors and the impact of cloudiness over snow on the albedo is drastically reduced, by a factor of 10 in the case of the NOAA-6 sensor. A significant solar zenith angle dependence is also shown for the NOAA-6 sensor
Author

A85-26928 **THE CURRENT USE OF TIROS-N SERIES OF METEOROLOGICAL SATELLITES FOR LAND-COVER STUDIES**

L. HAYES (Dundee, University, Dundee, Scotland) International Journal of Remote Sensing (ISSN 0143-1161), vol. 6, Jan. 1985, p. 35-45. refs

A literature survey of the use of data from the TIROS-N series of polar orbiting meteorological satellites in investigations outside the meteorological and oceanographic context is presented. Studies of the land surface using sensors aboard these satellites have

mostly used combinations of reflected wavelengths up to the present. These studies suggest that the Advanced Very High Resolution Radiometer (AVHRR) can provide valuable information on various surface features. Comparisons of data from the TIROS-N series platforms with data from Landsat lend support to this view. A review of previous work outlining differences between the TIROS-N and Landsat satellite systems is presented together with a summary of the various combinations of reflected wavelengths as applied to land surface studies. The final section summarizes the work undertaken in studies published. Author

A85-26929* National Aeronautics and Space Administration
Goddard Space Flight Center, Greenbelt, Md.
**COMPARISON OF LEVEL I LAND COVER CLASSIFICATION
ACCURACY FOR MSS AND AVHRR DATA**

J. C. GERVIN, A. G. KERBER, R. G. WITT (NASA, Goddard Space Flight Center, Greenbelt, MD), Y. C. LU, and R. SEKHON (Computer Sciences Corp., Silver Spring, MD) International Journal of Remote Sensing (ISSN 0143-1161), vol. 6, Jan. 1985, p. 47-57 refs

The capabilities of the Advanced Very-High-Resolution Radiometer (AVHRR) for land-cover mapping were investigated by comparing the accuracy of land-cover information for the Washington, DC area derived from NOAA-7 AVHRR data with that from Landsat Multispectral Scanner Subsystem (MSS) data. Unsupervised level I land-cover classifications were performed for MSS and AVHRR data sets collected on July 11, 1981. A detailed accuracy assessment was conducted based on ground data delineated on 12 U.S. Geological Survey 7-5 min series topographic maps. These results produced overall land-cover classification accuracies of 71.9 and 76.8 per cent for AVHRR and MSS, respectively. While the accuracies for predominant categories were similar for both sensors, land-cover discrimination for less commonly occurring and/or spatially heterogeneous categories was improved with the MSS data set. The AVHRR, however, performed as well as or better than the MSS in classifying large homogeneous areas. The application of AVHRR data with its lower processing cost and more frequent worldwide coverage appears promising for regional land-cover mapping. Author

A85-27057#

**SPAS-01 - SPACE FLIGHT TECHNOLOGY FOR THE GENERAL
USER [SPAS-01 - RAUMFLUGTECHNIK FUER
NORMALVERBRAUCHER]**

G. GREGER (Bundesministerium fuer Forschung und Technologie, Bonn, West Germany) Luft- und Raumfahrt (ISSN 0173-6264), vol. 5, 4th Quarter, 1984, p. 99-102 In German

The present paper is concerned with a space mission which involved the employment of the first, reusable 'Shuttle Pallet Satellite' (SPAS). A SPAS is taken into space by the Orbiter of the Space Shuttle system. It can be released to become an independent satellite of the earth. The SPAS 01 had been built by a West German aerospace company. Its first flight occurred in connection with a launch of the American Space Shuttle in June 1983. The experimental program of the SPAS-01 included a study of 'environmental pollution' in the vicinity of the Orbiter. Other experiments were related to the development of new, efficient methods for earth observation. The significance of SPAS-01 is evaluated. One important aspect is the aim to reduce the costs for experiments in space by launching a payload together with other payloads as part of the cargo of the Space Shuttle. A significant reduction of the involved costs would provide the basis for a more general utilization of the possibilities provided by the space environment. G.R.

A85-27059#

**MODULAR OPTOELECTRONIC MULTISPECTRAL SCANNER
(MOMS) TECHNOLOGICAL ASPECTS [MODULARER
OPTOELEKTRONISCHER MULTISPEKTRAL SCANNER (MOMS)
TECHNISCHE ASPEKTE]**

H. WINKENBACH (Deutsche Forschungs- und Versuchsanstalt fuer Luft- und Raumfahrt, Cologne, West Germany) and MEISSNER (Messerschmitt-Boelkow-Blohm GmbH, Bremen, West Germany) Luft- und Raumfahrt (ISSN 0173-6264), vol. 5, 4th Quarter, 1984, p. 105-108. In German. Research supported by the Bundesministerium fuer Forschung und Technologie. refs

MOMS has been developed by a German aerospace company for remote sensing applications involving the use of aircraft or spacecraft platforms. The scanning system is based on an employment of high-resolution linear charged coupled device (CCD) detectors. The space version of the instrument, called MOMS-01, has been employed on board of the Orbiter during the missions STS-7 and STS-11. The obtained digital image data show the highest resolution ever obtained with instruments located in space. A description is provided of the 'push-broom' scanning principles utilized in MOMS. Attention is also given to details regarding the design of the MOMS-01 system, the conduction of the two missions involving the use of the Space Shuttle, the current status of the MOMS program, and an outlook regarding future developments. G.R.

A85-27061#

**MOMS 1 AND ITS RESULTS [MOMS 1 UND SEINE
ERGEBNISSE]**

J. BODECHTEL, R. HAYDN, A. YAMANI, J. ZILGER (Muenchen, Universitaet, Munich, West Germany), P. SEIGE, and H. WINKENBACH (Deutsche Forschungs- und Versuchsanstalt fuer Luft- und Raumfahrt, Cologne, West Germany) Luft- und Raumfahrt (ISSN 0173-6264), vol. 5, 4th Quarter, 1984, p. 113-122 In German refs

The Modular Optoelectronic Multispectral Scanner (MOMS) is a new optoelectronic system intended for tasks of application-oriented remote sensing related to geology, forestry, agriculture, land utilization, and urban and regional planning. MOMS was developed by a German aerospace company. Missions of the two-channel MOMS-01 on board the Orbiter Challenger in connection with the flights STS-7 (June 1983) and STS-11 (February 1984) were conducted for a technological verification of the suitability of the sensor design and a demonstration of the capabilities of the instrument in map plotting applications up to a scale of 1:50,000. Attention is given to the MOMS concept and its technical specification in MOMS-01, details regarding the two MOMS-01 missions, the interpretation of the MOMS-01 data, the test area Bolivia, the test area Saudi Arabia, and plans for a further development of the MOMS family of instruments. Results obtained with MOMS-01 are illustrated with the aid of a number of graphs, taking into account a map of the city of Riyadh in Saudi Arabia. G.R.

A85-27698#

**AN AUTOMATIC HIGH-RESOLUTION PICTURE TRANSMISSION
RECEIVING STATION**

R. J. H. BRUSH and P. E. BAYLIS (Dundee, University, Dundee, Scotland) ESA Journal (ISSN 0379-2285), vol. 8, no. 4, 1984, p. 425-435. refs

A method to gather data from the NOAA series of meteorological satellites completely automatically, without the need for operator intervention, is described. The receiver, antenna mounting, high-density tape recorder, tracking computer, software, system operation and refinements, timing corrections, antenna pointing calculations, timing adjustments during a pass, autotrack system, and reliability are discussed. The system has been proved reliable and provides a most economical solution to the problems of automatic data collection from polar-orbiting satellites. C.D.

A85-27947* Cities Service Oil Co., Tulsa, Okla.
DEVELOPMENTS WITH MULTISPECTRAL THERMAL-IR AND ACTIVE MICROWAVE SYSTEMS - TIMS, SIR-A, SIR-B, AND RADARSAT

P. G. HARRISON (Cities Service Co., Tulsa, OK), A. B. KAHLE (California Institute of Technology, Jet Propulsion Laboratory, Pasadena, CA), F. F. SABINS (Chevron Oil Field Research Co., La Habra, CA), M. SETTLE (NASA, Washington, DC), V. R. SLANEY, and R. MORRITT IN: Frontiers for geological remote sensing from space; Geosat Workshop, 4th, Flagstaff, AZ, June 12-17, 1983, Report . Falls Church, VA, American Society of Photogrammetry, 1983, p. 49-55.

An update of current and future systems for spectral scanning of geological features in the thermal-IR, and active microwave bands is presented. The design characteristics of four individual systems are described, including the NASA Thermal Infrared Multispectral Scanner (TIMS); the Shuttle Imaging Radars A and B (SIRA-A and SIRA-B); and the Canadian RADARSAT satellite for geological mapping and ice monitoring. The applications of spectral data from the Side Looking Airborne Radar (SLAR), the GEMS 100 mapping system, and the Landsat RBV instrument to the mapping of large geological structures are also described.

I.H.

A85-29784
INTERCOMPARISONS OF TOMS, SBUV AND MFR SATELLITE OZONE MEASUREMENTS

J. E. LOVILL (California, University, Livermore, CA) (COSPAR, Topical Meeting on Intercomparison of Stratospheric/Mesospheric Data, Graz, Austria, June 25-July 7, 1984) Advances in Space Research (ISSN 0273-1177), vol. 4, no. 6, 1984, p. 57, 58.

A simultaneous intercomparison of ozone measurements by the Total Ozone Mapping System (TOMS), Satellite Backscattered Ultraviolet (SBUV), and Multichannel Filter Radiometer (MFR), obtained in July 1979, is presented. For all three data sets the largest difference is noted in the 55-75 deg N latitude region, where it is 30.6 DU between SBUV and MFR. The data sets compare most closely between 15 deg N and 60 deg S, with the difference between TOMS and MFR being within 3 percent (9.3 DU) in a 75-deg latitudinal span. The same general large-scale features were observed in all data sets, with maxima at 50-60 deg N and 40-60 deg S, and minima at 0-5 deg S.

L.T.

A85-29909
CONICAL MULTISPECTRAL SCANNER FOR THE STUDY OF EARTH RESOURCES [MNOGOZONAL'NYI SKANER S KONICHESKOI RAZVERTKOI DLIA ISSLEDOVANIIA PRIRODNYKH RESURSOV]

A. S. SELIVANOV, M. K. NARAEVA, B. I. NOSOV, A. S. PANFILOV, I. F. SINELNIKOVA, and B. A. SUVOROV Issledovanie Zemli iz Kosmosa (ISSN 0205-9614), Jan.-Feb. 1985, p. 66-72. In Russian refs

The design and operation of a four-band optomechanical scanner intended for the study of earth resources from the Meteor-Priroda satellites are described. The scanner covers a survey band of 600 km and has a scan rate of 48 lines per second, scanning is performed according to a conical law with a line-of-sight inclination of 39 deg. A relative radiometric accuracy of 1-1.5 percent is achieved in the spectral bands utilized, i.e., 0.5-0.6, 0.6-0.7, 0.7-0.8, and 0.8-1.1 micron. Diagrams of the optical system and video channel are presented along with the modulation curve.

B.J.

N85-16244*# SAR, Inc., Riverdale, Md.
CHARACTERIZING THE SCIENTIFIC POTENTIAL OF SATELLITE SENSORS

Dec 1984 13 p ERTS
 (Contract NAS5-28200)
 (E85-10044; NASA-CR-174221; NAS 1.26:174221) Avail: NTIS HC A02/MF A01 CSCL 08B

Eleven thematic mapper (TM) radiometric calibration programs were tested and evaluated in support of the task to characterize the potential of LANDSAT TM digital imagery for scientific

investigations in the Earth sciences and terrestrial physics. Three software errors related to integer overflow, divide by zero, and nonexistent file group were found and solved. Raw, calibrated, and corrected image groups that were created and stored on the Barker2 disk are enumerated. Black and white pixel print files were created for various subscenes of a San Francisco scene (ID 40392-18152). The development of linear regression software is discussed. The output of the software and its function are described. Future work in TM radiometric calibration, image processing, and software development is outlined.

R.S.F.

N85-16249*# SAR, Inc., Riverdale, Md.
CHARACTERIZING THE SCIENTIFIC POTENTIAL OF SATELLITE SENSORS

Nov. 1984 13 p Sponsored by NASA Original contains imagery Original photography may be purchased from the EROS Data Center, Sioux Falls, S.D. 57198 ERTS
 (E85-10053; NASA-CR-174227; NAS 1.26:174227) Avail: NTIS HC A02/MF A01 CSCL 08B

Analytical and programming support is to be provided to characterize the potential of the LANDSAT thematic mapper (TM) digital imagery for scientific investigations in the Earth sciences and in terrestrial physics. In addition, technical support to define lower atmospheric and terrestrial surface experiments for the space station and technical support to the Research Optical Sensor (ROS) study scientist for advanced studies in remote sensing are to be provided. Eleven radiometric calibration and correction programs are described. Coherent noise and bright target saturation correction are discussed along with image processing on the LAS/VAX and Hp-300/IDIMS. An image of San Francisco, California from TM band 2 is presented.

R.S.F.

N85-16250*# Arizona Univ., Tucson
LANDSAT-4 THEMATIC MAPPER MODULATION TRANSFER FUNCTION (MTF) EVALUATION Progress Report, 15 Jun. - 15 Sep. 1984

R. SCHOWENGERDT, Principal Investigator 16 Nov. 1984 8 p ERTS
 (Contract NCC2-234)
 (E85-10055; NASA-CR-174228; NAS 1.26:174228) Avail: NTIS HC A02/MF A01 CSCL 08B

The techniques used in the two-image comparison of TM data and 7-meter aerial data acquired over San Francisco on August 12, 1983 during LANDSAT 4 operation were refined. Analysis of one area is complete and reported herein; analysis of a second area is in progress. A large test target for measurement of the LANDSAT 5 MTF at the White Sands Missile Range, New Mexico was constructed.

R.S.R.

N85-16268*# Environmental Research Inst. of Michigan, Ann Arbor. Infrared and Optics Div.
STUDY OF SPECTRAL/RADIOMETRIC CHARACTERISTICS OF THE THEMATIC MAPPER FOR LAND USE APPLICATIONS

Quarterly Status Technical Progress Report, 21 Jun. - 20 Sep. 1984

W. A. MALILA, Principal Investigator and M. D. METZLER Oct. 1984 38 p refs ERTS
 (Contract NAS5-27346)
 (E85-10057; NASA-CR-174229; NAS 1.26:174229; ERIM-164000-13-P; QSTPR-8) Avail: NTIS HC A03/MF A01 CSCL 08B

Progress during the Environmental Research Institute of Michigan-ERIM's and 5 image data quality assessment program for the thematic mapper is described. Analyses of LANDSAT 5 TM radiometric characteristics were performed. Effects which had earlier been found in LANDSAT 4 TM data were found to be present in LANDSAT 5 data as well, including: (1) scan direction related signal droop, (2) scan correlated level shifts; and (3) low frequency coherent noise. Coincident LANDSAT 4 and 5 raw TM data were analyzed, and band by band relationships between the two sensors were derived. Earlier efforts which developed an information theoretic measure of multispectral information content

were continued, comparing TM and MSS information content.

Author

N85-16270*# Santa Barbara Research Center, Calif.
**THEMATIC MAPPER. VOLUME 1: CALIBRATION REPORT
FLIGHT MODEL, LANDSAT 5 Final Report**

R. C. COOLEY and J. C. LANSING Sep 1984 248 p ERTS
11 Vol.

(Contract NAS5-24200)

(E85-10059; NASA-CR-174231; NAS 1.26 174231;

HS236-9060-VOL-1) Avail: NTIS HC A11/MF A01 CSCL 14B

The calibration of the Flight 1 Model Thematic Mapper is discussed. Spectral response, scan profile, coherent noise, line spread profiles and white light leaks, square wave response, radiometric calibration, and commands and telemetry are specifically addressed. M.G.

N85-16271*# Santa Barbara Research Center, Calif.

**THEMATIC MAPPER. VOLUME 2: FLIGHT MODEL
PRESHIPMENT REVIEW**

23 Sep. 1982 250 p ERTS 11 Vol.

(Contract NAS5-24200)

(E85-10060; NASA-CR-174232; NAS 1.26 174232) Avail: NTIS
HC A11/MF A01 CSCL 14B

The various systems of the Thematic Mapper are reviewed and a comparison of measured and specified performance is given. Test methodologies are described. The specific instrument systems discussed include the power supply assembly, scan mirror, electronics module, focal plane assembly, radiometer, and radiation cooler M.G.

N85-16284# European Space Agency, Paris (France)
**ENHANCEMENT OF MULTISPECTRAL SCANNER IMAGES BY
DIGITAL FILTERING**

P. NOWAK May 1984 141 p refs Transl into ENGLISH of
"Bildverbesserung an multispektralen Scanneraufnahmen mit Hilfe
digitaler Filterverfahren", DFVLR, Oberpfaffenhofen, West Ger
Report DFVLR-FB-79-11, 1979

(ESA-TT-624; DFVLR-FB-79-11) Avail: NTIS HC A07/MF A01;
original German version available from DFVLR, Cologne DM 28

The possibilities for image enhancement of multispectral scanner images using two-dimensional digital filters were investigated. The theory of imaging system, possible distortions during image recording, and the theoretical basics of nonrecursive digital filtering were examined. Design techniques for digital filters are described. Results of the application of digital filter techniques to multispectral scanner data are presented. It is shown that the filtering and elimination of image distortions can have a favorable effect on subsequent image processing steps (e.g., multispectral classification). Author (ESA)

N85-17208*# Jet Propulsion Lab., California Inst. of Tech.,
Pasadena

THE SIR-B SCIENCE INVESTIGATIONS PLAN

1 Jul. 1984 210 p refs

(Contract NAS7-918)

(NASA-CR-174282; JPL-PUB-84-3; NAS 1.26.174282) Avail:
NTIS HC A10/MF A01 CSCL 171

Shuttle Imaging Radar-B (SIR-B) is the second synthetic aperture radar (SAR) to be flown on the National Aeronautics and Space Administration's Space Transportation System (Shuttle). It is the first spaceborne SAR to feature an antenna that allows acquisition of multincidence angle imagery. An international team of scientists will use SIR-B to conduct investigations in a wide range of disciplines. The radar, the mission, and the investigations are described.

N85-17250*# Kansas Univ. Center for Research, Inc.,
Lawrence.

**EVALUATION OF THE RADAR RESPONSE TO LAND
SURFACES AND VOLUMES: EXAMINATION OF THEORETICAL
MODELS, TARGET STATISTICS, AND APPLICATIONS**

F. T. ULABY, A. K. FUNG, M. C. DOBSON, and J. CHILAR (Canada
Centre for Remote Sensing, Ottawa) In JPL The SIR-B Sci.
Invest. Plan 3 p 1 Jul. 1984

Avail: NTIS HC A10/MF A01 CSCL 171

Four areas of L-band radar remote sensing of terrain were examined: (1) the behavior of the radar backscatter coefficient of distributed surface and volumes as a function of the targets' dielectric and geometric parameters and as a function of their physical parameters; (2) the correspondence of the angular behavior of the relative backscatter coefficient as extracted from SIR-B digital imagery and truck mounted L-band scatterometer measurements for about 100 fields, (3) the statistical behavior of SIR-B image density for targets that appear homogeneous on Thematic Mapper (TM) optical imagery and/or color IR photography, and (4) the applicability of SIR-B imagery both alone and in conjunction with TM imagery for the classification and monitoring of land cover and renewable resources. B.G.

N85-17350# Technical Univ. of Denmark, Lyngby. Inst. of
Electromagnetics.

**SPACEBORNE MICROWAVE RADIOMETERS: BACKGROUND
AND TECHNOLOGY REQUIREMENTS Final Report**

P. GUDMANDSEN, ed., N. SKOU, ed., and B. WOLFF, ed. Aug
1983 176 p refs Original contains color illustrations

(Contract ESTEC-4964/81/NL-MS(SC))

(LD-R-267; ESA-CR(P)-1928) Avail: NTIS HC A09/MF A01

Spaceborne microwave radiometer requirements in atmospheric, oceanographic, and cryospheric applications are discussed. Data processing is considered. Although still in a development phase, microwave radiometry shows examples of operational applications in the fields of atmospheric sounding and sea ice monitoring. The 10-channel Scanning Multichannel Microwave Radiometer on SEASAT and NIMBUS-7 is shown to have a good concept. However, experience suggests that improvements of the techniques, the calibration method, and the data retrieval are desirable. Developments over the past decade concern frequencies below 60 GHz and antenna and receiver techniques as well as development of suitable data retrieval methods. Author (ESA)

N85-17406# Royal Inst. of Tech., Stockholm (Sweden). Dept.
of Photogrammetry.

**PAPERS OF THE 15TH INTERNATIONAL SOCIETY FOR
PHOTOGRAMMETRY AND REMOTE SENSING (ISPRS)
CONGRESS**

1984 78 p refs Congr. held at Rio de Janeiro, Jun. 1984

(TRITA-FMI-9; ISSN-0071-8068) Avail: NTIS HC A05/MF A01;
Royal Institute of Technology, Stockholm SEK 150

Mathematical aspects of digital terrain information, comparative testing of photogrammetrically sampled digital elevation models; multimodel utilization; hierarchical data structures and algorithms for digital stereoscopic mensuration; an algorithm for computation of the inverse in bundle adjustment systems, digital elevation model computation using fast Poisson solutions; and sequential data processing for photogrammetric acquisition of digital elevation models were discussed.

N85-17409# Royal Inst. of Tech., Stockholm (Sweden). Dept.
of Photogrammetry.

**MULTIMODELS INCREASE ACCURACY: SUMMARY OF AN
EXPERIMENT**

K. TORLEGAARD In its Papers of the 15th Intern. Soc. for
Photogrammetry and Remote Sensing (ISPRS) Congr. p 24-33
1984 refs

Avail: NTIS HC A05/MF A01

Photogrammetry results based on multimodels formed by averaging two or more single stereomodels are presented. The single models are calculated without correction for lens distortion, atmospheric refraction and Earth curvature. Photographs were

08 INSTRUMENTATION AND SENSORS

taken from four flying altitudes, with different aircraft speed and flying directions. Accuracy was determined as rms errors, mean errors and standard deviations in planimetry and elevation. The classical theory of error propagation is confirmed. The precision of photogrammetric stereomodels can be decomposed into components related to ground coordinates, image coordinates and image motion due to aircraft speed. The accuracy improvement by multimodels is proportional to $1/\sqrt{n}$, n = number of models. The multimodel method increase of the accuracy is similar to the additional parameters in photogrammetric block adjustment, because both methods are based on multiple photographic coverage. Author (ESA)

N85-17469# Aerospace Corp., El Segundo, Calif.
AN AURORAL X-RAY IMAGING SPECTROMETER
P. F. MIZERA, W. A. KOLASINSKI, D. J. GORNEY, and J. L. ROEDER 30 Sep. 1984 13 p
(Contract F04701-83-C-0084)
(AD-A147756; TR-0084(4478-32)-4; SD-TR-84-39) Avail NTIS HC A02/MF A01 CSCL 04A

A scanning X-ray spectrometer was flown aboard the USAF-Defense Meteorological Satellite Program (DMSP-F6) satellite to image X-ray production in the Earth's atmosphere. One of the main objectives of this experiment was to image auroral signatures associated with electron precipitation at energies above a few keV. A brief description of the instrument is given and a sequence of auroral images is shown to demonstrate on-orbit performance and to illustrate the use of such data to remotely monitor ionization density perturbations in the Earth's atmosphere. Author (GRA)

N85-19385# Instituto de Pesquisas Espaciais, Sao Jose dos Campos (Brazil).
BRAZILIAN REMOTE SENSING SHUTTLE EXPERIMENT (BRESEX): CHARACTERISTICS AND FUTURE UTILIZATION ON SATELLITES
N. D. J. PARADA Oct 1984 11 p Presented at the 18th Intern. Symp. on Remote Sensing of the Environment, Paris, 1-5 Oct. 1984
(INPE-3313-PRE/620) Avail. NTIS HC A02/MF A01

Brazilian Space Program plans include the design, manufacturing, launching, operation of four satellites, two of which are designated for the remote sensing of Earth. A cooperative experiment with NASA provides the opportunity to use, in space, a prototype of the imaging instrument designed for these satellites. The objective of the Brazilian Remote Sensing Experiment (BRESEX) to be carried on space shuttle are listed. Specifications for the CCD, pushbroom mode, multispectral band camera are considered. A.R.H.

N85-19489# Environmental Research Inst. of Michigan, Ann Arbor.
STUDY OF SPECTRAL/RADIOMETRIC CHARACTERISTICS OF THE THEMATIC MAPPER FOR LAND USE APPLICATIONS
Quarterly Status Technical Progress Report, 21 Sep. - 20 Dec. 1984
W. A. MALILA and M. D. METZLER, Principal Investigators Jan. 1985 35 p refs ERTS
(Contract NAS5-27346)
(E85-10075; NASA-CR-174402; NAS 1.26:174402; ERIM-164000-14-P; QSTPR-9) Avail. NTIS HC A03/MF A01 CSCL 08B

The radiometric characteristics of LANDSAT 5 TM data were analyzed. Effects which were found earlier and quantified in LANDSAT 4 TM data were quantified for LANDSAT-5 data as well, including: scan-direction-related signal droop and scan correlated level shifts. Coincident LANDSAT 4 and 5 fully corrected (CCT-PT) TM data were analyzed, and band-by-band relationships between the two sensors were derived in terms of both signal counts and radiance. A.R.H.

N85-19491# Arizona Univ., Tucson. Optical Sciences Center.
SPECTRORADIOMETRIC CALIBRATION OF THE THEMATIC MAPPER AND MULTISPECTRAL SCANNER SYSTEM Quarterly Report, 1 Aug. - 31 Oct. 1984
P. N. SLATER and J. M. PALMER, Principal Investigators 4 Dec. 1984 39 p refs ERTS
(Contract NAS5-27382)
(E85-10077; NASA-CR-174404; NAS 1.26:174404, QR-8) Avail. NTIS HC A03/MF A01 CSCL 08B

Radiometric measurements were taken on the morning of the LANDSAT 5 Thematic Mapper overpass. The sky was cloud free and the sites were dry. Barnes multiband radiometer data were collected for a 4 x 4 pixel area and two fractional pixel areas of slightly higher and lower reflectances than the larger area. Helicopter color photography was obtained of all the ground areas. This photography will allow a detailed reflectance map of the 4 x 4 pixel area to be made and registered to the TM imagery to an accuracy of better than half a pixel. Spectropolarimeter data were also collected of the 4 x 4 pixel area from the helicopter. In addition, ground based solar radiometer data were collected to provide spectral extinction optical thickness values. The radiative transfer theory used in the development of the Herman code which was used in predicting the TM entrance pupil spectral radiances from the ground based measurements is described. B.G.

N85-19492# Santa Barbara Research Center, Goleta, Calif.
THEMATIC MAPPER: DESIGN THROUGH FLIGHT EVALUATION Final Report
Dec. 1984 208 p refs Revised Original contains imagery. Original photography may be purchased from the EROS Data Center, Sioux Falls, S.D. 57198 ERTS
(Contract NAS5-24200)
(E85-10078; NASA-CR-174405; NAS 1.26:174405) Avail. NTIS HC A10/MF A01 CSCL 14B

LANDSAT 4 and 5, launched in 1982 and 1984, not only carried the Thematic Mapper, but were redesigned to handle the increased data rates associated with it, and to communicate that data to Earth via geosynchronous orbiting Tracking and Data Relay Satellites (TDRS). The TM development program is summarized. A brief historical perspective is presented of the evolution of design requirements and hardware development. The basic performance parameters that serve as sensor design guidelines are presented. B.G.

N85-19501# Instituto de Pesquisas Espaciais, Sao Jose dos Campos (Brazil)
REMOTE SENSING ACTIVITIES IN LATIN AMERICA
N. D. J. PARADA Sep 1984 15 p Presented at the 18th Intern. Symp. on Remote Sensing of Environ., Paris, 1-5 Oct. 1984
(INPE-3297-PRE/612) Avail. NTIS HC A02/MF A01

The status of remote sensing in Latin America is discussed, including the reasons, motivations, and importance of remote sensing activities in the Latin American environment. In the field of data reception, processing, distribution, and utilization, the efforts made to improve those aspects which are vital to the whole process of remote sensing are presented. Specific countries with their programs and projects are mentioned briefly. The Brazilian remote sensing experiment (BRESEX) and its future utilization on the Brazilian complete space mission on board the shuttle is considered. Finally, the importance of regional societies, symposia, and training programs is addressed. R.S.F.

N85-20190# Joint Publications Research Service, Arlington, Va.
REMOTE SENSING TECHNOLOGY NOW PLAYING PRACTICAL ROLES
In its China Rept. Sci. and Technol. (JPRS-CST-84-026) p 1-6 18 Sep. 1984 Transl. into ENGLISH from Dianzi Shijie (Peking), no. 5, 1983 p 4-5
Avail: NTIS HC A03/MF A01

China has launched and recovered numerous scientific research satellites and has successfully developed many types of aerial remote sensors, including the highly sophisticated multiband

scanner and synthetic aperture lateral view radar. Rather high levels of development in designing and test producing optical image processors have been attained and the prospects of digital image processors being incorporated and assimilated in this area are promising. Many provinces, municipalities, and regions have been successful in experimenting with aerial remote sensing and satellite imagery analysis. Applications of remote sensing agriculture, evaluating mines and natural resources, and environmental monitoring are reviewed. A.R.H.

N85-20220# Joint Publications Research Service, Arlington, Va.
AIRBORNE REMOTE SENSING CCD IMAGING SYSTEM
 M. ZONGQUAN *In its* China Rept. Sci. and Technol (JPRS-CST-84-040) p 65-72 6 Dec 1984 refs Transl. into ENGLISH from Dianzi Xuebao (Beijing), no. 1, 1984 p 96-99
 Avail. NTIS HC A07/MF A01

An airborne remote sensing charge coupled device (CCD) imaging and transmission system is presented. Imaging formulas were derived. The equation express the signal to quantiz noise ratio with delta modulation is given. Experimental results are presented. The system described includes: a linear array CCD camera, digital video transmitter, receiver, terminal display, and recording device. The airborne portion is comprised of a camera, antenna and digital transmitter. The total weight is less than 5 kilograms and the power consumption is less than 12 W. E.A.K.

N85-20496*# National Aeronautics and Space Administration
 Goddard Space Flight Center, Greenbelt, Md
LANDSAT-4 SCIENCE CHARACTERIZATION EARLY RESULTS. VOLUME 1: MULTISPECTRAL SCANNER (MSS)
 J L BARKER, ed. Washington Jan. 1985 206 p refs Symp. held in Greenbelt, Md., 22-24 Feb 1983. Original contains imagery. Original photography may be purchased from the EROS Data Center, Sioux Falls, S.D. 57198 ERTS 4 Vol (E85-10067, NASA-CP-2355-VOL-1; REPT-85B0115-VOL-1; NAS 155-2355-VOL-1) Avail. NTIS HC A10/MF A01 CSCL 05B

LANDSAT 4 MSS data was characterized from a geometric, radiometric, geodetic, temporal, and spatial standpoint. Comparisons were made between LANDSAT 4 MSS data and similar data generated by earlier LANDSAT satellites. Error analyses were conducted on MSS data sets and band-to-band registration accuracy was evaluated.

N85-20499*# National Aeronautics and Space Administration.
 Goddard Space Flight Center, Greenbelt, Md.
SPECTRAL CHARACTERIZATION OF THE LANDAT-4 MSS SENSORS

B L MARKHAM and J L BARKER *In its* LANDSAT-4 Sci. Characterization Early Results, Vol. 1 p 23-56 Jan 1985 refs. Previously announced in IAA as A83-36575 ERTS
 Avail. NTIS HC A10/MF A01 CSCL 14B

Two multispectral scanner subsystems (MSS) have been fabricated and tested by an American aerospace company for the NASA LANDSAT program. One MSS, designated the protoflight (PF) model, was integrated into the LANDSAT-4 spacecraft, which was launched on July 16, 1982. The second, designated the flight (F) model, has been integrated into the LANDSAT-4 backup satellite, which is scheduled for possible launch in 1985. Each MSS has four bands in the reflective portion of the electromagnetic spectrum. The engineering test data which were collected included channel-by-channel spectral response curves. A description of the test procedure is included in Appendix A. This document is to make available to the LANDSAT user community data on the spectral characteristics of the two sensors. The LANDSAT-4 PF and F scanners were found to be essentially identical in mean spectral response. G.R. (IAA)

N85-20500*# Environmental Research Inst. of Michigan, Ann Arbor.

INVESTIGATION OF RADIOMETRIC PROPERTIES OF LANDSAT-4 MSS

D. P. RICE and W. A. MALILA *In* NASA Goddard Space Flight Center LANDSAT-4 Sci. Characterization Early Results, Vol. 1 p 57-76 Jan. 1985. Original contains imagery. Original photography may be purchased from the EROS Data Center, Sioux Falls, S.D. 57198 ERTS

Avail. NTIS HC A10/MF A01 CSCL 05B

Detector calibration and satellite-to-satellite calibration are discussed with respect to the characterization of LANDSAT 4 image data quality. LANDSAT data for California, North Carolina, South Carolina, and New England were utilized. Banding, quantization effects, coherent noise, relative calibration between LANDSAT 3 and 4, and geometric considerations are addressed. Evidence strongly suggests that LANDSAT 4 data are of the same high quality as previous LANDSATs, with a comparable dynamic range and target response, a good detector equalization procedure, and an accurate linear response to received radiance. A linear relationship between LANDSAT 3 and 4 was determined that renders LANDSAT 4 signals to have the same radiance response as LANDSAT 3 signals. Two artifacts, not noted in previous LANDSATs, were found and quantified. One is a geometric scan line length variation in LANDSAT A tapes, and was shown to be fairly well correctable. The other artifact is a coherent noise effect in all bands, having an amplitude of less than one count. R.S.F.

N85-20502*# National Aeronautics and Space Administration
 Earth Resources Labs., Bay St. Louis, Miss.

LANDSAT SCENE-TO-SCENE REGISTRATION ACCURACY ASSESSMENT

J. E. ANDERSON *In* NASA. Goddard Space Flight Center LANDSAT-4 Sci. Characterization Early Results, Vol. 1 p 119-122 Jan. 1985 ERTS

Avail. NTIS HC A10/MF A01 CSCL 05B

The scene-to-scene registration performance of the MSS on LANDSAT 4 relative to LANDSAT 1 through 3 MSS systems was evaluated. The temporal registration performance of LANDSAT 4 TM data sets was determined. A tabular comparison is presented of LANDSAT 2 and 4 element error, scan line error, registration RMS error, and indicated RMS error at the time of mapping equation development. The 1980/1982 registration resulted in an element error which was nearly twice as large as that obtained in the 1980/1981 registration (40 320 vs. 20 416 meters). This occurred even though the scan line errors were nearly identical (26.951 vs. 26 701 meters). Subsequent analysis indicated that the large element error encountered in the 1980/1982 temporal registration may be the result of less than adequate modeling of the LANDSAT 4 MSS scan mirror profile. R.S.F.

N85-20506*# National Aeronautics and Space Administration
 Ames Research Center, Moffett Field, Calif

IMPACT OF LANDSAT MSS SENSOR DIFFERENCES ON CHANGE DETECTION ANALYSIS

W C LIKENS and R. C. WRIGLEY *In* NASA. Goddard Space Flight Center LANDSAT-4 Sci. Characterization Early Results, Vol. 1 p 159-176 Jan. 1985 refs. Original contains imagery. Original photography may be purchased from the EROS Data Center, Sioux Falls, S.D. 57198 ERTS

Avail. NTIS HC A10/MF A01 CSCL 02F

Change detection techniques were used to pinpoint differences between LANDSAT 4 and earlier LANDSAT MSS sensors. Scattergrams between co-registered scenes were utilized to radiometrically compare data from the various MSS sensors. MSS data for San Francisco, CA; southeast New Mexico; Connecticut; and New Hampshire were compared. There appear to be no major problems preventing use of LANDSAT 4 MSS with previous MSS sensors for change detection, provided the interference noise can be removed or minimized. This noise may result in detection of spurious changes, as well as affect other uses of the data, including image classification. Analysis of dark (water and forests), rather than light, features is most impacted because the noise will form

a higher percentage of the total response at low DN values. The patterns are sweep dependent, and within a sweep it is not clear that they are completely systematic. R.S.F.

N85-20508*# National Aeronautics and Space Administration. Goddard Space Flight Center, Greenbelt, Md.

LANDSAT-4 SCIENCE CHARACTERIZATION EARLY RESULTS. VOLUME 2, PART 1: THEMATIC MAPPER (TM)

J. L. BARKER, ed. Washington Jan. 1985 482 p refs Symp. held in Greenbelt, Md., 22-24 Feb. 1983 Original contains imagery. Original photography may be purchased at the EROS Data Center, Sioux Falls, S.D. 57198 ERTS 4 Vol.

(E85-10068; NASA-CP-2355-VOL-2-PT-1, REPT-85B0115-VOL-2-PT-1; NAS 1.55:2355-VOL-2-PT-1) Avail: NTIS HC A21/MF A01 CSCL 08B

An overview of the LANDSAT 4 satellite is given. Spectral, radiometric, and geometric characteristics of the thematic mapper are discussed as well as methods for instrument calibration and data rectification.

N85-20509*# National Aeronautics and Space Administration. Goddard Space Flight Center, Greenbelt, Md.

AN OVERVIEW OF LANDSAT-4 AND THE THEMATIC MAPPER

J. R. IRONS *In its* LANDSAT-4 Sci. Characterization Early Results, Vol. 2, Pt. 1 p 15-46 Jan. 1985 refs ERTS

Avail: NTIS HC A21/MF A01 CSCL 08B

The LANDSAT-4 satellite, its sensor payload, its orbit, and the acquisition and processing of thematic mapper (TM) data are described. The satellite is designed to use the tracking and data relay satellite (TDRS) system to transmit both MSS and TM data to a ground station. The capability to transmit the data directly to ground stations is provided for the interim between the launch of LANDSAT-4 and the initiation TDRS operations. Unfortunately, after transmitting approximately 6000 TM scenes, the transmitter for TM data failed and additional TM data cannot often be received until routine TDRS operations begin. The available TM data are undergoing radiometric and geometric corrections to provide TM investigators with pictorial and digital image data. Early analyses of TM data indicate that the geometric and radiometric characteristics of the data exceed or are comparable to prelaunch specifications. A.R.H.

N85-20510*# National Aeronautics and Space Administration. Goddard Space Flight Center, Greenbelt, Md.

RADIOMETRIC CALIBRATION AND PROCESSING PROCEDURE FOR REFLECTIVE BANDS ON LANDSAT-4 PROTOFLIGHT THEMATIC MAPPER

J. L. BARKER, R. B. ABRAMS (Computer Sciences Corp., Silver Spring, Md.), D. L. BALL (Computer Sciences Corp., Silver Spring, Md.), and K. C. LEUNG (Computer Sciences Corp., Silver Spring, Md.) *In its* LANDSAT-4 Sci. Characterization Early Results, Vol. 2, Pt. 1 p 47-86 Jan. 1985 refs Previously announced as N84-31731 ERTS

Avail: NTIS HC A21/MF A01 CSCL 08B

The radiometric subsystem of NASA's LANDSAT-4 Thematic Mapper (TM) sensor is described. Special emphasis is placed on the internal calibrator (IC) pulse shapes and timing cycle. The procedures for the absolute radiometric calibration of the TM channels with a 122-centimeter integrating sphere and the transfer of radiometric calibration from the channels to the IC are reviewed. The use of the IC to calibrate TM data in the ground processing system consists of pulse integration, pulse averaging, IC state identification, linear regression analysis, and histogram equalization. An overview of the SCROUNGE-era (before August 1983) method is presented. Procedural differences between SCROUNGE and the TIPS-era (after July 1983) and the implications of these differences are discussed. Author

N85-20514*# National Aeronautics and Space Administration. Goddard Space Flight Center, Greenbelt, Md.

SPECTRAL CHARACTERIZATION OF THE LANDSAT THEMATIC MAPPER SENSORS

B. L. MARKHAM and J. L. BARKER *In its* LANDSAT-4 Sci. Characterization Early Results, Vol. 2, Pt. 1 p 235-276 Jan. 1985 refs Previously announced as N84-30402 ERTS

Avail: NTIS HC A21/MF A01 CSCL 08B

Relative spectral response data for the LANDSAT-4 and LANDSAT-4 backup multispectral scanner subsystems (MSS), the protoflight and flight models, are presented and compared to similar data for the LANDSAT 1, 2 and 3 scanners. Channel (six channels per band) outputs for soil and soybean targets were simulated and compared within each band and between scanners. Channel (six channels per band) outputs for soil and soybean targets were simulated and compared within each band and between scanners. The principal differences between the spectral responses of the LANDSAT-4 scanners and previous scanners are discussed. The simulated LANDSAT-4 scanner outputs were 3 to 10 percent lower in the red band and 3 to 11 percent higher in the first near-IR band than previous scanners for the soybeans targets. The LANDSAT-4 scanners were generally more uniform from channel to channel within bands than previous scanners. In the upper-band edge of the red band of the protoflight scanner, one channel was markedly different (12 nm) from the rest. For a soybeans target, this nonuniformity resulted in a within-band difference of 6.2 percent in simulated outputs between channels. A.R.H.

N85-20515*# National Aeronautics and Space Administration. Goddard Space Flight Center, Greenbelt, Md.

PRELAUNCH ABSOLUTE RADIOMETRIC CALIBRATION OF THE REFLECTIVE BANDS ON THE LANDSAT-4 PROTOFLIGHT THEMATIC MAPPER

J. L. BARKER, D. L. BALL (Computer Sciences Corp., Silver Spring, Md.), K. C. LEUNG (Computer Sciences Corp., Silver Spring, Md.), and J. A. WALKER (Santa Barbara Research Center, Goleta, Calif.) *In its* LANDSAT-4 Sci. Characterization Early Results, Vol. 2, Pt. 1 p 277-372 Jan. 1985 refs Previously announced as N84-31751 ERTS

Avail: NTIS HC A21/MF A01 CSCL 08B

The results of the absolute radiometric calibration of the LANDSAT 4 thematic mapper, as determined during pre-launch tests with a 122 cm integrating sphere, are presented. Results for the best calibration of the protoflight TM are given, as well as summaries of other tests performed on the sensor. The dynamic range of the TM is within a few percent of that required in all bands, except bands 1 and 3. Three detectors failed to pass the minimum SNR specified for their respective bands: band 5, channel 3 (dead), and band 2, channels 2 and 4 (noisy or slow response). Estimates of the absolute calibration accuracy for the TM show that the detectors are typically calibrated to 5% absolute error for the reflective bands: 10% full-scale accuracy was specified. Ten tests performed to transfer the detector absolute calibration to the internal calibrator show a 5% range at full scale in the transfer calibration, however, in two cases band 5 showed a 10% and a 7% difference. Author

N85-20516*# National Aeronautics and Space Administration. Goddard Space Flight Center, Greenbelt, Md.

CHARACTERIZATION OF RADIOMETRIC CALIBRATION OF LANDSAT-4 REFLECTIVE BANDS

J. L. BARKER, R. B. ABRAMS (Computer Sciences Corp., Silver Spring, Md.), D. L. BALL, and K. C. LEUNG (Computer Sciences Corp., Silver Spring, Md.) *In its* LANDSAT-4 Sci. Characterization Early Results, Vol. 2, Pt. 1 p 373-474 Jan. 1985 refs Previously announced as N84-31753 ERTS

Avail: NTIS HC A21/MF A01 CSCL 08B

Prelaunch and postlaunch internal calibrator, image, and background data is to characterize the radiometric performance of the LANDSAT-4 TM and to recommend improved procedures for radiometric calibration. All but two channels (band 2, channel 4; band 5, channel 3) behave normally. Gain changes relative to a postlaunch reference for channels within a band vary within 0.5

percent as a group. Instrument gain for channels in the cold focal plane oscillates. Noise in background and image data ranges from 0.5 to 1.7 counts. Average differences in forward and reverse image data indicate a need for separate calibration processing of forward and reverse scans. Precision is improved by increasing the pulse integration width from 31 to 41 minor frames, depending on the band. M A C.

N85-20776# Centre National d'Etudes Spatiales, Paris (France). Applications Program Division
THE SPOT OPERATIONAL REMOTE SENSING SATELLITE SYSTEM: CURRENT STATUS AND PERSPECTIVES
 G BRACHET *In* AGARD Space System Applications to Tactical Operations 13 p Oct. 1984
 Avail. NTIS HC A09/MF A01

The SPOT program, comprising Earth observation satellites and ground receiving stations is discussed. The first satellite, due for launch in 1985, will carry a payload of two identical high resolution visible instruments using CCD linear arrays technology. These will make images of the Earth with sampling step of 20 meters in three color bands in the visible range and in the near infrared, and with a sampling step of 10 meters in a broad, panchromatic band: i.e., in black and white. This configuration is suitable for observing the small agricultural plots found in many countries. It also satisfies some conventional cartographic requirements. Sidelooking capability will allow the satellite to observe any region of the Earth at intervals of one to several days, thus allowing relatively fast changing phenomena to be monitored. It will also be possible to provide for stereoscopic vision by associating views taken from different angles. R.J.F.

N85-20779# National Aeronautics and Space Administration, Washington, D C.
EARTH RESOURCES RESEARCH USING THE SHUTTLE IMAGING RADAR SYSTEM Abstract Only
 R. MONSON and C ELACHI (JPL) *In* AGARD Space System Applications to Tactical Operations 1 p Oct. 1984
 Avail. NTIS HC A09/MF A01

The Shuttle Imaging Radar (SIR) is an L-band synthetic radar that transmits and receives horizontally polarized microwave radiation. It was originally launched on the second Shuttle test flight (STS-2) in November 1981 with the antenna depression angle fixed at 43 deg. In this configuration, the radar system was referred to as SIR-A, and it collected more than then a million square kilometers of Earth imagery in a variety of areas situated between 38 deg north and south latitude. SIR-A data was optically recorded onboard the Shuttle, and it was subsequently correlated on the ground to produce imagery with a 50 kilometer swath width and a surface resolution of approximately 40 meters. The SIR is presently being upgraded into a new configuration termed SIR-B, in which the radar's antenna can be mechanically rotated in the Shuttle's payload bay during an orbital mission. SIR-B is currently scheduled for flight on the seventeenth Shuttle mission (STS-17) that is tentatively planned for August 1984. In its new configuration, the SIR-B can be used to image selected regions at different angles of incidence ranging from 15 deg to 60 deg (as measured from the local vertical). In principle, multiple incidence angle radar imagery of selected areas can be coregistered and used to differentiate surficial materials on the basis of their roughness characteristics. This procedure is conceptually similar to the use of multispectral imagery acquired at shorter wavelengths to discriminate surficial materials on the basis of their pigmentation. R.J.F.

N85-21724*# National Aeronautics and Space Administration. Goddard Space Flight Center, Greenbelt, Md.
LANDSAT-4 SCIENCE CHARACTERIZATION EARLY RESULTS. VOLUME 3, PART 2: THEMATIC MAPPER (TM)
 J. L. BARKER, ed. Washington Jan. 1985 591 p refs
 Symp. held in Greenbelt, Md., 22-24 Feb. 1983 Original contains imagery. Original photography may be purchased from the EROS Data Center, Sioux Falls, S.D. 57198 ERTS 4 Vol.
 (E85-10069; NASA-CP-2355-VOL-3-PT-2;
 REPT-85B0115-VOL-3-PT-2; NAS 1.55:2355-VOL-3-PT-2) Avail.
 NTIS HC A25/MF A01 CSCL 08B

The calibration of the LANDSAT 4 thematic mapper is discussed as well as the atmospheric, radiometric, and geometric accuracy and correction of data obtained with this sensor. Methods are given for assessing TM band to band registration.

N85-21725*# National Aeronautics and Space Administration. Goddard Space Flight Center, Greenbelt, Md.
RELATIVE RADIOMETRIC CALIBRATION OF LANDSAT TM REFLECTIVE BANDS
 J. L. BARKER *In* its LANDSAT-4 Sci. Characterization Early Results, Vol. 3, Pt. 2 p 1-219 Jan. 1985 refs Revised
 Previously announced as N84-31757 ERTS
 Avail. NTIS HC A25/MF A01 CSCL 14B

Results and recommendations pertaining to the characterization of the relative radiometric calibration of the preflight thematic mapper (TM/PF) on the LANDSAT-4 satellite are presented. Some preliminary pre-launch and in-orbit results are also included from the flight model (TM/F) on LANDSAT-5. A common scientific methodology and terminology is outlined for characterizing the radiometry of both TM sensors. The magnitude of the most significant sources of radiometric variability are discussed and methods are recommended for achieving the exceptional potential inherent in the radiometric precision and accuracy of the sensors. A.R.H.

N85-21727*# National Aeronautics and Space Administration. Goddard Space Flight Center, Greenbelt, Md.
THERMAL BAND CHARACTERIZATION OF THE LANDSAT-4 THEMATIC MAPPER
 J. C. LANSING (Santa Barbara Research Center, Calif.) and J. L. BARKER *In* its LANDSAT-4 Sci. Characterization Early Results, Vol. 3, Pt. 2 p 233-256 Jan. 1985 refs Original contains imagery. Original photography may be purchased from the EROS Data Center, Sioux Falls, S.D. 57198 ERTS
 Avail. NTIS HC A25/MF A01 CSCL 14B

The initial characterization of the Thematic Mapper (TM) thermal band is reported including gain stability, gain relation to internal calibration, corrections for channel-to-channel and scan direction differences, an approximate comparison to ground truth, and a calculation of noise equivalent temperature difference. Updated calibration information is also presented. A.R.H.

N85-21729*# Canada Centre for Remote Sensing, Ottawa (Ontario).
PRELIMINARY EVALUATION OF THE RADIOMETRIC CALIBRATION OF LANDSAT-4 THEMATIC MAPPER DATA BY THE CANADA CENTRE FOR REMOTE SENSING
 J. MURPHY, W. PARK, and A. FITZGERALD *In* its LANDSAT-4 Sci. Characterization Early Results, Vol. 3, Pt. 2 p 275-307 Jan. 1985 refs ERTS
 Avail. NTIS HC A25/MF A01 CSCL 14B

The radiometric characteristics of the LANDSAT-4 TM sensor are being studied with a view to developing absolute and relative radiometric calibration procedures. Preliminary results from several different approaches to the relative correction of all detectors within each band are reported. Topics covered include: the radiometric correction method; absolute calibration; the relative radiometric calibration algorithm; relative gain and offset calibration; relative gain and offset observations; and residual radiometric stripping. A.R.H.

N85-21730*# European Space Agency. ESRIN, Frascati (Italy). A PRELIMINARY ANALYSIS OF LANDSAT-4 THEMATIC MAPPER RADIOMETRIC PERFORMANCE

C. JUSTICE, L. FUSCO, and W. MEHL (Joint Research Centre of the European Communities) *In its LANDSAT-4 Sci. Characterization Early Results*, Vol. 3, Pt. 2 p 309-320 Jan. 1985 Original contains imagery. Original photography may be purchased from the EROS Data Center, Sioux Falls, S.D. 57198 ERTS

Avail: NTIS HC A25/MF A01 CSCL 14B

The NASA raw (BT) product, the radiometrically corrected (AT) product, and the radiometrically and geometrically corrected (PT) product of a TM scene were analyzed to examine the frequency distribution of the digital data; the statistical correlation between the bands; and the variability between the detectors within a band. The analyses were performed on a series of image subsets from the full scene. Results are presented from one 1024 x 1024 pixel subset of Reelfoot Lake, Tennessee which displayed a representative range of ground conditions and cover types occurring within the full frame image. From this cursory examination of one of the first seven channel TM data sets, it would appear that the radiometric performance of the system is most satisfactory and largely meets pre-launch specifications. Problems were noted with Band 5 Detector 3 and Band 2 Detector 4. Differences were observed between forward and reverse scan detector responses both for the BT and AT products. No systematic variations were observed between odd and even detectors A.R.H.

N85-21732*# European Space Agency. ESRIN, Frascati (Italy). TM GEOMETRIC PERFORMANCE: LINE TO LINE DISPLACEMENT ANALYSIS (LLDA)

L. FUSCO and W. MEHL *In its LANDSAT-4 Sci. Characterization Early Results*, Vol. 3, Pt. 2 p 359-388 Jan 1985 refs Previously announced as N84-19983 Original contains imagery. Original photography may be purchased from the EROS Data Center, Sioux Falls, S.D. 57198 ERTS

Avail: NTIS HC A25/MF A01 CSCL 05B

An early acquired TM data frame (track 23, frame 35 of 22 August 1982) was used to assess the geometric performance of the LANDSAT-4 thematic mapper instrument. The developed method consists in determining the displacements of adjacent lines by locating the maximum of the correlation profile between the two lines. Then the line to line displacement is used to characterize the TM instrument in respect to: scan to scan jitter and image skew, scan profile non-linearity, along scan jitter, detector to detector displacement, and band to band displacement. To verify the quality of the reported performance parameters, some extracted geometric parameters were used to correct the original raw data. Comparison between P-tape data and results of reprocessed data shows no significant differences in an area of 1024 x 1024 pixels.

A.R.H.

N85-21733*# Arizona Univ., Tucson. Optical Sciences Center. IN-PROGRESS ABSOLUTE RADIOMETRIC INFLIGHT CALIBRATION OF THE LANDSAT-4 SENSORS

K. R. CASTLE, M. DINGUIRARD (Centre d'Etudes et de Recherches de Toulouse), C. E. EZRA (Agricultural Research Service, Phoenix, Ariz.), R. G. HOLM, R. D. JACKSON (Agricultural Research Service, Phoenix, Ariz.), C. J. KASTNER, J. M. PALMER, R. SAVAGE (Atmospheric Sciences Lab.), and P. N. SLATER *In its LANDSAT-4 Sci. Characterization Early Results*, Vol. 3, Pt. 2 p 389-410 Jan. 1985 refs ERTS

(Contract NAS5-27382)

Avail: NTIS HC A25/MF A01 CSCL 14B

Using selected instrumented areas at White Sands Missile Range, New Mexico as reference, radiometric calibration is to be effected on the sensors of LANDSAT 4, particularly the thematic mapper. Optical measurements made during a TM overpass are discussed. The radiances of selected large ground areas are measured in the spectral bandpasses of the TM; the total optical thickness of the atmosphere is measured in nine narrow spectral intervals. Ground truth in the form of reflectances collected for

the alkalai flat region of gypsum and for the snow at White Sands is described. R.S.F

N85-21734*# National Oceanic and Atmospheric Administration, Washington, D. C. National Environmental Satellite, Data, and Information Service.

LANDSAT-4 THEMATIC MAPPER CALIBRATION AND ATMOSPHERIC CORRECTION

W. A. HOVIS *In its LANDSAT-4 Sci. Characterization Early Results*, Vol. 3, Pt. 2 p 411-420 Jan 1985 refs ERTS

Avail: NTIS HC A25/MF A01 CSCL 14B

The LANDSAT-4 thematic mapper, with its wide spectral coverage and digitization to 8 bits per word, is a large step forward in the direction of quantitative radiometry from the multispectral scanner (MSS). In order to utilize the quantitative accuracy built into the thematic mapper effectively, more attention must be paid to calibration before launch, changes of calibration with time in orbit, and atmospheric interference with the measurements, especially in the 450 to 520 nanometer band. Experience with the coastal zone color scanner (CZCS) program led to procedures wherein Rayleigh correction factors can be generated utilizing simultaneous surface truth data that empirically give correct upwelled surface radiances, despite errors in sensor calibration, solar spectral irradiance measurements, and reported values of Rayleigh optical depth. These techniques offer sensitive tests for change in calibration, especially at shorter wavelengths. Instruments, such as the CZCS, have shown that calibration changes first, and to the largest degree, at the shorter wavelengths, with lesser changes as wavelength increases. These techniques are utilized to calculate a Rayleigh correction factor that, together with geometric terms, should give an accurate correction for this portion of the atmospheric contribution to the signal R.S.F.

N85-21735*# Environmental Research Inst. of Michigan, Ann Arbor

SCAN ANGLE AND DETECTOR EFFECTS IN THEMATIC MAPPER RADIOMETRY

M. D. METZLER and W. A. MALILA *In its LANDSAT-4 Sci. Characterization Early Results*, Vol. 3, Pt. 2 p 421-442 Jan. 1985 refs ERTS

Avail: NTIS HC A25/MF A01 CSCL 20F

The effects of scan angle and interdetector differences on thematic mapper radiometry were analyzed. The data set used for this study consisted of computer compatible tapes (CCT's) of raw data (CCT-BT), radiometrically corrected data (CCT-AT), and geometrically corrected data (CCT-PT) for two scenes, 40049-16262 (north central Iowa) and 40037-16031 (Arkansas). Radiometric corrections currently performed were found to improve overall consistency of data, but some residual stripping remains in the corrected data due to the quantization of signal values and other effects. A new type of banding was discovered which is related to the bi-directional scanning of TM. An initial empirical model was developed for correcting this effect in band 1, but should receive additional development. The scan angle effects observed corresponded to those expected based on atmospheric considerations and scene characteristics. Low frequency scan-to-scan noise was detected in band 1, band 7, and to a lesser extent in bands 2 and 3. The band 1 detectors which exhibited this noise showed strong correlation in their variation.

R.S.F.

N85-21737*# Arizona Univ., Tucson. Remote Sensing Center

MTF ANALYSIS OF LANDSAT-4 THEMATIC MAPPER

R. SCHOWENGERDT *In its LANDSAT-4 Sci. Characterization Early Results*, Vol. 3, Pt. 2 p 467-470 Jan. 1985 refs

Previously announced as N83-33285 ERTS

Avail: NTIS HC A25/MF A01 CSCL 14D

The spatial radiance distribution of a ground target must be known to a resolution at least four to five times greater than that of the system under test when measuring a satellite sensor's modulation transfer function. Calibration of the target requires either the use of man-made special purpose targets with known properties, e.g., a small reflective mirror or a dark-light linear pattern

such as line or edge, or use of relatively high resolution underflight imagery to calibrate an arbitrary ground scene. Both approaches are to be used, in addition a technique that utilizes an analytical model of the scene spatial frequency power spectrum is being investigated as an alternative to calibration of the scene. A.R.H.

**N85-21738*# Geological Survey, Flagstaff, Ariz.
INTRABAND RADIOMETRIC PERFORMANCE OF THE
LANDSAT 4 THEMATIC MAPPER**

H. H. KIEFFER, E. M. ELIASON, and P. S. CHAVEZ, JR. *In its* LANDSAT-4 Sci. Characterization Early Results, Vol. 3, Pt. 2 p 471-496 Jan. 1985 refs Original contains imagery. Original photography may be purchased from the EROS Data Center, Sioux Falls, S.D. 57198 ERTS

Avail: NTIS HC A25/MF A01 CSCL 14B

Those radiometric characteristics of the LANDSAT 4 thematic mapper (TM) that could be established without absolute calibration of spectral data were examined. Radiometrically raw (B type) data of three daytime and two nighttime scenes were used, including TM scenes from Washington, DC, northeast Arkansas; Cape Cod, MA, Roanoke, VA, Richmond, VA; and Silver Bell, AZ. The effective resolution in radiance is degraded by a factor of about 2 by the irregular width of the digital levels. Underpopulated levels are consistent over all bands and detectors, and are spaced an average of 4 digital numbers (DN) apart. In band 6, level 127 is avoided by a factor 30. Several detectors exhibit a change of gain with a period of several scans, the largest effect is about 4%. At high contrast boundaries, some of the detectors in band 5 commonly overshoot by several DN and require about 30 samples to recover. The high frequency noise level of each detector was characterized by the standard deviation of the first derivative in the sample direction across a flat field. A coherent-sinusoidal-noise pattern is evident in detector 1 of band 3. The correlation between the six reflective bands was determined and used to select three groups of bands whose aggregate first principal components contain the greatest total information. A composite of the first components of bands 1, 2, 3, bands 5 and 7, and band 4, together containing 89% of the information in the reflectance bands, has reduced the effect of noise. R.S.F.

N85-21740*# Systems and Applied Sciences Corp., Hyattsville, Md

**THE USE OF LINEAR FEATURE DETECTION TO INVESTIGATE
THEMATIC MAPPER DATA PERFORMANCE AND
PROCESSING**

C. M. GURNEY *In its* LANDSAT-4 Sci. Characterization Early Results, Vol. 3, Pt. 2 p 513-526 Jan. 1985 refs Previously announced as N84-13680 Original contains imagery. Original photography may be purchased from the EROS Data Center, Sioux Falls, S.D. 57198 ERTS

Avail: NTIS HC A25/MF A01 CSCL 05B

The geometric and radiometric characteristics of thematic mapper data through analysis of linear features in the data are investigated. The particular aspects considered are: (1) thematic mapper ground IFUV; (2) radiometric contrast between linear features and background, (3) precision of system geometric correction; (4) band-to-band registration, and (5) potential utility of TM data for linear feature detection especially as compared to MSS data. It is shown that TM data may be used to estimate TM pixel size illustrate band: band mis-registration. M.G.

**N85-21741*# Purdue Univ., Lafayette, Ind.
SPATIAL RESOLUTION ESTIMATION OF LANDSAT-4
THEMATIC MAPPER DATA**

C. D. MCGILLEM, P. E. ANUTA, and E. MALARET *In its* LANDSAT-4 Sci. Characterization Early Results, Vol. 3, Pt. 2 p 527-536 Jan. 1985 refs ERTS

Avail: NTIS HC A25/MF A01 CSCL 14B

The problem of estimating the overall point-spread function (PSF) of multispectral scanner systems was studied using real scene data and known geometric structures in the scene. A direct solution to an approximate form of the PSF was made along with a method using the derivative of an estimated edge response.

Both results agreed closely. The TM scanner system specifications are given in line-spread function width and these values are listed with the experimental results in terms of meters. The estimated values are very reasonable, considering the number of factors which could be influencing the result. The atmosphere will have a blurring effect on the overall PSF as well as on cubic convolution resampling effects and possible electronic effects not accounted for in the specification. Also, the specific definition of the LSF specification is not known nor is the actual altitude at the instant the data were acquired. Thus the nominal overall PSF half-amplitude width of 39 m is reasonable; however, a greater sample of scene objects should be evaluated to further verify this result. Author

**N85-21742*# Research and Data Systems, Inc., Lanham, Md.
AN ANALYSIS OF THE HIGH FREQUENCY VIBRATIONS IN
EARLY THEMATIC MAPPER SCENES**

J. KOGUT and E. LARDUINAT *In its* LANDSAT-4 Sci. Characterization Early Results, Vol. 3, Pt. 2 p 537-552 Jan. 1985 refs ERTS

(Contract NAS5-27371)

Avail: NTIS HC A25/MF A01 CSCL 20K

The motion of the mirrors in the thematic mapper (TM) and multispectral scanner (MSS) instruments, and the motion of other devices, such as the TDRSS antenna drive, and solar array drives onboard LANDSAT-4 cause vibrations to propagate through the spacecraft. These vibrations as well as nonlinearities in the scanning motion of the TM mirror can cause the TM detectors to point away from their nominal positions. Two computer programs, JITTER and SCDFT, were developed as part of the LANDSAT-D Assessment System (LAS), Products and Procedures Analysis (PAPA) program to evaluate the potential effect of high frequency vibrations on the final TM image. The maximum overlap and underlap which were observed for early TM scenes are well within specifications for the ground processing system. The cross scan and scan high frequency vibrations are also within the specifications cited for the flight system B.G.

N85-21745*# Lockheed Engineering and Management Services Co., Inc., Houston, Tex.

**INVESTIGATION OF TM BAND-TO-BAND REGISTRATION
USING THE JSC REGISTRATION PROCESSOR**

S. S. YAO and M. L. AMIS *In its* LANDSAT-4 Sci. Characterization Early Results, Vol. 3, Pt. 2 p 571-580 Jan. 1985 refs ERTS

Avail: NTIS HC A25/MF A01 CSCL 05B

When the Thematic Mapper (TM) imagery was first received and displayed in the fall of 1982, its radiometric lucidity and geometric fidelity was judged far superior to the multispectral scanner (MSS) imagery. The MSS data from the LANDSAT series of satellites have served well as the mainstay of satellite imagery for the remote sensing community up to now. Therefore, there is great anticipation as to the utility of this new IM imagery to advance the field of remote sensing. The thematic mapper (TM) band to band registration accuracy evaluation was discussed. In particular, the band to band registration accuracies of the TM data in the subpixel region were evaluated using the Johnson Space Center (JSC) registration processor which is ideally suited for this task. The JSC registration processor was also used to register one acquisition to another acquisition of multitemporal TM data acquired over the same ground track. The approach and the rationale behind the task, the description of the data set, the evaluation results, and the preliminary conclusions are discussed. B.G.

08 INSTRUMENTATION AND SENSORS

N85-21756*# Arizona Univ., Tucson Optical Sciences Center.
SPECTRORADIOMETRIC CALIBRATION OF THE THEMATIC MAPPER AND MULTISPECTRAL SCANNER SYSTEM Quarterly Report, 1 Nov. 1984 - 28 Feb. 1985

J. M. PALMER and P. N. SLATER, Principal Investigators 28 Feb 1985 43 p refs ERTS
(Contract NAS5-27382)
(E85-10094, NASA-CR-175529; NAS 1.26:175529; QR-9) Avail: NTIS HC A03/MF A01 CSCL 08B

The effects of the atmosphere on propagating radiation must be known in order to calibrate an in orbit sensor using ground based measurements. A set of model atmosphere parameters, applicable to the White Sands (New Mexico) area is defined with particular attention given to those parameters which are required as input to the Herman Code. The radial size distribution, refractive index, vertical distribution, and visibility of aerosols are discussed as well as the molecular absorbers in the visible and near IR wavelength which produce strong absorption lines. Solar irradiance is also considered. A R.H.

N85-21873*# Pacific Northwest Lab., Richland, Wash.
ANALYSIS OF THE NASA/MSFC AIRBORNE DOPPLER LIDAR RESULTS FROM SAN GORGONIO PASS, CALIFORNIA Final Report

W. C. CLIFF, J. R. SKARDA, D. S. RENNE, and W. F. SANDUSKY Dec. 1984 70 p refs
(Contract NAS8-34733)
(NASA-CR-171355; NAS 1.26:171355) Avail: NTIS HC A04/MF A01 CSCL 04B

Two days during July of 1981 the NASA/MSFC Airborne Doppler Lidar System (ADLS) was flown aboard the NASA/AMES Convair 990 on the east side of San Geronio Pass California, near Palm Springs, to measure and investigate the accelerated atmospheric wind field discharging from the pass. The vertical and horizontal extent of the fast moving atmospheric flow discharging from the San Geronio Pass were examined. Conventional ground measurements were also taken during the tests to assist in validating the ADLS results. This particular region is recognized as a high wind resource region and, as such, a knowledge of the horizontal and vertical extent of this flow was of interest for wind energy applications. The statistics of the atmospheric flow field itself as it discharges from the pass and then spreads out over the desert were also of scientific interests. This data provided the first spatial data for ensemble averaging of spatial correlations to compute longitudinal and lateral integral length scales in the longitudinal and lateral directions for both components. Author

09

GENERAL

Includes economic analysis.

A85-19580#
ON REALIZING THE POTENTIAL OF THE EARTH-LOOKING VANTAGE POINT

D. LANDGREBE (Purdue University, West Lafayette, IN) American Institute of Aeronautics and Astronautics, Aerospace Sciences Meeting, 23rd, Reno, NV, Jan. 14-17, 1985. 6 p. refs (AIAA PAPER 85-0195)

Earth observational activities of the past have led to important new capabilities, several of which have become operational. Research-related activities of the field have been passing through a period of significantly diminished levels of effort in recent years. There are substantial signs that important new activities may begin again in the near future. In this paper, after postulating a context for the types of research needed in the area, some of these new activities now in the planning stage are reviewed briefly. Author

A85-20565
PERSPECTIVES OF REMOTE SENSING IN EUROPE AT THE END OF THE DECADE

G. FRAYSSE (Commission of the European Communities, Joint Research Centre, Ispra, Italy) Earth-Oriented Applications of Space Technology (ISSN 0277-4488), vol. 4, no. 4, 1984, p. 199-203

The availability of second generation earth-observation satellites (Landsat-5, Thematic Mapper, SPOT) will provide the European and developing countries with new possibilities for the monitoring of their natural resources. The actual situation where land and marine applications are considered respectively quasi-operational (Landsat in the USA) and experimental (MOS, ES-1/SAR) is discussed. The conditions which are necessary for the transfer of remote sensing to users, such as adequate performance, acceptable cost, data of reliable quality and short delay for the delivery of data are also considered. The various experimental and operational satellite missions are divided into three categories: (1) experimental Shuttle missions where new sensors are tested; only a limited number of scenes are acquired during these missions (NASA-SAR missions, MOMS, the Metric Camera and the MRSE); (2) experimental satellites when repetitive scenes are necessary to demonstrate the value of given applications (ERS-1); and (3) operational satellites when there is a guarantee of continuity (MSS Landsat, the French SPOT, and the European Meteosat) M.D.

A85-20566
INTERNATIONAL COOPERATION IN REMOTE SENSING APPLICATIONS

J. A. HOWARD (United Nations, Food and Agriculture Organization, Rome, Italy) Earth-Oriented Applications of Space Technology (ISSN 0277-4488), vol. 4, no. 4, 1984, p. 205-209. refs

The paper summarizes initially the organization of satellite remote sensing within the UN system and then briefly comments on FAO activities and the functions of the FAO Remote Sensing Center, which cover both satellite and airborne methods and techniques. It then reviews bilateral and multilateral international cooperation and notes major constraints. The paper proceeds to examine the content of international cooperation, covering education and training, institution building, equipment and follow-up activities to country based projects. In conclusion, it draws attention to the need to strengthen mechanisms of international cooperation, to expand training activities, to initiate pilot action studies in developing countries and to modify equipment to the conditions existing in many developing countries. Author

A85-20574
THE EDUCATIONAL ROLE OF SATELLITES

J. A. ALLAN (London, University, London, England) Earth-Oriented Applications of Space Technology (ISSN 0277-4488), vol. 4, no. 4, 1984, p. 265-270. refs

The paper reviews the extent to which satellite imagery of the past two decades has complemented and enhanced the conventional map which has an established place in secondary and tertiary education. After looking in some detail at the particular qualities of remotely sensed data which might be useful in teaching such subjects as climatology, meteorology, oceanography, geology, together with soil, vegetation and agricultural sciences and geography, the discussion moves on to emphasise the new opportunities made possible by the current and proposed remote sensing systems, in teaching the subjects associated with data acquisition, e.g. physics, and those associated with the application of such data in for example renewable resource monitoring and management. Author

A85-20640#**EDUCATION AND TRAINING IN SATELLITE REMOTE SENSING APPLICATIONS - GUIDE TO: EDUCATION AND TRAINING OPPORTUNITIES**

T WOLDAI (International Institute for Aerial Survey and Earth Sciences, Enschede, Netherlands) United Nations, International Meeting of Experts on Remote Sensing Information Systems, Feldafing and Oberpfaffenhofen, West Germany, May 7-11, 1984, Paper, 47 p. refs

A list is presented of education and training opportunities available in remote sensing throughout the world. For each country, the institutes or other training centers are named and their programs are described. The qualifications and requirements necessary for attending such programs are also mentioned wherever applicable

C D.

A85-20641#**THE U.S. CIVIL OPERATIONAL REMOTE SENSING PROGRAM OPPORTUNITIES FOR THE PRESENT AND FUTURE**

R. KOFFLER, B H NEEDHAM, and K. D HODGKINS (NOAA, National Environmental Satellite, Data, and Information Service, Washington, DC) United Nations, International Meeting of Experts on Remote Sensing Information Systems, Feldafing and Oberpfaffenhofen, West Germany, May 7-11, 1984, Paper 16 p.

It is pointed out that the National Environmental Satellite, Data, and Information Service (NESDIS) of the National Oceanic and Atmospheric Administration (NOAA) is the U.S. Government agency responsible for civil operational satellite remote sensing. NOAA/NESDIS operates the Geostationary Operational Environmental Satellites (GOES) and the Landsat-4 and 5 satellites. NOAA/NESDIS distributes also data from several other experimental remote sensing satellite missions. A review is provided of the remote sensing products and services available, taking into account also plans for future services, and current efforts to transfer the U.S. civil operational land system to the private sector. G R.

A85-20642#**COMMERCIALIZATION OF REMOTE SENSING DATA - ITS IMPACT ON THE CONTINUITY AND ACCESSIBILITY OF REMOTE SENSING DATA, INCLUDING RESPONSE TO STANDING ORDERS AS WELL AS ON THE STANDARDIZATION OF PRODUCTS**

G BRACHET (SPOT IMAGE, Toulouse, France) United Nations, International Meeting of Experts on Remote Sensing Information Systems, Feldafing and Oberpfaffenhofen, West Germany, May 7-11, 1984, Paper. 14 p.

A85-20646#**STATUS OF REMOTE SENSING INFORMATION SYSTEMS WITH SPECIAL EMPHASIS ON THEIR SPECIALIZATIONS, CAPABILITIES, ACCESSIBILITIES AND FUTURE DIRECTIONS**

L. MARELLI (ESA, European Space Research Institute, Frascati, Italy) United Nations, International Meeting of Experts on Remote Sensing Information Systems, Feldafing and Oberpfaffenhofen, West Germany, May 7-11, 1984, Paper. 12 p.

The status of remote sensing information systems is discussed, including Landsat, the SPOT mission, the Indian IRS-1 (planned for 1985) and the Japanese MOS-1 (planned for 1986). All missions include multispectral data in the visible and near infrared band and offer resolution varying from 80 x 80 to 10 x 10 m in the panchromatic mode. Four missions are planned for the end of the decade, which will provide global ocean/ice data. The acquisition, archiving and retrieval of the space remote sensing data are covered as well. The present usage of space sensing data comprises: cartographic mapping; geological and land-use map derivation; inventories; monitoring, and agricultural production forecasting. With the new generation of satellites, such as the Landsat 4/5 and SPOT, the availability of data worldwide on a continuous basis is possible.

L.T.

A85-25348* National Aeronautics and Space Administration, Washington, D. C.

USE OF SPACE STATION FOR EARTH AND PLANETARY EXPLORATION

W. L. PIOTROWSKI (NASA, Earth and Planetary Exploration Div., Washington, DC) IN: Optical engineering for cold environments; Proceedings of the Meeting, Arlington, VA, April 7, 8, 1983. Bellingham, WA, SPIE - The International Society for Optical Engineering, 1983, p. 162-178.

The Earth and Planetary Exploration program attempts to develop an understanding of the earth as a planet by utilizing the capability of instruments in space to explore the earth. Studies of the solar system are conducted to gain an understanding of its origin and evolution. The facilities for planetary observations will be greatly extended by making use of a Space Station. Special demands related to the appropriate utilization of a Space Station observatory are discussed, taking into account the employment of ultraviolet spectroscopy for the study of planetary atmospheres and comets, advantages provided by infrared spectroscopy, far-infrared and submillimeter spectroscopy and radiometry, and the search for other planetary systems. The capabilities provided by the Space Station for an investigation of earth resources are explored. Attention is given to vegetation research and observations, land cover dynamics, hydrologic cycle research, geological research, suitable instruments, and a study of crustal dynamics.

G.R

A85-27519**ASIAN CONFERENCE ON REMOTE SENSING, 4TH, COLOMBO, SRI LANKA, NOVEMBER 10-15, 1983, PROCEEDINGS**

Conference sponsored by the Ministry of Lands and Development of Sri Lanka, Japan Association of Remote Sensing, International Society for Photogrammetry and Remote Sensing, and Japan Society of Photogrammetry and Remote Sensing. Tokyo, Asian Association on Remote Sensing, 1984, 782 p. No individual items are abstracted in this volume.

The development and application of remote-sensing (RS) technology in Asian nations are discussed in national surveys, technical papers, and poster sessions. Topics examined include Space Shuttle RS experiments; RS in Indian forestry, land-use studies; RS for evaluation of overall resources, water resources, marine resources, and geology and geomorphology, and data processing and system design. Graphs, maps, tables, diagrams, and sample black-and-white and color images are provided. T K.

N85-20941# Council on Environmental Quality, Washington, D.C.

SOURCEBOOK: GAINING ACCESS TO US GOVERNMENT INFORMATION ON THE ENVIRONMENT AND NATURAL RESOURCES

F. M. OHARA, JR., comp and I. OHARA, comp. Nov. 1984. 127 p. refs.

(DE84-017419; DOE/PE-T1) Avail: NTIS HC A07/MF A01

Services and publications offered by the US government that provide information about the environment and natural resources are described. These sources of information include referral services, public-information offices, computerized data banks, information-analysis centers, and publication-distribution systems as well as published sources like bibliographies, abstract and index journals, reports, handbooks, and atlases. The subject matter covered by this sourcebook includes air pollution, meteorology, water resources and quality, fisheries, aquaculture, marine science, solid and hazardous waste treatment, land use, soil science, population and demography, anthropology, architecture, geography, urban studies, health, biology, agriculture, forestry, habitat, wildlife, geology, minerals, and related sciences and technologies. DOE

09 GENERAL

N85-20942# National Commission on Libraries and Information Science, Washington, D. C.

PRESERVE THE SENSE OF EARTH FROM SPACE

Aug. 1984 64 p refs

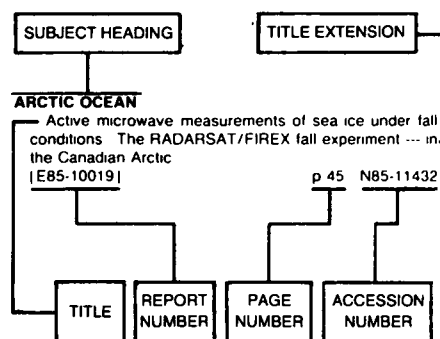
(PB85-124121; LC-84-18972) Avail: NTIS HC A04/MF A01

CSCL 05B

The results of a three-month effort by the panel on the information policy implications of archiving satellite data are presented. The findings and recommendations of the panel are as follows: (1) it is in the public interest to maintain an archive of land remote sensing satellite data for historical, scientific, and technical purposes; (2) the data in question are a national resource worthy of preservation for the advancement of science and other applications, and while the cost of archiving these data is not insignificant, it is extremely small relative to the investment in the space segments of the satellite remote sensing systems; (3) it is in the public interest to control the content and scope of the archive and to assure the quality, integrity, and continuity of the data; and (4) the maintenance of such an archive is, therefore, a responsibility that should be borne by the U.S. Government.

GRA

Typical Subject Index Listing



The subject heading is a key to the subject content of the document. The title is used to provide a description of the subject matter. When the title is insufficiently descriptive of the document content, the title extension is added, separated from the title by three hyphens. The (NASA or AIAA) accession number and the page number are included in each entry to assist the user in locating the abstract in the abstract section (of this supplement). If applicable, a report number is also included as an aid in identifying the document. Under any one subject heading, the accession numbers are arranged in sequence with the AIAA accession numbers appearing first.

A

ACCURACY

Geometric accuracy of LANDSAT-4 MSS image data p 53 N85-20503

ACID RAIN

Analysis of terrestrial conditions and dynamics [E85-10063] p 10 N85-17401

ACOUSTIC SCATTERING

Surface scattering effects at different spectral regions p 58 A85-23780

ADVECTION

Remote-sensing observations of advective eddies in the central part of the Baltic Sea p 38 A85-29915

AERIAL PHOTOGRAPHY

MASMAP, design for a project-oriented geo-information program package for urban upgrading schemes p 13 A85-20747

Method for sequential analysis of spatial development in a rural-urban fringe zone p 13 A85-20748

Population estimation from aerial photos for non-homogeneous urban residential areas p 14 A85-20749

Analysis of ACIR transparencies of citrus trees with a projecting spectral densitometer --- Aerial Color IR p 1 A85-21050

Resource measurement system p 47 A85-24258

EROS main image file - A picture perfect database for Landsat imagery and aerial photography p 48 A85-24521

Identification of the structure of soil-vegetation cover using aerial and space images p 5 A85-25656

Evaluation of aircraft MSS analytical block adjustment p 49 A85-26641

Estimation of the vegetation contribution to the 1.65-2.22 micron ratio in airborne thematic-mapper imagery of the Virginia Range, Nevada p 5 A85-26931

The utility of data from various airborne sensors for soil mapping p 5 A85-26932

Evidence accumulation for spatial reasoning p 50 N85-16261

Forest area estimates from LANDSAT MSS and forest inventory plot data [PB85-105617/GAR] p 9 N85-16290

Interactive digital image processing for terrain data extraction [AD-A148580] p 52 N85-17417

AERIAL RECONNAISSANCE

Near-infrared spectroscopy in geological reconnaissance and exploration p 22 A85-27944

AEROSOLS

Spectroradiometric calibration of the Thematic Mapper and Multispectral Scanner system [E85-10094] p 70 N85-21756

AEROSPACE ENVIRONMENTS

The space environment monitors onboard GOES [AIAA PAPER 85-0238] p 55 A85-19608

Earth observations and the polar platform [NOAA-TR-NESDIS-18] p 15 N85-20517

On the P1 data from GMS-SEM p 15 N85-21890

AFRICA

Satellite definition of the bio-optical and thermal variation of coastal eddies associated with the African current [AD-A147910] p 39 N85-16282

AGRICULTURE

Estimation of agronomic variables using spectral signatures p 2 A85-23753

Spectral response of different agricultural and penurban land-use units in the spectral windows at 1.55-1.75 and 2.08-2.35 microns p 4 A85-23787

Detecting agricultural to urban land use change from multi-temporal MSS digital data --- Salt Lake County, Utah [E85-10049] p 15 N85-16245

Exploring the use of structural models to improve remote sensing agricultural estimates p 9 N85-16259

Image variance and spatial structure in remotely sensed scenes --- South Dakota, California, Missouri, Kentucky, Louisiana, Tennessee, District of Columbia, and Oregon p 51 N85-16265

An integrated GIS/remote sensing data base in North Cache soil conservation district, Utah. A pilot project for the Utah Department of Agriculture's RIMS (Resource Inventory and Monitoring System) [E85-10073] p 11 N85-19487

Analysis of the quality of image data required by the LANDSAT-4 Thematic Mapper and Multispectral Scanner --- agricultural and forest cover types in California [E85-10074] p 11 N85-19488

Remote sensing technology now playing practical roles p 64 N85-20190

AGRICULTURE PROJECT

Shortwave infrared detection of vegetation [E85-10064] p 10 N85-17402

Analysis of data acquired by synthetic aperture radar and LANDSAT Multispectral Scanner over Kershaw County, South Carolina, during the summer season [E85-10071] p 11 N85-19485

NOAA-AISC user's guide for implementing CERES maize model for large area yield estimation [E85-10083] p 12 N85-21748

NOAA-AISC user's guide for implementing CERES wheat model for large area yield estimation [E85-10085] p 12 N85-21750

Estimating solar radiation for plant simulation models [E85-10089] p 13 N85-21751

AGROCLIMATOLOGY

An integrated remote sensing approach for identifying ecological range sites --- Parker Mountain [E85-10050] p 8 N85-16246

AGROMETEOROLOGY

The management of atmospheric resources in food production p 9 N85-16362

AIR SEA ICE INTERACTIONS

Ice sheet margins and ice shelves p 32 A85-24524

Passive microwave remote sensing for sea ice research [NASA-CR-175570] p 42 N85-21758

AIR WATER INTERACTIONS

Space radar observations of small-scale formations on the ocean surface p 27 A85-20086

Evaluation of the ocean/atmosphere thermal interaction in the Atlantic FGGE area p 28 A85-22175

Variations in atmospheric mixing height across oceanic thermal fronts p 34 A85-27704

AIRBORNE EQUIPMENT

A comparison of in situ and airborne radar observations of ocean wave directionality p 27 A85-20487

Aircraft measurements for calibration of an orbiting spacecraft sensor p 59 A85-24246

Performance of an airborne imaging 92/183 GHz radiometer during the Bering Sea Marginal Ice Zone Experiment (MIZEX-WEST) p 33 A85-24945

Airborne snow water equivalent and soil moisture measurement using natural terrestrial gamma radiation p 43 A85-25352

Prospecting from the skies p 23 A85-29405

Airborne remote sensing CCD imaging system p 65 N85-20220

AIRBORNE LASERS

The use of airborne lasers in terrestrial and water environments p 33 A85-25351

Automated measurements of terrain reflection and height variations using an airborne infrared laser system p 5 A85-26933

The reflection of airborne UV laser pulses from the ocean p 37 A85-29714

AIRBORNE SURVEILLANCE RADAR

Advanced SAR system maps Arctic regions p 35 A85-27841

Electromagnetic bias of 10-GHz radar altimeter measurements of MSL p 37 A85-29713

ALABAMA

Geodetic accuracy of LANDSAT 4 Multispectral Scanner and Thematic Mapper data --- Washington, DC, California, Alabama, South Dakota, and Illinois p 53 N85-20504

ALEUTIAN ISLANDS (US)

Satellite magnetic anomalies over subduction zones - The Aleutian Arc anomaly p 16 A85-21107

ALGORITHMS

Swell propagation in the North Atlantic ocean using SEASAT altimeter p 30 A85-23702

Information extraction and transmission techniques for spaceborne synthetic aperture radar images [NASA-CR-174341] p 52 N85-17256

ALTIMETERS

Altimeter measurements of ocean topography p 30 A85-23695

Gravity field investigation in the North Sea p 30 A85-23699

The altimetric geoid in the North Sea p 16 A85-23700

Spatial variation of significant wave-height p 30 A85-23704

A sampling strategy for altimeter measurements of the global statistics of mesoscale eddies p 32 A85-24553

Eddy kinetic energy distribution in the southern ocean from Seasat altimeter and FGGE drifting buoys p 32 A85-24554

Cosmic interpolation of terrestrial potential values p 18 A85-25476

A survey of oceanographic satellite altimetric missions p 36 A85-29703

The potential for ocean prediction and the role of altimeter data p 36 A85-29704

Regional mean sea surfaces based on GEOS-3 and SEASAT altimeter data p 38 A85-29716

A method for determining mesoscale dynamic topography [AD-D011412] p 40 N85-17506

Along-track deflection of the vertical from SEASAT GEBCO (General Bathymetric Chart of the Oceans) overlays p 42 N85-21767

AMAZON REGION (SOUTH AMERICA)

Deforestation, floodplain dynamics, and carbon biogeochemistry in the Amazon Basin p 44 N85-17216

Information for space radar designers Required dynamic range vs resolution and antenna calibration using the Amazon rain forest p 44 N85-17239

ANGLES (GEOMETRY)

- Investigation of SIR-B images for lithologic mapping p 25 N85-17241
- Australian Multispectral Assessment of SIR-B (AMAS) p 52 N85-17243

ANGULAR DISTRIBUTION

- Computing the foliage angle distribution from contact frequency data p 6 A85-29969

ANNUAL VARIATIONS

- Comparative seasonal evolution of the spectral signatures of broad-leaved and coniferous trees from Landsat data Comparison with other perennial surfaces p 2 A85-23757
- Structure and seasonal characteristics of the Gaspe current p 35 A85-27705
- Satellite definition of the bio-optical and thermal variation of coastal eddies associated with the African current [AD-A147910] p 39 N85-16282
- North American vegetation patterns observed with the NOAA-7 advanced very high resolution radiometer --- North America [E85-10062] p 10 N85-17400
- Growth and reflectance characteristics of winter wheat canopies [E85-10080] p 11 N85-19494

ANTARCTIC REGIONS

- Ice sheet margins and ice shelves p 32 A85-24524

ANTENNA RADIATION PATTERNS

- Information for space radar designers Required dynamic range vs resolution and antenna calibration using the Amazon rain forest p 44 N85-17239

ARCTIC OCEAN

- Satellite photographs suggest arctic volcano p 38 N85-16239
- Data report on variations in the composition of sea ice during MIZEX/East'83 with the Nimbus-7 SMMR [NASA-TM-86170] p 40 N85-18443

ARCTIC REGIONS

- Advanced SAR system maps Arctic regions p 35 A85-27841
- Satellite photographs suggest arctic volcano p 38 N85-16239
- MIZEX (Marginal Ice Zone Program) A program for mesoscale air-ice-ocean interaction experiments in Arctic marginal ice zones 5 MIZEX 84 Summer experiment PI (Principal Investigator) preliminary reports [AD-A148986] p 41 N85-19594

ARGENTINA

- Tectonic, volcanic, and climatic geomorphology study of the Sierras Pampeanas Andes, northwestern Argentina p 24 N85-17215

ARID LANDS

- Measuring spectra of arid lands p 20 A85-21975
- Inventory of geographically homogeneous zones by spectral modeling of diachronic Meteosat albedo or combined albedo/thermal-channel data - Applications to the Maghreb and to Sahelian Africa p 46 A85-23769
- Regional analysis from data from heterogeneous pixels - Remote sensing of total dry matter production in the Senegalese Sahel p 47 A85-23783
- Estimation of the vegetation contribution to the 1.65-2.22 micron ratio in airborne thematic-mapper imagery of the Virginia Range, Nevada p 5 A85-26931
- Australian Multispectral Assessment of SIR-B (AMAS) p 52 N85-17243

ARIZONA

- Intraband radiometric performance of the LANDSAT 4 Thematic Mapper --- Washington, DC, Arkansas, Massachusetts, Virginia, and Arizona p 69 N85-21738

ARKANSAS

- Scan angle and detector effects in Thematic Mapper radiometry --- Iowa and Arkansas p 68 N85-21735
- Intraband radiometric performance of the LANDSAT 4 Thematic Mapper --- Washington, DC, Arkansas, Massachusetts, Virginia, and Arizona p 69 N85-21738

ARTIFICIAL SATELLITES

- Passive microwave remote sensing for sea ice research [NASA-CR-175570] p 42 N85-21758

ASIA

- Asian Conference on Remote Sensing, 4th, Colombo, Sri Lanka, November 10-15, 1983, Proceedings p 71 A85-27519

ATLANTIC OCEAN

- Evaluation of the ocean/atmosphere thermal interaction in the Atlantic FGGE area p 28 A85-22175
- Validation and applications of SASS over JASIN --- wind scatterometer results in Atlantic NW of Scotland p 29 A85-23681
- Swell propagation in the North Atlantic ocean using SEASAT altimeter p 30 A85-23702
- The diurnal variation of Atlantic Ocean tropical cyclone cloud distribution inferred from geostationary satellite infrared measurements p 33 A85-24739
- Seafloor spreading anomalies in the Magsat field of the North Atlantic p 17 A85-26415

- The imaging of internal waves by the SEASAT-A synthetic aperture radar [AD-A149808] p 20 N85-21761

ATMOSPHERIC ATTENUATION

- A comparative analysis of some prediction methods for rain attenuation statistics in earth-to-space links p 42 A85-21130
- Comparison of modelled and empirical atmospheric propagation data p 46 A85-22678
- The influence of a scattering medium on the quality of an optical image p 48 A85-26294
- Evaluation of the radiometric integrity of LANDSAT 4 Thematic Mapper band 6 data p 54 N85-21726
- Spectroradiometric calibration of the Thematic Mapper and Multispectral Scanner system [E85-10094] p 70 N85-21756

ATMOSPHERIC BOUNDARY LAYER

- Variations in atmospheric mixing height across oceanic thermal fronts p 34 A85-27704
- Determination of monthly mean humidity in the atmospheric surface layer over oceans from satellite data p 35 A85-28007

ATMOSPHERIC CIRCULATION

- Analysis of the NASA/MSFC Airborne Doppler Lidar results from San Geronio Pass, California [NASA-CR-171355] p 70 N85-21873

ATMOSPHERIC COMPOSITION

- Intercomparisons of TOMS, SBUV and MFR satellite ozone measurements --- Satellite Backscattered Ultraviolet, Total Ozone Mapping System, Multichannel Filter Radiometer p 62 A85-29784

ATMOSPHERIC CORRECTION

- Demonstration, analysis, and correction of atmospheric effects on Landsat or SPOT multispectral data p 58 A85-23781
- LANDSAT-4 Thematic Mapper calibration and atmospheric correction p 68 N85-21734
- LANDSAT 4 band 6 data evaluation [E85-10093] p 55 N85-21755

ATMOSPHERIC EFFECTS

- Demonstration, analysis, and correction of atmospheric effects on Landsat or SPOT multispectral data p 58 A85-23781
- Lake ice occurrence as a possible detector of atmospheric CO2 effects on climate [DE85-002951] p 45 N85-20606

ATMOSPHERIC MODELS

- Spectroradiometric calibration of the Thematic Mapper and Multispectral Scanner system [E85-10094] p 70 N85-21756

ATMOSPHERIC MOISTURE

- The scanning multichannel microwave radiometer - An assessment p 57 A85-23705
- Determination of monthly mean humidity in the atmospheric surface layer over oceans from satellite data p 35 A85-28007

ATMOSPHERIC OPTICS

- The influence of a scattering medium on the quality of an optical image p 48 A85-26294

ATMOSPHERIC PHYSICS

- Observations of the earth using nighttime visible imagery p 48 A85-25350
- The use of principal components analysis techniques Nimbus-7 coastal zone color scanner data to define mesoscale ocean features through a warm humid atmosphere [AD-A148567] p 40 N85-17416

ATMOSPHERIC SCATTERING

- Performance of a coherent lidar remote sensor in snow and fog p 59 A85-25347
- The influence of a scattering medium on the quality of an optical image p 48 A85-26294
- Earth observation modeling based on layer scattering matrices p 7 A85-30091

ATMOSPHERIC TEMPERATURE

- Advances in microwave remote sensing of the ocean and atmosphere p 28 A85-21960

ATS 3

- Satellite data communication system for near real-time processing and distribution of marine fishery research data p 36 A85-28119

AUSTRALIA

- Evaluation of SIR-B imagery for geologic and geomorphic mapping, hydrology, and oceanography in Australia p 51 N85-17229

AUTOMATIC CONTROL

- An automatic high-resolution picture transmission receiving station p 61 A85-27698

AUTOREGRESSIVE PROCESSES

- Texture classification using autoregressive filtering p 50 N85-16254
- Autoregressive spectral estimation for two dimensional time series p 50 N85-16258

AZIMUTH

- Structural investigation of the Grenville Province by radar and other imaging and nonimaging sensors p 25 N85-17237

B

BACKSCATTERING

- Can optical measurements help in the interpretation of radar backscatter? p 29 A85-23683
- Microwave properties of vegetation canopies - An overview p 4 A85-23772
- Relations between the radar backscatter coefficient and the characteristics of a vegetation canopy - Analysis of the effect of structure p 4 A85-23774
- The analysis of backscattering properties from SAR data of mountain regions p 59 A85-24081
- The effect of a snow cover on microwave backscatter from sea ice p 32 A85-24083
- The reflection of airborne UV laser pulses from the ocean p 37 A85-29714
- Intermediate results of radar backscatter measurements from summer sea ice [AD-A147212] p 38 N85-15960
- Simultaneous ocean cross-section and rainfall measurements from space with a nadir-pointing radar [NASA-TM-86167] p 44 N85-16273
- The interpretation of SIR-B imagery of surface waves and other oceanographic features using in-situ, meteorological satellite, and infrared satellite data p 39 N85-17212
- Evaluation of the radar response to land surfaces and volumes Examination of theoretical models, target statistics, and applications p 63 N85-17250
- Ground truth for SIR-B images obtained by SIR system 8 impulse radar p 10 N85-17251
- Remote sensing of soil moisture p 10 N85-17252
- Oceanographic and meteorological research based on the data products of SEASAT [E85-10091] p 41 N85-21753

BATHYMETERS

- Expressions of bathymetry on Seasat synthetic radar images p 29 A85-23691
- The investigation of selected oceanographic applications of spaceborne synthetic-aperture radar p 39 N85-17233
- Along-track deflection of the vertical from SEASAT GEBCO (General Bathymetric Chart of the Oceans) overlays [PB85-129641] p 42 N85-21767

BAYES THEOREM

- Bayesian estimation of normal mixture parameters p 50 N85-16255
- Spatial estimation from remotely sensed data via empirical Bayes models p 8 N85-16256
- Multivariate spline methods in surface fitting p 50 N85-16257

BEAUFORT SEA (NORTH AMERICA)

- Atlas of the Beaufort Sea [AD-A149545] p 41 N85-20619

BEDS (GEOLOGY)

- Tidal current bedforms investigated by Seasat p 30 A85-23692

BIAS

- Electromagnetic bias of 10-GHz radar altimeter measurements of MSL p 37 A85-29713

BIBLIOGRAPHIES

- Sourcebook Gaining access to US government information on the environment and natural resources [DE84-017419] p 71 N85-20941

BIOGEOCHEMISTRY

- Deforestation, floodplain dynamics, and carbon biogeochemistry in the Amazon Basin p 44 N85-17216

BIOLUMINESCENCE

- Bio-optical variability in the Alboran Sea as assessed by Nimbus-7 coastal zone color scanner [AD-A147909] p 39 N85-16281

BIOMASS

- Regional analysis from data from heterogeneous pixels - Remote sensing of total dry matter production in the Senegalese Sahel p 47 A85-23783

BIOMETEOROLOGY

- Study of the correlation between the IRT band of the NOAA AVHRR and the factors conditioning the thermal behavior of bioclimatic areas on a regional scale p 58 A85-23768

BLACK AND WHITE PHOTOGRAPHY

- The utility of data from various airborne sensors for soil mapping p 5 A85-26932

BOUNDARY VALUE PROBLEMS

- Multivariate spline methods in surface fitting p 50 N85-16257

BRAGG ANGLE

- The Harp probe - An in situ Bragg scattering sensor
p 28 A85-22171

BRAZIL

- Integrated analysis of remote sensing products from basic geological surveys --- Brazil
[E85-10052] p 24 N85-16248
- Brazilian remote sensing receiving, recording and processing ground systems in the 1980's
[E85-10079] p 52 N85-19493
- The sharing of remote sensing techniques in Brazilian geographic research
[INPE-3307-PRE/617] p 15 N85-19502

BRAZILIAN SPACE PROGRAM

- Brazilian Remote Sensing Shuttle Experiment (BRESEX) Characteristics and future utilization on satellites
[INPE-3313-PRE/620] p 64 N85-19385
- Remote sensing activities in Latin America
[INPE-3297-PRE/612] p 64 N85-19501

BRIDGES (LANDFORMS)

- Viscous remanent magnetization model for the Broken Ridge satellite magnetic anomaly
p 22 A85-26423

BRIGHTNESS

- Correlation of spectral brightnesses measured using multispectral space images
p 60 A85-25659

BROADBAND

- Method of measuring sea surface water temperature with a satellite including wideband passive synthetic-aperture multichannel receiver
[NASA-CASE-NPO-15651-1] p 41 N85-21723

BUOYS

- Eddy kinetic energy distribution in the southern ocean from Seasat altimeter and FGGE drifting buoys
p 32 A85-24554

C**CALIBRATING**

- Aircraft measurements for calibration of an orbiting spacecraft sensor
p 59 A85-24246
- Thematic Mapper Volume 1 Calibration report flight model, LANDSAT 5
[E85-10059] p 63 N85-16270
- Evaluation of the L-band scattering characteristics of volcanic terrain in aid of lithologic identification, assessment of SIR-B calibration, and development of planetary geomorphic analogs
p 24 N85-17232
- Application and calibration of the subsurface mapping capability of SIR-B in desert regions
p 25 N85-17244
- Radiometric calibration and processing procedure for reflective bands on LANDSAT-4 prototype Thematic Mapper
p 66 N85-20510
- Prelaunch absolute radiometric calibration of the reflective bands on the LANDSAT-4 prototype Thematic Mapper
p 66 N85-20515
- Characterization of radiometric calibration of LANDSAT-4 reflective bands
p 66 N85-20516
- Thermal band characterization of the LANDSAT-4 Thematic Mapper
p 67 N85-21727
- Preliminary evaluation of the radiometric calibration of LANDSAT-4 Thematic Mapper data by the Canada Centre for Remote Sensing
p 67 N85-21729

CALIFORNIA

- Characterizing the scientific potential of satellite sensors --- San Francisco, California
[E85-10044] p 62 N85-16244
- Characterizing the scientific potential of satellite sensors --- San Francisco, California
[E85-10053] p 62 N85-16249
- LANDSAT-4 Thematic Mapper Modulation Transfer Function (MTF) evaluation --- California and New Mexico
[E85-10055] p 62 N85-16250
- Image variance and spatial structure in remotely sensed scenes --- South Dakota, California, Missouri, Kentucky, Louisiana, Tennessee, District of Columbia, and Oregon
p 51 N85-16265
- Image-to-image correspondence Linear structure matching
p 51 N85-16266
- Analysis of SIR-B radar illumination of geometry for depth of penetration and surface feature and vegetation detection, Nevada and California
p 25 N85-17248
- Analysis of the quality of image data required by the LANDSAT-4 Thematic Mapper and Multispectral Scanner --- agricultural and forest cover types in California
[E85-10074] p 11 N85-19488
- Investigation of radiometric properties of LANDSAT-4 MSS --- California, North Carolina, South Carolina, and New England
p 65 N85-20500
- Geodetic accuracy of LANDSAT 4 Multispectral Scanner and Thematic Mapper data --- Washington, DC, California, Alabama, South Dakota, and Illinois
p 53 N85-20504
- Impact of LANDSAT MSS sensor differences on change detection analysis --- New Mexico, San Francisco, CA, New Hampshire, and Connecticut
p 65 N85-20506

- Analysis of the NASA/MSFC Airborne Doppler Lidar results from San Geronio Pass, California
[NASA-CR-171355] p 70 N85-21873

CANADA

- Evaluation of the radar response to land surfaces and volumes Examination of theoretical models, target statistics, and applications
p 63 N85-17250
- Canadian plans for Thematic Mapper data
p 54 N85-20513

CANADIAN SHIELD

- Structural investigation of the Grenville Province by radar and other imaging and nonimaging sensors
p 25 N85-17237

CANADIAN SPACE PROGRAMS

- The Canadian SAR experience
p 46 A85-23689

CANOPES (VEGETATION)

- Angular and spatial variability of visible and NIR spectral data
p 2 A85-23752
- Estimation of agronomic variables using spectral signatures
p 2 A85-23753
- Light polarization measurements - A method to determine the specular and diffuse light-scattering properties of both leaves and plant canopies
p 2 A85-23754
- Microwave properties of vegetation canopies - An overview
p 4 A85-23772
- Relations between the radar backscatter coefficient and the characteristics of a vegetation canopy - Analysis of the effect of structure
p 4 A85-23774
- Identification of the structure of soil-vegetation cover using aerial and space images
p 5 A85-25656
- Spectral characterization of vegetation canopies in the visible and NIR - Application to remote sensing
p 5 A85-25670

- Detection of lowland flooding using active microwave systems
p 43 A85-29218
- Computing the foliage angle distribution from contact frequency data
p 6 A85-29969

- Effect of vegetation on soil moisture sensing observed from orbiting microwave radiometers
p 7 A85-30089
- Earth observation modeling based on layer scattering matrices
p 7 A85-30091

- Comparative study of Suits and SAIL canopy reflectance models
p 7 A85-30092
- Variation in spectral response of soybeans with respect to illumination, view, and canopy geometry
[E85-10040] p 8 N85-16241

- Spectral estimators of absorbed photosynthetically active radiation in corn canopies
[E85-10041] p 8 N85-16242
- Growth/reflectance model interface for wheat and corresponding model
[E85-10058] p 9 N85-16269

- Development and evaluation of techniques for using combined microwave and optical image data for vegetation studies
p 9 N85-17240
- The extension of an invertible coniferous forest canopy reflectance model using SIR-B and LANDSAT data
p 10 N85-17246

- Analysis of terrestrial conditions and dynamics
[E85-10063] p 10 N85-17401
- Shortwave infrared detection of vegetation
[E85-10064] p 10 N85-17402

- Growth and reflectance characteristics of winter wheat canopies
[E85-10080] p 11 N85-19494
- Techniques for measuring intercepted and absorbed PAR in corn canopies
[E85-10081] p 11 N85-19495

- Investigations of vegetation and soils information contained in LANDSAT Thematic Mapper and Multispectral Scanner data
[E85-10082] p 12 N85-21747

CARBON

- Deforestation, floodplain dynamics, and carbon biogeochemistry in the Amazon Basin
p 44 N85-17216

CARBON DIOXIDE

- Lake ice occurrence as a possible detector of atmospheric CO₂ effects on climate
[DE85-002951] p 45 N85-20606

CARIBBEAN REGION

- Neotectonics of the Caribbean
p 27 A85-21145

CELESTIAL GEODESY

- Altitude measurements of ocean topography
p 30 A85-23695
- Cosmic interpolation of terrestrial potential values
p 18 A85-26476

- Regional mean sea surfaces based on GEOS-3 and SEASAT altimeter data
p 38 A85-29716
- Methods of space geodesy and its role in earth studies
p 19 A85-30013

CENTER OF MASS

- Center of mass estimation in closed vortices - A verification in principle and practice
p 26 A85-19417

CEPSTRAL ANALYSIS

- Improvement of the accuracy of radar measurements of sea-ice thickness by cepstral processing of reflected signals
p 35 A85-27736

CHANNELS (DATA TRANSMISSION)

- Prelaunch absolute radiometric calibration of the reflective bands on the LANDSAT-4 prototype Thematic Mapper
p 66 N85-20515

CHARGE COUPLED DEVICES

- Airborne remote sensing CCD imaging system
p 65 N85-20220

CHINA

- Remote sensing technology now playing practical roles
p 64 N85-20190

CHINESE SPACE PROGRAM

- Remote sensing development in the People's Republic of China
p 56 A85-20643

CHLOROPHYLLS

- Estimating ocean primary production from satellite chlorophyll - Introduction to regional differences and statistics for the Southern California Bight
p 35 A85-28005

CIRCULATION DISTRIBUTION

- Lagrangian observations of surface circulation at the Emperor Seamount chain
p 35 A85-27710

CITIES

- An examination of some problems and solutions in monitoring urban areas from satellite platforms
p 14 A85-26935

- Detecting agricultural to urban land use change from multi-temporal MSS digital data --- Salt Lake County, Utah
[E85-10049] p 15 N85-16245

- Image variance and spatial structure in remotely sensed scenes --- South Dakota, California, Missouri, Kentucky, Louisiana, Tennessee, District of Columbia, and Oregon
p 51 N85-16265

CITRUS TREES

- Analysis of ACIR transparencies of citrus trees with a projecting spectral densitometer --- Aerial Color IR
p 1 A85-21050

CLASSIFICATIONS

- Estimating location parameters in a mixture
p 50 N85-16252
- Texture classification using autoregressive filtering
p 50 N85-16254

- Assessment of LANDSAT for rangeland mapping, Rush Valley, Utah
[E85-10072] p 15 N85-19486

CLASSIFIERS

- A computationally-efficient maximum-likelihood classifier employing prior probabilities for remotely-sensed data
p 49 A85-26948

CLEAN ENERGY

- The potential of solar power satellites for developing countries
p 59 A85-24654

CLEARINGS (OPENINGS)

- Relationship between forest clearing and biophysical factors in tropical environments Implications for the design of a forest change monitoring approach --- Costa Rica
[E85-10051] p 8 N85-16247

CLIMATE

- Lake ice occurrence as a possible detector of atmospheric CO₂ effects on climate
[DE85-002951] p 45 N85-20606

CLIMATOLOGY

- Study of the correlation between the IRT band of the NOAA AVHRR and the factors conditioning the thermal behavior of bioclimatic areas on a regional scale
p 58 A85-23768

- Ice sheet margins and ice shelves
p 32 A85-24524
- Satellite measurements of sea-surface temperature for climate research
p 32 A85-24555

CLOUD COVER

- On the separability of various classes from the GOES visible and infrared data --- of winter cloud and snow cover
p 45 A85-21138

- Separating clouds from ocean in infrared images
p 28 A85-22423

- The diurnal variation of Atlantic Ocean tropical cyclone cloud distribution inferred from geostationary satellite infrared measurements
p 33 A85-24739

- Dramatic contrast between low clouds and snow cover in daytime 3.7 micron imagery
p 48 A85-24740
- Comments on 'Inference of cloud temperature and thickness by microwave radiometry from space'
p 59 A85-25182

CLUSTER ANALYSIS

- Calibration or inverse regression Which is appropriate for crop surveys using LANDSAT data?
p 9 N85-16260

CLUTTER

- Land clutter models for radar design and analysis
p 49 A85-27827

COASTAL CURRENTS

- Satellite definition of the bio-optical and thermal variation of coastal eddies associated with the African current [AD-A147910] p 39 N85-16282

COASTAL WATER

- Development of water quality models applicable throughout the entire San Francisco Bay and Delta p 42 A85-21046
- Investigation of Krasnovodsk bay on the basis of space photographs p 28 A85-21669
- Remote sensing techniques for monitoring of pollution in coastal waters - Potential application to Saudi Arabia p 34 A85-27441

COASTAL ZONE COLOR SCANNER

- Aircraft measurements for calibration of an orbiting spacecraft sensor p 59 A85-24246
- Bio-optical variability in the Alboran Sea as assessed by Nimbus-7 coastal zone color scanner [AD-A147909] p 39 N85-16281
- The use of principal components analysis techniques Nimbus-7 coastal zone color scanner data to define mesoscale ocean features through a warm humid atmosphere [AD-A148567] p 40 N85-17416

COASTS

- Nautical charting with remotely sensed imagery, volume 1 [AD-A149361] p 41 N85-19503
- Nautical charting with remotely sensed imagery Volume 2 Case studies [AD-A149362] p 41 N85-19504

COHERENT RADAR

- Some properties of SAR speckle p 46 A85-23684
- Performance of a coherent lidar remote sensor in snow and fog p 59 A85-25347

COLD WEATHER

- Optical engineering for cold environments, Proceedings of the Meeting, Arlington, VA, April 7, 8, 1983 p 59 A85-25344
- Landsat-4 thematic mapper (TM) for cold environments p 60 A85-25349

COLOR PHOTOGRAPHY

- The utility of data from various airborne sensors for soil mapping p 5 A85-26932
- Bio-optical variability in the Alboran Sea as assessed by Nimbus-7 coastal zone color scanner [AD-A147909] p 39 N85-16281

COMMUNICATION EQUIPMENT

- Satellite data communication system for near real-time processing and distribution of marine fishery research data p 36 A85-28119

COMPILERS

- Investigations of the accuracy of the digital photogrammetry system DPS, a rigorous three dimensional compilation process for push broom imagery [MBB-UA-753/83-OE] p 60 A85-26393

COMPUTER AIDED MAPPING

- MASMAP, design for a project-oriented geo-information program package for urban upgrading schemes p 13 A85-20747
- Method for sequential analysis of spatial development in a rural-urban fringe zone p 13 A85-20748
- Geomorphology and remote sensing Numerical inventory of objects in Landsat, SPOT imagery and SIR-A data Applications to the Mopti-Bandiagara (Mali) region p 21 A85-23785

COMPUTER COMPATIBLE TAPES

- TM digital image products for applications p 54 N85-20512

COMPUTER GRAPHICS

- Resource measurement system p 47 A85-24258
- Nonparametric analysis of Minnesota spruce and aspen tree data and LANDSAT data p 8 N85-16253
- Tests of low-frequency geometric distortions in LANDSAT 4 images p 55 N85-21744

COMPUTER PROGRAMS

- An analysis of the high frequency vibrations in early Thematic Mapper scenes p 69 N85-21742

COMPUTER SYSTEMS PROGRAMS

- Characterizing the scientific potential of satellite sensors --- San Francisco, California [E85-10044] p 62 N85-16244

COMPUTERIZED SIMULATION

- The extension of an invertible coniferous forest canopy reflectance model using SIR-B and LANDSAT data p 10 N85-17246

CONFERENCES

- Spectral signatures of objects in remote sensing, International Conference, 2nd, Bordeaux, France, September 12-16, 1983, Reports p 57 A85-23751
- Large-scale oceanographic experiments and satellites, Proceedings of the Advanced Research Workshop, Porto Vecchio, Corse, France, October 3-7, 1983 p 32 A85-24551

- American Congress on Surveying and Mapping and American Society of Photogrammetry, Fall Convention, Salt Lake City, UT, September 19-23, 1983, Technical Papers p 14 A85-24950

- Optical engineering for cold environments, Proceedings of the Meeting, Arlington, VA, April 7, 8, 1983 p 59 A85-25344

- Mathematical modelling of the geomagnetic field and secular variation, and its applications, Proceedings of the Symposium, Hamburg, West Germany, August 15-27, 1983 p 16 A85-25689

- International Symposium on Microwave Signatures in Remote Sensing, 3rd, Toulouse, France, January 16-20, 1984, Proceedings p 6 A85-26942

- Asian Conference on Remote Sensing, 4th, Colombo, Sri Lanka, November 10-15, 1983, Proceedings p 71 A85-27519

- Frontiers for geological remote sensing from space, Geosast Workshop, 4th, Flagstaff, AZ, June 12-17, 1983, Report p 22 A85-27943

- Proceedings of the Second Annual Symposium on Mathematical Pattern Recognition and Image Analysis Program [E85-10056] p 50 N85-16251

- Papers of the 15th International Society for Photogrammetry and Remote Sensing (ISPRS) Congress --- conferences [TRITA-FMI-9] p 63 N85-17406

- LANDSAT-4 Science Characterization Early Results Volume 2, part 1 Thematic Mapper (TM) [E85-10068] p 66 N85-20508

CONIFERS

- Comparative seasonal evolution of the spectral signatures of broad-leaved and coniferous trees from Landsat data Comparison with other perennial surfaces p 2 A85-23757

CONNECTICUT

- Impact of LANDSAT MSS sensor differences on change detection analysis --- New Mexico, San Francisco, CA, New Hampshire, and Connecticut p 65 N85-20506

COORDINATES

- Geodetic accuracy of LANDSAT 4 Multispectral Scanner and Thematic Mapper data p 20 N85-21746

CORN

- An analysis of spectral discrimination between corn and soybeans using a row crop reflectance model p 7 A85-30086
- Application of Thematic Mapper data to corn and soybean development stage estimation p 7 A85-30093

- Spectral estimators of absorbed photosynthetically active radiation in corn canopies [E85-10041] p 8 N85-16242

- Shortwave infrared detection of vegetation [E85-10064] p 10 N85-17402

- Techniques for measuring intercepted and absorbed PAR in corn canopies [E85-10081] p 11 N85-19495

- NOAA-AISC user's guide for implementing CERES maize model for large area yield estimation [E85-10083] p 12 N85-21748

CORRELATION

- Analysis of subpixel registration p 51 N85-16267

CORRELATION COEFFICIENTS

- Investigation of the properties of natural objects by the canonical-correlation method p 49 A85-28973

COSMOS SATELLITES

- Complex studies of the environment by optical and radar methods p 56 A85-20081
- Space radar observations of small-scale formations on the ocean surface p 27 A85-20086

COST EFFECTIVENESS

- An example of Landsat cost effectiveness in mapping land-cover p 1 A85-20573

COSTA RICA

- Relationship between forest clearing and biophysical factors in tropical environments Implications for the design of a forest change monitoring approach --- Costa Rica [E85-10051] p 8 N85-16247

COTTON

- Effect of heliotropism on the bidirectional reflectance of irrigated cotton p 1 A85-22420

CROP GROWTH

- Estimation of wheat production on the basis of Landsat channel 5 and 7 radiometric measurements p 3 A85-23763

- Spectral estimators of absorbed photosynthetically active radiation in corn canopies [E85-10041] p 8 N85-16242

- Growth/reflectance model interface for wheat and corresponding model [E85-10058] p 9 N85-16269

- Growth and reflectance characteristics of winter wheat canopies [E85-10080] p 11 N85-19494

- NOAA-AISC user's guide for implementing CERES maize model for large area yield estimation [E85-10083] p 12 N85-21748

CROP IDENTIFICATION

- An analysis of spectral discrimination between corn and soybeans using a row crop reflectance model p 7 A85-30086

- Comparative study of Suits and SAIL canopy reflectance models p 7 A85-30092

- Application of Thematic Mapper data to corn and soybean development stage estimation p 7 A85-30093

CROP INVENTORIES

- Comparison of SPOT HRV and Landsat-4 TM for crop inventories p 3 A85-23762

- Use of satellite data in agricultural surveys p 4 A85-23782

- Calibration or inverse regression Which is appropriate for crop surveys using LANDSAT data? p 9 N85-16260

- Remote sensing research for agricultural applications --- San Joaquin County, California and Snake River Plain and Twin Falls area, Idaho [E85-10090] p 13 N85-21752

CROPS

- Thematic Mapper spectral dimensionality and data structure p 12 N85-21736

CRUDE OIL

- Analysis of mesofractures according to space images - Currents trends in the exploration for oil and gas deposits p 21 A85-25655

CYCLONES

- The diurnal variation of Atlantic Ocean tropical cyclone cloud distribution inferred from geostationary satellite infrared measurements p 33 A85-24739

D

DATA ACQUISITION

- Status of remote sensing information systems with special emphasis on their specializations, capabilities, accessibilities and future directions p 71 A85-20646

- SEASAT-data acquisition and processing by the Royal Aircraft Establishment p 57 A85-23678

- The near-earth magnetic field at 1980 determined from Magsat data p 16 A85-26408

- An overview of LANDSAT-4 and the Thematic Mapper p 66 N85-20509

- Building a functional, integrated GIS/remote sensing resource analysis and planning system --- Utah [E85-10092] p 15 N85-21754

DATA BASES

- EROS main image file - A picture perfect database for Landsat imagery and aerial photography p 48 A85-24521

- Sourcebook Gaining access to US government information on the environment and natural resources [DE84-017419] p 71 N85-20941

DATA COMPRESSION

- Multispectral data compression using staggered detector arrays p 47 A85-24277

- Information extraction and transmission techniques for spaceborne synthetic aperture radar images [NASA-CR-174341] p 52 N85-17256

DATA CORRELATION

- Digital correlation of images along quasi-epipolar lines by successive approximations p 48 A85-25671

- Characterization of radiometric calibration of LANDSAT-4 reflective bands p 66 N85-20516

- TM geometric performance Line to Line Displacement Analysis (LLDA) --- New Mexico p 68 N85-21732

- Investigation of TM band-to-band registration using the JSC registration processor p 69 N85-21745

DATA INTEGRATION

- An integrated remote sensing approach for identifying ecological range sites --- Parker Mountain [E85-10050] p 8 N85-16246

- LANDSAT 4 investigation of Thematic Mapper and Multispectral Scanner applications [E85-10076] p 52 N85-19490

- Spectroradiometric calibration of the Thematic Mapper and Multispectral Scanner system [E85-10077] p 64 N85-19491

DATA PROCESSING

- SEASAT-data acquisition and processing by the Royal Aircraft Establishment p 57 A85-23678

- Interpretation of thermal infrared data to augment spectral signatures p 47 A85-23791

- The near-earth magnetic field at 1980 determined from Magsat data p 16 A85-26408

- Data report on variations in the composition of sea ice during MIZEX/East'83 with the Nimbus-7 SMMR [NASA-TM-86170] p 40 N85-18443

SUBJECT INDEX

- Brazilian remote sensing receiving, recording and processing ground systems in the 1980's [E85-10079] p 52 N85-19493
- An overview of the Thematic Mapper geometric correction system p 53 N85-20511
- Canadian plans for Thematic Mapper data p 54 N85-20513
- An analysis of the high frequency vibrations in early Thematic Mapper scenes p 69 N85-21742
- DATA PROCESSING EQUIPMENT**
- Papers of the 15th International Society for Photogrammetry and Remote Sensing (ISPRS) Congress --- conferences [TRITA-FMI-9] p 63 N85-17406
- DATA TRANSMISSION**
- Satellite data communication system for near real-time processing and distribution of marine fishery research data p 36 A85-28119
- DAYTIME**
- Calculation of thermal inertia from day-night measurements separated by days or weeks p 45 A85-21048
- DEFLECTION**
- Along-track deflection of the vertical from SEASAT GEBCO (General Bathymetric Chart of the Oceans) overlays [PB85-129641] p 42 N85-21767
- DEFOCUSING**
- Effect of defocusing on the images of ocean waves p 29 A85-23688
- DEFORESTATION**
- Relationship between forest clearing and biophysical factors in tropical environments Implications for the design of a forest change monitoring approach --- Costa Rica [E85-10051] p 8 N85-16247
- Deforestation, floodplain dynamics, and carbon biogeochemistry in the Amazon Basin p 44 N85-17216
- DENSITOMETERS**
- Analysis of ACIR transparencies of citrus trees with a projecting spectral densitometer --- Aerial Color IR p 1 A85-21050
- DESERTIFICATION**
- Comprehensive desertification maps and methods for making such maps on the basis of space photographs p 14 A85-29907
- DESERTS**
- Application and calibration of the subsurface mapping capability of SIR-B in desert regions p 25 N85-17244
- DETECTION**
- Lake ice occurrence as a possible detector of atmospheric CO₂ effects on climate [DE85-002951] p 45 N85-20606
- DEVELOPING NATIONS**
- Needs and accessibility of developing countries for/to remote sensing information systems p 13 A85-20647
- MASMAP, design for a project-oriented geo-information program package for urban upgrading schemes p 13 A85-20747
- Population estimation from aerial photos for non-homogeneous urban residential areas p 14 A85-20749
- The potential of solar power satellites for developing countries p 59 A85-24654
- DIELECTRIC PROPERTIES**
- Microwave properties of vegetation canopies - An overview p 4 A85-23772
- DIGITAL DATA**
- The integrated use of digital cartographic data and remotely sensed imagery p 45 A85-20572
- Investigations of the accuracy of the digital photogrammetry system DPS, a rigorous three dimensional compilation process for push broom imagery [MBB-UA-753/83-OE] p 60 A85-26393
- Characterizing the scientific potential of satellite sensors --- San Francisco, California [E85-10044] p 62 N85-16244
- Detecting agricultural to urban land use change from multi-temporal MSS digital data --- Salt Lake County, Utah [E85-10049] p 15 N85-16245
- Image variance and spatial structure in remotely sensed scenes --- South Dakota, California, Missouri, Kentucky, Louisiana, Tennessee, District of Columbia, and Oregon p 51 N85-16265
- Analysis of subpixel registration p 51 N85-16267
- Interactive digital image processing for terrain data extraction [AD-A148580] p 52 N85-17417
- Radiometric accuracy assessment of LANDSAT 4 Multispectral Scanner data p 53 N85-20498
- LANDSAT scene-to-scene registration accuracy assessment p 65 N85-20502
- Geometric accuracy assessment of LANDSAT-4 Multispectral Scanner (MSS) data p 19 N85-20505

- TM digital image products for applications p 54 N85-20512
- A preliminary assessment of LANDSAT-4 Thematic Mapper data --- Windsor, Ontario and Medicine Hat areas, Canada p 54 N85-21728
- Preliminary evaluation of the radiometric calibration of LANDSAT-4 Thematic Mapper data by the Canada Centre for Remote Sensing p 67 N85-21729
- A preliminary analysis of LANDSAT-4 Thematic Mapper radiometric performance p 68 N85-21730
- DIGITAL FILTERS**
- Enhancement of multispectral scanner images by digital filtering [ESA-TT-624] p 63 N85-16284
- DIGITAL RADAR SYSTEMS**
- Realtime processor of SAR systems p 60 A85-25855
- DIGITAL SYSTEMS**
- Interactive digital image processing for terrain data extraction [AD-A148580] p 52 N85-17417
- DIGITAL TECHNIQUES**
- Automatic production of DTM data using digital off-line technique --- Digital Terrain Modelling p 45 A85-20750
- Interpretation of space images of the sea surface using the SVIT digital-processing complex p 34 A85-25654
- Features of the digital processing of radar images obtained with the sidelooking radar of the Cosmos-1500 satellite p 48 A85-25660
- Digital correlation of images along quasi-epipolar lines by successive approximations p 48 A85-25671
- The effects of image noise on digital correlation probability p 49 A85-29221
- Detecting agricultural to urban land use change from multi-temporal MSS digital data --- Salt Lake County, Utah [E85-10049] p 15 N85-16245
- Information extraction and transmission techniques for spaceborne synthetic aperture radar images [NASA-CR-174341] p 52 N85-17256
- Mathematical aspects of digital terrain information, Report from International Society for Photogrammetry and Remote Sensing (ISPRS) working group 3.3, 1980 - 1984 --- photogrammetry p 19 N85-17407
- A comparative test of photogrammetrically sampled digital elevation models p 52 N85-17408
- DIRECTION**
- A comparison of in situ and airborne radar observations of ocean wave directionality p 27 A85-20487
- DISPLAY DEVICES**
- An airborne infrared thermal scanning system for easy use on Navy P-3 aircraft [AD-A149690] p 42 N85-22143
- DISTORTION**
- Tests of low-frequency geometric distortions in LANDSAT 4 images p 55 N85-21744
- DISTRICT OF COLUMBIA**
- Image variance and spatial structure in remotely sensed scenes --- South Dakota, California, Missouri, Kentucky, Louisiana, Tennessee, District of Columbia, and Oregon p 51 N85-16265
- Geodetic accuracy of LANDSAT 4 Multispectral Scanner and Thematic Mapper data --- Washington, DC, California, Alabama, South Dakota, and Illinois p 53 N85-20504
- Geometric accuracy assessment of LANDSAT-4 Multispectral Scanner (MSS) data p 19 N85-20505
- Intraband radiometric performance of the LANDSAT 4 Thematic Mapper --- Washington, DC, Arkansas, Massachusetts, Virginia, and Arizona p 69 N85-21738
- DIURNAL VARIATIONS**
- The diurnal variation of Atlantic Ocean tropical cyclone cloud distribution inferred from geostationary satellite infrared measurements p 33 A85-24739
- DMSP SATELLITES**
- The influence of satellite spectral sensor response on the analysis of satellite imagery at high latitudes p 60 A85-26927
- DOCUMENTATION**
- Preserve the sense of Earth from space --- achieves of remote sensing data [PB85-124121] p 72 N85-20942
- DOPPLER RADAR**
- Analysis of the NASA/MSFC Airborne Doppler Lidar results from San Geronio Pass, California [NASA-CR-171355] p 70 N85-21873
- DYNAMIC RESPONSE**
- Intraband radiometric performance of the LANDSAT 4 Thematic Mapper --- Washington, DC, Arkansas, Massachusetts, Virginia, and Arizona p 69 N85-21738

EARTH OBSERVATIONS (FROM SPACE)

E

EARTH (PLANET)

- The near-earth magnetic field at 1980 determined from Magsat data p 16 A85-26408

EARTH ALBEDO

- Inventory of geographically homogeneous zones by spectral modeling of diachronic Meteosat albedo or combined albedo/thermal-channel data - Applications to the Maghreb and to Sahelian Africa p 46 A85-23769

EARTH CRUST

- The participation of the Netherlands in the NASA Crustal Dynamics Project p 15 A85-20035
- On the identification of Magsat anomaly charts as crustal part of the internal field p 17 A85-26412
- Seafloor spreading anomalies in the Magsat field of the North Atlantic p 17 A85-26415
- Extraction of magnetic anomalies of crustal origin from Magsat data over the area of the Japanese Islands p 21 A85-26419
- An estimation of continental crust magnetization and susceptibility from Magsat data for the conterminous United States p 22 A85-26420
- Crustal structure of the Churchill-Superior boundary zone between 80 and 98 deg W longitude from Magsat anomaly maps and stacked passes p 22 A85-26421
- Magsat and POGO magnetic anomalies over the Lord Howe Rise Evidence against a simple continental crustal structure p 18 A85-26422
- Viscous remanent magnetization model for the Broken Ridge satellite magnetic anomaly p 22 A85-26423
- United States crustal thickness p 18 A85-28011
- Estimation of lower crust magnetization from satellite derived anomaly field p 18 A85-28012

EARTH ENVIRONMENT

- Sourcebook Gaining access to US government information on the environment and natural resources [DE84-017419] p 71 N85-20941

EARTH HYDROSPHERE

- Monitoring Africa's Lake Chad basin with Landsat and NOAA satellite data p 43 A85-26930

EARTH OBSERVATIONS (FROM SPACE)

- Methodological study of spectral band selection for multispectral remote sensing p 55 A85-19363
- On realizing the potential of the earth-looking vantage point [AIAA PAPER 85-0195] p 70 A85-19580
- Complex studies of the environment by optical and radar methods p 56 A85-20081
- Ring structures observed on space radar images of the earth p 45 A85-20084
- Status of remote sensing information systems with special emphasis on their specializations, capabilities, accessibilities and future directions p 71 A85-20646
- Survey of multispectral imaging systems for earth observations p 56 A85-22424
- Status and future plans for ERS-1 p 31 A85-23707
- Radiogrammetry of Shuttle Imaging Radar-B experiment p 46 A85-23779
- Thematic evaluation of SPOT spectral bands p 58 A85-23794
- Review of earth observation satellite programs p 59 A85-23795
- Comments on 'Inference of cloud temperature and thickness by microwave radiometry from space' p 59 A85-25182
- Use of Space Station for Earth and Planetary Exploration p 71 A85-25348
- Observations of the earth using nighttime visible imagery p 48 A85-25350
- Effect of meteorological conditions on the characteristics of space radar images of the earth surface p 48 A85-25653
- Frontiers for geological remote sensing from space, Geosat Workshop, 4th, Flagstaff, AZ, June 12-17, 1983, Report p 22 A85-27943
- Space remote-sensing data in geology --- Russian book p 23 A85-28400
- A survey of oceanographic satellite altimetric missions p 36 A85-29703
- The use of a priori estimation of the conditions of the observation of the earth surface from space for a rational selection of the time at which the survey is conducted p 50 A85-29914
- Earth observation modeling based on layer scattering matrices p 7 A85-30091
- Brazilian Remote Sensing Shuttle Experiment (BRESEX) Characteristics and future utilization on satellites [INPE-3313-PRE/620] p 64 A85-19385
- The spot operational remote sensing satellite system Current status and perspectives p 67 A85-20776
- Earth resources research using the Shuttle Imaging Radar system p 67 A85-20779

F

EARTH RESOURCES

- Study on a regional geographical information system and application model p 13 A85-20644
- Investigation of Krasnovodsk bay on the basis of space photographs p 28 A85-21669
- Landsat-4 thematic mapper (TM) for cold environments p 60 A85-25349
- The use of airborne lasers in terrestrial and water environments p 33 A85-25351
- The current use of TIROS-N series of meteorological satellites for land-cover studies p 60 A85-26928
- Comparison of level I land cover classification accuracy for MSS and AVHRR data --- Advanced Very High Resolution Radiometers p 61 A85-26929
- Possibilities of using remote-sensing methods to improve the efficiency of oil and gas exploration p 24 A85-29905

- Comprehensive desertification maps and methods for making such maps on the basis of space photographs p 14 A85-29907

- Conical multispectral scanner for the study of earth resources p 62 A85-29909

- Remote sensing technology now playing practical roles p 64 A85-20190

- Sourcebook Gaining access to US government information on the environment and natural resources [DE84-017419] p 71 A85-20941

EARTH RESOURCES INFORMATION SYSTEMS

- Needs and accessibility of developing countries for/to remote sensing information systems p 13 A85-20647

EARTH RESOURCES PROGRAM

- Remote sensing development in the People's Republic of China p 56 A85-20643
- Resource measurement system p 47 A85-24258

EARTH RESOURCES SHUTTLE IMAGING RADAR

- Earth resources research using the Shuttle Imaging Radar system p 67 A85-20779

EARTH SATELLITES

- Perspectives of remote sensing in Europe at the end of the decade p 70 A85-20565
- Review of earth observation satellite programs p 59 A85-23795

EARTH SURFACE

- Thermal-inertia mapping from space p 21 A85-23766
- Observations of the earth using nighttime visible imagery p 48 A85-25350
- Land clutter models for radar design and analysis p 49 A85-27827
- The use of a priori estimation of the conditions of the observation of the earth surface from space for a rational selection of the time at which the survey is conducted p 50 A85-29914
- Evaluation of the radiometric quality of the TM data using clustering, linear transformations and multispectral distance measures --- Illinois p 54 A85-21731

EARTHNET

- SEASAT - A key element of the EARTHNET programme --- program for distribution of remote sensing data to Europe p 46 A85-23679

EARTHQUAKES

- Neotectonics of the Caribbean p 27 A85-21145

ECHO SOUNDING

- Improvement of the accuracy of radar measurements of sea-ice thickness by cepstral processing of reflected signals p 35 A85-27736

ECOLOGICAL

- Visual interpretation of SAR images of two areas in the Netherlands p 1 A85-23694
- The potential of satellite remote sensing of ecological conditions for survey and forecasting desert-locust activity p 5 A85-26934
- An integrated remote sensing approach for identifying ecological range sites --- parker mountain [E85-10050] p 8 A85-16246
- Relationship between forest clearing and biophysical factors in tropical environments. Implications for the design of a forest change monitoring approach --- Costa Rica [E85-10051] p 8 A85-16247
- Analysis of terrestrial conditions and dynamics [E85-10063] p 10 A85-17401

EDUCATION

- The educational role of satellites p 70 A85-20574
- Education and training in satellite remote sensing applications - Guide to education and training opportunities p 71 A85-20640

ELECTRO-OPTICS

- Modular Optoelectronic Multispectral Scanner (MOMS) Technological aspects p 61 A85-27059

ELECTROMAGNETIC NOISE

- Research on ocean floor electrical surveys [AD-A149831] p 42 A85-21920

ELECTROMAGNETIC PROPERTIES

- Research on ocean floor electrical surveys [AD-A149831] p 42 A85-21920

ELEVATION

- Automatic terrain elevation mapping and registration p 52 A85-17242
- A comparative test of photogrammetrically sampled digital elevation models p 52 A85-17408

ENERGY DISTRIBUTION

- Eddy kinetic energy distribution in the southern ocean from Seasat altimeter and FGGE drifting buoys p 32 A85-24554

ENERGY TECHNOLOGY

- The potential of solar power satellites for developing countries p 59 A85-24654

ENVIRONMENT MODELS

- A comparison between GEOS 1 magnetic-field measurements and some models of the geomagnetic field p 18 A85-27386
- Land clutter models for radar design and analysis p 49 A85-27827

ENVIRONMENTAL MONITORING

- The space environment monitors onboard GOES [AIAA PAPER 85-0238] p 55 A85-19608
- Complex studies of the environment by optical and radar methods p 56 A85-20081
- On the application of meteorological satellite imagery for monitoring the environment p 13 A85-20570
- An examination of some problems and solutions in monitoring urban areas from satellite platforms p 14 A85-26935
- Asian Conference on Remote Sensing, 4th, Colombo, Sri Lanka, November 10-15, 1983, Proceedings p 71 A85-27519
- Remote sensing technology now playing practical roles p 64 A85-20190
- On the P1 data from GMS-SEM p 15 A85-21890
- The development of image processing of NOAA AVHRR data and its application to sea surface temperature p 42 A85-21891

EPHEMERIS TIME

- Altimetry, orbits and tides [E85-10066] p 40 A85-17404

EQUATORIAL ELECTROJET

- The near-earth magnetic field at 1980 determined from Magsat data p 16 A85-26408

EROS (SATELLITES)

- EROS main image file - A picture perfect database for Landsat imagery and aerial photography p 48 A85-24521

EROSION

- Nautical charting with remotely sensed imagery, volume 1 [AD-A149361] p 41 A85-19503
- Nautical charting with remotely sensed imagery Volume 2 Case studies [AD-A149362] p 41 A85-19504

ERROR ANALYSIS

- Determination of the external-orientation elements of aerial and space photographs in the remote sensing of dynamic processes and phenomena p 56 A85-19998
- Investigations of the accuracy of the digital photogrammetry system DPS, a rigorous three dimensional compilation process for push broom imagery [MBB-JA-753/83-OE] p 60 A85-26393
- Altimetry, orbits and tides [E85-10066] p 40 A85-17404
- Multimodels increase accuracy Summary of an experiment --- photogrammetry p 63 A85-17409

ERS-1 (ESA SATELLITE)

- Status and future plans for ERS-1 p 31 A85-23707

ESTIMATES

- Forest area estimates from LANDSAT MSS and forest inventory plot data [PB85-105617/GAR] p 9 A85-16290

ESTIMATING

- Rain volume estimation over areas using satellite and radar data [NASA-CR-174434] p 44 A85-19568

ESTUARIES

- Remote sensing of water quality in the Neuse River Estuary, North Carolina p 43 A85-29219

EUROPEAN SPACE PROGRAMS

- Perspectives of remote sensing in Europe at the end of the decade p 70 A85-20565
- Status and future plans for ERS-1 p 31 A85-23707

EVALUATION

- Development and evaluation of techniques for using combined microwave and optical image data for vegetation studies p 9 A85-17240

EVAPOTRANSPIRATION

- Estimation of evapotranspiration on the basis of thermal IR p 3 A85-23765
- Effects of the experimental errors and conditions on the estimation of thermal inertia and evapotranspiration from METEOSAT data p 3 A85-23767

FARM CROPS

- Spatial estimation from remotely sensed data via empirical Bayes models p 8 A85-16256
- The management of atmospheric resources in food production p 9 A85-16362

FARMLANDS

- Satellite passive microwave rain rate measurement over croplands during spring, summer and fall p 4 A85-25181

- The potential of satellite remote sensing of ecological conditions for survey and forecasting desert-locust activity p 5 A85-26934
- Thermal structure of an agricultural region as seen by NOAA-7 AVHRR p 7 A85-30090

- Evaluation of SIR-B imagery for geologic and geomorphic mapping, hydrology, and oceanography in Australia p 51 A85-17229
- Remote sensing research for agricultural applications --- San Joaquin County, California and Snake River Plain and Twin Falls area, Idaho [E85-10090] p 13 A85-21752

- [E85-10090] p 13 A85-21752

FERTILIZERS

- Growth and reflectance characteristics of winter wheat canopies [E85-10080] p 11 A85-19494

FINLAND

- Retrieval of snow water equivalent from Nimbus-7 SMMR data Effect of land-cover categories and weather conditions p 43 A85-24082

FISHERIES

- Satellite data communication system for near real-time processing and distribution of marine fishery research data p 36 A85-28119

FLIGHT TESTS

- Aircraft measurements for calibration of an orbiting spacecraft sensor p 59 A85-24246

FLOOD PLAINS

- Deforestation, floodplain dynamics, and carbon biogeochemistry in the Amazon Basin p 44 A85-17216

FLOODS

- Detection of lowland flooding using active microwave systems p 43 A85-29218

FLUID DYNAMICS

- Analysis of the NASA/MSFC Airborne Doppler Lidar results from San Geronio Pass, California [NASA-CR-171355] p 70 A85-21873

FLUX DENSITY

- Techniques for measuring intercepted and absorbed PAR in corn canopies [E85-10081] p 11 A85-19495

FOG

- Performance of a coherent lidar remote sensor in snow and fog p 59 A85-25347

FOLDS (GEOLOGY)

- Structural investigation of the Grenville Province by radar and other imaging and nonimaging sensors p 25 A85-17237

FORESTS

- Comparative seasonal evolution of the spectral signatures of broad-leaved and coniferous trees from Landsat data Comparison with other perennial surfaces p 2 A85-23757

- Image variance and spatial structure in remotely sensed scenes --- South Dakota, California, Missouri, Kentucky, Louisiana, Tennessee, District of Columbia, and Oregon p 51 A85-16265

- Forest area estimates from LANDSAT MSS and forest inventory plot data [PB85-105617/GAR] p 9 A85-16290

- Microwave and optical remote sensing of forest vegetation p 9 A85-17228

- The extension of an invertible coniferous forest canopy reflectance model using SIR-B and LANDSAT data p 10 A85-17246

- Test plan for the forest-echo experiment [DE84-017175] p 10 A85-18447

- Analysis of data acquired by synthetic aperture radar and LANDSAT Multispectral Scanner over Kershaw County, South Carolina, during the summer season [E85-10071] p 11 A85-19485

- Analysis of the quality of image data required by the LANDSAT-4 Thematic Mapper and Multispectral Scanner --- agricultural and forest cover types in California [E85-10074] p 11 A85-19488

FREEZING

- Lake ice occurrence as a possible detector of atmospheric CO2 effects on climate [DE85-002951] p 45 A85-20606

FRENCH SPACE PROGRAMS

- CNES, INRA do joint remote-sensing research p 11 A85-19321

GAMMA RAYS

- Airborne snow water equivalent and soil moisture measurement using natural terrestrial gamma radiation p 43 A85-25352

GEOBOTANY

- Experimental evidence for spring and autumn windows for the detection of geobotanical anomalies through the remote sensing of overlying vegetation p 6 A85-26939
- The importance of geobotany in geological remote sensing applications p 23 A85-27948

GEOCHRONOLOGY

- Post-carboniferous tectonics in the Anadarko Basin, Oklahoma Evidence from side-looking radar imagery [NASA-CR-175458] p 26 A85-19498

GEODESY

- Altimetry, orbits and tides [E85-10066] p 40 A85-17404
- Mathematical aspects of digital terrain information, Report from International Society for Photogrammetry and Remote Sensing (ISPRS) working group 3 3, 1980 - 1984 --- photogrammetry p 19 A85-17407
- Using the global positioning system (GPS) phase observable for relative geodesy Modeling, processing, and results p 19 A85-18437
- Activities report of the Department of Applied Research 78 for satellite geodesy of the Technical University, Munich [ASTRON-GEODAET-ARB-45] p 19 A85-18440
- Geodetic accuracy of LANDSAT 4 Multispectral Scanner and Thematic Mapper data --- Washington, DC, California, Alabama, South Dakota, and Illinois p 53 A85-20504
- Geometric accuracy assessment of LANDSAT-4 Multispectral Scanner (MSS) data p 19 A85-20505
- Hybrid method of mapping and photogeodetic control network densification [PB85-133775] p 20 A85-21766

GEODETTIC ACCURACY

- Minimization of the effect of the earth's curvature in the projective transformation of space images into photoplans and photomaps p 16 A85-25662

GEODETTIC SURVEYS

- Hybrid method of mapping and photogeodetic control network densification [PB85-133775] p 20 A85-21766
- Planetary cartography in the next decade (1984 - 1994) [NASA-SP-475] p 20 A85-22323

GEODYNAMICS

- The participation of the Netherlands in the NASA Crustal Dynamics Project p 15 A85-20035
- Satellite magnetic anomalies over subduction zones - The Aleutian Arc anomaly p 16 A85-21107
- Activities report of the Department of Applied Research 78 for satellite geodesy of the Technical University, Munich [ASTRON-GEODAET-ARB-45] p 19 A85-18440

GEOGRAPHIC INFORMATION SYSTEMS

- Study on a regional geographical information system and application model p 13 A85-20644
- MASMAP, design for a project-oriented geo-information program package for urban upgrading schemes p 13 A85-20747
- Building a functional, integrated GIS/remote sensing resource analysis and planning system --- Utah [E85-10092] p 15 A85-21754

GEOGRAPHY

- Inventory of geographically homogeneous zones by spectral modeling of diachronic Meteosat albedo or combined albedo/thermal-channel data - Applications to the Maghreb and to Sahelian Africa p 46 A85-23769
- The sharing of remote sensing techniques in Brazilian geographic research [INPE-3307-PRE/617] p 15 A85-19502

GEOIDS

- The altimetric geoid in the North Sea p 16 A85-23700
- Use of ocean skewness measurements in calculating the accuracy of altimeter height measurements p 30 A85-23703
- Cosmic interpolation of terrestrial potential values p 18 A85-26476
- On the determination of the deflection of the vertical by satellite altimetry --- for marine geoid height estimates p 37 A85-29706

- Altimetry, orbits and tides [E85-10066] p 40 A85-17404

GEOLOGICAL FAULTS

- Analysis of SIR-B radar illumination of geometry for depth of penetration and surface feature and vegetation detection, Nevada and California p 25 A85-17248

- SIR-A imagery in geologic studies of the Sierra Madre Oriental, northeastern Mexico Part 1 (Regional stratigraphy) The use of morphostratigraphic units in remote sensing mapping [NASA-CR-175457] p 25 A85-19497
- Post-carboniferous tectonics in the Anadarko Basin, Oklahoma Evidence from side-looking radar imagery [NASA-CR-175458] p 26 A85-19498

GEOLOGICAL SURVEYS

- Neotectonics of the Caribbean Thermal-inertia mapping from space p 27 A85-21145
- Classification of the geological environments of Anticosti Island - An approach using a Landsat-4 spectral simulation p 21 A85-23790
- Frontiers for geological remote sensing from space, Geosat Workshop, 4th, Flagstaff, AZ, June 12-17, 1983, Report p 22 A85-27943
- Space remote-sensing data in geology --- Russian book p 23 A85-28400
- Prospecting from the skies p 23 A85-29405
- Identification of homogeneous regions with incomplete boundaries on an image p 24 A85-29912
- Image-scale and look-direction effects on the detectability of lineaments in radar images p 24 A85-30087
- Integrated analysis of remote sensing products from basic geological surveys --- Brazil [E85-10052] p 24 A85-16248
- LANDSAT 4 investigations of Thematic Mapper and Multispectral Scanner applications --- Drum Mountains, Utah and Tonopah, Nevada [E85-10095] p 26 A85-21757

GEOLOGY

- Evaluation of SIR-B imagery for geologic and geomorphic mapping, hydrology, and oceanography in Australia p 51 A85-17229

GEOMAGNETISM

- Satellite magnetic anomalies over subduction zones - The Aleutian Arc anomaly p 16 A85-21107
- Mathematical modelling of the geomagnetic field and secular variation, and its applications, Proceedings of the Symposium, Hamburg, West Germany, August 15-27, 1983 p 16 A85-25689
- Introduction to the special issue - A perspective on Magsat results p 16 A85-26401
- The near-earth magnetic field at 1980 determined from Magsat data p 16 A85-26408
- A review of problems and progress in studies of satellite magnetic anomalies p 17 A85-26409
- Mean ionospheric field correction for Magsat data p 17 A85-26411
- On the identification of Magsat anomaly charts as crustal part of the internal field p 17 A85-26412
- Comparison between the recent US composite magnetic anomaly map and Magsat anomaly data p 17 A85-26413
- Seafloor spreading anomalies in the Magsat field of the North Atlantic p 17 A85-26415
- Magsat scalar magnetic anomalies at northern high latitudes p 18 A85-26416
- Scalar magnetic anomalies of Canada and northern United States derived from Magsat data p 18 A85-26418
- Extraction of magnetic anomalies of crustal origin from Magsat data over the area of the Japanese Islands p 21 A85-26419
- A comparison between GEOS 1 magnetic-field measurements and some models of the geomagnetic field p 18 A85-27386
- Estimation of lower crust magnetization from satellite derived anomaly field p 18 A85-28012
- Research on ocean floor electrical surveys [AD-A149831] p 42 A85-21920

GEOMETRIC ACCURACY

- Canadian plans for Thematic Mapper data p 54 A85-20513
- LANDSAT-4 Science Characterization Early Results Volume 3, part 2 Thematic Mapper (TM) [E85-10069] p 67 A85-21724
- A preliminary assessment of LANDSAT-4 Thematic Mapper data --- Windsor, Ontario and Medicine Hat areas, Canada p 54 A85-21728
- TM geometric performance Line to Line Displacement Analysis (LLDA) --- New Mexico p 68 A85-21732
- A preliminary evaluation of LANDSAT-4 Thematic Mapper data for their geometric and radiometric accuracies p 54 A85-21739

GEOMETRIC RECTIFICATION (IMAGERY)

- Minimization of the effect of the earth's curvature in the projective transformation of space images into photoplans and photomaps p 16 A85-25662
- Evaluation of aircraft MSS analytical block adjustment p 49 A85-26641

- Rectification of single and multiple frames of satellite scanner imagery using points and edges as control p 51 A85-16263

- The influence of the number of ground control points on the scene-to-map registration accuracy --- Kansas, Louisiana, Mississippi, and Missouri p 51 A85-16264
- Analysis of the quality of image data required by the LANDSAT-4 Thematic Mapper and Multispectral Scanner --- agricultural and forest cover types in California [E85-10074] p 11 A85-19488

- Summary of MSS characterization investigations p 53 A85-20497
- Radiometric calibration and geocoded precision processing of LANDSAT-4 Multispectral Scanner products by the Canada Centre for Remote Sensing p 53 A85-20501

- Geometric accuracy of LANDSAT-4 MSS image data p 53 A85-20503

- Geometric accuracy assessment of LANDSAT-4 Multispectral Scanner (MSS) data p 19 A85-20505
- LS-4 MSS geometric correction Methods and results p 53 A85-20507

- An overview of the Thematic Mapper geometric correction system p 53 A85-20511

GEOMORPHOLOGY

- Geomorphology and remote sensing Numerical inventory of objects in Landsat, SPOT simulation, and SIR-A data Applications to the Mopti-Bandiagara (Mali) region p 21 A85-23785
- United States crustal thickness p 18 A85-28011
- The use of Salyut-5 photographs for regional geomorphological mapping p 23 A85-28999
- Tectonic, volcanic, and climatic geomorphology study of the Sierras Pampeanas Andes, northwestern Argentina p 24 A85-17215
- Geological, structural, and geomorphological analyses from SIR-B p 24 A85-17226
- Interlobate comparison of glacial-depositional style as evidenced by small-relief glacial landscape features in Illinois, Indiana, and Ohio, utilizing SIR-B p 39 A85-17231

- Evaluation of the L-band scattering characteristics of volcanic terrain in aid of lithologic identification, assessment of SIR-B calibration, and development of planetary geomorphic analogs p 24 A85-17232

- Assessment of LANDSAT for rangeland mapping, Rush Valley, Utah [E85-10072] p 15 A85-19486

- An integrated GIS/remote sensing data base in North Cache soil conservation district, Utah A pilot project for the Utah Department of Agriculture's RIMS (Resource Inventory and Monitoring System) [E85-10073] p 11 A85-19487

- Nautical charting with remotely sensed imagery, volume 1 [AD-A149361] p 41 A85-19503

- Nautical charting with remotely sensed imagery Volume 2 Case studies [AD-A149362] p 41 A85-19504

GEOPHYSICS

- Mathematical modelling of the geomagnetic field and secular variation, and its applications, Proceedings of the Symposium, Hamburg, West Germany, August 15-27, 1983 p 16 A85-25689
- MIZEX (Marginal Ice Zone Program) A program for mesoscale air-ice-ocean interaction experiments in Arctic marginal ice zones 5 MIZEX 84 Summer experiment PI (Principal Investigator) preliminary reports [AD-A148986] p 41 A85-19594

GEOPOTENTIAL

- Methods of space geodesy and its role in earth studies p 19 A85-30013

GEORGIA

- Geometric accuracy of LANDSAT-4 MSS image data p 53 A85-20503

GEOS 1 SATELLITE

- A comparison between GEOS 1 magnetic-field measurements and some models of the geomagnetic field p 18 A85-27386

GLACIAL DRIFT

- Mapping of glacial landforms from Seasat radar images p 36 A85-28027

GLACIOLOGY

- Interlobate comparison of glacial-depositional style as evidenced by small-relief glacial landscape features in Illinois, Indiana, and Ohio, utilizing SIR-B p 39 A85-17231

GLOBAL POSITIONING SYSTEM

- Using the global positioning system (GPS) phase observable for relative geodesy Modeling, processing, and results p 19 A85-18437
- Hybrid method of mapping and photogeodetic control network densification [PB85-133775] p 20 A85-21766

GLOBAL CLUSTERS

The secular period behavior of 38 RR Lyrae stars in the LMC globular cluster NGC 2257 p 14 A85-25070

GOES SATELLITES

The space environment monitors onboard GOES [AIAA PAPER 85-0238] p 55 A85-19608
The U.S. civil operational remote sensing program opportunities for the present and future p 71 A85-20641

On the separability of various classes from the GOES visible and infrared data --- of winter cloud and snow cover p 45 A85-21138

GOES 2

An intercalibration of Meteosat-1 and GOES-2 visible and infrared measurements p 26 A85-19420

GRAPHS (CHARTS)

Atlas of the Beaufort Sea [AD-A149545] p 41 N85-20619

GRAVIMETRY

Gravity field investigation in the North Sea p 30 A85-23699

GRAVITATIONAL FIELDS

Gravity field investigation in the North Sea p 30 A85-23699
Cosmic interpolation of terrestrial potential values p 18 A85-26476

GRAVITY WAVES

The interpretation of SIR-B imagery of surface waves and other oceanographic features using in-situ, meteorological satellite, and infrared satellite data p 39 N85-17212

GREENLAND

Airborne microwave measurements of the southern Greenland ice sheet p 28 A85-23644

GROUND STATIONS

Brazilian remote sensing receiving, recording and processing ground systems in the 1980's [E85-10079] p 52 N85-19493
The spot operational remote sensing satellite system Current status and perspectives p 67 N85-20776

GROUND TRUTH

Development of a SPOT-simulation radiometer p 57 A85-23759
Exploring the use of structural models to improve remote sensing agricultural estimates p 9 N85-16259
The influence of the number of ground control points on the scene-to-map registration accuracy --- Kansas, Louisiana, Mississippi, and Missouri p 51 N85-16264
Ground truth for SIR-B images obtained by SIR system 8 impulse radar p 10 N85-17251
Spectroradiometric calibration of the Thematic Mapper and Multispectral Scanner system [E85-10077] p 64 N85-19491
Preliminary evaluation of the airborne imaging spectrometer for vegetation analysis [NASA-CR-174440] p 12 N85-19496

GROWTH

User's guide to the TAMW wheat model as implemented on the IBM 360/195 computer [E85-10084] p 12 N85-21749

GULF STREAM

Abyssal eddies near the Gulf Stream p 34 A85-27701

H

HARMONIC ANALYSIS

Magsat vertical field anomalies above 40 deg N from spherical cap harmonic analysis p 18 A85-26417

HEAT BALANCE

Evaluation of the ocean/atmosphere thermal interaction in the Atlantic FGGE area p 28 A85-22175

HEAT CAPACITY MAPPING MISSION

Thermal-inertia mapping from space p 21 A85-23766
Use of HCMM thermal images in the study of microclimates in a mountainous region p 3 A85-23771

Generation of a Landsat-HCMM combined image and its application to geological cartography p 21 A85-23792

HIERARCHIES

Evidence accumulation for spatial reasoning p 50 N85-16261

HIGH RESOLUTION

An automatic high-resolution picture transmission receiving station p 61 A85-27698

HIGH RESOLUTION COVERAGE ANTENNAS

Information for space radar designers Required dynamic range vs resolution and antenna calibration using the Amazon rain forest p 44 N85-17239

HUMIDITY

Determination of monthly mean humidity in the atmospheric surface layer over oceans from satellite data p 35 A85-28007

HYDROGEOLOGY

Deforestation, floodplain dynamics, and carbon biogeochemistry in the Amazon Basin p 44 N85-17216

HYDROGRAPHY

Nautical charting with remotely sensed imagery, volume 1 [AD-A149361] p 41 N85-19503
Nautical charting with remotely sensed imagery Volume 2 Case studies [AD-A149362] p 41 N85-19504

HYDROLOGY

Influence of spatial variability of soil hydraulic characteristics on surface parameters obtained from remote-sensing data in thermal infrared and microwaves p 43 A85-23786

Detection of lowland flooding using active microwave systems p 43 A85-29218

Determination of water surfaces in northwest Bohemia on the basis of satellite data p 44 A85-29906

Evaluation of SIR-B imagery for geologic and geomorphic mapping, hydrology, and oceanography in Australia p 51 N85-17229

HYDROMETEOROLOGY

Satellite passive microwave rain rate measurement over croplands during spring, summer and fall p 4 A85-25181

ICE

MIZEX (Marginal Ice Zone Program) A program for mesoscale air-ice-ocean interaction experiments in Arctic marginal ice zones 5 MIZEX 84 Summer experiment PI (Principal Investigator) preliminary reports [AD-A148986] p 41 N85-19594
Lake ice occurrence as a possible detector of atmospheric CO2 effects on climate [DE85-002951] p 45 N85-20606

ICE ENVIRONMENTS

Landsat-4 thematic mapper (TM) for cold environments p 60 A85-25349

ICE MAPPING

Airborne microwave measurements of the southern Greenland ice sheet p 28 A85-23644
Performance of an airborne imaging 92/183 GHz radiometer during the Bering Sea Marginal Ice Zone Experiment (MIZEX-WEST) p 33 A85-24945
Determination of the physical parameters of sea ice on the basis of remote microwave measurements in the 0.3-18 cm range p 38 A85-29903

ICE REPORTING

Complex studies of the environment by optical and radar methods p 56 A85-20081
An algorithm to measure sea ice concentration with microwave radiometers p 27 A85-20492
Ultrashort-wave radar subsurface sounding of sea ice and earth covers p 34 A85-25594
Improvement of the accuracy of radar measurements of sea-ice thickness by cepstral processing of reflected signals p 35 A85-27736
Satellite observations of sea ice p 36 A85-28022
Data report on variations in the composition of sea ice during MIZEX-East'83 with the Nimbus-7 SMMR [NASA-TM-86170] p 40 N85-18443

ILLINOIS

Interlobate comparison of glacial-depositional style as evidenced by small-relief glacial landscape features in Illinois, Indiana, and Ohio, utilizing SIR-B p 39 N85-17231

Geodetic accuracy of LANDSAT 4 Multispectral Scanner and Thematic Mapper data --- Washington, DC, California, Alabama, South Dakota, and Illinois p 53 N85-20504

Evaluation of the radiometric quality of the TM data using clustering, linear transformations and multispectral distance measures --- Illinois p 54 N85-21731

IMAGE ANALYSIS

Method for sequential analysis of spatial development in a rural-urban fringe zone p 13 A85-20748
Separating clouds from ocean in infrared images p 28 A85-22423

The measurement of bidirectional reflectances by analysis of Landsat images p 2 A85-23756

Classification of vegetation types by analysis of X-band and C-band radar images p 4 A85-23775

Regional analysis from data from heterogeneous pixels - Remote sensing of total dry matter production in the Senegalese Sahel p 47 A85-23783

Independent variables in remote sensing as a function of landcover type p 47 A85-23788

Generation of a Landsat-HCMM combined image and its application to geological cartography p 21 A85-23792

Resource measurement system p 47 A85-24258

The influence of satellite spectral sensor response on the analysis of satellite imagery at high latitudes p 60 A85-26927

Thematic mapper data analysis p 23 A85-27946

Investigation of the properties of natural objects by the canonical-correlation method p 49 A85-28973

Identification of homogeneous regions with incomplete boundaries on an image p 24 A85-29912

Integrated analysis of remote sensing products from basic geological surveys --- Brazil [E85-10052] p 24 N85-16248

LANDSAT-4 Thematic Mapper Modulation Transfer Function (MTF) evaluation --- California and New Mexico [E85-10055] p 62 N85-16250

Proceedings of the Second Annual Symposium on Mathematical Pattern Recognition and Image Analysis Program [E85-10056] p 50 N85-16251

Estimating location parameters in a mixture p 50 N85-16252

Nonparametric analysis of Minnesota spruce and aspen tree data and LANDSAT data p 8 N85-16253

Texture classification using autoregressive filtering p 50 N85-16254

Bayesian estimation of normal mixture parameters p 50 N85-16255

Spatial estimation from remotely sensed data via empirical Bayes models p 8 N85-16256

Evidence accumulation for spatial reasoning p 50 N85-16261

Power spectral density of markov texture fields p 50 N85-16262

Rectification of single and multiple frames of satellite scanner imagery using points and edges as control p 51 N85-16263

The influence of the number of ground control points on the scene-to-map registration accuracy --- Kansas, Louisiana, Mississippi, and Missouri p 51 N85-16264

Image variance and spatial structure in remotely sensed scenes --- South Dakota, California, Missouri, Kentucky, Louisiana, Tennessee, District of Columbia, and Oregon p 51 N85-16265

Image-to-image correspondence Linear structure matching p 51 N85-16266

The interpretation of SIR-B imagery of surface waves and other oceanographic features using in-situ, meteorological satellite, and infrared satellite data p 39 N85-17212

Analysis of the quality of image data required by the LANDSAT-4 Thematic Mapper and Multispectral Scanner --- agricultural and forest cover types in California [E85-10074] p 11 N85-19488

Study of spectral/radiometric characteristics of the Thematic Mapper for land use applications [E85-10075] p 64 N85-19489

Geodetic accuracy of LANDSAT 4 Multispectral Scanner and Thematic Mapper data --- Washington, DC, California, Alabama, South Dakota, and Illinois p 53 N85-20504

Geometric accuracy assessment of LANDSAT-4 Multispectral Scanner (MSS) data p 19 N85-20505

Canadian plans for Thematic Mapper data p 54 N85-20513

The use of linear feature detection to investigate Thematic Mapper data performance and processing p 69 N85-21740

IMAGE ENHANCEMENT

Integration of the SPOT panchromatic channel into its multispectral mode for image sharpness enhancement p 49 A85-29217

Information extraction and transmission techniques for spaceborne synthetic aperture radar images [NASA-CR-174341] p 52 N85-17256

Resolution enhancement of multichannel microwave imagery from the Nimbus-7 SMMR for maritime rainfall analysis [NASA-CR-174367] p 44 N85-19221

IMAGE PROCESSING

Microcomputer systems for satellite image processing p 56 A85-20571

Remote sensing development in the People's Republic of China p 56 A85-20643

Automatic production of DTM data using digital off-line technique --- Digital Terrain Modelling p 45 A85-20750

Evaluation of an experimental system for spaceborne processing of multispectral image data p 46 A85-23144

Visual interpretation of SAR images of two areas in the Netherlands p 1 A85-23694

Use of satellite data in agricultural surveys p 4 A85-23782

Resource measurement system p 47 A85-24258

Interpretation of space images of the sea surface using the SVIT digital-processing complex p 34 A85-25654

Features of the digital processing of radar images obtained with the sidelooking radar of the Cosmos-1500 satellite p 48 A85-25660

Digital correlation of images along quasi-epipolar lines by successive approximations p 48 A85-25671

The effects of image noise on digital correlation probability p 49 A85-29221

Characterizing the scientific potential of satellite sensors --- San Francisco, California p 62 N85-16244 [E85-10044]

Integrated analysis of remote sensing products from basic geological surveys --- Brazil p 24 N85-16248 [E85-10052]

Enhancement of multispectral scanner images by digital filtering p 63 N85-16284 [ESA-TT-624]

Development and evaluation of techniques for using combined microwave and optical image data for vegetation studies p 9 N85-17240

Automatic terrain elevation mapping and registration p 52 N85-17242

Analysis of SIR-B radar illumination of geometry for depth of penetration and surface feature and vegetation detection, Nevada and California p 25 N85-17248

Information extraction and transmission techniques for spaceborne synthetic aperture radar images [NASA-CR-174341] p 52 N85-17256

Interactive digital image processing for terrain data extraction p 52 N85-17417 [AD-A148580]

An aural X-ray imaging spectrometer p 64 N85-17469 [AD-A147756]

LANDSAT 4 investigation of Thematic Mapper and Multispectral Scanner applications p 52 N85-19490 [E85-10076]

Thematic Mapper Design through flight evaluation p 64 N85-19492 [E85-10078]

LS-4 MSS geometric correction Methods and results p 53 N85-20507

An overview of LANDSAT-4 and the Thematic Mapper p 66 N85-20509

TM digital image products for applications p 54 N85-20512

Characterization of radiometric calibration of LANDSAT-4 reflective bands p 66 N85-20516

Relative radiometric calibration of LANDSAT TM reflective bands p 67 N85-21725

Preliminary evaluation of the radiometric calibration of LANDSAT-4 Thematic Mapper data by the Canada Centre for Remote Sensing p 67 N85-21729

The use of linear feature detection to investigate Thematic Mapper data performance and processing p 69 N85-21740

The development of image processing of NOAA AVHRR data and its application to sea surface temperature p 42 N85-21891

IMAGE RECONSTRUCTION

Multispectral data compression using staggered detector arrays p 47 A85-24277

IMAGE RESOLUTION

The influence of a scattering medium on the quality of an optical image p 48 A85-26294

Integration of the SPOT panchromatic channel into its multispectral mode for image sharpness enhancement p 49 A85-29217

Resolution enhancement of multichannel microwave imagery from the Nimbus-7 SMMR for maritime rainfall analysis [NASA-CR-174367] p 44 N85-19221

LANDSAT-4 Science Characterization Early Results Volume 3, part 2 Thematic Mapper (TM) [E85-10069] p 67 N85-21724

TM geometric performance Line to Line Displacement Analysis (LLDA) --- New Mexico p 68 N85-21732

A preliminary evaluation of LANDSAT-4 Thematic Mapper data for their geometric and radiometric accuracies p 54 N85-21739

IMAGERY

Image variance and spatial structure in remotely sensed scenes --- South Dakota, California, Missouri, Kentucky, Louisiana, Tennessee, District of Columbia, and Oregon p 51 N85-16265

Analysis of subpixel registration p 51 N85-16267

IMAGES

Development and evaluation of techniques for using combined microwave and optical image data for vegetation studies p 9 N85-17240

IMAGING TECHNIQUES

Synthetic apertures - An overview p 57 A85-22711

Imaging ocean surface waves by synthetic aperture radar - A review p 29 A85-23682

Image-to-image correspondence Linear structure matching p 51 N85-16266

Application and calibration of the subsurface mapping capability of SIR-B in desert regions p 25 N85-17244

Airborne remote sensing CCD imaging system p 65 N85-20220

IMPERIAL VALLEY (CA)

Investigation of radiometric properties of LANDSAT-4 MSS --- California, North Carolina, South Carolina, and New England p 65 N85-20500

INCIDENCE

Investigation of SIR-B images for lithologic mapping p 25 N85-17241

Australian Multiexperimental Assessment of SIR-B (AMAS) p 52 N85-17243

INCOHERENT SCATTERING

Surface scattering effects at different spectral regions p 58 A85-23780

INDIANA

Interlobate comparison of glacial-depositional style as evidenced by small-relief glacial landscape features in Illinois, Indiana, and Ohio, utilizing SIR-B p 39 N85-17231

INFORMATION DISSEMINATION

Education and training in satellite remote sensing applications - Guide to education and training opportunities p 71 A85-20640

INFORMATION SYSTEMS

The U S civil operational remote sensing program opportunities for the present and future p 71 A85-20641

Commercialization of remote sensing data - Its impact on the continuity and accessibility of remote sensing data, including response to standing orders as well as on the standardization of products p 71 A85-20642

Status of remote sensing information systems with special emphasis on their specializations, capabilities, accessibilities and future directions p 71 A85-20646

Sourcebook Gaining access to US government information on the environment and natural resources [DE84-017419] p 71 N85-20941

INFORMATION THEORY

Study of spectral/radiometric characteristics of the Thematic Mapper for land use applications [E85-10057] p 62 N85-16268

INFRARED IMAGERY

Analysis of ACIR transparencies of citrus trees with a projecting spectral densitometer --- Aerial Color IR p 1 A85-21050

On the separability of various classes from the GOES visible and infrared data --- of winter cloud and snow cover p 45 A85-21138

Separating clouds from ocean in infrared images p 28 A85-22423

Comparison of modelled and empirical atmospheric propagation data p 46 A85-22678

Study of the correlation between the IRT band of the NOAA AVHRR and the factors conditioning the thermal behavior of bioclimatic areas on a regional scale p 58 A85-23768

Dramatic contrast between low clouds and snow cover in daytime 3.7 micron imagery p 48 A85-24740

Double-angle method for measuring ocean surface temperature in the infrared p 34 A85-25658

Soil slaking and the possibilities to record with infrared line scanning p 5 A85-26936

An integrated remote sensing approach for identifying ecological range sites --- Parker Mountain [E85-10050] p 8 N85-16246

The interpretation of SIR-B imagery of surface waves and other oceanographic features using in-situ, meteorological satellite, and infrared satellite data p 39 N85-17212

Evaluation of the radar response to land surfaces and volumes Examination of theoretical models, target statistics, and applications p 63 N85-17250

LANDSAT 4 band 6 data evaluation [E85-10093] p 55 N85-21755

INFRARED INSTRUMENTS

An airborne infrared thermal scanning system for easy use on Navy P-3 aircraft [AD-A149690] p 42 N85-22143

INFRARED LASERS

Automated measurements of terrain reflection and height variations using an airborne infrared laser system p 5 A85-26933

INFRARED RADIATION

Variation in spectral response of soybeans with respect to illumination, view, and canopy geometry [E85-10040] p 8 N85-16241

INFRARED RADIOMETERS

An intercalibration of Meteosat-1 and GOES-2 visible and infrared measurements p 26 A85-19420

Study of the correlation between the IRT band of the NOAA AVHRR and the factors conditioning the thermal behavior of bioclimatic areas on a regional scale p 58 A85-23768

Interpretation of thermal infrared data to augment spectral signatures p 47 A85-23791

Thermal structure of an agricultural region as seen by NOAA-7 AVHRR p 7 A85-30090

INFRARED SCANNERS

The Thematic Mapper - Instrument overview and preliminary on-orbit results p 56 A85-22681

Large scan mirror assembly of the new Thematic Mapper developed for Landsat 4 earth resources satellite p 56 A85-22682

Satellite measurements of sea-surface temperature for climate research p 32 A85-24555

Satellite sea surface temperature determination from microwave and infrared radiometry p 33 A85-24556

Developments with multispectral thermal-IR and active microwave systems - TMS, SIR-A, SIR-B, and radarsat p 62 A85-27947

An airborne infrared thermal scanning system for easy use on Navy P-3 aircraft [AD-A149690] p 42 N85-22143

INFRARED SIGNATURES

Spectral signatures of soil, snow and sea ice as observed by passive microwave and thermal infrared techniques p 58 A85-23784

INFRARED SPECTRA

Spectral response of different agricultural and penurban land-use units in the spectral windows at 1.55-1.75 and 2.08-2.35 microns p 4 A85-23787

Thermal band characterization of the LANDSAT-4 Thematic Mapper p 67 N85-21727

INFRARED SPECTROMETERS

Preliminary evaluation of the airborne imaging spectrometer for vegetation analysis [NASA-CR-174440] p 12 N85-19496

INFRARED SPECTROSCOPY

Near-infrared spectroscopy in geological reconnaissance and exploration p 22 A85-27944

INSTRUMENT COMPENSATION

Electromagnetic bias of 36-GHz radar altimeter measurements of MSL --- Mean Sea Level p 37 A85-29712

INTEGRATED CIRCUITS

Multispectral data compression using staggered detector arrays p 47 A85-24277

INTERNAL WAVES

The investigation of selected oceanographic applications of spaceborne synthetic-aperture radar p 39 N85-17233

The imaging of internal waves by the SEASAT-A synthetic aperture radar [AD-A149808] p 20 N85-21761

INTERNATIONAL COOPERATION

The participation of the Netherlands in the NASA Coastal Dynamics Project p 15 A85-20035

International cooperation in remote sensing applications p 70 A85-20566

IONOSPHERIC CURRENTS

Mean ionospheric field correction for Magsat data p 17 A85-26411

IOWA

Shortwave infrared detection of vegetation [E85-10064] p 10 N85-17402

Scan angle and detector effects in Thematic Mapper radiometry --- Iowa and Arkansas p 68 N85-21735

Investigation of TM band-to-band registration using the JSC registration processor p 69 N85-21745

IRRIGATION

Effect of heliotropism on the bidirectional reflectance of irrigated cotton p 1 A85-22420

ISLANDS

Satellite photographs suggest arctic volcano p 38 N85-16239

J

JAPAN

Extraction of magnetic anomalies of crustal origin from Magsat data over the area of the Japanese Islands p 21 A85-26419

K

KANSAS

The influence of the number of ground control points on the scene-to-map registration accuracy --- Kansas, Louisiana, Mississippi, and Missouri p 51 N85-16264

KENTUCKY

Image variance and spatial structure in remotely sensed scenes --- South Dakota, California, Missouri, Kentucky, Louisiana, Tennessee, District of Columbia, and Oregon p 51 N85-16265

L

- LAKES**
Lake ice occurrence as a possible detector of atmospheric CO₂ effects on climate [E85-002951] p 45 N85-20606
- LAND**
Earth observations and the polar platform [NOAA-TR-NESDIS-18] p 15 N85-20517
- LAND ICE**
Airborne microwave measurements of the southern Greenland ice sheet p 28 A85-23644
Ice sheet margins and ice shelves p 32 A85-24524
Ultrasort-wave radar subsurface sounding of sea ice and earth covers p 34 A85-25594
- LAND USE**
Seasat over land p 57 A85-23693
Spectral response of different agricultural and penurban land-use units in the spectral windows at 1.55-1.75 and 2.08-2.35 microns p 4 A85-23787
Interpretation of thermal infrared data to augment spectral signatures p 47 A85-23791
The current use of TIROS-N series of meteorological satellites for land-cover studies p 60 A85-26928
Comparison of level I land cover classification accuracy for MSS and AVHRR data --- Advanced Very High Resolution Radiometers p 61 A85-26929
Effect of Landsat Thematic Mapper sensor parameters on land cover classification p 14 A85-30088
Detecting agricultural to urban land use change from multi-temporal MSS digital data --- Salt Lake County, Utah p 15 N85-16245
Calibration or inverse regression Which is appropriate for crop surveys using LANDSAT data? p 9 N85-16260
Study of spectral/radiometric characteristics of the Thematic Mapper for land use applications [E85-10057] p 62 N85-16268
Analysis of data acquired by synthetic aperture radar and LANDSAT Multispectral Scanner over Kershaw County, South Carolina, during the summer season [E85-10071] p 11 N85-19485
Assessment of LANDSAT for rangeland mapping, Rush Valley, Utah [E85-10072] p 15 N85-19486
An integrated GIS/remote sensing data base in North Cache soil conservation district, Utah A pilot project for the Utah Department of Agriculture's RIMS (Resource Inventory and Monitoring System) [E85-10073] p 11 N85-19487
Assessment of the quality of image data required by the LANDSAT-4 Thematic Mapper and Multispectral Scanner --- agricultural and forest cover types in California [E85-10074] p 11 N85-19488
Study of spectral/radiometric characteristics of the Thematic Mapper for land use applications [E85-10075] p 64 N85-19489
Building a functional, integrated GIS/remote sensing resource analysis and planning system --- Utah [E85-10092] p 15 N85-21754
- LANDFORMS**
Mapping of landforms from Landsat imagery - An example from eastern New South Wales, Australia p 21 A85-22422
Mapping of glacial landforms from Seasat radar images p 36 A85-28027
- LANDSAT SATELLITES**
An example of Landsat cost effectiveness in mapping land-cover p 1 A85-20573
Determining stretch parameters for lithologic discrimination on Landsat MSS band-ratio images p 20 A85-21047
Measuring spectra of and lands p 20 A85-21975
Mapping of landforms from Landsat imagery - An example from eastern New South Wales, Australia p 21 A85-22422
The Thematic Mapper - Instrument overview and preliminary on-orbit results p 56 A85-22681
The measurement of bidirectional reflectances by analysis of Landsat images p 2 A85-23756
Experiments concerning radiometric measurements and natural-object indicators in order to apply corrections to recordings of satellite remote sensing p 58 A85-23789
Generation of a Landsat-HCMM combined image and its application to geological cartography p 21 A85-23792
Characteristics of playa deposits as seen on SIR-A, Seasat and Landsat coregistered data p 21 A85-23793
Determination of visual range from Landsat data p 47 A85-24285
EROS main image file - A picture perfect database for Landsat imagery and aerial photography p 48 A85-24521
- Monitoring water quality conditions in a large western reservoir with Landsat imagery p 43 A85-29220
The extension of an invertible coniferous forest canopy reflectance model using SIR-B and LANDSAT data p 10 N85-17246
Assessment of LANDSAT for rangeland mapping, Rush Valley, Utah [E85-10072] p 15 N85-19486
An integrated GIS/remote sensing data base in North Cache soil conservation district, Utah A pilot project for the Utah Department of Agriculture's RIMS (Resource Inventory and Monitoring System) [E85-10073] p 11 N85-19487
- LANDSAT 4**
The U.S. civil operational remote sensing program opportunities for the present and future p 71 A85-20641
Comparison of modelled and empirical atmospheric propagation data p 46 A85-22678
Large scan mirror assembly of the new Thematic Mapper developed for Landsat 4 earth resources satellite p 56 A85-22682
Comparison of SPOT HRV and Landsat-4 TM for crop inventories p 3 A85-23762
Independent variables in remote sensing as a function of landcover type p 47 A85-23788
Classification of the geological environments of Anticosti Island - An approach using a Landsat-4 spectral simulation p 21 A85-23790
Landsat-4 thematic mapper (TM) for cold environments p 60 A85-25349
Thematic mapper data analysis p 23 A85-27946
Study of spectral/radiometric characteristics of the Thematic Mapper for land use applications [E85-10057] p 62 N85-16268
LANDSAT 4 investigation of Thematic Mapper and Multispectral Scanner applications [E85-10076] p 52 N85-19490
Thematic Mapper Design through flight evaluation [E85-10078] p 64 N85-19492
LANDSAT-4 Science Characterization Early Results Volume 1 Multispectral Scanner (MSS) [E85-10067] p 65 N85-20496
Spectral characterization of the LANDSAT-4 MSS sensors p 65 N85-20499
Investigation of radiometric properties of LANDSAT-4 MSS --- California, North Carolina, South Carolina, and New England p 65 N85-20500
LANDSAT scene-to-scene registration accuracy assessment p 65 N85-20502
Geometric accuracy of LANDSAT-4 MSS image data p 53 N85-20503
Impact of LANDSAT MSS sensor differences on change detection analysis --- New Mexico, San Francisco, CA, New Hampshire, and Connecticut p 65 N85-20506
LANDSAT-4 Science Characterization Early Results Volume 2, part 1 Thematic Mapper (TM) [E85-10068] p 66 N85-20508
An overview of LANDSAT-4 and the Thematic Mapper p 66 N85-20509
Radiometric calibration and processing procedure for reflective bands on LANDSAT-4 preflight Thematic Mapper p 66 N85-20510
An overview of the Thematic Mapper geometric correction system p 53 N85-20511
TM digital image products for applications p 54 N85-20512
Spectral characterization of the LANDSAT Thematic Mapper sensors p 66 N85-20514
Prelaunch absolute radiometric calibration of the reflective bands on the LANDSAT-4 preflight Thematic Mapper p 66 N85-20515
LANDSAT-4 Science Characterization Early Results Volume 3, part 2 Thematic Mapper (TM) [E85-10069] p 67 N85-21724
Relative radiometric calibration of LANDSAT TM reflective bands p 67 N85-21725
Evaluation of the radiometric integrity of LANDSAT 4 Thematic Mapper band 6 data p 54 N85-21726
Thermal band characterization of the LANDSAT-4 Thematic Mapper p 67 N85-21727
A preliminary assessment of LANDSAT-4 Thematic Mapper data --- Windsor, Ontario and Medicine Hat areas, Canada p 54 N85-21728
Preliminary evaluation of the radiometric calibration of LANDSAT-4 Thematic Mapper data by the Canada Centre for Remote Sensing p 67 N85-21729
A preliminary analysis of LANDSAT-4 Thematic Mapper radiometric performance p 68 N85-21730
TM geometric performance Line to Line Displacement Analysis (LLDA) --- New Mexico p 68 N85-21732
In-progress absolute radiometric in-flight calibration of the LANDSAT-4 sensors --- New Mexico p 68 N85-21733
LANDSAT-4 Thematic Mapper calibration and atmospheric correction p 68 N85-21734
- MTF analysis of LANDSAT-4 Thematic Mapper p 68 N85-21737
Intraband radiometric performance of the LANDSAT 4 Thematic Mapper --- Washington, DC, Arkansas, Massachusetts, Virginia, and Arizona p 69 N85-21738
A preliminary evaluation of LANDSAT-4 Thematic Mapper data for their geometric and radiometric accuracies p 54 N85-21739
The use of linear feature detection to investigate Thematic Mapper data performance and processing p 69 N85-21740
An analysis of the high frequency vibrations in early Thematic Mapper scenes p 69 N85-21742
Assessment of Thematic Mapper band-to-band registration by the block correlation method p 55 N85-21743
Tests of low-frequency geometric distortions in LANDSAT 4 images p 55 N85-21744
Investigation of TM band-to-band registration using the JSC registration processor p 69 N85-21745
Geometric accuracy of LANDSAT 4 Multispectral Scanner and Thematic Mapper data p 20 N85-21746
LANDSAT 4 band 6 data evaluation [E85-10093] p 55 N85-21755
- LANDSAT 5**
The U.S. civil operational remote sensing program opportunities for the present and future p 71 A85-20641
Study of spectral/radiometric characteristics of the Thematic Mapper for land use applications [E85-10057] p 62 N85-16268
Thematic Mapper Volume 1 Calibration report flight model, LANDSAT 5 [E85-10059] p 63 N85-16270
Thematic Mapper Volume 2 Flight model preshipment review [E85-10060] p 63 N85-16271
LANDSAT 4 investigation of Thematic Mapper and Multispectral Scanner applications [E85-10076] p 52 N85-19490
Spectroradiometric calibration of the Thematic Mapper and Multispectral Scanner system [E85-10077] p 64 N85-19491
Thematic Mapper Design through flight evaluation [E85-10078] p 64 N85-19492
- LASER APPLICATIONS**
Automated measurements of terrain reflection and height variations using an airborne infrared laser system p 5 A85-26933
- LEAVES**
Effect of heliotropism on the bidirectional reflectance of irrigated cotton p 1 A85-22420
Light polarization measurements - A method to determine the specular and diffuse light-scattering properties of both leaves and plant canopies p 2 A85-23754
Comparative study of Suits and SAIL canopy reflectance models p 7 A85-30092
- LIGHT SCATTERING**
Light polarization measurements - A method to determine the specular and diffuse light-scattering properties of both leaves and plant canopies p 2 A85-23754
Surface scattering effects at different spectral regions p 58 A85-23780
The reflection of airborne UV laser pulses from the ocean p 37 A85-29714
- LIMNOLOGY**
Monitoring Africa's Lake Chad basin with Landsat and NOAA satellite data p 43 A85-26930
Determination of water surfaces in northwest Bohemia on the basis of satellite data p 44 A85-29906
- LINEARITY**
Image-to-image correspondence Linear structure matching p 51 N85-16266
- LITHOLOGY**
Determining stretch parameters for lithologic discrimination on Landsat MSS band-ratio images p 20 A85-21047
Evaluation of the L-band scattering characteristics of volcanic terrain in aid of lithologic identification, assessment of SIR-B calibration, and development of planetary geomorphic analogs p 24 N85-17232
Investigation of SIR-B images for lithologic mapping p 25 N85-17241
LANDSAT 4 investigations of Thematic Mapper and Multispectral Scanner applications --- Drum Mountains, Utah and Tonopah, Nevada [E85-10095] p 26 N85-21757
- LITHOSPHERE**
Intermediate-wavelength magnetic anomaly field of the North Pacific and possible source distributions p 17 A85-26414

LOCUSTS

The potential of satellite remote sensing of ecological conditions for survey and forecasting desert-locust activity p 5 A85-26934

LOOK ANGLES (TRACKING)

Angular and spatial variability of visible and NIR spectral data p 2 A85-23752
Terrain and look angle effects upon multispectral scanner response p 60 A85-26642

LOUISIANA

The influence of the number of ground control points on the scene-to-map registration accuracy --- Kansas, Louisiana, Mississippi, and Missouri p 51 N85-16264
Image variance and spatial structure in remotely sensed scenes --- South Dakota, California, Missouri, Kentucky, Louisiana, Tennessee, District of Columbia, and Oregon p 51 N85-16265

LOW PASS FILTERS

An airborne infrared thermal scanning system for easy use on Navy P-3 aircraft [AD-A149690] p 42 N85-22143

LOW TEMPERATURE ENVIRONMENTS

Optical engineering for cold environments, Proceedings of the Meeting, Arlington, VA, April 7, 8, 1983 p 59 A85-25344

LUMINOSITY

The influence of a scattering medium on the quality of an optical image p 48 A85-26294

M

MAGNETIC ANOMALIES

Satellite magnetic anomalies over subduction zones - The Aleutian Arc anomaly p 16 A85-21107
The near-earth magnetic field at 1980 determined from Magsat data p 16 A85-26408
A review of problems and progress in studies of satellite magnetic anomalies p 17 A85-26409
On the identification of Magsat anomaly charts as crustal part of the internal field p 17 A85-26412
Comparison between the recent U.S. composite magnetic anomaly map and Magsat anomaly data p 17 A85-26413
Intermediate-wavelength magnetic anomaly field of the North Pacific and possible source distributions p 17 A85-26414

Seafloor spreading anomalies in the Magsat field of the North Atlantic p 17 A85-26415
Magsat scalar magnetic anomalies at northern high latitudes p 18 A85-26416
Magsat vertical field anomalies above 40 deg N from spherical cap harmonic analysis p 18 A85-26417
Scalar magnetic anomalies of Canada and northern United States derived from Magsat data p 18 A85-26418

Extraction of magnetic anomalies of crustal origin from Magsat data over the area of the Japanese Islands p 21 A85-26419

An estimation of continental crust magnetization and susceptibility from Magsat data for the conterminous United States p 22 A85-26420
Crustal structure of the Churchill-Superior boundary zone between 80 and 98 deg W longitude from Magsat anomaly maps and stacked passes p 22 A85-26421
Magsat and POGO magnetic anomalies over the Lord Howe Rise Evidence against a simple continental crustal structure p 18 A85-26422
Viscous remanent magnetization model for the Broken Ridge satellite magnetic anomaly p 22 A85-26423
Estimation of lower crust magnetization from satellite derived anomaly field p 18 A85-28012

Mean ionospheric field correction for Magsat data p 17 A85-26411

MAGNETIC DISTURBANCES

Mean ionospheric field correction for Magsat data p 17 A85-26411

MAGNETIC FIELDS

The near-earth magnetic field at 1980 determined from Magsat data p 16 A85-26408

MAGNETIC MEASUREMENT

A comparison between GEOS 1 magnetic-field measurements and some models of the geomagnetic field p 18 A85-27386

MAGNETIC SIGNATURES

Crustal structure of the Churchill-Superior boundary zone between 80 and 98 deg W longitude from Magsat anomaly maps and stacked passes p 22 A85-26421

MAGNETIC SURVEYS

Intermediate-wavelength magnetic anomaly field of the North Pacific and possible source distributions p 17 A85-26414

MAGNETIC VARIATIONS

Mathematical modelling of the geomagnetic field and secular variation, and its applications, Proceedings of the Symposium, Hamburg, West Germany, August 15-27, 1983 p 16 A85-25689

MAGNETIZATION

An estimation of continental crust magnetization and susceptibility from Magsat data for the conterminous United States p 22 A85-26420
Estimation of lower crust magnetization from satellite derived anomaly field p 18 A85-28012

MAGNETOSPHERE

A comparison between GEOS 1 magnetic-field measurements and some models of the geomagnetic field p 18 A85-27386

MAGSAT SATELLITES

Introduction to the special issue - A perspective on Magsat results p 16 A85-26401
A review of problems and progress in studies of satellite magnetic anomalies p 17 A85-26409
Mean ionospheric field correction for Magsat data p 17 A85-26411

On the identification of Magsat anomaly charts as crustal part of the internal field p 17 A85-26412
Comparison between the recent U.S. composite magnetic anomaly map and Magsat anomaly data p 17 A85-26413

Seafloor spreading anomalies in the Magsat field of the North Atlantic p 17 A85-26415
Magsat scalar magnetic anomalies at northern high latitudes p 18 A85-26416

Magsat vertical field anomalies above 40 deg N from spherical cap harmonic analysis p 18 A85-26417
Scalar magnetic anomalies of Canada and northern United States derived from Magsat data p 18 A85-26418

Extraction of magnetic anomalies of crustal origin from Magsat data over the area of the Japanese Islands p 21 A85-26419

An estimation of continental crust magnetization and susceptibility from Magsat data for the conterminous United States p 22 A85-26420
Crustal structure of the Churchill-Superior boundary zone between 80 and 98 deg W longitude from Magsat anomaly maps and stacked passes p 22 A85-26421
Magsat and POGO magnetic anomalies over the Lord Howe Rise Evidence against a simple continental crustal structure p 18 A85-26422

MAP MATCHING GUIDANCE

SIR-B cartography and stereo topographic mapping p 19 N85-17234

MAPPING

Mapping of landforms from Landsat imagery - An example from eastern New South Wales, Australia p 21 A85-22422

American Congress on Surveying and Mapping and American Society of Photogrammetry, Fall Convention, Salt Lake City, UT, September 19-23, 1983, Technical Papers p 14 A85-24950

SIR-B cartography and stereo topographic mapping p 19 N85-17234

Application and calibration of the subsurface mapping capability of SIR-B in desert regions p 25 N85-17244
Analysis of SIR-B radar illumination of geometry for depth of penetration and surface feature and vegetation detection, Nevada and California p 25 N85-17248

Hybrid method of mapping and photogeodetic control network densification [PB85-133775] p 20 N85-21766

MARINE BIOLOGY

Estimating ocean primary production from satellite chlorophyll - Introduction to regional differences and statistics for the Southern California Bight p 35 A85-28005

MARINE ENVIRONMENTS

An algorithm to measure sea ice concentration with microwave radiometers p 27 A85-20492
The use of airborne lasers in terrestrial and water environments p 33 A85-25351

MARINE METEOROLOGY

Evaluation of the ocean/atmosphere thermal interaction in the Atlantic FGGE area p 28 A85-22175
A review of SEASAT --- ocean surface imagery p 28 A85-23677

Determination of monthly mean humidity in the atmospheric surface layer over oceans from satellite data p 35 A85-28007

MARITIME SATELLITES

Large-scale oceanographic experiments and satellites, Proceedings of the Advanced Research Workshop, Porto Vecchio, Corse, France, October 3-7, 1983 p 32 A85-24551

MARKOV PROCESSES

Power spectral density of markov texture fields p 50 N85-16262

MASSACHUSETTS

Intraband radiometric performance of the LANDSAT 4 Thematic Mapper --- Washington, DC, Arkansas, Massachusetts, Virginia, and Arizona p 69 N85-21738

MATHEMATICAL MODELS

The near-earth magnetic field at 1980 determined from Magsat data p 16 A85-26408
Viscous remanent magnetization model for the Broken Ridge satellite magnetic anomaly p 22 A85-26423
Growth/reflection model interface for wheat and corresponding model [E85-10058] p 9 N85-16269

Papers of the 15th International Society for Photogrammetry and Remote Sensing (ISPRS) Congress --- conferences [TRITA-FMI-9] p 63 N85-17406

Mathematical aspects of digital terrain information, Report from International Society for Photogrammetry and Remote Sensing (ISPRS) working group 3 3, 1980 - 1984 --- photogrammetry p 19 N85-17407

A comparative test of photogrammetrically sampled digital elevation models p 52 N85-17408

Multimodels increase accuracy Summary of an experiment --- photogrammetry p 63 N85-17409

User's guide to the TAMW wheat model as implemented on the IBM 360/195 computer [E85-10084] p 12 N85-21749

MAXIMUM LIKELIHOOD ESTIMATES

A computationally-efficient maximum-likelihood classifier employing prior probabilities for remotely-sensed data p 49 A85-26948
Bayesian estimation of normal mixture parameters p 50 N85-16255

MEASURING INSTRUMENTS

The Harp probe - An in situ Bragg scattering sensor p 28 A85-22171

Abyssal eddies near the Gulf Stream p 34 A85-27701

MEDITERRANEAN SEA

Bio-optical variability in the Alboran Sea as assessed by Nimbus-7 coastal zone color scanner [AD-A147909] p 39 N85-16281

MESOSCALE PHENOMENA

A sampling strategy for altimeter measurements of the global statistics of mesoscale eddies p 32 A85-24553
Airborne Doppler estimates of the air motions associated with a developing, sea-breeze induced, mesoscale precipitation line p 36 A85-28783

The use of principal components analysis techniques Nimbus-7 coastal zone color scanner data to define mesoscale ocean features through a warm humid atmosphere [AD-A148567] p 40 N85-17416

A method for determining mesoscale dynamic topography [AD-D011412] p 40 N85-17506

Rain volume estimation over areas using satellite and radar data [NASA-CR-174434] p 44 N85-19568

METEOROLOGICAL PARAMETERS

Study of the correlation between the IRT band of the NOAA AVHRR and the factors conditioning the thermal behavior of bioclimatic areas on a regional scale p 58 A85-23768

Effect of meteorological conditions on the characteristics of space radar images of the earth surface p 48 A85-25653

MIZEX (Marginal Ice Zone Program) A program for mesoscale air-ice-ocean interaction experiments in Arctic marginal ice zones 5 MIZEX 84 Summer experiment PI (Principal Investigator) preliminary reports [AD-A148986] p 41 N85-19594

METEOROLOGICAL RADAR

Airborne Doppler estimates of the air motions associated with a developing, sea-breeze induced, mesoscale precipitation line p 36 A85-28783

Simultaneous ocean cross-section and rainfall measurements from space with a nadir pointing radar p 36 A85-28788

Simultaneous ocean cross-section and rainfall measurements from space with a nadir-pointing radar [NASA-TM-86167] p 44 N85-16273

METEOROLOGICAL SATELLITES

On the application of meteorological satellite imagery for monitoring the environment p 13 A85-20570

Determination of monthly mean humidity in the atmospheric surface layer over oceans from satellite data p 35 A85-28007

Satellite definition of the bio-optical and thermal variation of coastal eddies associated with the African current [AD-A147910] p 39 N85-16282

An auroral X-ray imaging spectrometer [AD-A147756] p 64 N85-17469

METEOSAT SATELLITE

An intercalibration of Meteosat-1 and GOES-2 visible and infrared measurements p 26 A85-19420

Effects of the experimental errors and conditions on the estimation of thermal inertia and evapotranspiration from METEOSAT data p 3 A85-23767

Inventory of geographically homogeneous zones by spectral modeling of diachronic Meteosat albedo or combined albedo/thermal-channel data - Applications to the Maghreb and to Sahelian Africa p 46 A85-23769

MEXICO

SIR-A imagery in geologic studies of the Sierra Madre Oriental, northeastern Mexico Part 1 (Regional stratigraphy) The use of morphostratigraphic units in remote sensing mapping [NASA-CR-175457] p 25 N85-19497

MICROCLIMATOLOGY

Use of HCMM thermal images in the study of microclimates in a mountainous region p 3 A85-23771

MICROCOMPUTERS

Microcomputer systems for satellite image processing p 56 A85-20571

MICROWAVE ATTENUATION

A comparative analysis of some prediction methods for rain attenuation statistics in earth-to-space links p 42 A85-21130

MICROWAVE EMISSION

The evaluation of SMMR retrieval algorithms --- Scanning Multichannel Microwave Radiometer p 31 A85-23706

Microwave properties of vegetation canopies - An overview p 4 A85-23772

Spectral signatures of soil, snow and sea ice as observed by passive microwave and thermal infrared techniques p 58 A85-23784

Data report on variations in the composition of sea ice during MIZEX/East'83 with the Nimbus-7 SMMR [NASA-TM-86170] p 40 N85-18443

MICROWAVE IMAGERY

Airborne microwave measurements of the southern Greenland ice sheet p 28 A85-23644

Satellite microwave remote sensing p 28 A85-23676

The interpretation of SIR-B imagery of surface waves and other oceanographic features using in-situ, meteorological satellite, and infrared satellite data p 39 N85-17212

Microwave and optical remote sensing of forest vegetation p 9 N85-17228

Development and evaluation of techniques for using combined microwave and optical image data for vegetation studies p 9 N85-17240

Automatic terrain elevation mapping and registration p 52 N85-17242

Resolution enhancement of multichannel microwave imagery from the Nimbus-7 SMMR for maritime rainfall analysis [NASA-CR-174367] p 44 N85-19221

Earth resources research using the Shuttle Imaging Radar system p 67 N85-20779

MICROWAVE RADIOMETERS

An algorithm to measure sea ice concentration with microwave radiometers p 27 A85-20492

The scanning multichannel microwave radiometer - An assessment p 57 A85-23705

The evaluation of SMMR retrieval algorithms --- Scanning Multichannel Microwave Radiometer p 31 A85-23706

Simultaneous radiometric and radar altimetric measurements of sea microwave signatures p 31 A85-24076

Radiophysical techniques employed for sea ice investigations p 31 A85-24077

Polarization effects in sea-ice signatures p 31 A85-24078

Microwave signatures of the sea ice in the East Greenland Current p 31 A85-24079

Interpretation of aircraft sea ice microwave data p 32 A85-24080

Retrieval of snow water equivalent from Nimbus-7 SMMR data Effect of land-cover categories and weather conditions p 43 A85-24082

Satellite measurements of sea-surface temperature for climate research p 32 A85-24555

Satellite sea surface temperature determination from microwave and infrared radiometry p 33 A85-24556

Performance of an airborne imaging 92/183 GHz radiometer during the Bering Sea Marginal Ice Zone Experiment (MIZEX-WEST) p 33 A85-24945

Comments on 'Inference of cloud temperature and thickness by microwave radiometry from space' p 59 A85-25182

Determination of the physical parameters of sea ice on the basis of remote microwave measurements in the 0.3-18 cm range p 38 A85-29903

Determination of soil moisture content by microwave radiometry with the use of a priori information p 6 A85-29910

Effect of vegetation on soil moisture sensing observed from orbiting microwave radiometers p 7 A85-30089

Spaceborne microwave radiometers Background and technology requirements [LD-R-267] p 63 N85-17350

MICROWAVE REFLECTOMETERS

Ultraslow-wave radar subsurface sounding of sea ice and earth covers p 34 A85-25594

MICROWAVE SCATTERING

Surface scattering effects at different spectral regions p 58 A85-23780

The effect of a snow cover on microwave backscatter from sea ice p 32 A85-24083

MICROWAVE SENSORS

Microwave properties of vegetation canopies - An overview p 4 A85-23772

Spectral signatures of soil, snow and sea ice as observed by passive microwave and thermal infrared techniques p 58 A85-23784

International Symposium on Microwave Signatures in Remote Sensing, 3rd, Toulouse, France, January 16-20, 1984, Proceedings p 6 A85-26942

The investigation of selected oceanographic applications of spaceborne synthetic-aperture radar p 39 N85-17233

Passive microwave remote sensing for sea ice research [NASA-CR-175570] p 42 N85-21758

MICROWAVE SOUNDING

Advances in microwave remote sensing of the ocean and atmosphere p 28 A85-21960

Satellite passive microwave rain rate measurement over croplands during spring, summer and fall p 4 A85-25181

MINERAL DEPOSITS

Prospecting from the skies p 23 A85-29405

LANDSAT 4 investigations of Thematic Mapper and Multispectral Scanner applications --- Drum Mountains, Utah and Tonopah, Nevada [E85-10095] p 26 N85-21757

MINERAL EXPLORATION

Analysis of mesofractures according to space images - Currents trends in the exploration for oil and gas deposits p 21 A85-25655

Near-infrared spectroscopy in geological reconnaissance and exploration p 22 A85-27944

Analysis of SIR-B radar illumination of geometry for depth of penetration and surface feature and vegetation detection, Nevada and California p 25 N85-17248

MINERALOGY

Imaging systems for the delineation of spectral properties of geologic materials in the visible and near-infrared p 22 A85-27945

MIRRORS

Large scan mirror assembly of the new Thematic Mapper developed for Landsat 4 earth resources satellite p 56 A85-22682

An analysis of the high frequency vibrations in early Thematic Mapper scenes p 69 N85-21742

MISSION PLANNING

The SIR-B science investigations plan [NASA-CR-174282] p 63 N85-17208

CNES, INRA do joint remote-sensing research p 11 N85-19321

MISSISSIPPI

The influence of the number of ground control points on the scene-to-map registration accuracy --- Kansas, Louisiana, Mississippi, and Missouri p 51 N85-16264

MISSISSIPPI DELTA (LA)

Geological, structural, and geomorphological analyses from SIR-B p 24 N85-17226

MISSOURI

The influence of the number of ground control points on the scene-to-map registration accuracy --- Kansas, Louisiana, Mississippi, and Missouri p 51 N85-16264

Image variance and spatial structure in remotely sensed scenes --- South Dakota, California, Missouri, Kentucky, Louisiana, Tennessee, District of Columbia, and Oregon p 51 N85-16265

MIXING HEIGHT

Variations in atmospheric mixing height across oceanic thermal fronts p 34 A85-27704

MOBILE COMMUNICATION SYSTEMS

Satellite data communication system for near real-time processing and distribution of marine fishery research data p 36 A85-28119

MODULATION TRANSFER FUNCTION

LANDSAT-4 Thematic Mapper Modulation Transfer Function (MTF) evaluation --- California and New Mexico [E85-10055] p 62 N85-16250

MTF analysis of LANDSAT-4 Thematic Mapper p 68 N85-21737

MONTE CARLO METHOD

The extension of an invertible coniferous forest canopy reflectance model using SIR-B and LANDSAT data p 10 N85-17246

MORPHOLOGY

Australian Multixperimental Assessment of SIR-B (AMAS) p 52 N85-17243

MOUNTAINS

Use of HCMM thermal images in the study of microclimates in a mountainous region p 3 A85-23771

The analysis of backscattering properties from SAR data of mountain regions p 59 A85-24081

Tectonic, volcanic, and climatic geomorphology study of the Sierras Pampeanas Andes, northwestern Argentina p 24 N85-17215

MULTIBEAM ANTENNAS

An analysis of a satellite multibeam altimeter p 38 A85-29715

MULTISPECTRAL BAND SCANNERS

Methodological study of spectral band selection for multispectral remote sensing p 55 A85-19363

Remote sensing development in the People's Republic of China p 56 A85-20643

Determining stretch parameters for lithologic discrimination on Landsat MSS band-ratio images p 20 A85-21047

Measuring spectra of and lands p 20 A85-21975

Survey of multispectral imaging systems for earth observations p 56 A85-22424

The Thematic Mapper - Instrument overview and preliminary on-orbit results p 56 A85-22681

Demonstration, analysis, and correction of atmospheric effects on Landsat or SPOT multispectral data p 58 A85-23781

Experiments concerning radiometric measurements and natural-object indicators in order to apply corrections to recordings of satellite remote sensing p 58 A85-23789

Determination of visual range from Landsat data p 47 A85-24285

Correlation of spectral brightnesses measured using multispectral space images p 60 A85-25659

Evaluation of aircraft MSS analytical block adjustment p 49 A85-26641

Terrain and look angle effects upon multispectral scanner response p 60 A85-26642

Comparison of level I land cover classification accuracy for MSS and AVHRR data --- Advanced Very High Resolution Radiometers p 61 A85-26929

Modular Optoelectronic Multispectral Scanner (MOMS) Technological aspects p 61 A85-27059

MOMS 1 and its results p 61 A85-27061

Investigation of the properties of natural objects by the canonical-correlation method p 49 A85-28973

Integration of the SPOT panchromatic channel into its multispectral mode for image sharpness enhancement p 49 A85-29217

Conical multispectral scanner for the study of earth resources p 62 A85-29909

Effect of Landsat Thematic Mapper sensor parameters on land cover classification p 14 A85-30088

Characterizing the scientific potential of satellite sensors --- San Francisco, California [E85-10053] p 62 N85-16249

Study of spectral/radiometric characteristics of the Thematic Mapper for land use applications [E85-10057] p 62 N85-16268

Thematic Mapper Volume 1 Calibration report flight model, LANDSAT 5 [E85-10059] p 63 N85-16270

Thematic Mapper Volume 2 Flight model preshipment review [E85-10060] p 63 N85-16271

Enhancement of multispectral scanner images by digital filtering [ESA-TT-624] p 63 N85-16284

Forest area estimates from LANDSAT MSS and forest inventory plot data [PB85-105617/GAR] p 9 N85-16290

Spectroradiometric calibration of the Thematic Mapper and Multispectral Scanner system [E85-10077] p 64 N85-19491

LANDSAT-4 Science Characterization Early Results Volume 1 Multispectral Scanner (MSS) [E85-10067] p 65 N85-20496

Spectral characterization of the LANDAT-4 MSS sensors p 65 N85-20499

Investigation of radiometric properties of LANDSAT-4 MSS --- California, North Carolina, South Carolina, and New England p 65 N85-20500

LANDSAT scene-to-scene registration accuracy assessment p 65 N85-20502

Geometric accuracy of LANDSAT-4 MSS image data p 53 N85-20503

Impact of LANDSAT MSS sensor differences on change detection analysis --- New Mexico, San Francisco, CA, New Hampshire, and Connecticut p 65 N85-20506

Spectral characterization of the LANDSAT Thematic Mapper sensors p 66 N85-20514

- Prelaunch absolute radiometric calibration of the reflective bands on the LANDSAT-4 prototype Thematic Mapper p 66 N85-20515
- The spot operational remote sensing satellite system Current status and perspectives p 67 N85-20776
- In-progress absolute radiometric inflight calibration of the LANDSAT-4 sensors --- New Mexico p 68 N85-21733
- LANDSAT-4 Thematic Mapper calibration and atmospheric correction p 68 N85-21734
- Thematic Mapper spectral dimensionality and data structure p 12 N85-21736
- Intraband radiometric performance of the LANDSAT 4 Thematic Mapper --- Washington, DC, Arkansas, Massachusetts, Virginia, and Arizona p 69 N85-21738
- The use of linear feature detection to investigate Thematic Mapper data performance and processing p 69 N85-21740
- Geodetic accuracy of LANDSAT 4 Multispectral Scanner and Thematic Mapper data p 20 N85-21746
- MULTISPECTRAL PHOTOGRAPHY**
- Evaluation of an experimental system for spaceborne processing of multispectral image data p 46 A85-23144
- Multispectral data compression using staggered detector arrays p 47 A85-24277
- Microwave and optical remote sensing of forest vegetation p 9 N85-17228
- N**
- NASA PROGRAMS**
- The participation of the Netherlands in the NASA Crustal Dynamics Project p 15 A85-20035
- NATIONAL PARKS**
- Investigation of Krasnovodsk bay on the basis of space photographs p 28 A85-21669
- NATURAL GAS**
- Analysis of mesofractures according to space images - Currents trends in the exploration for oil and gas deposits p 21 A85-25655
- NAVIGATION**
- Using the global positioning system (GPS) phase observable for relative geodesy Modeling, processing, and results p 19 N85-18437
- NAVY**
- An airborne infrared thermal scanning system for easy use on Navy P-3 aircraft [AD-A149690] p 42 N85-22143
- NEAR INFRARED RADIATION**
- Spectral characterization of vegetation canopies in the visible and NIR - Application to remote sensing p 5 A85-25670
- Variation in spectral response of soybeans with respect to illumination, view, and canopy geometry [E85-10040] p 8 N85-16241
- NETHERLANDS**
- The participation of the Netherlands in the NASA Crustal Dynamics Project p 15 A85-20035
- NEVADA**
- Analysis of SIR-B radar illumination of geometry for depth of penetration and surface feature and vegetation detection, Nevada and California p 25 N85-17248
- NEW ENGLAND (US)**
- Investigation of radiometric properties of LANDSAT-4 MSS --- California, North Carolina, South Carolina, and New England p 65 N85-20500
- NEW HAMPSHIRE**
- Impact of LANDSAT MSS sensor differences on change detection analysis --- New Mexico, San Francisco, CA, New Hampshire, and Connecticut p 65 N85-20506
- NEW MEXICO**
- LANDSAT-4 Thematic Mapper Modulation Transfer Function (MTF) evaluation --- California and New Mexico [E85-10055] p 62 N85-16250
- Spectroradiometric calibration of the Thematic Mapper and Multispectral Scanner system [E85-10077] p 64 N85-19491
- Impact of LANDSAT MSS sensor differences on change detection analysis --- New Mexico, San Francisco, CA, New Hampshire, and Connecticut p 65 N85-20506
- In-progress absolute radiometric inflight calibration of the LANDSAT-4 sensors --- New Mexico p 68 N85-21733
- NIGHT**
- Calculation of thermal inertia from day-night measurements separated by days or weeks p 45 A85-21048
- NIMBUS 7 SATELLITE**
- The evaluation of SMMR retrieval algorithms --- Scanning Multichannel Microwave Radiometer p 31 A85-23706
- Retrieval of snow water equivalent from Nimbus-7 SMMR data Effect of land-cover categories and weather conditions p 43 A85-24082
- Bio-optical variability in the Alboran Sea as assessed by Nimbus-7 coastal zone color scanner [AD-A147909] p 39 N85-16281
- Data report on variations in the composition of sea ice during MIZEX/East'83 with the Nimbus-7 SMMR [NASA-TM-86170] p 40 N85-18443
- NITROGEN**
- Growth and reflectance characteristics of winter wheat canopies [E85-10080] p 11 N85-19494
- NOAA SATELLITES**
- An automatic high-resolution picture transmission receiving station p 61 A85-27698
- The development of image processing of NOAA AVHRR data and its application to sea surface temperature p 42 N85-21891
- NOAA 6 SATELLITE**
- The influence of satellite spectral sensor response on the analysis of satellite imagery at high latitudes p 60 A85-26927
- NOAA 7 SATELLITE**
- Thermal structure of an agricultural region as seen by NOAA-7 AVHRR p 7 A85-30090
- NONPARAMETRIC STATISTICS**
- Nonparametric analysis of Minnesota spruce and aspen tree data and LANDSAT data p 8 N85-16253
- NORTH AMERICA**
- North American vegetation patterns observed with the NOAA-7 advanced very high resolution radiometer --- North America [E85-10062] p 10 N85-17400
- NORTH CAROLINA**
- Investigation of radiometric properties of LANDSAT-4 MSS --- California, North Carolina, South Carolina, and New England p 65 N85-20500
- NORTH SEA**
- Gravity field investigation in the North Sea p 30 A85-23699
- The altimetric geoid in the North Sea p 16 A85-23700
- NORTHERN HEMISPHERE**
- Magsat scalar magnetic anomalies at northern high latitudes p 18 A85-26416
- O**
- OCEAN BOTTOM**
- Neotectonics of the Caribbean p 27 A85-21145
- Seafloor spreading anomalies in the Magsat field of the North Atlantic p 17 A85-26415
- Abyssal eddies near the Gulf Stream p 34 A85-27701
- Satellite photographs suggest arctic volcano p 38 N85-16239
- Research on ocean floor electrical surveys [AD-A149831] p 42 N85-21920
- OCEAN CURRENTS**
- Center of mass estimation in closed vortices - A verification in principle and practice p 26 A85-19417
- Tidal current bedforms investigated by Seasat p 30 A85-23692
- Microwave signatures of the sea ice in the East Greenland Current p 31 A85-24079
- Eddy kinetic energy distribution in the southern ocean from Seasat altimeter and FGGE drifting buoys p 32 A85-24554
- Features characterizing the development of mushroom-shaped currents in the ocean, revealed by an analysis of satellite imagery p 34 A85-25651
- Abyssal eddies near the Gulf Stream p 34 A85-27701
- Structure and seasonal characteristics of the Gaspe current p 35 A85-27705
- The potential for ocean prediction and the role of altimeter data p 36 A85-29704
- Observing global ocean circulation with SEASAT altimeter data p 36 A85-29705
- Bio-optical variability in the Alboran Sea as assessed by Nimbus-7 coastal zone color scanner [AD-A147909] p 39 N85-16281
- Satellite definition of the bio-optical and thermal variation of coastal eddies associated with the African current [AD-A147910] p 39 N85-16282
- Atlas of the Beaufort Sea [AD-A149545] p 41 N85-20619
- OCEAN DATA ACQUISITIONS SYSTEMS**
- Lidar applications in remote sensing of ocean properties p 31 A85-23755
- Satellite data communication system for near real-time processing and distribution of marine fishery research data p 36 A85-28119
- Simultaneous ocean cross-section and rainfall measurements from space with a nadir pointing radar p 36 A85-28788
- Method of measuring sea surface water temperature with a satellite including wideband passive synthetic-aperture multichannel receiver [NASA-CASE-NPO-15651-1] p 41 N85-21723
- OCEAN DYNAMICS**
- A comparison of in situ and airborne radar observations of ocean wave directionality p 27 A85-20487
- The effect of a moving sea surface on SAR imagery p 29 A85-23685
- Swell propagation in the North Atlantic ocean using SEASAT altimeter p 30 A85-23702
- Structure and seasonal characteristics of the Gaspe current p 35 A85-27705
- Lagrangian observations of surface circulation at the Emperor Seamount chain p 35 A85-27710
- Observing global ocean circulation with SEASAT altimeter data p 36 A85-29705
- Remote-sensing observations of advective eddies in the central part of the Baltic Sea p 38 A85-29915
- Monitoring of the tidal dynamics of the Dutch Waddensea by SIR-B p 40 N85-17235
- OCEAN SURFACE**
- Predicting dangerous ocean waves with spaceborne synthetic aperture radar p 27 A85-19429
- Space radar observations of small-scale formations on the ocean surface p 27 A85-20086
- Aircraft and satellite measurement of ocean wave directional spectra using scanning-beam microwave radars p 27 A85-20486
- The Harp probe - An in situ Bragg scattering sensor p 28 A85-22171
- Separating clouds from ocean in infrared images p 28 A85-22423
- Satellite microwave remote sensing p 28 A85-23676
- Imaging ocean surface waves by synthetic aperture radar - A review p 29 A85-23682
- Can optical measurements help in the interpretation of radar backscatter? p 29 A85-23683
- Theory of SAR ocean wave imaging p 29 A85-23686
- Effect of defocusing on the images of ocean waves p 29 A85-23688
- Expressions of bathymetry on Seasat synthetic radar images p 29 A85-23691
- Altimeter measurements of ocean topography p 30 A85-23695
- The altimetric geoid in the North Sea p 16 A85-23700
- Wave measurements with the Seasat radar altimeter - A Review p 30 A85-23701
- Use of ocean skewness measurements in calculating the accuracy of altimeter height measurements p 30 A85-23703
- Spatial variation of significant wave-height p 30 A85-23704
- The evaluation of SMMR retrieval algorithms --- Scanning Multichannel Microwave Radiometer p 31 A85-23706
- Simultaneous radiometric and radar altimetric measurements of sea microwave signatures p 31 A85-24076
- A sampling strategy for altimeter measurements of the global statistics of mesoscale eddies p 32 A85-24553
- Wind speed and stress over the ocean - Scatterometer versus surface measurements p 33 A85-24557
- A summary of the wind data available from satellites from the past history to future sensors p 33 A85-24558
- Interpretation of space images of the sea surface using the SVIT digital-processing complex p 34 A85-25654
- Transformation of sea-wave spectrum into a synthetic-aperture-radar image spectrum p 34 A85-25661
- Intermediate-wavelength magnetic anomaly field of the North Pacific and possible source distributions p 17 A85-26414
- Cosmic interpolation of terrestrial potential values p 18 A85-26476
- Lagrangian observations of surface circulation at the Emperor Seamount chain p 35 A85-27710
- Determination of monthly mean humidity in the atmospheric surface layer over oceans from satellite data p 35 A85-28007
- On the determination of the deflection of the vertical by satellite altimetry --- for marine geoid height estimates p 37 A85-29706
- World ocean mean monthly waves, swell, and surface winds for July through October 1978 from SEASAT radar altimeter data p 37 A85-29707
- Swell in the Pacific Ocean observed by SEASAT radar altimeter p 37 A85-29708
- Electromagnetic bias of 36-GHz radar altimeter measurements of MSL --- Mean Sea Level p 37 A85-29712

- The reflection of airborne UV laser pulses from the ocean p 37 A85-29714
- Regional mean sea surfaces based on GEOS-3 and SEASAT altimeter data p 38 A85-29716
- The interpretation of SIR-B imagery of surface waves and other oceanographic features using in-situ, meteorological satellite, and infrared satellite data p 39 N85-17212
- The investigation of selected oceanographic applications of spaceborne synthetic-aperture radar p 39 N85-17233
- Oceanographic and meteorological research based on the data products of SEASAT [E85-10091] p 41 N85-21753
- OCEANOGRAPHIC PARAMETERS**
- A review of SEASAT --- ocean surface imagery p 28 A85-23677
- Validation and applications of SASS over JASIN --- wind scatterometer results in Atlantic NW of Scotland p 29 A85-23681
- The use of SEASAT-SAR data in oceanography at the IJP p 29 A85-23690
- Use of ocean skewness measurements in calculating the accuracy of altimeter height measurements p 30 A85-23703
- Performance of an airborne imaging 92/183 GHz radiometer during the Bering Sea Marginal Ice Zone Experiment (MIZEX-WEST) p 33 A85-24945
- The use of airborne lasers in terrestrial and water environments p 33 A85-25351
- Features characterizing the development of mushroom-shaped currents in the ocean, revealed by an analysis of satellite imagery p 34 A85-25651
- Structure and seasonal characteristics of the Gaspe current p 35 A85-27705
- A survey of oceanographic satellite altimetric missions p 36 A85-29703
- An analysis of a satellite multibeam altimeter p 38 A85-29715
- Atlas of the Beaufort Sea [AD-A149545] p 41 N85-20619
- OCEANOGRAPHY**
- Advances in microwave remote sensing of the ocean and atmosphere p 28 A85-21960
- Altimeter measurements of ocean topography p 30 A85-23695
- Large-scale oceanographic experiments and satellites, Proceedings of the Advanced Research Workshop, Porto Vecchio, Corse, France, October 3-7, 1983 p 32 A85-24551
- The interpretation of SIR-B imagery of surface waves and other oceanographic features using in-situ, meteorological satellite, and infrared satellite data p 39 N85-17212
- The spatial evolution of the directional wave spectrum in the Southern Ocean Its relation to extreme waves in Agulhas Current p 39 N85-17213
- Evaluation of SIR-B imagery for geologic and geomorphic mapping, hydrology, and oceanography in Australia p 51 N85-17229
- SEASAT 3 and 4 [AD-A148343] p 40 N85-17274
- Altimetry, orbits and tides p 40 N85-17404
- [E85-10066] p 40 N85-17404
- The use of principal components analysis techniques Nimbus-7 coastal zone color scanner data to define mesoscale ocean features through a warm humid atmosphere [AD-A148567] p 40 N85-17416
- Nautical charting with remotely sensed imagery, volume 1 [AD-A149361] p 41 N85-19503
- An airborne infrared thermal scanning system for easy use on Navy P-3 aircraft [AD-A149690] p 42 N85-22143
- OCEANS**
- Earth observations and the polar platform [NOAA-TR-NESDIS-18] p 15 N85-20517
- Along-track deflection of the vertical from SEASAT GEBCO (General Bathymetric Chart of the Oceans) overlays [PB85-129641] p 42 N85-21767
- OHIO**
- Interlobate companson of glacial-depositional style as evidenced by small-relief glacial landscape features in Illinois, Indiana, and Ohio, utilizing SIR-B p 39 N85-17231
- OIL EXPLORATION**
- Space remote-sensing data in geology --- Russian book p 23 A85-28400
- Possibilities of using remote-sensing methods to improve the efficiency of oil and gas exploration p 24 A85-29905

OKLAHOMA

- Post-carboniferous tectonics in the Anadarko Basin, Oklahoma Evidence from side-looking radar imagery [NASA-CR-175458] p 26 N85-19498

ONBOARD DATA PROCESSING

- Evaluation of an experimental system for spaceborne processing of multispectral image data p 46 A85-23144

OPTICAL DATA PROCESSING

- Development and evaluation of techniques for using combined microwave and optical image data for vegetation studies p 9 N85-17240

OPTICAL EQUIPMENT

- Airborne remote sensing CCD imaging system p 65 N85-20220

OPTICAL MEASUREMENT

- Can optical measurements help in the interpretation of radar backscatter? p 29 A85-23683

OPTICAL MEASURING INSTRUMENTS

- Optical engineering for cold environments, Proceedings of the Meeting, Arlington, VA, April 7, 8, 1983 p 59 A85-25344

OPTICAL PROPERTIES

- Bio-optical variability in the Alboran Sea as assessed by Nimbus-7 coastal zone color scanner [AD-A147909] p 39 N85-16281

OPTICAL RADAR

- Lidar applications in remote sensing of ocean properties p 31 A85-23755
- Performance of a coherent lidar remote sensor in snow and fog p 59 A85-25347
- Analysis of the NASA/MSFC Airborne Doppler Lidar results from San Geronio Pass, California [NASA-CR-171355] p 70 N85-21873

OPTICAL SCANNERS

- Complex studies of the environment by optical and radar methods p 56 A85-20081

ORBITAL SPACE STATIONS

- Earth observations and the polar platform [NOAA-TR-NESDIS-18] p 15 N85-20517

OREGON

- Image variance and spatial structure in remotely sensed scenes --- South Dakota, California, Missouri, Kentucky, Louisiana, Tennessee, District of Columbia, and Oregon p 51 N85-16265

OZONOMETRY

- Intercomparisons of TOMS, SBUV and MFR satellite ozone measurements --- Satellite Backscattered Ultraviolet, Total Ozone Mapping System, Multichannel Filter Radiometer p 62 A85-29784

P**P-3 AIRCRAFT**

- An airborne infrared thermal scanning system for easy use on Navy P-3 aircraft [AD-A149690] p 42 N85-22143

PACIFIC OCEAN

- Intermediate-wavelength magnetic anomaly field of the North Pacific and possible source distributions p 17 A85-26414
- On the determination of the deflection of the vertical by satellite altimetry --- for marine geoid height estimates p 37 A85-29706
- Swell in the Pacific Ocean observed by SEASAT radar altimeter p 37 A85-29708
- The spatial evolution of the directional wave spectrum in the Southern Ocean Its relation to extreme waves in Agulhas Current p 39 N85-17213

PALEOMAGNETISM

- A review of problems and progress in studies of satellite magnetic anomalies p 17 A85-26409

PARAMETER IDENTIFICATION

- Estimating location parameters in a mixture p 50 N85-16252
- Bayesian estimation of normal mixture parameters p 50 N85-16255

PARAMETERIZATION

- Spatial resolution estimation of LANDSAT-4 Thematic Mapper data p 69 N85-21741

PATTERN RECOGNITION

- Proceedings of the Second Annual Symposium on Mathematical Pattern Recognition and Image Analysis Program [E85-10056] p 50 N85-16251
- Multivariate spline methods in surface fitting p 50 N85-16257
- Calibration or inverse regression Which is appropriate for crop surveys using LANDSAT data? p 9 N85-16260
- Power spectral ensity of markov texture fields p 50 N85-16262
- Rectification of single and multiple frames of satellite scanner imagery using points and edges as control p 51 N85-16263

- The influence of the number of ground control points on the scene-to-map registration accuracy --- Kansas, Louisiana, Mississippi, and Missouri p 51 N85-16264
- Image variance and spatial structure in remotely sensed scenes --- South Dakota, California, Missouri, Kentucky, Louisiana, Tennessee, District of Columbia, and Oregon p 51 N85-16265
- Image-to-image correspondence Linear structure matching p 51 N85-16266
- Analysis of subpixel registration p 51 N85-16267
- Analysis of terrestrial conditions and dynamics [E85-10063] p 10 N85-17401
- Assessment of Thematic Mapper band-to-band registration by the block correlation method p 55 N85-21743

PATTERN REGISTRATION

- The influence of the number of ground control points on the scene-to-map registration accuracy --- Kansas, Louisiana, Mississippi, and Missouri p 51 N85-16264
- Analysis of subpixel registration p 51 N85-16267
- Investigation of TM band-to-band registration using the JSC registration processor p 69 N85-21745
- Geodetic accuracy of LANDSAT 4 Multispectral Scanner and Thematic Mapper data p 20 N85-21746

PENETRATION

- Application and calibration of the subsurface mapping capability of SIR-B in desert regions p 25 N85-17244
- Ground truth for SIR-B images obtained by SIR system 8 impulse radar p 10 N85-17251

PERFORMANCE TESTS

- Spectral characterization of the LANDAT-4 MSS sensors p 65 N85-20499

PERIODICALS

- Sourcebook Gaining access to US government information on the environment and natural resources [DE84-017419] p 71 N85-20941

PHASED ARRAYS

- Synthetic apertures - An overview p 57 A85-22711

PHENOLOGY

- NOAA-AISC user's guide for implementing CERES maize model for large area yield estimation [E85-10083] p 12 N85-21748
- User's guide to the TAMW wheat model as implemented on the IBM 360/195 computer [E85-10084] p 12 N85-21749
- NOAA-AISC user's guide for implementing CERES wheat model for large area yield estimation [E85-10085] p 12 N85-21750
- Estimating solar radiation for plant simulation models [E85-10089] p 13 N85-21751

PHOTO GEOLOGY

- Determining stretch parameters for lithologic discrimination on Landsat MSS band-ratio images p 20 A85-21047
- Mapping of landforms from Landsat imagery - An example from eastern New South Wales, Australia p 21 A85-22422
- Seasat over land p 57 A85-23693
- Generation of a Landsat-HCMM combined image and its application to geological cartography p 21 A85-23792

- Analysis of mesofractures according to space images - Currents trends in the exploration for oil and gas deposits p 21 A85-25655
- Frontiers for geological remote sensing from space, Geosat Workshop, 4th, Flagstaff, AZ, June 12-17, 1983, Report p 22 A85-27943
- Near-infrared spectroscopy in geological reconnaissance and exploration p 22 A85-27944
- Imaging systems for the delineation of spectral properties of geologic materials in the visible and near-infrared p 22 A85-27945
- Thematic mapper data analysis p 23 A85-27946
- The importance of geobotany in geological remote sensing applications p 23 A85-27948
- Space remote-sensing data in geology --- Russian book p 23 A85-28400
- Methods for the study of recent tectonics on the basis of remote sensing and ground data p 23 A85-29904
- Possibilities of using remote-sensing methods to improve the efficiency of oil and gas exploration p 24 A85-29905

- A preliminary evaluation of LANDSAT-4 Thematic Mapper data for their geometric and radiometric accuracies p 54 N85-21739
- LANDSAT 4 investigations of Thematic Mapper and Multispectral Scanner applications --- Drum Mountains, Utah and Tonopah, Nevada [E85-10095] p 26 N85-21757

PHOTOGRAMMETRY

- Determination of the external-orientation elements of arial and space photographs in the remote sensing of dynamic processes and phenomena p 56 A85-19998
- Automatic production of DTM data using digital off-line technique --- Digital Terrain Modelling p 45 A85-20750

- American Congress on Surveying and Mapping and American Society of Photogrammetry, Fall Convention, Salt Lake City, UT, September 19-23, 1983, Technical Papers p 14 A85-24950
- Minimization of the effect of the earth's curvature in the projective transformation of space images into photoplans and photomaps p 16 A85-25662
- Investigations of the accuracy of the digital photogrammetry system DPS, a rigorous three dimensional compilation process for push broom imagery [MBB-UA-753/83-OE] p 60 A85-26393
- Evaluation of aircraft MSS analytical block adjustment p 49 A85-26641
- Segmentation of half-tone remote-sensing images by the level lines method p 49 A85-29913
- The use of a priori estimation of the conditions of the observation of the earth surface from space for a rational selection of the time at which the survey is conducted p 50 A85-29914
- Papers of the 15th International Society for Photogrammetry and Remote Sensing (ISPRS) Congress --- conferences [TRITA-FMI-9] p 63 A85-17406
- Mathematical aspects of digital terrain information, Report from International Society for Photogrammetry and Remote Sensing (ISPRS) working group 3 3, 1980 - 1984 --- photogrammetry p 19 A85-17407
- A comparative test of photogrammetrically sampled digital elevation models p 52 A85-17408
- Multimodels increase accuracy Summary of an experiment --- photogrammetry p 63 A85-17409
- Hybrid method of mapping and photogeodetic control network densification [PB85-133775] p 20 A85-21766
- PHOTOINTERPRETATION**
- Ring structures observed on space radar images of the earth p 45 A85-20084
- Population estimation from aerial photos for non-homogeneous urban residential areas p 14 A85-20749
- Visual interpretation of SAR images of two areas in the Netherlands p 1 A85-23694
- Interpretation of space images of the sea surface using the SVIT digital-processing complex p 34 A85-25654
- Identification of homogeneous regions with incomplete boundaries on an image p 24 A85-29912
- Segmentation of half-tone remote-sensing images by the level lines method p 49 A85-29913
- Effect of Landsat Thematic Mapper sensor parameters on land cover classification p 14 A85-30088
- Integrated analysis of remote sensing products from basic geological surveys --- Brazil [E85-10052] p 24 A85-16248
- Evidence accumulation for spatial reasoning p 50 A85-16261
- Forest area estimates from LANDSAT MSS and forest inventory plot data [PB85-105617/GAR] p 9 A85-16290
- Assessment of LANDSAT for rangeland mapping, Rush Valley, Utah [E85-10072] p 15 A85-19486
- LANDSAT 4 investigation of Thematic Mapper and Multispectral Scanner applications [E85-10076] p 52 A85-19490
- PHOTOMAPPING**
- An example of Landsat cost effectiveness in mapping land-cover p 1 A85-20573
- Minimization of the effect of the earth's curvature in the projective transformation of space images into photoplans and photomaps p 16 A85-25662
- Comparison of level I land cover classification accuracy for MSS and AVHRR data --- Advanced Very High Resolution Radiometers p 61 A85-26929
- Advanced SAR system maps Arctic regions p 35 A85-27841
- Mapping of glacial landforms from Seasat radar images p 36 A85-28027
- The use of Salyut-5 photographs for regional geomorphological mapping p 23 A85-28999
- Comprehensive desertification maps and methods for making such maps on the basis of space photographs p 14 A85-29907
- PHOTOMETRY**
- Determination of reflectances of tropical vegetation by combined methods of radiometry and photometry p 2 A85-23760
- Planetary cartography in the next decade (1984 - 1994) [NASA-SP-475] p 20 A85-22323
- PHOTON ABSORPTIOMETRY**
- Techniques for measuring intercepted and absorbed PAR in corn canopies [E85-10081] p 11 A85-19495
- PHOTOSYNTHESIS**
- Spectral estimators of absorbed photosynthetically active radiation in corn canopies [E85-10041] p 8 A85-16242
- Techniques for measuring intercepted and absorbed PAR in corn canopies [E85-10081] p 11 A85-19495
- PHOTOTROPISM**
- Effect of heliotropism on the bidirectional reflectance of irrigated cotton p 1 A85-22420
- PHYSICAL PROPERTIES**
- Determination of the physical parameters of sea ice on the basis of remote microwave measurements in the 0.3-18 cm range p 38 A85-29903
- PLANETARY CRATERS**
- Geological, structural, and geomorphological analyses from SIR-B p 24 A85-17226
- PLANETARY MAPPING**
- Planetary cartography in the next decade (1984 - 1994) [NASA-SP-475] p 20 A85-22323
- PLANETARY STRUCTURE**
- Mathematical modelling of the geomagnetic field and secular variation, and its applications, Proceedings of the Symposium, Hamburg, West Germany, August 15-27, 1983 p 16 A85-25689
- PLANT STRESS**
- Analysis of ACIR transparencies of citrus trees with a projecting spectral densitometer --- Aerial Color IR p 1 A85-21050
- PLANTS (BOTANY)**
- Computing the foliage angle distribution from contact frequency data p 6 A85-29969
- Estimating solar radiation for plant simulation models [E85-10089] p 13 A85-21751
- PLATES (TECTONICS)**
- Delineation of major geologic structures in Turkey using SIR-B data p 25 A85-17249
- PLAYAS**
- Characteristics of playa deposits as seen on SIR-A, Seasat and Landsat coregistered data p 21 A85-23793
- POGO**
- Magsat and POGO magnetic anomalies over the Lord Howe Rise Evidence against a simple continental crustal structure p 18 A85-26422
- POINT SPREAD FUNCTIONS**
- Some properties of SAR speckle p 46 A85-23684
- Spatial resolution estimation of LANDSAT-4 Thematic Mapper data p 69 A85-21741
- POLAR REGIONS**
- The influence of satellite spectral sensor response on the analysis of satellite imagery at high latitudes p 60 A85-26927
- Satellite observations of sea ice p 36 A85-28022
- Passive microwave remote sensing for sea ice research [NASA-CR-175570] p 42 A85-21758
- POLARIMETRY**
- Light polarization measurements - A method to determine the specular and diffuse light-scattering properties of both leaves and plant canopies p 2 A85-23754
- POLARIZATION (WAVES)**
- Polarization effects in sea-ice signatures p 31 A85-24078
- POLLUTION MONITORING**
- Remote sensing techniques for monitoring of pollution in coastal waters - Potential application to Saudi Arabia p 34 A85-27441
- POPULATIONS**
- Population estimation from aerial photos for non-homogeneous urban residential areas p 14 A85-20749
- POSITION (LOCATION)**
- Determination of the external-orientation elements of aerial and space photographs in the remote sensing of dynamic processes and phenomena p 56 A85-19998
- Geodetic accuracy of LANDSAT 4 Multispectral Scanner and Thematic Mapper data --- Washington, DC, California, Alabama, South Dakota, and Illinois p 53 A85-20504
- POWER SPECTRA**
- Power spectral density of markov texture fields p 50 A85-16262
- MTF analysis of LANDSAT-4 Thematic Mapper p 68 A85-21737
- PRECAMBRIAN PERIOD**
- Structural investigation of the Canadian Shield by orbital radar and LANDSAT p 25 A85-17236
- PRECIPITATION (METEOROLOGY)**
- Airborne Doppler estimates of the air motions associated with a developing, sea-breeze induced, mesoscale precipitation line p 36 A85-28783
- PREDICTION ANALYSIS TECHNIQUES**
- A comparative analysis of some prediction methods for rain attenuation statistics in earth-to-space links p 42 A85-21130
- The potential for ocean prediction and the role of altimeter data p 36 A85-29704
- Exploring the use of structural models to improve remote sensing agricultural estimates p 9 A85-16259
- Evidence accumulation for spatial reasoning p 50 A85-16261
- PRINCIPAL COMPONENTS ANALYSIS**
- The use of principal components analysis techniques Nimbus-7 coastal zone color scanner data to define mesoscale ocean features through a warm humid atmosphere [AD-A148567] p 40 A85-17416
- PROBABILITY DENSITY FUNCTIONS**
- Multivariate spline methods in surface fitting p 50 A85-16257
- PROBABILITY THEORY**
- A computationally-efficient maximum-likelihood classifier employing prior probabilities for remotely-sensed data p 49 A85-26948
- Analysis of subpixel registration p 51 A85-16267
- PRODUCTION PLANNING**
- Estimating ocean primary production from satellite chlorophyll - Introduction to regional differences and statistics for the Southern California Bight p 35 A85-28005
- PRODUCTIVITY**
- North American vegetation patterns observed with the NOAA-7 advanced very high resolution radiometer --- North America [E85-10062] p 10 A85-17400
- PROTON DENSITY (CONCENTRATION)**
- On the P1 data from GMS-SEM p 15 A85-21890
- PULSED LASERS**
- The reflection of airborne UV laser pulses from the ocean p 37 A85-29714
- PUSHBROOM SENSOR MODES**
- Investigations of the accuracy of the digital photogrammetry system DPS, a rigorous three dimensional compilation process for push broom imagery [MBB-UA-753/83-OE] p 60 A85-26393
- Q**
- QUALITY CONTROL**
- Thematic Mapper Design through flight evaluation [E85-10078] p 64 A85-19492
- R**
- RADAR**
- Aircraft and satellite measurement of ocean wave directional spectra using scanning-beam microwave radars p 27 A85-20486
- RADAR CROSS SECTIONS**
- Simultaneous ocean cross-section and rainfall measurements from space with a nadir pointing radar p 36 A85-28788
- Simultaneous ocean cross-section and rainfall measurements from space with a nadir-pointing radar [NASA-TM-86167] p 44 A85-16273
- RADAR DATA**
- The use of SEASAT-SAR data in oceanography at the IOP p 29 A85-23690
- Ultrashort-wave radar subsurface sounding of sea ice and earth covers p 34 A85-25594
- Soil moisture content estimation by radar survey data during the sowing campaign p 6 A85-26947
- Rain volume estimation over areas using satellite and radar data [NASA-CR-174434] p 44 A85-19568
- RADAR DETECTION**
- Land clutter models for radar design and analysis p 49 A85-28727
- RADAR ECHOES**
- Relations between the radar backscatter coefficient and the characteristics of a vegetation canopy - Analysis of the effect of structure p 4 A85-23774
- Test plan for the forest-echo experiment [DE84-017175] p 10 A85-18447
- RADAR GEOLOGY**
- Ring structures observed on space radar images of the earth p 45 A85-20084
- Image-scale and look-direction effects on the detectability of lineaments in radar images p 24 A85-30087
- RADAR IMAGERY**
- Predicting dangerous ocean waves with spaceborne synthetic aperture radar p 27 A85-19429
- Ring structures observed on space radar images of the earth p 45 A85-20084

- Space radar observations of small-scale formations on the ocean surface p 27 A85-20086
- Imaging ocean surface waves by synthetic aperture radar - A review p 29 A85-23682
- The effect of a moving sea surface on SAR imagery p 29 A85-23685
- Theory of SAR ocean wave imaging p 29 A85-23686
- Effect of defocusing on the images of ocean waves p 29 A85-23688
- Expressions of bathymetry on Seasat synthetic radar images p 29 A85-23691
- Visual interpretation of SAR images of two areas in the Netherlands p 1 A85-23694
- A survey of some recent scientific results from the Seasat altimeter p 30 A85-23696
- Classification of vegetation types by analysis of X-band and C-band radar images p 4 A85-23775
- Radargrammetry of Shuttle Imaging Radar-B experiment p 46 A85-23779
- Effect of meteorological conditions on the characteristics of space radar images of the earth surface p 48 A85-25653
- Features of the digital processing of radar images obtained with the sidelooking radar of the Cosmos-1500 satellite p 48 A85-25660
- Transformation of sea-wave spectrum into a synthetic-aperture-radar image spectrum p 34 A85-25661
- Realtime processor of SAR systems p 60 A85-25855
- Land clutter models for radar design and analysis p 49 A85-27827
- Advanced SAR system maps Arctic regions p 35 A85-27841
- Developments with multispectral thermal-IR and active microwave systems - TIMS, SIR-A, SIR-B, and radarsat p 62 A85-27947
- Mapping of glacial landforms from Seasat radar images p 36 A85-28027
- Detection of lowland flooding using active microwave systems p 43 A85-29218
- Image-scale and look-direction effects on the detectability of lineaments in radar images p 24 A85-30087
- The SIR-B science investigations plan [NASA-CR-174282] p 63 A85-17208
- Microwave and optical remote sensing of forest vegetation p 9 A85-17228
- Evaluation of SIR-B imagery for geologic and geomorphic mapping, hydrology, and oceanography in Australia p 51 A85-17229
- Interlobate comparison of glacial-depositional style as evidenced by small-relief glacial landscape features in Illinois, Indiana, and Ohio, utilizing SIR-B p 39 A85-17231
- Information extraction and transmission techniques for spaceborne synthetic aperture radar images [NASA-CR-174341] p 52 A85-17256
- SEASAT 3 and 4 [AD-A148343] p 40 A85-17274
- Analysis of data acquired by synthetic aperture radar and LANDSAT Multispectral Scanner over Kershaw County, South Carolina, during the summer season [E85-10071] p 11 A85-19485
- Earth resources research using the Shuttle Imaging Radar system p 67 A85-20779
- The imaging of internal waves by the SEASAT-A synthetic aperture radar [AD-A149808] p 20 A85-21761
- RADAR MAPS**
- Radar mapping of the moisture of open soils p 6 A85-29911
- RADAR MEASUREMENT**
- Remote sensing by radar altimetry p 26 A85-19428
- A comparison of in situ and airborne radar observations of ocean wave directionality p 27 A85-20487
- Wave measurements with the Seasat radar altimeter - A Review p 30 A85-23701
- Lidar applications in remote sensing of ocean properties p 31 A85-23755
- Simultaneous radiometric and radar altimetric measurements of sea microwave signatures p 31 A85-24076
- Radiophysical techniques employed for sea ice investigations p 31 A85-24077
- Improvement of the accuracy of radar measurements of sea-ice thickness by cepstral processing of reflected signals p 35 A85-27736
- Simultaneous ocean cross-section and rainfall measurements from space with a nadir pointing radar p 36 A85-28788
- Intermediate results of radar backscatter measurements from summer sea ice [AD-A147212] p 38 A85-15960
- Simultaneous ocean cross-section and rainfall measurements from space with a nadir-pointing radar [NASA-TM-86167] p 44 A85-16273
- RADAR PHOTOGRAPHY**
- Determination of the heights of points of a place on the basis of radar-survey data p 19 A85-29000
- RADAR SCATTERING**
- The Harp probe - An in situ Bragg scattering sensor p 28 A85-22171
- Can optical measurements help in the interpretation of radar backscatter? p 29 A85-23683
- The analysis of backscattering properties from SAR data of mountain regions p 59 A85-24081
- The effect of a snow cover on microwave backscatter from sea ice p 32 A85-24083
- Simultaneous ocean cross-section and rainfall measurements from space with a nadir-pointing radar [NASA-TM-86167] p 44 A85-16273
- Evaluation of the L-band scattering characteristics of volcanic terrain in aid of lithologic identification, assessment of SIR-B calibration, and development of planetary geomorphic analogs p 24 A85-17232
- Oceanographic and meteorological research based on the data products of SEASAT [E85-10091] p 41 A85-21753
- RADAR SIGNATURES**
- Relations between the radar backscatter coefficient and the characteristics of a vegetation canopy - Analysis of the effect of structure p 4 A85-23774
- RADARSAT**
- Developments with multispectral thermal-IR and active microwave systems - TIMS, SIR-A, SIR-B, and radarsat p 62 A85-27947
- RADIANCE**
- Comparison of modelled and empirical atmospheric propagation data p 46 A85-22678
- Prelaunch absolute radiometric calibration of the reflective bands on the LANDSAT-4 prototype Thematic Mapper p 66 A85-20515
- Relative radiometric calibration of LANDSAT TM reflective bands p 67 A85-21725
- Evaluation of the radiometric integrity of LANDSAT 4 Thematic Mapper band 6 data p 54 A85-21726
- Thermal band characterization of the LANDSAT-4 Thematic Mapper p 67 A85-21727
- MTF analysis of LANDSAT-4 Thematic Mapper p 68 A85-21737
- RADIATION ABSORPTION**
- Spectral estimators of absorbed photosynthetically active radiation in corn canopies [E85-10041] p 8 A85-16242
- Techniques for measuring intercepted and absorbed PAR in corn canopies [E85-10081] p 11 A85-19495
- RADIATION COUNTERS**
- On the P1 data from GMS-SEM p 15 A85-21890
- RADIATION DETECTORS**
- Multispectral data compression using staggered detector arrays p 47 A85-24277
- RADIATIVE TRANSFER**
- Advances in microwave remote sensing of the ocean and atmosphere p 28 A85-21960
- The evaluation of SMMR retrieval algorithms - Scanning Multichannel Microwave Radiometer p 31 A85-23706
- Earth observation modeling based on layer scattering matrices p 7 A85-30091
- Evaluation of the radiometric integrity of LANDSAT 4 Thematic Mapper band 6 data p 54 A85-21726
- Spectroradiometric calibration of the Thematic Mapper and Multispectral Scanner system [E85-10094] p 70 A85-21756
- RADIO ALTIMETERS**
- Remote sensing by radar altimetry p 26 A85-19428
- A survey of some recent scientific results from the Seasat altimeter p 30 A85-23696
- Wave measurements with the Seasat radar altimeter - A Review p 30 A85-23701
- Use of ocean skewness measurements in calculating the accuracy of altimeter height measurements p 30 A85-23703
- Simultaneous radiometric and radar altimetric measurements of sea microwave signatures p 31 A85-24076
- Observing global ocean circulation with SEASAT altimeter data p 36 A85-29705
- On the determination of the deflection of the vertical by satellite altimetry - for marine geoid height estimates p 37 A85-29706
- World ocean mean monthly waves, swell, and surface winds for July through October 1978 from SEASAT radar altimeter data p 37 A85-29707
- Swell in the Pacific Ocean observed by SEASAT radar altimeter p 37 A85-29708
- Electromagnetic bias of 36-GHz radar altimeter measurements of MSL - Mean Sea Level p 37 A85-29712
- Electromagnetic bias of 10-GHz radar altimeter measurements of MSL p 37 A85-29713
- An analysis of a satellite multibeam altimeter p 38 A85-29715
- RADIO PHYSICS**
- Radiophysical techniques employed for sea ice investigations p 31 A85-24077
- RADIOMETERS**
- Analysis of ground radiometric measurements in the rice-growing site at Tamani (Republic of Mali) - Effect of certain yield parameters on the spectral signature p 2 A85-23758
- Development of a SPOT-simulation radiometer p 57 A85-23759
- Determination of reflectances of tropical vegetation by combined methods of radiometry and photometry p 2 A85-23760
- Estimation of wheat production on the basis of Landsat channel 5 and 7 radiometric measurements p 3 A85-23763
- RADIOMETRIC CORRECTION**
- Evaluation of an experimental system for spaceborne processing of multispectral image data p 46 A85-23144
- Experiments concerning radiometric measurements and natural-object indicators in order to apply corrections to recordings of satellite remote sensing p 58 A85-23789
- Characterizing the scientific potential of satellite sensors - San Francisco, California [E85-10044] p 62 A85-16244
- Characterizing the scientific potential of satellite sensors - San Francisco, California [E85-10053] p 62 A85-16249
- Study of spectral/radiometric characteristics of the Thematic Mapper for land use applications [E85-10057] p 62 A85-16268
- Study of spectral/radiometric characteristics of the Thematic Mapper for land use applications [E85-10075] p 64 A85-19489
- Radiometric accuracy assessment of LANDSAT 4 Multispectral Scanner data p 53 A85-20498
- Radiometric calibration and geocoded precision processing of LANDSAT-4 Multispectral Scanner products by the Canada Centre for Remote Sensing p 53 A85-20501
- Radiometric calibration and processing procedure for reflective bands on LANDSAT-4 prototype Thematic Mapper p 66 A85-20510
- A preliminary assessment of LANDSAT-4 Thematic Mapper data - Windsor, Ontario and Medicine Hat areas, Canada p 54 A85-21728
- Preliminary evaluation of the radiometric calibration of LANDSAT-4 Thematic Mapper data by the Canada Centre for Remote Sensing p 67 A85-21729
- In-progress absolute radiometric in-flight calibration of the LANDSAT-4 sensors - New Mexico p 68 A85-21733
- LANDSAT-4 Thematic Mapper calibration and atmospheric correction p 68 A85-21734
- Scan angle and detector effects in Thematic Mapper radiometry - Iowa and Arkansas p 68 A85-21735
- RADIOMETRIC RESOLUTION**
- Determination of visual range from Landsat data p 47 A85-24285
- Comparison of level I land cover classification accuracy for MSS and AVHRR data - Advanced Very High Resolution Radiometers p 61 A85-26929
- Study of spectral/radiometric characteristics of the Thematic Mapper for land use applications [E85-10075] p 64 A85-19489
- Summary of MSS characterization investigations p 53 A85-20497
- Radiometric accuracy assessment of LANDSAT 4 Multispectral Scanner data p 53 A85-20498
- Investigation of radiometric properties of LANDSAT-4 MSS - California, North Carolina, South Carolina, and New England p 65 A85-20500
- Impact of LANDSAT MSS sensor differences on change detection analysis - New Mexico, San Francisco, CA, New Hampshire, and Connecticut p 65 A85-20506
- Prelaunch absolute radiometric calibration of the reflective bands on the LANDSAT-4 prototype Thematic Mapper p 66 A85-20515
- Characterization of radiometric calibration of LANDSAT-4 reflective bands p 66 A85-20516
- LANDSAT-4 Science Characterization Early Results Volume 3, part 2 Thematic Mapper (TM) [E85-10069] p 67 A85-21724
- Relative radiometric calibration of LANDSAT TM reflective bands p 67 A85-21725
- Evaluation of the radiometric integrity of LANDSAT 4 Thematic Mapper band 6 data p 54 A85-21726

- Thermal band characterization of the LANDSAT-4 Thematic Mapper p 67 N85-21727
- A preliminary analysis of LANDSAT-4 Thematic Mapper radiometric performance p 68 N85-21730
- Evaluation of the radiometric quality of the TM data using clustering, linear transformations and multispectral distance measures --- Illinois p 54 N85-21731
- Intraband radiometric performance of the LANDSAT 4 Thematic Mapper --- Washington, DC, Arkansas, Massachusetts, Virginia, and Arizona p 69 N85-21738
- A preliminary evaluation of LANDSAT-4 Thematic Mapper data for their geometric and radiometric accuracies p 54 N85-21739
- The use of linear feature detection to investigate Thematic Mapper data performance and processing p 69 N85-21740
- Assessment of Thematic Mapper band-to-band registration by the block correlation method p 55 N85-21743
- LANDSAT 4 band 6 data evaluation [E85-10093] p 55 N85-21755
- Spectroradiometric calibration of the Thematic Mapper and Multispectral Scanner system [E85-10094] p 70 N85-21756
- RAIN**
- A comparative analysis of some prediction methods for rain attenuation statistics in earth-to-space links p 42 A85-21130
- Satellite passive microwave rain rate measurement over croplands during spring, summer and fall p 4 A85-25181
- Simultaneous ocean cross-section and rainfall measurements from space with a nadir-pointing radar [NASA-TM-86167] p 44 N85-16273
- Resolution enhancement of multichannel microwave imagery from the Nimbus-7 SMMR for maritime rainfall analysis [NASA-CR-174367] p 44 N85-19221
- Rain volume estimation over areas using satellite and radar data [NASA-CR-174434] p 44 N85-19568
- RAIN FORESTS**
- Relationship between forest clearing and biophysical factors in tropical environments. Implications for the design of a forest change monitoring approach --- Costa Rica [E85-10051] p 8 N85-16247
- Information for space radar designers. Required dynamic range vs resolution and antenna calibration using the Amazon rain forest p 44 N85-17239
- RAINDROPS**
- Simultaneous ocean cross-section and rainfall measurements from space with a nadir pointing radar p 36 A85-28788
- RANGELANDS**
- The potential of satellite remote sensing of ecological conditions for survey and forecasting desert-locust activity p 5 A85-26934
- An integrated remote sensing approach for identifying ecological range sites --- Parker mountain [E85-10050] p 8 N85-16246
- RAYLEIGH SCATTERING**
- LANDSAT-4 Thematic Mapper calibration and atmospheric correction p 68 N85-21734
- REAL TIME OPERATION**
- Realtime processor of SAR systems p 60 A85-25855
- RECEIVERS**
- Method of measuring sea surface water temperature with a satellite including wideband passive synthetic-aperture multichannel receiver [NASA-CASE-NPO-15651-1] p 41 N85-21723
- RECONNAISSANCE SPACECRAFT**
- A method for determining mesoscale dynamic topography [AD-D011412] p 40 N85-17506
- REFLECTANCE**
- Estimation of agronomic variables using spectral signatures p 2 A85-23753
- The measurement of bidirectional reflectances by analysis of Landsat images p 2 A85-23756
- Prospecting from the skies p 23 A85-29405
- The extension of an invertible coniferous forest canopy reflectance model using SIR-B and LANDSAT data p 10 N85-17246
- Preliminary evaluation of the airborne imaging spectrometer for vegetation analysis [NASA-CR-174440] p 12 N85-19496
- Radiometric calibration and processing procedure for reflective bands on LANDSAT-4 prototype Thematic Mapper p 66 N85-20510
- In-progress absolute radiometric inflight calibration of the LANDSAT-4 sensors --- New Mexico p 68 N85-21733
- Investigations of vegetation and soils information contained in LANDSAT Thematic Mapper and Multispectral Scanner data [E85-10082] p 12 N85-21747
- REGIONAL PLANNING**
- The management of atmospheric resources in food production p 9 N85-16362
- REGRESSION ANALYSIS**
- Exploring the use of structural models to improve remote sensing agricultural estimates p 9 N85-16259
- Calibration or inverse regression Which is appropriate for crop surveys using LANDSAT data? p 9 N85-16260
- REMANENCE**
- Viscous remanent magnetization model for the Broken Ridge satellite magnetic anomaly p 22 A85-26423
- REMOTE SENSING**
- Methodological study of spectral band selection for multispectral remote sensing p 55 A85-19363
- Remote sensing by radar altimetry p 26 A85-19428
- On realizing the potential of the earth-looking vantage point [AIAA PAPER 85-0195] p 70 A85-19580
- Determination of the external-orientation elements of aerial and space photographs in the remote sensing of dynamic processes and phenomena p 56 A85-19998
- Aircraft and satellite measurement of ocean wave directional spectra using scanning-beam microwave radars p 27 A85-20486
- Perspectives of remote sensing in Europe at the end of the decade p 70 A85-20565
- International cooperation in remote sensing applications p 70 A85-20566
- Status and plans for the SPOT program and the launch of SPOT 1 - Its on-ground processing and data dissemination to users p 56 A85-20568
- The integrated use of digital cartographic data and remotely sensed imagery p 45 A85-20572
- The educational role of satellites p 70 A85-20574
- Education and training in satellite remote sensing applications - Guide to education and training opportunities p 71 A85-20640
- The U.S. civil operational remote sensing program opportunities for the present and future p 71 A85-20641
- Commercialization of remote sensing data - Its impact on the continuity and accessibility of remote sensing data, including response to standing orders as well as on the standardization of products p 71 A85-20642
- Remote sensing development in the People's Republic of China p 56 A85-20643
- Study on a regional geographical information system and application model p 13 A85-20644
- Status of remote sensing information systems with special emphasis on their specializations, capabilities, accessibilities and future directions p 71 A85-20646
- Needs and accessibility of developing countries for/to remote sensing information systems p 13 A85-20647
- Calculation of thermal inertia from day-night measurements separated by days or weeks p 45 A85-21048
- Advances in microwave remote sensing of the ocean and atmosphere p 28 A85-21960
- Measuring spectra of and lands p 20 A85-21975
- The Harp probe - An in situ Bragg scattering sensor p 28 A85-22171
- Effect of heliotropism on the bidirectional reflectance of irrigated cotton p 1 A85-22420
- The Thematic Mapper - Instrument overview and preliminary on-orbit results p 56 A85-22681
- Large scan mirror assembly of the new Thematic Mapper developed for Landsat 4 earth resources satellite p 56 A85-22682
- Airborne microwave measurements of the southern Greenland ice sheet p 28 A85-23644
- Satellite microwave remote sensing p 28 A85-23676
- SEASAT - A key element of the EARTHNET programme --- program for distribution of remote sensing data to Europe p 46 A85-23679
- Seasat over land p 57 A85-23693
- A survey of some recent scientific results from the Seasat altimeter p 30 A85-23696
- Spectral signatures of objects in remote sensing, International Conference, 2nd, Bordeaux, France, September 12-16, 1983, Reports p 57 A85-23751
- Angular and spatial variability of visible and NIR spectral data p 2 A85-23752
- Estimation of agronomic variables using spectral signatures p 2 A85-23753
- Lidar applications in remote sensing of ocean properties p 31 A85-23755
- Comparative seasonal evolution of the spectral signatures of broad-leaved and coniferous trees from Landsat data Comparison with other perennial surfaces p 2 A85-23757
- Analysis of ground radiometric measurements in the rice-growing site at Taman (Republic of Mali) - Effect of certain yield parameters on the spectral signature p 2 A85-23758
- Comparison of SPOT HRV and Landsat-4 TM for crop inventories p 3 A85-23762
- Estimation of wheat production on the basis of Landsat channel 5 and 7 radiometric measurements p 3 A85-23763
- Estimation of evapotranspiration on the basis of thermal IR p 3 A85-23765
- Inventory of geographically homogeneous zones by spectral modeling of diachronic Meteorol albedo or combined albedo/thermal-channel data - Applications to the Maghreb and to Sahelian Africa p 46 A85-23769
- Microwave properties of vegetation canopies - An overview p 4 A85-23772
- Radargrammetry of Shuttle Imaging Radar-B experiment p 46 A85-23779
- Use of satellite data in agricultural surveys p 4 A85-23782
- Regional analysis from data from heterogeneous pixels - Remote sensing of total dry matter production in the Senegalese Sahel p 47 A85-23783
- Geomorphology and remote sensing Numerical inventory of objects in Landsat, SPOT simulation, and SIR-A data Applications to the Mopti-Bandiagara (Mali) region p 21 A85-23785
- Influence of spatial variability of soil hydraulic characteristics on surface parameters obtained from remote-sensing data in thermal infrared and microwaves p 43 A85-23786
- Independent variables in remote sensing as a function of landcover type p 47 A85-23788
- Experiments concerning radiometric measurements and natural-object indicators in order to apply corrections to recordings of satellite remote sensing p 58 A85-23789
- Classification of the geological environments of Anticosti Island - An approach using a Landsat-4 spectral simulation p 21 A85-23790
- Interpretation of thermal infrared data to augment spectral signatures p 47 A85-23791
- Review of earth observation satellite programs p 59 A85-23795
- Radiophysical techniques employed for sea ice investigations p 31 A85-24077
- Polarization effects in sea-ice signatures p 31 A85-24078
- Microwave signatures of the sea ice in the East Greenland Current p 31 A85-24079
- Interpretation of aircraft sea ice microwave data p 32 A85-24080
- Retrieval of snow water equivalent from Nimbus-7 SMMR data Effect of land-cover categories and weather conditions p 43 A85-24082
- EROS main image file - A picture perfect database for Landsat imagery and aerial photography p 48 A85-24521
- American Congress on Surveying and Mapping and American Society of Photogrammetry, Fall Convention, Salt Lake City, UT, September 19-23, 1983, Technical Papers p 14 A85-24950
- Satellite passive microwave rain rate measurement over croplands during spring, summer and fall p 4 A85-25181
- Comments on 'Inference of cloud temperature and thickness by microwave radiometry from space' p 59 A85-25182
- Airborne snow water equivalent and soil moisture measurement using natural terrestrial gamma radiation p 43 A85-25352
- Spectral characterization of vegetation canopies in the visible and NIR - Application to remote sensing p 5 A85-25670
- Realtime processor of SAR systems p 60 A85-25855
- Investigations of the accuracy of the digital photogrammetry system DPS, a rigorous three dimensional compilation process for push broom imagery [MBB-UA-753/83-OE] p 60 A85-26393
- The potential of satellite remote sensing of ecological conditions for survey and forecasting desert-locust activity p 5 A85-26934
- International Symposium on Microwave Signatures in Remote Sensing, 3rd, Toulouse, France, January 16-20, 1984, Proceedings p 6 A85-26942
- Soil moisture content estimation by radar survey data during the sowing campaign p 6 A85-26947
- A computationally-efficient maximum-likelihood classifier employing prior probabilities for remotely-sensed data p 49 A85-26948
- MOMS 1 and its results p 61 A85-27061
- Remote sensing techniques for monitoring of pollution in coastal waters - Potential application to Saudi Arabia p 34 A85-27441

Asian Conference on Remote Sensing, 4th, Colombo, Sri Lanka, November 10-15, 1983, Proceedings p 71 A85-27519

Frontiers for geological remote sensing from space, Geosat Workshop, 4th, Flagstaff, AZ, June 12-17, 1983, Report p 22 A85-27943

Near-infrared spectroscopy in geological reconnaissance and exploration p 22 A85-27944

Imaging systems for the delineation of spectral properties of geologic materials in the visible and near-infrared p 22 A85-27945

The importance of geobotany in geological remote sensing applications p 23 A85-27948

Detection of lowland flooding using active microwave systems p 43 A85-29218

Remote sensing of water quality in the Neuse River Estuary, North Carolina p 43 A85-29219

Monitoring water quality conditions in a large western reservoir with Landsat imagery p 43 A85-29220

The effects of image noise on digital correlation probability p 49 A85-29221

Prospecting from the skies p 23 A85-29405

Determination of the physical parameters of sea ice on the basis of remote microwave measurements in the 0-3-18 cm range p 38 A85-29903

Methods for the study of recent tectonics on the basis of remote sensing and ground data p 23 A85-29904

Possibilities of using remote-sensing methods to improve the efficiency of oil and gas exploration p 24 A85-29905

Determination of soil moisture content by microwave radiometry with the use of a priori information p 6 A85-29910

Radar mapping of the moisture of open soils p 6 A85-29911

Identification of homogeneous regions with incomplete boundaries on an image p 24 A85-29912

Segmentation of half-tone remote-sensing images by the level lines method p 49 A85-29913

The use of a priori estimation of the conditions of the observation of the earth surface from space for a rational selection of the time at which the survey is conducted p 50 A85-29914

Remote-sensing observations of advective eddies in the central part of the Baltic Sea p 38 A85-29915

Computing the foliage angle distribution from contact frequency data p 6 A85-29969

Comparative study of Suits and SAIL canopy reflectance models p 7 A85-30092

Intermediate results of radar backscatter measurements from summer sea ice p 38 A85-15960

[AD-A147212] p 38 A85-15960

Enhancement of multispectral scanner images by digital filtering [ESA-TT-624] p 63 A85-16284

Geological, structural, and geomorphological analyses from SIR-B p 24 A85-17226

Microwave and optical remote sensing of forest vegetation p 9 A85-17228

Evaluation of SIR-B imagery for geologic and geomorphic mapping, hydrology, and oceanography in Australia p 51 A85-17229

Interlobate comparison of glacial-depositional style as evidenced by small-relief glacial landscape features in Illinois, Indiana, and Ohio, utilizing SIR-B p 39 A85-17231

Evaluation of the L-band scattering characteristics of volcanic terrain in aid of lithologic identification, assessment of SIR-B calibration, and development of planetary geomorphic analogs p 24 A85-17232

The investigation of selected oceanographic applications of spaceborne synthetic-aperture radar p 39 A85-17233

Investigation of SIR-B images for lithologic mapping p 25 A85-17241

Remote sensing of soil moisture p 10 A85-17252

Spaceborne microwave radiometers Background and technology requirements p 63 A85-17350

[LD-R-267] p 63 A85-17350

Papers of the 15th International Society for Photogrammetry and Remote Sensing (ISPRS) Congress --- conferences p 63 A85-17406

[TRITA-FMI-9] p 63 A85-17406

Resolution enhancement of multichannel microwave imagery from the Nimbus-7 SMMR for maritime rainfall analysis [NASA-CR-174367] p 44 A85-19221

CNES, INRA do joint remote-sensing research p 11 A85-19321

Brazilian Remote Sensing Shuttle Experiment (BRESEX) Characteristics and future utilization on satellites [INPE-3313-PRE/620] p 64 A85-19385

Brazilian remote sensing receiving, recording and processing ground systems in the 1980's [E85-10079] p 52 A85-19493

Preliminary evaluation of the airborne imaging spectrometer for vegetation analysis [NASA-CR-174440] p 12 A85-19496

SIR-A imagery in geologic studies of the Sierra Madre Oriental, northeastern Mexico Part 1 (Regional stratigraphy) The use of morphostratigraphic units in remote sensing mapping [NASA-CR-175457] p 25 A85-19497

Remote sensing activities in Latin America [INPE-3297-PRE/612] p 64 A85-19501

The sharing of remote sensing techniques in Brazilian geographic research [INPE-3307-PRE/617] p 15 A85-19502

Nautical charting with remotely sensed imagery, volume 1 [AD-A149361] p 41 A85-19503

Nautical charting with remotely sensed imagery Volume 2 Case studies [AD-A149362] p 41 A85-19504

Remote sensing technology now playing practical roles p 64 A85-20190

Airborne remote sensing CCD imaging system p 65 A85-20220

Earth observations and the polar platform [NOAA-TR-NESDIS-18] p 15 A85-20517

The spot operational remote sensing satellite system Current status and perspectives p 67 A85-20776

Preserve the sense of Earth from space --- achieves of remote sensing data [PB85-124121] p 72 A85-20942

Passive microwave remote sensing for sea ice research [NASA-CR-175570] p 42 A85-21758

REMOTE SENSORS

Survey of multispectral imaging systems for earth observations p 56 A85-22424

SEASAT-data acquisition and processing by the Royal Aircraft Establishment p 57 A85-23678

Development of a SPOT-simulation radiometer p 57 A85-23759

Performance of a coherent lidar remote sensor in snow and fog p 59 A85-25347

The utility of data from various airborne sensors for soil mapping p 5 A85-26932

Modular Optoelectronic Multispectral Scanner (MOMS) Technological aspects p 61 A85-27059

MOMS 1 and its results p 61 A85-27061

Intercomparisons of TOMS, SBUV and MFR satellite ozone measurements --- Satellite Backscattered Ultraviolet, Total Ozone Mapping System, Multichannel Filter Radiometer p 62 A85-29784

Thematic Mapper Volume 1 Calibration report flight model, LANDSAT 5 [E85-10059] p 63 A85-16270

Thematic Mapper Volume 2 Flight model preshipment review [E85-10060] p 63 A85-16271

Nautical charting with remotely sensed imagery, volume 1 [AD-A149361] p 41 A85-19503

Spectral characterization of the LANDAT-4 MSS sensors p 65 A85-20499

LANDSAT-4 Science Characterization Early Results Volume 2, part 1 Thematic Mapper (TM) [E85-10068] p 66 A85-20508

An overview of LANDSAT-4 and the Thematic Mapper p 66 A85-20509

Spatial resolution estimation of LANDSAT-4 Thematic Mapper data p 69 A85-21741

RESEARCH AND DEVELOPMENT

On realizing the potential of the earth-looking vantage point [AIAA PAPER 85-0195] p 70 A85-19580

Remote sensing development in the People's Republic of China p 56 A85-20643

RESERVOIRS

Monitoring water quality conditions in a large western reservoir with Landsat imagery p 43 A85-29220

RESIDENTIAL AREAS

Population estimation from aerial photos for non-homogeneous urban residential areas p 14 A85-20749

RESOURCES MANAGEMENT

The management of atmospheric resources in food production p 9 A85-16362

An integrated GIS/remote sensing data base in North Cache soil conservation district, Utah A pilot project for the Utah Department of Agriculture's RIMS (Resource Inventory and Monitoring System) [E85-10073] p 11 A85-19487

Remote sensing technology now playing practical roles p 64 A85-20190

Remote sensing research for agricultural applications --- San Joaquin County, California and Snake River Plain and Twin Falls area, Idaho [E85-10090] p 13 A85-21752

Building a functional, integrated GIS/remote sensing resource analysis and planning system --- Utah [E85-10092] p 15 A85-21754

RING STRUCTURES

Ring structures observed on space radar images of the earth p 45 A85-20084

RIVER BASINS

Deforestation, floodplain dynamics, and carbon biogeochemistry in the Amazon Basin p 44 A85-17216

RIVERS

Determination of water surfaces in northwest Bohemia on the basis of satellite data p 44 A85-29906

Image-to-image correspondence Linear structure matching p 51 A85-16266

RURAL LAND USE

Method for sequential analysis of spatial development in a rural-urban fringe zone p 13 A85-20748

S

S MATRIX THEORY

Earth observation modeling based on layer scattering matrices p 7 A85-30091

SALINITY

Investigation of salty soils and salines on the basis of space remote-sensing methods p 6 A85-29908

SALT BEDS

Characteristics of playa deposits as seen on SIR-A, Seasat and Landsat coregistered data p 21 A85-23793

SAN FRANCISCO (CA)

Characterizing the scientific potential of satellite sensors --- San Francisco, California [E85-10044] p 62 A85-16244

Characterizing the scientific potential of satellite sensors --- San Francisco, California [E85-10053] p 62 A85-16249

Impact of LANDSAT MSS sensor differences on change detection analysis --- New Mexico, San Francisco, CA, New Hampshire, and Connecticut p 65 A85-20506

SAN FRANCISCO BAY (CA)

Development of water quality models applicable throughout the entire San Francisco Bay and Delta p 42 A85-21046

SATELLITE GROUND SUPPORT

Commercialization of remote sensing data - Its impact on the continuity and accessibility of remote sensing data, including response to standing orders as well as on the standardization of products p 71 A85-20642

SATELLITE GROUND TRACKS

Altitude, orbits and tides [E85-10066] p 40 A85-17404

SATELLITE IMAGERY

Methodological study of spectral band selection for multispectral remote sensing p 55 A85-19363

Complex studies of the environment by optical and radar methods p 56 A85-20081

On the application of meteorological satellite imagery for monitoring the environment p 13 A85-20570

Microcomputer systems for satellite image processing p 56 A85-20571

The integrated use of digital cartographic data and remotely sensed imagery p 45 A85-20572

An example of Landsat cost effectiveness in mapping land-cover p 1 A85-20573

The educational role of satellites p 70 A85-20574

Education and training in satellite remote sensing applications - Guide to education and training opportunities p 71 A85-20640

Development of water quality models applicable throughout the entire San Francisco Bay and Delta p 42 A85-21046

Determining stretch parameters for lithologic discrimination on Landsat MSS band-ratio images p 20 A85-21047

Calculation of thermal inertia from day-night measurements separated by days or weeks p 45 A85-21048

On the separability of various classes from the GOES visible and infrared data --- of winter cloud and snow cover p 45 A85-21138

African land-cover classification using satellite data p 1 A85-21174

Mapping of landforms from Landsat imagery - An example from eastern New South Wales, Australia p 21 A85-22422

Separating clouds from ocean in infrared images p 28 A85-22423

The Thematic Mapper - Instrument overview and preliminary on-orbit results p 56 A85-22681

Large scan mirror assembly of the new Thematic Mapper developed for Landsat 4 earth resources satellite p 56 A85-22682

- Satellite microwave remote sensing p 28 A85-23676
- A review of SEASAT --- ocean surface imagery p 28 A85-23677
- SEASAT-data acquisition and processing by the Royal Aircraft Establishment p 57 A85-23678
- SEASAT - A key element of the EARTHNET programme --- program for distribution of remote sensing data to Europe p 46 A85-23679
- Validation and applications of SASS over JASIN --- wind scatterometer results in Atlantic NW of Scotland p 29 A85-23681
- The Canadian SAR experience p 46 A85-23689
- Expressions of bathymetry on Seasat synthetic radar images p 29 A85-23691
- Tidal current bedforms investigated by Seasat p 30 A85-23692
- Spatial variation of significant wave-height p 30 A85-23704
- The measurement of bidirectional reflectances by analysis of Landsat images p 2 A85-23756
- Study of the correlation between the IRT band of the NOAA AVHRR and the factors conditioning the thermal behavior of bioclimatic areas on a regional scale p 58 A85-23768
- Inventory of geographically homogeneous zones by spectral modeling of diachronic Meteosat albedo or combined albedo/thermal-channel data - Applications to the Maghreb and to Sahelian Africa p 46 A85-23769
- Use of HCMM thermal images in the study of microclimates in a mountainous region p 3 A85-23771
- Demonstration, analysis, and correction of atmospheric effects on Landsat or SPOT multispectral data p 58 A85-23781
- Use of satellite data in agricultural surveys p 4 A85-23782
- Regional analysis from data from heterogeneous pixels - Remote sensing of total dry matter production in the Senegalese Sahel p 47 A85-23783
- Geomorphology and remote sensing Numerical inventory of objects in Landsat, SPOT simulation, and SIR-A data Applications to the Mopti-Bandiagara (Mali) region p 21 A85-23785
- Independent variables in remote sensing as a function of landcover type p 47 A85-23788
- Generation of a Landsat-HCMM combined image and its application to geological cartography p 21 A85-23792
- Characteristics of playa deposits as seen on SIR-A, Seasat and Landsat coregistered data p 21 A85-23793
- Multispectral data compression using staggered detector arrays p 47 A85-24277
- Determination of visual range from Landsat data p 47 A85-24285
- EROS main image file - A picture perfect database for Landsat imagery and aerial photography p 48 A85-24521
- Dramatic contrast between low clouds and snow cover in daytime 3.7 micron imagery p 48 A85-24740
- Observations of the earth using nighttime visible imagery p 48 A85-25350
- Features characterizing the development of mushroom-shaped currents in the ocean, revealed by an analysis of satellite imagery p 34 A85-25651
- Effect of meteorological conditions on the characteristics of space radar images of the earth surface p 48 A85-25653
- Interpretation of space images of the sea surface using the SVIT digital-processing complex p 34 A85-25654
- Analysis of mesofractures according to space images - Currents trends in the exploration for oil and gas deposits p 21 A85-25655
- Identification of the structure of soil-vegetation cover using aerial and space images p 5 A85-25656
- Correlation of spectral brightnesses measured using multispectral space images p 60 A85-25659
- Features of the digital processing of radar images obtained with the sidelooking radar of the Cosmos-1500 satellite p 48 A85-25660
- Digital correlation of images along quasi-epipolar lines by successive approximations p 48 A85-25671
- The influence of satellite spectral sensor response on the analysis of satellite imagery at high latitudes p 60 A85-26927
- The current use of TIROS-N series of meteorological satellites for land-cover studies p 60 A85-26928
- Monitoring Africa's Lake Chad basin with Landsat and NOAA satellite data p 43 A85-26930
- The potential of satellite remote sensing of ecological conditions for survey and forecasting desert-locust activity p 5 A85-26934
- Experimental evidence for spring and autumn windows for the detection of geobotanical anomalies through the remote sensing of overlying vegetation p 6 A85-26939
- Asian Conference on Remote Sensing, 4th, Colombo, Sri Lanka, November 10-15, 1983, Proceedings p 71 A85-27519
- An automatic high-resolution picture transmission receiving station p 61 A85-27698
- Imaging systems for the delineation of spectral properties of geologic materials in the visible and near-infrared p 22 A85-27945
- Thematic mapper data analysis p 23 A85-27946
- Developments with multispectral thermal-IR and active microwave systems - TMS, SIR-A, SIR-B, and radarsat p 62 A85-27947
- Mapping of glacial landforms from Seasat radar images p 36 A85-28027
- Space remote-sensing data in geology --- Russian book p 23 A85-28400
- Investigation of the properties of natural objects by the canonical-correlation method p 49 A85-28973
- Integration of the SPOT panchromatic channel into its multispectral mode for image sharpness enhancement p 49 A85-29217
- Remote sensing of water quality in the Neuse River Estuary, North Carolina p 43 A85-29219
- Monitoring water quality conditions in a large western reservoir with Landsat imagery p 43 A85-29220
- Determination of water surfaces in northwest Bohemia on the basis of satellite data p 44 A85-29906
- Investigation of salty soils and -salines on the basis of space remote-sensing methods p 6 A85-29908
- Segmentation of half-tone remote-sensing images by the level lines method p 49 A85-29913
- Thermal structure of an agricultural region as seen by NOAA-7 AVHRR p 7 A85-30090
- Application of Thematic Mapper data to corn and soybean development stage estimation p 7 A85-30093
- Characterizing the scientific potential of satellite sensors --- San Francisco, California p 62 A85-16244
- [E85-10044]
- Characterizing the scientific potential of satellite sensors --- San Francisco, California p 62 A85-16249
- [E85-10053]
- Landsat-4 Thematic Mapper Modulation Transfer Function (MTF) evaluation --- California and New Mexico p 62 A85-16250
- [E85-10055]
- Proceedings of the Second Annual Symposium on Mathematical Pattern Recognition and Image Analysis Program p 50 A85-16251
- [E85-10056]
- Exploring the use of structural models to improve remote sensing agricultural estimates p 9 A85-16259
- Calibration or inverse regression Which is appropriate for crop surveys using LANDSAT data? p 9 A85-16260
- Rectification of single and multiple frames of satellite scanner imagery using points and edges as control p 51 A85-16263
- The influence of the number of ground control points on the scene-to-map registration accuracy --- Kansas, Louisiana, Mississippi, and Missouri p 51 A85-16264
- Resolution enhancement of multichannel microwave imagery from the Nimbus-7 SMMR for maritime rainfall analysis p 44 A85-19221
- [NASA-CR-174367]
- Assessment of LANDSAT for rangeland mapping, Rush Valley, Utah p 15 A85-19486
- [E85-10072]
- Analysis of the quality of image data required by the Landsat-4 Thematic Mapper and Multispectral Scanner --- agricultural and forest cover types in California p 11 A85-19488
- [E85-10074]
- Thematic Mapper Design through flight evaluation p 64 A85-19492
- [E85-10078]
- The sharing of remote sensing techniques in Brazilian geographic research p 15 A85-19502
- [INPE-3307-PRE/617]
- Landsat-4 Science Characterization Early Results Volume 1 Multispectral Scanner (MSS) p 65 A85-20496
- [E85-10067]
- Summary of MSS characterization investigations p 53 A85-20497
- Radiometric accuracy assessment of Landsat 4 Multispectral Scanner data p 53 A85-20498
- Investigation of radiometric properties of Landsat-4 MSS --- California, North Carolina, South Carolina, and New England p 65 A85-20500
- Radiometric calibration and geocoded precision processing of Landsat-4 Multispectral Scanner products by the Canada Centre for Remote Sensing p 53 A85-20501
- Geodetic accuracy of Landsat 4 Multispectral Scanner and Thematic Mapper data --- Washington, DC, California, Alabama, South Dakota, and Illinois p 53 A85-20504
- Geometric accuracy assessment of Landsat-4 Multispectral Scanner (MSS) data p 19 A85-20505
- LS-4 MSS geometric correction Methods and results p 53 A85-20507
- Landsat-4 Science Characterization Early Results Volume 2, part 1 Thematic Mapper (TM) p 66 A85-20508
- [E85-10068]
- TM digital image products for applications p 54 A85-20512
- Canadian plans for Thematic Mapper data p 54 A85-20513
- Landsat-4 Science Characterization Early Results Volume 3, part 2 Thematic Mapper (TM) p 67 A85-21724
- [E85-10069]
- A preliminary assessment of Landsat-4 Thematic Mapper data --- Windsor, Ontario and Medicine Hat areas, Canada p 54 A85-21728
- Evaluation of the radiometric quality of the TM data using clustering, linear transformations and multispectral distance measures --- Illinois p 54 A85-21731
- TM geometric performance Line to Line Displacement Analysis (LLDA) --- New Mexico p 68 A85-21732
- In-progress absolute radiometric inflight calibration of the Landsat-4 sensors --- New Mexico p 68 A85-21733
- Scan angle and detector effects in Thematic Mapper radiometry --- Iowa and Arkansas p 68 A85-21735
- Thematic Mapper spectral dimensionality and data structure p 12 A85-21736
- Intraband radiometric performance of the Landsat 4 Thematic Mapper --- Washington, DC, Arkansas, Massachusetts, Virginia, and Arizona p 69 A85-21738
- Tests of low-frequency geometric distortions in Landsat 4 images p 55 A85-21744
- Investigation of TM band-to-band registration using the JSC registration processor p 69 A85-21745
- The development of image processing of NOAA AVHRR data and its application to sea surface temperature p 42 A85-21891
- SATELLITE INSTRUMENTS**
- Thematic Mapper Volume 1 Calibration report flight model, Landsat 5 p 63 A85-16270
- [E85-10059]
- Thematic Mapper Volume 2 Flight model preshipment review p 63 A85-16271
- [E85-10060]
- SATELLITE OBSERVATION**
- An intercalibration of Meteosat-1 and GOES-2 visible and infrared measurements p 26 A85-19420
- Remote sensing by radar altimetry p 26 A85-19428
- Satellite magnetic anomalies over subduction zones - The Aleutian Arc anomaly p 16 A85-21107
- African land-cover classification using satellite data p 1 A85-21174
- Altimeter measurements of ocean topography p 30 A85-23695
- Effects of the experimental errors and conditions on the estimation of thermal inertia and evapotranspiration from METEOSAT data p 3 A85-23767
- Review of earth observation satellite programs p 59 A85-23795
- Large-scale oceanographic experiments and satellites, Proceedings of the Advanced Research Workshop, Porto Vecchio, Corse, France, October 3-7, 1983 p 32 A85-24551
- A sampling strategy for altimeter measurements of the global statistics of mesoscale eddies p 32 A85-24553
- Satellite measurements of sea-surface temperature for climate research p 32 A85-24555
- Satellite sea surface temperature determination from microwave and infrared radiometry p 33 A85-24556
- Wind speed and stress over the ocean - Scatterometer versus surface measurements p 33 A85-24557
- A summary of the wind data available from satellites from the past history to future sensors p 33 A85-24558
- The diurnal variation of Atlantic Ocean tropical cyclone cloud distribution inferred from geostationary satellite infrared measurements p 33 A85-24739
- Satellite passive microwave rain rate measurement over croplands during spring, summer and fall p 4 A85-25181
- Comments on 'Inference of cloud temperature and thickness by microwave radiometry from space' p 59 A85-25182
- Spectral characterization of vegetation canopies in the visible and NIR - Application to remote sensing p 5 A85-25670
- Introduction to the special issue - A perspective on Magsat results p 16 A85-26401
- An estimation of continental crust magnetization and susceptibility from Magsat data for the conterminous United States p 22 A85-26420

- Crustal structure of the Churchill-Superior boundary zone between 80 and 98 deg W longitude from Magsat anomaly maps and stacked passes p 22 A85-26421
- Viscous remanent magnetization model for the Broken Ridge satellite magnetic anomaly p 22 A85-26423
- The 1982 El Chichon Volcano eruptions - A satellite perspective p 14 A85-27984
- Estimating ocean primary production from satellite chlorophyll - Introduction to regional differences and statistics for the Southern California Bight p 35 A85-28005
- Satellite observations of sea ice p 36 A85-28022
- Methods of space geodesy and its role in earth studies p 19 A85-30013
- Autoregressive spectral estimation for two dimensional time series p 50 A85-16258
- North American vegetation patterns observed with the NOAA-7 advanced very high resolution radiometer --- North America p 10 A85-17400
- [E85-10062] p 10 A85-17400
- Remote sensing activities in Latin America p 64 A85-19501
- [INPE-3297-PRE/612] p 64 A85-19501
- Rain volume estimation over areas using satellite and radar data p 44 A85-19568
- [NASA-CR-174434] p 44 A85-19568
- Preserve the sense of Earth from space --- achieves of remote sensing data p 72 A85-20942
- SATELLITE ORBITS**
- Altitude, orbits and tides p 40 A85-17404
- [E85-10066] p 40 A85-17404
- SATELLITE SOUNDING**
- Double-angle method for measuring ocean surface temperature in the infrared p 34 A85-25658
- An examination of some problems and solutions in monitoring urban areas from satellite platforms p 14 A85-26935
- A comparison between GEOS 1 magnetic-field measurements and some models of the geomagnetic field p 18 A85-27386
- Estimation of lower crust magnetization from satellite derived anomaly field p 18 A85-28012
- A survey of oceanographic satellite altimetric missions p 36 A85-29703
- Observing global ocean circulation with SEASAT altimeter data p 36 A85-29705
- World ocean mean monthly waves, swell, and surface winds for July through October 1978 from SEASAT radar altimeter data p 37 A85-29707
- Swell in the Pacific Ocean observed by SEASAT radar altimeter p 37 A85-29708
- Regional mean sea surfaces based on GEOS-3 and SEASAT altimeter data p 38 A85-29716
- Intercomparisons of TOMS, SBUV and MFR satellite ozone measurements --- Satellite Backscattered Ultraviolet, Total Ozone Mapping System, Multichannel Filter Radiometer p 62 A85-29784
- Effect of vegetation on soil moisture sensing observed from orbiting microwave radiometers p 7 A85-30089
- SATELLITE TRANSMISSION**
- A comparative analysis of some prediction methods for rain attenuation statistics in earth-to-space links p 42 A85-21130
- SATELLITE-BORNE INSTRUMENTS**
- The space environment monitors onboard GOES [AIAA PAPER 85-0238] p 55 A85-19608
- The U S civil operational remote sensing program opportunities for the present and future p 71 A85-20641
- Advances in microwave remote sensing of the ocean and atmosphere p 28 A85-21960
- Measuring spectra of arid lands p 20 A85-21975
- A review of SEASAT --- ocean surface imagery p 28 A85-23677
- A survey of some recent scientific results from the Seasat altimeter p 30 A85-23696
- Gravity field investigation in the North Sea p 30 A85-23699
- Swell propagation in the North Atlantic ocean using SEASAT altimeter p 30 A85-23702
- Use of ocean skewness measurements in calculating the accuracy of altimeter height measurements p 30 A85-23703
- The scanning multichannel microwave radiometer - An assessment p 57 A85-23705
- The evaluation of SMRR retrieval algorithms --- Scanning Multichannel Microwave Radiometer p 31 A85-23706
- Aircraft measurements for calibration of an orbiting spacecraft sensor p 59 A85-24246
- Imaging systems for the delineation of spectral properties of geologic materials in the visible and near-infrared p 22 A85-27945
- Prospecting from the skies p 23 A85-29405
- The potential for ocean prediction and the role of altimeter data p 36 A85-29704
- On the determination of the deflection of the vertical by satellite altimetry --- for marine geoid height estimates p 37 A85-29706
- An analysis of a satellite multibeam altimeter p 38 A85-29715
- Intercomparisons of TOMS, SBUV and MFR satellite ozone measurements --- Satellite Backscattered Ultraviolet, Total Ozone Mapping System, Multichannel Filter Radiometer p 62 A85-29784
- Conical multispectral scanner for the study of earth resources p 62 A85-29909
- Spaceborne microwave radiometers Background and technology requirements p 63 A85-17350
- [LD-R-267] p 63 A85-17350
- Method of measuring sea surface water temperature with a satellite including wideband passive synthetic-aperture multichannel receiver [NASA-CASE-NPO-15651-1] p 41 A85-21723
- Spatial resolution estimation of LANDSAT-4 Thematic Mapper data p 69 A85-21741
- On the P1 data from GMS-SEM p 15 A85-21890
- SATELLITE-BORNE PHOTOGRAPHY**
- Investigation of Krasnovodsk bay on the basis of space photographs p 28 A85-21669
- Minimization of the effect of the earth's curvature in the projective transformation of space images into photoplans and photomaps p 16 A85-25662
- Methods for the study of recent tectonics on the basis of remote sensing and ground data p 23 A85-29904
- Possibilities of using remote-sensing methods to improve the efficiency of oil and gas exploration p 24 A85-29905
- Comprehensive desertification maps and methods for making such maps on the basis of space photographs p 14 A85-29907
- The use of a priori estimation of the conditions of the observation of the earth surface from space for a rational selection of the time at which the survey is conducted p 50 A85-29914
- SATELLITE-BORNE RADAR**
- Remote sensing by radar altimetry p 26 A85-19428
- Predicting dangerous ocean waves with spaceborne synthetic aperture radar p 27 A85-19429
- Ring structures observed on space radar images of the earth p 45 A85-20084
- Wave measurements with the Seasat radar altimeter - A Review p 30 A85-23701
- Simultaneous ocean cross-section and rainfall measurements from space with a nadir pointing radar p 36 A85-28788
- Earth resources research using the Shuttle Imaging Radar system p 67 A85-20779
- SAUDI ARABIA**
- Remote sensing techniques for monitoring of pollution in coastal waters - Potential application to Saudi Arabia p 34 A85-27441
- SCATTERING COEFFICIENTS**
- The analysis of backscattering properties from SAR data of mountain regions p 59 A85-24081
- SCATTERING CROSS SECTIONS**
- The reflection of airborne UV laser pulses from the ocean p 37 A85-29714
- SCATTEROMETERS**
- The Harp probe - An in situ Bragg scattering sensor p 28 A85-22171
- Validation and applications of SASS over JASIN --- wind scatterometer results in Atlantic NW of Scotland p 29 A85-23681
- Wind speed and stress over the ocean - Scatterometer versus surface measurements p 33 A85-24557
- Information for space radar designers Required dynamic range vs resolution and antenna calibration using the Amazon rain forest p 44 A85-17239
- SCENE ANALYSIS**
- Use of satellite data in agricultural surveys p 4 A85-23782
- Texture classification using autoregressive filtering p 50 A85-16254
- SEA BREEZE**
- Airborne Doppler estimates of the air motions associated with a developing, sea-breeze induced, mesoscale precipitation line p 36 A85-28783
- SEA ICE**
- An algorithm to measure sea ice concentration with microwave radiometers p 27 A85-20492
- Spectral signatures of soil, snow and sea ice as observed by passive microwave and thermal infrared techniques p 58 A85-23784
- Radiophysical techniques employed for sea ice investigations p 31 A85-24077
- Polarization effects in sea-ice signatures p 31 A85-24078
- Microwave signatures of the sea ice in the East Greenland Current p 31 A85-24079
- Interpretation of aircraft sea ice microwave data p 32 A85-24080
- The effect of a snow cover on microwave backscatter from sea ice p 32 A85-24083
- Performance of an airborne imaging 92/183 GHz radiometer during the Bering Sea Marginal Ice Zone Experiment (MIZEX-WEST) p 33 A85-24945
- Ultrashort-wave radar subsurface sounding of sea ice and earth covers p 34 A85-25594
- Improvement of the accuracy of radar measurements of sea-ice thickness by cepstral processing of reflected signals p 35 A85-27736
- Satellite observations of sea ice p 36 A85-28022
- Determination of the physical parameters of sea ice on the basis of remote microwave measurements in the 0.3-18 cm range p 38 A85-29903
- Intermediate results of radar backscatter measurements from summer sea ice [AD-A147212] p 38 A85-15960
- Data report on variations in the composition of sea ice during MIZEX-East'83 with the Nimbus-7 SMRR [NASA-TM-86170] p 40 A85-18443
- Atlas of the Beaufort Sea [AD-A149545] p 41 A85-20619
- SEA LEVEL**
- Electromagnetic bias of 36-GHz radar altimeter measurements of MSL --- Mean Sea Level p 37 A85-29712
- Electromagnetic bias of 10-GHz radar altimeter measurements of MSL p 37 A85-29713
- SEA ROUGHNESS**
- Expressions of bathymetry on Seasat synthetic radar images p 29 A85-23691
- Surface scattering effects at different spectral regions p 58 A85-23780
- Simultaneous radiometric and radar altimetric measurements of sea microwave signatures p 31 A85-24076
- The spatial evolution of the directional wave spectrum in the Southern Ocean Its relation to extreme waves in Agulhas Current p 39 A85-17213
- SEA SURFACE TEMPERATURE**
- The scanning multichannel microwave radiometer - An assessment p 57 A85-23705
- Satellite measurements of sea-surface temperature for climate research p 32 A85-24555
- Satellite sea surface temperature determination from microwave and infrared radiometry p 33 A85-24556
- Double-angle method for measuring ocean surface temperature in the infrared p 34 A85-25658
- Variations in atmospheric mixing height across oceanic thermal fronts p 34 A85-27704
- Method of measuring sea surface water temperature with a satellite including wideband passive synthetic-aperture multichannel receiver [NASA-CASE-NPO-15651-1] p 41 A85-21723
- The development of image processing of NOAA AVHRR data and its application to sea surface temperature p 42 A85-21891
- SEA TRUTH**
- Gravity field investigation in the North Sea p 30 A85-23699
- SEA WATER**
- Estimating ocean primary production from satellite chlorophyll - Introduction to regional differences and statistics for the Southern California Bight p 35 A85-28005
- SEAMOUNTS**
- Intermediate-wavelength magnetic anomaly field of the North Pacific and possible source distributions p 17 A85-26414
- Lagrangian observations of surface circulation at the Emperor Seamount chain p 35 A85-27710
- SEASAT SATELLITES**
- Satellite microwave remote sensing p 28 A85-23676
- A review of SEASAT --- ocean surface imagery p 28 A85-23677
- SEASAT-data acquisition and processing by the Royal Aircraft Establishment p 57 A85-23678
- SEASAT - A key element of the EARTHNET programme --- program for distribution of remote sensing data to Europe p 46 A85-23679
- The effect of a moving sea surface on SAR imagery p 29 A85-23685
- The Canadian SAR experience p 46 A85-23689
- The use of SEASAT-SAR data in oceanography at the IFP p 29 A85-23690
- Seasat over land p 57 A85-23693
- A survey of some recent scientific results from the Seasat altimeter p 30 A85-23696
- The altimetric geoid in the North Sea p 16 A85-23700
- Wave measurements with the Seasat radar altimeter - A Review p 30 A85-23701
- Use of ocean skewness measurements in calculating the accuracy of altimeter height measurements p 30 A85-23703

- Characteristics of playa deposits as seen on SIR-A, Seasat and Landsat coregistered data p 21 A85-23793
- Eddy kinetic energy distribution in the southern ocean from Seasat altimeter and FGGE drifting buoys p 32 A85-24554
- SEASAT 3 and 4 [AD-A148343] p 40 N85-17274
- Along-track deflection of the vertical from SEASAT GEBCO (General Bathymetric Chart of the Oceans) overlays [PB85-129641] p 42 N85-21767
- SEASAT 1**
- Validation and applications of SASS over JASIN --- wind scatterometer results in Atlantic NW of Scotland p 29 A85-23681
- SECULAR VARIATIONS**
- The secular period behavior of 38 RR Lyrae stars in the LMC globular cluster NGC 2257 p 14 A85-25070
- SEDIMENTARY ROCKS**
- Tidal current bedforms investigated by Seasat p 30 A85-23692
- SEDIMENTS**
- SIR-A imagery in geologic studies of the Sierra Madre Oriental, northeastern Mexico Part 1 (Regional stratigraphy) The use of morphostratigraphic units in remote sensing mapping [NASA-CR-175457] p 25 N85-19497
- SENEGAL**
- Regional analysis from data from heterogeneous pixels - Remote sensing of total dry matter production in the Senegalese Sahel p 47 A85-23783
- SEQUENTIAL ANALYSIS**
- Method for sequential analysis of spatial development in a rural-urban fringe zone p 13 A85-20748
- SHALLOW WATER**
- The investigation of selected oceanographic applications of spaceborne synthetic-aperture radar p 39 N85-17233
- SHIPS**
- SEASAT 3 and 4 [AD-A148343] p 40 N85-17274
- SHUTTLE IMAGING RADAR**
- Radargrammetry of Shuttle Imaging Radar-B experiment p 46 A85-23779
- Characteristics of playa deposits as seen on SIR-A, Seasat and Landsat coregistered data p 21 A85-23793
- Developments with multispectral thermal-IR and active microwave systems - TIMS, SIR-A, SIR-B, and radarsat p 62 A85-27947
- The SIR-B science investigations plan [NASA-CR-174282] p 63 N85-17208
- The interpretation of SIR-B imagery of surface waves and other oceanographic features using in-situ, meteorological satellite, and infrared satellite data p 39 N85-17212
- The spatial evolution of the directional wave spectrum in the Southern Ocean Its relation to extreme waves in Agulhas Current p 39 N85-17213
- Tectonic, volcanic, and climatic geomorphology study of the Sierras Pampeanas Andes, northwestern Argentina p 24 N85-17215
- Deforestation, floodplain dynamics, and carbon biogeochemistry in the Amazon Basin p 44 N85-17216
- Geological, structural, and geomorphological analyses from SIR-B p 24 N85-17226
- Microwave and optical remote sensing of forest vegetation p 9 N85-17228
- Evaluation of SIR-B imagery for geologic and geomorphic mapping, hydrology, and oceanography in Australia p 51 N85-17229
- Interlobate comparison of glacial-depositional style as evidenced by small-relief glacial landscape features in Illinois, Indiana, and Ohio, utilizing SIR-B p 39 N85-17231
- Evaluation of the L-band scattering characteristics of volcanic terrain in aid of lithologic identification, assessment of SIR-B calibration, and development of planetary geomorphic analogs p 24 N85-17232
- The investigation of selected oceanographic applications of spaceborne synthetic-aperture radar p 39 N85-17233
- SIR-B cartography and stereo topographic mapping p 19 N85-17234
- Monitoring of the tidal dynamics of the Dutch Waddensea by SIR-B p 40 N85-17235
- Structural investigation of the Canadian Shield by orbital radar and LANDSAT p 25 N85-17236
- Structural investigation of the Grenville Province by radar and other imaging and nonimaging sensors p 25 N85-17237
- Information for space radar designers Required dynamic range vs resolution and antenna calibration using the Amazon rain forest p 44 N85-17239
- Development and evaluation of techniques for using combined microwave and optical image data for vegetation studies p 9 N85-17240
- Investigation of SIR-B images for lithologic mapping p 25 N85-17241
- Australian Multiexperimental Assessment of SIR-B (AMAS) p 52 N85-17243
- Application and calibration of the subsurface mapping capability of SIR-B in desert regions p 25 N85-17244
- The extension of an invertible coniferous forest canopy reflectance model using SIR-B and LANDSAT data p 10 N85-17246
- Analysis of SIR-B radar illumination of geometry for depth of penetration and surface feature and vegetation detection, Nevada and California p 25 N85-17248
- Delineation of major geologic structures in Turkey using SIR-B data p 25 N85-17249
- Evaluation of the radar response to land surfaces and volumes Examination of theoretical models, target statistics, and applications p 63 N85-17250
- Ground truth for SIR-B images obtained by SIR system 8 impulse radar p 10 N85-17251
- Remote sensing of soil moisture p 10 N85-17252
- SIR-A imagery in geologic studies of the Sierra Madre Oriental, northeastern Mexico Part 1 (Regional stratigraphy) The use of morphostratigraphic units in remote sensing mapping [NASA-CR-175457] p 25 N85-19497
- SHUTTLE PALLET SATELLITES**
- SPAS-01 - Space flight technology for the general user --- Shuttle Pallet Satellite (ESA) p 61 A85-27057
- Modular Optoelectronic Multispectral Scanner (MOMS) Technological aspects p 61 A85-27059
- MOMS 1 and its results p 61 A85-27061
- SIDE-LOOKING RADAR**
- Complex studies of the environment by optical and radar methods p 56 A85-20081
- Radiophysical techniques employed for sea ice investigations p 31 A85-24077
- Features of the digital processing of radar images obtained with the sidelooking radar of the Cosmos-1500 satellite p 48 A85-25660
- Soil moisture content estimation by radar survey data during the sowing campaign p 6 A85-26947
- Radar mapping of the moisture of open soils p 6 A85-29911
- SIGNAL TO NOISE RATIOS**
- The effects of image noise on digital correlation probability p 49 A85-29221
- SIGNATURE ANALYSIS**
- Crustal structure of the Churchill-Supenor boundary zone between 80 and 98 deg W longitude from Magsat anomaly maps and stacked passes p 22 A85-26421
- International Symposium on Microwave Signatures in Remote Sensing, 3rd, Toulouse, France, January 16-20, 1984, Proceedings p 6 A85-26942
- SIMULATION**
- NOAA-AISC user's guide for implementing CERES wheat model for large area yield estimation [E85-10085] p 12 N85-21750
- Estimating solar radiation for plant simulation models [E85-10089] p 13 N85-21751
- SIRS B SATELLITE**
- SIR-B cartography and stereo topographic mapping p 19 N85-17234
- Monitoring of the tidal dynamics of the Dutch Waddensea by SIR-B p 40 N85-17235
- SLOPES**
- Relationship between forest clearing and biophysical factors in tropical environments Implications for the design of a forest change monitoring approach --- Costa Rica [E85-10051] p 8 N85-16247
- SNOW**
- Performance of a coherent lidar remote sensor in snow and fog p 59 A85-25347
- SNOW COVER**
- On the separability of various classes from the GOES visible and infrared data --- of winter cloud and snow cover p 45 A85-21138
- Spectral signatures of soil, snow and sea ice as observed by passive microwave and thermal infrared techniques p 58 A85-23784
- Retrieval of snow water equivalent from Nimbus-7 SMMR data Effect of land-cover categories and weather conditions p 43 A85-24082
- The effect of a snow cover on microwave backscatter from sea ice p 32 A85-24083
- Dramatic contrast between low clouds and snow cover in daytime 3.7 micron imagery p 48 A85-24740
- Airborne snow water equivalent and soil moisture measurement using natural terrestrial gamma radiation p 43 A85-25352
- SOIL MAPPING**
- Visual interpretation of SAR images of two areas in the Netherlands p 1 A85-23694
- Influence of spatial variability of soil hydraulic characteristics on surface parameters obtained from remote-sensing data in thermal infrared and microwaves p 43 A85-23786
- Identification of the structure of soil-vegetation cover using aerial and space images p 5 A85-25656
- The utility of data from various airborne sensors for soil mapping p 5 A85-26932
- Soil slaking and the possibilities to record with infrared line scanning p 5 A85-26936
- Investigation of salty soils and salines on the basis of space remote-sensing methods p 6 A85-29908
- Evaluation of SIR-B imagery for geologic and geomorphic mapping, hydrology, and oceanography in Australia p 51 N85-17229
- SOIL MOISTURE**
- Spectral signatures of soil, snow and sea ice as observed by passive microwave and thermal infrared techniques p 58 A85-23784
- Influence of spatial variability of soil hydraulic characteristics on surface parameters obtained from remote-sensing data in thermal infrared and microwaves p 43 A85-23786
- Airborne snow water equivalent and soil moisture measurement using natural terrestrial gamma radiation p 43 A85-25352
- Soil moisture content estimation by radar survey data during the sowing campaign p 6 A85-26947
- Determination of soil moisture content by microwave radiometry with the use of a priori information p 6 A85-29910
- Radar mapping of the moisture of open soils p 6 A85-29911
- Effect of vegetation on soil moisture sensing observed from orbiting microwave radiometers p 7 A85-30089
- Evaluation of the radar response to land surfaces and volumes Examination of theoretical models, target statistics, and applications p 63 N85-17250
- Ground truth for SIR-B images obtained by SIR system 8 impulse radar p 10 N85-17251
- Remote sensing of soil moisture p 10 N85-17252
- Investigations of vegetation and soils information contained in LANDSAT Thematic Mapper and Multispectral Scanner data [E85-10082] p 12 N85-21747
- SOILS**
- An integrated remote sensing approach for identifying ecological range sites --- Parker Mountain [E85-10050] p 8 N85-16246
- Relationship between forest clearing and biophysical factors in tropical environments Implications for the design of a forest change monitoring approach --- Costa Rica [E85-10051] p 8 N85-16247
- Thematic Mapper spectral dimensionality and data structure p 12 N85-21736
- Remote sensing research for agricultural applications --- San Joaquin County, California and Snake River Plain and Twin Falls area, Idaho [E85-10090] p 13 N85-21752
- SOLAR CONSTANT**
- Spectroradiometric calibration of the Thematic Mapper and Multispectral Scanner system [E85-10094] p 70 N85-21756
- SOLAR POSITION**
- Terrain and look angle effects upon multispectral scanner response p 60 A85-26642
- SOLAR POWER SATELLITES**
- The potential of solar power satellites for developing countries p 59 A85-24654
- SOLAR RADIATION**
- Estimating solar radiation for plant simulation models [E85-10089] p 13 N85-21751
- SOUTH CAROLINA**
- Analysis of data acquired by synthetic aperture radar and LANDSAT Multispectral Scanner over Kershaw County, South Carolina, during the summer season [E85-10071] p 11 N85-19485
- Investigation of radiometric properties of LANDSAT-4 MSS --- California, North Carolina, South Carolina, and New England p 65 N85-20500
- SOUTH DAKOTA**
- Image variance and spatial structure in remotely sensed scenes --- South Dakota, California, Missouri, Kentucky, Louisiana, Tennessee, District of Columbia, and Oregon p 51 N85-16265
- Geodetic accuracy of LANDSAT 4 Multispectral Scanner and Thematic Mapper data --- Washington, DC, California, Alabama, South Dakota, and Illinois p 53 N85-20504
- SOYBEANS**
- An analysis of spectral discrimination between corn and soybeans using a row crop reflectance model p 7 A85-30086
- Application of Thematic Mapper data to corn and soybean development stage estimation p 7 A85-30093

- Variation in spectral response of soybeans with respect to illumination, view, and canopy geometry [E85-10040] p 8 N85-16241
- Shortwave infrared detection of vegetation [E85-10064] p 10 N85-17402
- SPACE BASED RADAR**
- Effect of meteorological conditions on the characteristics of space radar images of the earth surface p 48 A85-25653
- Realtime processor of SAR systems p 60 A85-25855
- SPACE COMMERCIALIZATION**
- Commercialization of remote sensing data - Its impact on the continuity and accessibility of remote sensing data, including response to standing orders as well as on the standardization of products p 71 A85-20642
- SPACE EXPLORATION**
- Use of Space Station for Earth and Planetary Exploration p 71 A85-25348
- Planetary cartography in the next decade (1984 - 1994) [NASA-SP-475] p 20 N85-22323
- SPACE MISSIONS**
- SPAS-01 - Space flight technology for the general user --- Shuttle Pallet Satellite (ESA) p 61 A85-27057
- The SIR-B science investigations plan [NASA-CR-174282] p 63 N85-17208
- SPACE PLATFORMS**
- Use of Space Station for Earth and Planetary Exploration p 71 A85-25348
- SPAS-01 - Space flight technology for the general user --- Shuttle Pallet Satellite (ESA) p 61 A85-27057
- Earth observations and the polar platform [NOAA-TR-NESDIS-18] p 15 N85-20517
- SPACE SHUTTLE PAYLOADS**
- SPAS-01 - Space flight technology for the general user --- Shuttle Pallet Satellite (ESA) p 61 A85-27057
- Brazilian Remote Sensing Shuttle Experiment (BRESEX) Characteristics and future utilization on satellites [INPE-3313-PRE/620] p 64 N85-19385
- SPACE SHUTTLES**
- Earth resources research using the Shuttle Imaging Radar system p 67 N85-20779
- SPACE STATIONS**
- Use of Space Station for Earth and Planetary Exploration p 71 A85-25348
- SPACEBORNE ASTRONOMY**
- Use of Space Station for Earth and Planetary Exploration p 71 A85-25348
- SPACEBORNE EXPERIMENTS**
- A method for determining mesoscale dynamic topography [AD-D011412] p 40 N85-17506
- SPACEBORNE PHOTOGRAPHY**
- Determination of the external-orientation elements of aerial and space photographs in the remote sensing of dynamic processes and phenomena p 56 A85-19998
- Synthetic apertures - An overview p 57 A85-22711
- Evaluation of an experimental system for spaceborne processing of multispectral image data p 46 A85-23144
- The use of Salyut-5 photographs for regional geomorphological mapping p 23 A85-28999
- SPATIAL DEPENDENCIES**
- Angular and spatial variability of visible and NIR spectral data p 2 A85-23752
- SPATIAL DISTRIBUTION**
- Spatial variation of significant wave-height p 30 A85-23704
- Estimating location parameters in a mixture p 50 N85-16252
- Spatial estimation from remotely sensed data via empirical Bayes models p 8 N85-16256
- MTF analysis of LANDSAT-4 Thematic Mapper p 68 N85-21737
- SPATIAL RESOLUTION**
- Rectification of single and multiple frames of satellite scanner imagery using points and edges as control p 51 N85-16263
- The influence of the number of ground control points on the scene-to-map registration accuracy --- Kansas, Louisiana, Mississippi, and Missouri p 51 N85-16264
- Image variance and spatial structure in remotely sensed scenes --- South Dakota, California, Missouri, Kentucky, Louisiana, Tennessee, District of Columbia, and Oregon p 51 N85-16265
- Analysis of subpixel registration p 51 N85-16267
- Resolution enhancement of multichannel microwave imagery from the Nimbus-7 SMMR for maritime rainfall analysis [NASA-CR-174367] p 44 N85-19221
- LANDSAT scene-to-scene registration accuracy assessment p 65 N85-20502

- Geodetic accuracy of LANDSAT 4 Multispectral Scanner and Thematic Mapper data --- Washington, DC, California, Alabama, South Dakota, and Illinois p 53 N85-20504
- Geometric accuracy assessment of LANDSAT-4 Multispectral Scanner (MSS) data p 19 N85-20505
- Scan angle and detector effects in Thematic Mapper radiometry --- Iowa and Arkansas p 68 N85-21735
- The use of linear feature detection to investigate Thematic Mapper data performance and processing p 69 N85-21740
- SPECKLE PATTERNS**
- Some properties of SAR speckle p 46 A85-23684
- SPECTRA**
- The spatial evolution of the directional wave spectrum in the Southern Ocean - Its relation to extreme waves in Agulhas Current p 39 N85-17213
- SPECTRAL BANDS**
- Methodological study of spectral band selection for multispectral remote sensing p 55 A85-19363
- Comparison of modelled and empirical atmospheric propagation data p 46 A85-22678
- Comparison of SPOT HRV and Landsat-4 TM for crop inventories p 3 A85-23762
- Spectral response of different agricultural and perurban land-use units in the spectral windows at 1.55-1.75 and 2.08-2.35 microns p 4 A85-23787
- Thematic evaluation of SPOT spectral bands p 58 A85-23794
- Study of spectral/radiometric characteristics of the Thematic Mapper for land use applications [E85-10075] p 64 N85-19489
- Prelaunch absolute radiometric calibration of the reflective bands on the LANDSAT-4 prototype Thematic Mapper p 66 N85-20515
- Relative radiometric calibration of LANDSAT TM reflective bands p 67 N85-21725
- Evaluation of the radiometric integrity of LANDSAT 4 Thematic Mapper band 6 data p 54 N85-21726
- Thermal band characterization of the LANDSAT-4 Thematic Mapper p 67 N85-21727
- A preliminary analysis of LANDSAT-4 Thematic Mapper radiometric performance p 68 N85-21730
- A preliminary evaluation of LANDSAT-4 Thematic Mapper data for their geometric and radiometric accuracies p 54 N85-21739
- Assessment of Thematic Mapper band-to-band registration by the block correlation method p 55 N85-21743
- LANDSAT 4 band 6 data evaluation [E85-10093] p 55 N85-21755
- LANDSAT 4 investigations of Thematic Mapper and Multispectral Scanner applications --- Drum Mountains, Utah and Tonopah, Nevada [E85-10095] p 26 N85-21757
- SPECTRAL CORRELATION**
- Correlation of spectral brightnesses measured using multispectral space images p 60 A85-25659
- SPECTRAL METHODS**
- Transformation of sea-wave spectrum into a synthetic-aperture-radar image spectrum p 34 A85-25661
- Autoregressive spectral estimation for two dimensional time series p 50 N85-16258
- SPECTRAL RECONNAISSANCE**
- Measuring spectra of lands p 20 A85-21975
- The spot operational remote sensing satellite system Current status and perspectives p 67 N85-20776
- SPECTRAL REFLECTANCE**
- Methodological study of spectral band selection for multispectral remote sensing p 55 A85-19363
- Effect of heliotropism on the bidirectional reflectance of irrigated cotton p 1 A85-22420
- Determination of reflectances of tropical vegetation by combined methods of radiometry and photometry p 2 A85-23760
- Surface scattering effects at different spectral regions p 58 A85-23780
- An analysis of spectral discrimination between corn and soybeans using a row crop reflectance model p 7 A85-30086
- Comparative study of Suits and SAIL canopy reflectance models p 7 A85-30092
- Variation in spectral response of soybeans with respect to illumination, view, and canopy geometry [E85-10040] p 8 N85-16241
- Spectral estimators of absorbed photosynthetically active radiation in corn canopies [E85-10041] p 8 N85-16242
- Growth/reflectance model interface for wheat and corresponding model [E85-10058] p 9 N85-16269
- North American vegetation patterns observed with the NOAA-7 advanced very high resolution radiometer --- North America [E85-10062] p 10 N85-17400

- Analysis of terrestrial conditions and dynamics [E85-10063] p 10 N85-17401
- Growth and reflectance characteristics of winter wheat canopies [E85-10080] p 11 N85-19494
- SPECTRAL RESOLUTION**
- LANDSAT-4 Science Characterization Early Results Volume 2, part 1 Thematic Mapper (TM) [E85-10068] p 66 N85-20508
- Spectral characterization of the LANDSAT Thematic Mapper sensors p 66 N85-20514
- LANDSAT-4 Science Characterization Early Results Volume 3, part 2 Thematic Mapper (TM) [E85-10069] p 67 N85-21724
- Thematic Mapper spectral dimensionality and data structure p 12 N85-21736
- SPECTRAL SENSITIVITY**
- The influence of satellite spectral sensor response on the analysis of satellite imagery at high latitudes p 60 A85-26927
- Thematic Mapper Volume 1 Calibration report flight model, LANDSAT 5 [E85-10059] p 63 N85-16270
- Spectral characterization of the LANDSAT-4 MSS sensors p 65 N85-20499
- SPECTRAL SIGNATURES**
- Spectral signatures of objects in remote sensing, International Conference, 2nd, Bordeaux, France, September 12-16, 1983, Reports p 57 A85-23751
- Angular and spatial variability of visible and NIR spectral data p 2 A85-23752
- Estimation of agronomic variables using spectral signatures p 2 A85-23753
- Light polarization measurements - A method to determine the specular and diffuse light-scattering properties of both leaves and plant canopies p 2 A85-23754
- Lidar applications in remote sensing of ocean properties p 31 A85-23755
- Comparative seasonal evolution of the spectral signatures of broad-leaved and coniferous trees from Landsat data Comparison with other perennial surfaces p 2 A85-23757
- Analysis of ground radiometric measurements in the rice-growing site at Tamani (Republic of Mali) - Effect of certain yield parameters on the spectral signature p 2 A85-23758
- Determination of reflectances of tropical vegetation by combined methods of radiometry and photometry p 2 A85-23760
- Relations between the radar backscatter coefficient and the characteristics of a vegetation canopy - Analysis of the effect of structure p 4 A85-23774
- Spectral signatures of soil, snow and sea ice as observed by passive microwave and thermal infrared techniques p 58 A85-23784
- Spectral response of different agricultural and perurban land-use units in the spectral windows at 1.55-1.75 and 2.08-2.35 microns p 4 A85-23787
- Independent variables in remote sensing as a function of landcover type p 47 A85-23788
- Interpretation of thermal infrared data to augment spectral signatures p 47 A85-23791
- Polarization effects in sea-ice signatures p 31 A85-24078
- Microwave signatures of the sea ice in the East Greenland Current p 31 A85-24079
- Spectral characterization of vegetation canopies in the visible and NIR - Application to remote sensing p 5 A85-25670
- Imaging systems for the delineation of spectral properties of geologic materials in the visible and near-infrared p 22 A85-27945
- The importance of geobotany in geological remote sensing applications p 23 A85-27948
- Analysis of data acquired by synthetic aperture radar and LANDSAT Multispectral Scanner over Kershaw County, South Carolina, during the summer season [E85-10071] p 11 N85-19485
- Radiometric calibration and processing procedure for reflective bands on LANDSAT-4 prototype Thematic Mapper p 66 N85-20510
- Investigations of vegetation and soils information contained in LANDSAT Thematic Mapper and Multispectral Scanner data [E85-10082] p 12 N85-21747
- Remote sensing research for agricultural applications --- San Joaquin County, California and Snake River Plain and Twin Falls area, Idaho [E85-10090] p 13 N85-21752
- SPECTRORADIOMETERS**
- An intercalibration of Meteosat-1 and GOES-2 visible and infrared measurements p 26 A85-19420

SUBJECT INDEX

- Experiments concerning radiometric measurements and natural-object indicators in order to apply corrections to recordings of satellite remote sensing p 58 A85-23789
- SPECTRUM ANALYSIS**
Thematic evaluation of SPOT spectral bands p 58 A85-23794
- SPECULAR REFLECTION**
Light polarization measurements - A method to determine the specular and diffuse light-scattering properties of both leaves and plant canopies p 2 A85-23754
TM digital image products for applications p 54 A85-20512
- SPHERICAL CAPS**
Magsat vertical field anomalies above 40 deg N from spherical cap harmonic analysis p 18 A85-26417
- SPLINE FUNCTIONS**
Multivariate spline methods in surface fitting p 50 A85-16257
- SPOT (FRENCH SATELLITE)**
Status and plans for the SPOT program and the launch of SPOT 1 - Its on-ground processing and data dissemination to users p 56 A85-20568
Commercialization of remote sensing data - Its impact on the continuity and accessibility of remote sensing data, including response to standing orders as well as on the standardization of products p 71 A85-20642
Development of a SPOT-simulation radiometer p 57 A85-23759
Comparison of SPOT HRV and Landsat-4 TM for crop inventories p 3 A85-23762
Integration of the SPOT panchromatic channel into its multispectral mode for image sharpness enhancement p 49 A85-29217
CNES, INRA do joint remote-sensing research p 11 A85-19321
The spot operational remote sensing satellite system Current status and perspectives p 67 A85-20776
- SQUALLS**
Airborne Doppler estimates of the air motions associated with a developing, sea-breeze induced, mesoscale precipitation line p 36 A85-28783
- STATISTICAL CORRELATION**
The effects of image noise on digital correlation probability p 49 A85-29221
Assessment of Thematic Mapper band-to-band registration by the block correlation method p 55 A85-21743
- STEREOPHOTOGRAPHY**
Determination of the heights of points of a place on the basis of radar-survey data p 19 A85-29000
- STEREOSCOPY**
SIR-B cartography and stereo topographic mapping p 19 A85-17234
Automatic terrain elevation mapping and registration p 52 A85-17242
- STRATIGRAPHY**
SIR-A imagery in geologic studies of the Sierra Madre Oriental, northeastern Mexico Part 1 (Regional stratigraphy) The use of morphostratigraphic units in remote sensing mapping [NASA-CR-175457] p 25 A85-19497
- STREAM FUNCTIONS (FLUIDS)**
Center of mass estimation in closed vortices - A verification in principle and practice p 26 A85-19417
- STRUCTURAL BASINS**
Monitoring Africa's Lake Chad basin with Landsat and NOAA satellite data p 43 A85-26930
Post-carboniferous tectonics in the Anadarko Basin, Oklahoma Evidence from side-looking radar imagery [NASA-CR-175458] p 26 A85-19498
- STRUCTURAL PROPERTIES (GEOLOGY)**
Analysis of mesofractures according to space images - Currents trends in the exploration for oil and gas deposits p 21 A85-25655
Space remote-sensing data in geology --- Russian book p 23 A85-28400
Image-scale and look-direction effects on the detectability of lineaments in radar images p 24 A85-30087
Geological, structural, and geomorphological analyses from SIR-B p 24 A85-17226
Structural investigation of the Canadian Shield by orbital radar and LANDSAT p 25 A85-17236
Structural investigation of the Grenville Province by radar and other imaging and nonimaging sensors p 25 A85-17237
Delineation of major geologic structures in Turkey using SIR-B data p 25 A85-17249
- SUBDUCTION (GEOLOGY)**
Satellite magnetic anomalies over subduction zones - The Aleutian Arc anomaly p 16 A85-21107
- SUBMARINES**
Research on ocean floor electrical surveys [AD-A149831] p 42 A85-21920

- SUN**
Variation in spectral response of soybeans with respect to illumination, view, and canopy geometry [E85-10040] p 8 A85-16241
- SURFACE PROPERTIES**
Australian Multixperimental Assessment of SIR-B (AMAS) p 52 A85-17243
- SURFACE ROUGHNESS**
Interactive digital image processing for terrain data extraction [AD-A148580] p 52 A85-17417
- SURFACE ROUGHNESS EFFECTS**
Surface scattering effects at different spectral regions p 58 A85-23780
Land clutter models for radar design and analysis p 49 A85-27827
- SURFACE TEMPERATURE**
Effects of the experimental errors and conditions on the estimation of thermal inertia and evapotranspiration from METEOSAT data p 3 A85-23767
Satellite definition of the bio-optical and thermal variation of coastal eddies associated with the African current [AD-A147910] p 39 A85-16282
- SURFACE WATER**
Determination of water surfaces in northwest Bohemia on the basis of satellite data p 44 A85-29906
A preliminary analysis of LANDSAT-4 Thematic Mapper radiometric performance p 68 A85-21730
- SURFACE WAVES**
Swell propagation in the North Atlantic ocean using SEASAT altimeter p 30 A85-23702
The investigation of selected oceanographic applications of spaceborne synthetic-aperture radar p 39 A85-17233
SEASAT 3 and 4 [AD-A148343] p 40 A85-17274
- SWEDEN**
Ground truth for SIR-B images obtained by SIR system 8 impulse radar p 10 A85-17251
- SYNOPTIC MEASUREMENT**
Swell in the Pacific Ocean observed by SEASAT radar altimeter p 37 A85-29708
- SYNOPTIC METEOROLOGY**
Oceanographic and meteorological research based on the data products of SEASAT [E85-10091] p 41 A85-21753
- SYNTHETIC APERTURE RADAR**
Predicting dangerous ocean waves with spaceborne synthetic aperture radar p 27 A85-19429
Imaging ocean surface waves by synthetic aperture radar - A review p 29 A85-23682
Some properties of SAR speckle p 46 A85-23684
The effect of a moving sea surface on SAR imagery p 29 A85-23685
Theory of SAR ocean wave imaging p 29 A85-23686
Effect of defocusing on the images of ocean waves p 29 A85-23688
The Canadian SAR experience p 46 A85-23689
The use of SEASAT-SAR data in oceanography at the IFP p 29 A85-23690
Expressions of bathymetry on Seasat synthetic radar images p 29 A85-23691
Tidal current bedforms investigated by Seasat p 30 A85-23692
Visual interpretation of SAR images of two areas in the Netherlands p 1 A85-23694
The analysis of backscattering properties from SAR data of mountain regions p 59 A85-24081
Transformation of sea-wave spectrum into a synthetic-aperture-radar image spectrum p 34 A85-25661
Realtime processor of SAR systems p 60 A85-25855
Advanced SAR system maps Arctic regions p 35 A85-27841
Mapping of glacial landforms from Seasat radar images p 36 A85-28027
Image-scale and look-direction effects on the detectability of lineaments in radar images p 24 A85-30087
The investigation of selected oceanographic applications of spaceborne synthetic-aperture radar p 39 A85-17233
SIR-B cartography and stereo topographic mapping p 19 A85-17234
Investigation of SIR-B images for lithologic mapping p 25 A85-17241
Automatic terrain elevation mapping and registration p 52 A85-17242
Australian Multixperimental Assessment of SIR-B (AMAS) p 52 A85-17243
Information extraction and transmission techniques for spaceborne synthetic aperture radar images [NASA-CR-174341] p 52 A85-17256

TERRAIN ANALYSIS

- Earth resources research using the Shuttle Imaging Radar system p 67 A85-20779
The imaging of internal waves by the SEASAT-A synthetic aperture radar [AD-A149808] p 20 A85-21761
- SYNTHETIC APERTURES**
Synthetic apertures - An overview p 57 A85-22711
- SYNTHETIC ARRAYS**
Synthetic apertures - An overview p 57 A85-22711
- T**
- TARGET RECOGNITION**
Research on ocean floor electrical surveys [AD-A149831] p 42 A85-21920
- TECHNOLOGY ASSESSMENT**
Automatic production of DTM data using digital off-line technique --- Digital Terrain Modelling p 45 A85-20750
Synthetic apertures - An overview p 57 A85-22711
- TECHNOLOGY UTILIZATION**
On realizing the potential of the earth-looking vantage point [AIAA PAPER 85-0195] p 70 A85-19580
The educational role of satellites p 70 A85-20574
Needs and accessibility of developing countries for/to remote sensing information systems p 13 A85-20647
- TECTONICS**
Neotectonics of the Caribbean p 27 A85-21145
Intermediate-wavelength magnetic anomaly field of the North Pacific and possible source distributions p 17 A85-26414
Methods for the study of recent tectonics on the basis of remote sensing and ground data p 23 A85-29904
Tectonic, volcanic, and climatic geomorphology study of the Sierras Pampeanas Andes, northwestern Argentina p 24 A85-17215
Post-carboniferous tectonics in the Anadarko Basin, Oklahoma Evidence from side-looking radar imagery [NASA-CR-175458] p 26 A85-19498
- TELEMETRY**
An overview of the Thematic Mapper geometric correction system p 53 A85-20511
- TELEPHOTOMETRY**
Determination of visual range from Landsat data p 47 A85-24285
- TELEVISION RECEIVERS**
An automatic high-resolution picture transmission receiving station p 61 A85-27698
- TELEVISION TRANSMISSION**
An automatic high-resolution picture transmission receiving station p 61 A85-27698
- TEMPERATURE MEASUREMENT**
Double-angle method for measuring ocean surface temperature in the infrared p 34 A85-25658
Method of measuring sea surface water temperature with a satellite including wideband passive synthetic-aperture multichannel receiver [NASA-CASE-NPO-15651-1] p 41 A85-21723
- TEMPORAL RESOLUTION**
LANDSAT scene-to-scene registration accuracy assessment p 65 A85-20502
Geometric accuracy assessment of LANDSAT-4 Multispectral Scanner (MSS) data p 19 A85-20505
- TENNESSEE**
Image variance and spatial structure in remotely sensed scenes --- South Dakota, California, Missouri, Kentucky, Louisiana, Tennessee, District of Columbia, and Oregon p 51 A85-16265
- TERRAIN**
Automatic terrain elevation mapping and registration p 52 A85-17242
Interactive digital image processing for terrain data extraction [AD-A148580] p 52 A85-17417
- TERRAIN ANALYSIS**
Automatic production of DTM data using digital off-line technique --- Digital Terrain Modelling p 45 A85-20750
Terrain and look angle effects upon multispectral scanner response p 60 A85-26642
Automated measurements of terrain reflection and height variations using an airborne infrared laser system p 5 A85-26933
Advanced SAR system maps Arctic regions p 35 A85-27841
Determination of the heights of points of a place on the basis of radar-survey data p 19 A85-29000
Evaluation of the L-band scattering characteristics of volcanic terrain in aid of lithologic identification, assessment of SIR-B calibration, and development of planetary geomorphic analogs p 24 A85-17232
Investigation of SIR-B images for lithologic mapping p 25 A85-17241

Mathematical aspects of digital terrain information, Report from International Society for Photogrammetry and Remote Sensing (ISPRS) working group 3.3, 1980 - 1984 --- photogrammetry p 19 N85-17407
SIR-A imagery in geologic studies of the Sierra Madre Oriental, northeastern Mexico Part 1 (Regional stratigraphy) The use of morphostratigraphic units in remote sensing mapping [NASA-CR-175457] p 25 N85-19497

TERRESTRIAL RADIATION

Airborne snow water equivalent and soil moisture measurement using natural terrestrial gamma radiation p 43 A85-25352

TEXTURES

Texture classification using autoregressive filtering p 50 N85-16254

THEMATIC MAPPING

The integrated use of digital cartographic data and remotely sensed imagery p 45 A85-20572
Study on a regional geographical information system and application model p 13 A85-20644
African land-cover classification using satellite data p 1 A85-21174

The Thematic Mapper - Instrument overview and preliminary on-orbit results p 56 A85-22681
Large scan mirror assembly of the new Thematic Mapper developed for Landsat 4 earth resources satellite p 56 A85-22682

Inventory of geographically homogeneous zones by spectral modeling of diachronic Meteorol albedo or combined albedo/thermal-channel data - Applications to the Maghreb and to Sahelian Africa p 46 A85-23769
Spectral response of different agricultural and penurban land-use units in the spectral windows at 1.55-1.75 and 2.08-2.35 microns p 4 A85-23787
Classification of the geological environments of Anticosti Island - An approach using a Landsat-4 spectral simulation p 21 A85-23790

Thematic evaluation of SPOT spectral bands p 58 A85-23794

Resource measurement system p 47 A85-24258
Landsat-4 thematic mapper (TM) for cold environments p 60 A85-25349

Magsat vertical field anomalies above 40 deg N from spherical cap harmonic analysis p 18 A85-26417
Estimation of the vegetation contribution to the 1.65-2.22 micron ratio in airborne thematic-mapper imagery of the Virginia Range, Nevada p 5 A85-26931

Experimental evidence for spring and autumn windows for the detection of geobotanical anomalies through the remote sensing of overlying vegetation p 6 A85-26939

Near-infrared spectroscopy in geological reconnaissance and exploration p 22 A85-27944
Thematic mapper data analysis p 23 A85-27946

The use of Salyut-5 photographs for regional geomorphological mapping p 23 A85-28999
Effect of Landsat Thematic Mapper sensor parameters on land cover classification p 14 A85-30088
Application of Thematic Mapper data to corn and soybean development stage estimation p 7 A85-30093

Evaluation of SIR-B imagery for geologic and geomorphic mapping, hydrology, and oceanography in Australia p 51 N85-17229
Structural investigation of the Grenville Province by radar and other imaging and nonimaging sensors p 25 N85-17237

Investigation of SIR-B images for lithologic mapping p 25 N85-17241

Analysis of terrestrial conditions and dynamics [E85-10063] p 10 N85-17401

Analysis of data acquired by synthetic aperture radar and LANDSAT Multispectral Scanner over Kershaw County, South Carolina, during the summer season [E85-10071] p 11 N85-19485

Study of spectral/radiometric characteristics of the Thematic Mapper for land use applications [E85-10075] p 64 N85-19489

Spectroradiometric calibration of the Thematic Mapper and Multispectral Scanner system [E85-10077] p 64 N85-19491

Thematic Mapper Design through flight evaluation [E85-10078] p 64 N85-19492

LANDSAT-4 Science Characterization Early Results Volume 2, part 1 Thematic Mapper (TM) [E85-10068] p 66 N85-20508

An overview of LANDSAT-4 and the Thematic Mapper p 66 N85-20509

Radiometric calibration and processing procedure for reflective bands on LANDSAT-4 preflight Thematic Mapper p 66 N85-20510

An overview of the Thematic Mapper geometric correction system p 53 N85-20511

TM digital image products for applications p 54 N85-20512

Canadian plans for Thematic Mapper data p 54 N85-20513

Characterization of radiometric calibration of LANDSAT-4 reflective bands p 66 N85-20516

LANDSAT-4 Science Characterization Early Results Volume 3, part 2 Thematic Mapper (TM) [E85-10069] p 67 N85-21724

Thermal band characterization of the LANDSAT-4 Thematic Mapper p 67 N85-21727

A preliminary assessment of LANDSAT-4 Thematic Mapper data --- Windsor, Ontario and Medicine Hat areas, Canada p 54 N85-21728

Preliminary evaluation of the radiometric calibration of LANDSAT-4 Thematic Mapper data by the Canada Centre for Remote Sensing p 67 N85-21729

A preliminary analysis of LANDSAT-4 Thematic Mapper radiometric performance p 68 N85-21730

A preliminary evaluation of LANDSAT-4 Thematic Mapper data for their geometric and radiometric accuracies p 54 N85-21739

Spatial resolution estimation of LANDSAT-4 Thematic Mapper data p 69 N85-21741

An analysis of the high frequency vibrations in early Thematic Mapper scenes p 69 N85-21742

Tests of low-frequency geometric distortions in LANDSAT 4 images p 55 N85-21744

Investigation of TM band-to-band registration using the JSC registration processor p 69 N85-21745

Geodetic accuracy of LANDSAT 4 Multispectral Scanner and Thematic Mapper data p 20 N85-21746

Investigations of vegetation and soils information contained in LANDSAT Thematic Mapper and Multispectral Scanner data [E85-10082] p 12 N85-21747

Remote sensing research for agricultural applications --- San Joaquin County, California and Snake River Plain and Twin Falls area, Idaho [E85-10090] p 13 N85-21752

LANDSAT 4 band 6 data evaluation [E85-10093] p 55 N85-21755

Spectroradiometric calibration of the Thematic Mapper and Multispectral Scanner system [E85-10094] p 70 N85-21756

LANDSAT 4 investigations of Thematic Mapper and Multispectral Scanner applications --- Drum Mountains, Utah and Tonopah, Nevada [E85-10095] p 26 N85-21757

THERMAL MAPPING

Calculation of thermal inertia from day-night measurements separated by days or weeks p 45 A85-21048

Estimation of evapotranspiration on the basis of thermal IR p 3 A85-23765

Thermal-inertia mapping from space p 21 A85-23766

Use of HCMM thermal images in the study of microclimates in a mountainous region p 3 A85-23771

Influence of spatial variability of soil hydraulic characteristics on surface parameters obtained from remote-sensing data in thermal infrared and microwaves p 43 A85-23786

Interpretation of thermal infrared data to augment spectral signatures p 47 A85-23791

Soil slaking and the possibilities to record with infrared line scanning p 5 A85-26936

Developments with multispectral thermal-IR and active microwave systems - TIMS, SIR-A, SIR-B, and radarsat p 62 A85-27947

Thermal structure of an agricultural region as seen by NOAA-7 AVHRR p 7 A85-30090

The use of principal components analysis techniques Nimbus-7 coastal zone color scanner data to define mesoscale ocean features through a warm humid atmosphere [AD-A148567] p 40 N85-17416

Evaluation of the radiometric quality of the TM data using clustering, linear transformations and multispectral distance measures --- Illinois p 54 N85-21731

THERMAL RESISTANCE

Calculation of thermal inertia from day-night measurements separated by days or weeks p 45 A85-21048

Effects of the experimental errors and conditions on the estimation of thermal inertia and evapotranspiration from METEOSAT data p 3 A85-23767

THERMODYNAMIC PROPERTIES

Effects of the experimental errors and conditions on the estimation of thermal inertia and evapotranspiration from METEOSAT data p 3 A85-23767

THERMOGRAPHY

Double-angle method for measuring ocean surface temperature in the infrared p 34 A85-25658

THICKNESS

Improvement of the accuracy of radar measurements of sea-ice thickness by cepstral processing of reflected signals p 35 A85-27736

TIDES

Monitoring of the tidal dynamics of the Dutch Waddensea by SIR-B p 40 N85-17235

Altimetry, orbits and tides [E85-10066] p 40 N85-17404

TIME SERIES ANALYSIS

Autoregressive spectral estimation for two dimensional time series p 50 N85-16258

TIROS N SERIES SATELLITES

The current use of TIROS-N series of meteorological satellites for land-cover studies p 60 A85-26928

TOPOGRAPHY

Relationship between forest clearing and biophysical factors in tropical environments Implications for the design of a forest change monitoring approach --- Costa Rica [E85-10051] p 8 N85-16247

Interlobate comparison of glacial-depositional style as evidenced by small-relief glacial landscape features in Illinois, Indiana, and Ohio, utilizing SIR-B p 39 N85-17231

SIR-B cartography and stereo topographic mapping p 19 N85-17234

Monitoring of the tidal dynamics of the Dutch Waddensea by SIR-B p 40 N85-17235

Application and calibration of the subsurface mapping capability of SIR-B in desert regions p 25 N85-17244

Mathematical aspects of digital terrain information, Report from International Society for Photogrammetry and Remote Sensing (ISPRS) working group 3.3, 1980 - 1984 --- photogrammetry p 19 N85-17407

A method for determining mesoscale dynamic topography [AD-D011412] p 40 N85-17506

Planetary cartography in the next decade (1984 - 1994) [NASA-SP-475] p 20 N85-22323

TRANSMITTANCE

Comparison of modelled and empirical atmospheric propagation data p 46 A85-22678

TRANSPORTATION NETWORKS

Relationship between forest clearing and biophysical factors in tropical environments Implications for the design of a forest change monitoring approach --- Costa Rica [E85-10051] p 8 N85-16247

TREES (PLANTS)

Nonparametric analysis of Minnesota spruce and aspen tree data and LANDSAT data p 8 N85-16253

TROPICAL REGIONS

Relationship between forest clearing and biophysical factors in tropical environments Implications for the design of a forest change monitoring approach --- Costa Rica [E85-10051] p 8 N85-16247

TROPICAL STORMS

The diurnal variation of Atlantic Ocean tropical cyclone cloud distribution inferred from geostationary satellite infrared measurements p 33 A85-24739

TURKEY

Delineation of major geologic structures in Turkey using SIR-B data p 25 N85-17249

U

ULTRAHIGH FREQUENCIES

Ultrashort-wave radar subsurface sounding of sea ice and earth covers p 34 A85-25594

Using the global positioning system (GPS) phase observable for relative geodesy Modeling, processing, and results p 19 N85-18437

UNITED NATIONS

Commercialization of remote sensing data - Its impact on the continuity and accessibility of remote sensing data, including response to standing orders as well as on the standardization of products p 71 A85-20642

UNITED STATES

An estimation of continental crust magnetization and susceptibility from Magsat data for the conterminous United States p 22 A85-26420

United States crustal thickness p 18 A85-28011

Evaluation of the radar response to land surfaces and volumes Examination of theoretical models, target statistics, and applications p 63 N85-17250

UPLINKING

A comparative analysis of some prediction methods for rain attenuation statistics in earth-to-space links p 42 A85-21130

URBAN DEVELOPMENT

Method for sequential analysis of spatial development in a rural-urban fringe zone p 13 A85-20748

URBAN PLANNING

- MASMAP, design for a project-oriented geo-information program package for urban upgrading schemes p 13 A85-20747
- An examination of some problems and solutions in monitoring urban areas from satellite platforms p 14 A85-26935

URBAN RESEARCH

- Population estimation from aerial photos for non-homogeneous urban residential areas p 14 A85-20749

USER MANUALS (COMPUTER PROGRAMS)

- NOAA-AISC user's guide for implementing CERES maize model for large area yield estimation [E85-10083] p 12 N85-21748
- User's guide to the TAMW wheat model as implemented on the IBM 360/195 computer [E85-10084] p 12 N85-21749
- NOAA-AISC user's guide for implementing CERES wheat model for large area yield estimation [E85-10085] p 12 N85-21750

UTAH

- Detecting agricultural to urban land use change from multi-temporal MSS digital data --- Salt Lake County, Utah [E85-10049] p 15 N85-16245
- An integrated remote sensing approach for identifying ecological range sites --- parker mountain [E85-10050] p 8 N85-16246
- Assessment of LANDSAT for rangeland mapping, Rush Valley, Utah [E85-10072] p 15 N85-19486
- An integrated GIS/remote sensing data base in North Cache soil conservation district, Utah A pilot project for the Utah Department of Agriculture's RIMS (Resource Inventory and Monitoring System) [E85-10073] p 11 N85-19487
- LANDSAT 4 investigation of Thematic Mapper and Multispectral Scanner applications [E85-10076] p 52 N85-19490

V

VARIABLE STARS

- The secular period behavior of 38 RR Lyrae stars in the LMC globular cluster NGC 2257 p 14 A85-25070

VEGETATION

- African land-cover classification using satellite data p 1 A85-21174
- Determination of reflectances of tropical vegetation by combined methods of radiometry and photometry p 2 A85-23760
- Classification of vegetation types by analysis of X-band and C-band radar images p 4 A85-23775
- Experimental evidence for spring and autumn windows for the detection of geobotanical anomalies through the remote sensing of overlying vegetation p 6 A85-26939
- An integrated remote sensing approach for identifying ecological range sites --- parker mountain [E85-10050] p 8 N85-16246
- Microwave and optical remote sensing of forest vegetation p 9 N85-17228
- Remote sensing of soil moisture p 10 N85-17252
- North American vegetation patterns observed with the NOAA-7 advanced very high resolution radiometer --- North America [E85-10062] p 10 N85-17400
- Shortwave infrared detection of vegetation [E85-10064] p 10 N85-17402
- An integrated GIS/remote sensing data base in North Cache soil conservation district, Utah A pilot project for the Utah Department of Agriculture's RIMS (Resource Inventory and Monitoring System) [E85-10073] p 11 N85-19487
- Preliminary evaluation of the airborne imaging spectrometer for vegetation analysis [NASA-CR-174440] p 12 N85-19496
- Thematic Mapper spectral dimensionality and data structure p 12 N85-21736
- Investigations of vegetation and soils information contained in LANDSAT Thematic Mapper and Multispectral Scanner data [E85-10082] p 12 N85-21747
- VEGETATION GROWTH**
- Estimation of the vegetation contribution to the 1.65-2.22 micron ratio in airborne thematic-mapper imagery of the Virginia Range, Nevada p 5 A85-26931
- Spectral characterization of the LANDSAT-4 MSS sensors p 65 N85-20499
- NOAA-AISC user's guide for implementing CERES wheat model for large area yield estimation [E85-10085] p 12 N85-21750
- Estimating solar radiation for plant simulation models [E85-10089] p 13 N85-21751

VEGETATIVE INDEX

- Computing the foliage angle distribution from contact frequency data p 6 A85-29969

VERTICAL DISTRIBUTION

- Magsat vertical field anomalies above 40 deg N from spherical cap harmonic analysis p 18 A85-26417

VERTICAL ORIENTATION

- Along-track deflection of the vertical from SEASAT GEBCO (General Bathymetric Chart of the Oceans) overlays [PB85-129641] p 42 N85-21767

VIBRATION

- An analysis of the high frequency vibrations in early Thematic Mapper scenes p 69 N85-21742

VIRGINIA

- Intraband radiometric performance of the LANDSAT 4 Thematic Mapper --- Washington, DC, Arkansas, Massachusetts, Virginia, and Arizona p 69 N85-21738

VISIBILITY

- Determination of visual range from Landsat data p 47 A85-24285

VISIBLE SPECTRUM

- Spectral characterization of vegetation canopies in the visible and NIR - Application to remote sensing p 5 A85-25670

VISUAL OBSERVATION

- Observations of the earth using nighttime visible imagery p 48 A85-25350

VOLCANOES

- The 1982 El Chichon Volcano eruptions - A satellite perspective p 14 A85-27984
- Satellite photographs suggest arctic volcano p 38 N85-16239

- Evaluation of the L-band scattering characteristics of volcanic terrain in aid of lithologic identification, assessment of SIR-B calibration, and development of planetary geomorphic analogs p 24 N85-17232

VOLCANOLOGY

- The 1982 El Chichon Volcano eruptions - A satellite perspective p 14 A85-27984
- Tectonic, volcanic, and climatic geomorphology study of the Sierras Pampeanas Andes, northwestern Argentina p 24 N85-17215

VORTICES

- Center of mass estimation in closed vortices - A verification in principle and practice p 26 A85-19417
- A sampling strategy for altimeter measurements of the global statistics of mesoscale eddies p 32 A85-24553
- Eddy kinetic energy distribution in the southern ocean from Seasat altimeter and FGGE drifting buoys p 32 A85-24554
- Abyssal eddies near the Gulf Stream p 34 A85-27701
- Lagrangian observations of surface circulation at the Emperor Seamount chain p 35 A85-27710
- Remote-sensing observations of advective eddies in the central part of the Baltic Sea p 38 A85-29915

W

WAKES

- SEASAT 3 and 4 [AD-A148343] p 40 N85-17274

WATER CIRCULATION

- Features characterizing the development of mushroom-shaped currents in the ocean, revealed by an analysis of satellite imagery p 34 A85-25651
- The potential for ocean prediction and the role of altimeter data p 36 A85-29704
- Observing global ocean circulation with SEASAT altimeter data p 36 A85-29705
- Remote-sensing observations of advective eddies in the central part of the Baltic Sea p 38 A85-29915

WATER POLLUTION

- Remote sensing techniques for monitoring of pollution in coastal waters - Potential application to Saudi Arabia p 34 A85-27441

WATER QUALITY

- Development of water quality models applicable throughout the entire San Francisco Bay and Delta p 42 A85-21046
- Remote sensing of water quality in the Neuse River Estuary, North Carolina p 43 A85-29219
- Monitoring water quality conditions in a large western reservoir with Landsat imagery p 43 A85-29220

WATER RESOURCES

- Estimating ocean primary production from satellite chlorophyll - Introduction to regional differences and statistics for the Southern California Bight p 35 A85-28005
- Building a functional, integrated GIS/remote sensing resource analysis and planning system --- Utah [E85-10092] p 15 N85-21754

WATER WAVES

- Predicting dangerous ocean waves with spaceborne synthetic aperture radar p 27 A85-19429
- Aircraft and satellite measurement of ocean wave directional spectra using scanning-beam microwave radars p 27 A85-20486
- A comparison of in situ and airborne radar observations of ocean wave directionality p 27 A85-20487
- Imaging ocean surface waves by synthetic aperture radar - A review p 29 A85-23682
- Can optical measurements help in the interpretation of radar backscatter? p 29 A85-23683
- The effect of a moving sea surface on SAR imagery p 29 A85-23685
- Theory of SAR ocean wave imaging p 29 A85-23686
- Effect of defocusing on the images of ocean waves p 29 A85-23688
- Wave measurements with the Seasat radar altimeter - A Review p 30 A85-23701
- Spatial variation of significant wave-height p 30 A85-23704
- Transformation of sea-wave spectrum into a synthetic-aperture-radar image spectrum p 34 A85-25661

- World ocean mean monthly waves, swell, and surface winds for July through October 1978 from SEASAT radar altimeter data p 37 A85-29707
- Electromagnetic bias of 36-GHz radar altimeter measurements of MSL --- Mean Sea Level p 37 A85-29712

- The interpretation of the SIR-B imagery of surface waves and other oceanographic features using in-situ, meteorological satellite, and infrared satellite data p 39 N85-17212
- The spatial evolution of the directional wave spectrum in the Southern Ocean Its relation to extreme waves in Agulhas Current p 39 N85-17213

- The imaging of internal waves by the SEASAT-A synthetic aperture radar [AD-A149808] p 20 N85-21761

WEATHER FORECASTING

- Rain volume estimation over areas using satellite and radar data [NASA-CR-174434] p 44 N85-19568

WEATHER MODIFICATION

- The management of atmospheric resources in food production p 9 N85-16362

WEST GERMANY

- Activities report of the Department of Applied Research 78 for satellite geodesy of the Technical University, Munich [ASTRON-GEODAET-ARB-45] p 19 N85-18440

WHEAT

- Estimation of wheat production on the basis of Landsat channel 5 and 7 radiometric measurements p 3 A85-23763
- Growth/reflectance model interface for wheat and corresponding model [E85-10058] p 9 N85-16269
- Growth and reflectance characteristics of winter wheat canopies [E85-10080] p 11 N85-19494
- User's guide to the TAMW wheat model as implemented on the IBM 360/195 computer [E85-10084] p 12 N85-21749
- NOAA-AISC user's guide for implementing CERES wheat model for large area yield estimation [E85-10085] p 12 N85-21750

WILDLIFE

- Investigation of Krasnovodsk bay on the basis of space photographs p 28 A85-21669

WIND EFFECTS

- Predicting dangerous ocean waves with spaceborne synthetic aperture radar p 27 A85-19429

WIND MEASUREMENT

- Validation and applications of SASS over JASIN --- wind scatterometer results in Atlantic NW of Scotland p 29 A85-23681
- A summary of the wind data available from satellites from the past history to future sensors p 33 A85-24558

- Airborne Doppler estimates of the air motions associated with a developing, sea-breeze induced, mesoscale precipitation line p 36 A85-28783

WIND PROFILES

- Oceanographic and meteorological research based on the data products of SEASAT [E85-10091] p 41 N85-21753

WIND VELOCITY

- Swell propagation in the North Atlantic ocean using SEASAT altimeter p 30 A85-23702
- The scanning multichannel microwave radiometer - An assessment p 57 A85-23705

WIND VELOCITY MEASUREMENT

SUBJECT INDEX

WIND VELOCITY MEASUREMENT

Wind speed and stress over the ocean - Scatterometer
versus surface measurements p 33 A85-24557
World ocean mean monthly waves, swell, and surface
winds for July through October 1978 from SEASAT radar
altimeter data p 37 A85-29707

X

X RAY SPECTROSCOPY

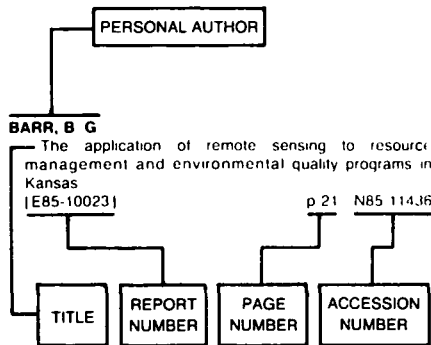
An auroral X-ray imaging spectrometer
[AD-A147756] p 64 N85-17469

Y

YIELD

NOAA-AISC user's guide for implementing CERES
maize model for large area yield estimation
[E85-10083] p 12 N85-21748

Typical Personal Author Index Listing



Listings in this index are arranged alphabetically by personal author. The title of the document provides the user with a brief description of the subject matter. The report number helps to indicate the type of document listed (e.g., NASA report, translation, NASA contractor report). The page and accession numbers are located beneath and to the right of the title. Under any one author's name the accession numbers are arranged in sequence with the AIAA accession numbers appearing first.

A

- AANSTOOS, J. V.**
Evaluation of an experimental system for spaceborne processing of multispectral image data p 46 A85-23144
- AARDOOM, L.**
The participation of the Netherlands in the NASA Crustal Dynamics Project p 15 A85-20035
- ABBOTT, M. R.**
Estimating ocean primary production from satellite chlorophyll - Introduction to regional differences and statistics for the Southern California Bight p 35 A85-28005
- ABDELLAOUI, A.**
Effects of the experimental errors and conditions on the estimation of thermal inertia and evapotranspiration from METEOSAT data p 3 A85-23767
- ABRAMENOK, G. A.**
Analysis of mesofractures according to space images - Currents trends in the exploration for oil and gas deposits p 21 A85-25655
- ABRAMS, M.**
Generation of a Landsat-HCMM combined image and its application to geological cartography p 21 A85-23792
- ABRAMS, R. B.**
Radiometric calibration and processing procedure for reflective bands on LANDSAT-4 protoflight Thematic Mapper p 66 N85-20510
TM digital image products for applications p 54 N85-20512
Characterization of radiometric calibration of LANDSAT-4 reflective bands p 66 N85-20516
- ADLER, R.**
Hybrid method of mapping and photogeodetic control network densification [PB85-133775] p 20 N85-21766
- AGREEN, R. W.**
Observing global ocean circulation with SEASAT altimeter data p 36 A85-29705
- AITKEN, G. W.**
Optical engineering for cold environments, Proceedings of the Meeting, Arlington, VA, April 7, 8, 1983 p 59 A85-25344

- ALCOCK, G. A.**
Altimeter measurements of ocean topography p 30 A85-23695
- ALFORD, W. L.**
Summary of MSS characterization investigations p 53 N85-20497
Radiometric accuracy assessment of LANDSAT 4 Multispectral Scanner data p 53 N85-20498
Geometric accuracy assessment of LANDSAT-4 Multispectral Scanner (MSS) data p 19 N85-20505
- ALLAN, J. A.**
The educational role of satellites p 70 A85-20574
- ALLAN, T.**
The interpretation of SIR-B imagery of surface waves and other oceanographic features using in-situ, meteorological satellite, and infrared satellite data p 39 N85-17212
- ALLAN, T. D.**
Satellite microwave remote sensing p 28 A85-23676
- ALLENBY, R. J.**
A review of SEASAT p 28 A85-23677
- ALLENBY, R. J.**
United States crustal thickness p 18 A85-28011
Estimation of lower crust magnetization from satellite derived anomaly field p 18 A85-28012
- ALLEY, R. E.**
Calculation of thermal inertia from day-night measurements separated by days or weeks p 45 A85-21048
- ALPERS, W.**
Imaging ocean surface waves by synthetic aperture radar - A review p 29 A85-23682
- AMATA, E.**
A comparison between GEOS 1 magnetic-field measurements and some models of the geomagnetic field p 18 A85-27386
- AMIS, M. L.**
Investigation of TM band-to-band registration using the JSC registration processor p 69 N85-21745
- AMURSKII, G. I.**
Analysis of mesofractures according to space images - Currents trends in the exploration for oil and gas deposits p 21 A85-25655
- ANDERSON, J. E.**
LANDSAT scene-to-scene registration accuracy assessment p 65 N85-20502
- ANDERSEN, R. S.**
Computing the foliage angle distribution from contact frequency data p 6 A85-29969
- ANGLADE, I.**
Study of the correlation between the IRT band of the NOAA AVHRR and the factors conditioning the thermal behavior of bioclimatic areas on a regional scale p 58 A85-23768
- ANIKOVICH, V. M.**
Determination of the physical parameters of sea ice on the basis of remote microwave measurements in the 0.3-18 cm range p 38 A85-29903
- ANUTA, P. E.**
Evaluation of the radiometric quality of the TM data using clustering, linear transformations and multispectral distance measures p 54 N85-21731
Spatial resolution estimation of LANDSAT-4 Thematic Mapper data p 69 N85-21741
- APEL, J. R.**
A survey of some recent scientific results from the Seasat altimeter p 30 A85-23696
- ARKANI-HAMED, J.**
Scalar magnetic anomalies of Canada and northern United States derived from Magsat data p 18 A85-26418
- ARNOLD, K.**
Cosmic interpolation of terrestrial potential values p 18 A85-26476
- ARNONE, R. A.**
Bio-optical variability in the Alboran Sea as assessed by Nimbus-7 coastal zone color scanner [AD-A147909] p 39 N85-16281
Satellite definition of the bio-optical and thermal variation of coastal eddies associated with the African current [AD-A147910] p 39 N85-16282

- ARP, G. K.**
The importance of geobotany in geological remote sensing applications p 23 A85-27948
- ATLAS, D.**
Simultaneous ocean cross-section and rainfall measurements from space with a nadir pointing radar p 36 A85-28788
Simultaneous ocean cross-section and rainfall measurements from space with a nadir-pointing radar [NASA-TM-86167] p 44 N85-16273
- AXELSSON, S.**
Ground truth for SIR-B images obtained by SIR system 8 impulse radar p 10 N85-17251

B

- BADHWAR, G. D.**
Comparative study of Suits and SAIL canopy reflectance models p 7 A85-30092
Application of Thematic Mapper data to corn and soybean development stage estimation p 7 A85-30093
- BAGG, M.**
The investigation of selected oceanographic applications of spaceborne synthetic-aperture radar p 39 N85-17233
- BAGG, M. M.**
The imaging of internal waves by the SEASAT-A synthetic aperture radar [AD-A149808] p 20 N85-21761
- BAILEY, B.**
Near-infrared spectroscopy in geological reconnaissance and exploration p 22 A85-27944
- BAKAI, G. G.**
The use of Salyut-5 photographs for regional geomorphological mapping p 23 A85-28999
- BAKER, P. L.**
Aircraft and satellite measurement of ocean wave directional spectra using scanning-beam microwave radars p 27 A85-20486
- BALL, D. L.**
Radiometric calibration and processing procedure for reflective bands on LANDSAT-4 protoflight Thematic Mapper p 66 N85-20510
TM digital image products for applications p 54 N85-20512
Prelaunch absolute radiometric calibration of the reflective bands on the LANDSAT-4 protoflight Thematic Mapper p 66 N85-20515
Characterization of radiometric calibration of LANDSAT-4 reflective bands p 66 N85-20516
- BARAN, W.**
Methods of space geodesy and its role in earth studies p 19 A85-30013
- BARBER, B. C.**
Some properties of SAR speckle p 46 A85-23684
The investigation of selected oceanographic applications of spaceborne synthetic-aperture radar p 39 N85-17233
- BARDINET, C.**
Inventory of geographically homogeneous zones by spectral modeling of diachronic Meteosat albedo or combined albedo/thermal-channel data - Applications to the Maghreb and to Sahelian Africa p 46 A85-23769
Geomorphology and remote sensing Numenal inventory of objects in Landsat, SPOT simulation, and SIR-A data Applications to the Mopt-Bandiagara (Mali) region p 21 A85-23785
- BARET, F.**
Estimation of wheat production on the basis of Landsat channel 5 and 7 radiometric measurements p 3 A85-23763
- BARKER, J. L.**
LANDSAT-4 Science Characterization Early Results Volume 1. Multispectral Scanner (MSS) [E85-10067] p 65 N85-20496
Spectral characterization of the LANDSAT-4 MSS sensors p 65 N85-20499
LANDSAT-4 Science Characterization Early Results Volume 2, part 1 Thematic Mapper (TM) [E85-10068] p 66 N85-20508

- Radiometric calibration and processing procedure for reflective bands on LANDSAT-4 protoflight Thematic Mapper p 66 N85-20510
TM digital image products for applications p 54 N85-20512
- Spectral characterization of the LANDSAT Thematic Mapper sensors p 66 N85-20514
Prelaunch absolute radiometric calibration of the reflective bands on the LANDSAT-4 protoflight Thematic Mapper p 66 N85-20515
Characterization of radiometric calibration of LANDSAT-4 reflective bands p 66 N85-20516
LANDSAT-4 Science Characterization Early Results Volume 3, part 2 Thematic Mapper (TM) [E85-10069] p 67 N85-21724
Relative radiometric calibration of LANDSAT TM reflective bands p 67 N85-21725
Thermal band characterization of the LANDSAT-4 Thematic Mapper p 67 N85-21727
- BARNES, M. B.**
The investigation of selected oceanographic applications of spaceborne synthetic-aperture radar p 39 N85-17233
- BARRACLOUGH, D. R.**
Mathematical modelling of the geomagnetic field and secular variation, and its applications, Proceedings of the Symposium, Hamburg, West Germany, August 15-27, 1983 p 16 A85-25689
- BARRY, R. G.**
Lake ice occurrence as a possible detector of atmospheric CO₂ effects on climate [DE85-002951] p 45 N85-20606
- BARTOLUCCI, L. A.**
Evaluation of the radiometric quality of the TM data using clustering, linear transformations and multispectral distance measures p 54 N85-21731
- BARTON, D. K.**
Land clutter models for radar design and analysis p 49 A85-27827
- BASKAKOV, A. I.**
Simultaneous radiometric and radar altimetric measurements of sea microwave signatures p 31 A85-24076
- BATSON, R. M.**
Tests of low-frequency geometric distortions in LANDSAT 4 images p 55 N85-21744
- BAUER, M. E.**
Variation in spectral response of soybeans with respect to illumination, view, and canopy geometry [E85-10040] p 8 N85-16241
Spectral estimators of absorbed photosynthetically active radiation in corn canopies [E85-10041] p 8 N85-16242
Microwave and optical remote sensing of forest vegetation p 9 N85-17228
Growth and reflectance characteristics of winter wheat canopies [E85-10080] p 11 N85-19494
- BAYLIS, P. E.**
An automatic high-resolution picture transmission receiving station p 61 A85-27698
- BEAL, R. C.**
Predicting dangerous ocean waves with spaceborne synthetic aperture radar p 27 A85-19429
The spatial evolution of the directional wave spectrum in the Southern Ocean Its relation to extreme waves in Agulhas Current p 39 N85-17213
- BECK, L. H.**
Remote sensing research for agricultural applications [E85-10090] p 13 N85-21752
- BECKER, F.**
Effects of the experimental errors and conditions on the estimation of thermal inertia and evapotranspiration from METEOSAT data p 3 A85-23767
- BEGIN, D.**
Classification of vegetation types by analysis of X-band and C-band radar images p 4 A85-23775
- BELEVICH, V. V.**
Evaluation of the ocean/atmosphere thermal interaction in the Atlantic FGGE area p 28 A85-22175
- BELIKOV, P. V.**
Determination of the heights of points of a place on the basis of radar-survey data p 19 A85-29000
- BELL, E. J.**
Analysis of SIR-B radar illumination of geometry for depth of penetration and surface feature and vegetation detection, Nevada and California p 25 N85-17248
- BELL, R.**
Experimental evidence for spring and autumn windows for the detection of geobotanical anomalies through the remote sensing of overlying vegetation p 6 A85-26939
- BELLE, K. C.**
Airborne Doppler estimates of the air motions associated with a developing, sea-breeze induced, mesoscale precipitation line p 36 A85-28783
- BENARD, M.**
Inventory of geographically homogeneous zones by spectral modeling of diachronic Meteosat albedo or combined albedo/thermal-channel data - Applications to the Maghreb and to Sahelian Africa p 46 A85-23769
Geomorphology and remote sensing Numerical inventory of objects in Landsat, SPOT simulation, and SIR-A data Applications to the Mopti-Bandiagara (Mali) region p 21 A85-23785
- BENDER, L. U.**
A preliminary evaluation of LANDSAT-4 Thematic Mapper data for their geometric and radiometric accuracies p 54 N85-21739
- BENNETT, D.**
Radiometric calibration and geocoded precision processing of LANDSAT-4 Multispectral Scanner products by the Canada Centre for Remote Sensing p 53 N85-20501
- BENNING, V. M.**
An example of Landsat cost effectiveness in mapping land-cover p 1 A85-20573
- BENOIT, J.**
Structure and seasonal characteristics of the Gaspe current p 35 A85-27705
- BERENSTEIN, C. A.**
Analysis of subpixel registration p 51 N85-16267
- BERNSTEIN, R. L.**
Satellite sea surface temperature determination from microwave and infrared radiometry p 33 A85-24556
- BEYER, E. P.**
An overview of the Thematic Mapper geometric correction system p 53 N85-20511
- BIEGEL, J. D.**
Comparison of modelled and empirical atmospheric propagation data p 46 A85-22678
- BIEL, L. L.**
Variation in spectral response of soybeans with respect to illumination, view, and canopy geometry [E85-10040] p 8 N85-16241
Microwave and optical remote sensing of forest vegetation p 9 N85-17228
- BIRDSEY, R. A.**
Forest area estimates from LANDSAT MSS and forest inventory plot data [PB85-105617/GAR] p 9 N85-16290
- BLANCHARD, A. J.**
Detection of lowland flooding using active microwave systems p 43 A85-29218
- BLANCHARD, B. J.**
Detection of lowland flooding using active microwave systems p 43 A85-29218
- BLAZQUEZ, C. H.**
Analysis of ACIR transparencies of citrus trees with a projecting spectral densitometer p 1 A85-21050
- BLEUER, N. K.**
Interlobate comparison of glacial-depositional style as evidenced by small-relief glacial landscape features in Illinois, Indiana, and Ohio, utilizing SIR-B p 39 N85-17231
- BLIVEN, L. F.**
The Harp probe - An in situ Bragg scattering sensor p 28 A85-22171
- BLODGET, H. W.**
Structural investigation of the Canadian Shield by orbital radar and LANDSAT p 25 N85-17236
Structural investigation of the Grenville Province by radar and other imaging and nonimaging sensors p 25 N85-17237
Automatic terrain elevation mapping and registration p 52 N85-17242
- BLOM, R.**
Application and calibration of the subsurface mapping capability of SIR-B in desert regions p 25 N85-17244
- BLOOM, A. L.**
Tectonic, volcanic, and climatic geomorphology study of the Sierras Pampeanas Andes, northwestern Argentina p 24 N85-17215
- BOBERG, D.**
Information extraction and transmission techniques for spaceborne synthetic aperture radar images [NASA-CR-174341] p 52 N85-17256
- BODECHTEL, J.**
MOMS 1 and its results p 61 A85-27061
- BOERWINKEL, E.**
Regional analysis from data from heterogeneous pixels - Remote sensing of total dry matter production in the Senegalese Sahel p 47 A85-23783
- BOGORODSKII, V. V.**
Interpretation of aircraft sea ice microwave data p 32 A85-24080
Improvement of the accuracy of radar measurements of sea-ice thickness by cepstral processing of reflected signals p 35 A85-27736
- BOIARSKII, V. I.**
Improvement of the accuracy of radar measurements of sea-ice thickness by cepstral processing of reflected signals p 35 A85-27736
- BOLDYREV, N. I.**
Interpretation of space images of the sea surface using the SVIT digital-processing complex p 34 A85-25654
- BONN, F.**
Classification of vegetation types by analysis of X-band and C-band radar images p 4 A85-23775
Spectral response of different agricultural and penurban land-use units in the spectral windows at 1.55-1.75 and 2.08-2.35 microns p 4 A85-23787
Classification of the geological environments of Anticosti Island - An approach using a Landsat-4 spectral simulation p 21 A85-23790
Integration of the SPOT panchromatic channel into its multispectral mode for image sharpness enhancement p 49 A85-29217
- BORENGASSER, M.**
Analysis of SIR-B radar illumination of geometry for depth of penetration and surface feature and vegetation detection, Nevada and California p 25 N85-17248
- BORG, C. G.**
Ground truth for SIR-B images obtained by SIR system 8 impulse radar p 10 N85-17251
- BORGESON, W. T.**
Tests of low-frequency geometric distortions in LANDSAT 4 images p 55 N85-21744
- BORN, G. H.**
A survey of oceanographic satellite altimetric missions p 36 A85-29703
- BRACHET, G.**
Commercialization of remote sensing data - Its impact on the continuity and accessibility of remote sensing data, including response to standing orders as well as on the standardization of products p 71 A85-20642
The spot operational remote sensing satellite system Current status and perspectives p 67 N85-20776
- BREED, C. S.**
Application and calibration of the subsurface mapping capability of SIR-B in desert regions p 25 N85-17244
- BRENNECKE, J.**
The altimetric geoid in the North Sea p 16 A85-23700
- BRETHERTON, F. P.**
A sampling strategy for altimeter measurements of the global statistics of mesoscale eddies p 32 A85-24553
- BROCHU, R.**
Classification of vegetation types by analysis of X-band and C-band radar images p 4 A85-23775
- BROOKS, D. R.**
An intercalibration of Meteosat-1 and GOES-2 visible and infrared measurements p 26 A85-19420
- BROOKS, J.**
LS-4 MSS geometric correction Methods and results p 53 N85-20507
- BROSSIER, C.**
World ocean mean monthly waves, swell, and surface winds for July through October 1978 from SEASAT radar altimeter data p 37 A85-29707
- BROWN, P. V. K.**
Remote sensing by radar altimetry p 26 A85-19428
- BROZIN, KH. IU.**
Remote-sensing observations of advective eddies in the central part of the Baltic Sea p 38 A85-29915
- BRUNET, Y.**
Influence of spatial variability of soil hydraulic characteristics on surface parameters obtained from remote-sensing data in thermal infrared and microwaves p 43 A85-23786
- BRUSH, R. J. H.**
An automatic high-resolution picture transmission receiving station p 61 A85-27698
- BRYAN, M. L.**
Deforestation, floodplain dynamics, and carbon biogeochemistry in the Amazon Basin p 44 N85-17216
- BUCKINGHAM, W.**
Near-infrared spectroscopy in geological reconnaissance and exploration p 22 A85-27944
- BUI, J. P.**
Development of a SPOT-simulation radiometer p 57 A85-23759
- BUNNIK, N. J. J.**
Comparative study of Suits and SAIL canopy reflectance models p 7 A85-30092
- BURKE, K.**
Neotectonics of the Caribbean p 27 A85-21145
- BURPÉE, R. W.**
Airborne Doppler estimates of the air motions associated with a developing, sea-breeze induced, mesoscale precipitation line p 36 A85-28783
- BUSH, G. B.**
An analysis of a satellite multibeam altimeter p 38 A85-29715

BYCHKOVA, I. A.

Remote-sensing observations of advective eddies in the central part of the Baltic Sea p 38 A85-29915

BYRNE, G.

Evaluation of SIR-B imagery for geologic and geomorphic mapping, hydrology, and oceanography in Australia p 51 N85-17229

C

CALLAN, C.

SEASAT 3 and 4 [AD-A148343] p 40 N85-17274

CAMPBELL, W. J.

World ocean mean monthly waves, swell, and surface winds for July through October 1978 from SEASAT radar altimeter data p 37 A85-29707

CANDE, S. C.

Intermediate-wavelength magnetic anomaly field of the North Pacific and possible source distributions p 17 A85-26414

CANDIDI, M.

A comparison between GEOS 1 magnetic-field measurements and some models of the geomagnetic field p 18 A85-27386

CANO, D.

Inventory of geographically homogeneous zones by spectral modeling of diachronic Meteosat albedo or combined albedo/thermal-channel data - Applications to the Maghreb and to Sahelian Africa p 46 A85-23769

CARD, D. H.

Assessment of Thematic Mapper band-to-band registration by the block correlation method p 55 N85-21743

CARIGNAN, M.

Spectral response of different agricultural and perurban land-use units in the spectral windows at 1.55-1.75 and 2.08-2.35 microns p 4 A85-23787

CARR, H.

SIR-B cartography and stereo topographic mapping p 19 N85-17234

CARROLL, T. R.

Airborne snow water equivalent and soil moisture measurement using natural terrestrial gamma radiation p 43 A85-25352

CARTWRIGHT, D. E.

Altimeter measurements of ocean topography p 30 A85-23695

CASE, K.

SEASAT 3 and 4 [AD-A148343] p 40 N85-17274

CASTLE, K. R.

In-progress absolute radiometric inflight calibration of the LANDSAT-4 sensors p 68 N85-21733

CATLOW, D. R.

The integrated use of digital cartographic data and remotely sensed imagery p 45 A85-20572

CAVALIERI, D. J.

Performance of an airborne imaging 92/183 GHz radiometer during the Bering Sea Marginal Ice Zone Experiment (MIZEX-WEST) p 33 A85-24945

CAVAYAS, F.

The measurement of bidirectional reflectances by analysis of Landsat images p 2 A85-23756

CHALLENGER, P. G.

Spatial variation of significant wave-height p 30 A85-23704

CHANCELLOR, J.

Intermediate results of radar backscatter measurements from summer sea ice [AD-A147212] p 38 N85-15960

CHARBONNEAU, L.

Spectral response of different agricultural and perurban land-use units in the spectral windows at 1.55-1.75 and 2.08-2.35 microns p 4 A85-23787

CHAUME, R.

Comparative seasonal evolution of the spectral signatures of broad-leaved and coniferous trees from Landsat data Comparison with other perennial surfaces p 2 A85-23757

CHAVEZ, P.

Thematic mapper data analysis p 23 A85-27946

CHAVEZ, P. S., JR.

Intraband radiometric performance of the LANDSAT 4 Thematic Mapper p 69 N85-21738

CHEEVASUVIT, F.

Thermal structure of an agricultural region as seen by NOAA-7 AVHRR p 7 A85-30090

CHEN, W.

Remote sensing development in the People's Republic of China p 56 A85-20643

CHENEY, R. E.

Regional mean sea surfaces based on GEOS-3 and SEASAT altimeter data p 38 A85-29716

CHESHIRE, H. M.

Remote sensing of water quality in the Neuse River Estuary, North Carolina p 43 A85-29219

CHHIKARA, R. S.

Calibration or inverse regression Which is appropriate for crop surveys using LANDSAT data? p 9 N85-16260

CHI, T.

Study on a regional geographical information system and application model p 13 A85-20644

CHIN, R. T.

Resolution enhancement of multichannel microwave imagery from the Nimbus-7 SMMR for maritime rainfall analysis [NASA-CR-174367] p 44 N85-19221

CHING, N. P.

An example of Landsat cost effectiveness in mapping land-cover p 1 A85-20573

CHOROWICZ, J.

Generation of a Landsat-HCMM combined image and its application to geological cartography p 21 A85-23792
Thematic evaluation of SPOT spectral bands p 58 A85-23794

CHOY, L. W.

Electromagnetic bias of 10-GHz radar altimeter measurements of MSL p 37 A85-29713

CICONE, R. C.

Thematic Mapper spectral dimensionality and data structure p 12 N85-21736

CIHLAR, J.

Evaluation of the radar response to land surfaces and volumes Examination of theoretical models, target statistics, and applications p 63 N85-17250

CLARK, J.

Forest area estimates from LANDSAT MSS and forest inventory plot data [PB85-105617/GAR] p 9 N85-16290

CLARK, S. C.

Satellite magnetic anomalies over subduction zones - The Aleutian Arc anomaly p 16 A85-21107

CLICHE, G.

Integration of the SPOT panchromatic channel into its multispectral mode for image sharpness enhancement p 49 A85-29217

CLIFF, W. C.

Analysis of the NASA/MSFC Airborne Doppler Lidar results from San Geronio Pass, California [NASA-CR-171355] p 70 N85-21873

COLES, R. L.

Magsat scalar magnetic anomalies at northern high latitudes p 18 A85-26416

COLLINS, A. B.

Canadian plans for Thematic Mapper data p 54 N85-20513

COLLINS, W.

Near-infrared spectroscopy in geological reconnaissance and exploration p 22 A85-27944
The importance of geobotany in geological remote sensing applications p 23 A85-27948

COLOMBO, O. L.

Altimetry, orbits and tides [E85-10066] p 40 N85-17404

COLWELL, J. E.

Investigations of vegetation and soils information contained in LANDSAT Thematic Mapper and Multispectral Scanner data [E85-10082] p 12 N85-21747

COLWELL, R. N.

Analysis of the quality of image data required by the LANDSAT-4 Thematic Mapper and Multispectral Scanner [E85-10074] p 11 N85-19488

Remote sensing research for agricultural applications [E85-10090] p 13 N85-21752

COMBEAU, A.

Comparative seasonal evolution of the spectral signatures of broad-leaved and coniferous trees from Landsat data Comparison with other perennial surfaces p 2 A85-23757

COOLEY, R. C.

Thematic Mapper Volume 1 Calibration report flight model, LANDSAT 5 [E85-10059] p 63 N85-16270

CORDIER, P.

Comparison of SPOT HRV and Landsat-4 TM for crop inventories p 3 A85-23762

COVER, W.

Nautical charting with remotely sensed imagery, volume 1 [AD-A149361] p 41 N85-19503

Nautical charting with remotely sensed imagery Volume 2 Case studies [AD-A149362] p 41 N85-19504

CRIST, E.

Investigations of vegetation and soils information contained in LANDSAT Thematic Mapper and Multispectral Scanner data [E85-10082] p 12 N85-21747

CRIST, E. P.

Thematic Mapper spectral dimensionality and data structure p 12 N85-21736

CUDDAPAH, P.

Remote sensing of soil moisture p 10 N85-17252

D

DANIAULT, N.

Eddy kinetic energy distribution in the southern ocean from Seasat altimeter and FGGE drifting buoys p 32 A85-24554

DAROVSKIKH, A. N.

Interpretation of aircraft sea ice microwave data p 32 A85-24080

DASHEN, R.

SEASAT 3 and 4 [AD-A148343] p 40 N85-17274

DASILVAFAGUNDESFILHO, E.

Integrated analysis of remote sensing products from basic geological surveys [E85-10052] p 24 N85-16248

DAUGHTRY, C. S. T.

Spectral estimators of absorbed photosynthetically active radiation in corn canopies [E85-10041] p 8 N85-16242

Growth and reflectance characteristics of winter wheat canopies [E85-10080] p 11 N85-19494

Techniques for measuring intercepted and absorbed PAR in corn canopies [E85-10081] p 11 N85-19495

DAVIS, L. S.

Evidence accumulation for spatial reasoning p 50 N85-16261

DAVIS, R.

SEASAT 3 and 4 [AD-A148343] p 40 N85-17274

DE BOER, TH. A.

Visual interpretation of SAR images of two areas in the Netherlands p 1 A85-23694

DE BRUIJN, C. A.

MASMAP, design for a project-oriented geo-information program package for urban upgrading schemes p 13 A85-20747

DE MASSON DAUTUME, G.

Digital correlation of images along quasi-epipolar lines by successive approximations p 48 A85-25671

DEALMEIDA, F. C.

The management of atmospheric resources in food production p 9 N85-16362

DEAN, M. E.

Evaluation of the radiometric quality of the TM data using clustering, linear transformations and multispectral distance measures p 54 N85-21731

DEANE, G. C.

Seasat over land p 57 A85-23693

DEGLORIA, S. D.

Remote sensing research for agricultural applications [E85-10090] p 13 N85-21752

DELEONIBUS, P.

The spatial evolution of the directional wave spectrum in the Southern Ocean Its relation to extreme waves in Agulhas Current p 39 N85-17213

DELNORE, V. E.

Airborne microwave measurements of the southern Greenland ice sheet p 28 A85-23644

DENNEN, R. S.

Determination of visual range from Landsat data p 47 A85-24285

DESCHAMPS, P. Y.

Demonstration, analysis, and correction of atmospheric effects on Landsat or SPOT multispectral data p 58 A85-23781

DESTAERKE, D.

The use of SEASAT-SAR data in oceanography at the IFF p 29 N85-23690

DEVRIES, D. J.

Geodetic accuracy of LANDSAT 4 Multispectral Scanner and Thematic Mapper data p 53 N85-20504

Geodetic accuracy of LANDSAT 4 Multispectral Scanner and Thematic Mapper data p 20 N85-21746

DICKINSON, K.

A preliminary assessment of LANDSAT-4 Thematic Mapper data p 54 N85-21728

DIEBEL-LANGOHR, D.

Lidar applications in remote sensing of ocean properties p 31 A85-23755

- DIEDERIX, H.**
Needs and accessibility of developing countries for/to remote sensing information systems p 13 A85-20647
- DINGUIRARD, M.**
In-progress absolute radiometric inflight calibration of the LANDSAT-4 sensors p 68 N85-21733
- DOBSON, E. B.**
An analysis of a satellite multibeam altimeter p 38 A85-29715
- DOBSON, M. C.**
Evaluation of the radar response to land surfaces and volumes Examination of theoretical models, target statistics, and applications p 63 N85-17250
- DOLIER, B.**
The investigation of selected oceanographic applications of spaceborne synthetic-aperture radar p 39 N85-17233
- DOMIK, G.**
SIR-B cartography and stereo topographic mapping p 19 N85-17234
- DONEAUD, A. A.**
Rain volume estimation over areas using satellite and radar data [NASA-CR-174434] p 44 N85-19568
- DOUGLAS, B. C.**
Observing global ocean circulation with SEASAT altimeter data p 36 A85-29705
- DOUGLASS, G. E.**
Assessment of LANDSAT for rangeland mapping, Rush Valley, Utah [E85-10072] p 15 N85-19486
- DOW, D. D.**
The influence of the number of ground control points on the scene-to-map registration accuracy p 51 N85-16264
- DOYLE, F. J.**
Review of earth observation satellite programs p 59 A85-23795
- DRANOVSKII, V. I.**
Complex studies of the environment by optical and radar methods p 56 A85-20081
- DROFA, A. S.**
The influence of a scattering medium on the quality of an optical image p 48 A85-26294
- DUBE, C.**
Classification of vegetation types by analysis of X-band and C-band radar images p 4 A85-23775
- DUBINOVSKII, V. B.**
Determination of the external-orientation elements of aerial and space photographs in the remote sensing of dynamic processes and phenomena p 56 A85-19998
- DUCHOSSOIS, G.**
Status and future plans for ERS-1 p 31 A85-23707
- DUHAUT, P.**
Demonstration, analysis, and correction of atmospheric effects on Landsat or SPOT multispectral data p 58 A85-23781
- DUNNE, T.**
Deforestation, floodplain dynamics, and carbon biogeochemistry in the Amazon Basin p 44 N85-17216
- DUPONT, O.**
Spectral response of different agricultural and penurban land-use units in the spectral windows at 1.55-1.75 and 2.08-2.35 microns p 4 A85-23787
- DWIVEDI, R. S.**
The utility of data from various airborne sensors for soil mapping p 5 A85-26932
- DYE, D. G.**
North American vegetation patterns observed with the NOAA-7 advanced very high resolution radiometer [E85-10062] p 10 N85-17400
- DZYUBA, O.**
Satellite photographs suggest arctic volcano p 38 N85-16239

E

- EDWARDS, G. J.**
Analysis of ACIR transparencies of citrus trees with a projecting spectral densitometer p 1 A85-21050
- EFIMOV, V. B.**
Complex studies of the environment by optical and radar methods p 56 A85-20081
Features of the digital processing of radar images obtained with the sidelooking radar of the Cosmos-1500 satellite p 48 A85-25660
- EHLERS, M.**
The effects of image noise on digital correlation probability p 49 A85-29221
- EKGREN, B.**
Ground truth for SIR-B images obtained by SIR system 8 impulse radar p 10 N85-17251

- EL-SABH, M. I.**
Structure and seasonal characteristics of the Gaspe current p 35 A85-27705
- ELACHI, C.**
Earth resources research using the Shuttle Imaging Radar system p 67 N85-20779
- ELENSKII, L. V.**
Features of the digital processing of radar images obtained with the sidelooking radar of the Cosmos-1500 satellite p 48 A85-25660
- ELIASON, E. M.**
Intraband radiometric performance of the LANDSAT 4 Thematic Mapper p 69 N85-21738
- ELIUSHKIN, V. G.**
Determination of the heights of points of a place on the basis of radar-survey data p 19 A85-29000
- ELVIDGE, C.**
The importance of geobotany in geological remote sensing applications p 23 A85-27948
- ELVIDGE, C. D.**
Estimation of the vegetation contribution to the 1.65-2.22 micron ratio in airborne thematic-mapper imagery of the Virginia Range, Nevada p 5 A85-26931
- ENGEL, J. L.**
The Thematic Mapper - Instrument overview and preliminary on-orbit results p 56 A85-22681
- ENGLAND, C. F.**
An intercalibration of Meteosat-1 and GOES-2 visible and infrared measurements p 26 A85-19420
- EPPLEY, R. W.**
Estimating ocean primary production from satellite chlorophyll - Introduction to regional differences and statistics for the Southern California Bight p 35 A85-28005
- ESTES, R. H.**
The near-earth magnetic field at 1980 determined from Magsat data p 16 A85-26408
- ETKIN, V. S.**
Determination of the physical parameters of sea ice on the basis of remote microwave measurements in the 0.3-18 cm range p 38 A85-29903
- EVERETT, J. R.**
Thematic mapper data analysis p 23 A85-27946
- EZRA, C. E.**
In-progress absolute radiometric inflight calibration of the LANDSAT-4 sensors p 68 N85-21733

F

- FAKHOURY, E.**
Remote sensing research for agricultural applications [E85-10090] p 13 N85-21752
- FALCONE, N.**
A preliminary evaluation of LANDSAT-4 Thematic Mapper data for their geometric and radiometric accuracies p 54 N85-21739
- FARRAKHOV, E. G.**
Methods for the study of recent tectonics on the basis of remote sensing and ground data p 23 A85-29904
- FEDOR, L. S.**
An algorithm to measure sea ice concentration with microwave radiometers p 27 A85-20492
- FEDOROV, K. N.**
Features characterizing the development of mushroom-shaped currents in the ocean, revealed by an analysis of satellite imagery p 34 A85-25651
- FEIGIN, M. M.**
Segmentation of half-tone remote-sensing images by the level lines method p 49 A85-29913
- FENDER, J. S.**
Synthetic apertures - An overview p 57 A85-22711
- FERNIS, D. C.**
Microcomputer systems for satellite image processing p 56 A85-20571
- FERRARI, G. M.**
Analysis of ground radiometric measurements in the rice-growing site at Tamani (Republic of Mali) - Effect of certain yield parameters on the spectral signature p 2 A85-23758
- FETT, R.**
Variations in atmospheric mixing height across oceanic thermal fronts p 34 A85-27704
- FIELDING, E. J.**
Tectonic, volcanic, and climatic geomorphology study of the Sierras Pampeanas Andes, northwestern Argentina p 24 N85-17215
- FIEUX, M.**
Large-scale oceanographic experiments and satellites, Proceedings of the Advanced Research Workshop, Porto Vecchio, Corse, France, October 3-7, 1983 p 32 A85-24551
- FINKELSHTEIN, M. I.**
Ultrasound-wave radar subsurface sounding of sea ice and earth covers p 34 A85-25594

- FITZGERALD, A.**
Preliminary evaluation of the radiometric calibration of LANDSAT-4 Thematic Mapper data by the Canada Centre for Remote Sensing p 67 N85-21729
- FLEMING, E. A.**
A preliminary assessment of LANDSAT-4 Thematic Mapper data p 54 N85-21728
- FLORENSKII, P. V.**
Space remote-sensing data in geology p 23 A85-28400
- FOERSTNER, W.**
Rectification of single and multiple frames of satellite scanner imagery using points and edges as control p 51 N85-16263
- FONTANEL, A.**
Status and plans for the SPOT program and the launch of SPOT 1 - Its on-ground processing and data dissemination to users p 56 A85-20568
- FORD, J. P.**
Mapping of glacial landforms from Seasat radar images p 36 A85-28027
- FORD, P.**
Delineation of major geologic structures in Turkey using SIR-B data p 25 N85-17249
- FORSTER, B. C.**
An examination of some problems and solutions in monitoring urban areas from satellite platforms p 14 A85-26935
Australian Multispectral Assessment of SIR-B (AMAS) p 52 N85-17243
- FOSTER, J. L.**
Observations of the earth using nighttime visible imagery p 48 A85-25350
- FOURNIER, P.**
Comparison of SPOT HRV and Landsat-4 TM for crop inventories p 3 A85-23762
- FRANCIS, C. R.**
The evaluation of SMMR retrieval algorithms p 31 A85-23706
- FRASER, G. S.**
Interlobate comparison of glacial-depositional style as evidenced by small-relief glacial landscape features in Illinois, Indiana, and Ohio, utilizing SIR-B p 39 N85-17231
- FRAYSSE, G.**
Perspectives of remote sensing in Europe at the end of the decade p 70 A85-20565
- FREIDLIN, A. A.**
Methods for the study of recent tectonics on the basis of remote sensing and ground data p 23 A85-29904
- FRENCH, V.**
Estimating solar radiation for plant simulation models [E85-10089] p 13 N85-21751
- FREY, H.**
Satellite magnetic anomalies over subduction zones - The Aleutian Arc anomaly p 16 A85-21107
Magsat and POGO magnetic anomalies over the Lord Howe Rise Evidence against a simple continental crustal structure p 18 A85-26422
- FROST, V. S.**
Information for space radar designers Required dynamic range vs resolution and antenna calibration using the Amazon rain forest p 44 N85-17239
Information extraction and transmission techniques for spaceborne synthetic aperture radar images [NASA-CR-174341] p 52 N85-17256
- FU, L.**
Remote sensing development in the People's Republic of China p 56 A85-20643
- FUKUSHIMA, N.**
Extraction of magnetic anomalies of crustal origin from Magsat data over the area of the Japanese Islands p 21 A85-26419
- FUNG, A. K.**
Surface scattering effects at different spectral regions p 58 A85-23780
Evaluation of the radar response to land surfaces and volumes Examination of theoretical models, target statistics, and applications p 63 N85-17250
- FUSCO, L.**
A preliminary analysis of LANDSAT-4 Thematic Mapper radiometric performance p 68 N85-21730
TM geometric performance Line to Line Displacement Analysis (LLDA) p 68 N85-21732
- GAFFIELD, T.**
Advanced SAR system maps Arctic regions p 35 A85-27841
- GAGARIN, S. P.**
Simultaneous radiometric and radar altimetric measurements of sea microwave signatures p 31 A85-24076

G

- GAGLIANO, J. A.**
Performance of an airborne imaging 92/183 GHz radiometer during the Bering Sea Marginal Ice Zone Experiment (MIZEX-WEST) p 33 A85-24945
- GAIAZOVA, A. K.**
Possibilities of using remote-sensing methods to improve the efficiency of oil and gas exploration p 24 A85-29905
- GALEANO, R. E.**
Needs and accessibility of developing countries for/to remote sensing information systems p 13 A85-20647
- GALLO, K. P.**
Spectral estimators of absorbed photosynthetically active radiation in corn canopies [E85-10041] p 8 N85-16242
Techniques for measuring intercepted and absorbed PAR in corn canopies [E85-10081] p 11 N85-19495
- GARDNER, S.**
Information extraction and transmission techniques for spaceborne synthetic aperture radar images [NASA-CR-174341] p 52 N85-17256
- GASTON, A.**
Regional analysis from data from heterogeneous pixels - Remote sensing of total dry matter production in the Senegalese Sahel p 47 A85-23783
- GAUTIER, C.**
Large-scale oceanographic experiments and satellites, Proceedings of the Advanced Research Workshop, Porto Vecchio, Corse, France, October 3-7, 1983 p 32 A85-24551
- GELLER, A. G.**
Soil moisture content estimation by radar survey data during the sowing campaign p 6 A85-26947
- GENTRY, R. C.**
The diurnal variation of Atlantic Ocean tropical cyclone cloud distribution inferred from geostationary satellite infrared measurements p 33 A85-24739
- GERVIN, J. C.**
Landsat-4 thematic mapper (TM) for cold environments p 60 A85-25349
Comparison of level 1 land cover classification accuracy for MSS and AVHRR data p 61 A85-26929
- GINZBURG, A. I.**
Features characterizing the development of mushroom-shaped currents in the ocean, revealed by an analysis of satellite imagery p 34 A85-25651
- GIRARD, C. J.**
Classification of vegetation types by analysis of X-band and C-band radar images p 4 A85-23775
- GLOERSEN, P.**
Data report on variations in the composition of sea ice during MIZEX/East'83 with the Nimbus-7 SMMR [NASA-TM-86170] p 40 N85-18443
- GOEL, N. S.**
Estimation of agronomic variables using spectral signatures p 2 A85-23753
- GOETZ, A. F. H.**
Imaging systems for the delineation of spectral properties of geologic materials in the visible and near-infrared p 22 A85-27945
- GOFF, T. E.**
African land-cover classification using satellite data p 1 A85-21174
- GOGINENI, S.**
Intermediate results of radar backscatter measurements from summer sea ice [AD-A147212] p 38 N85-15960
- GOLDFINGER, A.**
The spatial evolution of the directional wave spectrum in the Southern Ocean. Its relation to extreme waves in Agulhas Current p 39 N85-17213
- GONELLA, J.**
Eddy kinetic energy distribution in the southern ocean from Seasat altimeter and FGGE drifting buoys p 32 A85-24554
- GOODENOUGH, D. G.**
Canadian plans for Thematic Mapper data p 54 N85-20513
A preliminary assessment of LANDSAT-4 Thematic Mapper data p 54 N85-21728
- GORBUSHINA, E. A.**
Correlation of spectral brightnesses measured using multispectral space images p 60 A85-25659
- GORNEY, D. J.**
An auroral X-ray imaging spectrometer [AD-A147756] p 64 N85-17469
- GOROZHANKINA, S. M.**
Identification of the structure of soil-vegetation cover using aerial and space images p 5 A85-25656
- GOWARD, S. N.**
North American vegetation patterns observed with the NOAA-7 advanced very high resolution radiometer [E85-10062] p 10 N85-17400
Analysis of terrestrial conditions and dynamics [E85-10063] p 10 N85-17401
- Shortwave infrared detection of vegetation [E85-10064] p 10 N85-17402
- GRAFF, G.**
Prospecting from the skies p 23 A85-29405
- GRANT, L.**
Light polarization measurements - A method to determine the specular and diffuse light-scattering properties of both leaves and plant canopies p 2 A85-23754
- GRAY, R. T.**
Multispectral data compression using staggered detector arrays p 47 A85-24277
- GREEN, M. J.**
An airborne infrared thermal scanning system for easy use on Navy P-3 aircraft [AD-A149690] p 42 N85-22143
- GREEN, T., III**
An airborne infrared thermal scanning system for easy use on Navy P-3 aircraft [AD-A149690] p 42 N85-22143
- GREGER, G.**
SPAS-01 - Space flight technology for the general user p 61 A85-27057
- GREGOIRE, J. M.**
Analysis of ground radiometric measurements in the rice-growing site at Tamani (Republic of Mali) - Effect of certain yield parameters on the spectral signature p 2 A85-23758
- GRIEVE, R. A. F.**
Geological, structural, and geomorphological analyses from SIR-B p 24 N85-17226
- GRISHIN, G. A.**
Interpretation of space images of the sea surface using the SVIT digital-processing complex p 34 A85-25654
- GROLLIER, M. J.**
Application and calibration of the subsurface mapping capability of SIR-B in desert regions p 25 N85-17244
- GRUBB, R. N.**
The space environment monitors onboard GOES [AIAA PAPER 85-0238] p 55 A85-19608
- GUDDANDSEN, P.**
Spaceborne microwave radiometers Background and technology requirements [LD-R-267] p 63 N85-17350
- GUENTHER, K.**
Lidar applications in remote sensing of ocean properties p 31 A85-23755
- GUERTIN, F. E.**
Radiometric calibration and geocoded precision processing of LANDSAT-4 Multispectral Scanner products by the Canada Centre for Remote Sensing p 53 N85-20501
Canadian plans for Thematic Mapper data p 54 N85-20513
- GULEN, L.**
Delineation of major geologic structures in Turkey using SIR-B data p 25 N85-17249
- GUNST, R. F.**
Exploring the use of structural models to improve remote sensing agricultural estimates p 9 N85-16259
- GUNTHER, F. J.**
TM digital image products for applications p 54 N85-20512
- GURNEY, C. M.**
The use of linear feature detection to investigate Thematic Mapper data performance and processing p 69 N85-21740
- GUSEMAN, L. F., JR.**
Proceedings of the Second Annual Symposium on Mathematical Pattern Recognition and Image Analysis Program [E85-10056] p 50 N85-16251
Multivariate spline methods in surface fitting p 50 N85-16257
- GUYMER, T.**
The interpretation of SIR-B imagery of surface waves and other oceanographic features using in-situ, meteorological satellite, and infrared satellite data p 39 N85-17212
- GUYMER, T. H.**
Validation and applications of SASS over JASIN p 29 A85-23681
- GUYOT, G.**
Spectral signatures of objects in remote sensing, International Conference, 2nd, Bordeaux, France, September 12-16, 1983, Reports p 57 A85-23751
Angular and spatial variability of visible and NIR spectral data p 2 A85-23752
Development of a SPOT-simulation radiometer p 57 A85-23759
Estimation of wheat production on the basis of Landsat channel 5 and 7 radiometric measurements p 3 A85-23763
Spectral characterization of vegetation canopies in the visible and NIR - Application to remote sensing p 5 A85-25670
- GWYN, Q. H. J.**
Classification of the geological environments of Anticosti Island - An approach using a Landsat-4 spectral simulation p 21 A85-23790

H

- HACHMEISTER, L. E.**
Atlas of the Beaufort Sea [AD-A149545] p 41 N85-20619
- HAGAN, D. E.**
Lagrangian observations of surface circulation at the Emperor Seamount chain p 35 A85-27710
- HAHN, A.**
On the identification of Magsat anomaly charts as crustal part of the internal field p 17 A85-26412
- HAINES, G. V.**
Magsat vertical field anomalies above 40 deg N from spherical cap harmonic analysis p 18 A85-26417
- HALL, D. H.**
Crustal structure of the Churchill-Superior boundary zone between 80 and 98 deg W longitude from Magsat anomaly maps and stacked passes p 22 A85-26421
- HALL, F. G.**
Use of satellite data in agricultural surveys p 4 A85-23782
- HALL, J. R.**
Assessment of Thematic Mapper band-to-band registration by the block correlation method p 55 N85-21743
- HALLIKAINEN, M. T.**
Retrieval of snow water equivalent from Nimbus-7 SMMR data Effect of land-cover categories and weather conditions p 43 A85-24082
- HAMMAK, J.**
SIR-B cartography and stereo topographic mapping p 19 N85-17234
- HAMMOND, D. L.**
Electromagnetic bias of 10-GHz radar altimeter measurements of MSL p 37 A85-29713
- HANCOCK, D. W., III**
Electromagnetic bias of 36-GHz radar altimeter measurements of MSL p 37 A85-29712
- HANCOCK, J. F.**
Development of a SPOT-simulation radiometer p 57 A85-23759
- HARDESTY, R. M.**
Performance of a coherent lidar remote sensor in snow and fog p 59 A85-25347
- HARDY, D.**
SEASAT-data acquisition and processing by the Royal Aircraft Establishment p 57 A85-23678
- HARIHARAN, T. A.**
Advances in microwave remote sensing of the ocean and atmosphere p 28 A85-21960
- HARRISON, P. G.**
Developments with multispectral thermal-IR and active microwave systems - TIMS, SIR-A, SIR-B, and radarsat p 62 A85-27947
- HAYDN, R.**
MOMS 1 and its results p 61 A85-27061
- HAYES, L.**
The current use of TIROS-N series of meteorological satellites for land-cover studies p 60 A85-26928
- HAYES, P. S.**
Airborne microwave measurements of the southern Greenland ice sheet p 28 A85-23644
- HAYNES, C. V.**
Application and calibration of the subsurface mapping capability of SIR-B in desert regions p 25 N85-17244
- HAZEN-LILLER, M. L.**
The secular period behavior of 38 RR Lyrae stars in the LMC globular cluster NGC 2257 p 14 A85-25070
- HE, J.**
Study on a regional geographical information system and application model p 13 A85-20644
- HEAD, J. W., III**
Geological, structural, and geomorphological analyses from SIR-B p 24 N85-17226
- HENDERSON-SELLERS, A.**
The influence of satellite spectral sensor response on the analysis of satellite imagery at high latitudes p 60 A85-26927
- HENDERSON, F. B.**
Frontiers for geological remote sensing from space, Geosat Workshop, 4th, Flagstaff, AZ, June 12-17, 1983, Report p 22 A85-27943
- HENDERSON, K. E.**
Application of Thematic Mapper data to corn and soybean development stage estimation p 7 A85-30093
- HERD, J. S.**
Airborne microwave measurements of the southern Greenland ice sheet p 28 A85-23644

HESSER, J. E.

The secular period behavior of 38 RR Lyrae stars in the LMC globular cluster NGC 2257 p 14 A85-25070

HEYDORN, R. P.

Estimating location parameters in a mixture p 50 N85-16252

HEYDT, H.

Interactive digital image processing for terrain data extraction [AD-A148580] p 52 N85-17417

HEYMAN, U.

Estimating ocean primary production from satellite chlorophyll - Introduction to regional differences and statistics for the Southern California Bight p 35 A85-28005

HIELKEMA, J. U.

The potential of satellite remote sensing of ecological conditions for survey and forecasting desert-locust activity p 5 A85-26934

HILL, J. R.

Spatial estimation from remotely sensed data via empirical Bayes models p 8 N85-16256

HINES, D. E.

Electromagnetic bias of 36-GHz radar altimeter measurements of MSL p 37 A85-29712

HINKLEY, D. V.

Spatial estimation from remotely sensed data via empirical Bayes models p 8 N85-16256

HINTON, B.

A summary of the wind data available from satellites from the past history to future sensors p 33 A85-24558

HINZE, W. J.

Comparison between the recent U.S. composite magnetic anomaly map and Magsat anomaly data p 17 A85-26413

HINZMAN, L. D.

Growth and reflectance characteristics of winter wheat canopies [E85-10080] p 11 N85-19494

HODGES, T.

NOAA-AISC user's guide for implementing CERES maize model for large area yield estimation [E85-10083] p 12 N85-21748

User's guide to the TAMW wheat model as implemented on the IBM 360/195 computer [E85-10084] p 12 N85-21749

NOAA-AISC user's guide for implementing CERES wheat model for large area yield estimation [E85-10085] p 12 N85-21750

Estimating solar radiation for plant simulation models [E85-10089] p 13 N85-21751

HODGKINS, K. D.

The U.S. civil operational remote sensing program opportunities for the present and future p 71 A85-20641

HOFFER, R. M.

Microwave and optical remote sensing of forest vegetation p 9 N85-17228

HOFFMANN, O.

Investigations of the accuracy of the digital photogrammetry system DPS, a rigorous three dimensional compilation process for push broom imagery [MBB-UA-753/83-OE] p 60 A85-26393

HOGE, F. E.

The reflection of airborne UV laser pulses from the ocean p 37 A85-29714

HOLM, R. G.

In-progress absolute radiometric inflight calibration of the LANDSAT-4 sensors p 68 N85-21733

HOLTZMAN, J. C.

Power spectral density of markov texture fields p 50 N85-16262

HOLYER, R. J.

The use of principal components analysis techniques Nimbus-7 coastal zone color scanner data to define mesoscale ocean features through a warm humid atmosphere [AD-A148567] p 40 N85-17416

HONEY, F. R.

Evaluation of SIR-B imagery for geologic and geomorphic mapping, hydrology, and oceanography in Australia p 51 N85-17229

HOOKER, L. K.

Experimental evidence for spring and autumn windows for the detection of geobotanical anomalies through the remote sensing of overlying vegetation p 6 A85-26939

HOOKER, S. B.

Center of mass estimation in closed vortices - A verification in principle and practice p 26 A85-19417

HORAI, K.

On the determination of the deflection of the vertical by satellite altimetry p 37 A85-29706

HORN, D. A.

MIZEX (Marginal Ice Zone Program) A program for mesoscale air-ice-ocean interaction experiments in Arctic marginal ice zones 5 MIZEX 84 Summer experiment PI (Principal Investigator) preliminary reports [AD-A148986] p 41 N85-19594

HORWITZ, R.

Evaluation of SIR-B imagery for geologic and geomorphic mapping, hydrology, and oceanography in Australia p 51 N85-17229

HOSCHITZKY, H.

Monitoring of the tidal dynamics of the Dutch Waddensea by SIR-B p 40 N85-17235

HOUSTON, A. G.

Use of satellite data in agricultural surveys p 4 A85-23782

Calibration or inverse regression Which is appropriate for crop surveys using LANDSAT data? p 9 N85-16260

HOVIS, W. A.

Aircraft measurements for calibration of an orbiting spacecraft sensor p 59 A85-24246

LANDSAT-4 Thematic Mapper calibration and atmospheric correction p 68 N85-21734

HOWARD, J. A.

International cooperation in remote sensing applications p 70 A85-20566

HSU, S. A.

Variations in atmospheric mixing height across oceanic thermal fronts p 34 A85-27704

HSU, S. Y.

Development and evaluation of techniques for using combined microwave and optical image data for vegetation studies p 9 N85-17240

HUANG, N. E.

The Harp probe - An in situ Bragg scattering sensor p 28 A85-22171

HUFEN, J. H.

On the identification of Magsat anomaly charts as crustal part of the internal field p 17 A85-26412

HUNT, B. R.

Multispectral data compression using staggered detector arrays p 47 A85-24277

HUNT, G. E.

An intercalibration of Meteosat-1 and GOES-2 visible and infrared measurements p 26 A85-19420

On the application of meteorological satellite imagery for monitoring the environment p 13 A85-20570

HUNTINGTON, J.

Evaluation of SIR-B imagery for geologic and geomorphic mapping, hydrology, and oceanography in Australia p 51 N85-17229

HURLBURT, H. E.

The potential for ocean prediction and the role of altimeter data p 36 A85-29704

HWANG, V. S. S.

Evidence accumulation for spatial reasoning p 50 N85-16261

ILIN, I. U. P.

Interpretation of space images of the sea surface using the SVIT digital-processing complex p 34 A85-25654

ILINSKI, R. V.

Interpretation of space images of the sea surface using the SVIT digital-processing complex p 34 A85-25654

IMHOFF, M. L.

Summary of MSS characterization investigations p 53 N85-20497

Radiometric accuracy assessment of LANDSAT 4 Multispectral Scanner data p 53 N85-20498

Geometric accuracy assessment of LANDSAT-4 Multispectral Scanner (MSS) data p 19 N85-20505

INKSTER, R.

Advanced SAR system maps Arctic regions p 35 A85-27841

IRONS, J. R.

An overview of LANDSAT-4 and the Thematic Mapper p 66 N85-20509

IRVINE, D.

The spatial evolution of the directional wave spectrum in the Southern Ocean Its relation to extreme waves in Agulhas Current p 39 N85-17213

ISHANOV, M. K.

Possibilities of using remote-sensing methods to improve the efficiency of oil and gas exploration p 24 A85-29905

ISHAQ, A. M.

Remote sensing techniques for monitoring of pollution in coastal waters - Potential application to Saudi Arabia p 34 A85-27441

ISSAWI, B.

Application and calibration of the subsurface mapping capability of SIR-B in desert regions p 25 N85-17244

IUOV, V. I.

Investigation of the properties of natural objects by the canonical-correlation method p 49 A85-28973

IUSHIN, V. I.

Possibilities of using remote-sensing methods to improve the efficiency of oil and gas exploration p 24 A85-29905

IVANOV, A. V.

Transformation of sea-wave spectrum into a synthetic-aperture-radar image spectrum p 34 A85-25661

J

JACK, R. F.

EROS main image file - A picture perfect database for Landsat imagery and aerial photography p 48 A85-24521

JACKETT, D. R.

Computing the foliage angle distribution from contact frequency data p 6 A85-29969

JACKSON, F. C.

Aircraft and satellite measurement of ocean wave directional spectra using scanning-beam microwave radars p 27 A85-20486

A comparison of in situ and airborne radar observations of ocean wave directionality p 27 A85-20487

JACKSON, R. D.

In-progress absolute radiometric inflight calibration of the LANDSAT-4 sensors p 68 N85-21733

JACKSON, T. J.

Remote sensing of soil moisture p 10 N85-17252

JARRARD, R. D.

Intermediate-wavelength magnetic anomaly field of the North Pacific and possible source distributions p 17 A85-26414

JASENTULIYANA, N.

The potential of solar power satellites for developing countries p 59 A85-24654

JAYNES, R. A.

Detecting agricultural to urban land use change from multi-temporal MSS digital data [E85-10049] p 15 N85-16245

An integrated remote sensing approach for identifying ecological range sites [E85-10050] p 8 N85-16246

JEE, R.

Nonparametric analysis of Minnesota spruce and aspen tree data and LANDSAT data p 8 N85-16253

JELINEK, D. A.

Test plan for the forest-echo experiment [DE84-017175] p 10 N85-18447

JIMENEZ, O. H.

SIR-A imagery in geologic studies of the Sierra Madre Oriental, northeastern Mexico Part 1 (Regional stratigraphy) The use of morphostratigraphic units in remote sensing mapping [NASA-CR-175457] p 25 N85-19497

JOHANNESSEN, O. M.

MIZEX (Marginal Ice Zone Program) A program for mesoscale air-ice-ocean interaction experiments in Arctic marginal ice zones 5 MIZEX 84 Summer experiment PI (Principal Investigator) preliminary reports [AD-A148986] p 41 N85-19594

JOHNSON, B. D.

A review of problems and progress in studies of satellite magnetic anomalies p 17 A85-26409

Viscous remanent magnetization model for the Broken Ridge satellite magnetic anomaly p 22 A85-26423

JOHNSON, K. I.

The imaging of internal waves by the SEASAT-A synthetic aperture radar [AD-A149808] p 20 N85-21761

JOHNSON, W. H.

Interlobate comparison of glacial-depositional style as evidenced by small-relief glacial landscape features in Illinois, Indiana, and Ohio, utilizing SIR-B p 39 N85-17231

JONES, O. D.

A preliminary evaluation of LANDSAT-4 Thematic Mapper data for their geometric and radiometric accuracies p 54 N85-21739

JONES, W. L.

Airborne microwave measurements of the southern Greenland ice sheet p 28 A85-23644

JORGENSEN, D. P.

Airborne Doppler estimates of the air motions associated with a developing, sea-breeze induced, mesoscale precipitation line p 36 A85-28783

JOSELYN, J. A.

The space environment monitors onboard GOES [AIAA PAPER 85-0238] p 55 A85-19608

JOYCE, A. T.

- Relationship between forest clearing and biophysical factors in tropical environments Implications for the design of a forest change monitoring approach [E85-10051] p 8 N85-16247

JUSTICE, C.

- A preliminary analysis of LANDSAT-4 Thematic Mapper radiometric performance p 68 N85-21730

K

KAHLE, A. B.

- Calculation of thermal inertia from day-night measurements separated by days or weeks p 45 A85-21048
Measuring spectra of and lands p 20 A85-21975
Thematic mapper data analysis p 23 A85-27946
Developments with multispectral thermal-IR and active microwave systems - TMS, SIR-A, SIR-B, and radarsat p 62 A85-27947

KALINKEVICH, A. A.

- Simultaneous radiometric and radar altimetric measurements of sea microwave signatures p 31 A85-24076

KALMYKOV, A. I.

- Complex studies of the environment by optical and radar methods p 56 A85-20081
Ring structures observed on space radar images of the earth p 45 A85-20084
Space radar observations of small-scale formations on the ocean surface p 27 A85-20086
Features of the digital processing of radar images obtained with the sidelooking radar of the Cosmos-1500 satellite p 48 A85-25660

KANAL, L. N.

- Analysis of subpixel registration p 51 N85-16267

KAPITONOVA, N. V.

- The use of a priori estimation of the conditions of the observation of the earth surface from space for a rational selection of the time at which the survey is conducted p 50 A85-29914

KARASEV, A. B.

- Double-angle method for measuring ocean surface temperature in the infrared p 34 A85-25658

KARKHANIS, V.

- Interactive digital image processing for terrain data extraction [AD-A148580] p 52 N85-17417

KASTNER, C. J.

- In-progress absolute radiometric inflight calibration of the LANDSAT-4 sensors p 68 N85-21733

KAUFMAN, A. A.

- Research on ocean floor electrical surveys [AD-A149831] p 42 N85-21920

KAUPP, V.

- SIR-B cartography and stereo topographic mapping p 19 N85-17234

KAUPP, V. H.

- Evaluation of the L-band scattering characteristics of volcanic terrain in aid of lithologic identification, assessment of SIR-B calibration, and development of planetary geomorphic analogs p 24 N85-17232

KAUTH, R. J.

- Investigations of vegetation and soils information contained in LANDSAT Thematic Mapper and Multispectral Scanner data [E85-10082] p 12 N85-21747

KELLER, G. V.

- Research on ocean floor electrical surveys [AD-A149831] p 42 N85-21920

KELLEY, E.

- Abyssal eddies near the Gulf Stream p 34 A85-27701

KELLY, K. A.

- Separating clouds from ocean in infrared images p 28 A85-22423

KENNEY, J. E.

- Electromagnetic bias of 36-GHz radar altimeter measurements of MSL p 37 A85-29712

KENYON, N. H.

- Tidal current bedforms investigated by Seasat p 30 A85-23692

KERBER, A. G.

- Comparison of level I land cover classification accuracy for MSS and AVHRR data p 61 A85-26929

KEYTE, G. E.

- The investigation of selected oceanographic applications of spaceborne synthetic-aperture radar p 39 N85-17233

KHARIN, N. G.

- Comprehensive desertification maps and methods for making such maps on the basis of space photographs p 14 A85-29907

KHMYROV, B. E.

- Complex studies of the environment by optical and radar methods p 56 A85-20081

KHORRAM, S.

- Development of water quality models applicable throughout the entire San Francisco Bay and Delta p 42 A85-21046
Remote sensing of water quality in the Neuse River Estuary, North Carolina p 43 A85-29219

KIDDER, S. Q.

- Dramatic contrast between low clouds and snow cover in daytime 3.7 micron imagery p 48 A85-24740

KIEFFER, H. H.

- Thematic mapper data analysis p 23 A85-27946
Intraband radiometric performance of the LANDSAT 4 Thematic Mapper p 69 N85-21738

KILGUS, C. C.

- Remote sensing by radar altimetry p 26 A85-19428
An analysis of a satellite multibeam altimeter p 38 A85-29715

KIM, Y.-S.

- The effect of a snow cover on microwave backscatter from sea ice p 32 A85-24083

KIMES, D. S.

- Effect of heliotropism on the bidirectional reflectance of irrigated cotton p 1 A85-22420

KIMMER, E.

- LS-4 MSS geometric correction Methods and results p 53 N85-20507

KIRKHNER, K.

- Determination of water surfaces in northwest Bohemia on the basis of satellite data p 44 A85-29906

KISELEV, E. M.

- Investigation of Krasnovodsk bay on the basis of space photographs p 28 A85-21669

KITCHO, C. A.

- Thematic mapper data analysis p 23 A85-27946

KLEIFORTH, H.

- Analysis of SIR-B radar illumination of geometry for depth of penetration and surface feature and vegetation detection, Nevada and California p 25 N85-17248

KLEINER, E.

- Analysis of SIR-B radar illumination of geometry for depth of penetration and surface feature and vegetation detection, Nevada and California p 25 N85-17248

KNEPPER, D. H., JR.

- Determining stretch parameters for lithologic discrimination on Landsat MSS band-ratio images p 20 A85-21047

KNOLL, J. S.

- Aircraft measurements for calibration of an orbiting spacecraft sensor p 59 A85-24246

KOBICK, M.

- SIR-B cartography and stereo topographic mapping p 19 N85-17234

KOFFLER, R.

- The U S civil operational remote sensing program opportunities for the present and future p 71 A85-20641

KOGUT, J.

- An analysis of the high frequency vibrations in early Thematic Mapper scenes p 69 N85-21742

KOLARZH, I. A.

- Determination of water surfaces in northwest Bohemia on the basis of satellite data p 44 A85-29906

KOLASINSKI, W. A.

- An auroral X-ray imaging spectrometer [AD-A147756] p 64 N85-17469

KONO, M.

- Mean ionospheric field correction for Magsat data p 17 A85-26411

KONSTANTINOV, V. D.

- Identification of the structure of soil-vegetation cover using aerial and space images p 5 A85-25656

KOOPMANS, B. N.

- Monitoring of the tidal dynamics of the Dutch Waddensea by SIR-B p 40 N85-17235

KORAK, J.

- Nautical charting with remotely sensed imagery, volume 1 [AD-A149361] p 41 N85-19503
Nautical charting with remotely sensed imagery Volume 2 Case studies [AD-A149362] p 41 N85-19504

KOSTAL, H.

- Spatial estimation from remotely sensed data via empirical Bayes models p 8 N85-16256

KOTTSOV, V. A.

- Correlation of spectral brightnesses measured using multispectral space images p 60 A85-25659
Investigation of the properties of natural objects by the canonical-correlation method p 49 A85-28973

KRABILL, W. B.

- The use of airborne lasers in terrestrial and water environments p 33 A85-25351

- The reflection of airborne UV laser pulses from the ocean p 37 A85-29714

KRECKEL, K.

- Resource measurement system p 47 A85-24258

KRUPENIO, N. N.

- Radar mapping of the moisture of open soils p 6 A85-29911

KUREKIN, A. S.

- Features of the digital processing of radar images obtained with the sidelooking radar of the Cosmos-1500 satellite p 48 A85-25660

KURSKAIA, A. A.

- Radiophysical techniques employed for sea ice investigations p 31 A85-24077

KUTUZA, B. G.

- Simultaneous radiometric and radar altimetric measurements of sea microwave signatures p 31 A85-24076

- Radiophysical techniques employed for sea ice investigations p 31 A85-24077

KUZINA, A. M.

- Minimization of the effect of the earth's curvature in the projective transformation of space images into photoplans and photomaps p 16 A85-25662

L

LA VIOLETTE, P. E.

- Variations in atmospheric mixing height across oceanic thermal fronts p 34 A85-27704

LABAUGH, R. J.

- Evaluation of an experimental system for spaceborne processing of multispectral image data p 46 A85-23144

LABOVITZ, M. L.

- Experimental evidence for spring and autumn windows for the detection of geobotanical anomalies through the remote sensing of overlying vegetation p 6 A85-26939

- The importance of geobotany in geological remote sensing applications p 23 A85-27948

LABRECQUE, J. L.

- Intermediate-wavelength magnetic anomaly field of the North Pacific and possible source distributions p 17 A85-26414

- Seafloor spreading anomalies in the Magsat field of the North Atlantic p 17 A85-26415

LAGOUARDE, J. P.

- Use of HCMM thermal images in the study of microclimates in a mountainous region p 3 A85-23771

LAKSHMINARAYANAN, M. Y.

- Exploring the use of structural models to improve remote sensing agricultural estimates p 9 N85-16259

LALLEMAND, C.

- Independent variables in remote sensing as a function of landcover type p 47 A85-23788

LAME, D. B.

- A survey of oceanographic satellite altimetric missions p 36 A85-29703

LAMERS, J. G.

- Soil slaking and the possibilities to record with infrared line scanning p 5 A85-26936

LANDGREBE, D.

- On realizing the potential of the earth-looking vantage point [AIAA PAPER 85-0195] p 70 A85-19580

LANGEL, R. A.

- Introduction to the special issue - A perspective on Magsat results p 16 A85-26401

- The near-earth magnetic field at 1980 determined from Magsat data p 16 A85-26408

- Comparison between the recent U S composite magnetic anomaly map and Magsat anomaly data p 17 A85-26413

LANSING, J. C.

- Thematic Mapper Volume 1 Calibration report flight model, LANDSAT 5 [E85-10059] p 63 N85-16270

- Thermal band characterization of the LANDSAT-4 Thematic Mapper p 67 N85-21727

LARDUINAT, E.

- An analysis of the high frequency vibrations in early Thematic Mapper scenes p 69 N85-21742

LARGE, W. G.

- Wind speed and stress over the ocean - Scatterometer versus surface measurements p 33 A85-24557

LARRABEE, J.

- NOAA-AISC user's guide for implementing CERES maize model for large area yield estimation [E85-10083] p 12 N85-21748

- User's guide to the TAMW wheat model as implemented on the IBM 360/195 computer [E85-10084] p 12 N85-21749

- NOAA-AISC user's guide for implementing CERES wheat model for large area yield estimation [E85-10085] p 12 N85-21750
- LARSEN, C. A.**
Experimental evidence for spring and autumn windows for the detection of geobotanical anomalies through the remote sensing of overlying vegetation p 6 A85-26939
- LAUER, D. T.**
LANDSAT 4 investigation of Thematic Mapper and Multispectral Scanner applications [E85-10076] p 52 N85-19490
LANDSAT 4 investigations of Thematic Mapper and Multispectral Scanner applications [E85-10095] p 26 N85-21757
- LAURIN, R.**
Investigations of vegetation and soils information contained in LANDSAT Thematic Mapper and Multispectral Scanner data [E85-10082] p 12 N85-21747
- LAVENTU, F.**
Thematic evaluation of SPOT spectral bands p 58 A85-23794
- LAVINE, D.**
Analysis of subpixel registration p 51 N85-16267
- LAVIOLETTE, P. E.**
Bio-optical variability in the Alboran Sea as assessed by Nimbus-7 coastal zone color scanner [AD-A147909] p 39 N85-16281
Satellite definition of the bio-optical and thermal variation of coastal eddies associated with the African current [AD-A147910] p 39 N85-16282
The use of principal components analysis techniques Nimbus-7 coastal zone color scanner data to define mesoscale ocean features through a warm humid atmosphere [AD-A148567] p 40 N85-17416
- LAWTON, W. M.**
Texture classification using autoregressive filtering p 50 N85-16254
- LE TOAN, T.**
Relations between the radar backscatter coefficient and the characteristics of a vegetation canopy - Analysis of the effect of structure p 4 A85-23774
- LEBERI, F.**
SIR-B cartography and stereo topographic mapping p 19 N85-17234
- LECKIE, D.**
Automated measurements of terrain reflection and height variations using an airborne infrared laser system p 5 A85-26933
- LEDUC, S.**
Estimating solar radiation for plant simulation models [E85-10089] p 13 N85-21751
- LEE, M.**
Texture classification using autoregressive filtering p 50 N85-16254
- LEGENDRE, G.**
Independent variables in remote sensing as a function of landcover type p 47 A85-23788
- LELGEMANN, D.**
The altimetric geoid in the North Sea p 16 A85-23700
- LEUNG, K. C.**
Radiometric calibration and processing procedure for reflective bands on LANDSAT-4 protoflight Thematic Mapper p 66 N85-20510
Prelaunch absolute radiometric calibration of the reflective bands on the LANDSAT-4 protoflight Thematic Mapper p 66 N85-20515
Characterization of radiometric calibration of LANDSAT-4 reflective bands p 66 N85-20516
- LEUNG, S.**
Advanced SAR system maps Arctic regions p 35 A85-27841
- LIKENS, W. C.**
Impact of LANDSAT MSS sensor differences on change detection analysis p 65 N85-20506
- LINDGREN, R.**
A comparative test of photogrammetrically sampled digital elevation models p 52 N85-17408
- LINK, L. E.**
The use of airborne lasers in terrestrial and water environments p 33 A85-25351
- LISSAUER, I. M.**
Atlas of the Beaufort Sea [AD-A149545] p 41 N85-20619
- LIU, W. T.**
Determination of monthly mean humidity in the atmospheric surface layer over oceans from satellite data p 35 A85-28007
- LLEWELLYN-JONES, D. T.**
Satellite measurements of sea-surface temperature for climate research p 32 A85-24555
- LODGE, D. W. S.**
Expressions of bathymetry on Seasat synthetic radar images p 29 A85-23691
- LONG, S. R.**
The Harp probe - An in situ Bragg scattering sensor p 28 A85-22171
- LONGORIA, J. F.**
SIR-A imagery in geologic studies of the Sierra Madre Oriental, northeastern Mexico Part 1 (Regional stratigraphy) The use of morphostratigraphic units in remote sensing mapping [NASA-CR-175457] p 25 N85-19497
- LONGUET-HIGGINS, M. S.**
Can optical measurements help in the interpretation of radar backscatter? p 29 A85-23683
- LOPES, A.**
Relations between the radar backscatter coefficient and the characteristics of a vegetation canopy - Analysis of the effect of structure p 4 A85-23774
- LOSINSKII, V. N.**
Remote-sensing observations of advective eddies in the central part of the Baltic Sea p 38 A85-29915
- LOUGHEED, J.**
Automated measurements of terrain reflection and height variations using an airborne infrared laser system p 5 A85-26933
- LOVILL, J. E.**
Intercomparisons of TOMS, SBUV and MFR satellite ozone measurements p 62 A85-29784
- LOWMAN, P. D., JR.**
Structural investigation of the Canadian Shield by orbital radar and LANDSAT p 25 N85-17236
Structural investigation of the Grenville Province by radar and other imaging and nonimaging sensors p 25 N85-17237
- LU, Y. C.**
Comparison of level I land cover classification accuracy for MSS and AVHRR data p 61 A85-26929
- LUDWIG, R. A.**
The potential of solar power satellites for developing countries p 59 A85-24654
- LUGASKI, T. P.**
Analysis of SIR-B radar illumination of geometry for depth of penetration and surface feature and vegetation detection, Nevada and California p 25 N85-17248
- LUKASHEVICH, E. L.**
The use of a priori estimation of the conditions of the observation of the earth surface from space for a rational selection of the time at which the survey is conducted p 50 A85-29914
- LUTCHMAN, H. T. J.**
Method for sequential analysis of spatial development in a rural-urban fringe zone p 13 A85-20748
- LYDEN, J.**
The spatial evolution of the directional wave spectrum in the Southern Ocean Its relation to extreme waves in Agulhas Current p 39 N85-17213
- LYNN, N.**
The investigation of selected oceanographic applications of spaceborne synthetic-aperture radar p 39 N85-17233
- LYON, R. J. P.**
Estimation of the vegetation contribution to the 1.65-2.22 micron ratio in airborne thematic-mapper imagery of the Virginia Range, Nevada p 5 A85-26931
The importance of geobotany in geological remote sensing applications p 23 A85-27948
- LYZENG, D.**
The spatial evolution of the directional wave spectrum in the Southern Ocean Its relation to extreme waves in Agulhas Current p 39 N85-17213
- M**
- MACARTHUR, J. L.**
Remote sensing by radar altimetry p 26 A85-19428
- MACCHIARELLA, G.**
A comparative analysis of some prediction methods for rain attenuation statistics in earth-to-space links p 42 A85-21130
- MACDONALD, H. C.**
Evaluation of the L-band scattering characteristics of volcanic terrain in aid of lithologic identification, assessment of SIR-B calibration, and development of planetary geomorphic analogs p 24 N85-17232
SIR-B cartography and stereo topographic mapping p 19 N85-17234
- MAETZLER, C.**
Polarization effects in sea-ice signatures p 31 A85-24078
- MAITRE, H.**
Thermal structure of an agricultural region as seen by NOAA-7 AVHRR p 7 A85-30090
- MAKAROV, V. I.**
Space remote-sensing data in geology p 23 A85-28400
- MAKAROVIC, B.**
Automatic production of DTM data using digital off-line technique p 45 A85-20750
- MALARET, E.**
Spatial resolution estimation of LANDSAT-4 Thematic Mapper data p 69 N85-21741
- MALAYAUD, A.**
Relations between the radar backscatter coefficient and the characteristics of a vegetation canopy - Analysis of the effect of structure p 4 A85-23774
- MALESHEKOV, G. N.**
Possibilities of using remote-sensing methods to improve the efficiency of oil and gas exploration p 24 A85-29905
- MALILA, W. A.**
Study of spectral/radiometric characteristics of the Thematic Mapper for land use applications [E85-10057] p 62 N85-16268
Study of spectral/radiometric characteristics of the Thematic Mapper for land use applications [E85-10075] p 64 N85-19489
Investigation of radiometric properties of LANDSAT-4 MSS p 65 N85-20500
Scan angle and detector effects in Thematic Mapper radiometry p 68 N85-21735
- MAMEDOV, E. A.**
Investigation of salty soils and salines on the basis of space remote-sensing methods p 6 A85-29908
- MANDESCU, E.**
Experiments concerning radiometric measurements and natural-object indicators in order to apply corrections to recordings of satellite remote sensing p 58 A85-23789
- MANN, P.**
Neotectonics of the Caribbean p 27 A85-21145
- MAO, Y.**
Methodological study of spectral band selection for multispectral remote sensing p 55 A85-19363
- MARELLI, L.**
Status of remote sensing information systems with special emphasis on their specializations, capabilities, accessibilities and future directions p 71 A85-20646
SEASAT - A key element of the EARTHNET programme p 46 A85-23679
- MARKHAM, B. L.**
Spectral characterization of the LANDSAT-4 MSS sensors p 65 N85-20499
Spectral characterization of the LANDSAT Thematic Mapper sensors p 66 N85-20514
- MARSH, J. G.**
Regional mean sea surfaces based on GEOS-3 and SEASAT altimeter data p 38 A85-29716
- MARSH, S.**
Near-infrared spectroscopy in geological reconnaissance and exploration p 22 A85-27944
- MARSH, S. E.**
Imaging systems for the delineation of spectral properties of geologic materials in the visible and near-infrared p 22 A85-27945
- MARTENS, A.**
Resource measurement system p 47 A85-24258
- MARTIN-KAYE, P. H.**
Seasat over land p 57 A85-23693
- MARTIN, M. V.**
Estimating location parameters in a mixture p 50 N85-16252
- MARTIN, T. V.**
Regional mean sea surfaces based on GEOS-3 and SEASAT altimeter data p 38 A85-29716
- MASUOKA, E. J.**
Experimental evidence for spring and autumn windows for the detection of geobotanical anomalies through the remote sensing of overlying vegetation p 6 A85-26939
- MASURENKOV, Y.**
Satellite photographs suggest arctic volcano p 38 N85-16239
- MATHER, P. M.**
A computationally-efficient maximum-likelihood classifier employing prior probabilities for remotely-sensed data p 49 A85-26948
- MATSON, M.**
The 1982 El Chichon Volcano eruptions - A satellite perspective p 14 A85-27984
- MATSUYAMA, T.**
Evidence accumulation for spatial reasoning p 50 N85-16261
- MATYSKIELA, R.**
An analysis of a satellite multibeam altimeter p 38 A85-29715
- MAYHEW, M. A.**
A review of problems and progress in studies of satellite magnetic anomalies p 17 A85-26409

- MCCARTHY, J. J.**
Regional mean sea surfaces based on GEOS-3 and SEASAT altimeter data p 38 A85-29716
- MCCAULEY, J. F.**
Application and calibration of the subsurface mapping capability of SIR-B in desert regions p 25 N85-17244
- MCDONOUGH, M.**
Seasat over land p 57 A85-23693
- MCLEROY, J. H.**
Earth observations and the polar platform [NOAA-TR-NESDIS-18] p 15 N85-20517
- MCGILLEM, C. D.**
Spatial resolution estimation of LANDSAT-4 Thematic Mapper data p 69 N85-21741
- MCGINNIS, D. F., JR.**
Monitoring Africa's Lake Chad basin with Landsat and NOAA satellite data p 43 A85-26930
- MCGILONE, J. C.**
Evaluation of aircraft MSS analytical block adjustment p 49 A85-26641
- MCHAIL, R.**
Resource measurement system p 47 A85-24258
- MCHUGH, W.**
Application and calibration of the subsurface mapping capability of SIR-B in desert regions p 25 N85-17244
- MCKIM, H. L.**
Landsat-4 thematic mapper (TM) for cold environments p 60 A85-25349
- MCNALLY, G. J.**
Lagrangian observations of surface circulation at the Emperor Seamount chain p 35 A85-27710
- MCSHEEHY, J. J.**
Performance of an airborne imaging 92/183 GHz radiometer during the Bering Sea Marginal Ice Zone Experiment (MIZEX-WEST) p 33 A85-24945
- MEHL, W.**
A preliminary analysis of LANDSAT-4 Thematic Mapper radiometric performance p 68 N85-21730
TM geometric performance Line to Line Displacement Analysis (LLDA) p 68 N85-21732
- MEISSNER**
Modular Optoelectronic Multispectral Scanner (MOMS) Technological aspects p 61 A85-27059
- MELACK, J.**
Deforestation, floodplain dynamics, and carbon biogeochemistry in the Amazon Basin p 44 N85-17216
- MENARD, Y.**
Eddy kinetic energy distribution in the southern ocean from Seasat altimeter and FGGE drifting buoys p 32 A85-24554
- MENEGHINI, R.**
Simultaneous ocean cross-section and rainfall measurements from space with a nadir pointing radar p 36 A85-28788
Simultaneous ocean cross-section and rainfall measurements from space with a nadir-pointing radar [NASA-TM-86167] p 44 N85-16273
- MEREDITH, B. D.**
Evaluation of an experimental system for spaceborne processing of multispectral image data p 46 A85-23144
- MEROLA, J. A.**
Detecting agricultural to urban land use change from multi-temporal MSS digital data p 15 N85-16245
An integrated GIS/remote sensing data base in North Cache soil conservation district, Utah: A pilot project for the Utah Department of Agriculture's RIMS (Resource Inventory and Monitoring System) [E85-10073] p 11 N85-19487
- MERTZ, F. C.**
Assessment of Thematic Mapper band-to-band registration by the block correlation method p 55 N85-21743
- METZLER, M. D.**
Study of spectral/radiometric characteristics of the Thematic Mapper for land use applications [E85-10057] p 62 N85-16268
Study of spectral/radiometric characteristics of the Thematic Mapper for land use applications [E85-10075] p 64 N85-19489
Scan angle and detector effects in Thematic Mapper radiometry p 68 N85-21735
- MEYER-ROUX, J.**
Comparison of SPOT HRV and Landsat-4 TM for crop inventories p 3 A85-23762
- MEYER, J.**
On the identification of Magsat anomaly charts as crustal part of the internal field p 17 A85-26412
- MIGUET, J. N.**
Estimation of wheat production on the basis of Landsat channel 5 and 7 radiometric measurements p 3 A85-23763
- MIKHAIL, E. M.**
Evaluation of aircraft MSS analytical block adjustment p 49 A85-26641
Rectification of single and multiple frames of satellite scanner imagery using points and edges as control p 51 N85-16263
- MILLAR, T. W.**
Crustal structure of the Churchill-Superior boundary zone between 80 and 98 deg W longitude from Magsat anomaly maps and stacked passes p 22 A85-26421
- MILLER, W. F.**
Forest area estimates from LANDSAT MSS and forest inventory plot data [PB85-105617/GAR] p 9 N85-16290
- MILNE, A. K.**
Australian Multitextural Assessment of SIR-B (AMAS) p 52 N85-17243
- MILTON, N. M.**
Thematic mapper data analysis p 23 A85-27946
The importance of geobotany in geological remote sensing applications p 23 A85-27948
- MINDEN, G. J.**
Information extraction and transmission techniques for spaceborne synthetic aperture radar images [NASA-CR-174341] p 52 N85-17256
- MINNETT, P. J.**
Satellite measurements of sea-surface temperature for climate research p 32 A85-24555
- MINNIS, P.**
An intercalibration of Meteosat-1 and GOES-2 visible and infrared measurements p 26 A85-19420
- MINSKII, D. E.**
Segmentation of half-tone remote-sensing images by the level lines method p 49 A85-29913
- MITCHELL, J. L.**
A survey of oceanographic satellite altimetric missions p 36 A85-29703
A method for determining mesoscale dynamic topography [AD-D011412] p 40 N85-17506
- MIZERA, P. F.**
An auroral X-ray imaging spectrometer [AD-A147756] p 64 N85-17469
- MO, T.**
Remote sensing of soil moisture p 10 N85-17252
- MOGNARD, N. M.**
Swell propagation in the North Atlantic ocean using SEASAT altimeter p 30 A85-23702
World ocean mean monthly waves, swell, and surface winds for July through October 1978 from SEASAT radar altimeter data p 37 A85-29707
Swell in the Pacific Ocean observed by SEASAT radar altimeter p 37 A85-29708
- MOLLO-CHRISTENSEN, E.**
The Harp probe - An in situ Bragg scattering sensor p 28 A85-22171
- MONALDO, F.**
The spatial evolution of the directional wave spectrum in the Southern Ocean: Its relation to extreme waves in Agulhas Current p 39 N85-17213
- MONGET, J. M.**
Inventory of geographically homogeneous zones by spectral modeling of diachronic Meteosat albedo or combined albedo/thermal-channel data - Applications to the Maghreb and to Sahelian Africa p 46 A85-23769
Geomorphology and remote sensing Numerical inventory of objects in Landsat, SPOT simulation, and SIR-A data Applications to the Mopti-Bandiagara (Mali) region p 21 A85-23785
- MONSON, R.**
Earth resources research using the Shuttle Imaging Radar system p 67 N85-20779
- MOORE, R. K.**
The effect of a snow cover on microwave backscatter from sea ice p 32 A85-24083
International Symposium on Microwave Signatures in Remote Sensing, 3rd, Toulouse, France, January 16-20, 1984, Proceedings p 6 A85-26942
Intermediate results of radar backscatter measurements from summer sea ice [AD-A147212] p 38 N85-15960
Information for space radar designers Required dynamic range vs resolution and antenna calibration using the Amazon rain forest p 44 N85-17239
- MOROZOV, A. A.**
Determination of the external-orientation elements of aerial and space photographs in the remote sensing of dynamic processes and phenomena p 56 A85-19998
- MORRIS, C. N.**
Spatial estimation from remotely sensed data via empirical Bayes models p 8 N85-16256
- MORRITT, R.**
Developments with multispectral thermal-IR and active microwave systems - TIMS, SIR-A, SIR-B, and radarsat p 62 A85-27947
- MORSON, B. J.**
Atlas of the Beaufort Sea [AD-A149545] p 41 N85-20619
- MOSHKOV, A. V.**
Transformation of sea-wave spectrum into a synthetic-aperture-radar image spectrum p 34 A85-25661
- MOUAT, D. A.**
Thematic mapper data analysis p 23 A85-27946
The importance of geobotany in geological remote sensing applications p 23 A85-27948
- MOUGINIS-MARK, P. J.**
Geological, structural, and geomorphological analyses from SIR-B p 24 N85-17226
Evaluation of the L-band scattering characteristics of volcanic terrain in aid of lithologic identification, assessment of SIR-B calibration, and development of planetary geomorphic analogs p 24 N85-17232
- MROCYNSKI, R. P.**
Microwave and optical remote sensing of forest vegetation p 9 N85-17228
- MUEKSCH, M. C.**
Determination of reflectances of tropical vegetation by combined methods of radiometry and photometry p 2 A85-23760
- MULLER, P.**
The interpretation of SIR-B imagery of surface waves and other oceanographic features using in-situ, meteorological satellite, and infrared satellite data p 39 N85-17212
- MUNK, W.**
SEASAT 3 and 4 [AD-A148343] p 40 N85-17274
- MURPHY, J.**
Radiometric calibration and geocoded precision processing of LANDSAT-4 Multispectral Scanner products by the Canada Centre for Remote Sensing p 53 N85-20501
Preliminary evaluation of the radiometric calibration of LANDSAT-4 Thematic Mapper data by the Canada Centre for Remote Sensing p 67 N85-21729
- MURRAY, C. W.**
Automatic terrain elevation mapping and registration p 52 N85-17242
- MURRAY, N. D.**
Evaluation of an experimental system for spaceborne processing of multispectral image data p 46 A85-23144
- MUSATOV, V. A.**
Investigation of Krasnovodsk bay on the basis of space photographs p 28 A85-21669

N

- NAGAI, T.**
On the P1 data from GMS-SEM p 15 N85-21890
- NAKAGAWA, I.**
Extraction of magnetic anomalies of crustal origin from Magsat data over the area of the Japanese Islands p 21 A85-26419
- NARAEVA, M. K.**
Conical multispectral scanner for the study of earth resources p 62 A85-29909
- NARAGHI, M.**
Characteristics of playa deposits as seen on SIR-A, Seasat and Landsat coregistered data p 21 A85-23793
- NEEDHAM, B. H.**
The US civil operational remote sensing program opportunities for the present and future p 71 A85-20641
- NELEPO, A. B.**
Interpretation of space images of the sea surface using the SVIT digital-processing complex p 34 A85-25654
- NELSON, R. F.**
Experimental evidence for spring and autumn windows for the detection of geobotanical anomalies through the remote sensing of overlying vegetation p 6 A85-26939
- NEMEC, J. M.**
The secular period behavior of 38 RR Lyrae stars in the LMC globular cluster NGC 2257 p 14 A85-25070
- NEWCOMB, W. W.**
Effect of heliotropism on the bidirectional reflectance of irrigated cotton p 1 A85-22420
- NEWTON, H. J.**
Autoregressive spectral estimation for two dimensional time series p 50 N85-16258
- NIBLACK, W.**
Generation of a Landsat-HCMM combined image and its application to geological cartography p 21 A85-23792
- NICHOLS, A.**
Advanced SAR system maps Arctic regions p 35 A85-27841

NIELSEN, K. C.

Post-carboniferous tectonics in the Anadarko Basin, Oklahoma Evidence from side-looking radar imagery [NASA-CR-175458] p 26 N85-19498

NIELER, P. P.

Determination of monthly mean humidity in the atmospheric surface layer over oceans from satellite data p 35 A85-28007

NIKOLAIEVA, E. M.

The use of Salyut-5 photographs for regional geomorphological mapping p 23 A85-28999

NILSSON, C.

Evaluation of SIR-B imagery for geologic and geomorphic mapping, hydrology, and oceanography in Australia p 51 N85-17229

NOBLE, I. A.

Crustal structure of the Churchill-Superior boundary zone between 80 and 98 deg W longitude from Magsat anomaly maps and stacked passes p 22 A85-26421

NOSOV, B. I.

Conical multispectral scanner for the study of earth resources p 62 A85-29909

NOVO, E. M. L. D.

The shanning of remote sensing techniques in Brazilian geographic research [INPE-3307-PRE/617] p 15 N85-19502

NOWAK, P.

Enhancement of multispectral scanner images by digital filtering [ESA-TT-624] p 63 N85-16284

O

ODENWELLER, J.

Growth/reflectance model interface for wheat and corresponding model [E85-10058] p 9 N85-16269

OESTMAN, A.

A comparative test of photogrammetrically sampled digital elevation models p 52 N85-17408

OGANESIAN, A. G.

Improvement of the accuracy of radar measurements of sea-ice thickness by cepstral processing of reflected signals p 35 A85-27736

OHARA, F. M., JR.

Sourcebook Gaining access to US government information on the environment and natural resources [DE84-017419] p 71 N85-20941

OHARA, I.

Sourcebook Gaining access to US government information on the environment and natural resources [DE84-017419] p 71 N85-20941

OLORY-HECHINGER, E.

Effects of the experimental errors and conditions on the estimation of thermal inertia and evapotranspiration from METEOSAT data p 3 A85-23767

OLSON, D. B.

Center of mass estimation in closed vortices - A verification in principle and practice p 26 A85-19417

OLSON, E. C.

Analysis of subpixel registration p 51 N85-16267

OLSON, W. S.

Resolution enhancement of multichannel microwave imagery from the Nimbus-7 SMMR for maritime rainfall analysis [NASA-CR-174367] p 44 N85-19221

ONSTOTT, R. G.

The effect of a snow cover on microwave backscatter from sea ice p 32 A85-24083
Intermediate results of radar backscatter measurements from summer sea ice [AD-A147212] p 38 N85-15960

OPRESCU, N.

Experiments concerning radiometric measurements and natural-object indicators in order to apply corrections to recordings of satellite remote sensing p 58 A85-23789

ORFEL, R.

A comparison between GEOS 1 magnetic-field measurements and some models of the geomagnetic field p 18 A85-27386

ORMSBY, J. P.

Detection of lowland flooding using active microwave systems p 43 A85-29218

OTTERSTEN, H.

Ground truth for SIR-B images obtained by SIR system 8 impulse radar p 10 N85-17251

OUCHI, K.

Effect of defocusing on the images of ocean waves p 29 A85-23688

P

PADERES, F. C., JR.

Rectification of single and multiple frames of satellite scanner imagery using points and edges as control p 51 N85-16263

PAIA, S.

Structural investigation of the Canadian Shield by orbital radar and LANDSAT p 25 N85-17236
Structural investigation of the Grenville Province by radar and other imaging and nonimaging sensors p 25 N85-17237

PAIN, C. F.

Mapping of landforms from Landsat imagery - An example from eastern New South Wales, Australia p 21 A85-22422

PALMER, J. M.

Spectroradiometric calibration of the Thematic Mapper and Multispectral Scanner system [E85-10077] p 64 N85-19491
In-progress absolute radiometric inflight calibration of the LANDSAT-4 sensors p 68 N85-21733
Spectroradiometric calibration of the Thematic Mapper and Multispectral Scanner system [E85-10094] p 70 N85-21756

PANDEY, P. C.

Advances in microwave remote sensing of the ocean and atmosphere p 28 A85-21960

PANFILOV, A. S.

Conical multispectral scanner for the study of earth resources p 62 A85-29909

PARADA, N. D. J.

Brazilian Remote Sensing Shuttle Experiment (BRESEX) Characteristics and future utilization on satellites [INPE-3313-PRE/620] p 64 N85-19385
Brazilian remote sensing receiving, recording and processing ground systems in the 1980's [E85-10079] p 52 N85-19493
Remote sensing activities in Latin America [INPE-3297-PRE/612] p 64 N85-19501

PARIS, J. F.

Development and evaluation of techniques for using combined microwave and optical image data for vegetation studies p 9 N85-17240

PARK, W.

Preliminary evaluation of the radiometric calibration of LANDSAT-4 Thematic Mapper data by the Canada Centre for Remote Sensing p 67 N85-21729

PARR, J. T.

Investigation of SIR-B images for lithologic mapping p 25 N85-17241

PARRISH, J.

The importance of geobotany in geological remote sensing applications p 23 A85-27948

PARSELL, R. J.

The integrated use of digital cartographic data and remotely sensed imagery p 45 A85-20572

PASSAUER, J.

Nautical charting with remotely sensed imagery, volume 1 [AD-A149361] p 41 N85-19503
Nautical charting with remotely sensed imagery Volume 2 Case studies [AD-A149362] p 41 N85-19504

PEDERSEN, L. T.

Microwave signatures of the sea ice in the East Greenland Current p 31 A85-24079

PENG, C. Y.

A comparison of in situ and airborne radar observations of ocean wave directionality p 27 A85-20487

PEREVOZCHIKOV, A. V.

Interpretation of space images of the sea surface using the SVIT digital-processing complex p 34 A85-25654

PERRAS, S.

Classification of the geological environments of Anticosti Island - An approach using a Landsat-4 spectral simulation p 21 A85-23790

PETERFREUND, A. R.

Geological, structural, and geomorphological analyses from SIR-B p 24 N85-17226

PETERS, C.

Bayesian estimation of normal mixture parameters p 50 N85-16255

PETERSON, C.

Interactive digital image processing for terrain data extraction [AD-A148580] p 52 N85-17417

PETERSON, F. F.

Analysis of SIR-B radar illumination of geometry for depth of penetration and surface feature and vegetation detection, Nevada and California p 25 N85-17248

PETTINGILL, G. H.

Delineation of major geologic structures in Turkey using SIR-B data p 25 N85-17249

PHILLIPS, J. D.

Comparison between the recent US composite magnetic anomaly map and Magsat anomaly data p 17 A85-26413

PICHUGIN, A. P.

Complex studies of the environment by optical and radar methods p 56 A85-20081
Ring structures observed on space radar images of the earth p 45 A85-20084
Space radar observations of small-scale formations on the ocean surface p 27 A85-20086
Effect of meteorological conditions on the characteristics of space radar images of the earth surface p 48 A85-25653
Features of the digital processing of radar images obtained with the sidelooking radar of the Cosmos-1500 satellite p 48 A85-25660

PIERSON, W. J., JR.

Oceanographic and meteorological research based on the data products of SEASAT [E85-10091] p 41 N85-21753

PIOTROWSKI, W. L.

Use of Space Station for Earth and Planetary Exploration p 71 A85-25348

PLAKHI, S.

Determination of water surfaces in northwest Bohemia on the basis of satellite data p 44 A85-29906

PODAIRE, A.

Comparison of SPOT HRV and Landsat-4 TM for crop inventories p 3 A85-23762

PODWYSOCKI, M. H.

Imaging systems for the delineation of spectral properties of geologic materials in the visible and near-infrared p 22 A85-27945
A preliminary evaluation of LANDSAT-4 Thematic Mapper data for their geometric and radiometric accuracies p 54 N85-21739

POLLE, V. F. L.

Population estimation from aerial photos for non-homogeneous urban residential areas p 14 A85-20749

PRICE, J.

Interpretation of thermal infrared data to augment spectral signatures p 47 A85-23791

PRICE, K. P.

Assessment of LANDSAT for rangeland mapping, Rush Valley, Utah [E85-10072] p 15 N85-19486

PRONIN, B. V.

Determination of the heights of points of a place on the basis of radar-survey data p 19 A85-29000

R

RABU, Y.

Generation of a Landsat-HCMM combined image and its application to geological cartography p 21 A85-23792

RAFFY, M.

Effects of the experimental errors and conditions on the estimation of thermal inertia and evapotranspiration from METEOSAT data p 3 A85-23767

RAGGAM, J.

SIR-B cartography and stereo topographic mapping p 19 N85-17234

RAGUSKY, M.

Nautical charting with remotely sensed imagery, volume 1 [AD-A149361] p 41 N85-19503
Nautical charting with remotely sensed imagery Volume 2 Case studies [AD-A149362] p 41 N85-19504

RAINES, G. L.

Determining stretch parameters for lithologic discrimination on Landsat MSS band-ratio images p 20 A85-21047

RAIZER, V. I.

Determination of the physical parameters of sea ice on the basis of remote microwave measurements in the 0.3-18 cm range p 38 A85-29903

RAMAPRIYAN, H. K.

Automatic terrain elevation mapping and registration p 52 N85-17242

RAMM, N. S.

Minimization of the effect of the earth's curvature in the projective transformation of space images into photoplans and photomaps p 16 A85-25662

RAMSEIER, R. O.

An algorithm to measure sea ice concentration with microwave radiometers p 27 A85-20492
Polarization effects in sea-ice signatures p 31 A85-24078

RANEY, R. K.

The Canadian SAR experience p 46 A85-23689

- RANSON, K. J.**
Variation in spectral response of soybeans with respect to illumination, view, and canopy geometry
[E85-10040] p 8 N85-16241
- RAYMOND, C. A.**
Seafloor spreading anomalies in the Magsat field of the North Atlantic p 17 A85-26415
- REBILLARD, PH.**
Characteristics of playa deposits as seen on SIR-A, Seasat and Landsat coregistered data p 21 A85-23793
- REMONDI, B. W.**
Using the global positioning system (GPS) phase observable for relative geodesy Modeling, processing, and results p 19 N85-18437
- RENNE, D. S.**
Analysis of the NASA/MSFC Airborne Doppler Lidar results from San Geronio Pass, California
[NASA-CR-171355] p 70 N85-21873
- REUTER, R.**
Lidar applications in remote sensing of ocean properties p 31 A85-23755
- REUTOV, E. A.**
Determination of soil moisture content by microwave radiometry with the use of a priori information p 6 A85-29910
- RIBE, N. M.**
On the determination of the deflection of the vertical by satellite altimetry p 37 A85-29706
- RICE, D. P.**
Investigation of radiometric properties of LANDSAT-4 MSS p 65 N85-20500
- RICHARDS, J. A.**
Australian Multiexperimental Assessment of SIR-B (AMAS) p 52 N85-17243
- RICHEY, J.**
Deforestation, floodplain dynamics, and carbon biogeochemistry in the Amazon Basin p 44 N85-17216
- RIDD, M. K.**
Detecting agricultural to urban land use change from multi-temporal MSS digital data
[E85-10049] p 15 N85-16245
Assessment of LANDSAT for rangeland mapping, Rush Valley, Utah
[E85-10072] p 15 N85-19486
An integrated GIS/remote sensing data base in North Cache soil conservation district, Utah A pilot project for the Utah Department of Agriculture's RIMS (Resource Inventory and Monitoring System)
[E85-10073] p 11 N85-19487
Building a functional, integrated GIS/remote sensing resource analysis and planning system
[E85-10092] p 15 N85-21754
- RITTER, P. R.**
Remote sensing research for agricultural applications
[E85-10090] p 13 N85-21752
- ROBERTSON, C.**
The use of SEASAT-SAR data in oceanography at the IFP p 29 A85-23690
- ROCHON, G.**
The measurement of bidirectional reflectances by analysis of Landsat images p 2 A85-23756
- ROCK, B. N.**
Frontiers for geological remote sensing from space, Geosat Workshop, 4th, Flagstaff, AZ, June 12-17, 1983, Report p 22 A85-27943
The importance of geobotany in geological remote sensing applications p 23 A85-27948
Development and evaluation of techniques for using combined microwave and optical image data for vegetation studies p 9 N85-17240
- RODGERS, E. B.**
The diurnal variation of Atlantic Ocean tropical cyclone cloud distribution inferred from geostationary satellite infrared measurements p 33 A85-24739
- ROEDER, J. L.**
An auroral X-ray imaging spectrometer
[AD-A147756] p 64 N85-17469
- ROFFEY, J.**
The potential of satellite remote sensing of ecological conditions for survey and forecasting desert-locust activity p 5 A85-26934
- ROTHERAM, S.**
Theory of SAR ocean wave imaging p 29 A85-23686
- ROTT, H.**
The analysis of backscattering properties from SAR data of mountain regions p 59 A85-24081
- ROUQUET, M. C.**
Demonstration, analysis, and correction of atmospheric effects on Landsat or SPOT multispectral data p 58 A85-23781
- RUFENACH, C.**
The spatial evolution of the directional wave spectrum in the Southern Ocean Its relation to extreme waves in Agulhas Current p 39 N85-17213
- RUMMEL, R.**
Gravity field investigation in the North Sea p 30 A85-23699
- ## S
- SAADI, M.**
Geomorphology and remote sensing Numencal inventory of objects in Landsat, SPOT simulation, and SIR-A data Applications to the Mopt-Bandiagara (Mali) region p 21 A85-23785
- SABINS, F. F.**
Developments with multispectral thermal-IR and active microwave systems - TMS, SIR-A, SIR-B, and radarsat p 62 A85-27947
- SADER, S. A.**
Relationship between forest clearing and biophysical factors in tropical environments Implications for the design of a forest change monitoring approach
[E85-10051] p 8 N85-16247
- SAFONOV, I. U. G.**
Space remote-sensing data in geology p 23 A85-28400
- SAILOR, R. V.**
Investigation of SIR-B images for lithologic mapping p 25 N85-17241
- SAINT, G.**
Development of a SPOT-simulation radiometer p 57 A85-23759
Comparison of SPOT HRV and Landsat-4 TM for crop inventories p 3 A85-23762
Thematic evaluation of SPOT spectral bands p 58 A85-23794
- SALISBURY, J. W.**
Near-infrared spectroscopy in geological reconnaissance and exploration p 22 A85-27944
- SALOMONSON, V. V.**
Landsat-4 thematic mapper (TM) for cold environments p 60 A85-25349
- SANDUSKY, W. F.**
Analysis of the NASA/MSFC Airborne Doppler Lidar results from San Geronio Pass, California
[NASA-CR-171355] p 70 N85-21873
- SANDWELL, D. T.**
Observing global ocean circulation with SEASAT altimeter data p 36 A85-29705
Along-track deflection of the vertical from SEASAT GEBCO (General Bathymetric Chart of the Oceans) overlays
[PB85-129641] p 42 N85-21767
- SAVAGE, R.**
In-progress absolute radiometric inflight calibration of the LANDSAT-4 sensors p 68 N85-21733
- SAVASTANO, K. J.**
Satellite data communication system for near real-time processing and distribution of marine fishery research data p 36 A85-28119
- SCARPACE, F. L.**
An airborne infrared thermal scanning system for easy use on Navy P-3 aircraft
[AD-A149690] p 42 N85-22143
- SCHAAKE, J. C., JR.**
Airborne snow water equivalent and soil moisture measurement using natural terrestrial gamma radiation p 43 A85-25352
- SCHABER, G. G.**
Application and calibration of the subsurface mapping capability of SIR-B in desert regions p 25 N85-17244
- SCHANDA, E.**
International Symposium on Microwave Signatures in Remote Sensing, 3rd, Toulouse, France, January 16-20, 1984, Proceedings p 6 A85-26942
- SCHMUGGE, T.**
Spectral signatures of soil, snow and sea ice as observed by passive microwave and thermal infrared techniques p 58 A85-23784
- SCHMUGGE, T. J.**
Remote sensing of soil moisture p 10 N85-17252
- SCHNEIDER, M.**
Activities report of the Department of Applied Research 78 for satellite geodesy of the Technical University, Munich
[ASTRON-GEODAET-ARB-45] p 19 N85-18440
- SCHNEIDER, S. R.**
Monitoring Africa's Lake Chad basin with Landsat and NOAA satellite data p 43 A85-26930
Earth observations and the polar platform
[NOAA-TR-NESDIS-18] p 15 N85-20517
- SCHNETZLER, C. C.**
Comparison between the recent US composite magnetic anomaly map and Magsat anomaly data p 17 A85-26413
An estimation of continental crust magnetization and susceptibility from Magsat data for the conterminous United States p 22 A85-26420
United States crustal thickness p 18 A85-28011
Estimation of lower crust magnetization from satellite derived anomaly field p 18 A85-28012
- SCHOEPS, D.**
Cosmic interpolation of terrestrial potential values p 18 A85-26476
- SCHOTT, J. R.**
Comparison of modelled and empirical atmospheric propagation data p 46 A85-22678
Evaluation of the radiometric integrity of LANDSAT 4 Thematic Mapper band 6 data p 54 N85-21726
- SCHOTTER, R.**
Realtime processor of SAR systems p 60 A85-25855
- SCHOWENGERDT, R.**
LANDSAT-4 Thematic Mapper Modulation Transfer Function (MTF) evaluation
[E85-10055] p 62 N85-16250
MTF analysis of LANDSAT-4 Thematic Mapper p 68 N85-21737
- SCHREIER, H.**
Automated measurements of terrain reflection and height variations using an airborne infrared laser system p 5 A85-26933
- SCHUMAKER, L. L.**
Multivariate spline methods in surface fitting p 50 N85-16257
- SCHUTT, J. B.**
Effect of heliotropism on the bidirectional reflectance of irrigated cotton p 1 A85-22420
- SCOTT, D. W.**
Nonparametric analysis of Minnesota spruce and aspen tree data and LANDSAT data p 8 N85-16253
- SEGUIN, B.**
Estimation of evapotranspiration on the basis of thermal IR p 3 A85-23765
- SEIGE, P.**
MOMS 1 and its results p 61 A85-27061
- SEKHON, R.**
Comparison of level I land cover classification accuracy for MSS and AVHRR data p 61 A85-26929
- SELIVANOV, A. S.**
Complex studies of the environment by optical and radar methods p 56 A85-20081
Conical multispectral scanner for the study of earth resources p 62 A85-29909
- SETTLE, M.**
Thematic mapper data analysis p 23 A85-27946
Developments with multispectral thermal-IR and active microwave systems - TMS, SIR-A, SIR-B, and radarsat p 62 A85-27947
- SHANMUGAN, K. S.**
Power spectral density of markov texture fields p 50 N85-16262
Information extraction and transmission techniques for spaceborne synthetic aperture radar images
[NASA-CR-174341] p 52 N85-17256
- SHESTOPALOV, V. P.**
Complex studies of the environment by optical and radar methods p 56 A85-20081
Ring structures observed on space radar images of the earth p 45 A85-20084
Space radar observations of small-scale formations on the ocean surface p 27 A85-20086
- SHINE, K. P.**
The influence of satellite spectral sensor response on the analysis of satellite imagery at high latitudes p 60 A85-26927
- SHIUE, J. C.**
Remote sensing of soil moisture p 10 N85-17252
- SHUCHMAN, R.**
The spatial evolution of the directional wave spectrum in the Southern Ocean Its relation to extreme waves in Agulhas Current p 39 N85-17213
- SHUTKO, A. M.**
Determination of soil moisture content by microwave radiometry with the use of a priori information p 6 A85-29910
- SIEBERT, M.**
On the identification of Magsat anomaly charts as crustal part of the internal field p 17 A85-26412
- SIERON, R.**
Growth/reflectance model interface for wheat and corresponding model
[E85-10058] p 9 N85-16269
- SIGNORINI, C.**
A comparison between GEOS 1 magnetic-field measurements and some models of the geomagnetic field p 18 A85-27386

SIMONETT, D.

Deforestation, floodplain dynamics, and carbon biogeochemistry in the Amazon Basin p 44 N85-17216

SIMONETT, D. S.

The extension of an invertible coniferous forest canopy reflectance model using SIR-B and LANDSAT data p 10 N85-17246

SIMPSON, C. J.

Evaluation of SIR-B imagery for geologic and geomorphic mapping, hydrology, and oceanography in Australia p 51 N85-17229

SINELNIKOVA, I. F.

Conical multispectral scanner for the study of earth resources p 62 A85-29909

SINGHROY, V. H.

Structural investigation of the Canadian Shield by orbital radar and LANDSAT p 25 N85-17236
Structural investigation of the Grenville Province by radar and other imaging and nonimaging sensors p 25 N85-17237

SKARDA, J. R.

Analysis of the NASA/MSFC Airborne Doppler Lidar results from San Geronio Pass, California [NASA-CR-171355] p 70 N85-21873

SKORODUMOV, A. P.

Minimization of the effect of the earth's curvature in the projective transformation of space images into photoplans and photomaps p 16 A85-25662

SKOU, N.

Microwave signatures of the sea ice in the East Greenland Current p 31 A85-24079
Spaceborne microwave radiometers Background and technology requirements [LD-R-267] p 63 N85-17350

SLANEY, V. R.

Developments with multispectral thermal-IR and active microwave systems - TMS, SIR-A, SIR-B, and radarsat p 62 A85-27947
Structural investigation of the Canadian Shield by orbital radar and LANDSAT p 25 N85-17236
Structural investigation of the Grenville Province by radar and other imaging and nonimaging sensors p 25 N85-17237

SLATER, P. N.

Survey of multispectral imaging systems for earth observations p 56 A85-22424
Imaging systems for the delineation of spectral properties of geologic materials in the visible and near-infrared p 22 A85-27945
Spectroradiometric calibration of the Thematic Mapper and Multispectral Scanner system [E85-10077] p 64 N85-19491
In-progress absolute radiometric flight calibration of the LANDSAT-4 sensors p 68 N85-21733
Spectroradiometric calibration of the Thematic Mapper and Multispectral Scanner system [E85-10094] p 70 N85-21756

SLEMMONS, D. B.

Analysis of SIR-B radar illumination of geometry for depth of penetration and surface feature and vegetation detection, Nevada and California p 25 N85-17248

SLUD, E.

Analysis of subpixel registration p 51 N85-16267

SMITH, G. B.

Image-to-image correspondence Linear structure matching p 51 N85-16266

SMITH, G. R.

Aircraft measurements for calibration of an orbiting spacecraft sensor p 59 A85-24246

SMITH, R. H.

Forest area estimates from LANDSAT MSS and forest inventory plot data [PB85-105617/GAR] p 9 N85-16290

SMITH, W. B.

Autoregressive spectral estimation for two dimensional time series p 50 N85-16258

SOLOVEV, N. N.

Analysis of mesofractures according to space images Currents trends in the exploration for oil and gas deposits p 21 A85-25655

SPENCER, R. W.

Satellite passive microwave rain rate measurement over croplands during spring, summer and fall p 4 A85-25181

SPIRIDONOV, I. U. G.

Complex studies of the environment by optical and radar methods p 56 A85-20081
Ring structures observed on space radar images of the earth p 45 A85-20084
Effect of meteorological conditions on the characteristics of space radar images of the earth surface p 48 A85-25653

STACEY, J. M.

Method of measuring sea surface water temperature with a satellite including wideband passive synthetic-aperture multichannel receiver [NASA-CASE-NPO-15651-1] p 41 N85-21723

STARKUS, C. J.

Large scan mirror assembly of the new Thematic Mapper developed for Landsat 4 earth resources satellite p 56 A85-22682

STEPHENS, G.

Monitoring Africa's Lake Chad basin with Landsat and NOAA satellite data p 43 A85-26930

STERANKA, J.

The diurnal variation of Atlantic Ocean tropical cyclone cloud distribution inferred from geostationary satellite infrared measurements p 33 A85-24739

STERN, R. J.

Post-carboniferous tectonics in the Anadarko Basin, Oklahoma Evidence from side-looking radar imagery [NASA-CR-175458] p 26 N85-19498

STEWART, E.

Estimating ocean primary production from satellite chlorophyll - Introduction to regional differences and statistics for the Southern California Bight p 35 A85-28005

STOGER, L. B.

Satellite data communication system for near real-time processing and distribution of marine fishery research p 36 A85-28119

STOHR, C. J.

Terrain and look angle effects upon multispectral scanner response p 60 A85-26642

STRAHLER, A. H.

Image variance and spatial structure in remotely sensed scenes p 51 N85-16265
The extension of an invertible coniferous forest canopy reflectance model using SIR-B and LANDSAT data p 10 N85-17246
Preliminary evaluation of the airborne imaging spectrometer for vegetation analysis [NASA-CR-174440] p 12 N85-19496

STRANG VAN HEES, G. L.

Gravity field investigation in the North Sea p 30 A85-23699

STRANGWAY, D. W.

Scalar magnetic anomalies of Canada and northern United States derived from Magsat data p 18 A85-26418

STRECKER, M. R.

Tectonic, volcanic, and climatic geomorphology study of the Sierras Pampeanas Andes, northwestern Argentina p 24 N85-17215

STROME, W. M.

Canadian plans for Thematic Mapper data p 54 N85-20513

STRONG, J. P.

Automatic terrain elevation mapping and registration p 52 N85-17242

SU, J.

LS-4 MSS geometric correction Methods and results p 53 N85-20507

SUITS, G. H.

An analysis of spectral discrimination between corn and soybeans using a row crop reflectance model p 7 A85-30086

Growth/reflectance model interface for wheat and corresponding model [E85-10058] p 9 N85-16269

SULLIVAN, K. D.

Geological, structural, and geomorphological analyses from SIR-B p 24 N85-17226

SUVOROV, B. A.

Conical multispectral scanner for the study of earth resources p 62 A85-29909

SVENDSEN, E.

Polarization effects in sea-ice signatures p 31 A85-24078

SWIFT, C. T.

An algorithm to measure sea ice concentration with microwave radiometers p 27 A85-20492
Airborne microwave measurements of the southern Greenland ice sheet p 28 A85-23644

SWIFT, R. N.

The use of airborne lasers in terrestrial and water environments p 33 A85-25351
The reflection of airborne UV laser pulses from the ocean p 37 A85-29714

T

TACONET, O.

Thermal structure of an agricultural region as seen by NOAA-7 AVHRR p 7 A85-30090

TAKAHASHI, S.

The development of image processing of NOAA AVHRR data and its application to sea surface temperature p 42 N85-21891

TANG, C. L.

Structure and seasonal characteristics of the Gaspe current p 35 A85-27705

TANRE, D.

Demonstration, analysis, and correction of atmospheric effects on Landsat or SPOT multispectral data p 58 A85-23781

TARANIK, J. V.

Analysis of SIR-B radar illumination of geometry for depth of penetration and surface feature and vegetation detection, Nevada and California p 25 N85-17248

TAYLOR, G. R.

Australian Multiexperimental Assessment of SIR-B (AMAS) p 52 N85-17243

TAYLOR, P. K.

The scanning multichannel microwave radiometer - An assessment p 57 A85-23705

TAYLOR, P. T.

Comparison between the recent US composite magnetic anomaly map and Magsat anomaly data p 17 A85-26413

TEILLET, P.

The measurement of bidirectional reflectances by analysis of Landsat images p 2 A85-23756
Integration of the SPOT panchromatic channel into its multispectral mode for image sharpness enhancement p 49 A85-29217

TEREKHOV, V. A.

Simultaneous radiometric and radar altimetric measurements of sea microwave signatures p 31 A85-24076

THOMAS, D. P.

The evaluation of SMMR retrieval algorithms p 31 A85-23706

THOMAS, H. H.

Satellite magnetic anomalies over subduction zones - The Aleutian Arc anomaly p 16 A85-21107

THOMAS, I. L.

An example of Landsat cost effectiveness in mapping land-cover p 1 A85-20573

THOMAS, R. H.

Ice sheet margins and ice shelves p 32 A85-24524
Satellite observations of sea ice p 36 A85-28022

THOMAS, R. W.

Remote sensing research for agricultural applications [E85-10090] p 13 N85-21752

THOMPSON, R. L.

Estimation of agronomic variables using spectral signatures p 2 A85-23753

THORMODSGARD, J. M.

Geodetic accuracy of LANDSAT 4 Multispectral Scanner and Thematic Mapper data p 53 N85-20504
Geodetic accuracy of LANDSAT 4 Multispectral Scanner and Thematic Mapper data p 20 N85-21746

TIAN, G.

Methodological study of spectral band selection for multispectral remote sensing p 55 A85-19363

TILLEY, D.

The spatial evolution of the directional wave spectrum in the Southern Ocean Its relation to extreme waves in Agulhas Current p 39 N85-17213

TOKSOZ, M. N.

Delineation of major geologic structures in Turkey using SIR-B data p 25 N85-17249

TOKUNO, M.

The development of image processing of NOAA AVHRR data and its application to sea surface temperature p 42 N85-21891

TOLL, D. L.

Effect of Landsat Thematic Mapper sensor parameters on land cover classification p 14 A85-30088

TONG, Q.

Methodological study of spectral band selection for multispectral remote sensing p 55 A85-19363

TORLEGAARD, K.

Mathematical aspects of digital terrain information, Report from International Society for Photogrammetry and Remote Sensing (ISPRS) working group 3 3, 1980 - 1984 p 19 N85-17407

A comparative test of photogrammetrically sampled digital elevation models p 52 N85-17408
Multimodels increase accuracy Summary of an experiment p 63 N85-17409

TOTTEN, S. M.

Interlobate comparison of glacial-depositional style as evidenced by small-relief glacial landscape features in Illinois, Indiana, and Ohio, utilizing SIR-B p 39 N85-17231

TOWNSEND, K.

Information extraction and transmission techniques for spaceborne synthetic aperture radar images [NASA-CR-174341] p 52 N85-17256

- TOWNSEND, T. E.**
Imaging systems for the delineation of spectral properties of geologic materials in the visible and near-infrared p 22 A85-27945
- TOWNSHEND, J. R. G.**
African land-cover classification using satellite data p 1 A85-21174
- TRAVLOS, A. J.**
Remote sensing research for agricultural applications [E85-10090] p 13 A85-21752
- TRICART, J.**
Geomorphology and remote sensing Numerical inventory of objects in Landsat, SPOT simulation, and SIR-A data Applications to the Mopti-Bandiagara (Mali) region p 21 A85-23785
- TRIFONOV, V. G.**
Space remote-sensing data in geology p 23 A85-28400
- TRINDER, J. C.**
Australian Multiexperimental Assessment of SIR-B (AMAS) p 52 A85-17243
- TROENSEGAARD, K. W.**
Experimental evidence for spring and autumn windows for the detection of geobotanical anomalies through the remote sensing of overlying vegetation p 6 A85-26939
- TSONIS, A. A.**
On the separability of various classes from the GOES visible and infrared data p 45 A85-21138
- TSYMBAL, V. N.**
Space radar observations of small-scale formations on the ocean surface p 27 A85-20086
- TUCHIN, I. U. M.**
Complex studies of the environment by optical and radar methods p 56 A85-20081
- TUCKER, C.**
Automated measurements of terrain reflection and height variations using an airborne infrared laser system p 5 A85-26933
- TUCKER, C. J.**
African land-cover classification using satellite data p 1 A85-21174
Regional analysis from data from heterogeneous pixels - Remote sensing of total dry matter production in the Senegalese Sahel p 47 A85-23783
The potential of satellite remote sensing of ecological conditions for survey and forecasting desert-locust activity p 5 A85-26934
North American vegetation patterns observed with the NOAA-7 advanced very high resolution radiometer [E85-10062] p 10 A85-17400
- TUCKER, M. J.**
The effect of a moving sea surface on SAR imagery p 29 A85-23685
- U**
- ULABY, F. T.**
Microwave properties of vegetation canopies - An overview p 4 A85-23772
Evaluation of the radar response to land surfaces and volumes Examination of theoretical models, target statistics, and applications p 63 A85-17250
- ULIANA, E. A.**
Electromagnetic bias of 10-GHz radar altimeter measurements of MSL p 37 A85-29713
- ULRIKSEN, P.**
Ground truth for SIR-B images obtained by SIR system 8 impulse radar p 10 A85-17251
- URQUHART, W. E. S.**
Scalar magnetic anomalies of Canada and northern United States derived from Magsat data p 18 A85-26418
- USERY, E. L.**
Geometric accuracy of LANDSAT-4 MSS image data p 53 A85-20503
- V**
- VANDERBILT, V. C.**
Light polarization measurements - A method to determine the specular and diffuse light-scattering properties of both leaves and plant canopies p 2 A85-23754
- VANDERZEE, D.**
Monitoring of the tidal dynamics of the Dutch Waddensea by SIR-B p 40 A85-17235
- VANE, G.**
Imaging systems for the delineation of spectral properties of geologic materials in the visible and near-infrared p 22 A85-27945
- VANPRAET, C.**
Regional analysis from data from heterogeneous pixels - Remote sensing of total dry matter production in the Senegalese Sahel p 47 A85-23783
- VASTANO, A. C.**
Lagrangian observations of surface circulation at the Emperor Seamount chain p 35 A85-27710
- VAUCLIN, M.**
Influence of spatial variability of soil hydraulic characteristics on surface parameters obtained from remote-sensing data in thermal infrared and microwaves p 43 A85-23786
- VERBRUGGHE, M.**
Spectral signatures of objects in remote sensing, International Conference, 2nd, Bordeaux, France, September 12-16, 1983, Reports p 57 A85-23751
- VERDIN, J. P.**
Monitoring water quality conditions in a large western reservoir with Landsat imagery p 43 A85-29220
- VERHOEFF, W.**
Earth observation modeling based on layer scattering matrices p 7 A85-30091
Comparative study of Suits and SAIL canopy reflectance models p 7 A85-30092
- VERSLUUIS, H. W.**
Gravity field investigation in the North Sea p 30 A85-23699
- VERSTAPPEN, A. T.**
Monitoring of the tidal dynamics of the Dutch Waddensea by SIR-B p 40 A85-17235
- VESECKY, J.**
SEASAT 3 and 4 [AD-A148343] p 40 A85-17274
- VIDAL-MADJAR, D.**
Thermal structure of an agricultural region as seen by NOAA-7 AVHRR p 7 A85-30090
- VIKTOROV, S. V.**
Remote-sensing observations of advective eddies in the central part of the Baltic Sea p 38 A85-29915
- VINCENT, P.**
Spectral response of different agricultural and penurban land-use units in the spectral windows at 1.55-1.75 and 2.08-2.35 microns p 4 A85-23787
- VINOGRADOV, V. V.**
Remote-sensing observations of advective eddies in the central part of the Baltic Sea p 38 A85-29915
- VLASOV, V. P.**
Double-angle method for measuring ocean surface temperature in the infrared p 34 A85-25658
- VOLCHEGURSKII, L. F.**
Methods for the study of recent tectonics on the basis of remote sensing and ground data p 23 A85-29904
- VOLNISTOVA, L. P.**
The influence of a scattering medium on the quality of an optical image p 48 A85-26294
- VONDERHAAR, T. H.**
Rain volume estimation over areas using satellite and radar data [NASA-CR-174434] p 44 A85-19568
- VREELAND, H.**
Analysis of SIR-B radar illumination of geometry for depth of penetration and surface feature and vegetation detection, Nevada and California p 25 A85-17248
- VREELAND, P.**
Analysis of SIR-B radar illumination of geometry for depth of penetration and surface feature and vegetation detection, Nevada and California p 25 A85-17248
- W**
- WADSWORTH, A.**
The use of SEASAT-SAR data in oceanography at the IFF p 29 A85-23690
- WAITE, W. P.**
Evaluation of the L-band scattering characteristics of volcanic terrain in aid of lithologic identification, assessment of SIR-B calibration, and development of planetary geomorphic analogs p 24 A85-17232
SIR-B cartography and stereo topographic mapping p 19 A85-17234
- WAKKER, K. F.**
The participation of the Netherlands in the NASA Coastal Dynamics Project p 15 A85-20035
- WALKER, A. S.**
Application and calibration of the subsurface mapping capability of SIR-B in desert regions p 25 A85-17244
- WALKER, J. A.**
Prelaunch absolute radiometric calibration of the reflective bands on the LANDSAT-4 protoflight Thematic Mapper p 66 A85-20515
- WALL, S. L.**
Remote sensing research for agricultural applications [E85-10090] p 13 A85-21752
- WALSH, E. J.**
Electromagnetic bias of 36-GHz radar altimeter measurements of MSL p 37 A85-29712
An analysis of a satellite multibeam altimeter p 38 A85-29715
- WALTON, W. T.**
Aircraft and satellite measurement of ocean wave directional spectra using scanning-beam microwave radars p 27 A85-20486
A comparison of in situ and airborne radar observations of ocean wave directionality p 27 A85-20487
- WANG, J. R.**
Effect of vegetation on soil moisture sensing observed from orbiting microwave radiometers p 7 A85-30089
Remote sensing of soil moisture p 10 A85-17252
- WASILEWSKI, P. J.**
A review of problems and progress in studies of satellite magnetic anomalies p 17 A85-26409
- WATSON, E.**
Information extraction and transmission techniques for spaceborne synthetic aperture radar images [NASA-CR-174341] p 52 A85-17256
- WATSON, J.**
Information extraction and transmission techniques for spaceborne synthetic aperture radar images [NASA-CR-174341] p 52 A85-17256
- WATSON, K.**
Thermal-inertia mapping from space p 21 A85-23766
SEASAT 3 and 4 [AD-A148343] p 40 A85-17274
- WATTS, A. B.**
On the determination of the deflection of the vertical by satellite altimetry p 37 A85-29706
- WEATHERLY, G. L.**
Abyssal eddies near the Gulf Stream p 34 A85-27701
- WEBB, D. J.**
Wave measurements with the Seasat radar altimeter - A Review p 30 A85-23701
- WEBSTER, W. J., JR.**
Structural investigation of the Canadian Shield by orbital radar and LANDSAT p 25 A85-17236
Structural investigation of the Grenville Province by radar and other imaging and nonimaging sensors p 25 A85-17237
- WEINMAN, J. A.**
Resolution enhancement of multichannel microwave imagery from the Nimbus-7 SMMR for maritime rainfall analysis [NASA-CR-174367] p 44 A85-19221
- WELCH, R.**
SIR-B cartography and stereo topographic mapping p 19 A85-17234
Geometric accuracy of LANDSAT-4 MSS image data p 53 A85-20503
- WEST, T. R.**
Terrain and look angle effects upon multispectral scanner response p 60 A85-26642
- WHEELER, D. J.**
An integrated GIS/remote sensing data base in North Cache soil conservation district, Utah A pilot project for the Utah Department of Agriculture's RIMS (Resource Inventory and Monitoring System) p 11 A85-19487
Building a functional, integrated GIS/remote sensing resource analysis and planning system [E85-10092] p 15 A85-21754
- WHITE, G.**
Use of ocean skewness measurements in calculating the accuracy of altimeter height measurements p 30 A85-23703
- WHITE, G. C.**
The investigation of selected oceanographic applications of spaceborne synthetic-aperture radar p 39 A85-17233
- WICKLAND, D. E.**
The importance of geobotany in geological remote sensing applications p 23 A85-27948
- WILHELM, J.**
Advanced SAR system maps Arctic regions p 35 A85-27841
- WINDSOR, E. P. L.**
The evaluation of SMMR retrieval algorithms p 31 A85-23706
- WINKENBACH, H.**
Modular Optoelectronic Multispectral Scanner (MOMS) Technological aspects p 61 A85-27059
MOMS 1 and its results p 61 A85-27061
- WITT, R. G.**
Comparison of level I land cover classification accuracy for MSS and AVHRR data p 61 A85-26929
- WOLDAI, T.**
Education and training in satellite remote sensing applications - Guide to education and training opportunities p 71 A85-20640

WOLF, H. C.

- Monitoring of the tidal dynamics of the Dutch Waddensea by SIR-B p 40 N85-17235
- WOLF, H. C.**
Image-to-image correspondence Linear structure matching p 51 N85-16266
- WOLFF, B.**
Spaceborne microwave radiometers Background and technology requirements [LD-R-267] p 63 N85-17350
- WOODCOCK, C. E.**
Image variance and spatial structure in remotely sensed scenes p 51 N85-16265
Preliminary evaluation of the airborne imaging spectrometer for vegetation analysis [NASA-CR-174440] p 12 N85-19496
- WOODWELL, G.**
Deforestation, floodplain dynamics, and carbon biogeochemistry in the Amazon Basin p 44 N85-17216
- WRIGLEY, R. C.**
Impact of LANDSAT MSS sensor differences on change detection analysis p 65 N85-20506
Assessment of Thematic Mapper band-to-band registration by the block correlation method p 55 N85-21743
- WU, H.-T.**
Dramatic contrast between low clouds and snow cover in daytime 3.7 micron imagery p 48 A85-24740
- WU, S. S. C.**
Radargrammetry of Shuttle Imaging Radar-B experiment p 46 A85-23779
- WU, S. T.**
Analysis of data acquired by synthetic aperture radar and LANDSAT Multispectral Scanner over Kershaw County, South Carolina, during the summer season [E85-10071] p 11 N85-19485
- WYATT, B. K.**
The integrated use of digital cartographic data and remotely sensed imagery p 45 A85-20572
- WYLIE, D.**
A summary of the wind data available from satellites from the past history to future sensors p 33 A85-24558

Y

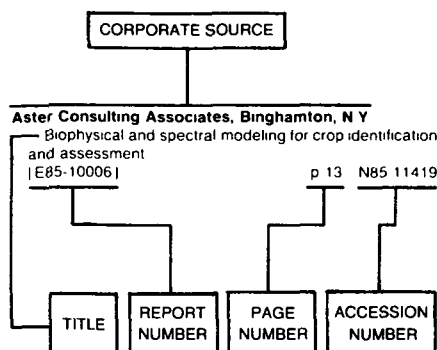
- YAMAGUCHI, Y.**
Image-scale and look-direction effects on the detectability of lineaments in radar images p 24 A85-30087
- YAMANI, A.**
MOMS 1 and its results p 61 A85-27061
- YANAGISAWA, M.**
Mean ionospheric field correction for Magsat data p 17 A85-26411
- YANG, S.**
Remote sensing development in the People's Republic of China p 56 A85-20643
- YAO, S. S.**
Investigation of TM band-to-band registration using the JSC registration processor p 69 N85-21745
- YEH, C. L.**
Resolution enhancement of multichannel microwave imagery from the Nimbus-7 SMMR for maritime rainfall analysis [NASA-CR-174367] p 44 N85-19221
- YEH, H.-Y. M.**
Comments on 'Inference of cloud temperature and thickness by microwave radiometry from space' p 59 A85-25182
- YEN, S.**
Study on a regional geographical information system and application model p 13 A85-20644
- YUKUTAKE, T.**
Extraction of magnetic anomalies of crustal origin from Magsat data over the area of the Japanese Islands p 21 A85-26419
- YUROVSKY, L.**
Information extraction and transmission techniques for spaceborne synthetic aperture radar images [NASA-CR-174341] p 52 N85-17256

Z

- ZACHARIASEN, F.**
SEASAT 3 and 4 [AD-A148343] p 40 N85-17274
- ZAITSOVA, I. G.**
Determination of the physical parameters of sea ice on the basis of remote microwave measurements in the 0.3-18 cm range p 38 A85-29903
- ZAVODY, A. M.**
Satellite measurements of sea-surface temperature for climate research p 32 A85-24555

ZBINDEN, R.

- Thematic evaluation of SPOT spectral bands p 58 A85-23794
- ZHAO, S.-X.**
Study on a regional geographical information system and application model p 13 A85-20644
- ZHENG, L.**
Remote sensing development in the People's Republic of China p 56 A85-20643
- ZILGER, J.**
MOMS 1 and its results p 61 A85-27061
- ZISK, S. H.**
Geological, structural, and geomorphological analyses from SIR-B p 24 N85-17226
Evaluation of the L-band scattering characteristics of volcanic terrain in aid of lithologic identification, assessment of SIR-B calibration, and development of planetary geomorphic analogs p 24 N85-17232
- ZLATOPOLSKII, A. A.**
Identification of homogeneous regions with incomplete boundaries on an image p 24 A85-29912
- ZONGQUAN, M.**
Airborne remote sensing CCD imaging system p 65 N85-20220
- ZOTOVA, E. N.**
Soil moisture content estimation by radar survey data during the sowing campaign p 6 A85-26947

Typical Corporate Source
Index Listing

The title of the document is used to provide a brief description of the subject matter. The page number and the accession number are included in each entry to assist the user in locating the abstract in the abstract section. If applicable, a report number is also included as an aid in identifying the document.

A

- Admiralty Research Establishment, Portland (England).**
The imaging of internal waves by the SEASAT-A synthetic aperture radar
[AD-A149808] p 20 N85-21761
- Aerospace Corp., El Segundo, Calif.**
An auroral X-ray imaging spectrometer
[AD-A147756] p 64 N85-17469
- Analytic Sciences Corp., Reading, Mass.**
Investigation of SIR-B images for lithologic mapping
p 25 N85-17241
- Applied Physics Lab., Johns Hopkins Univ., Laurel, Md.**
Predicting dangerous ocean waves with spaceborne synthetic aperture radar p 27 A85-19429
An analysis of a satellite multibeam altimeter p 38 A85-29715
The spatial evolution of the directional wave spectrum in the Southern Ocean. Its relation to extreme waves in Agulhas Current p 39 N85-17213
- Arizona Univ., Tucson.**
Survey of multispectral imaging systems for earth observations p 56 A85-22424
Imaging systems for the delineation of spectral properties of geologic materials in the visible and near-infrared p 22 A85-27945
LANDSAT-4 Thematic Mapper Modulation Transfer Function (MTF) evaluation [E85-10055] p 62 N85-16250
Spectroradiometric calibration of the Thematic Mapper and Multispectral Scanner system [E85-10077] p 64 N85-19491
In-progress absolute radiometric inflight calibration of the LANDSAT-4 sensors p 68 N85-21733
MTF analysis of LANDSAT-4 Thematic Mapper p 68 N85-21737
Spectroradiometric calibration of the Thematic Mapper and Multispectral Scanner system [E85-10094] p 70 N85-21756

Arkansas Univ., Fayetteville.

Evaluation of the L-band scattering characteristics of volcanic terrain in aid of lithologic identification, assessment of SIR-B calibration, and development of planetary geomorphic analogs p 24 N85-17232

Army Cold Regions Research and Engineering Lab., Hanover, N. H.

LandSAT-4 thematic mapper (TM) for cold environments p 60 A85-25349
MIZEX (Marginal Ice Zone Program) A program for mesoscale air-ice-ocean interaction experiments in Arctic marginal ice zones 5 MIZEX 84 Summer experiment PI (Principal Investigator) preliminary reports [AD-A148986] p 41 N85-19594

Army Engineer Waterways Experiment Station, Vicksburg, Miss.

The use of airborne lasers in terrestrial and water environments p 33 A85-25351

B

Bayerische Akademie der Wissenschaften, Munich (West Germany)

Activities report of the Department of Applied Research 78 for satellite geodesy of the Technical University, Munich [ASTRON-GEODATA-ARB-45] p 19 N85-18440

Boston Univ., Mass.

Image variance and spatial structure in remotely sensed scenes p 51 N85-16265

Brown Univ., Providence, R. I.

Geological, structural, and geomorphological analyses from SIR-B p 24 N85-17226

Business and Technological Systems, Inc., Seabrook, Md.

The near-earth magnetic field at 1980 determined from Magsat data p 16 A85-26408

C

California Univ., Berkeley.

Analysis of the quality of image data required by the LANDSAT-4 Thematic Mapper and Multispectral Scanner [E85-10074] p 11 N85-19488
Remote sensing research for agricultural applications [E85-10090] p 13 N85-21752

California Univ., Santa Barbara

The extension of an invertible coniferous forest canopy reflectance model using SIR-B and LANDSAT data p 10 N85-17246

Cambridge Univ. (England).

The near-earth magnetic field at 1980 determined from Magsat data p 16 A85-26408

Canada Centre for Remote Sensing, Ottawa (Ontario).

Radiometric calibration and geocoded precision processing of LANDSAT-4 Multispectral Scanner products by the Canada Centre for Remote Sensing p 53 N85-20501
Canadian plans for Thematic Mapper data p 54 N85-20513

Preliminary evaluation of the radiometric calibration of LANDSAT-4 Thematic Mapper data by the Canada Centre for Remote Sensing p 67 N85-21729

Centre National d'Etudes Spatiales, Paris (France).

The spot operational remote sensing satellite system Current status and perspectives p 67 N85-20776

Chevron Oil Field Research Co., La Habra, Calif.

Developments with multispectral thermal-IR and active microwave systems - TMS, SIR-A, SIR-B, and radarsat p 62 A85-27947

Cities Service Oil Co., Tulsa, Okla.

Developments with multispectral thermal-IR and active microwave systems - TMS, SIR-A, SIR-B, and radarsat p 62 A85-27947

City Coll. of the City Univ. of New York.

Oceanographic and meteorological research based on the data products of SEASAT [E85-10091] p 41 N85-21753

Clemson Univ., S.C.

The diurnal variation of Atlantic Ocean tropical cyclone cloud distribution inferred from geostationary satellite infrared measurements p 33 A85-24739

Coast Guard Research and Development Center, Groton, Conn.

Atlas of the Beaufort Sea [AD-A149545] p 41 N85-20619

Colorado School of Mines, Golden.

Research on ocean floor electrical surveys [AD-A149831] p 42 N85-21920

Colorado Univ., Boulder.

Lake ice occurrence as a possible detector of atmospheric CO₂ effects on climate [DE85-002951] p 45 N85-20606

Commonwealth Scientific and Industrial Research Organization, Wembley (Australia).

Evaluation of SIR-B imagery for geologic and geomorphic mapping, hydrology, and oceanography in Australia p 51 N85-17229

Computer Sciences Corp., Silver Spring, Md.

Aircraft and satellite measurement of ocean wave directional spectra using scanning-beam microwave radars p 27 A85-20486

Comparison of level 1 land cover classification accuracy for MSS and AVHRR data p 61 A85-26929

Cornell Univ., Ithaca, N.Y.

Tectonic, volcanic, and climatic geomorphology study of the Sierras Pampeanas Andes, northwestern Argentina p 24 N85-17215

Council on Environmental Quality, Washington, D.C.

Sourcebook Gaining access to US government information on the environment and natural resources [DE84-017419] p 71 N85-20941

D

Department of Energy, Mines, and Resources, Ottawa (Ontario).

A preliminary assessment of LANDSAT-4 Thematic Mapper data p 54 N85-21728

Department of the Navy, Washington, D.C.

A method for determining mesoscale dynamic topography [AD-D011412] p 40 N85-17506

E

Earth Satellite Corp., Chevy Chase, Md.

Thematic mapper data analysis p 23 A85-27946

EG and G Washington Analytical Services Center, Inc., Pocomoke City, Md.

The use of airborne lasers in terrestrial and water environments p 33 A85-25351

The reflection of airborne UV laser pulses from the ocean p 37 A85-29714

EG & G Washington Analytical Services Center, Inc., Riverdale, Md.

Regional mean sea surfaces based on GEOS-3 and SEASAT altimeter data p 38 A85-29716

Environmental Research Inst. of Michigan, Ann Arbor.

An analysis of spectral discrimination between corn and soybeans using a row crop reflectance model p 7 A85-30086

Study of spectral/radiometric characteristics of the Thematic Mapper for land use applications [E85-10057] p 62 N85-16268

Growth/reflectance model interface for wheat and corresponding model [E85-10058] p 9 N85-16269

Study of spectral/radiometric characteristics of the Thematic Mapper for land use applications [E85-10075] p 64 N85-19489

Investigation of radiometric properties of LANDSAT-4 MSS p 65 N85-20500

Scan angle and detector effects in Thematic Mapper radiometry p 68 N85-21735

Thematic Mapper spectral dimensionality and data structure p 12 N85-21736

Investigations of vegetation and soils information contained in LANDSAT Thematic Mapper and Multispectral Scanner data
[E85-10082] p 12 N85-21747

EROS Data Center, Sioux Falls, S. Dak.

LANDSAT 4 investigation of Thematic Mapper and Multispectral Scanner applications
[E85-10076] p 52 N85-19490

Geodetic accuracy of LANDSAT 4 Multispectral Scanner and Thematic Mapper data p 53 N85-20504

Geodetic accuracy of LANDSAT 4 Multispectral Scanner and Thematic Mapper data p 20 N85-21746

LANDSAT 4 investigations of Thematic Mapper and Multispectral Scanner applications
[E85-10095] p 26 N85-21757

European Space Agency, Paris (France).

Enhancement of multispectral scanner images by digital filtering
[ESA-TT-624] p 63 N85-16284

European Space Agency ESRI, Frascati (Italy).

A preliminary analysis of LANDSAT-4 Thematic Mapper radiometric performance p 68 N85-21730

TM geometric performance Line to Line Displacement Analysis (LLDA) p 68 N85-21732

F**Food and Agriculture Organization of the United Nations, Rome (Italy).**

The potential of satellite remote sensing of ecological conditions for survey and forecasting desert locust activity p 5 A85-26934

Forest Service, New Orleans, La.

Forest area estimates from LANDSAT MSS and forest inventory plot data
[PB85-105617/GAR] p 9 N85-16290

G**General Electric Co., Lanham, Md.**

Interactive digital image processing for terrain data extraction
[AD-A148580] p 52 N85-17417

LS-4 MSS geometric correction Methods and results p 53 N85-20507

General Electric Co., Philadelphia, Pa.

An overview of the Thematic Mapper geometric correction system p 53 N85-20511

General Software Corp., Landover, Md.

The diurnal variation of Atlantic Ocean tropical cyclone cloud distribution inferred from geostationary satellite infrared measurements p 33 A85-24739

Geological Survey, Flagstaff, Ariz.

Thematic mapper data analysis p 23 A85-27946

Application and calibration of the subsurface mapping capability of SIR-B in desert regions p 25 N85-17244

Intraband radiometric performance of the LANDSAT 4 Thematic Mapper p 69 N85-21738

Tests of low-frequency geometric distortions in LANDSAT 4 images p 55 N85-21744

Geological Survey, Reston, Va.

Comparison between the recent US composite magnetic anomaly map and Magsat anomaly data p 17 A85-26413

Imaging systems for the delineation of spectral properties of geologic materials in the visible and near-infrared p 22 A85-27945

Thematic mapper data analysis p 23 A85-27946

The importance of geobotany in geological remote sensing applications p 23 A85-27948

A preliminary evaluation of LANDSAT-4 Thematic Mapper data for their geometric and radiometric accuracies p 54 N85-21739

Geological Survey of Canada, Ottawa (Ontario).

Developments with multispectral thermal-IR and active microwave systems - TMS, SIR-A, SIR-B, and radarsat p 62 A85-27947

Georgia Inst. of Tech., Atlanta.

Performance of an airborne imaging 92/183 GHz radiometer during the Bering Sea Marginal Ice Zone Experiment (MIZEK-WEST) p 33 A85-24945

Georgia Univ., Athens.

Geometric accuracy of LANDSAT-4 MSS image data p 53 N85-20503

Geosat Committee, Inc., San Francisco, Calif.

Frontiers for geological remote sensing from space, Geosat Workshop, 4th, Flagstaff, AZ, June 12-17, 1983, Report p 22 A85-27943

H**Houston Univ., Tex.**

Neotectonics of the Caribbean p 27 A85-21145

Bayesian estimation of normal mixture parameters p 50 N85-16255

Hunter Coll., New York.

Preliminary evaluation of the airborne imaging spectrometer for vegetation analysis
[NASA-CR-174440] p 12 N85-19496

I**Illinois Univ., Urbana.**

Interlobate comparison of glacial-depositional style as evidenced by small-relief glacial landscape features in Illinois, Indiana, and Ohio, utilizing SIR-B p 39 N85-17231

Imperial Coll. of Science and Technology, London

(England). An intercalibration of Meteosat-1 and GOES-2 visible and infrared measurements p 26 A85-19420

Institute of Oceanographic Sciences, Wormley

(England). The interpretation of SIR-B imagery of surface waves and other oceanographic features using in-situ, meteorological satellite, and infrared satellite data p 39 N85-17212

Instituto de Pesquisas Espaciais, Sao Jose dos

Campos (Brazil). Integrated analysis of remote sensing products from basic geological surveys p 24 N85-16248

The management of atmospheric resources in food production p 9 N85-16362

Brazilian Remote Sensing Shuttle Experiment (BRESEX) Characteristics and future utilization on satellites [INPE-3313-PRE/620] p 64 N85-19385

Brazilian remote sensing receiving, recording and processing ground systems in the 1980's [E85-10052] p 52 N85-19493

Remote sensing activities in Latin America [INPE-3297-PRE/612] p 64 N85-19501

The sharing of remote sensing techniques in Brazilian geographic research [INPE-3307-PRE/617] p 15 N85-19502

International Inst. for Aerial Survey and Earth

Sciences, Enschede (Netherlands). Monitoring of the tidal dynamics of the Dutch Waddensea by SIR-B p 40 N85-17235

J**Jet Propulsion Lab., California Inst. of Tech.,**

Pasadena. Calculation of thermal inertia from day-night measurements separated by days or weeks p 45 A85-21048

Measuring spectra of and lands p 20 A85-21975

Characteristics of playa deposits as seen on SIR-A, Seasat and Landsat coregistered data p 21 A85-23793

Ice sheet margins and ice shelves p 32 A85-24524

Lagrangian observations of surface circulation at the Emperor Seamount chain p 35 A85-27710

Frontiers for geological remote sensing from space, Geosat Workshop, 4th, Flagstaff, AZ, June 12-17, 1983, Report p 22 A85-27943

Imaging systems for the delineation of spectral properties of geologic materials in the visible and near-infrared p 22 A85-27945

Thematic mapper data analysis p 23 A85-27946

Developments with multispectral thermal-IR and active microwave systems - TMS, SIR-A, SIR-B, and radarsat p 62 A85-27947

The importance of geobotany in geological remote sensing applications p 23 A85-27948

Estimating ocean primary production from satellite chlorophyll - Introduction to regional differences and statistics for the Southern California Bight p 35 A85-28005

Determination of monthly mean humidity in the atmospheric surface layer over oceans from satellite data p 35 A85-28007

Satellite observations of sea ice p 36 A85-28022

Mapping of glacial landforms from Seasat radar images p 36 A85-28027

A survey of oceanographic satellite altimetric missions p 36 A85-29703

Texture classification using autoregressive filtering p 50 N85-16254

The SIR-B science investigations plan [NASA-CR-174282] p 63 N85-17208

Deforestation, floodplain dynamics, and carbon biogeochemistry in the Amazon Basin p 44 N85-17216

SIR-B cartography and stereo topographic mapping p 19 N85-17234

Development and evaluation of techniques for using combined microwave and optical image data for vegetation studies p 9 N85-17240

Application and calibration of the subsurface mapping capability of SIR-B in desert regions p 25 N85-17244

Preliminary evaluation of the airborne imaging spectrometer for vegetation analysis [NASA-CR-174440] p 12 N85-19496

SIR-A imagery in geologic studies of the Sierra Madre Oriental, northeastern Mexico Part 1 (Regional stratigraphy) The use of morphostratigraphic units in remote sensing mapping [NASA-CR-175457] p 25 N85-19497

Post-carboniferous tectonics in the Anadarko Basin, Oklahoma Evidence from side-looking radar imagery [NASA-CR-175458] p 26 N85-19498

Method of measuring sea surface water temperature with a satellite including wideband passive synthetic-aperture multichannel receiver [NASA-CASE-NPO-15651-1] p 41 N85-21723

Joint Publications Research Service, Arlington, Va.

Satellite photographs suggest arctic volcano p 38 N85-16239

CNES, INRA do joint remote-sensing research p 11 N85-19321

Remote sensing technology now playing practical roles p 64 N85-20190

Airborne remote sensing CCD imaging system p 65 N85-20220

K**Kansas Univ., Lawrence.**

Power spectral density of markov texture fields p 50 N85-16262

Kansas Univ. Center for Research, Inc., Lawrence.

Surface scattering effects at different spectral regions p 58 A85-23780

Intermediate results of radar backscatter measurements from summer sea ice [AD-A147212] p 38 N85-15960

Information for space radar designers Required dynamic range vs resolution and antenna calibration using the Amazon rain forest p 44 N85-17239

Evaluation of the radar response to land surfaces and volumes Examination of theoretical models, target statistics, and applications p 63 N85-17250

Information extraction and transmission techniques for spaceborne synthetic aperture radar images [NASA-CR-174341] p 52 N85-17256

L**Lamont-Doherty Geological Observatory, Palisades, N. Y.**

Intermediate-wavelength magnetic anomaly field of the North Pacific and possible source distributions p 17 A85-26414

LNK Corp., Silver Spring, Md. Analysis of subpixel registration p 51 N85-16267

Lockheed Engineering and Management Services Co., Inc., Houston, Tex. Investigation of TM band-to-band registration using the JSC registration processor p 69 N85-21745

Lunar and Planetary Inst., Houston, Tex. Neotectonics of the Caribbean p 27 A85-21145

Lund Technical Univ. (Sweden). Ground truth for SIR-B images obtained by SIR system 8 impulse radar p 10 N85-17251

M**MacQuarie Univ., North Ryde (Australia).**

A review of problems and progress in studies of satellite magnetic anomalies p 17 A85-26409

Viscous remanent magnetization model for the Broken Ridge satellite magnetic anomaly p 22 A85-26423

Manitoba Univ., Winnipeg.

Crustal structure of the Churchill-Superior boundary zone between 80 and 98 deg W longitude from Magsat anomaly maps and stacked passes p 22 A85-26421

Martin Marietta Aerospace, Denver, Colo. Evaluation of an experimental system for spaceborne processing of multispectral image data p 46 A85-23144

Maryland Univ., College Park. Aircraft and satellite measurement of ocean wave directional spectra using scanning-beam microwave radars p 27 A85-20486

A comparison of in situ and airborne radar observations of ocean wave directionality p 27 A85-20487

- Experimental evidence for spring and autumn windows for the detection of geobotanical anomalies through the remote sensing of overlying vegetation p 6 A85-26939
- Evidence accumulation for spatial reasoning p 50 N85-16261
- Analysis of subpixel registration p 51 N85-16267
- North American vegetation patterns observed with the NOAA-7 advanced very high resolution radiometer [E85-10062] p 10 N85-17400
- Analysis of terrestrial conditions and dynamics [E85-10063] p 10 N85-17401
- Shortwave infrared detection of vegetation [E85-10064] p 10 N85-17402
- Massachusetts Inst. of Tech., Cambridge.**
- Delineation of major geologic structures in Turkey using SIR-B data p 25 N85-17249
- Meteorological Research Inst., Tokyo (Japan).**
- On the P1 data from GMS-SEM p 15 N85-21890
- Meteorological Satellite Center, Tokyo (Japan).**
- The development of image processing of NOAA AVHRR data and its application to sea surface temperature p 42 N85-21891
- Miami Univ., Fla.**
- Center of mass estimation in closed vortices - A verification in principle and practice p 26 A85-19417
- Mitre Corp., McLean, Va.**
- SEASAT 3 and 4 [AD-A148343] p 40 N85-17274
- N**
- National Aeronautics and Space Administration, Washington, D. C.**
- Ice sheet margins and ice shelves p 32 A85-24524
- Use of Space Station for Earth and Planetary Exploration p 71 A85-25348
- Thematic mapper data analysis p 23 A85-27946
- Developments with multispectral thermal-IR and active microwave systems - TMS, SIR-A, SIR-B, and radarsat p 62 A85-27947
- Satellite observations of sea ice p 36 A85-28022
- Earth resources research using the Shuttle Imaging Radar system p 67 N85-20779
- Planetary cartography in the next decade (1984 - 1994) p 20 N85-22323
- [NASA-SP-475] p 20 N85-22323
- National Aeronautics and Space Administration, Ames Research Center, Moffett Field, Calif.**
- Thematic mapper data analysis p 23 A85-27946
- The importance of geobotany in geological remote sensing applications p 23 A85-27948
- Impact of LANDSAT MSS sensor differences on change detection analysis p 65 N85-20506
- Assessment of Thematic Mapper band-to-band registration by the block correlation method p 55 N85-21743
- National Aeronautics and Space Administration, Earth Resources Labs., Bay St. Louis, Miss.**
- Relationship between forest clearing and biophysical factors in tropical environments Implications for the design of a forest change monitoring approach [E85-10051] p 8 N85-16247
- The influence of the number of ground control points on the scene-to-map registration accuracy p 51 N85-16264
- Analysis of data acquired by synthetic aperture radar and LANDSAT Multispectral Scanner over Kershaw County, South Carolina, during the summer season [E85-10071] p 11 N85-19485
- LANDSAT scene-to-scene registration accuracy assessment p 65 N85-20502
- National Aeronautics and Space Administration, Goddard Space Flight Center, Greenbelt, Md.**
- Aircraft and satellite measurement of ocean wave directional spectra using scanning-beam microwave radars p 27 A85-20486
- A comparison of in situ and airborne radar observations of ocean wave directionality p 27 A85-20487
- Satellite magnetic anomalies over subduction zones - The Aleutian Arc anomaly p 16 A85-21107
- African land-cover classification using satellite data p 1 A85-21174
- The Harp probe - An in situ Bragg scattering sensor p 28 A85-22171
- Effect of heliotropism on the bidirectional reflectance of irrigated cotton p 1 A85-22420
- Regional analysis from data from heterogeneous pixels - Remote sensing of total dry matter production in the Senegalese Sahel p 47 A85-23783
- Spectral signatures of soil, snow and sea ice as observed by passive microwave and thermal infrared techniques p 58 A85-23784

- The diurnal variation of Atlantic Ocean tropical cyclone cloud distribution inferred from geostationary satellite infrared measurements p 33 A85-24739
- Performance of an airborne imaging 92/183 GHz radiometer during the Bering Sea Marginal Ice Zone Experiment (MIZEX-WEST) p 33 A85-24945
- Comments on 'Inference of cloud temperature and thickness by microwave radiometry from space' p 59 A85-25182
- Landsat-4 thematic mapper (TM) for cold environments p 60 A85-25349
- Observations of the earth using nighttime visible imagery p 48 A85-25350
- Introduction to the special issue - A perspective on Magsat results p 16 A85-26401
- The near-earth magnetic field at 1980 determined from Magsat data p 16 A85-26408
- A review of problems and progress in studies of satellite magnetic anomalies p 17 A85-26409
- Comparison between the recent U.S. composite magnetic anomaly map and Magsat anomaly data p 17 A85-26413
- An estimation of continental crust magnetization and susceptibility from Magsat data for the continuous United States p 22 A85-26420
- Magsat and POGO magnetic anomalies over the Lord Howe Rise Evidence against a simple continental crustal structure p 18 A85-26422
- Viscous remanent magnetization model for the Broken Ridge satellite magnetic anomaly p 22 A85-26423
- Comparison of level I land cover classification accuracy for MSS and AVHRR data p 61 A85-26929
- The potential of satellite remote sensing of ecological conditions for survey and forecasting desert-locust activity p 5 A85-26934
- Experimental evidence for spring and autumn windows for the detection of geobotanical anomalies through the remote sensing of overlying vegetation p 6 A85-26939
- The importance of geobotany in geological remote sensing applications p 23 A85-27948
- United States crustal thickness p 18 A85-28011
- Estimation of lower crust magnetization from satellite derived anomaly field p 18 A85-28012
- Simultaneous ocean cross-section and rainfall measurements from space with a nadir pointing radar p 36 A85-28788
- Detection of lowland flooding using active microwave systems p 43 A85-29218
- Regional mean sea surfaces based on GEOS-3 and SEASAT altimeter data p 38 A85-29716
- Effect of Landsat Thematic Mapper sensor parameters on land cover classification p 14 A85-30088
- Effect of vegetation on soil moisture sensing observed from orbiting microwave radiometers p 7 A85-30089
- Simultaneous ocean cross-section and rainfall measurements from space with a nadir-pointing radar [NASA-TM-86167] p 44 A85-16273
- The spatial evolution of the directional wave spectrum in the Southern Ocean Its relation to extreme waves in Agulhas Current p 39 N85-17213
- Structural investigation of the Canadian Shield by orbital radar and LANDSAT p 25 N85-17236
- Structural investigation of the Grenville Province by radar and other imaging and nonimaging sensors p 25 N85-17237
- Automatic terrain elevation mapping and registration p 52 N85-17242
- Remote sensing of soil moisture p 10 N85-17252
- North American vegetation patterns observed with the NOAA-7 advanced very high resolution radiometer [E85-10062] p 10 N85-17400
- Altimetry, orbits and tides p 40 N85-17404
- Data report on variations in the composition of sea ice during MIZEX-East'83 with the Nimbus-7 SMMR [NASA-TM-86170] p 40 N85-18443
- LANDSAT-4 Science Characterization Early Results Volume 1 Multispectral Scanner (MSS) [E85-10067] p 65 N85-20496
- Summary of MSS characterization investigations p 53 N85-20497
- Radiometric accuracy assessment of LANDSAT 4 Multispectral Scanner data p 53 N85-20498
- Spectral characterization of the LANDSAT-4 MSS sensors p 65 N85-20499
- Geometric accuracy assessment of LANDSAT-4 Multispectral Scanner (MSS) data p 19 N85-20505
- LANDSAT-4 Science Characterization Early Results Volume 2, part 1 Thematic Mapper (TM) [E85-10068] p 66 N85-20508
- An overview of LANDSAT-4 and the Thematic Mapper p 66 N85-20509
- Radiometric calibration and processing procedure for reflective bands on LANDSAT-4 prototype Thematic Mapper p 66 N85-20510

- TM digital image products for applications p 54 N85-20512
- Spectral characterization of the LANDSAT Thematic Mapper sensors p 66 N85-20514
- Prelaunch absolute radiometric calibration of the reflective bands on the LANDSAT-4 prototype Thematic Mapper p 66 N85-20515
- Characterization of radiometric calibration of LANDSAT-4 reflective bands p 66 N85-20516
- LANDSAT-4 Science Characterization Early Results Volume 3, part 2 Thematic Mapper (TM) [E85-10069] p 67 N85-21724
- Relative radiometric calibration of LANDSAT TM reflective bands p 67 N85-21725
- Thermal band characterization of the LANDSAT-4 Thematic Mapper p 67 N85-21727
- National Aeronautics and Space Administration, Lyndon B. Johnson Space Center, Houston, Tex.**
- Use of satellite data in agricultural surveys p 4 A85-23782
- Comparative study of Suits and SAIL canopy reflectance models p 7 A85-30092
- Application of Thematic Mapper data to corn and soybean development stage estimation p 7 A85-30093
- Estimating location parameters in a mixture p 50 N85-16252
- Calibration or inverse regression Which is appropriate for crop surveys using LANDSAT data? p 9 N85-16260
- Geological, structural, and geomorphological analyses from SIR-B p 24 N85-17226
- National Aeronautics and Space Administration, Langley Research Center, Hampton, Va.**
- An intercalibration of Meteosat-1 and GOES-2 visible and infrared measurements p 26 A85-19420
- Evaluation of an experimental system for spaceborne processing of multispectral image data p 46 A85-23144
- National Aeronautics and Space Administration, Marshall Space Flight Center, Huntsville, Ala.**
- Satellite passive microwave rain rate measurement over croplands during spring, summer and fall p 4 A85-25181
- National Aeronautics and Space Administration, Pasadena Office, Calif.**
- Method of measuring sea surface water temperature with a satellite including wideband passive synthetic-aperture multichannel receiver [NASA-CASE-NPO-15651-1] p 41 N85-21723
- National Aeronautics and Space Administration, Wallops Flight Center, Wallops Island, Va.**
- The use of airborne lasers in terrestrial and water environments p 33 A85-25351
- Electromagnetic bias of 36-GHz radar altimeter measurements of MSL p 37 A85-29712
- The reflection of airborne UV laser pulses from the ocean p 37 A85-29714
- An analysis of a satellite multibeam altimeter p 38 A85-29715
- National Aerospace Lab., Amsterdam (Netherlands).**
- Comparative study of Suits and SAIL canopy reflectance models p 7 A85-30092
- National Commission on Libraries and Information Science, Washington, D. C.**
- Preserve the sense of Earth from space [PB85-124121] p 72 N85-20942
- National Geodetic Survey, Rockville, Md.**
- Regional mean sea surfaces based on GEOS-3 and SEASAT altimeter data p 38 A85-29716
- Hybrid method of mapping and photogeodetic control network densification [PB85-133775] p 20 N85-21766
- Along-track deflection of the vertical from SEASAT GEBCO (General Bathymetric Chart of the Oceans) overlays [PB85-129641] p 42 N85-21767
- National Oceanic and Atmospheric Administration, Columbia, Mo.**
- NOAA-AISC user's guide for implementing CERES maize model for large area yield estimation [E85-10083] p 12 N85-21748
- User's guide to the TAMW wheat model as implemented on the IBM 360/195 computer [E85-10084] p 12 N85-21749
- NOAA-AISC user's guide for implementing CERES wheat model for large area yield estimation [E85-10085] p 12 N85-21750
- Estimating solar radiation for plant simulation models [E85-10089] p 13 N85-21751
- National Oceanic and Atmospheric Administration, Washington, D. C.**
- Earth observations and the polar platform [NOAA-TR-NESDIS-18] p 15 N85-20517
- LANDSAT-4 Thematic Mapper calibration and atmospheric correction p 68 N85-21734

National Science Foundation, Washington, D.C.

A review of problems and progress in studies of satellite magnetic anomalies p 17 A85-26409

Naval Ocean Research and Development Activity, Bay St. Louis, Miss.

A survey of oceanographic satellite altimetric missions p 36 A85-29703

Bio-optical variability in the Alboran Sea as assessed by Nimbus-7 coastal zone color scanner [AD-A147909] p 39 N85-16281

Satellite definition of the bio-optical and thermal variation of coastal eddies associated with the African current [AD-A147910] p 39 N85-16282

The use of principal components analysis techniques Nimbus-7 coastal zone color scanner data to define mesoscale ocean features through a warm humid atmosphere [AD-A148567] p 40 N85-17416

Naval Research Lab., Washington, D. C.

Electromagnetic bias of 36-GHz radar altimeter measurements of MSL p 37 A85-29712

Electromagnetic bias of 10-GHz radar altimeter measurements of MSL p 37 A85-29713

Nevada Univ., Reno.

Analysis of SIR-B radar illumination of geometry for depth of penetration and surface feature and vegetation detection, Nevada and California p 25 N85-17248

New South Wales Univ., Kensington (Australia).

Australian Multispectral Assessment of SIR-B (AMAS) p 52 N85-17243

P**Pacific Northwest Lab., Richland, Wash.**

Analysis of the NASA/MSFC Airborne Doppler Lidar results from San Geronio Pass, California [NASA-CR-171355] p 70 N85-21873

Pennsylvania State Univ., University Park.

The importance of geobotany in geological remote sensing applications p 23 A85-27948

Purdue Univ., Lafayette, Ind.

Light polarization measurements - A method to determine the specular and diffuse light-scattering properties of both leaves and plant canopies p 2 A85-23754

Comparison between the recent US composite magnetic anomaly map and Magsat anomaly data p 17 A85-26413

Variation in spectral response of soybeans with respect to illumination, view, and canopy geometry [E85-10040] p 8 N85-16241

Spectral estimators of absorbed photosynthetically active radiation in corn canopies [E85-10041] p 8 N85-16242

Rectification of single and multiple frames of satellite scanner imagery using points and edges as control p 51 N85-16263

Microwave and optical remote sensing of forest vegetation p 9 N85-17228

Growth and reflectance characteristics of winter wheat canopies [E85-10080] p 11 N85-19494

Techniques for measuring intercepted and absorbed PAR in corn canopies [E85-10081] p 11 N85-19495

Evaluation of the radiometric quality of the TM data using clustering, linear transformations and multispectral distance measures p 54 N85-21731

Spatial resolution estimation of LANDSAT-4 Thematic Mapper data p 69 N85-21741

R**Reading Univ. (England).**

African land-cover classification using satellite data p 1 A85-21174

Research and Data Systems, Inc., Lanham, Md.

An analysis of the high frequency vibrations in early Thematic Mapper scenes p 69 N85-21742

Research Triangle Inst., Research Triangle Park, N.C.

Evaluation of an experimental system for spaceborne processing of multispectral image data p 46 A85-23144

Rice Univ., Houston, Tex.

Nonparametric analysis of Minnesota spruce and aspen tree data and LANDSAT data p 8 N85-16253

Rochester Inst. of Tech., N. Y.

Comparison of modelled and empirical atmospheric propagation data p 46 A85-22678

Evaluation of the radiometric integrity of LANDSAT 4 Thematic Mapper band 6 data p 54 N85-21726

LANDSAT 4 band 6 data evaluation [E85-10093] p 55 N85-21755

Royal Aircraft Establishment, Farnborough (England).

The investigation of selected oceanographic applications of spaceborne synthetic-aperture radar p 39 N85-17233

Royal Inst. of Tech., Stockholm (Sweden)

Papers of the 15th International Society for Photogrammetry and Remote Sensing (ISPRS) Congress [TRITA-FMI-9] p 63 N85-17406

Mathematical aspects of digital terrain information, Report from International Society for Photogrammetry and Remote Sensing (ISPRS) working group 3.3, 1980 - 1984 p 19 N85-17407

A comparative test of photogrammetrically sampled digital elevation models p 52 N85-17408

Multimodels increase accuracy Summary of an experiment p 63 N85-17409

S**Sandia Labs., Albuquerque, N. Mex.**

Test plan for the forest-echo experiment [DE84-017175] p 10 N85-18447

Santa Barbara Research Center, Calif.

Thematic Mapper Volume 1 Calibration report flight model, LANDSAT 5 [E85-10059] p 63 N85-16270

Thematic Mapper Volume 2 Flight model preshipment review [E85-10060] p 63 N85-16271

Santa Barbara Research Center, Goleta, Calif.

Thematic Mapper Design through flight evaluation [E85-10078] p 64 N85-19492

SAR, Inc., Riverdale, Md.

Characterizing the scientific potential of satellite sensors [E85-10044] p 62 N85-16244

Characterizing the scientific potential of satellite sensors [E85-10053] p 62 N85-16249

Science Systems and Applications, Inc., Seabrook, Md.

A comparison of in situ and airborne radar observations of ocean wave directionality p 27 A85-20487

Scripps Institution of Oceanography, La Jolla, Calif.

Lagrangian observations of surface circulation at the Emperor Seamount chain p 35 A85-27710

Estimating ocean primary production from satellite chlorophyll - Introduction to regional differences and statistics for the Southern California Bight p 35 A85-28005

Determination of monthly mean humidity in the atmospheric surface layer over oceans from satellite data p 35 A85-28007

South Dakota School of Mines and Technology, Rapid City.

Rain volume estimation over areas using satellite and radar data [NASA-CR-174434] p 44 N85-19568

Southern Methodist Univ., Dallas, Tex.

Exploring the use of structural models to improve remote sensing agricultural estimates p 9 N85-16259

SRI International Corp., Menlo Park, Calif.

Image-to-image correspondence Linear structure matching p 51 N85-16266

Stanford Univ., Calif.

The importance of geobotany in geological remote sensing applications p 23 A85-27948

State Univ. of New York, Binghamton.

Estimation of agronomic variables using spectral signatures p 2 A85-23753

Systems and Applied Sciences Corp., Hyattsville, Md.

Experimental evidence for spring and autumn windows for the detection of geobotanical anomalies through the remote sensing of overlying vegetation p 6 A85-26939

The use of linear feature detection to investigate Thematic Mapper data performance and processing p 69 N85-21740

T**Technical Univ. of Denmark, Lyngby.**

Spaceborne microwave radiometers Background and technology requirements p 63 N85-17350

Texas A&M Univ., College Station.

Lagrangian observations of surface circulation at the Emperor Seamount chain p 35 A85-27710

Detection of lowland flooding using active microwave systems p 43 A85-29218

Proceedings of the Second Annual Symposium on Mathematical Pattern Recognition and Image Analysis Program [E85-10056] p 50 N85-16251

Multivariate spline methods in surface fitting p 50 N85-16257

Autoregressive spectral estimation for two dimensional time series p 50 N85-16258

Texas Univ., Austin.

Neotectonics of the Caribbean p 27 A85-21145

A survey of oceanographic satellite altimetric missions p 36 A85-29703

Spatial estimation from remotely sensed data via empirical Bayes models p 8 N85-16256

Using the global positioning system (GPS) phase observable for relative geodesy Modeling, processing, and results p 19 N85-18437

Texas Univ., Dallas.

SIR-A imagery in geologic studies of the Sierra Madre Oriental, northeastern Mexico Part 1 (Regional stratigraphy) The use of morphostratigraphic units in remote sensing mapping [NASA-CR-175457] p 25 N85-19497

Post-carboniferous tectonics in the Anadarko Basin, Oklahoma Evidence from side-looking radar imagery [NASA-CR-175458] p 26 N85-19498

Titan Systems, Inc., Vienna, Va.

Nautical charting with remotely sensed imagery, volume 1 [AD-A149361] p 41 N85-19503

Nautical charting with remotely sensed imagery Volume 2 Case studies [AD-A149362] p 41 N85-19504

U**Uppsala Univ. (Sweden).**

Estimating ocean primary production from satellite chlorophyll - Introduction to regional differences and statistics for the Southern California Bight p 35 A85-28005

Utah Univ., Salt Lake City.

Detecting agricultural to urban land use change from multi-temporal MSS digital data [E85-10049] p 15 N85-16245

An integrated remote sensing approach for identifying ecological range sites [E85-10050] p 8 N85-16246

Assessment of LANDSAT for rangeland mapping, Rush Valley, Utah [E85-10072] p 15 N85-19486

An integrated GIS/remote sensing data base in North Cache soil conservation district, Utah A pilot project for the Utah Department of Agriculture's RIMS (Resource Inventory and Monitoring System) [E85-10073] p 11 N85-19487

Building a functional, integrated GIS/remote sensing resource analysis and planning system [E85-10092] p 15 N85-21754

W**Washington Univ., Seattle.**

Passive microwave remote sensing for sea ice research [NASA-CR-175570] p 42 N85-21758

Wisconsin Univ., Madison.

Satellite passive microwave rain rate measurement over croplands during spring, summer and fall p 4 A85-25181

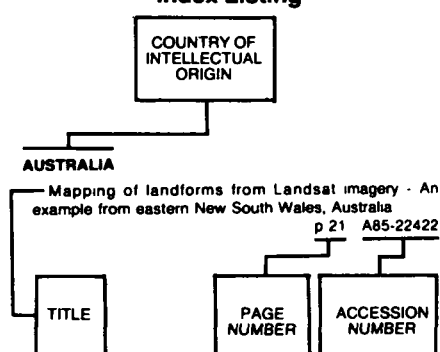
Resolution enhancement of multichannel microwave imagery from the Nimbus-7 SMMR for maritime rainfall analysis [NASA-CR-174367] p 44 N85-19221

An airborne infrared thermal scanning system for easy use on Navy P-3 aircraft [AD-A149690] p 42 N85-22143

Woodard-Clyde Consultants, San Francisco, Calif.

Thematic mapper data analysis p 23 A85-27946

Typical Foreign Technology Index Listing



Listings in this index are arranged alphabetically by country of intellectual origin. The title of the document is used to provide a brief description of the subject matter. The page number and the accession number are included in each entry to assist the user in locating the citation in the abstract section.

A

AUSTRALIA

- Mapping of landforms from Landsat imagery - An example from eastern New South Wales, Australia p 21 A85-22422
- An examination of some problems and solutions in monitoring urban areas from satellite platforms p 14 A85-26935
- Computing the foliage angle distribution from contact frequency data p 6 A85-29969
- Evaluation of SIR-B imagery for geologic and geomorphic mapping, hydrology, and oceanography in Australia p 51 N85-17229
- Australian Multiexperimental Assessment of SIR-B (AMAS) p 52 N85-17243

AUSTRIA

- The analysis of backscattering properties from SAR data of mountain regions p 59 A85-24081

B

BRAZIL

- Integrated analysis of remote sensing products from basic geological surveys [E85-10052] p 24 N85-16248
- The management of atmospheric resources in food production p 9 N85-16362
- Brazilian Remote Sensing Shuttle Experiment (BRESEX) Characteristics and future utilization on satellites [INPE-3313-PRE/620] p 64 N85-19385
- Brazilian remote sensing receiving, recording and processing ground systems in the 1980's [E85-10079] p 52 N85-19493
- Remote sensing activities in Latin America [INPE-3297-PRE/612] p 64 N85-19501

The sharing of remote sensing techniques in Brazilian geographic research [INPE-3307-PRE/617] p 15 N85-19502

C

CANADA

- On the separability of various classes from the GOES visible and infrared data p 45 A85-21138
- The Canadian SAR experience p 46 A85-23689
- The measurement of bidirectional reflectances by analysis of Landsat images p 2 A85-23756
- Classification of vegetation types by analysis of X-band and C-band radar images p 4 A85-23775
- Spectral response of different agricultural and penurban land-use units in the spectral windows at 1.55-1.75 and 2.08-2.35 microns p 4 A85-23787
- Classification of the geological environments of Anticosti Island - An approach using a Landsat-4 spectral simulation p 21 A85-23790
- The secular period behavior of 38 RR Lyrae stars in the LMC globular cluster NGC 2257 p 14 A85-25070
- Magsat scalar magnetic anomalies at northern high latitudes p 18 A85-26416
- Magsat vertical field anomalies above 40 deg N from spherical cap harmonic analysis p 18 A85-26417
- Scalar magnetic anomalies of Canada and northern United States derived from Magsat data p 18 A85-26418
- Crustal structure of the Churchill-Superior boundary zone between 80 and 98 deg W longitude from Magsat anomaly maps and stacked passes p 22 A85-26421
- Automated measurements of terrain reflection and height variations using an airborne infrared laser system p 5 A85-26933
- Structure and seasonal characteristics of the Gaspé current p 35 A85-27705
- Integration of the SPOT panchromatic channel into its multispectral mode for image sharpness enhancement p 49 A85-29217
- Radiometric calibration and geocoded precision processing of LANDSAT-4 Multispectral Scanner products by the Canada Centre for Remote Sensing p 53 N85-20501
- A preliminary assessment of LANDSAT-4 Thematic Mapper data p 54 A85-21728
- Preliminary evaluation of the radiometric calibration of LANDSAT-4 Thematic Mapper data by the Canada Centre for Remote Sensing p 67 N85-21729

CHINA, PEOPLE'S REPUBLIC OF

- Methodological study of spectral band selection for multispectral remote sensing p 55 A85-19363
- Remote sensing development in the People's Republic of China p 56 A85-20643
- Study on a regional geographical information system and application model p 13 A85-20644
- Remote sensing technology now playing practical roles p 64 N85-20190
- Airborne remote sensing CCD imaging system p 65 N85-20220

COLOMBIA

- Needs and accessibility of developing countries for/to remote sensing information systems p 13 A85-20647

CZECHOSLOVAKIA

- Determination of water surfaces in northwest Bohemia on the basis of satellite data p 44 A85-29906

D

DENMARK

- Microwave signatures of the sea ice in the East Greenland Current p 31 A85-24079
- Spaceborne microwave radiometers Background and technology requirements [LD-R-267] p 63 N85-17350

F

FINLAND

- Retrieval of snow water equivalent from Nimbus-7 SMMR data Effect of land-cover categories and weather conditions p 43 A85-24082

FRANCE

- Status and plans for the SPOT program and the launch of SPOT 1 - Its on-ground processing and data dissemination to users p 56 A85-20568
- Commercialization of remote sensing data - Its impact on the continuity and accessibility of remote sensing data, including response to standing orders as well as on the standardization of products p 71 A85-20642
- The use of SEASAT-SAR data in oceanography at the IFF p 29 A85-23690
- Swell propagation in the North Atlantic ocean using SEASAT altimeter p 30 A85-23702
- Spectral signatures of objects in remote sensing, International Conference, 2nd, Bordeaux, France, September 12-16, 1983, Reports p 57 A85-23751
- Angular and spatial variability of visible and NIR spectral data p 2 A85-23752
- Comparative seasonal evolution of the spectral signatures of broad-leaved and coniferous trees from Landsat data Comparison with other perennial surfaces p 2 A85-23757
- Development of a SPOT-simulation radiometer p 57 A85-23759
- Comparison of SPOT HRV and Landsat-4 TM for crop inventories p 3 A85-23762
- Estimation of wheat production on the basis of Landsat channel 5 and 7 radiometric measurements p 3 A85-23763
- Estimation of evapotranspiration on the basis of thermal IR p 3 A85-23765
- Effects of the experimental errors and conditions on the estimation of thermal inertia and evapotranspiration from METEOSAT data p 3 A85-23767
- Study of the correlation between the IRT band of the NOAA AVHRR and the factors conditioning the thermal behavior of bioclimatic areas on a regional scale p 58 A85-23768
- Inventory of geographically homogeneous zones by spectral modeling of diachronic Meteosat albedo or combined albedo/thermal-channel data - Applications to the Maghreb and to Sahelian Africa p 46 A85-23769
- Use of HCMM thermal images in the study of microclimates in a mountainous region p 3 A85-23771
- Relations between the radar backscatter coefficient and the characteristics of a vegetation canopy - Analysis of the effect of structure p 4 A85-23774
- Demonstration, analysis, and correction of atmospheric effects on Landsat or SPOT multispectral data p 58 A85-23781
- Geomorphology and remote sensing Numerical inventory of objects in Landsat, SPOT simulation, and SIR-A data Applications to the Mopti-Bandiagara (Mali) region p 21 A85-23785
- Influence of spatial variability of soil hydraulic characteristics on surface parameters obtained from remote-sensing data in thermal infrared and microwaves p 43 A85-23786
- Independent variables in remote sensing as a function of landcover type p 47 A85-23788
- Generation of a Landsat-HCMM combined image and its application to geological cartography p 21 A85-23792
- Thematic evaluation of SPOT spectral bands p 58 A85-23794
- Eddy kinetic energy distribution in the southern ocean from Seasat altimeter and FGGE drifting buoys p 32 A85-24554
- Spectral characterization of vegetation canopies in the visible and NIR - Application to remote sensing p 5 A85-25670
- Digital correlation of images along quasi-epipolar lines by successive approximations p 48 A85-25671
- World ocean mean monthly waves, swell, and surface winds for July through October 1978 from SEASAT radar altimeter data p 37 A85-29707

- Swell in the Pacific Ocean observed by SEASAT radar altimeter p 37 A85-29708
Thermal structure of an agricultural region as seen by NOAA-7 AVHRR p 7 A85-30090
CNES, INRA do joint remote-sensing research p 11 N85-19321
The spot operational remote sensing satellite system Current status and perspectives p 67 N85-20776

G

GERMANY, FEDERAL REPUBLIC OF

- Imaging ocean surface waves by synthetic aperture radar - A review p 29 A85-23682
The altimetric geoid in the North Sea p 16 A85-23700
Lidar applications in remote sensing of ocean properties p 31 A85-23755
Determination of reflectances of tropical vegetation by combined methods of radiometry and photometry p 2 A85-23760
Realtime processor of SAR systems p 60 A85-25855
Investigations of the accuracy of the digital photogrammetry system DPS, a rigorous three dimensional compilation process for push broom imagery [MBB-UA-753/83-OE] p 60 A85-26393
On the identification of Magsat anomaly charts as crustal part of the internal field p 17 A85-26412
SPAS-01 - Space flight technology for the general user p 61 A85-27057
Modular Optoelectronic Multispectral Scanner (MOMS) Technological aspects p 61 A85-27059
MOMS 1 and its results p 61 A85-27061
Enhancement of multispectral scanner images by digital filtering [ESA-TT-624] p 63 N85-16284
Activities report of the Department of Applied Research 78 for satellite geodesy of the Technical University, Munich p 19 N85-18440
[ASTRON-GEODAET-ARB-45] p 19 N85-18440
GERMANY, PEOPLES DEMOCRATIC REPUBLIC OF
Cosmic interpolation of terrestrial potential values p 18 A85-26476

I

INDIA

- Advances in microwave remote sensing of the ocean and atmosphere p 28 A85-21960
The utility of data from various airborne sensors for soil mapping p 5 A85-26932

INTERNATIONAL ORGANIZATION

- Perspectives of remote sensing in Europe at the end of the decade p 70 A85-20565
International cooperation in remote sensing applications p 70 A85-20566
Status of remote sensing information systems with special emphasis on their specializations, capabilities, accessibilities and future directions p 71 A85-20646
SEASAT - A key element of the EARTHNET programme p 46 A85-23679
Status and future plans for ERS-1 p 31 A85-23707
Analysis of ground radiometric measurements in the rice-growing site at Tamani (Republic of Mali) - Effect of certain yield parameters on the spectral signature p 2 A85-23758
The potential of solar power satellites for developing countries p 59 A85-24654

ITALY

- A comparative analysis of some prediction methods for rain attenuation statistics in earth-to-space links p 42 A85-21130
A comparison between GEOS 1 magnetic-field measurements and some models of the geomagnetic field p 18 A85-27386
A preliminary analysis of LANDSAT-4 Thematic Mapper radiometric performance p 68 N85-21730
TM geometric performance Line to Line Displacement Analysis (LLDA) p 68 N85-21732

J

JAPAN

- Mean ionospheric field correction for Magsat data p 17 A85-26411
Extraction of magnetic anomalies of crustal origin from Magsat data over the area of the Japanese Islands p 21 A85-26419
Asian Conference on Remote Sensing, 4th, Colombo, Sri Lanka, November 10-15, 1983, Proceedings p 71 A85-27519
On the determination of the deflection of the vertical by satellite altimetry p 37 A85-29706

D-2

- Image-scale and look-direction effects on the detectability of lineaments in radar images p 24 A85-30087
On the P1 data from GMS-SEM p 15 N85-21890
The development of image processing of NOAA AVHRR data and its application to sea surface temperature p 42 N85-21891

N

NETHERLANDS

- The participation of the Netherlands in the NASA Crustal Dynamics Project p 15 A85-20035
Education and training in satellite remote sensing applications - Guide to education and training opportunities p 71 A85-20640
MASMAP, design for a project-oriented geo-information program package for urban upgrading schemes p 13 A85-20747
Method for sequential analysis of spatial development in a rural-urban fringe zone p 13 A85-20748
Population estimation from aerial photos for non-homogeneous urban residential areas p 14 A85-20749
Automatic production of DTM data using digital off-line technique p 45 A85-20750
Visual interpretation of SAR images of two areas in the Netherlands p 1 A85-23694
Gravity field investigation in the North Sea p 30 A85-23699
Large-scale oceanographic experiments and satellites, Proceedings of the Advanced Research Workshop, Porto Vecchio, Corse, France, October 3-7, 1983 p 32 A85-24551
Mathematical modelling of the geomagnetic field and secular variation, and its applications, Proceedings of the Symposium, Hamburg, West Germany, August 15-27, 1983 p 16 A85-25689
Soil slaking and the possibilities to record with infrared line scanning p 5 A85-26936
Earth observation modeling based on layer scattering matrices p 7 A85-30091

P

POLAND

- Methods of space geodesy and its role in earth studies p 19 A85-30013

R

ROMANIA (RUMANIA)

- Experiments concerning radiometric measurements and natural-object indicators in order to apply corrections to recordings of satellite remote sensing p 58 A85-23789

S

SAUDI ARABIA

- Remote sensing techniques for monitoring of pollution in coastal waters - Potential application to Saudi Arabia p 34 A85-27441

SWEDEN

- Ground truth for SIR-B images obtained by SIR system 8 impulse radar p 10 N85-17251
Papers of the 15th International Society for Photogrammetry and Remote Sensing (ISPRS) Congress [TRITA-FMI-9] p 63 N85-17406
Mathematical aspects of digital terrain information, Report from International Society for Photogrammetry and Remote Sensing (ISPRS) working group 3.3, 1980 - 1984 p 19 N85-17407
A comparative test of photogrammetrically sampled digital elevation models p 52 N85-17408
Multimodels increase accuracy Summary of an experiment p 63 N85-17409

SWITZERLAND

- Polarization effects in sea-ice signatures p 31 A85-24078

U

U.S.S.R.

- Determination of the external-orientation elements of aerial and space photographs in the remote sensing of dynamic processes and phenomena p 56 A85-19998
Complex studies of the environment by optical and radar methods p 56 A85-20081
Ring structures observed on space radar images of the earth p 45 A85-20084

- Space radar observations of small-scale formations on the ocean surface p 27 A85-20086
Investigation of Krasnovodsk bay on the basis of space photographs p 28 A85-21669
Evaluation of the ocean/atmosphere thermal interaction in the Atlantic FGGE area p 28 A85-22175
Simultaneous radiometric and radar altimetric measurements of sea microwave signatures p 31 A85-24076
Radiophysical techniques employed for sea ice investigations p 31 A85-24077
Interpretation of aircraft sea ice microwave data p 32 A85-24080
Ultrashort-wave radar subsurface sounding of sea ice and earth covers p 34 A85-25594
Features characterizing the development of mushroom-shaped currents in the ocean, revealed by an analysis of satellite imagery p 34 A85-25651
Effect of meteorological conditions on the characteristics of space radar images of the earth surface p 48 A85-25653
Interpretation of space images of the sea surface using the SVIT digital-processing complex p 34 A85-25654
Analysis of mesofractures according to space images - Currents trends in the exploration for oil and gas deposits p 21 A85-25655
Identification of the structure of soil-vegetation cover using aerial and space images p 5 A85-25656
Double-angle method for measuring ocean surface temperature in the infrared p 34 A85-25658
Correlation of spectral brightnesses measured using multispectral space images p 60 A85-25659
Features of the digital processing of radar images obtained with the sidelooking radar of the Cosmos-1500 satellite p 48 A85-25660
Transformation of sea-wave spectrum into a synthetic-aperture-radar image spectrum p 34 A85-25661
Minimization of the effect of the earth's curvature in the projective transformation of space images into photoplans and photomaps p 16 A85-25662
The influence of a scattering medium on the quality of an optical image p 48 A85-26294
Soil moisture content estimation by radar survey data during the sowing campaign p 6 A85-26947
Improvement of the accuracy of radar measurements of sea-ice thickness by cepstral processing of reflected signals p 35 A85-27736
Space remote-sensing data in geology p 23 A85-28400
Investigation of the properties of natural objects by the canonical-correlation method p 49 A85-28973
The use of Salyut-5 photographs for regional geomorphological mapping p 23 A85-28999
Determination of the heights of points of a place on the basis of radar-survey data p 19 A85-29000
Determination of the physical parameters of sea ice on the basis of remote microwave measurements in the 0.3-18 cm range p 38 A85-29903
Methods for the study of recent tectonics on the basis of remote sensing and ground data p 23 A85-29904
Possibilities of using remote-sensing methods to improve the efficiency of oil and gas exploration p 24 A85-29905
Comprehensive desertification maps and methods for making such maps on the basis of space photographs p 14 A85-29907
Investigation of salty soils and salines on the basis of space remote-sensing methods p 6 A85-29908
Conical multispectral scanner for the study of earth resources p 62 A85-29909
Determination of soil moisture content by microwave radiometry with the use of a priori information p 6 A85-29910
Radar mapping of the moisture of open soils p 6 A85-29911
Identification of homogeneous regions with incomplete boundaries on an image p 24 A85-29912
Segmentation of half-tone remote-sensing images by the level lines method p 49 A85-29913
The use of a priori estimation of the conditions of the observation of the earth surface from space for a rational selection of the time at which the survey is conducted p 50 A85-29914
Remote-sensing observations of advective eddies in the central part of the Baltic Sea p 38 A85-29915
Satellite photographs suggest arctic volcano p 38 N85-16239
UNITED KINGDOM
On the application of meteorological satellite imagery for monitoring the environment p 13 A85-20570
Microcomputer systems for satellite image processing p 56 A85-20571
The integrated use of digital cartographic data and remotely sensed imagery p 45 A85-20572

An example of Landsat cost effectiveness in mapping land-cover p 1 A85-20573

The educational role of satellites p 70 A85-20574

Satellite microwave remote sensing p 28 A85-23676

A review of SEASAT p 28 A85-23677

SEASAT-data acquisition and processing by the Royal Aircraft Establishment p 57 A85-23678

Validation and applications of SASS over JASIN p 29 A85-23681

Can optical measurements help in the interpretation of radar backscatter? p 29 A85-23683

Some properties of SAR speckle p 46 A85-23684

The effect of a moving sea surface on SAR imagery p 29 A85-23685

Theory of SAR ocean wave imaging p 29 A85-23686

Effect of defocusing on the images of ocean waves p 29 A85-23688

Expressions of bathymetry on Seasat synthetic radar images p 29 A85-23691

Tidal current bedforms investigated by Seasat p 30 A85-23692

Seasat over land p 57 A85-23693

Altimeter measurements of ocean topography p 30 A85-23695

Wave measurements with the Seasat radar altimeter - A Review p 30 A85-23701

Use of ocean skewness measurements in calculating the accuracy of altimeter height measurements p 30 A85-23703

Spatial variation of significant wave-height p 30 A85-23704

The scanning multichannel microwave radiometer - An assessment p 57 A85-23705

The evaluation of SMMR retrieval algorithms p 31 A85-23706

Satellite measurements of sea-surface temperature for climate research p 32 A85-24555

The influence of satellite spectral sensor response on the analysis of satellite imagery at high latitudes p 60 A85-26927

The current use of TIROS-N series of meteorological satellites for land-cover studies p 60 A85-26928

International Symposium on Microwave Signatures in Remote Sensing, 3rd, Toulouse, France, January 16-20, 1984, Proceedings p 6 A85-26942

A computationally-efficient maximum-likelihood classifier employing prior probabilities for remotely-sensed data p 49 A85-26948

An automatic high-resolution picture transmission receiving station p 61 A85-27698

The interpretation of SIR-B imagery of surface waves and other oceanographic features using in-situ, meteorological satellite, and infrared satellite data p 39 N85-17212

The investigation of selected oceanographic applications of spaceborne synthetic-aperture radar p 39 N85-17233

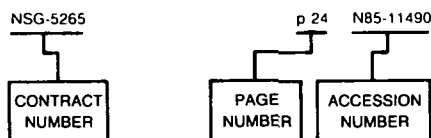
The imaging of internal waves by the SEASAT-A synthetic aperture radar [AD-A149808] p 20 N85-21761

CONTRACT NUMBER INDEX

EARTH RESOURCES / A Continuing Bibliography (Issue 46)

JULY 1985

Typical Contract Number Index Listing



Listings in this index are arranged alphanumerically by contract number. Under each contract number, the accession numbers denoting documents that have been produced as a result of research done under that contract are arranged in ascending order with the AIAA accession numbers appearing first. The accession number denotes the number by which the citation is identified in the abstract section. Preceding the accession number is the page number on which the citation may be found.

AF-AFOSR-81-0170 p 47 A85-24277
 AIR TASK A370370G/058C/2 p 37 A85-29713
 DAAG29-80-K-0018 p 58 A85-23780
 DAAK70-79-C-0153 p 52 N85-17417
 DE-AC02-83ER-60106 p 45 N85-20606
 DE-AC04-76DP-00789 p 10 N85-18447
 DE-AT03-82ER-60031 p 35 A85-28005
 DMA800-83-C-0056 p 41 N85-19503
 DOT-FH-7565 p 41 N85-19504
 ESTEC-4964/81/NL-MS(SC) p 60 A85-26642
 F04701-83-C-0084 p 63 N85-17350
 F19628-84-C-0001 p 64 N85-17469
 F59-553 p 40 N85-17274
 JPL-956430 p 39 N85-16281
 JPL-956432 p 26 N85-19498
 JPL-956435 p 25 N85-19497
 JPL-956582 p 12 N85-19496
 MDA903-83-C-0027 p 51 N85-16266
 NAGW-266 p 41 N85-21753
 NAGW-273 p 26 A85-19417
 NAGW-380 p 44 N85-19221
 NAGW-381 p 52 N85-17256
 NAGW-458 p 35 A85-28005
 NAGW-95 p 15 N85-16245
 p 8 N85-16246
 p 15 N85-19486
 p 11 N85-19487
 NAG5-155 p 27 A85-21145
 NAG5-196 p 56 A85-22424
 NAG5-268 p 58 A85-23780
 NAG5-269 p 2 A85-23754
 NAG5-386 p 44 N85-19568
 NASA ORDER S-10757-C p 52 N85-19490
 p 26 N85-21757
 NASW-3389 p 27 A85-21145
 NAS5-16538 p 12 N85-21736
 NAS5-24200 p 63 N85-16270
 p 63 N85-16271
 p 64 N85-19492
 NAS5-25300 p 53 N85-20511
 NAS5-25891 p 17 A85-26414
 NAS5-26074 p 17 A85-26409
 NAS5-26328 p 17 A85-26409
 NAS5-26616 p 17 A85-26409
 NAS5-27323 p 46 A85-22678
 NAS5-27346 p 55 N85-21755
 p 62 N85-16268
 NAS5-27371 p 64 N85-19489
 NAS5-27377 p 69 N85-21742
 NAS5-27382 p 11 N85-19488
 p 64 N85-19491

NAS5-27383
 NAS5-27385
 NAS5-28200
 NAS5-83
 NAS7-918
 NAS8-34733
 NAS9-14970
 NAS9-15800
 NAS9-16528

NAS9-16538
 NAS9-16664

NAVY PROJECT RR1452-SB-000
 NCC2-205
 NCC2-234
 NCC5-26

NOAA-NA-80SAC00742
 NOAA-04-7-158-44128
 NSERC-7526
 NSF AST-83-14961
 NSF ATM-80-18898
 NSF ATM-83-05502
 NSF OCE-78-20766
 NSF OCE-80-16991
 NSF OCE-80-18736
 NSF OCE-83-17174
 N00014-75-C-0300
 N00014-75-C-0537
 N00014-76-C-1105
 N00014-79-C-0066
 N00014-80-C-0042
 N00014-80-C-0098
 N00014-80-C-0768
 N00014-82-0404
 N00024-83-C-5301
 PROJ AGRISTARS

p 68 N85-21733
 p 70 N85-21756
 p 53 N85-20503
 p 33 A85-24945
 p 62 N85-16244
 p 9 N85-16269
 p 63 N85-17208
 p 70 N85-21873
 p 2 A85-23754
 p 9 N85-16260
 p 8 N85-16241
 p 8 N85-16242
 p 11 N85-19494
 p 11 N85-19495
 p 12 N85-21747
 p 50 N85-16251
 p 50 N85-16262
 p 51 N85-16263
 p 51 N85-16266
 p 37 A85-29713
 p 13 N85-21752
 p 62 N85-16250
 p 10 N85-17400
 p 10 N85-17401
 p 4 A85-25181
 p 49 A85-26641
 p 21 A85-23790
 p 14 A85-25070
 p 60 A85-26927
 p 48 A85-24740
 p 35 A85-28007
 p 26 A85-19417
 p 26 A85-19417
 p 17 A85-26414
 p 17 A85-26415
 p 28 A85-22423
 p 35 A85-27710
 p 38 N85-15960
 p 42 N85-22143
 p 26 A85-19417
 p 37 A85-29706
 p 42 N85-21920
 p 34 A85-27701
 p 37 A85-29712
 p 11 N85-19485
 p 12 N85-21748
 p 12 N85-21749
 p 12 N85-21750
 p 13 N85-21751

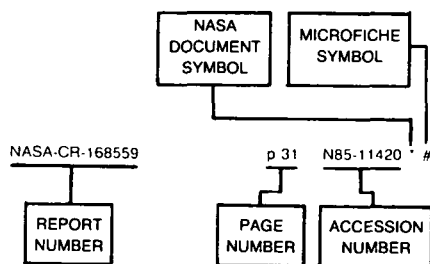
CONTRACT

REPORT/ACCESSION NUMBER INDEX

EARTH RESOURCES / A Continuing Bibliography (Issue 46)

JULY 1985

Typical Report/Accession Number Index Listing



Listings in this index are arranged alphabetically by report number. The page number indicates the page on which the citation is located. The accession number denotes the number by which the citation is identified. An asterisk (*) indicates that the item is a NASA report. A pound sign (#) indicates that the item is available on microfiche.

AD-A147212 p 38 N85-15960 #
 AD-A147756 p 64 N85-17469 #
 AD-A147909 p 39 N85-16281 #
 AD-A147910 p 39 N85-16282 #
 AD-A148343 p 40 N85-17274 #
 AD-A148567 p 40 N85-17416 #
 AD-A148580 p 52 N85-17417 #
 AD-A148986 p 41 N85-19594 #
 AD-A149361 p 41 N85-19503 #
 AD-A149362 p 41 N85-19504 #
 AD-A149545 p 41 N85-20619 #
 AD-A149690 p 42 N85-22143 #
 AD-A149808 p 20 N85-21761 #
 AD-A149831 p 42 N85-21920 #
 AD-D011412 p 40 N85-17506 #
 AD-E301513 p 41 N85-19594 #
 AD-F300533 p 41 N85-19503 #
 AD-F300533 p 41 N85-19504 #
 AIAA PAPER 85-0195 p 70 A85-19580 #
 AIAA PAPER 85-0238 p 55 A85-19608 #
 ARE/TN-720/84 p 20 N85-21761 #
 ASTRON-GEODAET-ARB-45 p 19 N85-18440 #
 CGR/DC-17/84 p 41 N85-20619 #
 CRREL-SR-84-29 p 41 N85-19594 #
 CRSC-84-8 p 11 N85-19487 * #
 CRSC-84-9 p 15 N85-19486 * #
 DC-Y2-04374 p 11 N85-19485 * #
 DE84-017175 p 10 N85-18447 #
 DE84-017419 p 71 N85-20941 #
 DE85-002951 p 45 N85-20606 #
 DFVLR-FB-79-11 p 63 N85-16284 #
 DOE/ER-60106/1 p 45 N85-20606 #
 DOE/PE-T1 p 71 N85-20941 #
 DRIC-BR-93397 p 20 N85-21761 #
 ERIM-160300-101-F p 12 N85-21747 * #
 ERIM-164000-13-P p 62 N85-16268 * #
 ERIM-164000-14-P p 64 N85-19489 * #
 ERIM-166500-4-F p 9 N85-16269 * #

ESA-CR(P)-1928

ESA-TT-624

ETL-0374

E85-10040
 E85-10041
 E85-10044
 E85-10049
 E85-10050
 E85-10051
 E85-10052
 E85-10053
 E85-10055
 E85-10056
 E85-10057
 E85-10058
 E85-10059
 E85-10060
 E85-10062
 E85-10063
 E85-10064
 E85-10066
 E85-10067
 E85-10068
 E85-10069
 E85-10071
 E85-10072
 E85-10073
 E85-10074
 E85-10075
 E85-10076
 E85-10077
 E85-10078
 E85-10079
 E85-10080
 E85-10081
 E85-10082
 E85-10083
 E85-10084
 E85-10085
 E85-10089
 E85-10090
 E85-10091
 E85-10092
 E85-10093
 E85-10094
 E85-10095

FSRP/SO-211

FTR-596-5

HS236-9060-VOL-1

INPE-3243-PRE/589
 INPE-3297-PRE/612
 INPE-3307-PRE/617
 INPE-3312-PRE/619
 INPE-3313-PRE/620

ISBN-3-7696-9788-X

ISSN-0071-8068

ISSN-0340-7691

JPL-PUB-84-3

JPL-9950-956
 JPL-9950-982
 JPL-9950-983

JSC-20236

JSC-20237

JSC-20238

JSC-20239

JSR-84-203

LARS-TR-062984

LARS-TR-073184

LARS-TR-111284

p 63 N85-17350 #

p 63 N85-16284 #

p 52 N85-17417 #

p 8 N85-16241 * #

p 8 N85-16242 * #

p 62 N85-16244 * #

p 15 N85-16245 * #

p 8 N85-16246 * #

p 8 N85-16247 * #

p 24 N85-16248 * #

p 62 N85-16249 * #

p 60 N85-16250 * #

p 52 N85-16251 * #

p 62 N85-16268 * #

p 9 N85-16269 * #

p 63 N85-16270 * #

p 63 N85-16271 * #

p 10 N85-17400 * #

p 10 N85-17401 * #

p 10 N85-17402 * #

p 40 N85-17404 * #

p 65 N85-20496 * #

p 66 N85-20508 * #

p 67 N85-21724 * #

p 11 N85-19485 * #

p 15 N85-19486 * #

p 11 N85-19487 * #

p 11 N85-19488 * #

p 64 N85-19489 * #

p 52 N85-19490 * #

p 64 N85-19491 * #

p 64 N85-19492 * #

p 52 N85-19493 * #

p 11 N85-19494 * #

p 11 N85-19495 * #

p 12 N85-21747 * #

p 12 N85-21748 * #

p 12 N85-21749 * #

p 12 N85-21750 * #

p 13 N85-21751 * #

p 13 N85-21752 * #

p 41 N85-21753 * #

p 15 N85-21754 * #

p 55 N85-21755 * #

p 70 N85-21756 * #

p 26 N85-21757 * #

p 9 N85-16290 #

p 52 N85-17256 * #

p 63 N85-16270 * #

p 24 N85-16248 * #

p 64 N85-19501 #

p 15 N85-19502 #

p 52 N85-19493 * #

p 64 N85-19385 #

p 19 N85-18440 #

p 63 N85-17406 #

p 19 N85-18440 #

p 63 N85-17208 * #

p 12 N85-19496 * #

p 26 N85-19498 * #

p 25 N85-19497 * #

p 12 N85-21750 * #

p 12 N85-21748 * #

p 12 N85-21749 * #

p 13 N85-21751 * #

p 40 N85-17274 #

p 8 N85-16242 * #

p 8 N85-16241 * #

p 11 N85-19495 * #

LARS-TR-111484

LC-84-18972

LD-R-267

M8B-UA-753/83-OE

NAS 1 15 86167

NAS 1 15 86170

NAS 1 15 86180

NAS 1 15 87402

NAS 1 15 87405

NAS 1 15 87413

NAS 1 21 475

NAS 1 26 171355

NAS 1 26 171819

NAS 1 26 171821

NAS 1 26 171822

NAS 1 26 171842

NAS 1 26 171843

NAS 1 26 171857

NAS 1 26 174188

NAS 1 26 174221

NAS 1 26 174225

NAS 1 26 174226

NAS 1 26 174227

NAS 1 26 174228

NAS 1 26 174229

NAS 1 26 174230

NAS 1 26 174231

NAS 1 26 174232

NAS 1 26 174282

NAS 1 26 174312

NAS 1 26 174313

NAS 1 26 174341

NAS 1 26 174367

NAS 1 26 174399

NAS 1 26 174400

NAS 1 26 174401

NAS 1 26 174402

NAS 1 26 174403

NAS 1 26 174404

NAS 1 26 174405

NAS 1 26 174406

NAS 1 26 174434

NAS 1 26 174440

NAS 1 26 175457

NAS 1 26 175458

NAS 1 26 175518

NAS 1 26 175519

NAS 1 26 175520

NAS 1 26 175524

NAS 1 26 175525

NAS 1 26 175526

NAS 1 26 175527

NAS 1 26 175528

NAS 1 26 175529

NAS 1 26 175530

NAS 1 26 175537

NAS 1 55 2355-VOL-1

NAS 1 55 2355-VOL-2-PT-1

NAS 1 55 2355-VOL-3-PT-2

NAS 1 71 NPO-15651-1

NASA-CASE-NPO-15651-1

NASA-CP-2355-VOL-1

NASA-CP-2355-VOL-2-PT-1

NASA-CP-2355-VOL-3-PT-2

NASA-CR-171355

NASA-CR-171819

NASA-CR-171821

NASA-CR-171822

NASA-CR-171842

NASA-CR-171843

NASA-CR-171857

NASA-CR-174188

NASA-CR-174221

NASA-CR-174225

NASA-CR-174226

NASA-CR-174227

p 11 N85-19494 * #

p 72 N85-20942 #

p 63 N85-17350 #

p 60 A85-26393 #

p 44 N85-16273 * #

p 40 N85-18443 * #

p 40 N85-17404 * #

p 10 N85-17400 * #

p 8 N85-16247 * #

p 11 N85-19485 * #

p 20 N85-22323 * #

p 70 N85-21873 * #

p 50 N85-16251 * #

p 8 N85-16241 * #

p 8 N85-16242 * #

p 11 N85-19495 * #

p 11 N85-19494 * #

p 12 N85-21747 * #

p 24 N85-16248 * #

p 62 N85-16244 * #

p 15 N85-16245 * #

p 8 N85-16246 * #

p 62 N85-16249 * #

p 62 N85-16250 * #

p 62 N85-16268 * #

p 9 N85-16269 * #

p 63 N85-16270 * #

p 63 N85-16271 * #

p 63 N85-17208 * #

p 10 N85-17401 * #

p 10 N85-17402 * #

p 52 N85-17256 * #

p 44 N85-19221 * #

p 15 N85-19486 * #

p 11 N85-19487 * #

p 11 N85-19488 * #

p 64 N85-19489 * #

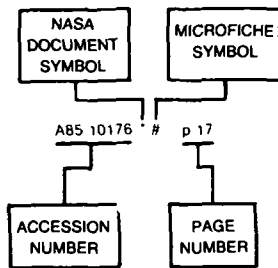
p 52 N85-19490 * #

NASA-CR-174228

REPORT NUMBER INDEX

NASA-CR-174228	p 62	N85-16250 * #	YM-15-00400	p 12	N85-21750 * #
NASA-CR-174229	p 62	N85-16268 * #	YM-15-00401	p 12	N85-21748 * #
NASA-CR-174230	p 9	N85-16269 * #	YM-15-00402	p 12	N85-21749 * #
NASA-CR-174231	p 63	N85-16270 * #	YM-15-00403	p 13	N85-21751 * #
NASA-CR-174232	p 63	N85-16271 * #			
NASA-CR-174282	p 63	N85-17208 * #			
NASA-CR-174312	p 10	N85-17401 * #			
NASA-CR-174313	p 10	N85-17402 * #			
NASA-CR-174341	p 52	N85-17256 * #			
NASA-CR-174367	p 44	N85-19221 * #			
NASA-CR-174399	p 15	N85-19486 * #			
NASA-CR-174400	p 11	N85-19487 * #			
NASA-CR-174401	p 11	N85-19488 * #			
NASA-CR-174402	p 64	N85-19489 * #			
NASA-CR-174403	p 52	N85-19490 * #			
NASA-CR-174404	p 64	N85-19491 * #			
NASA-CR-174405	p 64	N85-19492 * #			
NASA-CR-174406	p 52	N85-19493 * #			
NASA-CR-174434	p 44	N85-19568 * #			
NASA-CR-174440	p 12	N85-19496 * #			
NASA-CR-175457	p 25	N85-19497 * #			
NASA-CR-175458	p 26	N85-19498 * #			
NASA-CR-175518	p 12	N85-21748 * #			
NASA-CR-175519	p 12	N85-21749 * #			
NASA-CR-175520	p 12	N85-21750 * #			
NASA-CR-175524	p 13	N85-21751 * #			
NASA-CR-175525	p 13	N85-21752 * #			
NASA-CR-175526	p 41	N85-21753 * #			
NASA-CR-175527	p 15	N85-21754 * #			
NASA-CR-175528	p 55	N85-21755 * #			
NASA-CR-175529	p 70	N85-21756 * #			
NASA-CR-175530	p 26	N85-21757 * #			
NASA-CR-175570	p 42	N85-21758 * #			
NASA-SP-475	p 20	N85-22323 * #			
NASA-TM-86167	p 44	N85-16273 * #			
NASA-TM-86170	p 40	N85-18443 * #			
NASA-TM-86180	p 40	N85-17404 * #			
NASA-TM-87402	p 10	N85-17400 * #			
NASA-TM-87405	p 8	N85-16247 * #			
NASA-TM-87413	p 11	N85-19485 * #			
NOAA-TM-NOS-NGS-40	p 42	N85-21767 #			
NOAA-TM-NOS-NGS-41	p 20	N85-21766 #			
NOAA-TR-NESDIS-18	p 15	N85-20517 #			
NORDA-TN-283	p 39	N85-16281 #			
NORDA-TN-291	p 39	N85-16282 #			
NORDA-60	p 40	N85-17416 #			
NSTL/ERL-213	p 11	N85-19485 * #			
NSTL/ERL-230	p 8	N85-16247 * #			
PB85-105617/GAR	p 9	N85-16290 #			
PB85-124121	p 72	N85-20942 #			
PB85-129641	p 42	N85-21767 #			
PB85-133775	p 20	N85-21766 #			
PCN902-91548	p 52	N85-19490 * #			
PCN902-91548	p 26	N85-21757 * #			
QR-10	p 55	N85-21755 * #			
QR-8	p 64	N85-19491 * #			
QR-9	p 70	N85-21756 * #			
QSTPR-8	p 62	N85-16268 * #			
QSTPR-9	p 64	N85-19489 * #			
REPT-85B0115-VOL-1	p 65	N85-20496 * #			
REPT-85B0115-VOL-2-PT-1	p 66	N85-20508 * #			
REPT-85B0115-VOL-3-PT-2	p 67	N85-21724 * #			
RSL-TR-3311-2	p 38	N85-15960 #			
SAND-83-2195	p 10	N85-18447 #			
SD-TR-84-39	p 64	N85-17469 #			
TR-0084(4478-32)-4	p 64	N85-17469 #			
TRITA-FMI-9	p 63	N85-17406 #			
US-PATENT-APPL-SN-375620	p 41	N85-21723 * #			
US-PATENT-APPL-SN-582412	p 40	N85-17506 #			
US-PATENT-CLASS-343-352	p 41	N85-21723 * #			
US-PATENT-CLASS-374-122	p 41	N85-21723 * #			
US-PATENT-4,499,470	p 41	N85-21723 * #			
USCG-D-33-84	p 41	N85-20619 #			
UTD-CONTRIB-471	p 26	N85-19498 * #			

Typical Accession Number Index Listing



Listings in this index are arranged alphanumerically by accession number. The page number listed to the right indicates the page on which the citation is located. An asterisk (*) indicates that the item is a NASA report. A pound sign (#) indicates that the item is available on microfiche.

A85-19363	#	p 55	A85-22711	#	p 57	A85-26476	#	p 18	A85-30013	#	p 19
A85-19417	*	p 26	A85-23144	*	p 46	A85-26641	#	p 49	A85-30086	*	p 7
A85-19420	*	p 26	A85-23644	#	p 28	A85-26642	#	p 60	A85-30087	*	p 24
A85-19428	*	p 26	A85-23676	#	p 28	A85-26927	#	p 60	A85-30088	*	p 14
A85-19429	*	p 27	A85-23677	#	p 28	A85-26928	#	p 60	A85-30089	*	p 7
A85-19580	#	p 70	A85-23678	#	p 57	A85-26929	*	p 61	A85-30090	*	p 7
A85-19608	#	p 55	A85-23679	#	p 46	A85-26930	#	p 43	A85-30091	#	p 7
A85-19998	#	p 56	A85-23681	#	p 29	A85-26931	#	p 5	A85-30092	*	p 7
A85-20035	#	p 15	A85-23682	#	p 29	A85-26932	#	p 5	A85-30093	*	p 7
A85-20081	#	p 56	A85-23683	#	p 29	A85-26933	#	p 5			
A85-20084	#	p 45	A85-23684	#	p 46	A85-26934	*	p 5	N85-15960	#	p 38
A85-20086	#	p 27	A85-23685	#	p 29	A85-26935	#	p 14	N85-16239	#	p 38
A85-20486	*	p 27	A85-23686	#	p 29	A85-26936	#	p 5	N85-16241	#	p 8
A85-20487	*	p 27	A85-23688	#	p 29	A85-26939	*	p 6	N85-16242	#	p 8
A85-20492	#	p 27	A85-23689	#	p 46	A85-26942	#	p 6	N85-16244	#	p 62
A85-20565	#	p 70	A85-23690	#	p 29	A85-26947	#	p 6	N85-16245	#	p 15
A85-20566	#	p 70	A85-23691	#	p 29	A85-26948	#	p 49	N85-16246	#	p 8
A85-20568	#	p 56	A85-23692	#	p 30	A85-27057	#	p 61	N85-16247	#	p 8
A85-20570	#	p 13	A85-23693	#	p 57	A85-27059	#	p 61	N85-16248	#	p 24
A85-20571	#	p 56	A85-23694	#	p 1	A85-27061	#	p 61	N85-16249	#	p 62
A85-20572	#	p 45	A85-23695	#	p 30	A85-27066	#	p 18	N85-16250	#	p 62
A85-20573	#	p 1	A85-23696	#	p 30	A85-27386	#	p 18	N85-16251	#	p 50
A85-20574	#	p 70	A85-23699	#	p 30	A85-27441	#	p 34	N85-16252	#	p 50
A85-20640	#	p 71	A85-23700	#	p 16	A85-27519	#	p 71	N85-16253	#	p 8
A85-20641	#	p 71	A85-23701	#	p 30	A85-27698	#	p 61	N85-16254	#	p 50
A85-20642	#	p 71	A85-23702	#	p 30	A85-27701	#	p 34	N85-16255	#	p 50
A85-20643	#	p 56	A85-23703	#	p 30	A85-27704	#	p 34	N85-16256	#	p 8
A85-20644	#	p 13	A85-23704	#	p 30	A85-27705	#	p 35	N85-16257	#	p 50
A85-20646	#	p 71	A85-23705	#	p 57	A85-27710	*	p 35	N85-16258	#	p 50
A85-20647	#	p 13	A85-23706	#	p 31	A85-27736	#	p 35	N85-16259	#	p 9
A85-20747	#	p 13	A85-23707	#	p 31	A85-27827	#	p 49	N85-16260	#	p 9
A85-20748	#	p 13	A85-23751	#	p 57	A85-27841	#	p 35	N85-16261	#	p 50
A85-20749	#	p 14	A85-23752	#	p 2	A85-27943	*	p 22	N85-16262	#	p 50
A85-20750	#	p 45	A85-23753	*	p 2	A85-27944	#	p 22	N85-16263	#	p 51
A85-21046	#	p 42	A85-23754	*	p 2	A85-27945	*	p 22	N85-16264	#	p 51
A85-21047	#	p 20	A85-23755	#	p 31	A85-27946	*	p 23	N85-16265	#	p 51
A85-21048	*	p 45	A85-23756	#	p 2	A85-27947	*	p 62	N85-16266	#	p 51
A85-21050	#	p 1	A85-23757	#	p 2	A85-27948	*	p 23	N85-16267	#	p 51
A85-21107	*	p 16	A85-23758	#	p 2	A85-27984	#	p 14	N85-16268	#	p 62
A85-21130	#	p 42	A85-23759	#	p 57	A85-28005	*	p 35	N85-16269	#	p 9
A85-21138	#	p 45	A85-23760	#	p 2	A85-28007	*	p 35	N85-16270	#	p 63
A85-21145	*	p 27	A85-23761	#	p 3	A85-28011	#	p 18	N85-16271	#	p 63
A85-21174	*	p 1	A85-23762	#	p 3	A85-28012	#	p 18	N85-16273	#	p 44
A85-21669	#	p 28	A85-23763	#	p 3	A85-28022	#	p 36	N85-16281	#	p 39
A85-21960	#	p 28	A85-23765	#	p 3	A85-28027	#	p 36	N85-16282	#	p 39
A85-21975	*	p 20	A85-23766	#	p 21	A85-28119	#	p 36	N85-16284	#	p 63
A85-22171	*	p 28	A85-23767	#	p 3	A85-28400	#	p 23	N85-16290	#	p 9
A85-22175	#	p 28	A85-23768	#	p 58	A85-28783	#	p 36	N85-16362	#	p 9
A85-22420	*	p 1	A85-23769	#	p 46	A85-28788	#	p 36	N85-17208	#	p 63
A85-22422	#	p 21	A85-23771	#	p 3	A85-28973	#	p 49	N85-17212	#	p 39
A85-22423	#	p 28	A85-23772	#	p 4	A85-28999	#	p 23	N85-17213	#	p 39
A85-22424	*	p 56	A85-23774	#	p 4	A85-29000	#	p 19	N85-17215	#	p 24
A85-22678	#	p 46	A85-23775	#	p 4	A85-29217	#	p 49	N85-17216	#	p 44
A85-22681	#	p 56	A85-23779	#	p 46	A85-29218	#	p 43	N85-17226	#	p 24
A85-22682	#	p 56	A85-23780	*	p 58	A85-29219	#	p 43	N85-17228	#	p 9
			A85-23781	#	p 58	A85-29220	#	p 43	N85-17229	#	p 51
						A85-29221	#	p 49	N85-17231	#	p 39
						A85-29405	#	p 23	N85-17232	#	p 24
						A85-29703	*	p 36	N85-17233	#	p 39
						A85-29704	#	p 36	N85-17234	#	p 19
						A85-29705	#	p 36	N85-17235	#	p 40
						A85-29706	#	p 37	N85-17236	#	p 25
						A85-29707	#	p 37	N85-17237	#	p 25
						A85-29708	#	p 37	N85-17239	#	p 44
						A85-29712	#	p 37	N85-17240	#	p 9
						A85-29713	#	p 37	N85-17241	#	p 25
						A85-29714	*	p 37	N85-17242	#	p 52
						A85-29715	#	p 38	N85-17243	#	p 52
						A85-29716	#	p 38	N85-17244	#	p 25
						A85-29784	#	p 62	N85-17246	#	p 10
						A85-29903	#	p 38	N85-17248	#	p 25
						A85-29904	#	p 23	N85-17249	#	p 25
						A85-29905	#	p 24	N85-17250	#	p 63
						A85-29906	#	p 44	N85-17251	#	p 10
						A85-29907	#	p 14	N85-17252	#	p 10
						A85-29908	#	p 6	N85-17256	#	p 52
						A85-29909	#	p 62	N85-17274	#	p 40
						A85-29910	#	p 6	N85-17350	#	p 63
						A85-29911	#	p 6	N85-17400	#	p 10
						A85-29912	#	p 24	N85-17401	#	p 10
						A85-29913	#	p 49	N85-17402	#	p 10
						A85-29914	#	p 50	N85-17404	#	p 40
						A85-29915	#	p 38	N85-17406	#	p 63
						A85-29969	#	p 6			

N85-17407

ACCESSION NUMBER INDEX

N85-17407 # p 19
 N85-17408 # p 52
 N85-17409 # p 63
 N85-17416 # p 40
 N85-17417 # p 52
 N85-17469 # p 64
 N85-17506 # p 40
 N85-18437 # p 19
 N85-18440 # p 19
 N85-18443 * # p 40
 N85-18447 # p 10
 N85-19221 * # p 44
 N85-19321 # p 11
 N85-19385 # p 64
 N85-19485 * # p 11
 N85-19486 * # p 15
 N85-19487 * # p 11
 N85-19488 * # p 11
 N85-19489 * # p 64
 N85-19490 * # p 52
 N85-19491 * # p 64
 N85-19492 * # p 64
 N85-19493 * # p 52
 N85-19494 * # p 11
 N85-19495 * # p 11
 N85-19496 * # p 12
 N85-19497 * # p 25
 N85-19498 * # p 26
 N85-19501 # p 64
 N85-19502 # p 15
 N85-19503 # p 41
 N85-19504 # p 41
 N85-19568 * # p 44
 N85-19594 # p 41
 N85-20190 # p 64
 N85-20220 # p 65
 N85-20496 * # p 65
 N85-20497 * # p 53
 N85-20498 * # p 53
 N85-20499 * # p 65
 N85-20500 * # p 65
 N85-20501 * # p 53
 N85-20502 * # p 65
 N85-20503 * # p 53
 N85-20504 * # p 53
 N85-20505 * # p 19
 N85-20506 * # p 65
 N85-20507 * # p 53
 N85-20508 * # p 66
 N85-20509 * # p 66
 N85-20510 * # p 66
 N85-20511 * # p 53
 N85-20512 * # p 54
 N85-20513 * # p 54
 N85-20514 * # p 66
 N85-20515 * # p 66
 N85-20516 * # p 66
 N85-20517 # p 15
 N85-20606 # p 45
 N85-20619 # p 41
 N85-20776 # p 67
 N85-20779 # p 67
 N85-20941 # p 71
 N85-20942 # p 72
 N85-21723 * # p 41
 N85-21724 * # p 67
 N85-21725 * # p 67
 N85-21726 * # p 54
 N85-21727 * # p 67
 N85-21728 * # p 54
 N85-21729 * # p 67
 N85-21730 * # p 68
 N85-21731 * # p 54
 N85-21732 * # p 68
 N85-21733 * # p 68
 N85-21734 * # p 68
 N85-21735 * # p 68
 N85-21736 * # p 12
 N85-21737 * # p 68
 N85-21738 * # p 69
 N85-21739 * # p 54
 N85-21740 * # p 69
 N85-21741 * # p 69
 N85-21742 * # p 69
 N85-21743 * # p 55
 N85-21744 * # p 55
 N85-21745 * # p 69
 N85-21746 * # p 20
 N85-21747 * # p 12
 N85-21748 * # p 12
 N85-21749 * # p 12
 N85-21750 * # p 12
 N85-21751 * # p 13
 N85-21752 * # p 13
 N85-21753 * # p 41
 N85-21754 * # p 15

N85-21755 * # p 55
 N85-21756 * # p 70
 N85-21757 * # p 26
 N85-21758 * # p 42
 N85-21761 # p 20
 N85-21766 # p 20
 N85-21767 # p 42
 N85-21873 * # p 70
 N85-21890 # p 15
 N85-21891 # p 42
 N85-21920 # p 42
 N85-22143 # p 42
 N85-22323 * # p 20

1. Report No. NASA SP-7041 (46)	2. Government Accession No.	3. Recipient's Catalog No.	
4. Title and Subtitle EARTH RESOURCES A Continuing Bibliography (Issue 46)		5. Report Date July 1985	
		6. Performing Organization Code	
7. Author(s)		8. Performing Organization Report No.	
		10. Work Unit No.	
9. Performing Organization Name and Address National Aeronautics and Space Administration Washington, D.C. 20546		11. Contract or Grant No.	
		13. Type of Report and Period Covered	
12. Sponsoring Agency Name and Address		14. Sponsoring Agency Code	
15. Supplementary Notes			
16. Abstract <p>This bibliography lists 467 reports, articles and other documents introduced into the NASA scientific and technical information system between April 1 and June 30, 1985. Emphasis is placed on the use of remote sensing and geophysical instrumentation in spacecraft and aircraft to survey and inventory natural resources and urban areas. Subject matter is grouped according to agriculture and forestry, environmental changes and cultural resources geodesy and cartography, geology and mineral resources, hydrology and water management, data processing and distribution systems, instrumentation and sensors, and economical analysis.</p>			
17. Key Words (Suggested by Author(s)) Bibliographies Earth Resources Remote Sensors		18. Distribution Statement Unclassified - Unlimited	
19. Security Classif. (of this report) Unclassified	20. Security Classif. (of this page) Unclassified	21. No. of Pages 140	22. Price* \$12.00 HC

FEDERAL DEPOSITORY LIBRARY PROGRAM

The Federal Depository Library Program provides Government publications to designated libraries throughout the United States. The Regional Depository Libraries listed below receive and retain at least one copy of nearly every Federal Government publication, either in printed or microfilm form, for use by the general public. These libraries provide reference services and inter-library loans; however, they are *not* sales outlets. You may wish to ask your local library to contact a Regional Depository to help you locate specific publications, or you may contact the Regional Depository yourself.

ARKANSAS STATE LIBRARY

One Capitol Mall
Little Rock, AR 72201
(501) 371-2326

AUBURN UNIV. AT MONTGOMERY LIBRARY

Documents Department
Montgomery, AL 36193
(205) 279-9110, ext 253

UNIV. OF ALABAMA LIBRARY

Documents Dept —Box S
University, AL 35486
(205) 348-7369

DEPT. OF LIBRARY, ARCHIVES AND PUBLIC RECORDS

Third Floor—State Cap
1700 West Washington
Phoenix, AZ 85007
(602) 255-4121

UNIVERSITY OF ARIZONA LIB.

Government Documents Dept
Tucson, AZ 85721
(602) 626-5233

CALIFORNIA STATE LIBRARY

Govt. Publications Section
P O Box 2037
Sacramento, CA 95809
(916) 322-4572

UNIV. OF COLORADO LIB.

Government Pub. Division
Campus Box 184
Boulder, CO 80309
(303) 492-8834

DENVER PUBLIC LIBRARY

Govt. Pub. Department
1357 Broadway
Denver, CO 80203
(303) 571-2131

CONNECTICUT STATE LIBRARY

Government Documents Unit
231 Capitol Avenue
Hartford, CT 06106
(203) 566-4971

UNIV. OF FLORIDA LIBRARIES

Library West
Documents Department
Gainesville, FL 32611
(904) 392-0367

UNIV. OF GEORGIA LIBRARIES

Government Reference Dept
Athens, Ga 30602
(404) 542-8951

UNIV. OF HAWAII LIBRARY

Govt. Documents Collection
2550 The Mall
Honolulu, HI 96822
(808) 948-8230

UNIV. OF IDAHO LIBRARY

Documents Section
Moscow, ID 83843
(208) 885-6344

ILLINOIS STATE LIBRARY

Information Services Branch
Centennial Building
Springfield, IL 62706
(217) 782-5185

INDIANA STATE LIBRARY

Serials Documents Section
140 North Senate Avenue
Indianapolis, IN 46204
(317) 232-3686

UNIV. OF IOWA LIBRARIES

Govt. Documents Department
Iowa City, IA 52242
(319) 353-3318

UNIVERSITY OF KANSAS

Doc. Collect.—Cpencer Lib
Lawrence, KS 66045
(913) 864-4662

UNIV. OF KENTUCKY LIBRARIES

Govt. Pub. Department
Lexington, KY 40506
(606) 257-3139

LOUISIANA STATE UNIVERSITY

Middleton Library
Govt. Docs Dept
Baton Rouge, LA 70803
(504) 388-2570

LOUISIANA TECHNICAL UNIV. LIBRARY

Documents Department
Ruston, LA 71272
(318) 257-4962

UNIVERSITY OF MAINE

Raymond H. Fogler Library
Tri-State Regional Documents
Depository
Orono, ME 04469
(207) 581-1680

UNIVERSITY OF MARYLAND

McKeldin Lib.—Doc. Div
College Park, MD 20742
(301) 454-3034

BOSTON PUBLIC LIBRARY

Government Docs. Dept
Boston, MA 02117
(617) 536-5400 ext 226

DETROIT PUBLIC LIBRARY

Sociology Department
5201 Woodward Avenue
Detroit, MI 48202
(313) 833-1409

MICHIGAN STATE LIBRARY

P O Box 30007
Lansing, MI 48909
(517) 373-0640

UNIVERSITY OF MINNESOTA

Government Pubs. Division
409 Wilson Library
309 19th Avenue South
Minneapolis, MN 55455
(612) 373-7813

UNIV. OF MISSISSIPPI LIB

Documents Department
University, MS 38677
(601) 232-5857

UNIV. OF MONTANA

Mansfield Library
Documents Division
Missoula, MT 59812
(406) 243-6700

NEBRASKA LIBRARY COMM.

Federal Documents
1420 P Street
Lincoln, NE 68508
(402) 471-2045
In cooperation with University of
Nebraska-Lincoln

UNIVERSITY OF NEVADA LIB.

Govt. Pub. Department
Reno, NV 89557
(702) 784-6579

NEWARK PUBLIC LIBRARY

5 Washington Street
Newark, NJ 07101
(201) 733-7812

UNIVERSITY OF NEW MEXICO

Zimmerman Library
Government Pub. Dept
Albuquerque, NM 87131
(505) 277-5441

NEW MEXICO STATE LIBRARY

Reference Department
325 Don Gaspar Avenue
Santa Fe, NM 87501
(505) 827-2033, ext 22

NEW YORK STATE LIBRARY

Empire State Plaza
Albany, NY 12230
(518) 474-5563

UNIVERSITY OF NORTH CAROLINA AT CHAPEL HILL

Wilson Library
BA/SS Documents Division
Chapel Hill, NC 27515
(919) 962-1321

UNIVERSITY OF NORTH DAKOTA

Chester Fritz Library
Documents Department
Grand Forks, ND 58202
(701) 777-2617, ext 27
(In cooperation with North
Dakota State Univ. Library)

STATE LIBRARY OF OHIO

Documents Department
65 South Front Street
Columbus, OH 43215
(614) 462-7051

OKLAHOMA DEPT. OF LIB.

Government Documents
200 NE 18th Street
Oklahoma City, OK 73105
(405) 521-2502

OKLAHOMA STATE UNIV. LIB.

Documents Department
Stillwater, OK 74078
(405) 624-6546

PORTLAND STATE UNIV. LIB

Documents Department
P O Box 1151
Portland, OR 97207
(503) 229-3673

STATE LIBRARY OF PENN.

Government Pub. Section
P O Box 1601
Harrisburg, PA 17105
(717) 787-3752

TEXAS STATE LIBRARY

Public Services Department
P O Box 12927—Cap. Sta
Austin, TX 78753
(512) 471-2996

TEXAS TECH UNIV. LIBRARY

Govt. Documents Department
Lubbock, TX 79409
(806) 742-2268

UTAH STATE UNIVERSITY

Merrill Library, U M C 30
Logan, UT 84322
(801) 750-2682

UNIVERSITY OF VIRGINIA

Alderman Lib.—Public Doc
Charlottesville, VA 22901
(804) 924-3133

WASHINGTON STATE LIBRARY

Documents Section
Olympia, WA 98504
(206) 753-4027

WEST VIRGINIA UNIV. LIB.

Documents Department
Morgantown, WV 26506
(304) 293-3640

MILWAUKEE PUBLIC LIBRARY

814 West Wisconsin Avenue
Milwaukee, WI 53233
(414) 278-3000

ST. HIST. LIB. OF WISCONSIN

Government Pub. Section
816 State Street
Madison, WI 53706
(608) 262-4347

WYOMING STATE LIBRARY

Supreme Ct. & Library Bld
Cheyenne, WY 82002
(307) 777-6344

National Aeronautics and
Space Administration

Washington, D.C.
20546

Official Business

Penalty for Private Use, \$300

BULK RATE
POSTAGE & FEES PAID
NASA Washington, DC
Permit No. G-27

NASA

POSTMASTER: If Undeliverable (Section 158
Postal Manual) Do Not Return
